Ultrasonography in Obstetrics and Gynecology

A Practical Approach to Clinical Problems

Carol B. Benson
Edward I. Bluth

Second Edition

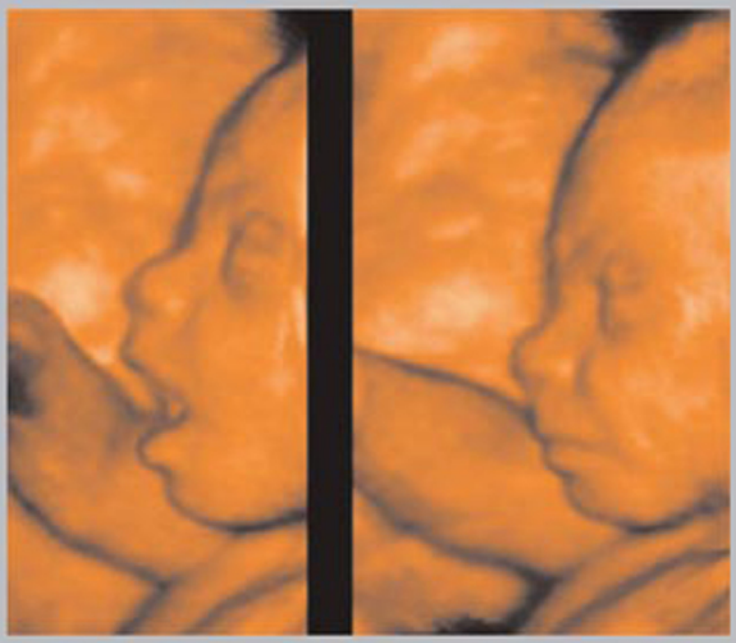

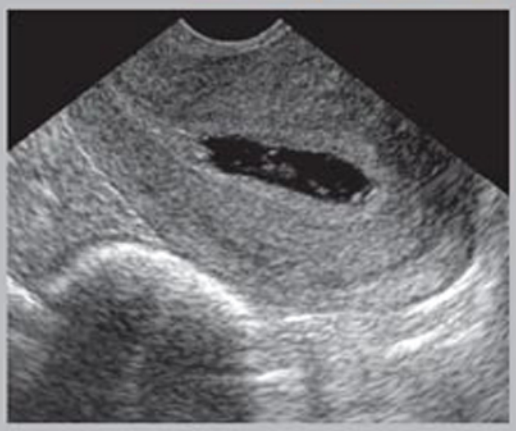

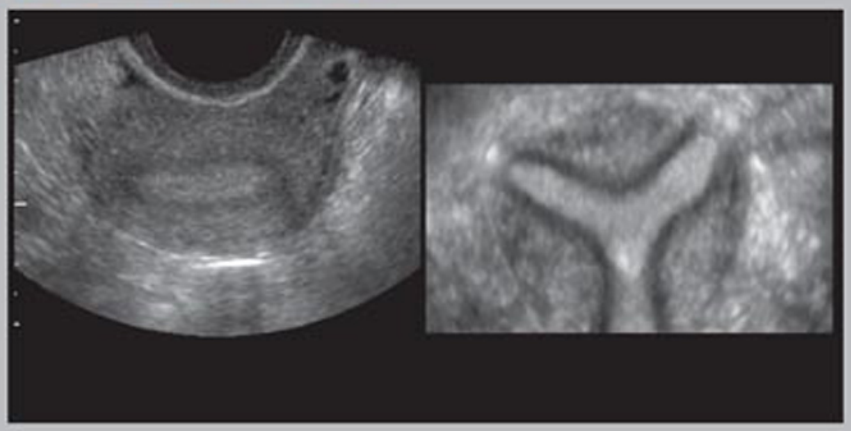

Thieme

Ultrasonography in Obstetrics and Gynecology

A Practical Approach to Clinical Problems

Second Edition

Carol B. Benson, M.D.
Professor
Department of Radiology
Harvard Medical School
Director of Ultrasound
Co-Director of High Risk Obstetrical Ultrasound
Brigham and Women's Hospital
Boston, Massachusetts

Edward I. Bluth, M.D., F.A.C.R.
Chairman Emeritus
Department of Radiology
Ochsner Health System
New Orleans, Louisiana

Thieme
New York • Stuttgart

Thieme Medical Publishers, Inc.
333 Seventh Ave.
New York, NY 10001

Editor: Timothy Hiscock
Editorial Assistant: David Price
Vice President, Production and Electronic Publishing: Anne T. Vinnicombe
Production Editor: Print Matters, Inc.
Vice President, International Marketing: Cornelia Schulze
Chief Financial Officer: Peter van Woerden
President: Brian D. Scanlan
Compositor: Compset, Inc.
Printer: Everbest Printing Co.

Library of Congress Cataloging-in-Publication Data

Ultrasonography in obstetrics and gynecology / [edited by] Carol B. Benson, Edward I. Bluth. — 2nd ed.
p.; cm.
Includes bibliographical references and index.
ISBN-13: 978-1-58890-612-0 (alk. paper)
1. Generative organs, Female—Ultrasonic imaging. 2. Fetus—Diseases—Diagnosis. 3. Ultrasonics in obstetrics. I. Benson, Carol B. II. Bluth, Edward I.
[DNLM: 1. Genital Diseases, Female—ultrasonography. 2. Fetal Diseases—ultrasonography. 3. Pregnancy Complications—ultrasonography. 4. Ultrasonography—methods. WP 141 U462 2007]
RG107.5.U4U485 2007
618'.047543—dc22 2006051488

Important note: Medical knowledge is ever-changing. As new research and clinical experience broaden our knowledge, changes in treatment and drug therapy may be required. The authors and editors of the material herein have consulted sources believed to be reliable in their efforts to provide information that is complete and in accord with the standards accepted at the time of publication. However, in view of the possibility of human error by the authors, editors, or publisher of the work herein or changes in medical knowledge, neither the authors, editors, or publisher, nor any other party who has been involved in the preparation of this work, warrants that the information contained herein is in every respect accurate or complete, and they are not responsible for any errors or omissions or for the results obtained from use of such information. Readers are encouraged to confirm the information contained herein with other sources. For example, readers are advised to check the product information sheet included in the package of each drug they plan to administer to be certain that the information contained in this publication is accurate and that changes have not been made in the recommended dose or in the contraindications for administration. This recommendation is of particular importance in connection with new or infrequently used drugs.

Some of the product names, patents, and registered designs referred to in this book are in fact registered trademarks or proprietary names even though specific reference to this fact is not always made in the text. Therefore, the appearance of a name without designation as proprietary is not to be construed as a representation by the publisher that it is in the public domain.

Printed in China

5 4 3 2 1

The Americas ISBN 978-1-58890-612-0
Rest of the World ISBN 978-3-13-125362-0

We dedicate this book to our families and friends, who supported us in this project:

Carol Benson to her husband, Peter, and her children, Nicole and Benjamin.

Ed Bluth to Elissa, Rachel, Jonathan, Marjorie, Irene, and Lawry
with gratitude and love.

Contents

Preface ix

Contributors x

1 Asymptomatic Palpable Adnexal Masses 1
Jill E. Langer and Peter H. Arger

2 Acute Pelvic Pain. 11
John S. Pellerito

3 Abnormal Premenopausal Vaginal Bleeding. 21
Edward A. Lyons

4 Infertility 39
Mary C. Frates

5 Amenorrhea in the Adolescent or Young Adult 50
Anna E. Nidecker, Harris L. Cohen, and Harry L. Zinn

6 Postmenopausal Vaginal Bleeding 65
Peter M. Doubilet

7 Family History of Ovarian Carcinoma. 76
Andrew M. Fried and Carol B. Benson

8 Tamoxifen. 90
Beverly G. Coleman

9 First-Trimester Pain or Bleeding or Both 103
Arthur C. Fleischer

10 Second- and Third-Trimester Bleeding 110
Barbara S. Hertzberg

11 Premature Labor 121
Geoffrey Wong and Deborah Levine

12 Estimating Fetal Gestational Age 133
Chaitali Shah and Ashok Bhanushali

13 Uterine Size Greater than Dates. 143
Beryl Benacerraf

14 Uterine Size Less than Dates: A Clinical Dilemma. 156
Alfred Abuhamad

15 Ruling Out Fetal Anomalies 161
Carol B. Benson

16 Family History of Congenital Heart Disease 174
Douglas L. Brown

17 Pregnant Women with High Maternal Serum–Alpha-Fetoprotein 187
Andrea L. Fick and Ruth B. Goldstein

18 Maternal Serum Screening Test Positive for Down Syndrome 199
Thomas D. Shipp

19 Diabetes Mellitus and Pregnancy 208
Peter W. Callen

20 Teratogen Exposure 216
Mark A. Kliewer

21 Postpartum Complications 237
Donald N. Di Salvo

Index 251

Preface

We have been pleased by the considerable popularity achieved by the first edition of *Ultrasonography in Obstetrics and Gynecology: A Practical Approach to Clinical Problems*. The second edition builds on the foundation that was originally laid at the Special Course on Ultrasound at the Meeting of the Radiological Society of North America in 1996, and then was further developed in the first edition of this text published in 2000. This new edition greatly expands and updates that previous work.

The overall aim of this textbook is to help the clinician assess and decide whether sonography or another imaging modality is the most appropriate for evaluating a clinical problem. In contrast to standard textbooks, our chapters are divided according to clinical questions rather than by organ systems. Our aim is to review the most important clinical issues faced by clinicians in their daily practice and to outline approaches for the effective use of sonography and other imaging modalities. Most chapters in the second edition have been extensively revised with new illustrations and images being added. The authors have attempted to incorporate the latest advances in ultrasound as well as to revise earlier recommendations based on advances in MRI, CT, and PET.

Each editor has a special area of interest and all of the authors are recognized authorities in the fields of ultrasound and radiology. The role of the radiologist, obstetrician, and gynecologist as a sonologist is changing. It is important to develop not only accurate diagnostic skills, but also the appropriate consultative skills to help direct the workup of clinical problems. It is hoped that this textbook will assist radiologists, obstetricians, gynecologists, residents, medical students and mid-level providers in developing their consultative skills regarding the use of ultrasound.

Although some of what is included in this book might be considered an opinion, our goal for the second edition of *Ultrasonography in Obstetrics and Gynecology: A Practical Approach to Clinical Problems* is to provide a readable and manageable book which will offer guidance for clinicians and diagnosticians on the appropriate use of sonography to solve important clinical problems.

Acknowledgments

The authors would like to thank Drs. Peter Arger, Barbara Hertzberg, William Middleton, and Carol Stelling for their help with the conceptual origins for this project. Additionally, the authors would like to thank Dr. Peter Arger for his role as an editor of the first edition.

Contributors

Alfred Abuhamad, M.D.
Mason C. Andrews Professor and Chairman
Department of Obstetrics and Gynecology
Eastern Virginia Medical School
Norfolk, Virginia

Peter H. Arger, M.D.
Professor
Department of Radiology
Hospital of the University of Pennsylvania
Philadelphia, Pennsylvania

Beryl Benacerraf, M.D.
Professor
Department of Obstetrics, Gynecology,
and Reproductive Biology
Harvard Medical School
Brigham and Women's Hospital
Boston, Massachusetts

Carol B. Benson, M.D.
Professor
Department of Radiology
Harvard Medical School
Director of Ultrasound
Co-Director of High Risk Obstetrical Ultrasound
Brigham and Women's Hospital
Boston, Massachusetts

Ashok Bhanushali, M.D.
Department of Radiology
Columbia University College of Physicians and Surgeons
New York Presbyterian Hospital
New York, New York

Douglas L. Brown, M.D.
Professor
Department of Radiology
Mayo Clinic College of Medicine
Rochester, Minnesota

Peter W. Callen, M.D.
Professor
Department of Radiology
University of California—San Francisco
San Francisco, California

Harris L. Cohen, M.D.
Professor of Radiology
Division of Body Imaging
Department of Radiology
Stony Brook University Medical Center
Visiting Professor of Radiology
The Johns Hopkins University School of Medicine
Baltimore, Maryland

Beverly G. Coleman, M.D.
Professor
Radiology Department
University of Pennsylvania School of Medicine
Associate Chairman, Abdominal Imaging
Chief of Ultrasound
Hospital of the University of Pennsylvania
Philadelphia, Pennsylvania

Donald N. Di Salvo, M.D.
Assistant Professor
Department of Radiology
Harvard Medical School
Director of Ultrasound Services
Dana Farber Cancer Institute
Boston, Massachusetts

Peter M. Doubilet, M.D., Ph.D.
Professor and Vice Chair
Department of Radiology
Harvard Medical School
Brigham and Women's Hospital
Boston, Massachusetts

Andrea L. Fick, M.D.
Clinical Fellow
Maternal–Fetal Medicine
Department of Obstetrics, Gynecology,
and Reproductive Sciences
University of California–San Francisco
San Francisco, California

Arthur C. Fleischer, M.D.
Professor
Departments of Radiology and Radiological Sciences,
and Obstetrics and Gynecology
Vanderbilt University Medical Center
Nashville, Tennessee

Mary C. Frates, M.D.
Associate Professor
Department of Radiology
Harvard Medical School
Boston, Massachusetts

Andrew M. Fried, M.D.
Professor
Department of Diagnostic Radiology
University of Kentucky Medical Center
Lexington, Kentucky

Ruth B. Goldstein, M.D.
Professor
Department of Radiology
University of California–San Francisco
San Francisco, California

Barbara S. Hertzberg, M.D., F.A.C.R.
Professor of Radiology
Associate Professor of Obstetrics and Gynecology
Department of Radiology
Duke University Medical Center
Durham, North Carolina

Mark A. Kliewer, M.D.
Professor
Department of Radiology
University of Wisconsin Hospital
Madison, Wisconsin

Jill E. Langer, M.D.
Associate Professor
Department of Radiology
University of Pennsylvania School of Medicine
Division of Ultrasound
Hospital of the University of Pennsylvania
Philadelphia, Pennsylvania

Deborah Levine, M.D.
Associate Professor
Department of Radiology
Harvard Medical School
Beth Israel Deaconess Medical Center
Boston, Massachusetts

Edward A. Lyons, M.D.
Professor
Departments of Radiology, Obstetrics and Gynecology,
and Anatomy
University of Manitoba
Health Sciences Centre
Winnipeg, Canada

Anna E. Nidecker, M.D.
Resident
Department of Radiology
Stony Brook University Medical Center
Stony Brook, New York

John S. Pellerito, M.D.
Chief
Department of Radiology
Division of Ultrasound, CT, and MRI
North Shore Hospital
Manhasset, New York

Chaitali Shah, M.D.
Managing Editor
www.sonoworld.com
Philadelphia, Pennsylvania

Thomas D. Shipp, M.D.
Associate Professor
Department of Obstetrics, Gynecology,
and Reproductive Biology
Harvard Medical School
Diagnostic Ultrasound Associates, P.C.
Boston, Massachusetts

Geoffrey Wong, M.D.
Assistant Professor
Department of Obstetrics and Gynecology
Beth Israel Deaconess Medical Center
Boston, Massachusetts

Harry L. Zinn, M.D.
Associate Professor
Department of Radiology
State University of New York–Downstate
Brooklyn, New York

1 Asymptomatic Palpable Adnexal Masses

Jill E. Langer and Peter H. Arger

Differential Diagnosis, Imaging, and Treatment

Various lesions can present as an asymptomatic, palpable, adnexal mass on routine gynecologic examination, such as physiological ovarian cysts, endometriomas, benign, and less commonly malignant ovarian tumors, as well as a variety of nonovarian adnexal lesions. The patient's age and menstrual status, the apparent size of the mass, and the feel of the mass will influence the diagnostic evaluation. The prevalence of palpable adnexal masses in young women is high, and the vast majority of these will be benign and often physiological in nature. If the mass is relatively small or has a soft feel, the examining physician may decide to evaluate the premenopausal patient with a repeat physical examination after one or two menstrual cycles; if the lesion has resolved, it was likely a physiological cyst. If a palpable mass is large, feels firm, persists or increases in size on follow-up physical exam, then a transvaginal ultrasound is the usual next diagnostic step for further characterization of the lesion. A serum cancer antigen 125 (CA 125) level or other imaging study such as magnetic resonance imaging (MRI) is rarely done in the premenopausal patient as part of the initial evaluation, but may be obtained when the ultrasound findings are inconclusive. Because the risk of malignancy is higher in a postmenopausal woman, a transvaginal ultrasound examination and CA 125 level are generally obtained when a mass is palpated in these patients.

Sonography allows discrimination between those adnexal lesions that are likely to be physiological and can be observed from those lesions that require surgery. Transvaginal ultrasound (TVUS), particularly with the use of color Doppler, carries a relatively high accuracy in the discrimination of benign from malignant ovarian masses.[1–3] If the sonographic characteristics of a mass are inconclusive, yet are associated with a low risk of malignancy, the patient can be treated with laparoscopic removal of the mass.

Laparoscopic surgery has become the gold standard for the treatment of known or presumed benign adnexal masses because of its shorter convalescence and reduced morbidity compared with laparotomy.[4,5] If, on sonography, a mass has features suggestive of a malignant ovarian neoplasm, the patient can be referred to a gynecologic surgeon capable of performing more comprehensive surgery. The sonographic features and etiologic aspects of some of the more common palpable masses are described in the following sections of this chapter. Exophytic fibroids are a common cause of an asymptomatic palpable adnexal mass.

Diagnostic Evaluation

Etiology and Ultrasound Imaging

Physiological Cysts

An asymptomatic physiological cyst is a common cause of a palpable adnexal mass in premenopausal adult women. In the first half of the menstrual cycle one or more dominant follicles will develop, grow to a diameter of ~20 to 25 mm, and then rupture at ovulation. In a small number of women, a mature follicle will fail to ovulate and continue to enlarge, occasionally reaching large size.[6] However, regardless of size, the typical follicular cyst will appear as a simple cyst on ultrasound, with thin walls, sharply defined borders, and containing anechoic fluid (**Fig. 1–1**). Small

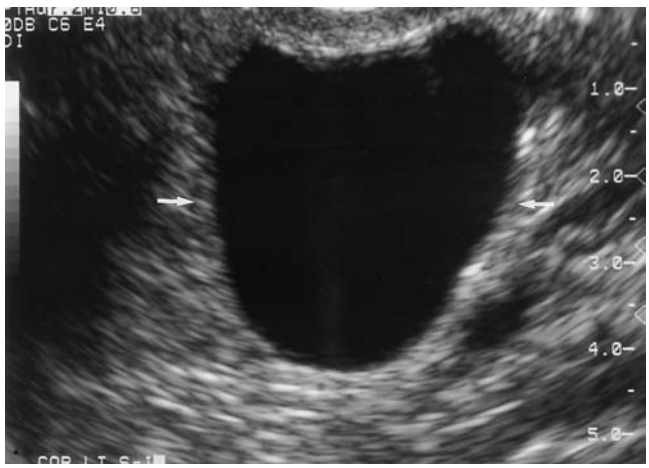

Figure 1–1 Simple ovarian cyst. Transvaginal sonogram of the ovary shows a smooth-walled, anechoic mass with good sound transmission (*white arrow*).

(< 3 cm), simple-appearing follicular cysts typically do not need further diagnostic evaluation. Larger, unilocular cysts should be evaluated by repeating the ultrasound exam after one or two menstrual cycles because most follicular cysts will disappear.[7,8]

In premenopausal women, ~30% of persistent, simple-appearing cysts will be neoplasms, the overwhelming majority of which will be benign.[9] Large lesion size (> 5 or 6 cm) raises concern for a neoplasm. However, the majority of large, simple-appearing cystic lesions in women of reproductive age are still more likely to be a functional cyst or other benign etiology rather than a malignant neoplasm.[7,9,10] Whereas the vast majority of follicular cysts will appear anechoic and unilocular, 14% may have septa and 3% may have nonvascular mural nodules.[7] These slightly more complicated lesions may be indistinguishable from other ovarian cystic masses at the time of the initial sonographic exam.

Corpus luteum cysts evolve from the remnant of the mature follicle following ovulation. These lesions have a thin (2 to 3 mm) echogenic and often highly vascular wall. Although well defined from the surrounding parenchyma, the corpus luteum may have an irregular outline if in the process of involuting. Typically, the corpus luteum cyst is under 2.5 cm in maximal dimension, reflecting its origin as a follicle, but it may be larger, particularly if complicated by internal hemorrhage[6,7] (**Fig. 1–2**).

Although the postmenopausal pelvis was thought to be hormonally quiescent, simple ovarian cysts are detected in 10 to 15% of all postmenopausal women undergoing transvaginal sonography.[9] The majority of these cysts are small and tend to resolve spontaneously. If the lesion size is less than 5 cm, or more conservatively 3 cm, and completely simple in appearance, some clinicians will elect to follow a simple-appearing cyst in a postmenopausal patient with serial ultrasound exams. If the lesion enlarges, it is considered suspect for a neoplasm and should be removed.[11] Larger postmenopausal cystic lesions usually undergo surgical excision. Fortunately, because the majority will be benign, the patients may still be treated with laparoscopic removal.[12]

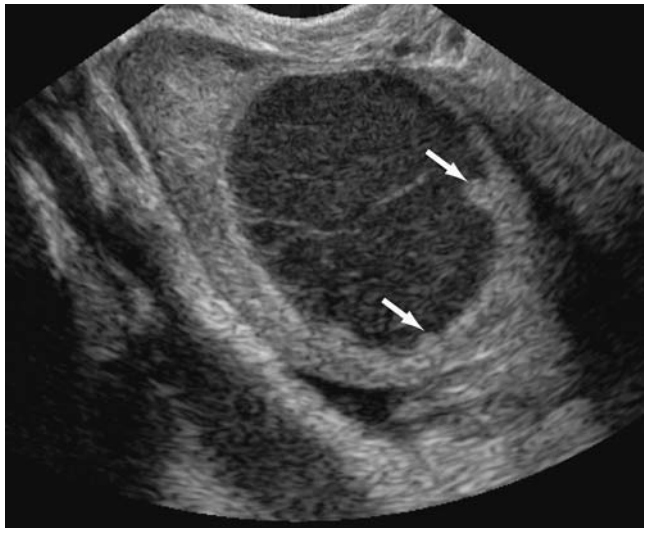

Figure 1–2 Corpus luteum cyst. This predominantly cystic mass has faint internal septations, low-level echoes, and small echogenic mural nodules (*white arrows*). The mass completely disappeared after two menstrual cycles, confirming the diagnosis of a hemorrhagic physiological corpus luteum cyst.

Hemorrhagic Cysts

Hemorrhagic cysts occur as a result of bleeding into a follicular cyst or corpus luteum cyst and can happen at anytime during the menstrual cycle. Hemorrhage within the

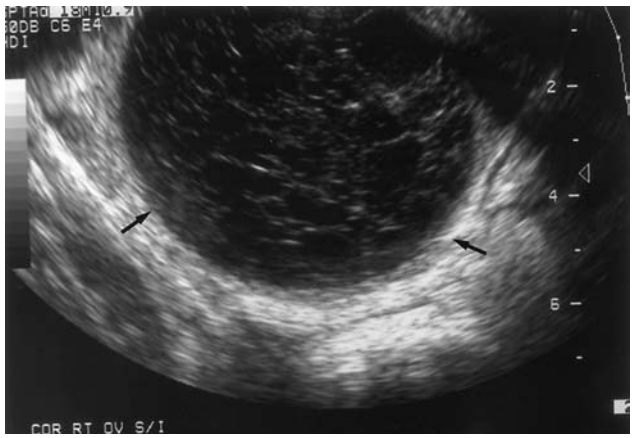

A

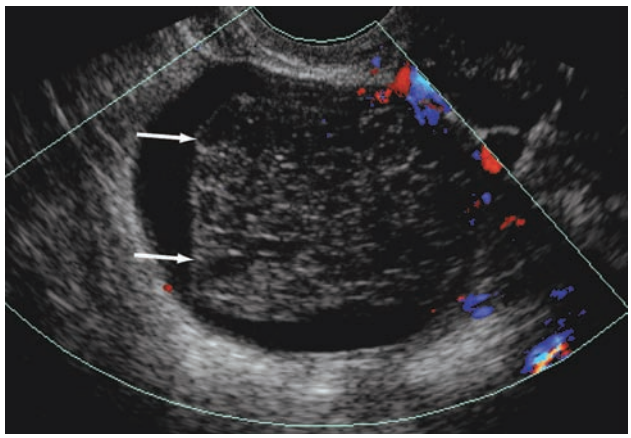

B

Figure 1–3 Hemorrhagic cyst evaluation. **(A)** A 6 cm complex cystic mass of the right ovary with an internal reticular pattern was noted in this asymptomatic 26-year-old patient (*black arrows*). On follow-up sonography, the lesion had decreased in size and the fibrin strands resorbed, confirming a hemorrhagic cyst. **(B)** This hemorrhagic cyst contains a retracting avascular thrombus with a straight border (*arrows*).

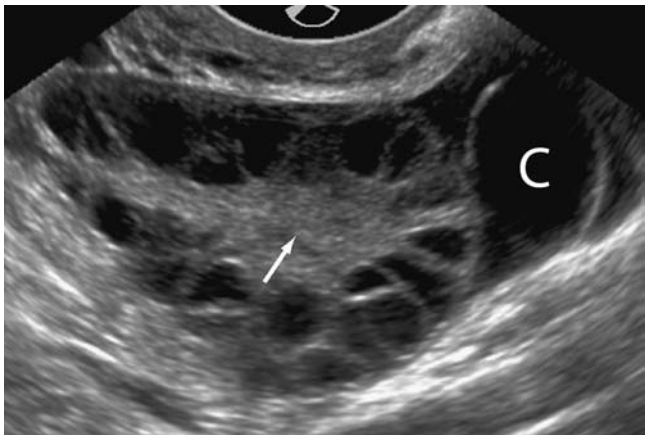

Figure 1–4 Polycystic ovary syndrome (PCOS). Enlarged ovaries with multiple peripheral follicles and echogenic central stromal tissue (*arrow*) were seen in this patient with a hormone profile consistent with PCOS. Incidentally noted is a small adjacent paraovarian cyst (C).

cyst subsequently interferes with the normal physiological involution and regression which would have occurred in that menstrual cycle. Variable characteristics can be seen in these hemorrhagic cysts, depending on the stage of clot formation, lysis, and retraction. Multiple fibrous strands, and retracting clot with convex or straight borders, suggest the presence of hemorrhage, which allows a confident diagnosis of a functional hemorrhagic cyst[13–15] (**Fig. 1–3**). The interdigitating strands of fibrin, often called a fish net or reticular pattern, differ from true septations by their thin size (< 1 mm), lack of vascularity, and poor reflectivity of sound, making them only faintly visible.[13,14] A dependent clot may simulate a solid component or mural nodule, but will fail to show vascular flow on Doppler exam.[13] The most common clinical presentation is the abrupt onset of acute pelvic pain; less commonly the patient is asymptomatic. Because hemorrhagic cysts will resolve or demonstrate regression, repeat sonography in 4 to 6 weeks should be recommended if hemorrhagic cyst is considered as a possible diagnosis for a complex adnexal mass in a premenopausal patient.

Polycystic Ovarian Syndrome

Patients with polycystic ovarian syndrome (PCOS) have complex clinical, laboratory, and ultrasound findings with heterogeneous symptoms that may vary over time. The original description by Stein and Leventhal in 1935 required direct visualization of the ovaries and histologic confirmation on wedge biopsy. More recently, biochemical criteria have become the mainstay for diagnosis.[16] Most women with PCOS present with menstrual cycle disturbances, hirsutism, acne, male pattern baldness, along with metabolic alterations such as obesity and insulin resistance.[16,17] The ovaries in patients with PCOS are typically enlarged, often over 14 cm^3, and demonstrate an excess of small follicles, arrested at the 6 to 9 mm stage of maturation (**Fig. 1–4**).

Other common ovarian features are a spherical shape and prominent central echogenic stroma tissue. However, the clinical and biochemical features may vary widely; some women with polycystic ovaries on sonography do not have the clinical stigmata of PCOS and some women with classic symptoms have normal-appearing ovaries. A consensus conference held in 2003 established criteria for the diagnosis of PCOS as the presence of two of the following three criteria: (1) oligomenorrhea or anovulation; (2) hyperandrogynism; (3) polycystic ovaries, defined as containing either 12 or more immature follicles, each measuring 2 to 9 mm in diameter, or an increased ovarian volume of over 10 cm^3.[17] These features carried the highest sensitivity and specificity for the differentiation of PCOS from an ovary with many follicles, such as may be seen during puberty and in women recovering from hypothalamic amenorrhea. It is worth noting that a single ovary meeting the criteria is sufficient for the diagnosis of PCOS and that a unilateral presentation can be seen in up to 35% of patients.[17,18] If there is a dominant follicle (710 mm) or a corpus luteum, the scan should be repeated.[17]

Paraovarian and Paratubal Cysts

Paraovarian and paratubal cysts arise from mesothelial tissue found in the broad ligament. They are most common in premenopausal women but have been shown to occur in women of all ages. Most commonly they are small and simple in appearance, and detected incidentally. However, larger lesions, particularly paraovarian cysts, may be palpable or noted during pelvic sonography. If a clear tissue plane can be demonstrated between the cyst and the adjacent ovary, the lesion can be correctly diagnosed as a paraovarian cyst (**Fig. 1–4, Fig. –5**). Others may be difficult to distinguish from exophytic ovarian lesions. These le-

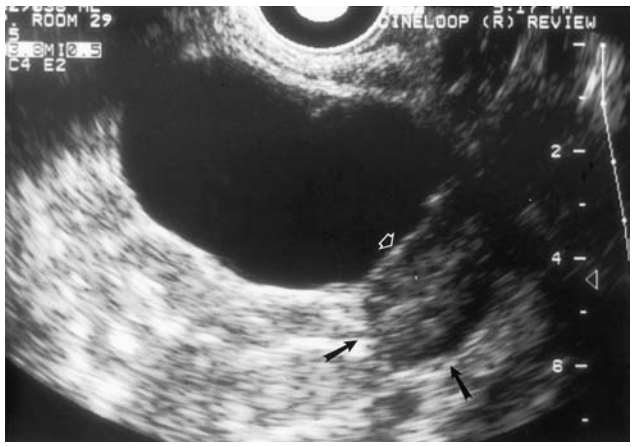

Figure 1–5 Paraovarian cyst. Endovaginal exam shows tissue plane (*open arrow*) separating this simple adnexal cyst from the ovary (*closed black arrows*).

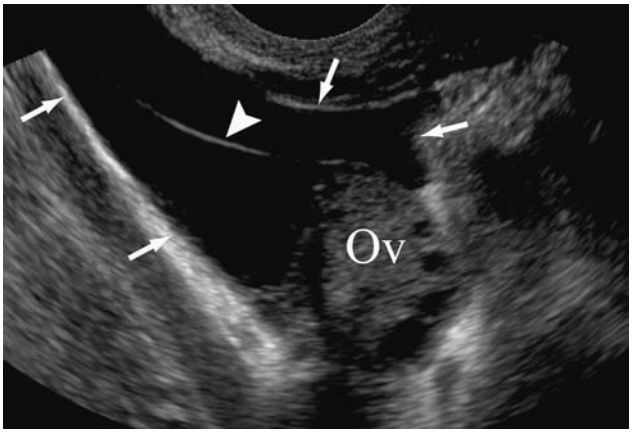

Figure 1–6 Peritoneal inclusion cyst. An irregularly shaped cyst (*long arrows*) conforming to the anatomical borders of the pelvis with a thin septation (*arrowhead*) is present adjacent to a normal-appearing ovary (Ov) in this patient with prior pelvic surgery.

sions will persist on repeat sonogram and if not correctly diagnosed are often referred for surgical excision.[19–21]

Peritoneal Inclusion Cyst

Peritoneal inclusion cysts occur when ovulatory fluid produced by the normal ovary is unable to be absorbed by the peritoneum secondary to prior infection, inflammation, or mechanical injury. These lesions, also called peritoneal pseudocysts, occur in premenopausal women, typically with a history of prior pelvic surgery, pelvic inflammatory disease, and/or endometriosis.[22–24] Over time, the ovulated fluid accumulates and becomes trapped by peritoneal adhesions, forming loculated fluid collections surrounding the ovary. They are typically large when detected by palpation, with a mean size of 11.6 cm. The lesions may be anechoic or contain only a few internal septations and may be ovoid or irregular in shape, conforming to the anatomical boundaries of the pelvis (**Fig. 1–6**). With extensive adhesions, the septations may be thicker and irregular and even have low-resistance vascular flow mimicking a cystic neoplasm.[24] The key to the diagnosis is the recognition of a normal-appearing ovary within the inclusion cyst, often displaced to the pelvic sidewall. If asymptomatic, these lesions do not require intervention. If painful, percutaneous drainage appears to be the best treatment option after a high rate of recurrence following surgical resection.

Hydrosalpinx

A dilated fallopian tube (hydrosalpinx) may occur as a result of a previous pyosalpinx in which the prior infection has resolved; the fallopian tube remains dilated and tortuous, but the fluid content becomes simple. Hydrosalpinx may also result from the accumulation of secretions following tubal ligation and after hysterectomy if the distal portion of the tube becomes blocked by adhesions. The ultrasound appearance is a tubular, anechoic structure with a folded configuration.[25,26] The tube is not typically uniformly dilated; often the ampullary segments are markedly dilated, whereas the proximal tube is less distended. The mildly inflamed mucosal lining of the tube may appear as prominent rugal folds, which produce echogenic or polypoid protrusions into the lumen of the tube, resulting in the so-called cog wheel appearance. A significantly scarred and dilated fallopian tube may easily be mistaken for a multilocular cystic ovarian mass and raise concern for a neoplasm. Scanning in multiple planes on TVUS is usually successful in elucidating the tubular configuration of a hydrosalpinx by noting that the

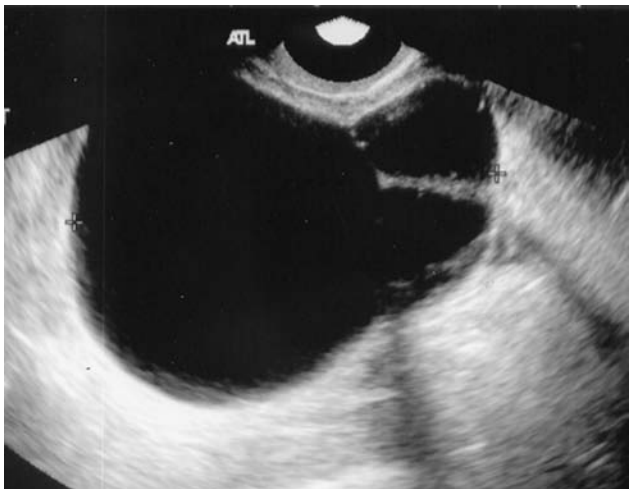

A

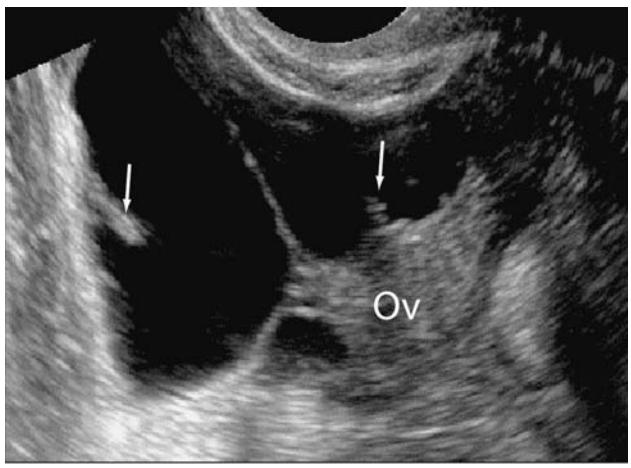

B

Figure 1–7 Hydrosalpinx. **(A)** A transverse image of the adnexa shows what appears to be a multilocular mass (outlined by electronic calipers). **(B)** Oblique scan through the same adnexa shows that the "mass" is a dilated fallopian tube. Thickened folds (*arrows*) or the walls of the folded tube may simulate septations. Ov, normal adjacent ovary.

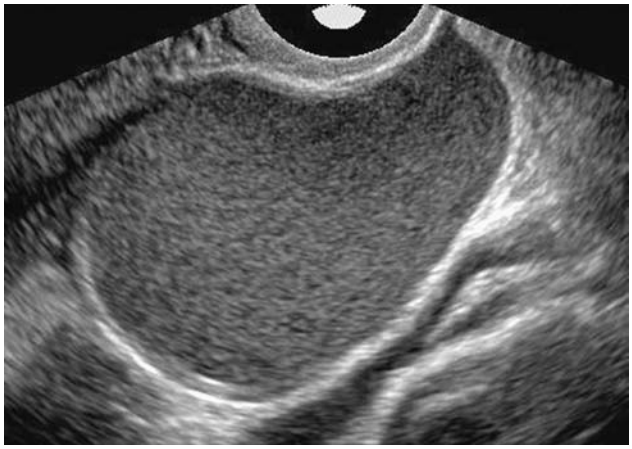

Figure 1–8 Endometrioma. This ovarian lesion demonstrates the "ground-glass" appearance of homogeneous low-level internal echoes with good sound transmission seen in many endometriomas.

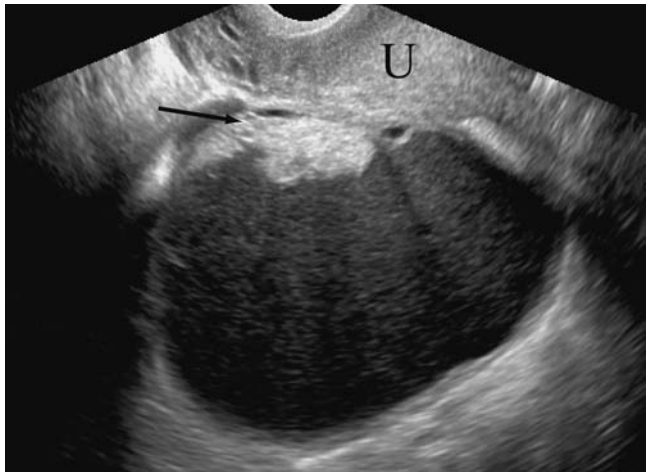

Figure 1–9 Endometrioma. This large endometrioma had an echogenic mural nodule (*black arrow*) and low-level echoes. The appearance is nonspecific and would overlap with a dermoid or other ovarian neoplasm. U, uterus.

perceived septa are incomplete and that the fluid-containing compartments can be connected (**Fig. 1–7**).

Endometriomas

Endometriomas occur as a complication of endometriosis, a common disorder usually seen in women of reproductive age, in which functional foci of endometrial tissue are implanted outside the uterus, most commonly in the adnexa and cul-de-sac. Cyclical bleeding may occur into these hormonally sensitive endometrial implants, forming lesions called endometriomas. Endometriomas contain dark, gelatinous blood products surrounded by a fibrous wall of variable thickness and are often multiple and bilateral. The most characteristic appearance of an endometrioma is a cystic lesion with homogeneous low-level echoes and good through-sound transmission ("ground-glass" appearance) without internal vascular flow (**Fig. 1–8**).[27,28]

However, some endometriomas have a more complex appearance with dependent and retracting clot, debris levels, thick septations, and wall nodularity. The sonographic appearance of endometriomas is therefore nonspecific and overlaps with a wide variety of other lesions, including hemorrhagic cyst, dermoid cysts, and ovarian neoplasms (**Fig. 1–9**). A follow-up ultrasound at 6 weeks may show an interval decrease in size in some endometriomas. In problematic cases, MRI can demonstrate the hemorrhagic characteristics of this entity, as well as other pelvic implants common in this disorder.[27,29]

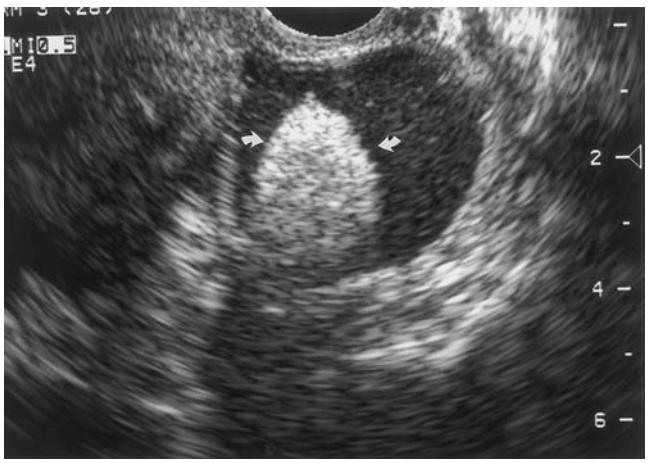

Figure 1–10 Dermoid cyst. A complex cystic lesion with a well-defined echogenic nodule (*arrows*) is seen.

Dermoid Cysts

A dermoid cyst (mature cystic teratoma) is benign tumor composed of well-differentiated derivations of at least two of the three germ cell layers (ectoderm, mesoderm, and endoderm). This commonly encountered lesion accounts for 20% of all ovarian tumors in adults and 50% of all ovarian tumors in children and is the most common benign tumor in women less than 45 years of age. They are often quite large when detected by physical exam, and bilateral lesions are noted in 10 to 15% of patients. Depending on the mixture of sebum, fat, hair, and epithelial tissue within a dermoid, the sonographic appearance ranges from purely cystic to complex cystic to an entirely solid, often hyperechoic mass.[30,31] Many dermoids contain an excrescence containing hair or bone fragments, called the dermoid plug or Rokitansky nodule, which appears as an echogenic mural nodule with distal acoustic shadowing (**Fig. 1–10**). Other common sonographic features are re-

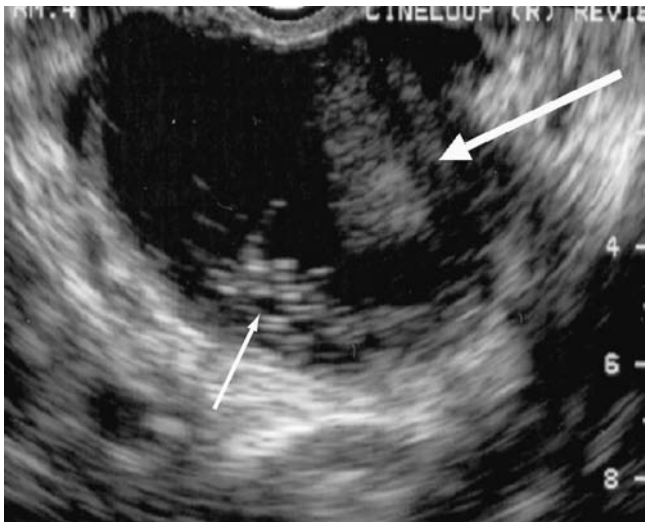

Figure 1–11 Dermoid cyst. The dermoid contains hyperechoic lines and dots (*thin arrow*) and a hyperechoic soft tissue nodule (*thick arrow*). The combination of these two features within the lesion is strongly predictive of a dermoid cyst.

gional diffuse bright echoes, hyperechoic lines and dots, and a fat-fluid level (**Fig. 1–11**).

Despite the wide variety of appearances, the identification of two or more characteristic sonographic features allows a highly confident diagnosis of a dermoid and at the same time a confident exclusion of malignancy, allowing the patient to proceed to laparoscopic removal.[5,30,31] If the sonographic exam is not conclusive, and a complex mass is noted in a young patient, MRI may be helpful to identify the lipid component found in the majority of these lesions.[32]

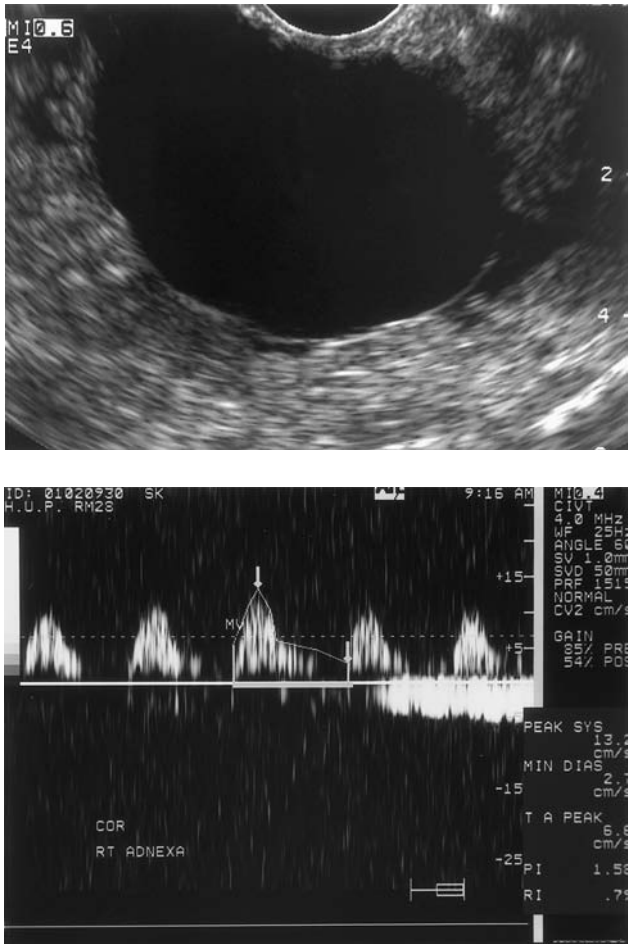

Figure 1–12 Benign serous cystadenoma. **(A)** This benign tumor appears as a unilocular cyst with minimal wall irregularity; no loculations or nodules are seen. **(B)** Color-guided duplex Doppler in wall of mass shows pulsatility index (PI) = 1.58 and resistive index (RI) = 0.79 in benign range.

Ovarian Neoplasms

When an adnexal mass is palpated on pelvic exam, there is always the concern that the lesion may be an ovarian neoplasm, and potentially, an ovarian carcinoma. Ovarian cancer is less common than either cervical or endometrial cancer, but it is the leading cause of death related to gynecologic malignancies because it tends to be diagnosed at a more advanced stage. Approximately 80% of ovarian tumors that occur in adult women are benign, 10 to 15% are primary ovarian malignancies, and 5% are due to ovarian metastases.[33–35] The majority of ovarian neoplasms that are found in younger women are benign, whereas the incidence of malignancy increases dramatically around the time of menopause and continues to rise such that ~40% of tumors in postmenopausal women are malignant.[9]

Primary ovarian tumors are classified based on their tissue origin as epithelial tumors, germ cell tumors, or sex cord–stromal tumors. Epithelial tumors account for 60% of all ovarian neoplasms, but over 85% of all malignancies. The two most common histologic subtypes of epithelial tumors are serous and mucinous lesions.

Serous fluid-containing tumors are more common than mucinous tumors and account for 50% of all ovarian carcinomas and 25% of benign ovarian neoplasms. Approximately 60% of serous tumors are benign cystadenomas, 25% are malignant cystadenocarcinomas, and 15% are classified as lesions of low malignant potential (LMP).[34,35] LMP lesions, also called borderline tumors, are true malignancies, but tend to have minimal invasion on histologic analysis. They tend to affect younger women and present with early stage I disease and therefore carry a better prognosis than ovarian malignancies of higher grade.[36] Benign serous tumors tend to be predominantly cystic lesions with minimally complicated fluid, thin septations, and small papillary projections (**Fig. 1–12**). Serous cystadenocarcinomas are usually more complex-appearing with multiple loculations, large papillary projections, and thicker septations (**Fig. 1–13**).

Approximately 20 to 25% of ovarian tumors are mucinous in origin; 80% of mucinous lesions are benign, 10% are malignant, and 10% are tumors of LMP. Mucinous tumors

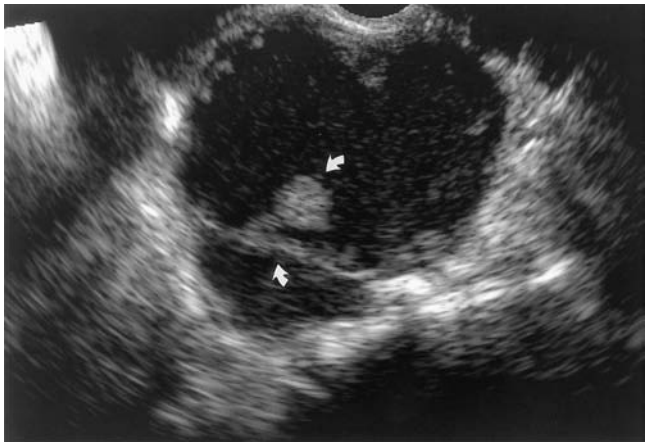

Figure 1–13 Papillary serous cystadenocarcinoma. This malignant tumor has thick septations with soft tissue nodularity (*curved white arrows*) and wall nodularity.

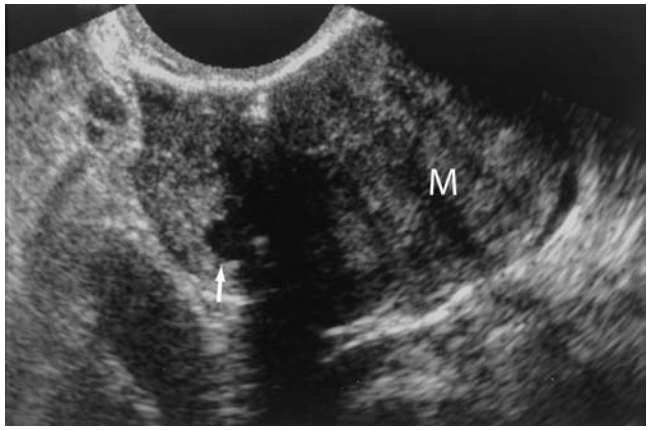

Figure 1–14 Fibroma. A uniformly solid mass (M) is seen surrounded by a rim of ovarian tissue that contains a follicle (*arrow*). Identification of the ovarian parenchyma surrounding the lesion confirms an intraovarian location of this lesion and differentiates it from an exophytic myoma.

are usually multiloculated masses, often with one or more locules containing complex or echogenic fluid. Serous tumors are more likely to be bilateral than mucinous tumors (20 vs. 5%) and when malignant are more likely to present with evidence of metastatic disease such as ascites or peritoneal implants. Endometrioid carcinoma represents ~10 to 15% of all ovarian carcinomas, with bilateral tumors noted in 30 to 50% of patients. They are typically a large, complex, mixed cystic and solid lesion and may be associated with endometrial hyperplasia or endometrial carcinoma. Clear cell carcinoma comprises ~5% of all ovarian malignancies and varies from a predominantly cystic appearance with minimal solid elements to a more solid appearance.[33–35]

Approximately 10 to 15% of ovarian tumors are germ cell tumors, with benign mature cystic teratomas (dermoid cysts) comprising 95% of this type (see preceding discussion). The other 5% are more likely to be malignant and include dysgerminomas, immature teratomas, and endodermal sinus tumor. These tumors are often large, complex lesions with a predominant solid component.

Sex cord and stromal tumors account for 5 to 10% of all ovarian neoplasms and affect all age groups. The most common type of sex cord tumor is the benign ovarian fibroma or fibrothecoma, which is typically a solid mass composed predominantly of fibroblasts with varying amounts of theca cells (**Fig. 1–14**). Some fibromas are so dense as to cause complete attenuation of the sound beam, a feature not typical of other solid ovarian masses.[37] The remainder of lesions in this category are called granulosa cell tumors and are hormonally active tumors that contain a mixture of granulosa cells, theca cells, Leydig cells, Sertoli cells and fibroblasts. They account for 2 to 3% of all adult ovarian cancers and, although usually malignant, carry high survival rates because many are confined to the ovary at the time of diagnosis. On ultrasound scan, these tumors appear as solid echogenic or heterogeneous tumor masses with cystic spaces (**Fig. 1–15**). An exophytic myoma presenting as a solid adnexal mass should always be considered when a solid adnexal mass is observed. Identification

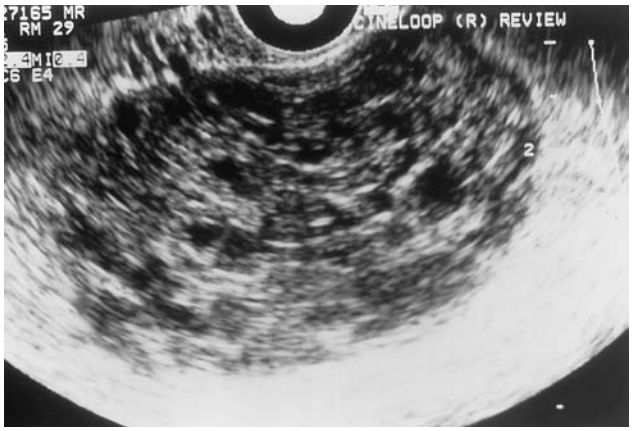

A

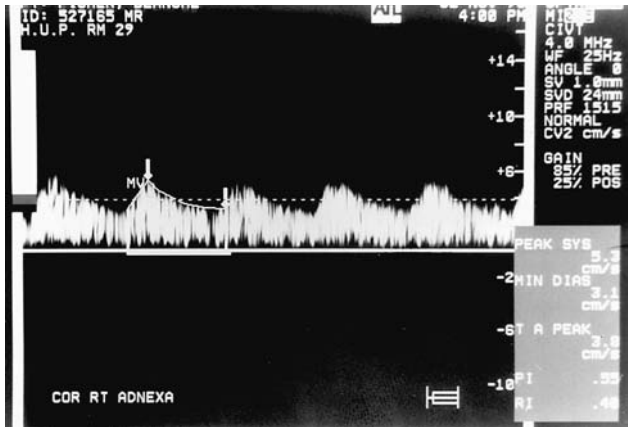

B

Figure 1–15 Granulosa cell tumor. **(A)** This tumor is primarily solid with small cystic areas. **(B)** Doppler of internal vessels shows pulsatility index (PI) = 0.55 and resistive index (RI) = 0.40, both in malignant range.

of the ipsilateral ovary helps to distinguish a pedunculated myoma from a solid ovarian mass.

Evaluation of Ovarian Lesions

Several investigators have used a variety of factors in an effort to predict whether an ovarian lesion is malignant, including sonographic gray-scale features,[1,2,38–42] Doppler analysis,[2–4,43–47] as well as serum tumor markers such as CA 125 levels.[7,48]

Clearly, there is no specific, clinical, gray-scale, or Doppler feature that allows reliable discrimination between a benign and a malignant lesion. Elevated CA 125 levels have been found to be more useful in predicting malignancy in postmenopausal patients with ovarian masses as compared with premenopausal patients because CA 125 is elevated in a variety of benign conditions, such as endometriosis, pelvic infection, and menstruation.[48] On gray-scale, the features that raise concern for a neoplasm include predominantly solid echotexture, a cystic lesion with a nonechogenic solid component, thick or irregular septations, and wall nodularity.[1,2,38–42] For example, the risk of a multilocular lesion with solid elements is as high as 75%, whereas the risk of malignancy of a unilocular cyst is extremely low, regardless of the patient's age.[2,9,10,47]

Experienced sonographers can often correctly diagnose many complex lesions, such as a dermoid, endometrioma, or hemorrhagic cyst, using the features already described.[4,49] However, many of these common lesions may have atypical features and there is overlap in the appearance of benign cystadenomas and cystic malignancies. This has led investigators to explore the use of spectral and color Doppler analysis to increase the specificity of sonography.

It is known that malignant tumors grow via a process called neoangiogenesis in which small, disorganized vessels are formed in the tumor that have low-resistance flow.[48] Early investigators found that the detection of low impedance vascular flow within ovarian masses with a pulsatility index (PI) of 1.0 or less and a resistive index (RI) under 0.4 indicated the presence of malignant neovascularity with relatively high accuracy.[45] These results have not proven to be universally reproducible with other investigators finding overlap in the flow velocity indices of benign and malignant ovarian masses, particularly in premenopausal patients.[49–52]

Additionally, the technique of obtaining adequate Doppler arterial resistance signals is often time-consuming and technically challenging; hence, this technique has not gained wide acceptance.[3,48] Attention has now turned to the location of vascularity within a lesion. The identification of vascular flow within the central aspect of a mass, either within a nonechogenic solid component or within septations, has been shown to correlate with an increased risk of malignancy as compared with peripheral flow within the wall of a lesion[2,46,48,53] (**Fig. 1–16**).

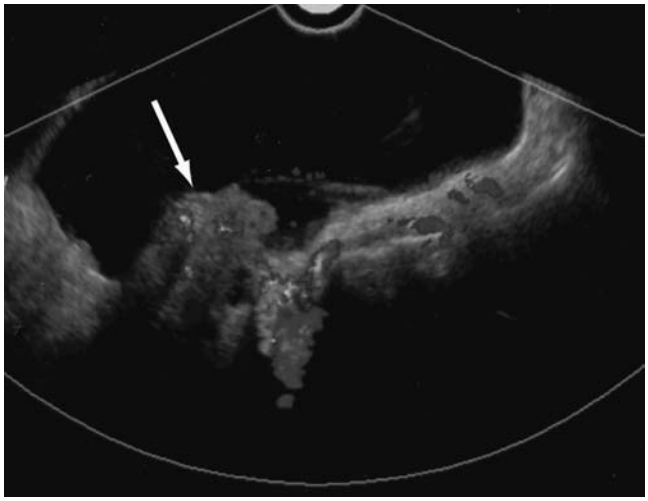

Figure 1–16 Serous ovarian carcinoma. A vascular mural nodule (*arrow*) was noted in this malignancy.

Management Guidelines

In general, the goal of the sonographic evaluation of the asymptomatic palpable adnexal mass is to determine if the lesion is likely physiological, likely benign, or in the case of malignancy, to plan the appropriate diagnostic plan for that patient. The sonographer should try to determine if the lesion may possibly be arising outside the ovary because many extraovarian cysts are benign, such as hydrosalpinges, paraovarian cysts, and peritoneal inclusion cysts. Identifying normal follicle-containing ovarian parenchyma surrounding a mass, "the ovarian crescent sign," is helpful to document an intraovarian origin of a lesion,[54] whereas identification of a separate and distinct ipsilateral ovary indicates that the mass does not arise from the ovary.[23] The multiplanar capabilities of MRI may be helpful for confirming the extraovarian location of some lesions when the sonogram is equivocal.

Large and complex cystic lesions in the premenopausal patient can be managed with follow-up sonography or physical exam to assess for interval decrease in size. The two most common persistent lesions in the premenopausal patient are dermoids and endometriomas.[4,55] In many instances, there may be characteristic features of these lesions. If the sonographic features are inconclusive, MRI may be helpful because it may offer a more specific diagnosis.[29,32,56]

Many authors feel that laparoscopic removal may be performed when a persistent minimally complicated cystic ovarian mass is identified because the risk of an invasive carcinoma is low in these lesions.[4,5] In the small percentage

that are malignant, they are often low grade or nonaggressive. Identification of a nonechogenic or vascular solid component in an ovarian mass is highly concerning for a neoplasm, particularly in a postmenopausal patient. The identification of complex ascites, a marked amount of simple ascites, and/or soft tissue implants carries a very high likelihood of metastatic ovarian malignancy requiring gynecologic oncological surgical evaluation.[52] (The majority of solid ovarian lesions will be neoplastic and usually warrant removal unless the lesions can be proven to be an exophytic myoma or benign ovarian fibroma.)

References

1. Ferrazzi E, Zanetta G, Dordoni D, Berlanda N, Mezzopane R, Lissoni G. Transvaginal ultrasonographic characterization of ovarian masses: comparison of five scoring systems in a multicenter study. Ultrasound Obstet Gynecol 1997;10:192–197
2. Brown DL, Doubilet PM, Miller F, et al. Benign and malignant ovarian masses: selection of the most discriminating gray-scale and Doppler sonographic features. Radiology 1998;208:103–110
3. Kinkel K, Hricak H, Lu Y, Tsuda K, Filly RA. US characterization of ovarian masses: a meta-analysis. Radiology 2000;217:803–811
4. Guerriero S, Ajossa S, Garau N, et al. Ultrasonography and color Doppler–based triage for adnexal masses to provide the most appropriate surgical approach. Am J Obstet Gynecol 2005;192:401–406
5. Canis M, Botchorishvilli R, Manhes H, et al. Management of adnexal masses. Semin Surg Oncol 2000;19:28–35
6. Ritchie WGM. Sonographic evaluation of normal and induced ovulation. Radiology 1986;161:1–10
7. Guerriero S, Ajossa S, Lai MP, et al. The diagnosis of functional ovarian cysts using transvaginal ultrasound combined with clinical parameters, CA 125 determinations, and color Doppler. Eur J Obstet Gynecol Reprod Biol 2003;110:83–88
8. Turan C, Zorlu CG, Ugur M, et al. Expectant management of functional ovarian cysts: an alternative to hormonal therapy. Int J Gynaecol Obstet 1994;47:257–260
9. Ekerhovd E, Wienerroith H, Staudach A, Granberg S. Preoperative assessment of unilocular adnexal cysts by transvaginal ultrasonography: a comparison between ultrasonographic morphologic imaging and histopathologic diagnosis. Am J Obstet Gynecol 2001; 184:48–54
10. Modesitt SC, Pavlik EJ, Ueland FR, et al. Risk of malignancy in unilocular ovarian cystic tumor less than 10 centimeters in diameter. Obstet Gynecol 2003;102:594–599
11. Levine D, Gosink BB, Wolf SI, Feldesman MR, Pretorius DH. Simple adnexal cysts: the natural history in postmenopausal women. Radiology 1992;184:653–659
12. Conway C, Zalud I, Dilena M, et al. Simple cyst in the postmenopausal patient: detection and management. J Ultrasound Med 1998;17:369–372
13. Jain KA. Sonographic spectrum of hemorrhagic ovarian cysts. J Ultrasound Med 2002;21:879–886
14. Patel MD, Feldstein VA, Filly RA. The likelihood ratio of sonographic findings for the diagnosis of hemorrhagic ovarian cysts. J Ultrasound Med 2005;24:607–614
15. Baltarowich OH, Kurtz AB, Pasto ME, Rifkin MD, Needleman L, Goldberg BB. The spectrum of sonographic findings in hemorrhagic cysts. AJR Am J Roentgenol 1987;148:901–905
16. Ehrmann DA. Polycystic ovary syndrome. N Engl J Med 2005; 352:1223–1236
17. Balen AH, Laven JS, Tan SL, Dewailly D. Ultrasound assessment of the polycystic ovary: international consensus definitions. Hum Reprod Update 2003;9:505–514
18. Battaglia C, Regnani G, Petraglia F, Primavera MR, Salvatori M, Volpe A. Polycystic ovary syndrome: is it always bilateral? Ultrasound Obstet Gynecol 1999;14:183–187
19. Alpern MB, Sandler MA, Madrazo BL. Sonographic features of parovarian cysts and their complications. AJR Am J Roentgenol 1984;143:157–160
20. Athey PA, Cooper NB. Sonographic features of parovarian cysts. AJR Am J Roentgenol 1985;144:83–86
21. Barloon TJ, Brown BP, Abu-Yousef MM, Warnock NG. Paraovarian and paratubal cysts: preoperative diagnosis using transabdominal and transvaginal sonography. J Clin Ultrasound 1996;24:117–122
22. Sohaey R, Gardner T, Woodward PJ, Peterson CM. Sonographic diagnosis of peritoneal inclusion cysts. J Ultrasound Med 1995;14: 913–917
23. Kim JS, Lee HJ, Woo S, Lee TS. Peritoneal inclusions cysts and their relationship to the ovaries: evaluation with sonography. Radiology 1997;204:481–484
24. Guerriero S, Ajossa S, Mais V, et al. Role of transvaginal sonography in the diagnosis of peritoneal inclusion cysts. J Ultrasound Med 2004;23:1193–1200
25. Benjaminov O, Atri M. Sonography of the abnormal fallopian tube. AJR Am J Roentgenol 2004;183:737–742
26. Rowling SE, Ramchandani P. Imaging of the fallopian tube. Semin Roentgenol 1996;31:299–311
27. Patel MD, Feldstein VA, Chen DC, Lipson SD, Filly RA. Endometriomas: diagnostic performance of US. Radiology 1999;210:739–745
28. Moore J, Copley S, Morris J, Lindsell D, Golding S, Kennedy S. A systematic review of the accuracy of ultrasound in the diagnosis of endometriosis. Ultrasound Obstet Gynecol 2002;20:630–634
29. Outwater E, Schiebler ML, Owen RS, Schnall MD. Characterization of hemorrhagic adnexal lesions with MR imaging: blinded reader study. Radiology 1993;186:489–494
30. Patel MD, Feldstein VA, Lipson SD, Chen DC, Filly RA. Cystic teratomas of the ovary: diagnostic value of sonography. AJR Am J Roentgenol 1998;171:1061–1065
31. Mais V, Guerriero S, Ajossa S, Angiolucci M, Paoletti AM, Melis GB. Transvaginal ultrasonography in the diagnosis of cystic teratoma. Obstet Gynecol 1995;85:48–52
32. Outwater EK, Siegelman ES, Hunt JL. Ovarian teratomas: tumor types and imaging characteristics. Radiographics 2001;21:475–490
33. Jung SE, Lee JM, Rha SE, Byun JY, Jung JI, Hahn ST. CT and MR imaging of ovarian tumors with emphasis on differential diagnosis. Radiographics 2002;22:1305–1325
34. Sutton CL, McKinney CD, Jones JE, Gay S. Ovarian masses revisited: radiologic and pathologic correlation. Radiographics 1992;12:853–877
35. Koonings PP, Campbell K, Mishell DR Jr, Grimes DA. Relative frequency of primary ovarian neoplasms: a 10-year review. Obstet Gynecol 1989;74:921–926
36. Pascual MA, Tresserra F, Grases PJ, Labastida R, Dexeus S. Borderline cystic tumors of the ovary: gray-scale and color Doppler findings. J Clin Ultrasound 2002;30:76–82
37. Athey PA, Malone RS. Sonography of ovarian fibromas/thecomas. J Ultrasound Med 1987;6:431–436

38. DePriest PD, Shenson D, Fried A, et al. A morphology index based on sonographic findings in ovarian cancer. Gynecol Oncol 1993; 51:7–11
39. Granberg S, Wikland M, Jansson I. Macroscopic characterization of ovarian tumors and their relationship to the histological diagnosis: criteria to be used for ultrasound evaluation. Gynecol Oncol 1989;35:139–144
40. Sassone AM, Timor-Tritsch IE, Artner A, Westhoff C. Transvaginal sonographic characterization of ovarian disease: evaluation of a new scoring system to predict ovarian malignancy. Obstet Gynecol 1991;78:70–76
41. Twickler DM, Forte TB, Santos-Ramos R, et al. The ovarian tumor index predicts risk for malignancy. Cancer 1999;86:2280–2290
42. Lerner JP, Timor-Tritsch IE, Federman A, Abramovich G. Transvaginal ultrasonographic characterization of ovarian masses with an improved weighted scoring system. Am J Obstet Gynecol 1994; 170:81–85
43. Kurjak A, Zalud I, Alfirevic Z. Evaluation of adnexal masses with transvaginal color Doppler ultrasound. J Ultrasound Med 1991;10: 295–297
44. Bourne T, Campbell S, Steer C, et al. Transvaginal color flow imaging: a possible new screening technique for ovarian cancer. BMJ 1989;299:1367–1370
45. Kurjak A, Predanic M. New scoring system for predication of ovarian malignancy based on transvaginal color Doppler sonography. J Ultrasound Med 1992;11:631–638
46. Buy JN, Ghossain MA, Hugol D, et al. Characterization of adnexal masses: combination of color Doppler and conventional sonography compared with spectral Doppler analysis alone and conventional sonography alone. AJR Am J Roentgenol 1996;166:385–393
47. Schelling M, Braun M, Kuhn W, et al. Combined transvaginal B-mode and color Doppler sonography for differential diagnosis of ovarian tumors: results of a multivariate logistic regression analysis. Gynecol Oncol 2000;77:78–86
48. Alcazar JL, Errasti T, Zornoza A, et al. Transvaginal color Doppler ultrasonography and CA-125 in suspicious adnexal masses. Int J Gynaecol Obstet 1999;66:255–261
49. Levine D, Feldstein VA, Babcook CJ, Filly RA. Sonography of ovarian masses: poor sensitivity of resistive index for identifying malignant lesions. AJR Am J Roentgenol 1994;162:1355–1359
50. Stein SM, Laifer-Narin S, Johnson MB, et al. Differentiation of benign and malignant adnexal masses: relative value of gray-scale, color Doppler, and spectral Doppler sonography. AJR Am J Roentgenol 1995;164:381–386
51. Hamper UM, Sheth S, Abbas FM, et al. Transvaginal color Doppler sonography of adnexal masses: differences in blood flow impedance in benign and malignant lesions. AJR Am J Roentgenol 1993;160:1225–1228
52. Kurtz AB, Tsimikas JV, Tempany CM, et al. The comparative values of Doppler/US, CT and MR in ovarian cancer diagnosis and staging: correlation with surgery and pathology. A report of the Radiology Diagnostic Oncology Group. Radiology 1999;212:19–27
53. Guerriero S, Alcazar JL, Coccia ME, et al. Complex pelvic mass as a target of evaluation of vessel distribution by color Doppler sonography for the diagnosis of adnexal malignancies: results of a multicenter European study. J Ultrasound Med 2002;21:1105–1111
54. Hillaby K, Aslam N, Salim R, et al. The value of the detection of normal ovarian tissue ("the ovarian crescent sign") in the differential diagnosis of adnexal masses. Ultrasound Obstet Gynecol 2004;23: 63–67
55. Timmerman D, Schwarzler P, Collins WP, et al. Subjective assessment of adnexal masses with the use of ultrasonography: an analysis of interobserver variability and experience. Ultrasound Obstet Gynecol 1999;13:11–16
56. Rieber A, Nussle K, Stohr I, et al. Preoperative diagnosis of ovarian tumors with MR imaging: comparison with transvaginal sonography, positron emission tomography, and histologic findings. AJR Am J Roentgenol 2001;177:123–129

2 Acute Pelvic Pain

John S. Pellerito

Acute pelvic pain is a common problem seen in everyday practice. There are multiple possible causes of acute pelvic pain, and a quick, cost-effective evaluation is desirable for timely diagnosis. Because ultrasound can distinguish between many of the diagnostic possibilities noninvasively, it is the preferred initial imaging modality performed to evaluate this condition. This chapter addresses the role of ultrasound in the clinical evaluation of acute pelvic pain. The value of other diagnostic modalities is also discussed.

Differential Diagnosis

Causes of acute pelvic pain can be divided into gynecologic and nongynecologic etiologies. Gynecologic causes of pelvic pain include ovarian cysts, pelvic inflammatory disease, ectopic pregnancy, and ovarian torsion. Less commonly, benign or malignant adnexal masses, such as fibroids or ovarian cancer, and endometriosis, may produce acute pelvic pain. Nongynecologic causes of pelvic pain include appendicitis, urinary calculi, mesenteric adenitis, inflammatory bowel disease, bowel obstruction, metastatic disease, and diverticulitis.

Diagnostic Evaluation

Nonimaging Tests

The evaluation of the patient with acute pelvic pain begins with the clinical history and physical examination. The value of any imaging technique is enhanced by the addition of clinical information. Because multiple disease processes may present with a similar clinical syndrome, the differential diagnosis is constructed from data obtained from the clinical history, including the age of the patient and menopausal status. The duration and recurrence of the problem as well as current medications are important considerations. Significant historical information concerning prior urinary or gynecologic problems also guide the diagnostic evaluation. For example, a prior history of ectopic pregnancy will focus the workup to exclude recurrence of the disease.

This diagnostic evaluation is also supported by the physical examination. The location of pain as well as signs of pelvic mass limit the differential diagnoses. Signs of infection, including fever and rebound tenderness, suggest inflammatory etiologies such as appendicitis or tubo-ovarian abscess (TOA). Sudden decrease in blood pressure or change in mental status portend more serious conditions prompting immediate diagnostic or surgical examinations.

The differential diagnosis is also informed by laboratory information. Hematologic and blood chemistry studies are obviously important tools to determine the origin of pain. An elevated white blood cell count and sedimentation rate support an infectious or inflammatory etiology for pain. Abnormal renal or liver function tests may suggest a specific cause for pain or point to a generalized process such as diffuse metastatic disease. Urine or serum pregnancy tests are essential in premenopausal patients, whereas serum tumor markers may be helpful in postmenopausal women.

Ultrasound Imaging

Ultrasound is the primary imaging modality utilized to distinguish between the different causes of acute pelvic pain. It is a noninvasive examination with no known adverse effects. Other advantages of ultrasound include ready availability, low cost, and high sensitivity for many disease processes.

Endovaginal sonography (EVS) has proven highly accurate for the diagnosis of many gynecologic conditions. EVS offers improved visualization of the pelvic structures compared with the transabdominal approach. EVS demonstrates adnexal masses, collections, free fluid, hydroureter, and other important clues to diagnosis.

Duplex and color flow Doppler techniques demonstrate physiological as well as anatomical information and may provide important diagnostic clues. Detection of tissue vascularity and characterization of specific flow patterns improve diagnostic accuracy and provide specific findings not possible with gray-scale imaging alone. For example, the detection of high-velocity, low-resistance flow signals allows the detection of placental flow in the uterus and adnexa even in the absence of significant gray-scale information. Conversely, the absence of ovarian flow is consistent with ovarian torsion.

Ovarian Cysts

The most common gynecologic cause of acute pelvic pain is the growth of ovarian cysts. The occurrence of pain is closely associated with follicular rupture during the midportion of the menstrual cycle.[1] Mittelschmerz (middle pain) was initially thought to be due to peritoneal irritation

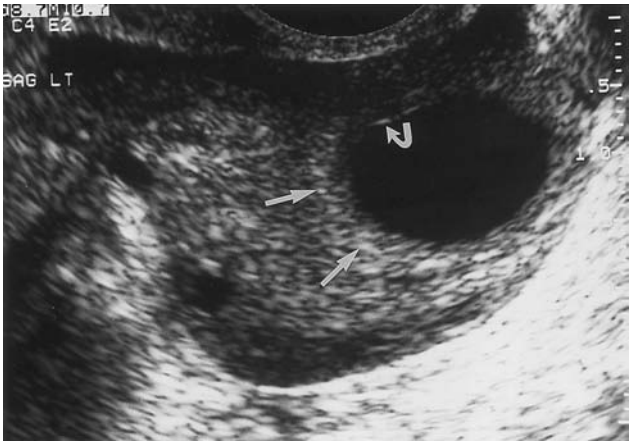

Figure 2–1 Ovarian cyst. A well-circumscribed cyst is identified within the ovary. Note the thickened rim (*arrows*) surrounding the cyst and the echogenic focus (*curved arrow*) consistent with the cumulus oophorus.

from release of blood and follicular contents during ovulation. This coincides with follicle-stimulating hormone/luteinizing hormone (FSH/LH) surge during days 14 through 16 of the menstrual cycle. Sonographic monitoring of midcycle ovaries has shown that the symptoms precede follicular rupture in 97% of cases.[2,3] The pain is usually noted on the side of the dominant follicle and is probably related to follicular enlargement.

Characteristic sonographic findings are associated with the periovulatory period. Prior to ovulation, the mature follicle demonstrates a mean diameter of 20 to 24 mm.[4,5] The cyst will demonstrate an echogenic rim (**Fig. 2–1**). Irregularity of the inner lining of the cyst may be seen when ovulation is imminent.[1] A small echogenic focus or rim may be seen along the wall of the mature follicle. This represents the cumulus oophorus and confirms that the follicle contains the oocyte. Ovulation usually occurs within 36 hours of visualization of the cumulus oophorus.

Following ovulation, the size of the follicular cyst usually decreases. Fluid is commonly seen in the cul-de-sac and surrounding adnexae. This is thought to be due to exudation from the ovary and has been measured to be ~15 to 25 mL at laparoscopy.[6]

Color and pulsed Doppler examination of the mature follicle demonstrates a rim of increased vascularity surrounding the cyst (**Fig. 2–2**). This is best visualized during endovaginal color flow imaging and is helpful in the identification of the corpus luteum.[7] The ring of vascularity ("ring of fire") is initially seen during day 8 of the menstrual cycle and continues through day 24. Although the ring of fire sign was originally described for the peripheral vascularity associated with an extrauterine gestational sac,

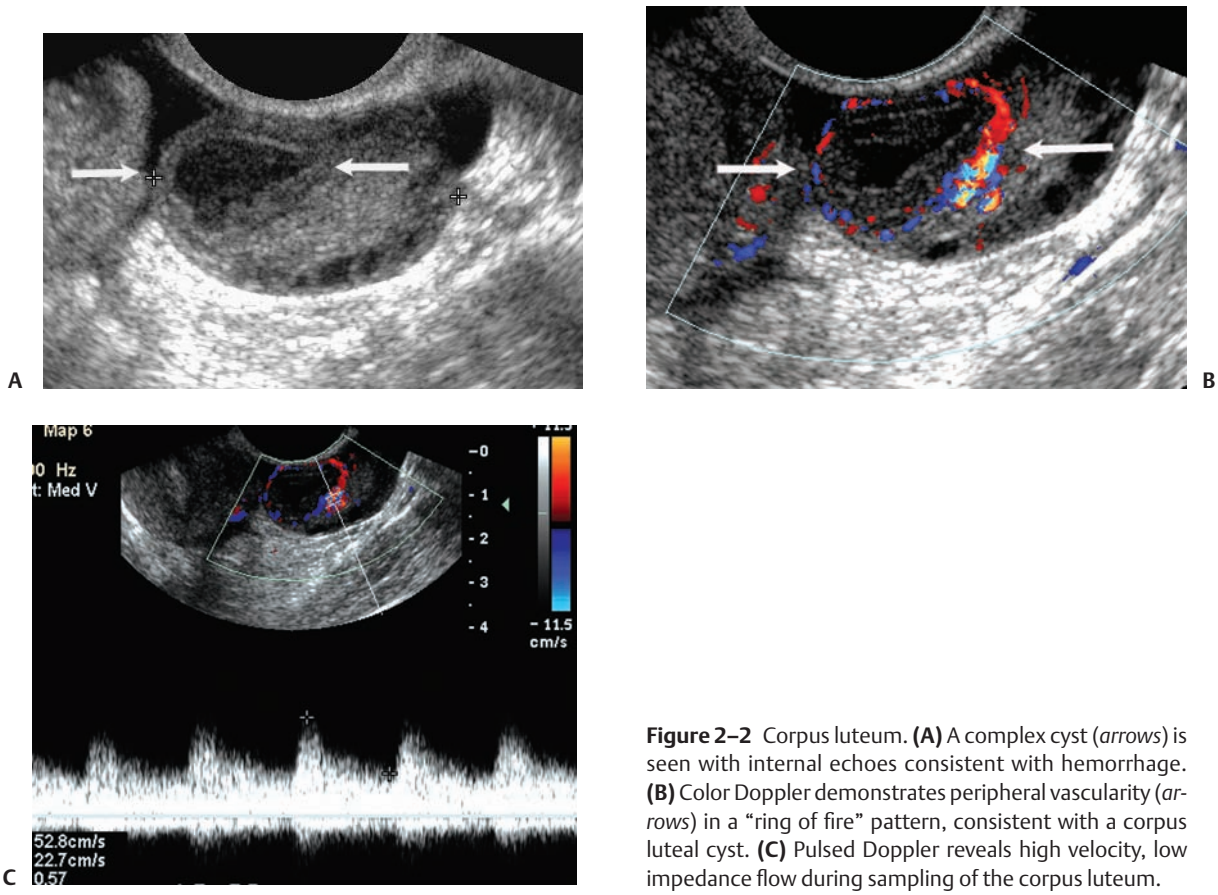

Figure 2–2 Corpus luteum. **(A)** A complex cyst (*arrows*) is seen with internal echoes consistent with hemorrhage. **(B)** Color Doppler demonstrates peripheral vascularity (*arrows*) in a "ring of fire" pattern, consistent with a corpus luteal cyst. **(C)** Pulsed Doppler reveals high velocity, low impedance flow during sampling of the corpus luteum.

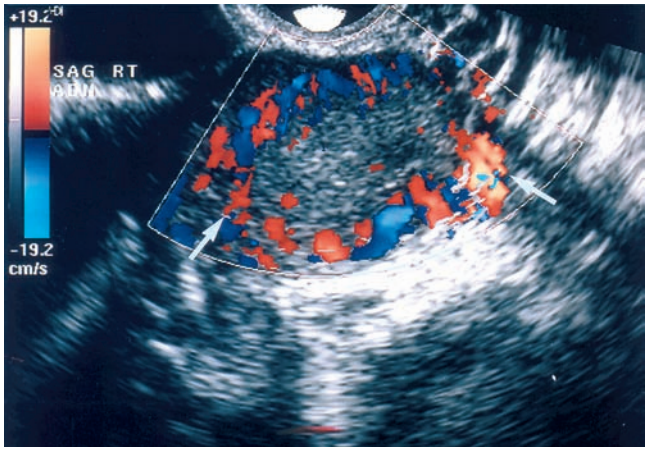

Figure 2–3 Hemorrhagic luteal cyst. A ring of vascularity (*arrows*) surrounds the hemorrhagic corpus luteum, which is isoechoic to the ovarian parenchyma.

the appearance is routinely identified in corpus luteal cysts. Peripheral vascularization of the corpus luteum may persist through the first trimester.

Color Doppler aids in the identification of the hemorrhagic corpus luteum. The cystic component may not be visualized if the hemorrhage within the cyst is isoechoic to the adjacent ovarian parenchyma. Increased vascularity is identified around the periphery of the isoechoic ovarian mass (**Fig. 2–3**). The detection of vascularity in the rim of the cyst, and not in the hemorrhagic component, is an important discriminator between a complex cyst and a solid ovarian mass. The finding of peripheral vascularity in a complex midcycle cyst warrants interval follow-up in 4 to 6 weeks, during the first week of a subsequent menstrual cycle, to confirm interval resolution of the cyst.

Pulsed Doppler sampling of the corpus luteum reveals higher-velocity, low-impedance flow from the vascular ring.[8] Dillon et al demonstrated a peak systolic velocity of 27 ± 10 cm/s and resistive index (RI) = 0.44 ± 0.09 for corpus luteal flow.[9] This low-impedance flow pattern should not be confused with low-resistance flow associated with ovarian cancer. The pain associated with formation of the dominant follicle and ovulation is self-limited, not requiring treatment in most cases.

Ectopic Pregnancy

Ectopic pregnancy is one of the most common indications for pelvic sonography in patients with acute pelvic pain. Ectopic pregnancy represents approximately[1] 4% of all reported pregnancies, with 75,000 cases occurring in the United States each year.[10] The risk of maternal death from ectopic pregnancy is 10 times greater than that from natural childbirth.

Important risk factors include pelvic inflammatory disease, endometriosis, prior tubal surgery and prior ectopic pregnancy. This is probably related to mechanical obstruction of the fallopian tube. Other risk factors include in vitro fertilization and embryo transfer as well as ovulation induction with gonadotropins.

Less than 50% of patients present with the classic clinical presentation of adnexal pain, pelvic mass, and vaginal bleeding.[11,12] Patients typically present with one or more of these nonspecific signs or symptoms. The menstrual history and pregnancy test are essential in the evaluation for ectopic pregnancy. A positive pregnancy test increases the suspicion for ectopic pregnancy. The differential diagnosis includes threatened abortion and gestational trophoblastic neoplasia.

Prompt sonographic examination is indicated to diagnose ectopic pregnancy because delayed diagnosis may result in life-threatening hemorrhage from tubal rupture. Endovaginal sonography is the preferred initial examination because it can diagnose intrauterine and ectopic pregnancy earlier than the transabdominal approach.[13–15] Culdocentesis is no longer considered a first-line diagnostic examination because a negative test does not exclude ectopic pregnancy. Uterine curettage and laparoscopy are useful but should be delayed pending the sonographic results.

The definitive diagnosis of ectopic pregnancy is made based on the observation of an extrauterine embryo or fetal cardiac pulsations (**Fig. 2–4**). If these findings are not identified, then a thorough evaluation of the uterus, adnexae, and cul-de-sac is performed to look for other evidence of pregnancy.

The uterus is evaluated first for evidence of an intrauterine pregnancy. If an intrauterine pregnancy is identified, then the likelihood of a concomitant or heterotopic ectopic pregnancy is low, occurring in one of 30,000 spontaneous pregnancies. The frequency of heterotopic pregnancy increases if the patient has undergone ovulation induction. If the uterus fails to demonstrate evidence of pregnancy, the adnexae are carefully surveyed for signs of ectopic pregnancy. Other possibilities include a complete

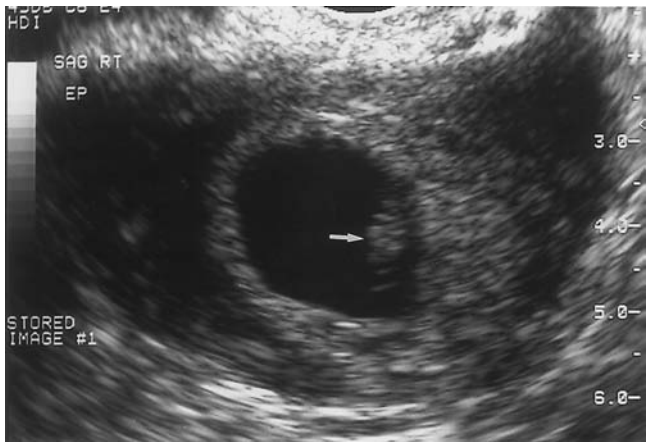

Figure 2–4 Ectopic embryo. An embryo (*arrow*) is identified within the ectopic gestational sac. Cardiac activity was noted.

abortion or very early intrauterine pregnancy (less than 5 weeks gestational age). Careful correlation with menstrual data and serum human chorionic gonadotropin (HCG) titers is helpful in distinguishing these entities. A subnormal rise or plateau of the serum HCG titers suggests a diagnosis of ectopic pregnancy.

An abnormal sac in the endometrial canal may represent an abnormal intrauterine pregnancy such as an incomplete abortion or a pseudogestational sac associated with an ectopic pregnancy. Duplex and color Doppler can distinguish these entities by demonstrating placental flow.[16] Endovaginal color flow imaging demonstrates placental flow as an area of increased vascularity around the periphery of the true gestational sac. Taylor et al described placental flow as a relatively high-velocity, low-impedance signal localized to the site of placentation during pulsed Doppler sampling.[17] He theorized that placental flow is related to the invasion of maternal tissues by trophoblastic villi. As the developing placenta invades the myometrium, maternal spiral arteries shunt blood into the intervillous space across a pressure gradient of ~60 mm Hg. This results in the low-resistance flow pattern observed during color and pulsed Doppler imaging.

Dillon et al showed that placental flow is noted in an intrauterine pregnancy ~36 days after the last menstrual period.[16] A velocity cut-off value of 21 cm/s was found to distinguish an intrauterine pregnancy from a pseudogestational sac. Pulsed Doppler sampling is performed with 0 degrees angle correction with manual manipulation of the transducer to obtain maximal Doppler velocity shifts.

The pseudogestational sac appears as an irregular saclike structure or thickening of the endometrial canal. This is related to a decidual reaction from an associated ectopic pregnancy. Unlike a normal gestational sac, the pseudogestational sac does not exhibit a double decidual lining, yolk sac, or fetal pole. Placental flow will not be identified around a pseudogestational sac.

The most specific sonographic appearance for ectopic pregnancy is an extrauterine sac or "tubal ring" (**Fig. 2–5**). The sac usually demonstrates a thick echogenic ring and may contain a yolk sac or fetal pole. The mass should be separate from the ovary to avoid confusion with a corpus luteum cyst. If the mass is not separate from the ovary, then follow-up endovaginal scans and serum HCG titers may be necessary for diagnosis.

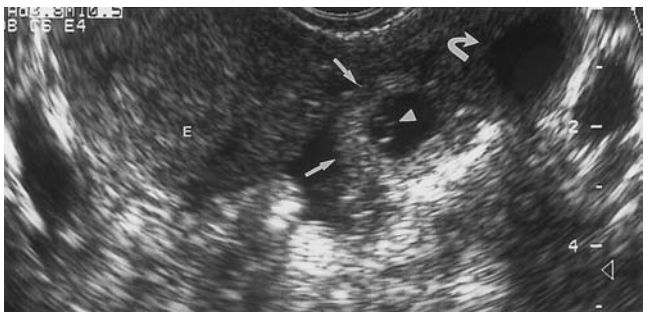

Figure 2–5 Ectopic gestational sac. An extrauterine gestational sac (*straight arrows*) with a yolk sac (*arrowhead*) is identified. Also note endometrial thickening (E) and left corpus luteal cyst (*curved arrow*).

Solid and complex adnexal masses may also represent an ectopic pregnancy in conjunction with an empty uterus and positive serum HCG titer. Placental flow may be demonstrated within these complex masses during endovaginal color flow imaging[7] (**Fig. 2–6**). These masses usually represent hemorrhage into the ectopic gestational sac or a ruptured ectopic pregnancy in the fallopian tube. They may also present as free intraperitoneal hematomas. Any extraovarian mass is suspicious for ectopic pregnancy in a pregnant patient without findings of intrauterine gestation.

In a recent study, placental flow was found in 55 (85%) of 65 ectopic pregnancies.[7] There was a sensitivity of 95% and specificity of 85% for the diagnosis of ectopic pregnancy with endovaginal color flow imaging. Detection of placental flow in an adnexal mass separate from the ovary is diagnostic of ectopic pregnancy. A velocity cutoff value is not required for the detection of placental flow in the adnexae. The detection of placental flow in adnexal lesions has been helpful in the diagnosis of ectopic pregnancy in the absence of an extrauterine sac or tubal ring.

Treatment of ectopic pregnancy includes surgical excision, preferably under laparoscopic guidance. Salpingectomy and salpingostomy are the most commonly performed procedures. There is a trend toward nonsurgical treatment utilizing methotrexate or expectant management. Methotrexate has been found to be efficacious in several series.[18,19] The risk of recurrent ectopic pregnancy is increased following tubal surgery, and close surveillance is recommended in subsequent pregnancies.

Ovarian Torsion

Ovarian torsion accounts for ~3% of gynecologic emergencies. Torsion usually occurs in premenopausal patients and is often associated with an ovarian mass. The mass serves as the focal point for the torsion, which involves both the ovary and the fallopian tube. Twenty percent of patients are pregnant at the time of diagnosis. Torsion can also occur in postmenopausal patients and may be associated with an ovarian neoplasm. Torsion of normal adnexa is uncommon but may be related to pregnancy or pelvic mass.

Patients with ovarian torsion present with acute, severe onset of unilateral pelvic pain. The right ovary is more commonly involved than the left.[20] Pain may be accompanied with nausea and vomiting, which mimics other conditions, including appendicitis or small bowel obstruction. Recurrent, intermittent bouts of pain may precede the current episode by days to weeks.

Sonography is the primary noninvasive examination for the diagnosis of ovarian torsion. Sonographic findings in ovarian torsion are variable. Most patients with torsion

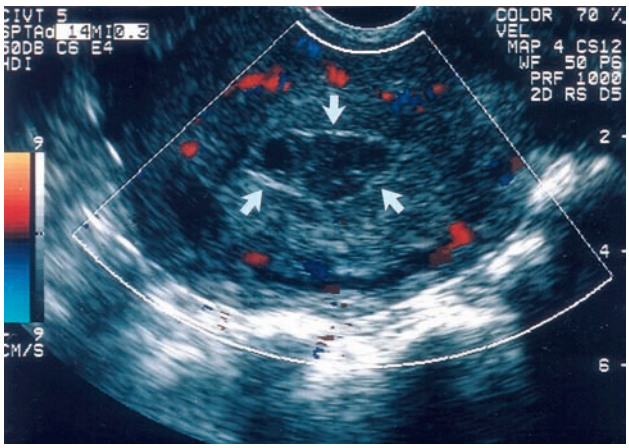

A

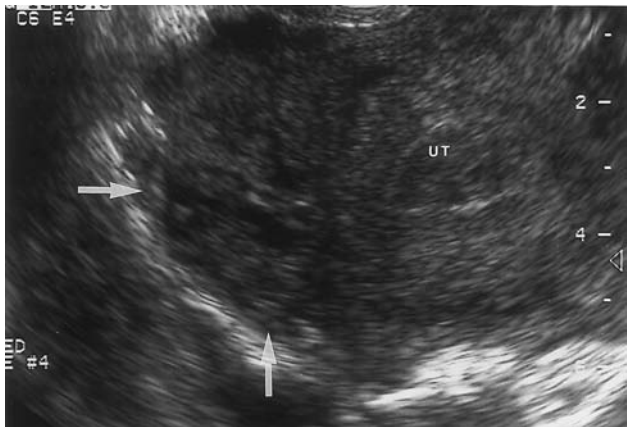

B

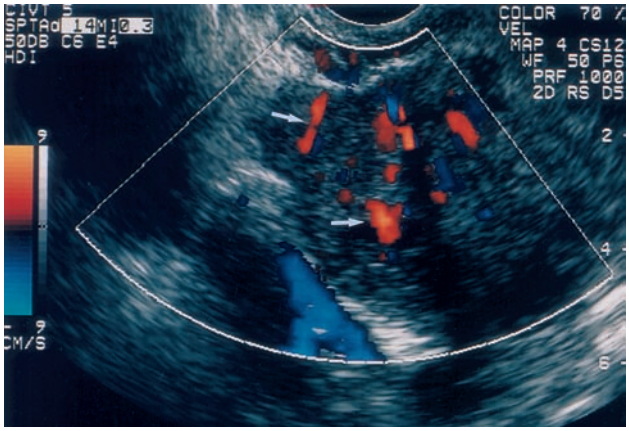

C

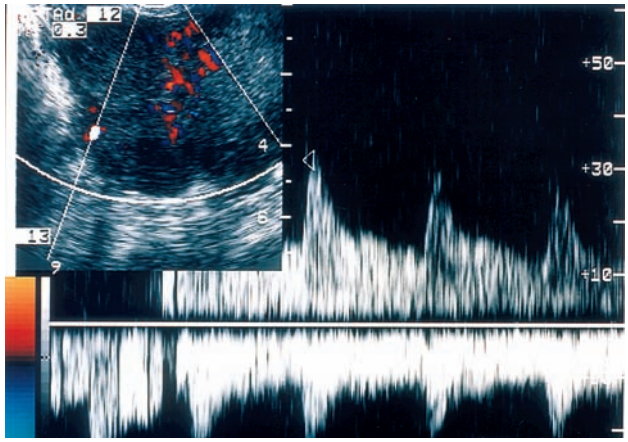

D

Figure 2–6 Solid ectopic with placental flow. **(A)** A pseudogestational sac (*arrows*) is seen in the uterus. Color flow imaging demonstrates no flow within the pseudogestational sac. **(B)** An ill-defined mass (arrows) is seen adjacent to the uterus (UT). The findings suggest small bowel, hematoma, or ectopic pregnancy. **(C)** Color flow imaging reveals flow (*arrows*) within the mass, confirming the location of the ectopic pregnancy. **(D)** Spectral analysis demonstrates low-impedance flow consistent with placental flow.

present with an enlarged ovary or mass. The sonographic appearance of the mass can vary from cystic to complex to completely solid.[20] The torsed ovary may contain hypoechoic areas representing hemorrhage or infarction. Venous and lymphatic obstruction produce edema and free intraperitoneal fluid. Clues to ovarian torsion include the presence of an enlarged ovary in an unusual location such as the cul-de-sac or above the uterus. The finding of a twisted or coiled vascular pedicle ("slinky sign") is also helpful. With partial torsion, the ovary can attain massive size due to edema from lymphatic obstruction. In pediatric patients, two sonographic patterns have emerged. In prepubertal girls, torsion tends to occur in enlarged, complex cystic masses, whereas in pubertal girls torsion occurs predominantly in solid, enlarged adnexal masses.[21]

The diagnosis of ovarian torsion is confirmed by the failure to detect arterial or venous flow from within ovarian parenchyma with color and pulsed Doppler (**Fig. 2–7**). The absence of flow within the torsed ovary during color flow, power, and pulsed Doppler is diagnostic. All color flow parameters must be optimized to ensure that the absence of flow is not related to technical factors such as high pulse repetition frequency (PRF), high wall filter, or low color gain settings. Arterial flow may be seen only around the periphery of the ovary with chronic torsion due to reactive inflammation. Decreased vascularity may be seen within the ovary with partial torsion. Several authors have described the presence of venous and arterial signals within surgically proven torsed ovaries.[21–23] This is likely related to the dual blood supply to the ovary from the ovarian artery and branches of the uterine artery. Thus, it is necessary to incorporate clinical and sonographic information to consider the diagnosis of ovarian torsion in difficult cases. The presence of an adnexal mass in a patient presenting with acute or recurrent pelvic pain should suggest the diagnosis of ovarian torsion.

Diagnostic laparoscopy is usually performed for ovarian torsion following sonographic evaluation. If the ovary appears viable, it is detorsed with removal of ovarian mass, if present. The ovary may be secured to prevent recurrent torsion. The ovary is removed if found to be nonviable or gangrenous.

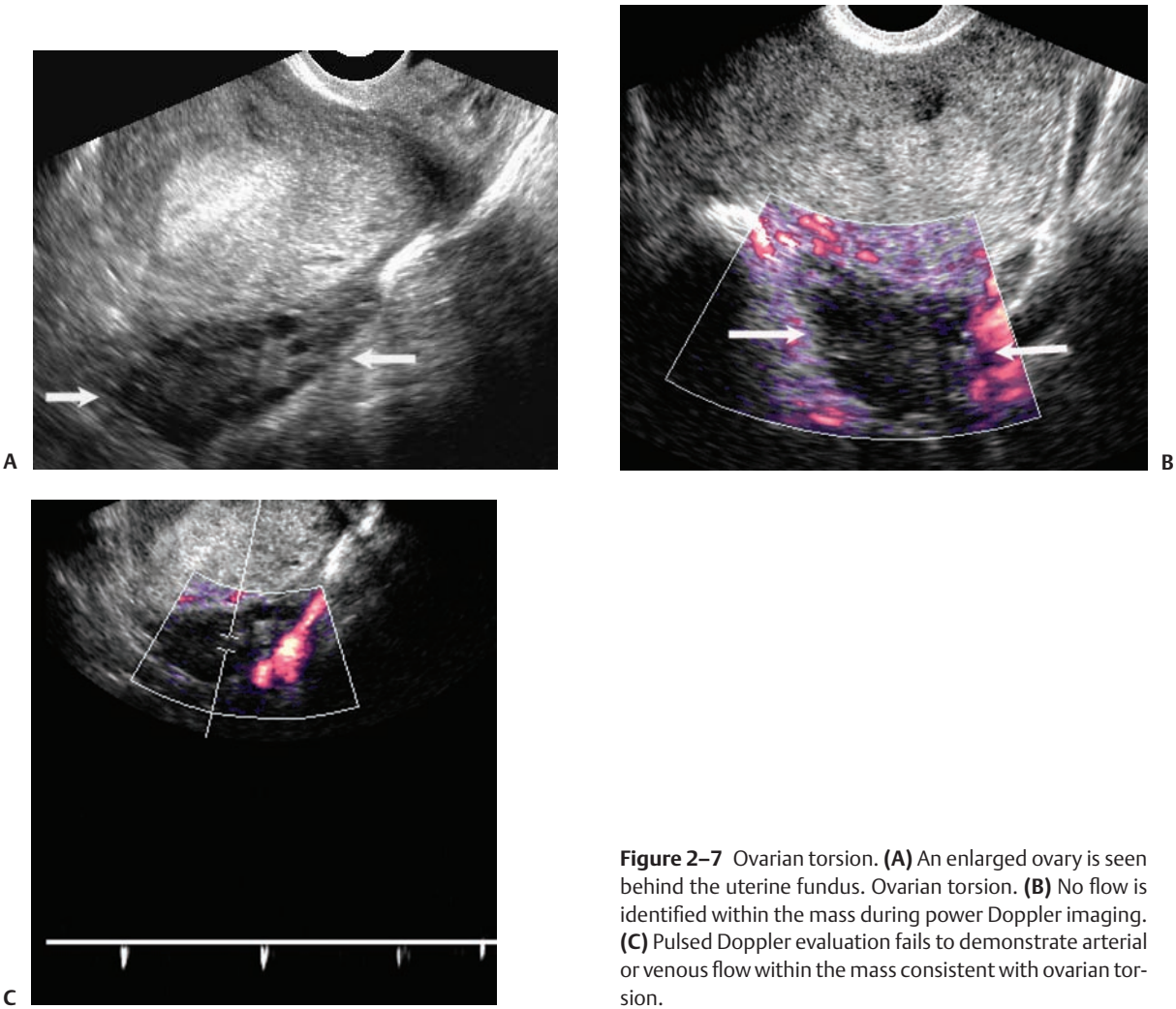

Figure 2–7 Ovarian torsion. **(A)** An enlarged ovary is seen behind the uterine fundus. Ovarian torsion. **(B)** No flow is identified within the mass during power Doppler imaging. **(C)** Pulsed Doppler evaluation fails to demonstrate arterial or venous flow within the mass consistent with ovarian torsion.

Pelvic Inflammatory Disease

Most cases of pelvic inflammatory disease (PID) are due to an ascending infection from the cervix to the endometrium. Continued spread to the fallopian tubes may occur due to reflux of menstrual blood with the eventual spill of exudate into the peritoneal cavity. Signs of a lower genital tract infection usually precede symptoms of PID. Most patients are premenopausal, with a typical history of multiple sexual partners and gonococcal or chlamydial infection.

TOA represents a severe complication of PID, occurring in ~15% of cases. This results from exudation of pus and microorganisms from the tube to the adjacent ovary or surrounding pelvic structures. This exudation leads to tissue destruction and the formation of loculations or abscess cavities affecting the tube, ovary, uterus, and bowel.

The most frequent symptom is bilateral lower abdominal or pelvic pain or tenderness. There may be associated nausea, vomiting, and fever, which reflect peritoneal inflammation. Physical examination may demonstrate cervical motion tenderness, palpable, tender adnexae, and leukorrhea. Laboratory data consistent with PID include leukocytosis, elevated erythrocyte sedimentation rate, and positive cultures for *Neisseria gonorrhoeae* or *Chlamydia trachomatis.*

Ultrasound is not reliable to detect subtle signs of salpingitis but can identify other signs of inflammation, including endometritis, pyosalpinx, TOA, and pelvic collections. The endovaginal examination is particularly uncomfortable and frequently results in the "chandelier sign." Sonographic signs of endometritis include fluid or gas within the endometrial cavity. Fluid or debris within the fallopian tube is suspicious for pyosalpinx. The tube typically tapers as it enters the uterus and distends distally. TOA appears as a cystic mass, which may demonstrate fluid levels or echogenic debris within the collection (**Fig. 2–8**). Occasionally, they may have a complex appearance with solid regions, nodularity, and septations. The ovary may not be identified separate from the mass. These masses may be hypervascular, a nonspecific finding.

Endometrial biopsy and laparoscopy are useful for confirming the diagnosis and obtaining cultures of the upper genital tract. These studies are particularly useful for patients failing antibiotic therapy due to severe disease or incorrect diagnosis.

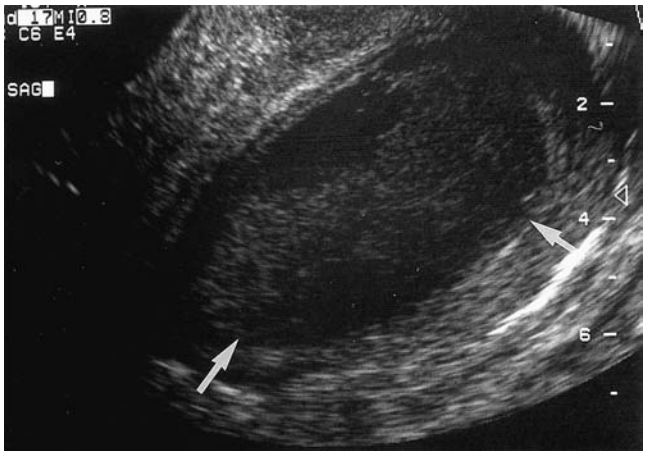

Figure 2–8 Tubo-ovarian abscess. A large complex mass (*arrows*) is filled with echogenic debris. The ovary was not identified separate from the mass.

Treatment for PID requires antibiotic therapy. Severe PID and TOA require hospitalization for intravenous administration of broad-spectrum antibiotics and percutaneous drainage. Surgical exploration is considered for patients who do not respond to medical therapy within 72 to 96 hours. Surgical drainage or total abdominal hysterectomy bilateral salpingo-oophorectomy (TAH-BSO) may be performed for impending abscess rupture or overwhelming sepsis.

Endometriosis

Endometriosis results from ectopic location of endometrial tissue outside the uterus within the peritoneal cavity and on the surfaces of pelvic organs and ligaments. Endometriosis less commonly presents with acute pelvic pain. The pain is described as aching and constant, beginning 2 to 7 days before the onset of menses and increasing in severity during menstruation. The patient may give a history of similar prior episodes of dysmenorrhea. Patients may also complain of infertility, dyspareunia, back pain, and uterine bleeding. Symptoms may relate to endometriosis at multiple sites, causing tenesmus, rectal bleeding, dysuria, flank pain, and urgency. Physical findings are variable and may include tenderness, nodularity, parametrial thickening, and adnexal masses.

Endometriosis is difficult to detect sonographically when the implants are small (< 5 mm). These implants may bleed and produce cystic or complex masses, which can be seen with ultrasound. These represent endometriomas and may contain low-level internal echoes consistent with hemorrhage (**Fig. 2–9**). The masses may contain nodules or septations that may simulate ovarian neoplasms. They may wax and wane in size and vascularity from cycle to cycle. These periodic changes are seen when comparing serial examinations and are diagnostic for this disease. Magnetic resonance imaging (MRI) confirms the presence of blood products within these adnexal masses and may find smaller implants in locations difficult to assess with ultrasound. Laparoscopy is considered the gold standard for this diagnosis because there is direct visualization and sampling of small implants.

The choice of treatment depends on the severity of symptoms and the extent of disease. Implants may be cauterized and adhesions lysed at laparoscopy. Hormonal suppression is reserved for invasive disease or cases resistant to laparoscopic treatment. Hysterectomy and oophorectomy are also options for severe cases.

Adnexal Tumors

Adnexal tumors are another uncommon cause of acute pelvic pain. Pain usually results from infection, torsion, or hemorrhage into the pelvic mass. Both benign and malignant ovarian tumors may torse. Acute pain and adnexal swelling with a decrease in the hematocrit are consistent with hemorrhage into a pelvic mass. Similarly, an elevated

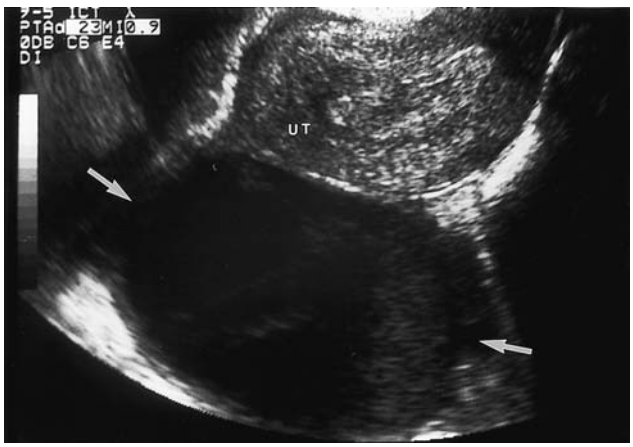

A

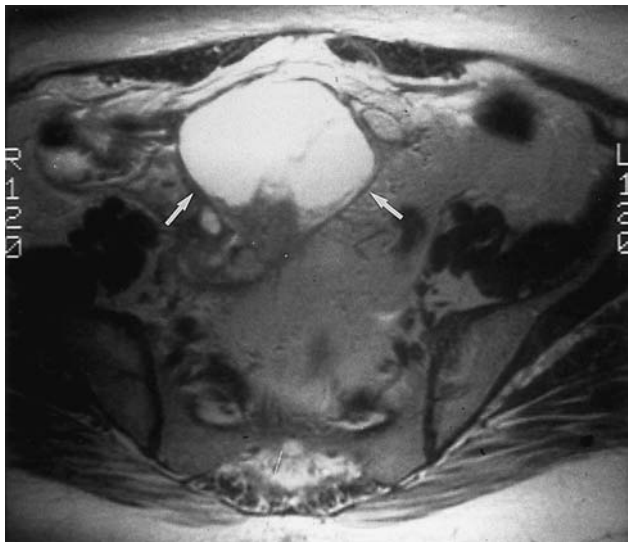

B

Figure 2–9 Endometrioma. **(A)** A complex cystic mass (*arrows*) is noted adjacent to the uterus (UT). **(B)** Magnetic resonance imaging demonstrates increased signal within the mass (*arrows*) consistent with hemorrhage.

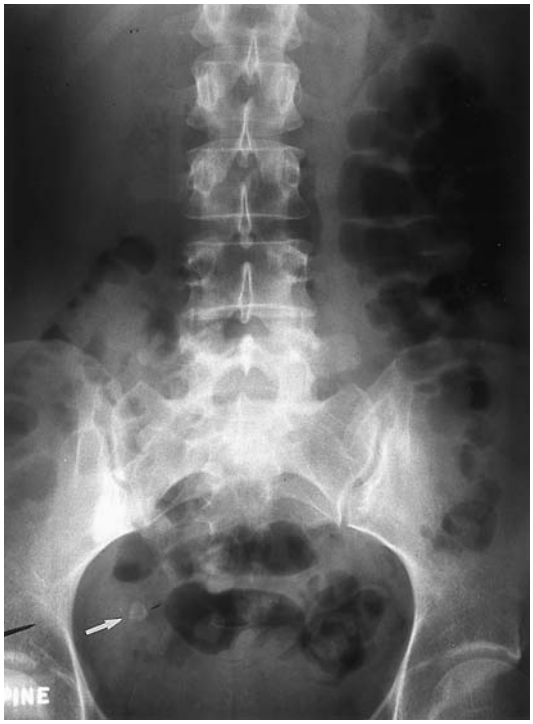

A

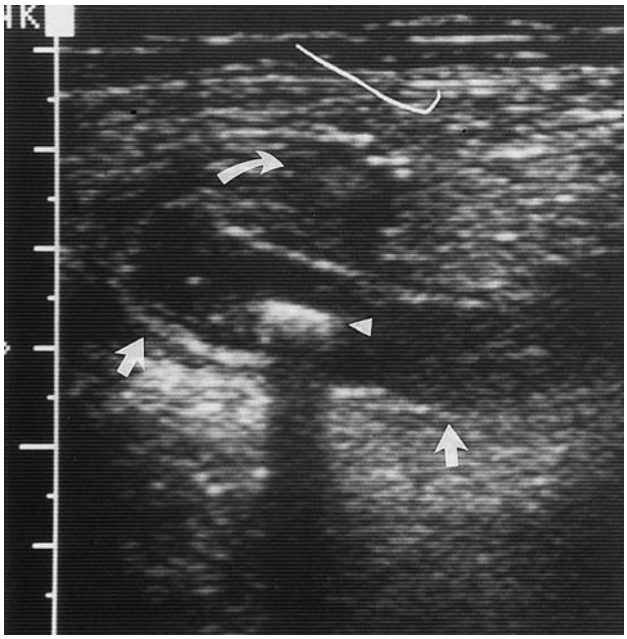

B

Figure 2–10 Appendicitis. **(A)** Abdominal radiograph demonstrates focal calcification (*arrow*) in the right lower quadrant consistent with an appendicolith. **(B)** A noncompressible, distended loop (*arrows*) is identified at the site of maximal tenderness. Note periappendiceal fluid (*curved arrow*) and fecalith (*arrowhead*).

white blood cell count, fever, and pelvic tenderness associated with an adnexal mass suggest superimposed infection.

Uterine fibroids can also undergo torsion, infection, or hemorrhage. MRI is helpful for identification of an adnexal mass as a fibroid. It is necessary to identify the uterine pedicle attachment of a pedunculated fibroid to distinguish a torsed fibroid from other adnexal masses. Color Doppler is particularly useful in demonstrating the vascular pedicle connection of the fibroid to the uterus.

Appendicitis

Appendicitis is one of the most common causes of acute abdominal/pelvic pain and is the most common indication for emergency laparotomy. Patients present with right lower-quadrant pain, which may be accompanied by fever, leukocytosis, and tenderness. Unfortunately, the clinical features are not specific. Thirty percent of patients will have an atypical presentation resulting in a high (20 to 46%) negative appendectomy rate.[24,25] The differential diagnosis includes all the gynecologic problems discussed earlier, as well as urolithiasis, diverticulitis, bowel obstruction, and other inflammatory conditions. A pregnancy test and endovaginal sonography are helpful to exclude other conditions.

Because appendicitis can mimic other clinical entities, the diagnostic evaluation should include the abdomen and pelvis. Radiography, ultrasound, and computed tomography (CT) are useful in the imaging workup. Plain-film radiographs may demonstrate right lower-quadrant calcification consistent with an appendicolith or findings suggestive of another process such as obstruction, ileus, or ureteral calculus.

Sonography is effective in the diagnosis of acute appendicitis with sensitivity of 80 to 89% and accuracy of 90 to 95%.[26–28] A graded compression technique is performed to demonstrate a distended, noncompressible appendix. A high-frequency (5 to 7 MHz) linear array transducer is used to gradually compress and disperse overlying bowel loops over the site of maximum tenderness. The inflamed appendix will appear as a noncompressible, aperistaltic blind loop on sagittal and transverse views (**Fig. 2–10**). The inflamed appendix demonstrates a "target" appearance on the transverse view with a diameter greater than 6 mm. An appendicolith is occasionally seen within the appendix. Sonography will also detect loculated periappendiceal fluid consistent with perforation and abscess formation. Gas can be seen within the appendix or adjacent abscess. Loss of the echogenic submucosal ring is associated with advanced infection and perforation.

CT is recommended for patients with suspected appendiceal perforation on clinical or sonographic grounds. CT can better define the extent of inflammation compared with ultrasound, and help guide percutaneous drainage procedures. Similarly, CT can better define abscesses or collections related to diverticulitis or Crohn's disease. CT should also be performed in patients with persistent symptoms without a diagnosis.

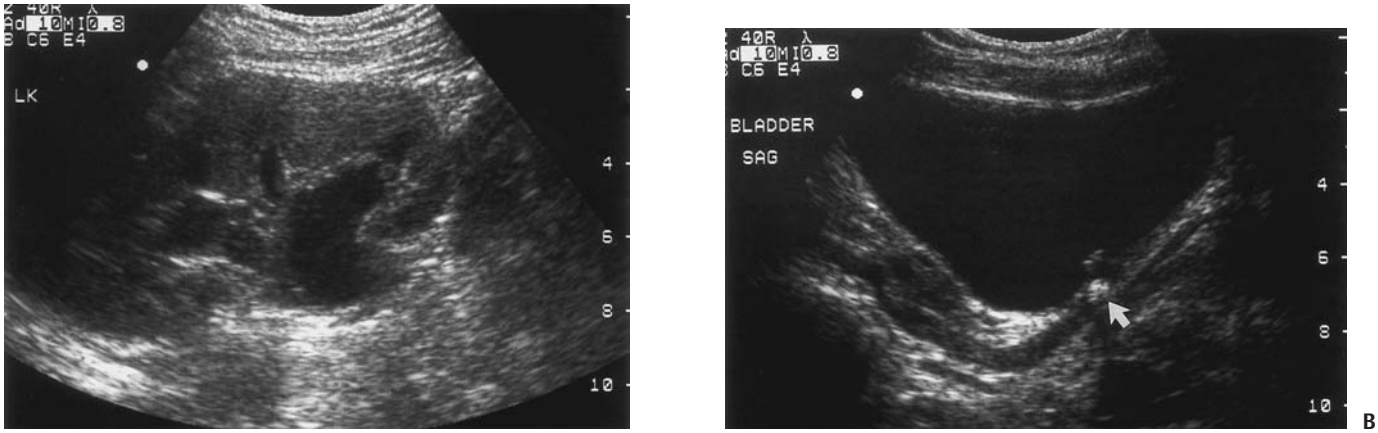

A B

Figure 2–11 Ureteral calculus. **(A)** There is moderate left hydronephrosis. No obstructing calculus is seen. **(B)** Transvesical examination of the pelvis reveals a calculus (*arrow*) at the ureterovesical junction.

Ureteral Calculus

Patients with urinary obstruction related to ureteral calculus may also present with acute lower quadrant or pelvic pain. The pain is unilateral and may radiate to the back, flank, or pelvis. There may be associated hematuria, fever, and leukocytosis.

When the clinical presentation is nonspecific, the diagnostic evaluation should include the abdominal and pelvic organs. A KUB may demonstrate renal or ureteral calculi. Like appendicitis, sonography is employed to distinguish between gynecologic and nongynecologic processes. Although ultrasound may demonstrate dilatation of the renal collecting system, there may be minimal or no hydronephrosis with early obstruction.[29] Ultrasound is less sensitive than intravenous urography for the diagnosis of acute renal obstruction. Sonography and KUB may replace intravenous urography in patients with renal insufficiency or contrast allergy.[30] Unenhanced helical CT has proven accurate and reliable for the detection of ureteral calculi in patients with flank pain. A recent study demonstrated a 98% sensitivity and 100% specificity for the detection of ureteral calculi with noncontrast-enhanced spiral CT in patients referred with acute flank pain.[31]

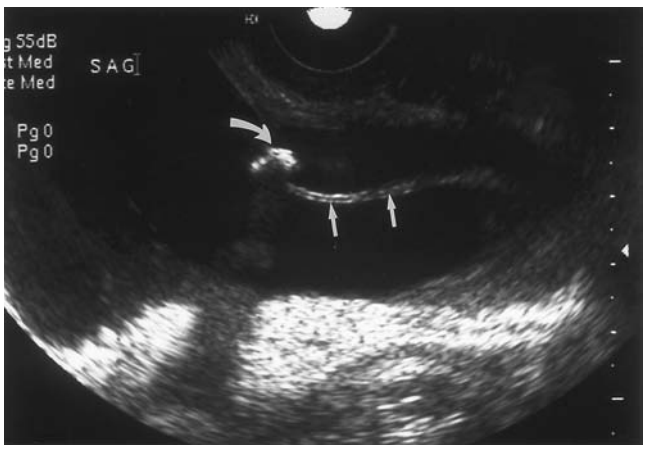

Figure 2–12 Ureteral calculus. Endovaginal sonogram reveals a calculus (*curved arrow*) in the distal ureter (*straight arrows*).

When renal colic is suspected, a search for the level of obstruction should be performed. Careful sonographic examination of the pelvis, including the region of the ureterovesical junction (UVJ) may reveal the obstructing calculus (**Fig. 2–11**). Endovaginal sonography may be helpful in identification of the distal ureteral stone. The transducer is directed toward the posteroinferior aspect of the bladder at the level of the UVJ. A dilated distal ureter can be followed to the level of obstruction. An obstructing calculus appears as an echogenic structure with acoustic shadowing (**Fig. 2–12**). In patients without obstruction, an intermittent ureteral jet can be identified at the UVJ with color flow imaging. An absent or persistent ureteral jet suggests ureteral obstruction.

Summary

Acute pelvic pain is a common clinical problem with many possible etiologies. The clinical history, physical examination, and laboratory data are necessary to formulate the differential diagnosis. Ultrasound is the preferred first-line noninvasive imaging examination due to ready availability, low cost, and high diagnostic accuracy. Ultrasound can distinguish between gynecologic and nongynecologic causes of pelvic pain. Duplex and color Doppler may add important diagnostic information to improve diagnosis.

References

1. Ritchie WG. Sonographic evaluation of normal and induced ovulation. Radiology 1986;161:1–10
2. Hackeloer BJ, Fleming R, Robinson HP, et al. Correlation of ultrasonic and endocrinologic assessment of human follicular development. Am J Obstet Gynecol 1979;135:122–128
3. O'Herlihy C, Robinson HP, deCrispigny LJ. Mittelschmerz is a preovulatory symptom. BMJ 1980;280:986
4. Kerin JF, Edmonds DK, Warnes GM, et al. Morphological and functional relations of graafian follicle growth to ovulation in women

using ultrasonic, laparoscopic and biochemical measurements. Br J Obstet Gynaecol 1981;88:81–90
5. Queenan JT, O'Brien GD, Bains LM, et al. Ultrasound scanning of ovaries to detect ovulation in women. Fertil Steril 1980;34:99–105
6. Koninckx PR, Renaer M, Brosens IA. Origin of peritoneal fluid in women: an ovarian exudation product. Br J Obstet Gynaecol 1980; 87:177–183
7. Pellerito JS, Taylor KJW, Quedens-Case C, et al. Ectopic pregnancy: evaluation with endovaginal color flow imaging. Radiology 1992; 183:407–411
8. Taylor KJ, Burns P, Wells PNT. Ultrasound Doppler flow studies of the ovarian and uterine arteries. Br J Obstet Gynaecol 1985;92: 240–246
9. Dillon EH, Quedens-Case C, Ramos IM, et al. Endovaginal pulsed and color flow Doppler in first trimester pregnancy. Ultrasound Med Biol 1993;19:517–525
10. Centers for Disease Control. Ectopic pregnancy: United States, 1986. MMWR Morb Mortal Wkly Rep 1989;38:481–484
11. Weckstein LN. Clinical diagnosis of ectopic pregnancy. Clin Obstet Gynecol 1987;30:236–244
12. Halpin TF. Ectopic pregnancy: the problem of diagnosis. Am J Obstet Gynecol 1970;106:227–236
13. Nyberg DA, Mack LA, Jeffrey RB, Laing FC. Endovaginal sonographic evaluation of ectopic pregnancy: a prospective study. AJR Am J Roentgenol 1987;149:1181–1186
14. Dashefsky SM, Lyons EA, Levi CS, et al. Suspected ectopic pregnancy: endovaginal and transvesical US. Radiology 1988;169:181–184
15. Cacciatore B, Stenman UH, Ylostalo P. Comparison of abdominal and vaginal sonography in suspected ectopic pregnancy. Obstet Gynecol 1989;73:770–774
16. Dillon EH, Feyock AL, Taylor KJW. Pseudogestational sacs: Doppler US differentiation from normal or abnormal intrauterine pregnancies. Radiology 1990;176:359–364
17. Taylor KJ, Ramos IM, Feyock AL, et al. Ectopic pregnancy: duplex Doppler evaluation. Radiology 1989;173:93–97
18. Stovall TG, Ling FW, Carson SA, Buster JE. Nonsurgical diagnosis and treatment of tubal pregnancy. Fertil Steril 1990;54:537–538
19. Kojima E, Abe Y, Morita M, et al. The treatment of unruptured tubal pregnancy with intratubal methotrexate injection under laparoscopic control. Obstet Gynecol 1990;75:723–725
20. Warner MA, Fleischer AC, Edell SL, et al. Uterine adnexal torsion: sonographic findings. Radiology 1985;154:773–775
21. Stark JE, Siegel MJ. Ovarian torsion in prepubertal and pubertal girls: sonographic findings. AJR Am J Roentgenol 1994;163:1479–1482
22. Rosado WM, Trambert MA, Gosink BB, Pretorius DH. Adnexal torsion: diagnosis by using Doppler sonography. AJR Am J Roentgenol 1992;159:1251–1253
23. Fleischer AC, Stein SM, Cullinan JA, Warner MA. Color Doppler sonography of adnexal torsion. J Ultrasound Med 1995;14:523–528
24. Abu-Yousef MM, Franken EA. An overview of graded compression sonography in the diagnosis of acute appendicitis. Semin Ultrasound CT MR 1989;10:352–363
25. Lewis FR, Holcroft JW, Boey J, et al. Appendicitis: a critical review of diagnosis and treatment in 1,000 cases. Arch Surg 1975;110:677–684
26. Abu-Yousef MM, Bleicher JJ, Maher JW, et al. High-resolution sonography of acute appendicitis. AJR Am J Roentgenol 1987;149: 53–58
27. Puylaert JBCM. Acute appendicitis: US evaluation using graded compression. Radiology 1986;158:355–360
28. Jeffrey RB, Laing FC, Lewis FR. Acute appendicitis: high-resolution real-time US findings. Radiology 1987;163:11–14
29. Laing FC, Jeffrey RB, Wing VW. Ultrasound versus excretory urography in evaluating acute flank pain. Radiology 1985;154:613–616
30. Haddad MC, Sharif HS, Shahed MS, et al. Renal colic: diagnosis and outcome. Radiology 1992;184:83–88
31. Fielding JR, Steele G, Fox LA, et al. Spiral computerized tomography in the evaluation of acute flank pain: a replacement for excretory urography. J Urol 1997;157:2071–2073

3 Abnormal Premenopausal Vaginal Bleeding

Edward A. Lyons

Diagnostic Evaluation

The Initial Assessment

Abnormal uterine bleeding in a patient during her reproductive years is more commonly than not associated with a pregnancy. The clinician will first assess the likelihood of pregnancy and will do a qualitative or quantitative pregnancy test to detect the presence of the β subunit of human chorionic gonadotrophin (hCG).

The Pregnancy Test

Human chorionic gonadotrophin is produced by the syncytiotrophoblast of the chorionic sac as it invades and implants in the decidual layer of the endometrium. Implantation takes place on or about day 22, or 8 days after fertilization, and hCG can be detected in maternal serum as early as 9 days postfertilization or day 23. The commonly used tests in the office and those available as home pregnancy tests are immunologic tests based on the antigenic properties of the hCG protein and are positive 4 to 7 days after the first missed period. Testing time varies from 2 minutes to 2 hours. The most sensitive test is a radioimmunoassay for hCG, which can detect serum levels as low as 2 to 4 mU/mL. It requires 24 to 48 hours of incubation time and gives a quantitative analysis.

It is important to remember that the half-life of β hCG in maternal serum is 1.5 days. After termination of pregnancy, spontaneous or induced, the test will remain positive for a period of time relative to the initial level. At 10 weeks menstrual age, the level of β hCG may be as high as 100,000 mIU/mL and will be detectable for 24 days after termination.

Further Evaluation

Abnormal uterine bleeding during the reproductive years is a common occurrence. The gynecologist can evaluate the patient completely in the office and the patient may never present for imaging evaluation.

History

The history should focus on the potential or actuality of pregnancy; the date of the last normal menstrual period; the volume, duration, and color of the bleeding; and associated pain, cramps, mass, infection, or intrauterine contraceptive device (IUCD).

Physical Exam

The physical exam of the gynecologist may detect uterine enlargement commonly from pregnancy, fibroids, or adenomyosis, but also possibly from endometrial carcinoma. A mass lesion in the adnexa or localizing tenderness may indicate presence of blood in the peritoneal cavity. Vulvar, vaginal, and cervical lesions, as well as the type of bleeding in those areas can be visualized directly upon speculum exam and cervical dilatation. Pain on cervical motion may be an important indicator of an ectopic pregnancy.

Nonimaging and Imaging Test Other than Ultrasound

Cytological Exam

The cervical or Pap smear may detect abnormal cervical mucosal changes or, in some cases, abnormal endometrial cells from carcinoma.

Endometrial Biopsy

As an office procedure, the introduction of a fine endometrial curette or suction curette (Pipelle) may sample abnormal sites of endometrium, but more often than not, misses *focal* abnormalities or mass lesions. The curette is a flexible polypropylene cannula with an outer diameter of 3.1 mm, which is introduced without the need for cervical dilatation or anesthesia. These have replaced a large number of dilation and curettages (D&Cs) as the method of choice for the diagnosis of abnormal uterine bleeding. Histological examination is performed on the tissue obtained.

Hysterosalpingography

This has been used for a wide variety of conditions, but is being requested less commonly in favor of ultrasound and direct hysteroscopy.

Office Hysteroscopy

With the advent of small, thin, flexible hysteroscopes, this is becoming a more common office procedure, whereas previously it was done only in hospitals. Local anesthesia is

frequently used via a paracervical block to dilate the cervix, particularly in postmenopausal women.

Dilatation and Curettage

This has always been the gold standard for abnormal bleeding. It is done mainly as day-surgery with local anesthesia or conscious sedation.

Ultrasound Imaging

This is being used to advantage by some knowledgeable clinicians in the office in addition to the clinical exam. Office-based ultrasound is frequently limited by a less expensive, lower-resolution scanner, which often lacks color Doppler. New and fully functional scanners are now available and are relatively inexpensive, making them affordable for the private office setting. One should always begin with a transabdominal exam with or without a full bladder. This portion of the exam is focused on finding large masses that may be obscured during the endovaginal study or will be out of the field of view. Solid ovarian dermoid tumors may not be appreciated during the endovaginal study because of the echogenic fat that may resemble bowel.

The endovaginal exam is essential for the most complete evaluation of the nongravid uterus. It provides the operator with a magnified view of the uterus, myometrium, endometrial canal, and adnexa. The endovaginal probe also provides a unique opportunity to palpate the pelvic organs and to "visualize" the site of any pain or tenderness. It is also useful in assessing mobility of structures and therefore their relationship. With additional pressure on the anterior abdominal wall, normal ovaries or masses may be visualized to better advantage.

Bleeding in the Nonpregnant Patient

In patients who are not pregnant, abnormal uterine bleeding can be due to abnormal menstruation, systemic or local disease, or urinary or gastrointestinal tract bleeding that is misinterpreted as vaginal. The sonologist should be aware of this when evaluating the pelvic sonogram.

Causes of Abnormal Menstrual Flow

Menorrhagia or Hypermenorrhea

Menstrual flow characterized by an increased volume or duration of flow sometimes associated with a clot is always abnormal. The usual causes are adenomyosis, early pregnancy loss, submucous fibroids, or just dysfunctional bleeding. Endometrial hyperplasia and malignant tumors are less common.[1]

Fibroids

Fibroids or leiomyomata are said to be present in 20 to 25% of women in the reproductive age group, increasing with age and decreasing with parity. They are more common in blacks than whites or Asians.[2] The age-standardized rates of ultrasound- or hysterectomy-confirmed diagnoses per 1000 woman-years were 8.9 among white women and 30.6 among black women. A 2.2 times increase in the incidence of fibroids among first-degree relatives has also been reported.[3]

Fibroids are often asymptomatic and grow only during the reproductive years under the influence of estrogen. During pregnancy they may enlarge and become tender, whereas postpartum they shrink and calcify. In menopause they tend to shrink and may even disappear. There are frequently multiple fibroids of varying sizes. Abnormal uterine bleeding is said to be present in 30% of patients with fibroids.

A fibroid located in the submucous region is the likely site when bleeding occurs and may be due to vascular engorgement and/or erosion of the overlying endometrial membrane. Abnormal bleeding can also occur with intramural fibroids where there is no direct contact with the endometrium. The mechanism is not well understood.

Pathologically, a fibroid is a rounded, firm, gray-white tumor, with the characteristic whorled pattern of smooth muscle bundles. As fibroid tumors grow, they push the myometrium aside and compress it, forming a pseudocapsule. This provides a cleavage plane for a fibroid to be shelled out at surgery or hysteroscopy. When the uterus is incised, the fibroid tends to pop out but not detach, as the myometrium tries to assume its normal configuration (**Fig. 3–1**).

Sonographically, the features of fibroids include:

- A discrete, well-defined mass with a hypoechoic periphery. The fibroid displaces and does not invade myometrium. The hypoechoic periphery may only be a few mm thick and represents compressed myometrium (**Fig. 3–2**). They may distort the endometrial cavity or the serosal surface (**Fig. 3–3**) or extend partially (**Fig. 3–4**) or even lie entirely within the endometrial canal, occasionally prolapsing out of the cervix (**Fig. 3–5**).
- They may be hypo-, iso-, or hyperechoic. The hyperechoic masses are usually due to hydropic degeneration and are soft on palpation and easily distorted by the endovaginal probe (**Fig. 3–6**) Lipoleiomyoma can also present as an echogenic mass within the myometrium, often with distal shadowing.
- Cystic areas of degeneration are uncommon in fibroids although they certainly do occur. Their etiology is not clearly understood; however, if there is associated rapid growth, sarcomatous change, although uncommon, should be considered. The cystic changes may also be overlooked because the fluid usually has

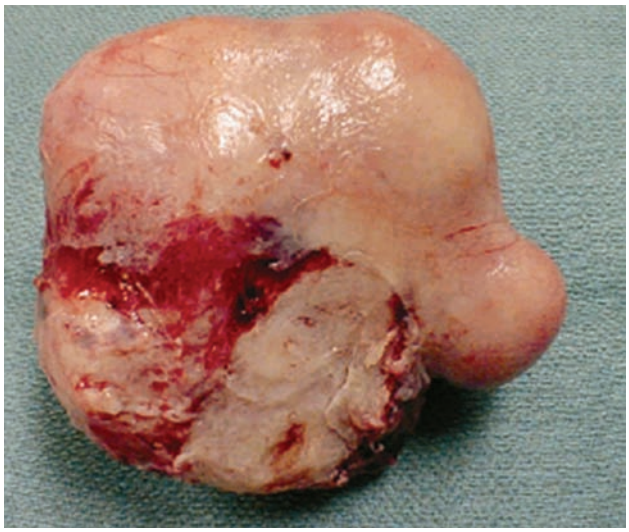

A

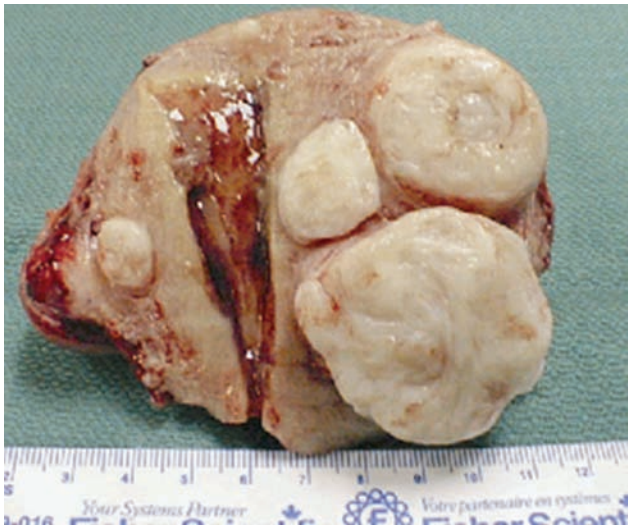

B

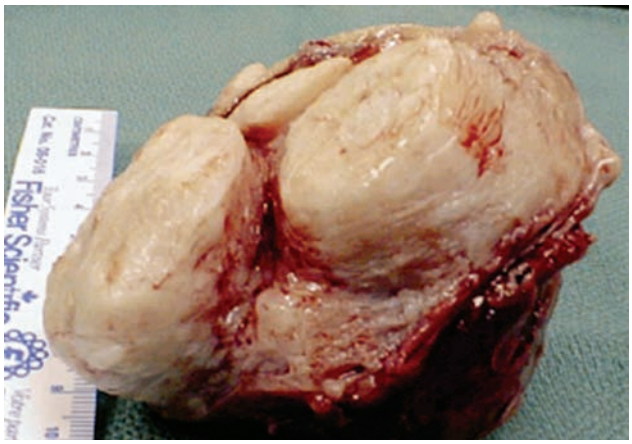

C

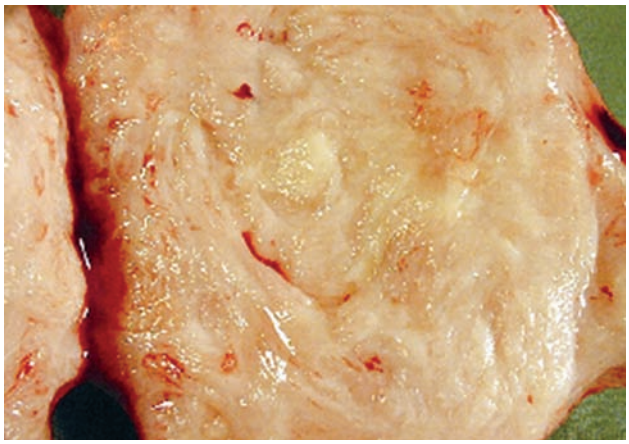

D

Figure 3–1 Fibroid uterus at pathology. This enlarged uterus contains four fibroids. **(A)** The intact uterus showing the typical lobulated appearance. **(B)** The uterus sectioned in the coronal plane. The large fibroids are seen displacing the endometrial canal to the right. **(C)** A side view of the sectioned uterus is showing the bulging of the fibroids above the cut surface. **(D)** A close-up view of a fibroid showing the typical disorganized and whorled appearance of the muscle bundles.

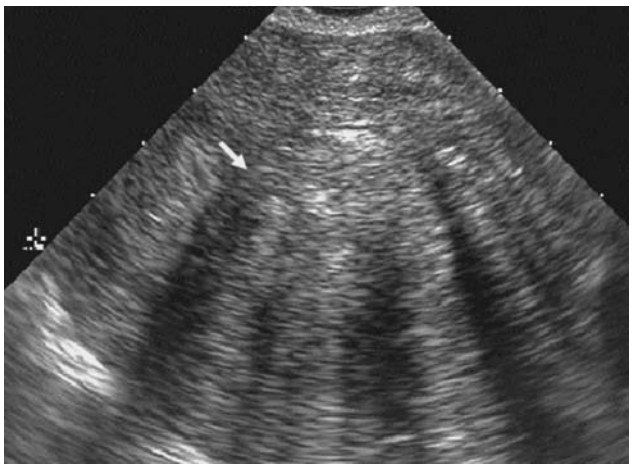

A

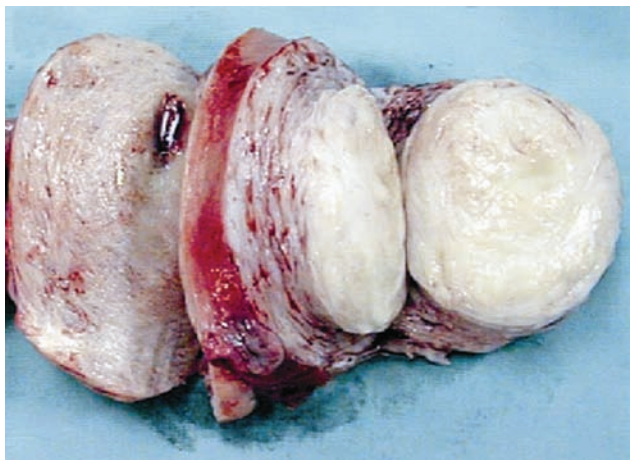

B

Figure 3–2 Fibroid with hypoechoic periphery. **(A)** There is a large, relatively isoechoic mass within the uterus on this coronal scan. A hypoechoic line (arrow) can be seen around the periphery. This also exhibits distal shadowing, another characteristic feature. **(B)** The gross specimen is showing the well-defined fibroid.

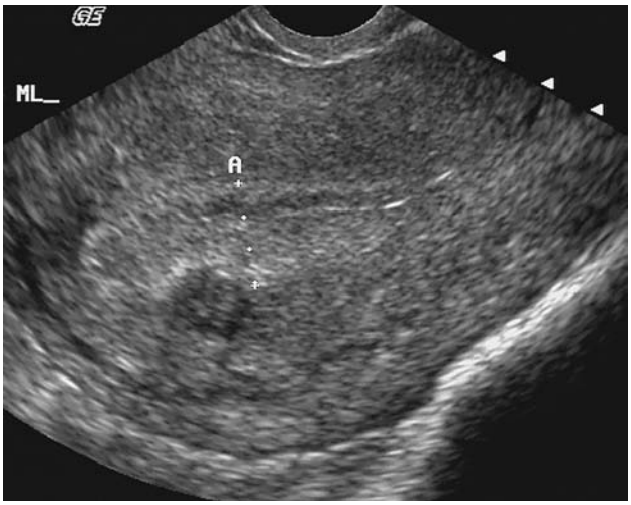

A

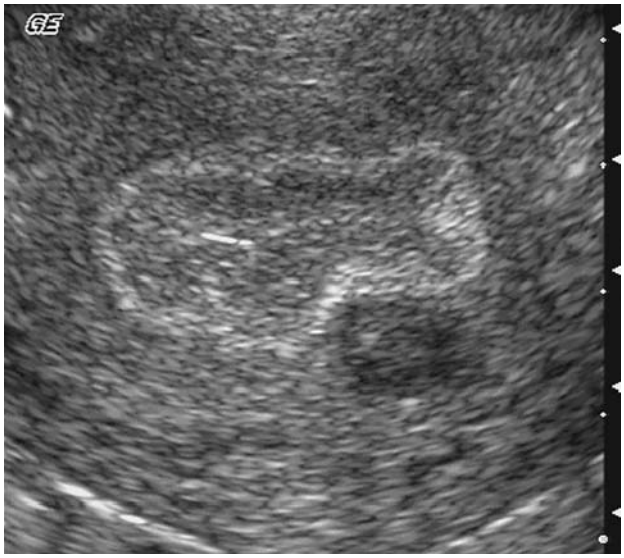

B

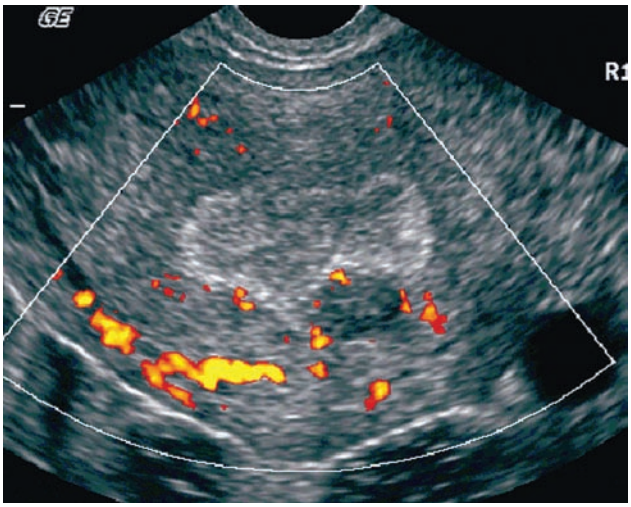

C

Figure 3–3 Submucous fibroid shown on **(A)** sagittal and **(B)** coronal scans that is distorting the echogenic endometrium posteriorly. The fibroid is 9 mm in diameter and shows a typical hypoechoic pattern. Notice the subtle shadow behind the fibroid on the sagittal scan. **(C)** This color flow coronal scan shows the vessels that surround the fibroid; none are seen within it.

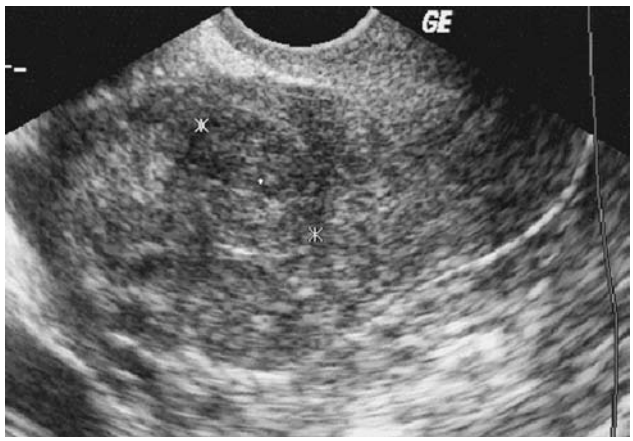

A

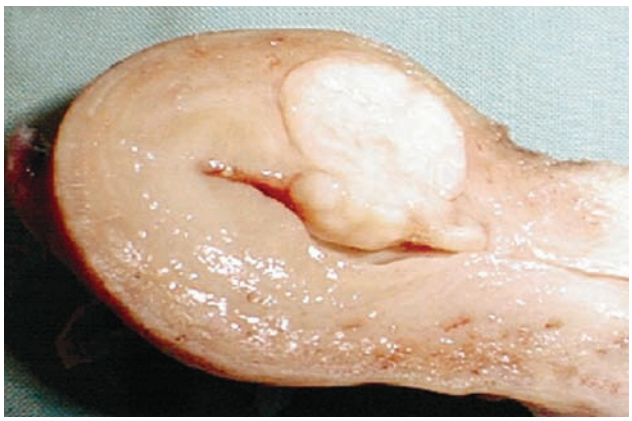

B

Figure 3–4 Submucous fibroid shown in **(A)** sagittal scan and **(B)** the gross specimen. The sonogram shows an isoechoic mass (calipers) distorting the anterior myometrium and displacing the endometrial canal. The gross specimen shows the intraluminal extension of the fibroid.

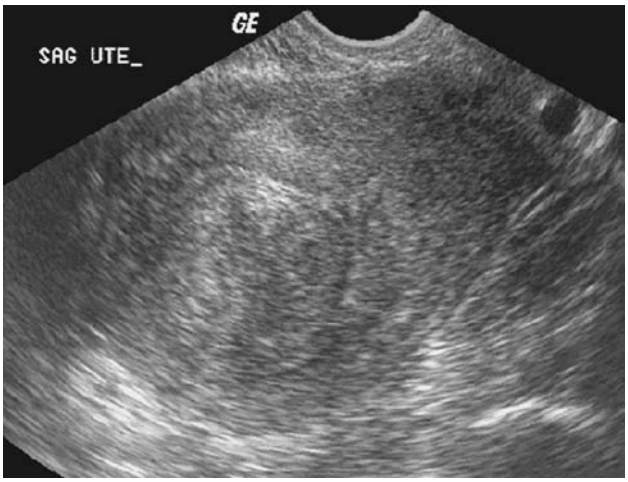

A

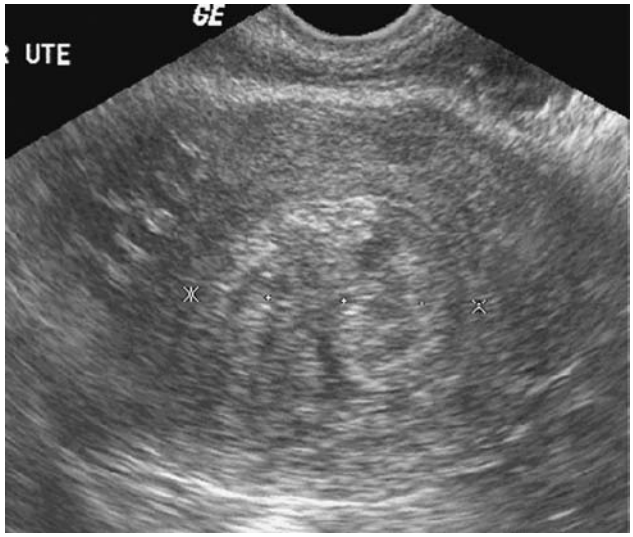

B

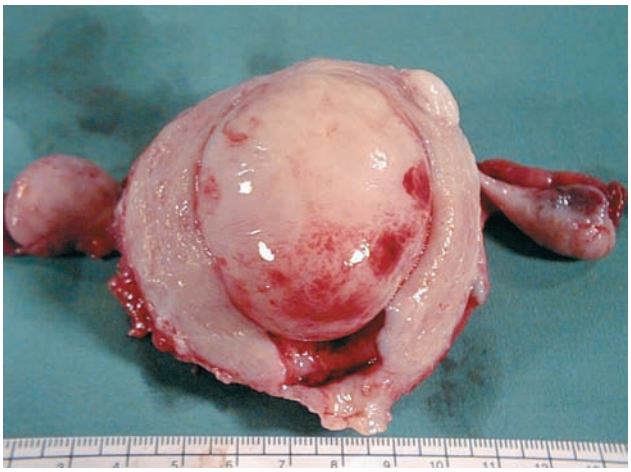

C

Figure 3–5 This is a submucous fibroid that lies entirely within the endometrial canal and is attached only by a short stalk (not visible). **(A)** Sagittal scan showing the somewhat heterogeneous fibroid within the fundal portion of the endometrial canal. **(B)** A coronal scan through the body shows the fibroid (calipers) situated centrally. **(C)** The gross specimen shows the 5 cm polypoid fibroid mass. Notice the ecchymotic areas that may have been the site of the patient's spotting.

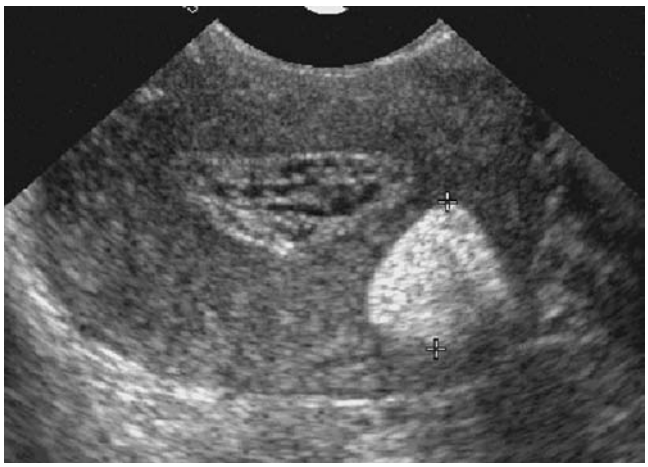

Figure 3–6 This coronal scan through the uterine body of a 50-year-old with cystic hyperplasia of the endometrium shows a brightly echogenic mural mass on the left with distal shadowing. This is due to hydropic degeneration of the fibroid.

echogenic debris within it. Compression of the fibroid with the endovaginal probe will create movement of the debris and distortion of the mass and should allow for the real-time confirmation of the cystic changes.

- Diffuse shadowing or distal attenuation of sound is commonly seen.
- Vessels are usually seen in the periphery of fibroids and occasionally within the fibroid as well (**Fig. 3–3C**) Tsuda et al[4] found in 70 women that only 6.1% of fibroids without a visible peripheral artery on endovaginal exam increased in volume over a 1 year period. This is compared with an increase in 46.2% of those with an artery. Of the 101 leiomyomata, an artery was detected in 51.5%.
- Fibroids are seldom tender except those that infarct and those that have undergone red degeneration during pregnancy.

- Calcification, likely dystrophic, is common, especially after a pregnancy and in postmenopausal women. It may have a curvilinear or flocculate appearance. The calcific deposits are usually clumps ~0.5 to 1 cm and seldom small.

For many years, sonologists have produced reports that read, "The myometrium is diffusely inhomogeneous. This may be due to the presence of multiple small fibroids." I cannot yet say that this statement is never true, but the occurrence is certainly close to never. Fibroids are *discrete* masses and do not give an ill-defined, inhomogeneous appearance. This appearance is almost certainly due to adenomyosis not fibroids.

Treatment of fibroids in general is done on a basis of symptomatology. If there is a large mass causing pressure, pain, or bleeding, a hysterectomy may be done in women who have completed their childbearing. To preserve the uterus and its reproductive capacity, a myomectomy may be done. The initial therapy is often medical, with the administration of gonadotropin-releasing hormone (GnRH) agonists to shrink the mass enough to relieve symptoms or in preparation for surgery. GnRH agonist therapy is used only temporarily because it induces an artificial menopause.

Fibroids in a submucous location that are causing bleeding or are contributing to recurrent spontaneous abortion can be removed under direct visualization with hysteroscopy. This is now a commonplace procedure.

Fibroids are sensitive to ischemia. There are several techniques that are now used to induce transient ischemia, which also result in significant shrinkage of the fibroid mass and reduction or cessation of any abnormal bleeding. Angiographic embolization of both uterine arteries or just the main fibroid feeding vessels is done with polyvinyl alcohol, a powderlike plastic material that is injected. Success rates of 88% have been reported, with an average decrease in size of 39% and relief of symptoms.[5] Premature ovarian failure is an uncommon but recognized complication due to embolization of the ovaries through the ovarian branch of the uterine arteries. New work has suggested that temporary, noninvasive clamping of the uterine arteries through the vaginal wall may give similar results to embolization.

High-intensity focused ultrasound (HIFU) is also used to ablate fibroids in a noninvasive manner. Therapeutic ultrasound units are attached to a magnetic resonance imaging (MRI) scanner, which is used to localize the lesion as well as to monitor the temperature rise within the fibroid.[6]

The accuracy of the ultrasound diagnosis of fibroids has not been confirmed in the literature. Ultrasound in the hands of knowledgeable users is currently the most sensitive and cost-effective diagnostic modality for fibroid detection. They are readily detectable by MRI and computed tomography, but these are less commonly used for the evaluation of pelvic pathology in the reproductive years. The gold standard would be pathological confirmation. It is recognized that the very small masses of less than 1 cm and those that are isoechoic with normal myometrium will be harder to identify. If these masses are not distorting the endometrial cavity or the serosal surface, they may go unrecognized; on the other hand, they are unlikely to be causing any symptoms and would not need therapy. It may also be difficult to recognize fibroids growing outside of the uterus either as free polypoid masses or within the broad ligament.

Adenomyosis or Endometriosis Interna

This is a condition characterized pathologically by nests of endometrial glands and stroma within the myometrium at least one high-power field (2 mm) deep to the endomyometrial junction. Adenomyosis must also be associated with compensatory hypertrophy of the myometrium surrounding the ectopic endometrium. Grossly, the uterus is enlarged and feels boggy. The cut surface through the area of adenomyosis is often congested with a focal bulging (**Fig. 3–7**). It is more infiltrative and does not have the discrete mass effect of a fibroid. Adenomyosis is a common finding, varying from 5 to 70% in routine sampling of uteri following hysterectomy.[7] This wide variation may depend on the age of the patients and on how meticulous the uterus was sectioned. It may be focal or diffuse and may be totally asymptomatic.

The cause of adenomyosis is unknown, although it may be related to pregnancy or childbirth because it is uncommon in nulliparous women. It is most common in multiparous women over 30 years of age, with the majority being in the fourth and fifth decades of life. There is no relationship between the incidence and the type of delivery, vaginal or cesarean, but it does tend to be higher in women reporting abortions, either spontaneous or induced.[8]

The most common complaints are reported as menorrhagia (40 to 50%), dysmenorrhea (15 to 30%), and dyspareunia or pelvic tenderness (7%).[7] In our center, 50% of women who presented with pelvic pain had sonographically visible adenomyosis as their cause of the pain and tenderness.

- Menorrhagia or heavy periods. These are often associated with clots and may even be reported as gushing of blood. Onset of these can usually be traced back to a time after childbirth.

- Dysmenorrhea or painful periods. These may vary in length from 1 or 2 days to lasting throughout the cycle. They may be cramping or continuous in nature.

- Pelvic tenderness or dyspareunia. Painful intercourse is often an indication of a tender uterus or adnexa. One should try to elicit tenderness during the endovaginal

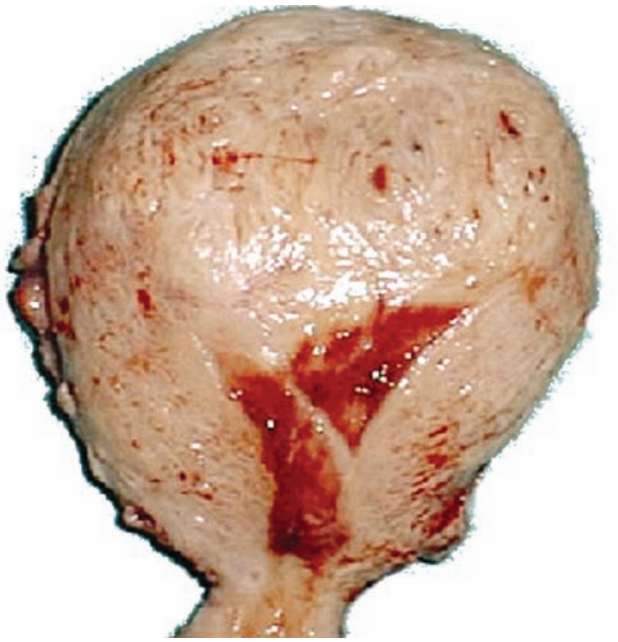

A

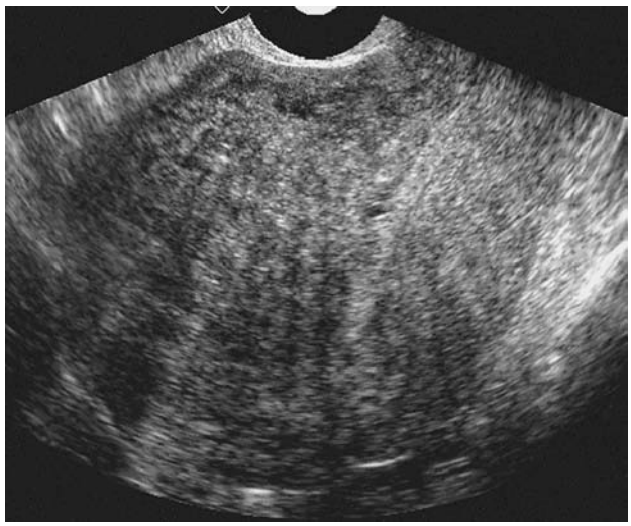

B

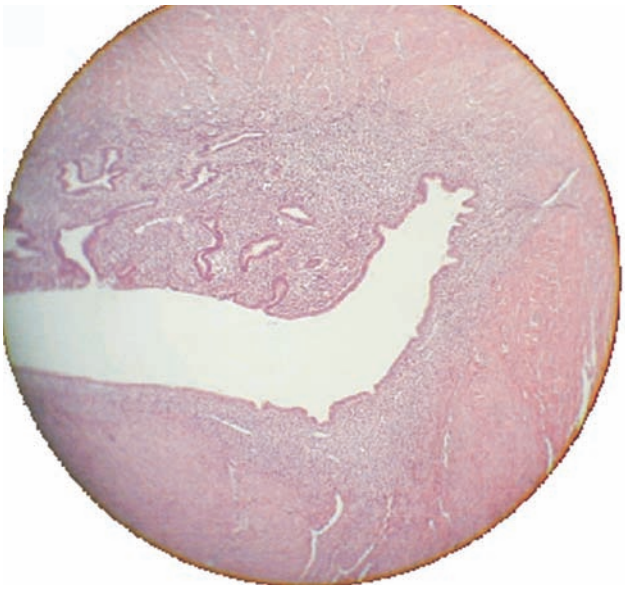

C

Figure 3–7 Adenomyosis involving the anterior myometrium and fundus. **(A)** A gross specimen showing the fundal myometrial thickening. Numerous vessels can be seen throughout the involved area. There is also a bulging of the myometrium, commonly seen in adenomyosis. This is an infiltrative process and is easily differentiated from fibroids. **(B)** A sagittal sonogram of the same uterus showing the thick inhomogeneous anterior myometrium, streaky shadowing, and small cysts. **(C)** A photomicrograph showing a dilated endometrial gland, seen as a cyst on a sonogram.

exam applying pressure to different parts of the uterus. Focal tenderness is very common in women who are not on any medication.

- Diagnosis may be difficult and it is important to take a good history at the time of scanning.
- MRI is a commonly used method for establishing the diagnosis and may show ill-defined areas of low signal intensity and/or focal or diffuse thickening of the junctional zone greater than 5 mm.
- Sonographically, the characteristic features are:
- Ill-defined areas of abnormally decreased or increased echogenicity. They vary in size from a few millimeters to a large mass of several centimeters. There can be numerous areas or a single mass, referred to as an adenomyoma. This is an infiltrative process as compared with a fibroid that is a well-defined mass (**Fig. 3–7**, **Fig. 3–8**).
- Asymmetrical myometrial thickening. This is commonly seen and may be quite pronounced. It has been reported that the posterior uterus is more often involved than the anterior portion.
- Myometrial cysts. They may be single or multiple, often in a subendometrial location and ranging in size from 0.2 to 1.5 cm (**Fig. 3–9**). Around menstruation, there may be echogenic blood filling the cyst, making

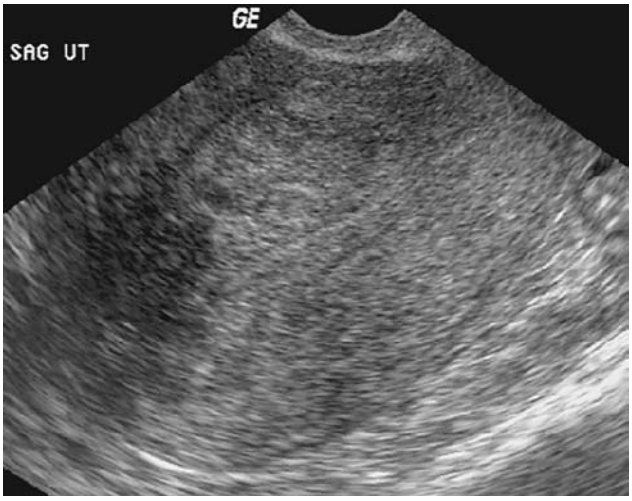

Figure 3–8 A midsagittal scan of the uterus with a more focal area of inhomogeneity just anterior to the endometrial canal. This was a focal area of adenomyosis at hysterectomy.

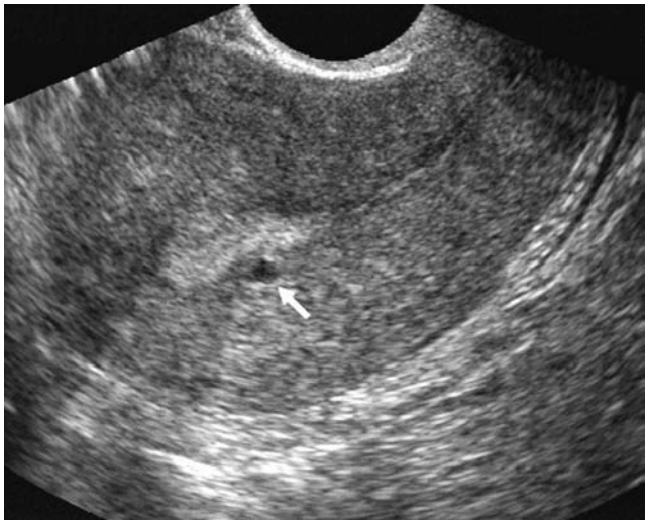

Figure 3–9 A sagittal scan of a uterus on day 19 of the menstrual cycle. The subendometrial cyst (arrow) is seen with an echogenic periphery.

it more difficult to visualize. The presence of myometrial cysts has been shown to be highly specific for adenomyosis. Reinhold et al[9] found cysts in 13 of 28 (46%) of patients with histologically proven adenomyosis. No cysts were found in the group without adenomyosis. Most important was that patients with cysts all had adenomyosis. The cysts were shown to be dilated endometrial glands, which would be most prominent in the secretory phase. We now try to examine patients with a suggestive history or myometrial inhomogeneity in the secretory phase around day 19.

- Central vascularity. The vessels are spread throughout the mass and are less well organized than those in normal myometrium. The cysts seen are *not* vessels (**Fig. 3–10**).
- Streaky shadowing. There is a streaky type of shadow with small bands of shadow interspersed between more normal areas. Some of this may be associated with cysts, but not all. Remember that in sagittal section at the lateral aspect of the uterus, one may normally get some irregular shadowing. This type of shadowing is different from the diffuse shadowing seen behind a fibroid.
- Tender on palpation. This is an important sign to elicit. During the endovaginal exam, push lightly on the uterus in various areas and ask the patient if it is tender. The patient may well feel the same discomfort she experiences during intercourse. Tenderness is focal and may be felt in some areas and not others. Often the areas with cysts or inhomogeneity are tender. After treatment or at different times during the normal cycle, the tenderness may subside.
- Don't calcify. I have never seen an area of adenomyosis with calcification, whereas fibroids, may calcify, especially after embolization therapy.

  Endometriosis is associated with adenomyosis in only ~15% of cases and may also be associated with fibroids.

The results of Reinhold et al[9] for the detection of adenomyosis are impressive (**Table 3–1**). They are based on histopathologic correlation with a 95% confidence interval. Their criteria are as follows:

Endovaginal ultrasound:

- A poorly defined area of abnormal echotexture (increased, decreased, mixed, and/ or myometrial cysts)
- Central vasculature, tender.

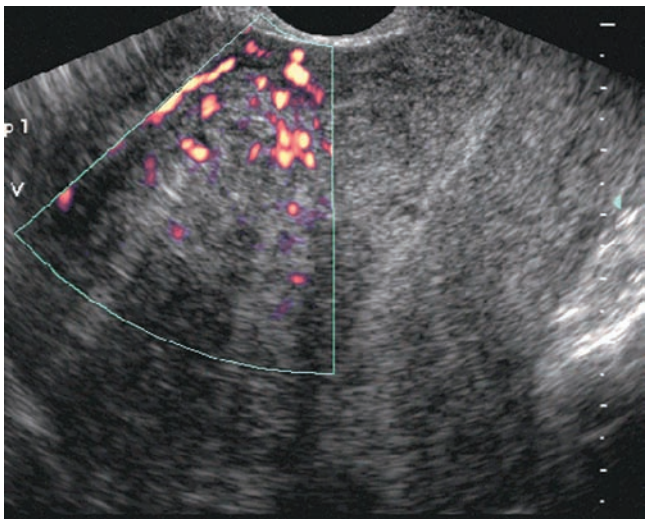

Figure 3–10 A midsagittal color Doppler scan of the uterus with diffuse adenomyosis as seen in **Fig. 3–7**, showing vascularity within the involved area.

Table 3–1 Sensitivity of Detection of Adenomyosis by Endovaginal Ultrasound and Magnetic Resonance Imaging

	Sensitivity	Specificity	PPV	NPV
Endovaginal ultrasound (%)	89	89	71	96
Magnetic resonance imaging (%)	86	86	65	95

Magnetic resonance imaging:

- A subjective opinion of localized or diffuse thickening of the uterine junctional zone or the presence of a low signal intensity myometrial mass with ill-defined borders.

In North America, the diagnosis of adenomyosis is still seldom made with ultrasound. The diagnosis is more reliably made when there are sonographic findings, physical findings, and an appropriate history. The history will include menorrhagia, often with clots, pelvic pain, and tenderness, often during intercourse. The sonographic findings include myometrial inhomogeneity, cysts, asymmetrical myometrial thickening, and streaky shadowing. The physical findings are of focal uterine tenderness determined by pressure using the endovaginal probe.

Sonologists should look for myometrial inhomogeneity and cysts, should ask the patient about menorrhagia and dysmenorrhea, and should be making the diagnosis. Adenomyosis is a common cause of vaginal bleeding and pelvic pain. If you are missing the diagnosis then a potentially treatable condition is being overlooked.

The sonographic differences between fibroids and adenomyosis are important to remember and are summarized in **Table 3–2**.

Treatment is ultimately by hysterectomy or menopause because it naturally regresses after menopause with the lack of estrogen. It may be reactivated with hormone replacement therapy and tamoxifen therapy for breast cancer. Antiinflammatory agents such as Naprosin have been found to be very useful in decreasing the pain and tenderness and even the menorrhagia. The use of GnRH agonists such as danazol and Lupron Depot (TAP Pharmaceutical Products Inc., Lake Forest, Illinois) are being used successfully with low doses relieving the symptoms. They are generally used only for 6 months at a time. The Mirena IUCD (Berlex, Wayne, New Jersey) has levo-norgesterol imbedded into the shaft of the device. This is released slowly over 3 months and acts locally. It has been reported that there is relief of symptoms due to atrophy of the ectopic endometrial glands and stroma. This may be the best therapeutic approach inasmuch as all of the medication is delivered locally, with little or no systemic effects.

Chemotherapy has generally not been successful and oral contraceptives tend to accentuate the pain or bleeding.

Table 3–2 Sonographic Characteristics of Uterine Fibroids and Adenomyosis

Fibroids	Adenomyosis
Often in nulliparous women	Usually multiparous
Discrete mass	Ill defined
Hypoechoic periphery	Asymmetric myometrial thickening
Hypo-, iso-, or hyperechoic	Mixed echogenicity
Cysts are uncommon	Small cysts are common
Vessels peripheral	Vessels usually central
Diffuse shadowing	Streaky shadowing
Nontender on palpation	Focal tenderness on palpation
Calcify late or after pregnancy	Don't calcify

Dysfunctional Uterine Bleeding

This is defined as the absence of an identifiable pathology and is a diagnosis of exclusion. The endometrium likely outgrows its blood supply and is sloughed in an irregular manner. It occurs more commonly in adolescents and perimenopausal women. A higher than normal dose of oral contraceptives is commonly used for three to six cycles.

Hypomenorrhea

Decreased volume or duration of menstrual flow may be normal in women on oral contraceptives. A mechanical obstruction such as an imperforate hymen or cervical stenosis may occur, although rarely in the premenopausal female.

Metrorrhagia

Intermenstrual bleeding occurs any time between normal menstrual periods. The most common cause is spotting associated with ovulation, which can be documented with a rise in basal body temperature. Endometrial polyps are the next most common cause, followed by carcinoma of the endometrium or cervix.

Endometrial Polyps

These are protruding stromal cores with mucosal surfaces projecting into the endometrial canal. Histologically they are of two types: (1) functional endometrium that mimics the adjacent endometrium in its cyclic changes and (2) hyperplastic endometrium, which is the most common. They respond to the growth effects of estrogen, but do not regress with progesterone. They may be sessile or polypoid on a stalk. These are common at all ages, but increase in frequency after 50 years of age. They may be single or multiple and generally measure 0.5 to 3.0 cm in diameter. Most arise in the fundus and project downward. Adenocarcinoma rarely develops in a polyp.

The endovaginal scan is the most effective noninvasive method of assessment, but must be performed only in the first half of the cycle (before day 7), when the endometrium is thin and hypoechoic. Scans done in the secretory phase or the second half of the cycle are seldom if ever diagnostic. The endometrium is normally thick and echogenic and often has polypoid changes, which will be sloughed during menstruation. The secretory endometrium is echogenic and often masks the presence of a true polyp. Some patients have continuous bleeding and may not have a well-defined menstrual flow. The best approach is for the gynecologist to induce a period medically with a course of progesterone, followed by sonographic assessment 5 to 7 days after the onset of bleeding.

Polyps within the endocervical canal can be confused with normal changes in the endocervix. Small polyps may be seen, whereas others are overlooked due to an inadequate assessment of the endocervical canal. If the endovaginal probe is too close to the cervix or is on the lower uterine segment, a large polyp may be overlooked, particularly if it is protruding through the cervical os, where it is obvious to the clinician during a speculum examination. The sonographer has to be aware that large polyps can be missed and that the endocervical canal must be examined in cases where no other cause for the vaginal bleeding has been demonstrated.

The diagnosis can be made sonographically. The transvesical examination is least sensitive. Endovaginal features include:

- An oblong echogenic mass occasionally with fluid around it. It is best visualized in the first half of the menstrual cycle, the secretory phase when the endometrium is less echogenic (**Fig. 3–11**, **Fig. 3–12**).
- Distention of the endometrial canal by the mass.
- Cyst or cysts in the endometrium. These are most often within a polyp.
- A prominent artery or feeding vessel on color Doppler. The vessel is less apparent and may be absent in postmenopausal women.
- An echogenic line seen on the anterior and posterior surfaces, representing the interface between the mass and the endometrial surface. The line will be seen only on one side if there is a broad-based polypoid mass.
- The moving mass. One can or should record a cine clip of the mass with the vaginal probe held steady in the sagittal plane of the uterus for 10 seconds. When the clip is played back at high speed, you can "see" the mass move within the endometrial canal in response to myometrial contractions.
- Nothing at all. Occasionally the mass may not be apparent on the sonogram.

Hysterosonography or fluid installation into the endometrial canal is helpful and usually diagnostic. This will detect even small polyps that are virtually invisible by other sonographic studies. The following is a saline hysterosonography technique that I use.

1. Informed consent is obtained prior to beginning the procedure.
2. I use a disposable plastic speculum with a light source incorporated into the handle.
3. The cervix is cleaned using a sterile forceps and 4 × 4 gauze pads soaked in an iodine-based solution such as Povidone. I then wipe the cervix with clean gauze to remove any excess iodine solution.

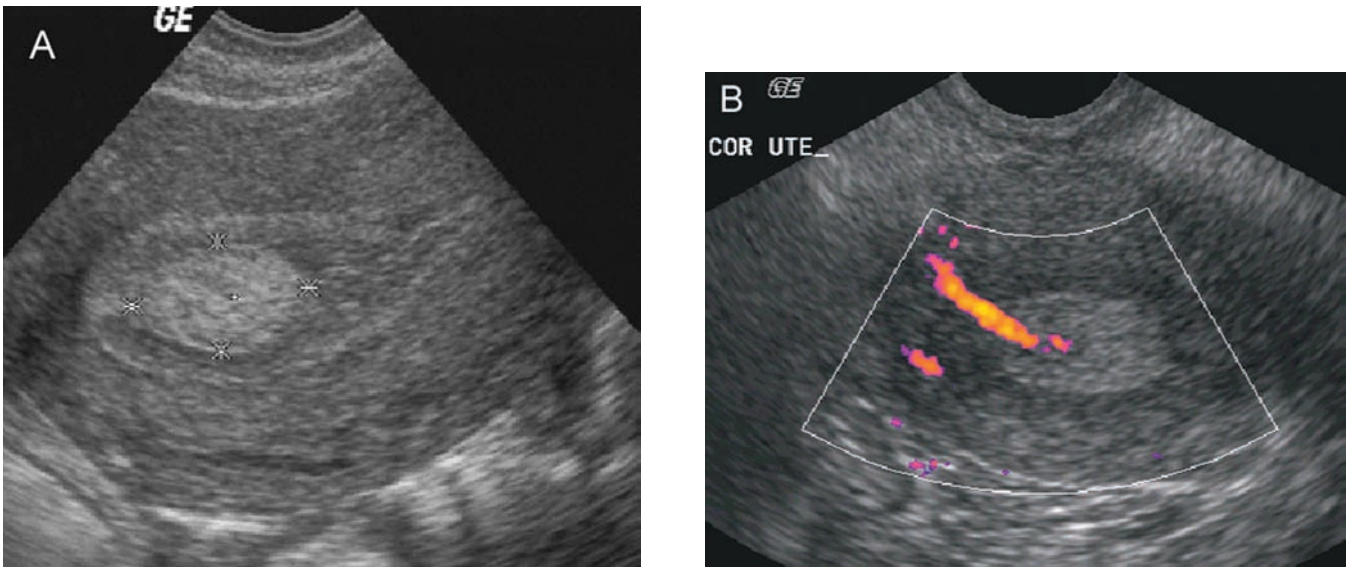

Figure 3–11 Endometrial polyp in a woman at midcycle presenting with spotting. **(A)** A sagittal scan showing an echogenic mass (calipers) in the endometrial canal. This patient is **(B)** A color Doppler scan showing the prominent feeding artery.

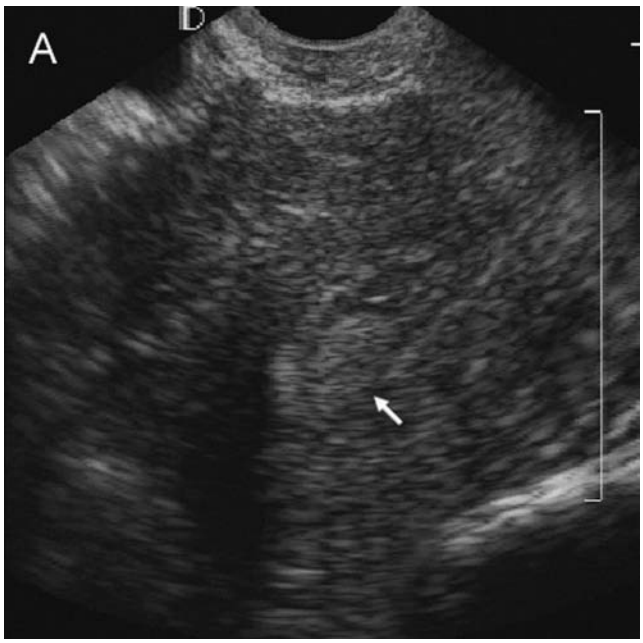

A

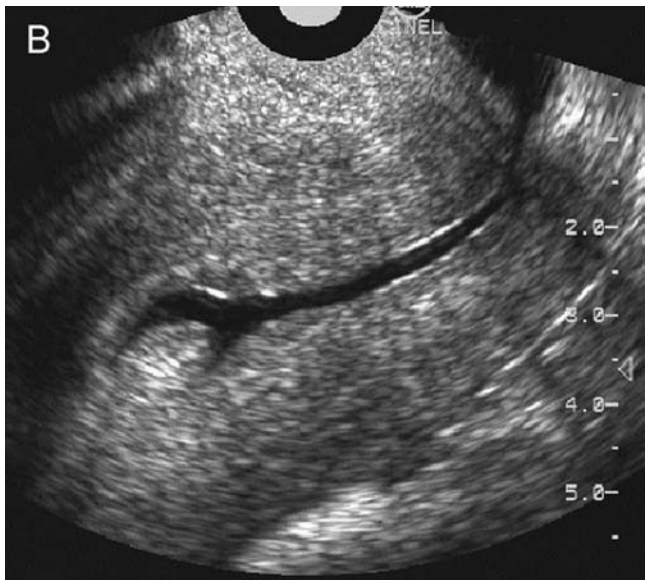

B

Figure 3–12 Endometrial polyp in a 48-year-old with heavy metrorrhagia. **(A)** The echogenic polyp (arrow) is visible in the endometrial canal but could not be appreciated 3 months earlier. **(B)** A hysterosonogram was done to outline the mass and shows it to be attached to the fundal portion of the cavity.

4. Under direct visualization, I use a second sterile long forceps to grasp a 5 French Ackrad catheter (Cooper-Surgical, Inc., Trumbull, Connecticut) ~2 cm from the tip. The catheter is introduced through the external cervical os and pushed up into the canal near the fundus. The balloon is then filled with ~2 mL of sterile saline once the catheter is clearly in the endometrial canal. Pull the catheter back to the lower segment. Some practitioners use a catheter without a balloon tip, which I personally have not found to be helpful in that there is often inadequate filling of the endometrial canal. The balloon-tipped catheters are more expensive than the others, which may be a consideration.
5. Sterile saline is instilled into the canal to provide some distension. One has to evaluate the amount of fluid to instill based on adequacy of visualizing the endometrial canal and the amount of discomfort that the patient is experiencing. Endometrial cavity distension is often better tolerated by multiparous than nulliparous women. Distension may be difficult in uteri with multiple fibroids or extensive adenomyosis, which makes the uterus semirigid.
6. Recording of the scan can be done in several ways. One may note the findings during the procedure and take only a few representative images. Recording cine sweeps in the sagittal and transverse planes is helpful for later review. We use a three-dimensional (3-D) scanner to acquire a volume dataset that can be reviewed later with possibly the best postprocedure visualization of the canal.
7. The polyp is measured in two planes and the location and size of the site of attachment are noted.
8. After assessing the fundal and body portions of the endometrial canal, I deflate the balloon, instill more fluid, and examine the endometrial canal in the lower segment and cervix.
9. The catheter is removed and discarded together with the plastic speculum and light holder.
10. The patient is observed in the waiting room for pain or vasovagal attacks. Some patients will require some medication for cramps, the best being an antiprostaglandins medication such as Advil (ibuprofen).

Hysteroscopy is also an excellent method of visualization and diagnosis. It is being used more frequently, particularly in the office and in place of radiographic hysterosalpingography.

Some polyps may be shed during the menstrual flow, especially if they are small within the endometrium. These may be seen as small, echogenic masses that spontaneously disappear at follow-up sonogram 1 month later.

Treatment may be by dilation and curettage (D&C), with a special Overstreet polyp forceps or, more commonly now, direct visualization and removal during hysteroscopy.

Polymenorrhea

This is bleeding that occurs too frequently and is usually associated with anovulation.

Menometrorrhagia

This is bleeding at irregular intervals in varying amounts. It may be due to various causes whose symptoms include

intermenstrual bleeding (e.g., polyps and carcinoma). The complications of pregnancy may also present this way.

Oligomenorrhea

Oligomenorrhea menses that occur more than 35 days apart are infrequent. The causes are generally systemic (like excessive weight loss) or endocrine (pregnancy, menopause, or estrogen-secreting tumors).

Contact Bleeding

Contact bleeding most commonly presents with a history of postcoital spotting. Although cervical cancer can be a cause, it is most commonly secondary to infection, vaginal or cervical.

Causes of Nonmenstrual Bleeding

Discussion of the specific disease entities that cause nonmenstrual bleeding occurs elsewhere in this chapter or in chapter 6 on postmenopausal bleeding. A list of possible causes based on the site of the bleeding follows.

- Vulva and vagina

  Atrophic vaginitis, vulvitis, trauma, infection (*Trichomonas, Chlamydia*), cancer (uncommon in this age group).
- Cervix

  Polyps, cancer, and pedunculated fibroids.
- Uterus

  Endometritis particularly after instrumentation (D&C), hyperplasia, cancer, polyps, adenomyosis, submucous fibroids, oral contraceptives, IUCDs.
- Fallopian tubes

  Salpingitis, tumors, ectopic pregnancy.
- Ovaries

  Estrogen-producing tumors, other cancers, functional ovarian cysts.
- Systemic, nongynecologic causes of bleeding

  Hypothyroidism; liver disease, which interferes with estrogen metabolism; blood dyscrasias or coagulopathies; administration of anticoagulants or steroids.

Bleeding in the Pregnant Patient

Many people recommend the routine use of ultrasound in early pregnancy. The differential diagnosis of bleeding in the first trimester includes:

- Intrauterine gestation (normal, normal with a subchorionic bleed, early failure)
- Extrauterine gestation (ectopic pregnancy)
- Heterotopic pregnancy

  To differentiate these, the ultrasound study, and in particular, an endovaginal exam, is almost 100% diagnostic. The recognition of an intrauterine sac alone or with a yolk sac confirms an intrauterine gestation. It does not guarantee the "viability" of the gestation (i.e., whether the pregnancy will go to term). It does, however, rule out an ectopic in all but one of 6000 cases of "heterotopic" gestation will occur. Heterotopic pregnancies regnancies are much more common in cases of assisted reproduction, especially in vitro fertilization and embryo transfer, where the incidence can be as high as 1%.[10] This information must be part of the history taking for the imaging specialist because the information may fail to be transmitted or appreciated if the patient presents to the emergency room.

The patient history is a vital part of the imaging exam, particularly an ultrasound exam, where the studies rely so heavily on the individual performing it. In fact, if the sonographer fails to document the key diagnostic images, then the interpreting physician may not be able to make the correct interpretation.

Intrauterine Gestation

Normal

First-trimester bleeding is one of the most common obstetrical complications, occurring in 15 to 25% of all pregnancies.[11] Even in a normal pregnancy, spotting can occur from bleeding at the implantation site 6 days after fertilization and last until 29 to 35 days after the last normal period.

Sonographically, a pregnancy presenting with bleeding can have an entirely normal-looking gestational sac, yolk sac, and embryo (**Fig. 3–13**).

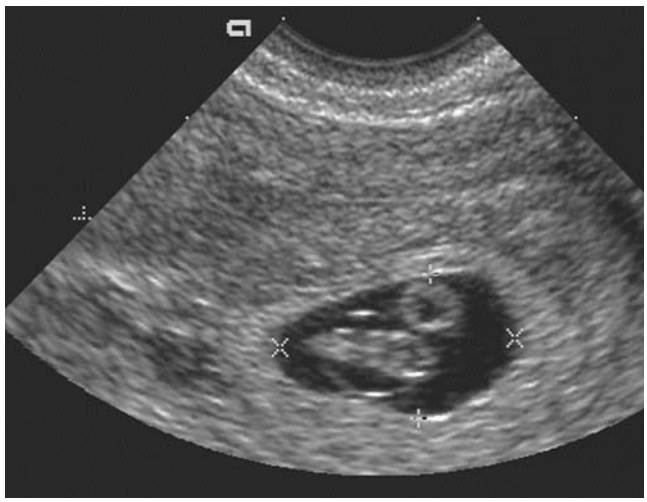

Figure 3–13 Normal intrauterine gestation 7 weeks menstrual age. The patient presented with spotting but went on to a full-term delivery. The fetus can be seen with the amniotic membrane surrounding it and the yolk sac anterior to it.

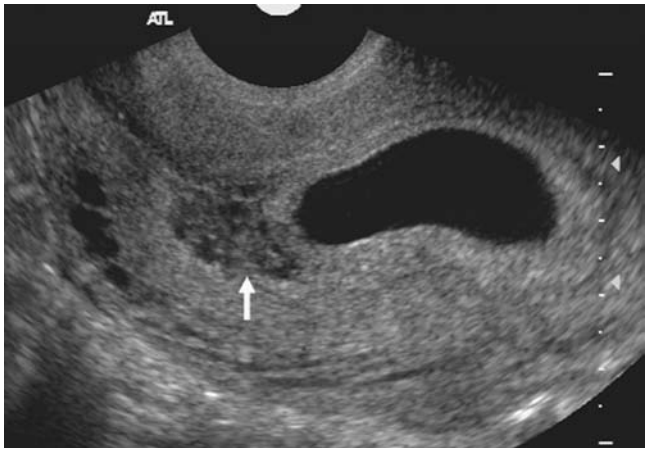

Figure 3–14 Normal intrauterine gestation 7 weeks menstrual age, with a small echogenic subchorionic hemorrhage (arrow). The pregnancy carried on to term.

Normal with a Subchorionic Hemorrhage

Subchorionic hemorrhage can be seen in a pregnancy that continues to term, but there is an increased risk of pregnancy failure depending on the size of the bleed (**Fig. 3–14**). Not all patients with a subchorionic hemorrhage will present with bleeding. If near the internal os, the subchorionic hemorrhage is more likely to be associated with vaginal bleeding than if it is near the fundus and remains concealed.

Sonographically, there may be a small fluid collection beneath the membranes that is the cause of the vaginal bleeding. The collection of blood can look echogenic initially, become echo-free, and may then disappear as the blood is reabsorbed (**Fig. 3–15**).

This is also discussed later in relation to early pregnancy failure.

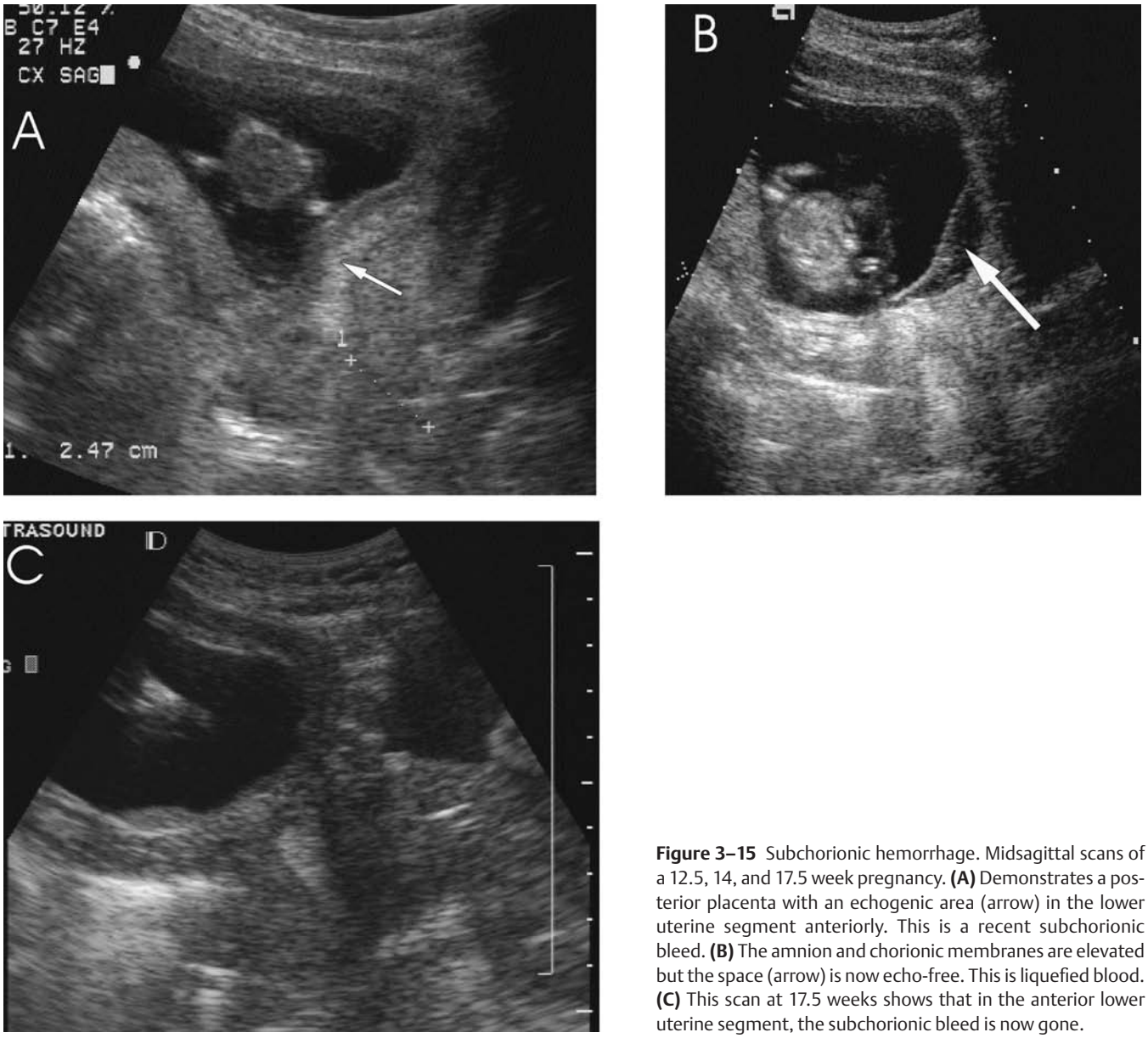

Figure 3–15 Subchorionic hemorrhage. Midsagittal scans of a 12.5, 14, and 17.5 week pregnancy. **(A)** Demonstrates a posterior placenta with an echogenic area (arrow) in the lower uterine segment anteriorly. This is a recent subchorionic bleed. **(B)** The amnion and chorionic membranes are elevated but the space (arrow) is now echo-free. This is liquefied blood. **(C)** This scan at 17.5 weeks shows that in the anterior lower uterine segment, the subchorionic bleed is now gone.

Early Failure

Bleeding is also the hallmark of the abnormal pregnancy, occurring in most cases of early pregnancy failure. Approximately half of the women who bleed in early pregnancy will ultimately abort. In almost 40% of patients, a failed early pregnancy will be diagnosed by the initial ultrasound examination.[12]

Bleeding alone has a better prognosis than bleeding with pain and cramps. The pain of abortion may simulate that of labor, being anterior and rhythmic. It may, however, be only an ache or simulate low back pain.

The treatment of non-life threatening bleeding in early pregnancy is mostly expectant. The physical exam will rule out local, more superficial causes. An ultrasound examination will identify the site and size of the gestation and may indicate the likelihood for a successful outcome. In the otherwise uncomplicated gestation with bleeding, bed rest and occasionally intramuscular injections of progesterone are used. The scientific efficacy for the use of synthetic progestational agents is not strong.

The etiology of first-trimester pregnancy loss is still not fully understood. There is a multitude of known and suspected causes. The spontaneous failure rate is ~75% of all pregnancies. About 15% of fertilized ova fail to divide, 15% are lost prior to implantation, 30% during implantation, 13 to 16% after implantation and before the first missed period,[13] and 9 to 10% following the first missed period. Multiple authors have found a postimplantation failure rate of 18 to 31%. The higher numbers may reflect the use of a more sensitive pregnancy test to detect a greater number of preclinical losses, which otherwise had a following implantation and spontaneous abortion.

Causes of First-Trimester Pregnancy Loss

Fetal (70%)

- Nonrecurring chromosomal abnormalities are the most common cause. X monosomy or trisomy may be seen due to errors at the time of gonadogenesis during meiosis. Triploidy may occur during fertilization, with two sperm entering the egg. Tetraploidy or mosaics will occur during the first division of the zygote.
- Abnormal placental formation.

Maternal (30%)

- Maternal age over 35 years.[14]
- Paternal age over 35 years.
- Systemic influences—insulin-dependent diabetes, smoking, alcohol consumption.
- Luteal phase defect or corpus luteum failure.[15]

Immunologic Disorders—Antisperm or Anticonception antibodies

- Antiphospholipid antibodies (APAs)
- Anticardiolipin antibodies
  The role of APAs and anticardiolipin antibodies is a matter of some debate. In 238 women, Simpson et al[16] found that, these antibodies were present before and at 21 days of gestation, the time of implantation. They found no increase in the levels when comparing women who delivered normally with those who had single or recurrent abortions.
- Lupus anticoagulant
- Thyroid-thyroglobulin and microsomal antibodies (TGT)
- Embryotoxic factor (ETA)
- Natural killer cells-systemic CD56 and CD16 cell
- Deficiency in transforming growth factor β-2 producing suppressor cells in uterine tissue near the placental attachment site
- Uterine defects that affect implantation—scarring, myomata,[17] congenitally small or distorted cavity caused by a uterine septum[18]
- Unknown

First-Trimester Pregnancy Loss Without Bleeding

Goldstein[19] studied 232 first-trimester private practice patients with an endovaginal scan at the first visit to determine the incidence of pregnancy loss. All patients had a positive urinary pregnancy test and no history of vaginal bleeding. All patients were followed to delivery or spontaneous abortion. In the embryonic period (i.e., 70 days from last menstrual period), 27 (11.5%) losses occurred and 4 (1.7%) losses in the fetal period. Specifically, the losses during the first 10 weeks can be further broken down based on what was visible sonographically by endovaginal scanning (**Table 3–3**). With each landmark, there was a reduction in

Table 3–3 First-Trimester Pregnancy Loss in Private Patients without Bleeding[19]

Sonographically Visible	Loss Rate (%)
Gestational sac	11.5
Yolk sac	8.5
Embryo < 5 mm CRL	7.2
Embryo 6–10 mm CRL	3.3
Embryo > 10 mm CRL	0.5
From 8.5 to 14 weeks	0
Fetal period 14 to 20 weeks	2.0

Abbreviations: CRL, Crown rump length.

the loss rate. Once an embryo had achieved a crown-rump length (CRL) of greater than 6 mm or 7 weeks menstrual age (MA), the loss rate until term was between 0 and 3%.

First-Trimester Pregnancy Loss with Bleeding

In the world of the primary care physician, bleeding in early pregnancy is still defined in terms of the amount of bleeding, passage of tissue, size of the uterus, and whether the external cervical os is open. Nonetheless, it is important for the sonologist to understand the traditional definitions and classification. Remember that these designations are used only prior to the sonographic evaluation.

Clinical Classification of First-Trimester Bleeding and Potential Pregnancy Loss[20]

Spontaneous abortion—Termination of a pregnancy prior to the 20th week gestation or 139 days. Spontaneous abortion implies the expulsion of any or all of the products of conception.

Complete abortion—Expulsion of all of the products of conception before the 20th week of gestation.

Incomplete abortion—The expulsion of only some of the products of conception up to the 20th week.

Threatened abortion—Uterine bleeding before the 20th week, with or without uterine contractions, or expulsion of products of conception and without dilatation of the cervix.

Inevitable abortion—Uterine bleeding before the 20th week of gestation with continuous and progressive cervical dilatation and without expulsion of products of conception.

Missed abortion—The embryo or fetus dies in utero before the 20th week and is retained for 8 weeks or more.

Subclinical spontaneous abortion—The pregnancy is aborted or resorbed before it has been recognized. The incidence is ~16% in the normal fertile population.

Infected abortion—Abortion associated with infection of the genital organs.

Septic abortion—An infected abortion with generalized spread through the maternal circulation.

Studies of Pregnancy Loss with Bleeding

In 1987, Stabile et al[12] reported on 624 women referred to an emergency gynecological clinic with a provisional diagnosis of threatened abortion. They all had a history of amenorrhea and vaginal bleeding, with or without pain. No pregnancy was present in 25% (158/624), with the most common causes of bleeding being follicular/luteal cyst (32) and pelvic inflammatory disease (26). Ectopic pregnancy was diagnosed in 9.6% (60/624). The remaining 406 patients were pregnant and of these, 61.5% (250/406) presented between 7 and 10 weeks. All women underwent a transabdominal ultrasound study through a full urinary bladder with a 3.5 MHz transducer. The clinical outcome resulted in 55.9% live births and 44.1% failed pregnancies, a significantly higher proportion than the 11.5% abortion rate of nonbleeding patients in the Goldstein[19] study (**Table 3–4**).

Table 3–4 Clinical Outcome of 406 Pregnant Patients with Bleeding[12]

Results	Number	Percent	Ultrasound
Normal pregnancy	227	55.9	Live fetus
Anembryonic pregnancy	67	16.5	
Incomplete abortion	41	10.1	
Missed abortion	34	8.4	
Therapeutic abortion	26	6.4	Live fetus
Spontaneous abortion	6	1.5	Live fetus
Complete abortion	4	1.0	
Molar pregnancy	1	0.2	

If one discounts the patients who had a subsequent abortion (therapeutic or spontaneous), then 36% (146/406) of patients with a threatened miscarriage had a nonviable pregnancy (i.e., no live fetus) diagnosed at first presentation by transabdominal ultrasound. This study since its publication is 13 years old and does not include studies investigated with the more sensitive endovaginal technique.

Falco et al[21] prospectively studied a group of 270 patients with transvaginal ultrasound between 5 and 12 weeks gestation with first-trimester bleeding. Forty-five percent were excluded, revealing a nonviable pregnancy, a sac without an embryo, or multiple gestation. The exact numbers of each were not recorded. Of the 149 remaining patients with demonstrable fetal cardiac activity, 15% (23/149) patients aborted. They predicted the probability of abortion based on the following abnormal sonographic findings:

- Slow embryonic heart rate (less than −1.2 SD from the mean).
- This varied with CRL from 90 bpm at 10 mm to 120 bpm at 30 mm and was the best criterion. This sign was not very sensitive (0.30), but when present was highly specific (0.93).
- Mean gestational sac diameter minus crown rump length less than −0.5 SD of the mean.
- Small sac size was the next most important finding, although it was seldom present (sensitivity of 0.39 and specificity of 0.88). A difference of less than 5 mm was associated with pregnancy failure in 80 to 90% of cases.[22] A discrepancy of 5 to 8 mm also had an increased risk.
- Discrepancy between menstrual and sonographic age of $>$ 1 week due to slow embryonic growth.
- Subchorionic hematoma was seen in 17% of cases, equally common in continuing and aborted pregnancies, but of no value in predicting outcome.

Table 3–5 Summary of the Rates of Spontaneous Abortion in Women with and without Bleeding

Author	Gestational Age (Weeks)	Number	Indication	Abortion Rate (%)
Goldstein (1994)[19]	5–10	232	Routine	11.5
Pandya et al (1996)[24]	10–13	17,870	Routine	2.8
Stabile et al (1987)[12]	5–16	624	Bleeding	45.0
Falco et al (1996)[21]	5–12	270	Bleeding	51.5
Falco et al (1996)[21]	5–12	149	Bleeding + live fetus	15.0
Pandya et al (1996)[24]	10–13	17,870	Bleeding	15.6
Johns, Jauniaux (2006)[26]	7–13	214	Bleeding	9.3

Bennett et al[23] found that the presence of a subchorionic bleed was associated with a higher incidence of pregnancy failure. In a retrospective study of 516 first-trimester patients with bleeding, a live fetus, and a subchorionic hematoma, they found a loss rate of 18.8% for a large hematoma involving two thirds of the chorionic sac. This was double their overall loss rate of 9.3%. Pandya et al[24] supported this association in a screening study, finding a pregnancy failure rate with bleeding of 5.1% with spotting, and 10.5% with heavy bleeding. The risk of spontaneous abortion was increased by 2.3 times when spotting occured, and 4.7 times when there was heavy bleeding.

In a screening study of 17,870 women between 10 and 13 weeks gestation, Pandya et al[24] found the early pregnancy failure rate in London, England, to be 2.8%. Of the 501 cases, 313 (62.5%) were missed abortions with a dead embryo visible and 188 (37.5%) were anembryonic with an empty sac. These were patients invited to participate in a study of fetal nuchal fold thickness and included patients with and without bleeding. A transabdominal study was routinely done and if no fetal heart was detected then a transvaginal exam was performed. The risk of spontaneous abortion, compared with the normal group, was increased with vaginal bleeding and maternal age over 40 years (2.48 times). The risk was not significantly affected by previous pregnancy loss or smoking, and decreased with increasing gestational age. The latter association (i.e., gestational age) is understandable if one remembers that there is a high reported incidence (45 to 70%) of chromosomal abnormalities, most commonly autosomal trisomies in miscarriages. The lethal forms will abort early in pregnancy, giving a decreased rate of failure later in the first trimester.

Ball et al[25] found an increased risk of miscarriage (odds ratio 2.8, 95% confidence interval 1.7 to 7.4), stillbirth (4.5, 1.5 to 13.2), abruptio placentae (11.2, 2.7 to 46.4), and preterm labor (2.6, 1.5 to 4.6), when cases were compared with controls without subchorionic hemorrhage or bleeding. It is important to remember that bleeding alone in early pregnancy increases the risk of miscarriage.

In a prospective, cohort-controlled study of 214 women presenting with first-trimester bleeding, Johns and Jauniaux[26] found a first-trimester miscarriage rate of 9.3%, an increased risk of preterm delivery between 34 and 37 weeks (5.6 vs. 11.9%), and increased prelabor rupture of membranes (1.9 vs. 7%).

The rate of spontaneous abortion in the studies of women with and without bleeding is summarized in **Table 3–5**.

Sonographic Findings of Early Pregnancy Failure

1. Small gestational sac size before 9 weeks; associated with triploidy and trisomy 16.[27]
2. 3-D sac volume that is smaller than expected.[28]
3. No embryonic cardiac activity, with a CRL > 5 mm.[29]
4. Embryonic bradycardia relative to CRL.[30]
   There is a 100% loss rate if: (a) the CRL is < 5 mm and the rate is < 80 bpm, (b) the CRL is 5 to 9 mm and the rate is < 100 bpm, or (c) the CRL is 10 to 15 mm and the rate is < 110 bpm.
5. Gestational sac larger than 8 mm without a yolk sac.
6. Gestational sac larger than 16 mm without an embryo.
7. Mean sac diameter minus CRL is less than 5 mm (**Fig. 3–16**).
8. CRL that is smaller than expected.[31]
9. Poor sac growth.
   The sac grows normally at a rate of 1 mm mean sac diameter per day. If the patient is followed for 4 to 7 days and the sac fails to grow appropriately, a failed pregnancy will most likely result.
10. Large yolk sac (> 5.6 mm prior to 10 weeks).
11. Abnormally large or floppy amniotic sac.[32]

The description of a failed pregnancy based on the ultrasound examination should be more descriptive than has been customary in the past. I favor the term *early pregnancy failure* to describe when there is an intrauterine gestational sac but no clearly visible embryo, although there may be a yolk sac and even an amniotic sac present. This term is much more appropriate than the conventional terms of *blighted ovum* or *missed abortion*.

If an embryo is present having a CRL > 5 mm, but with no demonstrable cardiac activity, then I refer to it as an *early embryonic demise*. In the second trimester, this would, by definition, be called a *fetal demise*.

The routine use of ultrasound in early pregnancy has helped clinicians manage cases of bleeding in early

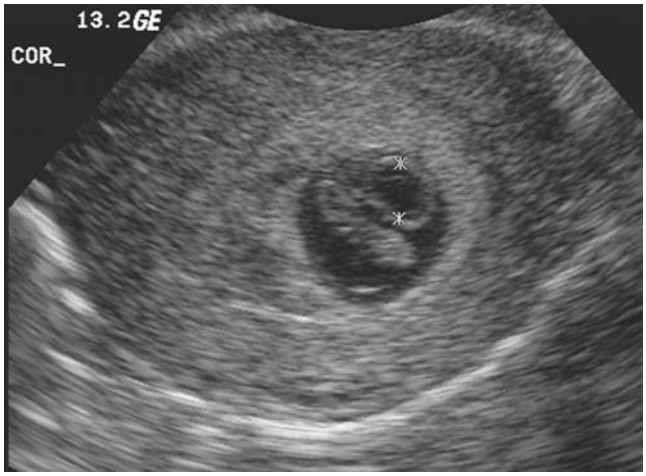

Figure 3–16 Scan of a 7-week gestation with a normal-sized embryo, but a small mean gestational sac diameter. The yolk sac is also larger than normal. There was cardiac activity that ceased 1 week later.

pregnancy, but the pregnancy outcome is difficult to predict accurately and requires careful counseling and timely followup.[33] Most women will opt for conservative management of an early pregnancy failure.

Extrauterine Gestation (Ectopic Pregnancy)

Abnormal uterine bleeding occurs in 75% of ectopics and is due to involution of the endometrium and sloughing of the decidua. It may be associated with pain and the presence of an adnexal mass. The pregnancy test is not always available to the sonologist at the time of the study and, when available, is not always helpful or positive.

The sonographic signs of an ectopic pregnancy are:

1. An empty, nongravid uterus
2. A live embryo in the adnexa
3. An adnexal mass with a tubal ring (gestational sac) ± yolk sac
4. An adnexal mass with no definite tubal ring
5. Echogenic free fluid
6. Decidual cyst (Ackerman et al[34])

The utility of the various signs is listed in **Table 3–6**, which shows the sensitivity, specificity, negative predictive value (NPV), and positive predictive value (PPV) of each. The data have been derived principally from two authors.[34]

Heterotopic Pregnancy

The heterotopic gestation with an intrauterine and extrauterine pregnancy is uncommon, with a rate of one per 6000 pregnancies. In our laboratory, we can expect to see one case a year. The incidence increases to 1% in cases of in vitro fertilization and embryo transfer.

A heterotopic gestation is difficult to recognize because one seldom has an increased level of suspicion. An ectopic, on the other hand, presents with a positive pregnancy test and an empty uterus, so there must be a pregnancy somewhere. The ectopic sac may be difficult to visualize if it is very early and small, or if it is within a hemorrhagic mass. In a Danish survey of 13 cases, five were diagnosed by ultrasound at 6- to 9-weeks gestation and eight were diagnosed at surgery for acute abdominal pain. Of all of the cases, four (30%) presented with vaginal bleeding. Ten (77%) of these cases ended satisfactorily in a term pregnancy.

The overall incidence of bleeding is hard to determine because the literature contains mostly case reports.

Summary

Bleeding during the reproductive years can pose a dilemma for the imaging specialist. Most often the patient has already been assigned to a pregnant or nonpregnant category. It is then up to the imaging team to detect the exact cause of the bleeding using ultrasound as the primary diagnostic modality because it is still the least invasive and most informative in this situation.

Table 3–6 Sensitivity and Specificity of Sonographic Criteria for Ectopic Pregnancy

Sonographic Criterion for Ectopic Pregnancy[35]	Sensitivity	Specificity	PPV	NPV
Adnexal embryo with heartbeat	20.1	100	100	78.5
Adnexal mass with yolk sac or embryo	36.1	100	100	82.2
Adnexal mass with tubal ring	64.6	99.5	97.8	89.1
Any adnexal mass, not a simple cyst	84.4	98.9	96.3	94.8
Decidual cyst (from Ackerman et al[34])	21	92	80	42

Abbreviations: PPV, positive predictive valve; NPV, negative predictive valve.

References

1. Gerbie MV. Complications of menstruation: abnormal uterine bleeding. In: DeCherney AH, Pernoll ML, eds. Current Obstetric and Gynecologic Diagnosis and Treatment. 8th ed. Norwalk, CT: Appleton & Lange; 1994:662–669
2. Marshall LM, Spiegelman D, Barbieri RL, et al. Variation in the incidence of uterine leiomyoma among premenopausal women by age and race. Obstet Gynecol 1997;90:967–973
3. Vikhlyaeva EM, Khodzhaeva ZS, Fantschenko ND. Familial predisposition to uterine leiomyomas. Int J Gynaecol Obstet 1995;51: 127–131
4. Tsuda H, Kawabata M, Nakamoto O, Yamamoto K. Clinical predictors in the natural history of uterine leiomyoma: preliminary study. J Ultrasound Med 1998;17:17–20
5. Goodwin et al—reported at the Society of Cardiovascular and Interventional Radiology 1998
6. Hindley J, Gedroyc WM, Regan L, et al. MRI guidance of focused ultrasound therapy of uterine fibroids: early results. AJR Am J Roentgenol 2004;183:1713–1719
7. Azziz R. Adenomyosis: current perspectives. Obstet Gynecol Clin North Am 1989;16:221–232
8. Vercellini P, Parazzini F, Oldani S, Panazza S, Bramante T, Crisinami PG. Adenomyosis at hysterectomy: a study on frequency distribution and patient characteristics. Hum Reprod 1995;10: 1160–1162
9. Reinhold C, McCarthy S, Bret P, et al. Diffuse adenomyosis: comparison of endovaginal US and MR imaging with histopathologic correlation. Radiology 1996;199:151–158
10. Svare J, Norup P, Grove Thomsen S, et al. Heterotopic pregnancies after in-vitro fertilization and embryo transfer: a Danish survey. Hum Reprod 1993;8:116–118
11. Vaginal bleeding in early pregnancy [editorial]. BMJ 1980;280:470
12. Stabile I, Campbell S, Grudzinskas JG. Ultrasonic assessment of complication during first trimester of pregnancy. Lancet 1987;2: 1237–1240
13. Bateman BG, Felder R, Kolp LA, Burkett B, Nunley WC Jr. Subclinical pregnancy loss in clomiphene citrate treated women. Fertil Steril 1992;57:25–27
14. Sterzik K, Dallenbach C, Schneider V, Sasse V, Dallenbach-Hellweg G. In vitro fertilisation: the degree of endometrial insufficiency varies with the type of ovarian stimulation. Fertil Steril 1988;50: 457–462
15. Blumenfeld Z, Ruach M. Early pregnancy wastage: the role of repetitive human chorionic gonadotrophin supplementation during the first 8 weeks of gestation. Fertil Steril 1992;58:19–23
16. Simpson JL, Carson SA, Chesney C, et al. Lack of association between antiphospholipid antibodies and first trimester spontaneous abortion: prospective study of pregnancies detected within 21 days of conception. Fertil Steril 1998;69:814–820
17. Benson CB, Doubilet PM, Cooney MJ, Frates MC, David V, Hornstein MD. Early singleton pregnancy outcome: effects of maternal age and mode of conception. Radiology 1997;203:399–403
18. Kupesic S, Kurjak A, Skenderovic S, Bjelos D. Screening for uterine abnormalities by 3D ultrasound improves perinatal outcome. J Perinat Med 2002;30:9–17
19. Goldstein SR. Embryonic death in early pregnancy: a new look at the first trimester. Obstet Gynecol 1994;84:294–297
20. Pernoll ML, Garmel SH. Early pregnancy risks. In: DeCherney AH, Pernoll ML, eds. Current Obstetric and Gynecologic Diagnosis and Treatment. Norwalk, CT: Appleton & Lange; 1994:306–330
21. Falco P, Milano V, Pilu G, et al. Sonography of pregnancies with first trimester bleeding and a viable embryo: a study of prognostic indicators by logistic regression analysis. Ultrasound Obstet Gynecol 1996;7:165–169
22. Bromley B, Harlow BL, Laboda LA, Benacerraf BR. Small sac size in the first trimester: a predictor of poor fetal outcome. Radiology 1991;178:375–377
23. Bennett GL, Bromley B, Lieberman E, Benacerraf BR. Subchorionic hemorrhage in first-trimester pregnancies: prediction of pregnancy outcome with sonography. Radiology 1996;200:803–806
24. Pandya PP, Snijders RJM, Psara N, Hilbert L, Nicolaides KH. The prevalence of non-viable pregnancy at 10-13 weeks of gestation. Ultrasound Obstet Gynecol 1996;7:170–173
25. Ball RH, Ade CM, Schoenborn JA, Crane JP. The clinical significance of ultrasonographically detected subchorionic hemorrhages. Am J Obstet Gynecol 1996;174:996–1002
26. Johns J, Jauniaux E. Threatened miscarriage as a predictor of obstetric outcome. Obstet Gynecol 2006;107:845–850
27. Dickey RP, Gasser R, Olar TT, et al. Relationship of initial chorionic sac diameter and abortion and abortus karyotype based on new growth curves for the 16th to 49th post-ovulation day. Hum Reprod 1994;9:559–565
28. Babinszki A, Nyari T, Jordan S, Nasseri A, Mukherjee T, Copperman AB. Three-dimensional measurement of gestational and yolk sac volumes as predictors of pregnancy outcome in the first trimester. Am J Perinatol 2001;18:203–212
29. Levi CS, Lyons EA, Zheng XH, et al. Endovaginal ultrasound: demonstration of cardiac activity in embryos of less than 5.0 mm in crown-rump length. Radiology 1990;176:71–74
30. Doubilet PM, Benson CB. Embryonic heart rate in the early first trimester: what rate is normal? J Ultrasound Med 1995;14:431–434
31. Reljic M. The significance of crown-rump length measurement for predicting adverse pregnancy outcome of threatened abortion. Ultrasound Obstet Gynecol 2004;17:510–512
32. Horrow MM. Enlarged amniotic cavity: a new sonographic sign of early embryonic death. AJR Am J Roentgenol 1992;158:359–362
33. Jauniaux E, Johns J, Burton GJ. The role of ultrasound imaging in diagnosing and investigating early pregnancy failure. Ultrasound Obstet Gynecol 2005;25:613–624
34. Ackerman TE, Levi CS, Lyons EA, et al. Decidual cyst: endovaginal sign of ectopic pregnancy. Radiology 1993;189:727–731
35. Brown DL, Doubilet PM. Transvaginal sonography for diagnosing ectopic pregnancy: positivity criteria and performance characteristics. J Ultrasound Med 1994;13:259–266

4 Infertility

Mary C. Frates

Infertility is defined as the absence of one term birth after 1 year of unprotected intercourse. It affects ~20% of women up to the age of 44 years. Age is an extremely important variable because maximum fertility occurs early and declines steadily.[1] The diagnosis and management of the infertile couple has become increasingly important, as reproductive endocrinologists all over the world assist patients who are attempting to conceive. Transvaginal sonography (TVS) is a cornerstone in diagnosis and treatment because it provides very detailed and reproducible imaging of the female pelvis. The use of ultrasound in the management of infertility can be divided into three main categories: (1) diagnosis, (2) monitoring of treatment, and (3) evaluation of early pregnancy.

Diagnosis

Sonography is an important component of the initial evaluation of women with impaired fertility. Initial evaluation of each patient should begin with a brief transabdominal image of the pelvis to evaluate for an enlarged uterus or large masses that may extend beyond the reach (penetration) of the high-frequency transvaginal probe. The presence of two normal-appearing kidneys should be confirmed in all patients. The pelvic examination then continues via the transvaginal approach. The uterus, ovaries, and fallopian tubes are evaluated carefully with transvaginal sonography for congenital anomalies and pathological entities. The presence of free intraperitoneal fluid can be noted. Because standard transvaginal probe covers and sonographic gel have both been shown to be embryotoxic,[2] nonsterile clear plastic bags should be used to cover the transvaginal transducer, and water should be used as a lubricant in this patient population.

Evaluation of the Uterus

The uterus is imaged in longitudinal and coronal planes. Particular care should be taken to include the entire fundus and full length of the cervix. The normal uterine shape is somewhat oval, with a rounded fundus. Often the initial workup of the infertility patient begins with hysterosalpingography for tubal patency evaluation, and uterine anomalies are identified at that time. In other patients, ultrasound is the initial imaging choice, and it has been shown to be highly accurate in the evaluation of infertility.[3,4] Congenital uterine malformations (lateral fusion defects) such as a didelphys or a bicornuate or septate uterus can be identified at transvaginal sonography[5] (**Fig. 4–1A**). In the coronal plane, the endometrial stripe is followed from the

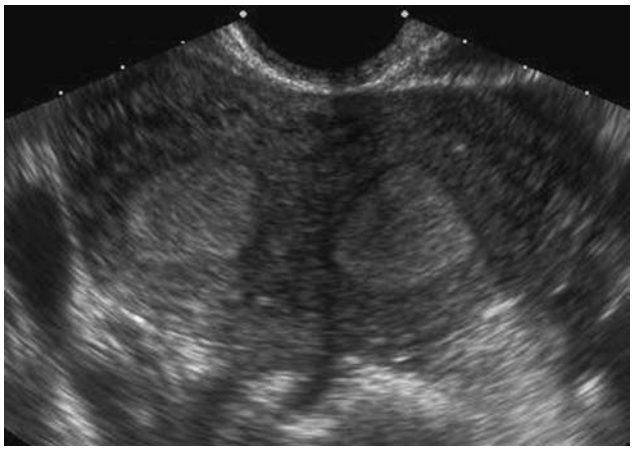

A

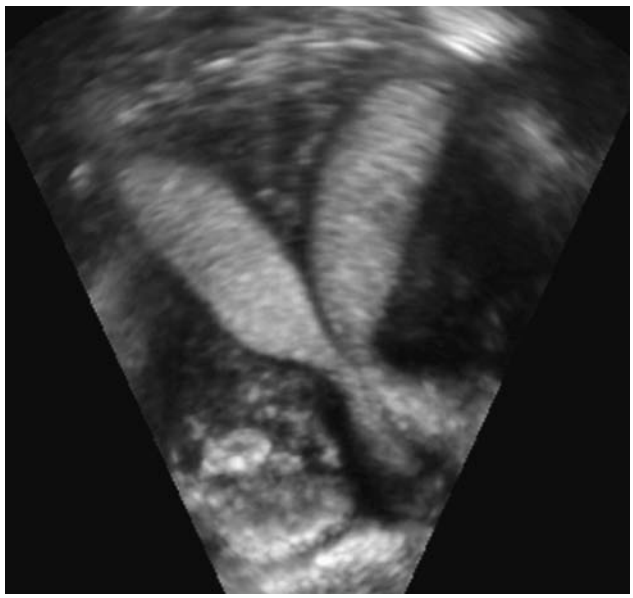

B

Figure 4–1 Uterine anomaly. **(A)** Transvaginal coronal image of a complete septate uterus. Two separate echogenic endometrial cavities are seen, separated by hypoechoic myometrium. **(B)** Transvaginal three-dimensional coronal reconstructed image of a complete septate uterus [same patient as **(A)**]. The echogenic endometrial canal is divided into two components. The hypoechoic septum is seen to extend through the cervical canal.

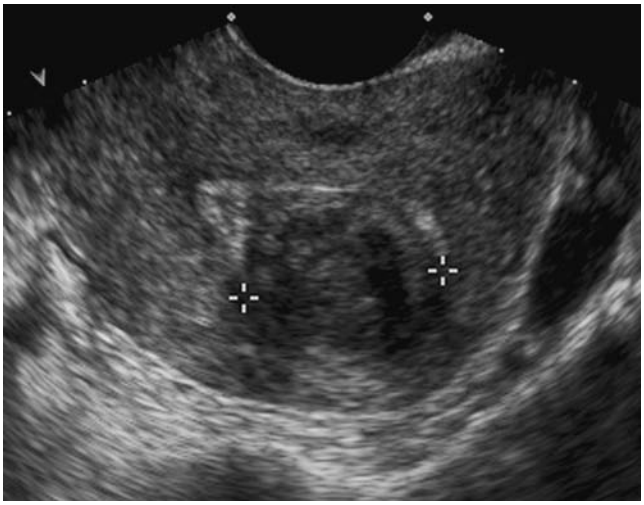

Figure 4–2 Transvaginal coronal image of a fibroid (calipers) shows a typical circumferential swirling pattern with well-defined borders. This fibroid is submucosal in location.

cervix to the fundus, and if the stripe bifurcates into separate left- and right-sided structures, an anomaly may be suspected. This can range from the normal variant arcuate uterus to the extreme of complete uterus didelphys. The thickness of the fundus and overall uterine shape can help the imager determine which anomaly may be present. In addition, three-dimensional (3-D) sonography can be used to particular advantage in the evaluation of uterine anomalies[6] (**Fig. 4–1B**). Some imagers may find it useful to perform TVS for suspected uterine anomalies during the secretory phase of the cycle because the hyperechoic endometrium may allow improved delineation of the shape of the cavity or cavities compared with other phases of the cycle. If transvaginal sonography with the addition of 3-D imaging is not definitive, magnetic resonance imaging (MRI), hysterosalpingography, or even laparoscopic evaluation may be required.

Pathology of the myometrium, such as the presence of leiomyomata, can be readily identified with ultrasound (**Fig. 4–2**). Fibroids demonstrate a typical circumferential swirling pattern with usually well-defined borders at sonography. Characteristic shadowing from the fibroid further confirms the diagnosis.[7] Most importantly for the infertility patient, the location of the fibroids in relation to the endometrial cavity, lower uterine segment, or uterine fundus should be evaluated. Myomata impinging into the endometrial cavity appear to be of clinical significance with respect to infertility and should be carefully excluded during the preliminary workup of the infertile patient. Submucosal fibroids interfere with implantation[8] and are associated with an increased rate of first trimester pregnancy loss. In some studies, in vitro fertilization (IVF) pregnancy success rates are lower in patients with intramural fibroids as small as 2 to 3 cm in diameter,[8,9] and lower in patients with any fibroid that distorts the endometrial stripe.[8,10] Resection of these fibroids appears to enhance fertility.[11] However, some studies show no difference in implantation rates or ongoing pregnancy rates in the presence of fibroids[12,13] and no improvement in fertility success after myomectomy.[14] Therefore, the management of fibroids in infertility patients remains controversial.

The endometrium is evaluated in both planes, with thickness measured on the sagittal long-axis view (**Fig. 4–3A**).

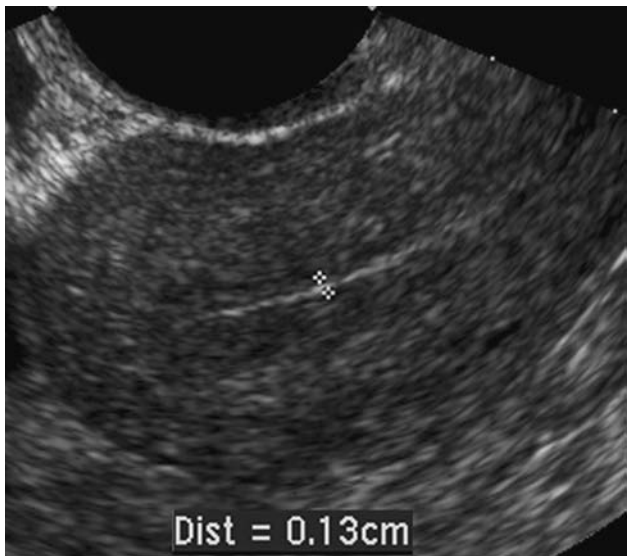

A

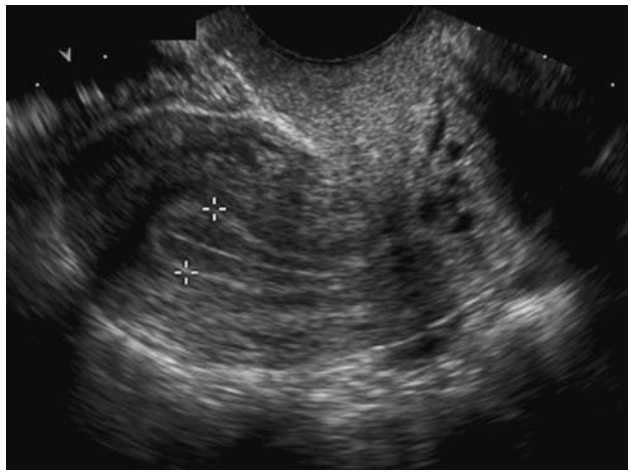

B

Figure 4–3 Various endometrial appearances. **(A)** Sagittal transvaginal image of the uterus shows a linear endometrium measuring less than 2 mm (calipers). **(B)** Sagittal transvaginal image of a uterus with a multilayered endometrium (calipers) during the proliferative phase of the menstrual cycle.

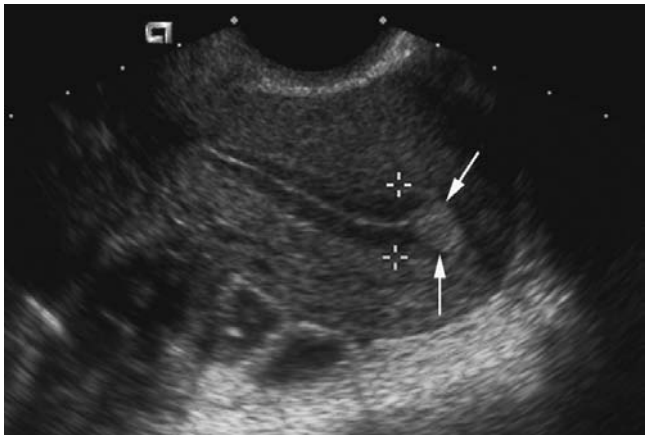

Figure 4–4 Sagittal transvaginal image of a multilayered endometrium with a focal echogenic lesion at the fundus consistent with a polyp.

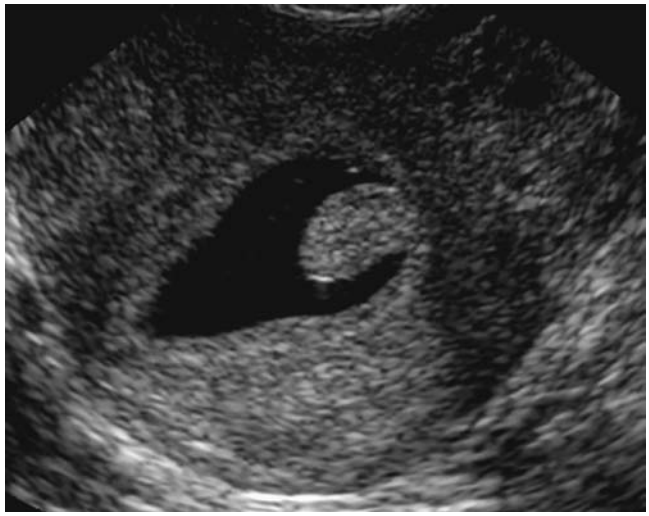

Figure 4–5 Coronal transvaginal image from a sonohysterogram. An echogenic polyp projects from the left uterine wall into the saline-filled endometrial cavity.

If fluid is found in the uterine cavity, the measurement should exclude the fluid interface. The endometrium increases in thickness throughout the follicular phase in response to rising serum estrogen concentrations. In the first days of the menstrual cycle, the endometrial stripe is linear and echogenic, typically < 5 mm. In the days preceding ovulation, a trilaminar pattern is apparent (**Fig. 4–3B**). During the luteal phase of the menstrual cycle, high serum progesterone levels cause the endometrium to transform into a secretory histological pattern, characterized by increased echogenicity and thickness and loss of the trilaminar pattern. Irregularities or deformities of the endometrial stripe suggest intracavitary lesions such as endometrial polyps or submucosal myomata (**Fig. 4–4**). These are typically resected prior to the initiation of fertility treatment because their removal appears to increase pregnancy rates.[11] Treatment of other potential sources of endometrial pathology such as squamous metaplasia or retained bony fragments can improve fertility as well.[15] If additional evaluation of the endometrium for filling defects is required, sonohysterography may be useful[16,17] (**Fig. 4–5**). Sonohysterography is best performed in the early proliferative phase of a woman's menstrual cycle when the endometrium is thin.

One area of ongoing investigation is the evaluation of blood flow to both uterus and ovaries. Using color, pulsed, and power Doppler, occasionally together with 3-D imaging, researchers have found that patients suffering from infertility have less flow to the endometrium and subendometrium during the early luteal phase than control patients.[18–20] In addition, among patients treated for infertility, those with higher blood flow rates in the uterine arteries and intraovarian vessels have more successful pregnancies than the group with less flow.[21]

Evaluation of the Fallopian Tubes

Under normal circumstances, the fallopian tube cannot be visualized with ultrasound. However, in a pathological state, the fallopian tube is readily identifiable. The ultrasonographic finding of fluid in a tubular-shaped adnexal structure suggests the presence of a hydrosalpinx (**Fig. 4–6**). The accurate identification of a hydrosalpinx is very important because its presence signifies a nonpatent tube, which will influence the choice of infertility treatment. Additionally, the presence of a hydrosalpinx decreases the success rate of in vitro fertilization and increases the risk of ectopic pregnancy, and toxins in the

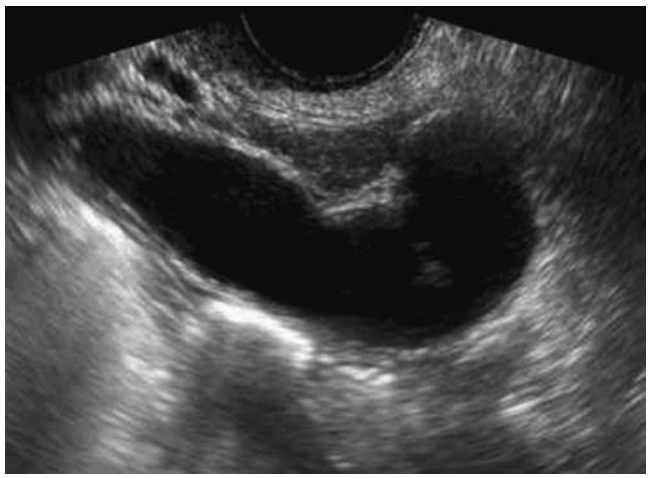

Figure 4–6 Coronal transvaginal image of a tubular fluid-filled structure adjacent to the uterus consistent with a hydrosalpinx. The fluid is nearly anechoic, with a barely perceptible wall.

fluid that fill a blocked fallopian tube are toxic to the developing embryo.[22] A known hydrosalpinx is often aspirated at the time of egg retrieval, or resected prior to an assisted reproduction cycle.[23,24] If fluid debris levels are noted within a hydrosalpinx, the possibility of a tuboovarian abscess should be considered in the appropriate clinical situation.

Investigation continues into the assessment of fallopian tube patency with the use of ultrasound. Using high-resolution ultrasound in combination with injection of normal saline, air, or contrast material, the patency of the fallopian tubes can be assessed by visualizing bubbles or contrast passing through the fallopian tube or the accumulation of air in the peritoneal cavity.[16,25–27] Although technology is improving in the sonographic visualization of the fallopian tube, currently, these techniques suffer from the inability to distinguish unilateral from bilateral tubal patency. Other limitations include the inability to keep the entire tube in a single imaging plane due to tortuosity, and the overlapping appearance of contrast in the tubes with peristalsing bowel. The addition of 3-D imaging to sonography with contrast injection may prove valuable in the future.[28] However, at the present time, hysterosalpingography, the traditional technique for evaluation of the fallopian tube, with the unique advantage of improved pregnancy rates following the procedure,[29] remains the gold standard in assessing fallopian tube patency.[30]

Evaluation of the Ovaries

Transvaginal ultrasound can be used to identify and describe the location, mobility, and appearance of the ovaries. Ovarian follicles are easily recognized by their characteristic anechoic, circular appearance within the capsule of the ovary. The number and size of follicles on each ovary can be documented. For proper interpretation of ultrasound findings, it is critical to know the stage of the menstrual cycle at the time the ultrasound is being performed. Ovarian findings, such as the presence or absence of a dominant follicle, the presence of a corpus luteum, or a sonographic appearance that may suggest the presence of polycystic ovarian syndrome, provide important information for the infertility patient.

The presence of ovarian follicles is a normal physiological finding. Antral ovarian follicles can be identified when they are as small as 3 to 5 mm. As folliculogenesis progresses, some of the follicles will start to mature, and the follicular size will increase. When an ovarian follicle has reached a minimum size of ~10 mm it should be considered to be among the cohort of follicles that may ovulate during the current cycle. By day 9 or 10 of the menstrual cycle, a dominant follicle ranging in size from 12 to 20 mm should be apparent. The other follicles regress, and the dominant follicle increases in size to ~20 to 25 mm before ovulation (**Fig. 4–7**). Ovulation usually occurs on day 14 or 15 of a 28 day menstrual cycle.

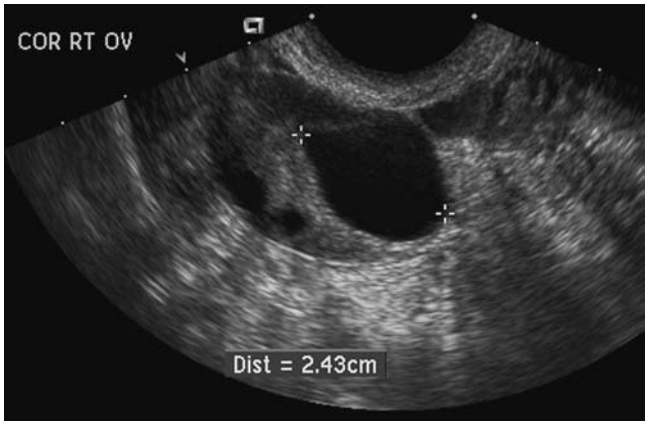

Figure 4–7 Coronal transvaginal image of the right ovary with a 24 mm simple cyst (calipers), which represents a dominant follicle. Other tiny follicles can be seen along the surface of the ovary.

At the time of ovulation, the dominant follicle ruptures and subsequently collapses. A small amount of free fluid can be seen at TVS following ovulation, and there is typically some bleeding into the center of the follicle. The wall of the follicle thickens and the cells begin to secrete progesterone as the cyst transitions from dominant follicle into the corpus luteum. At TVS, the corpus luteum has the characteristic appearance of a thick-walled cyst with a central cobweb appearance, ranging in size from 1.5 to 3 cm, with an intense vascular ring at color Doppler sonography (**Fig. 4–8**).

During the initial evaluation of the infertile woman, TVS may frequently identify abnormalities of the ovary. Most often, these prove to be functional follicular or corpus luteum cysts, but other pathology, such as endometri-

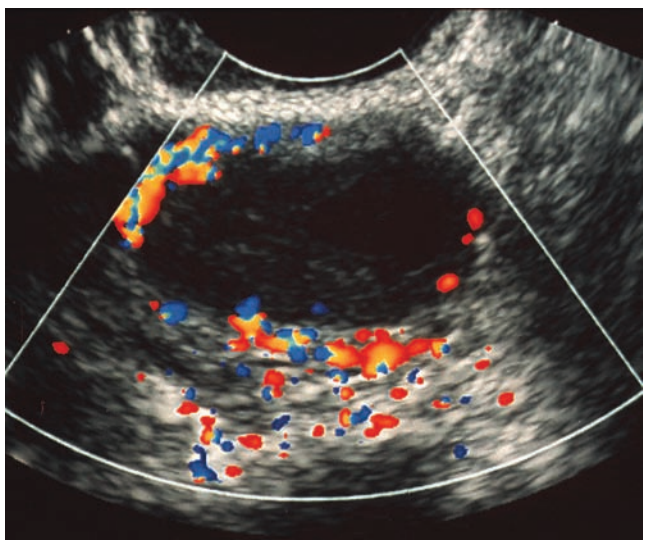

Figure 4–8 Coronal transvaginal image of the ovary, which contains a hypoechoic complex cyst with a thick wall and a prominent vascular ring. This is a corpus luteum cyst found in early pregnancy.

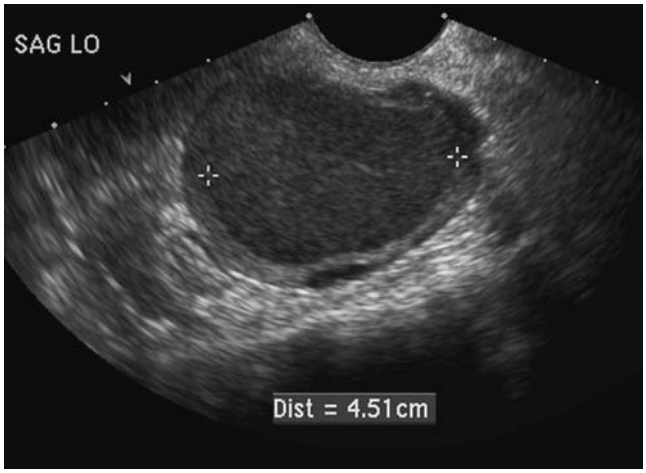

Figure 4–9 Sagittal transvaginal image of the left ovary, which contains a complex cyst (calipers). The cyst is filled with homogeneous internal echoes, which is characteristic of an endometrioma.

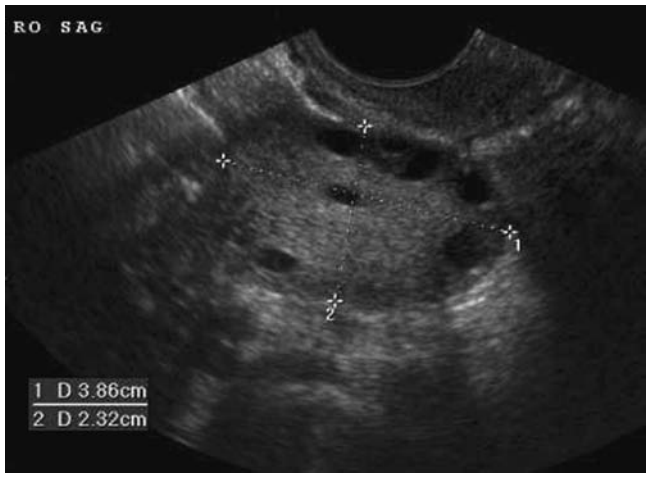

Figure 4–10 Sagittal transvaginal image of the right ovary (calipers) of a patient with polycystic ovarian syndrome. The ovary has an echogenic, solid-appearing center, with multiple tiny subcapsular follicles.

omas, dermoids, or malignant ovarian neoplasms is possible. The size and sonographic characteristics of all ovarian lesions should be identified and reported. Characteristic findings of a functional ovarian cyst include a simple, thin, regular wall and anechoic center. Size range is extremely variable. The classic sonographic appearance of an endometrioma is that of a complex cyst with homogeneous internal echoes or "ground-glass" appearance (**Fig. 4–9**), but endometriosis can have a wide range of appearances that can overlap with other entities, both benign and malignant. Complex ovarian masses with cystic and solid components, internal excrescences or mural nodules, multiple thick (> 3 mm) septations, a thick wall, and lack of mobility are worrisome for neoplasm. Most ovarian lesions are benign and change appearance rapidly, and often a repeat ultrasound examination following the patient's menses or following hormonal suppression with oral contraceptives or gonadotropin-releasing hormone analogs will show resolution of the lesion. If, after treatment, the mass has failed to regress or has grown, surgical excision is the preferred approach to obtain a histological diagnosis.

Polycystic ovarian syndrome (PCOS), the clinical triad of amenorrhea, hirsutism, and obesity, is commonly associated with infertility.[31] PCOS can be diagnosed at sonography if the ovaries are enlarged (volume > 10 mL), and one ovary contains at least 12 subcapsular follicles measuring 4 to 6 mm[32,33] (**Fig. 4–10**). The sonographic criteria should be considered in combination with the clinical findings.

Ultrasound can also be used to determine the mobility of the ovaries. The normal ovary is mobile, and movement of the ovary can be appreciated using real-time ultrasound with direct pressure by the transvaginal probe or while providing abdominal pressure with a free hand. A fixed ovary may suggest the presence of adhesions from endometriosis, previous infection, or surgery.

Monitoring Infertility Treatments

Ultrasound has an important role in monitoring endometrial and follicular development in the patient undergoing fertility treatment. Careful monitoring of induced ovarian stimulation allows adjustment of gonadotropin dosing to attempt to limit the percentage of women who develop ovarian hyperstimulation syndrome. Additionally, sonography is an integral part of IVF treatment, allowing real-time guidance for transvaginal ovum retrieval and optimizing the transfer of embryos into the uterus. The role for sonographic monitoring during the treatment cycle is clear. However, once a cycle has been completed, it is not necessary to reevaluate every patient with sonography prior to initiating a subsequent cycle.[34]

Evaluation of the Uterus

Transvaginal ultrasound can accurately identify the thickness of the endometrium as it responds to estrogen. During ovulation induction therapy, the endometrium progressively thickens, and characteristic sonographic patterns are seen. The endometrial stripe begins as a 2 to 3 mm thin, linear stripe, and changes to a 12 to 14 mm multilayered to trilaminar endometrium. This pattern has been associated with successful implantation after in vitro fertilization and ovulation induction.[35] Although the absence of at least an 8 mm trilaminar endometrial stripe may decrease the chance of pregnancy during that particular cycle,[35,36] it remains inconclusive because others have found no difference in pregnancy rates for infertility patients with thin versus thick endometria.[37–39] Some uncertainty exists regarding the upper normal endometrial thickness for successful conception; a successful outcome

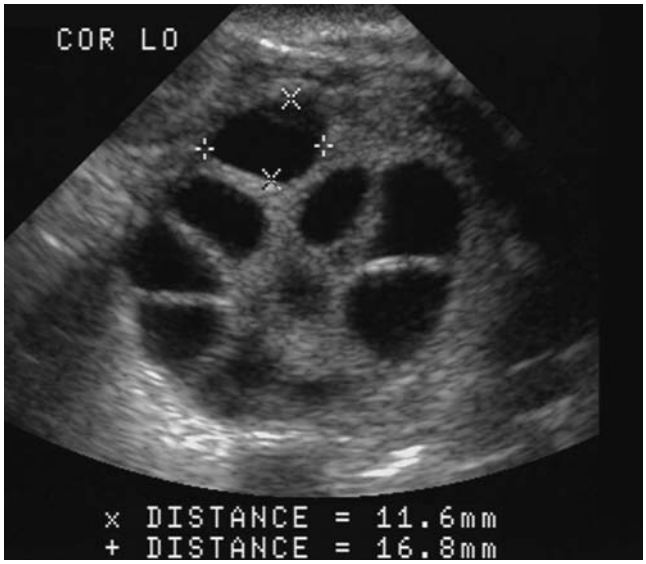

Figure 4–11 Coronal transvaginal image of the left ovary from a patient who has undergone follicular stimulation. Multiple anechoic follicles distend the ovary. One follicle is marked by calipers.

has recently been reported with an endometrial thickness of 20 mm on the day of embryo transfer.[40] Color Doppler showing higher blood flow rates to the endometrium and subendometrium on the day of embryo transfer may predict higher conception success, whereas absent flow to both suggests a poor uterine environment and significantly lower pregnancy rates.[41]

Evaluation of the Ovaries

One of the most important roles of ultrasound in the management of patients undergoing infertility treatment is the monitoring of ovulation induction techniques. Ultrasound is commonly used to assess the process of folliculogenesis during controlled ovarian stimulation with clomiphene citrate, or, most commonly, parenterally administered gonadotropins. Additionally, ultrasound can be used to track the development of a dominant follicle in a cycle without pharmacological intervention.

Controlled ovarian stimulation begins with a baseline ultrasound to ensure that the process of folliculogenesis has not already selected a dominant follicle and to exclude the presence of an ovarian cyst or mass. Ovarian stimulation with either clomiphene citrate or gonadotropins is initiated on days 3 to 5 of a normal menstrual cycle. It is expected that multiple follicles will enlarge in contrast to the emergence of a single dominant follicle in the natural menstrual cycle. TVS is used to document the number as well as the growth of the follicles. Sonographic monitoring of follicle growth is performed intermittently throughout the follicular phase. Imaging early in the follicular phase confirms adequate follicular recruitment. Continued monitoring of the follicles in conjunction with serum estradiol determinations on days 7 through 10 helps determine the optimal timing of ovulation. When ultrasound has identified the optimal follicular size, intramuscular human chorionic gonadotropin (hCG) is administered as a substitute for luteinizing hormone to trigger ovulation. This allows for the optimal timing of intrauterine insemination or oocyte retrieval for in vitro fertilization. A dominant follicle should reach ~25 mm in women stimulated with clomiphene citrate. The optimal development of follicles in a woman stimulated with gonadotropins is at least two follicles of 18 mm diameter each. In the case of in vitro fertilization, as many as 20 or more follicles may be recruited, and ovulation is triggered when at least four follicles are 19 to 20 mm or greater (**Fig. 4–11**).

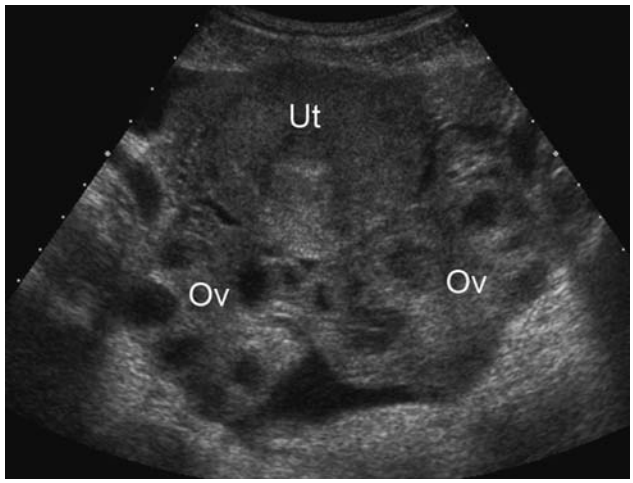

A

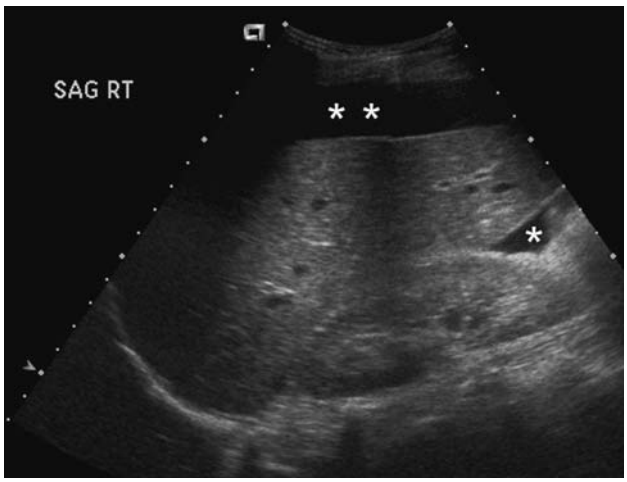

B

Figure 4–12 Ovarian hyperstimulation syndrome. **(A)** Transverse transabdominal image of the uterus and ovaries. The posterior aspect of the uterus (Ut) is surrounded by the markedly enlarged ovaries (Ov), which contain multiple complex cysts. **(B)** Sagittal image of the right upper quadrant showing a moderate amount of ascites (**) anterior to the right lobe of the liver, and between the liver and right kidney in Morison's pouch (*).

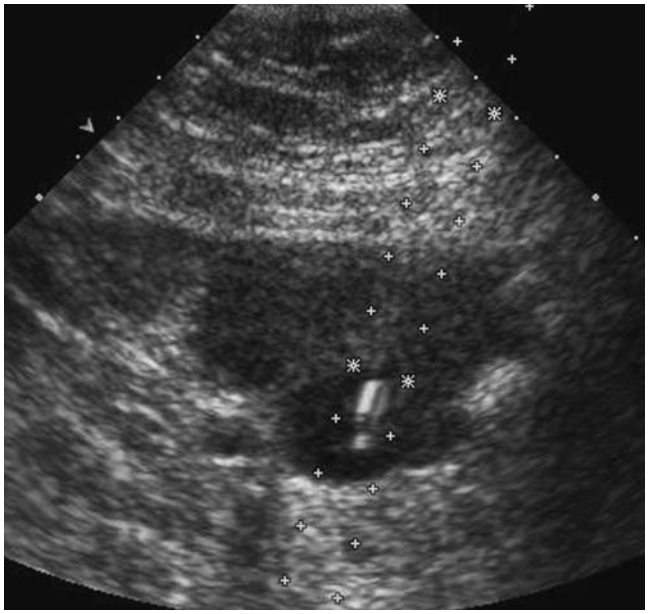

Figure 4–13 Transabdominal oocyte retrieval. The needle is identified within the guide markers, with the tip in an ovarian follicle. The fluid will be aspirated and searched for an oocyte.

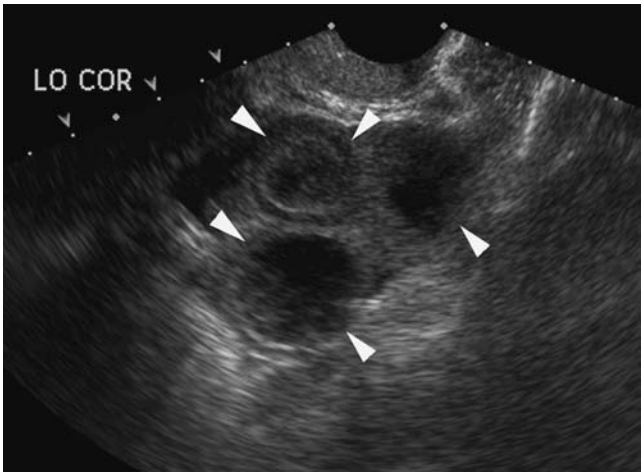

Figure 4–14 Coronal transvaginal image of the left ovary, which contains multiple complex and thick-walled cysts (arrowheads). These cysts are seen following needle aspiration of follicles due to hemorrhage from the needle puncture and may persist for several weeks.

One complication of ovulation induction with gonadotropins is ovarian hyperstimulation syndrome (OHSS).[42–44] The syndrome is composed of enlarged ovaries, weight gain, and third spacing of fluid resulting in ascites, pleural fluid, hemoconcentration, and oliguria. This entity occurs if too many follicles have developed. In these patients, withholding hCG may prevent the full-blown syndrome. If ovarian hyperstimulation does occur, ultrasound can be used to document free intraperitoneal fluid, evaluate for the presence of pleural fluid, and measure ovarian size (**Fig. 4–12**). In most cases, both ovaries are affected. A transabdominal scanning approach is usually needed when evaluating for ovarian hyperstimulation because the vaginal probe cannot penetrate far enough to image the often markedly enlarged ovaries. The ovaries are filled with complex cysts of varying sizes, and ovarian diameter is often > 10 cm. The ovaries are at increased risk for torsion or rupture. Paracentesis may be indicated as part of the treatment for OHSS, and transabdominal ultrasound can localize a site for safe access.

The role of TVS continues during in vitro fertilization treatment. Once an appropriate number of follicles are found during ovulation induction monitoring, transvaginal ultrasound provides real-time guidance for the aspiration of ovarian follicles during ovum retrieval. The ultrasound probe is fitted with a guide for a specialized needle. Under direct ultrasound guidance, the ovarian follicles are punctured, their contents are aspirated, and the oocyte is retrieved after microscopic examination of the aspirated follicular fluid. In some patients, the location of the ovary high in the abdomen requires the retrieval to be performed via a transabdominal approach, still with ultrasound guidance (**Fig. 4–13**). After fertilization, embryos are transferred into the endometrial cavity. Ultrasound is used to map the endometrial cavity and determine the optimal length and direction a catheter should be inserted to atraumatically transfer the embryos. When real-time ultrasound is used to guide embryo placement into the endometrial cavity, the implantation rate and subsequent successful pregnancy rate are both increased when compared to clinical touch embryo transfer.[45,46]

Complications of oocyte retrieval are rare, but include bleeding and infection.[47,48] Some bleeding is inevitable due to the multiple needle punctures of both ovaries and vaginal wall, and in most instances, it is self-limited, in the range of 10 to 20 mL.[49] The amount of pelvic fluid correlates with the number of oocytes retrieved. Multiple complex cysts of varying size are typically seen in the ovary postretrieval, representing hemorrhage into each of the aspirated follicles (**Fig. 4–14**). Rarely, a larger vessel may be injured during the retrieval. TVS may demonstrate complex fluid in the cul-de-sac and adnexa suggestive of hemoperitoneum. In these patients, additional imaging of the upper abdomen is necessary to evaluate for large amounts of blood that may flow into the upper abdomen (**Fig. 4–15**), out of the range of the transvaginal probe, particularly if the patient is in the lithotomy position. Correlation with the hematocrit level will help differentiate a large amount of blood loss from the ascites associated with ovarian hyperstimulation. Another rare complication of oocyte retrieval is infection, or tuboovarian abscess. This is reported in far less than 1% of retrievals and may be related to preexisting abnormalities such as hydrosalpinx.

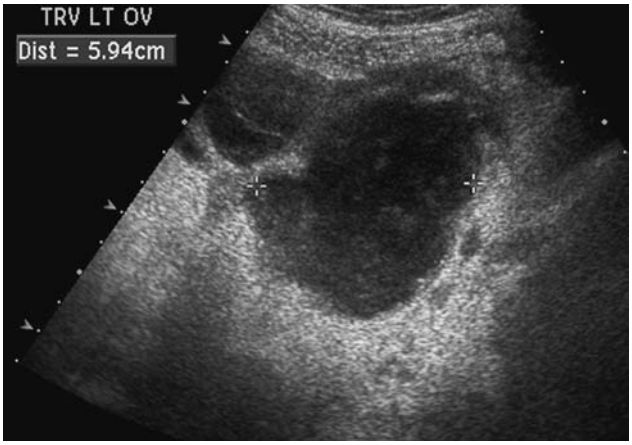

A

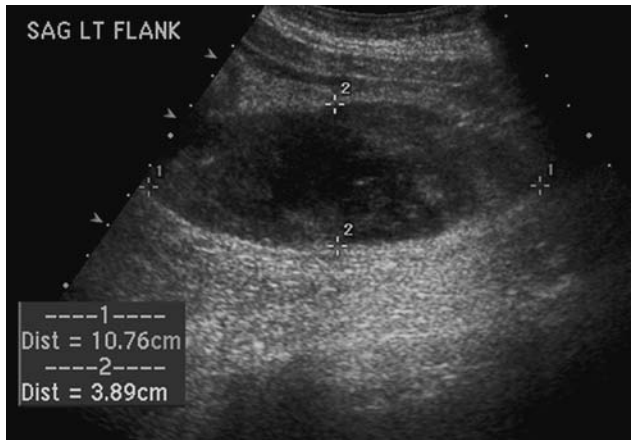

B

Figure 4–15 Hemorrhage following in vitro fertilization (2 weeks postprocedure). **(A)** Transverse transabdominal image of large complex collection (calipers) within the left ovary, representing an intraovarian hemorrhage. **(B)** Sagittal image of a large complex fluid collection (calipers) in the left flank consistent with hematoma.

Diagnosis of Early Pregnancy

Ultrasound has revolutionized the diagnosis and management of early pregnancy. An intrauterine gestational sac can be visualized with transvaginal ultrasound at 3 weeks from conception, or 5 weeks menstrual age (MA). An early pregnancy sac is characterized by a sonolucent center (the chorionic cavity) containing the amnion and eventually the embryonic disk and yolk sac and a symmetrical thick echogenic ring formed by primary trophoblasts. The gestational sac implants into the decidualized endometrium. If fluid is present in the endometrial cavity, the asymmetric nature of implantation can be appreciated. Until a yolk sac or embryonic pole with cardiac activity is visualized, an intrauterine pregnancy might be impossible to differentiate from a small endometrial cyst or a pseudosac associated with an ectopic pregnancy.

Once an intrauterine pregnancy has been identified, its growth can be assessed by serial ultrasounds. The mean diameter of a gestational sac increases ~1 mm a day during early pregnancy.[50] The yolk sac is a round structure with an echogenic rim inside the gestational sac that appears next, typically at 5.5 weeks MA. Cardiac activity is first identified at TVS at 6 weeks MA, at times before the embryonic pole is definitively seen. Assessment of the embryonic heart rate may provide a useful early predictor of pregnancy outcome.[51,52] After the appearance of the embryo, the crown– rump length can be used to determine gestational age and to monitor pregnancy progression. In IVF patients, the date of retrieval is used for pregnancy dating. Delay in pregnancy development in relation to retrieval dating is a poor prognostic indicator.

Assessment of Early Pregnancy Failure

Ultrasound can also assist the infertility physician in determining the continued well-being of a pregnancy. A pregnancy complicated by bleeding through a closed cervical os is considered a threatened abortion. To assess the status of a threatened abortion, serial ultrasounds can be used. Unless an ectopic pregnancy is still in question, following quantitative hCG values is only of limited value. Serial ultrasound examination can detect an abnormal or failed pregnancy by detecting a distorted gestational sac, a collapsed fragmented sac, or a lack of continued growth and expected landmarks.[53] If an embryo is < 5 mm long and no cardiac activity is discernible, a follow-up scan conducted at an appropriate interval should be performed to confirm a failed pregnancy consistent with an embryonic demise. Cardiac activity should be visible in all embryos measuring > 5 mm. Additionally, the absence of cardiac activity, when it had been detected previously, confirms a failed pregnancy.

Assessment of Ectopic Pregnancy

One of the most common complications of infertility treatment is an ectopic pregnancy. A history of infertility or infertility treatments are recognized risk factors for the development of ectopic pregnancy. Thus, all infertility patients achieving pregnancy are routinely followed with TVS until an ectopic pregnancy has been excluded. Ultrasound is very sensitive in identifying a intrauterine pregnancy, which virtually eliminates an ectopic pregnancy with the exception of heterotopic pregnancy. The presence of simultaneous intrauterine and extrauterine pregnancies is extremely rare; however, in women undergoing assisted reproduction, the rate of heterotopic

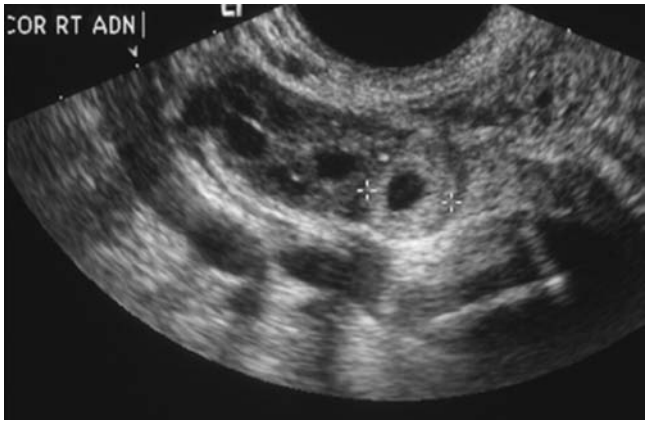

Figure 4–16 Coronal transvaginal image of the right adnexa. The echogenic tubal ring of an ectopic pregnancy (calipers) can be seen adjacent to the normal right ovary.

pregnancy is reported to be as high as 1%.[54,55] An ectopic pregnancy should remain in the differential for all patients who have undergone assisted reproduction and present with pelvic pain.

The detection of an extrauterine pregnancy relies on thorough evaluation of the adnexa at TVS.[56] The entire pelvis should be searched for an adnexal mass, which is often found between the uterus and ovary, in the expected location of the fallopian tube. Any mass that is not a simple cyst and that is separate from the ovary has a high specificity (98.9%) and high sensitivity (84.4%) for being an ectopic pregnancy.[57] An intraovarian lesion is most likely the corpus luteum. A simple cyst that is separate from the ovary is most likely a paratubal cyst. The presence of free fluid, particularly if it contains echoes suggesting that it is blood, increases the likelihood that there is an ectopic pregnancy.[56,58,59] An adnexal or tubal ring, the classic finding suggesting an ectopic pregnancy, represents the actual extrauterine gestational sac, often surrounded by fallopian tube (**Fig. 4–16**). The echogenic walls of the sac or ring are a clue to the diagnosis,[60] as well as the extraovarian location. Close investigation of the tubal ring may reveal a central yolk sac or even an embryo with cardiac activity. The corpus luteum of early pregnancy can be recognized as such and differentiated from an ectopic by its intraovarian location and typically hypoechoic rim.[60,61] Following treatment for ectopic pregnancy, fertility declines, and the risk for future ectopic pregnancy increases.[62]

Conclusion

Ultrasound has become an important clinical tool in the management of a couple being evaluated and treated for infertility. Transvaginal ultrasound provides high-resolution imaging of the pelvic structures. It can be used to diagnose existing uterine, tubal, or ovarian anomalies, to monitor infertility treatment, and to assist in ovum retrieval and embryo transfer. TVS remains the gold standard for the identification of an early intrauterine pregnancy, for the discrimination between a normal and an abnormal gestation, and for the diagnosis of ectopic pregnancy.

References

1. Jones HW Jr. Overview of infertility: the scope of the problem. In: Goldstein SR, Benson CB, eds. Imaging of the Infertile Couple. London: Martin Dunitz; 2001:1–6
2. Van der Auwera I, D'Hooghe TM. Ultrasound covers and sonographic gels are embryo-toxic and could be replaced by nontoxie polyethylene bags and paraffin oil. Hum Reprod 1998;13:2234–2237
3. Shalev J, Meizner I, Bar-Hava I, Dicker D, Mashiach R, Ben-Rafael Z. Predictive value of transvaginal sonography performed before routine diagnostic hysteroscopy for evaluation of infertility. Fertil Steril 2000;73:412–417
4. Loverro G, Nappi L, Vicino M, Carriero C, Vimercati A, Selvaggi L. Uterine cavity assessment in infertile women: comparison of transvaginal sonography and hysteroscopy. Eur J Obstet Gynecol Reprod Biol 2001;100:67–71
5. Kupesic S, Kurjak A. Septate uterus: detection and prediction of obstetrical complications by different forms of ultrasonography. J Ultrasound Med 1998;17:631–636
6. Benacerraf BR, Benson CB, Abuhamad AZ, et al. Three- and 4-dimensional ultrasound in obstetrics and gynecology: proceedings of the American Institute of Ultrasound in Medicine consensus conference. J Ultrasound Med 2005;24:1587–1597
7. Caoili EM, Hertzberg BS, Kliewer MA, DeLong D, Bowie JD. Refractory shadowing from pelvic masses on sonography: a useful diagnostic sign for uterine leiomyomas. AJR Am J Roentgenol 2000;174:97–101
8. Eldar-Geva T, Meagher S, Healy D. Effect of intramural, subserosal, and submucosal uterine fibroids on the outcome of assisted reproductive technology treatment. Fertil Steril 1998;70:687–691
9. Hart R, Khalaf Y, Yeong C-T, Seed P, Taylor A, Braude P. A prospective controlled study of the effect of intramural uterine fibroids on the outcome of assisted conception. Hum Reprod 2001;16:2411–2417
10. Gianroli L, Gordts S, D'Angelo A, et al. Effect of inner myometrium fibroid on reproductive outcome after IVF. Reprod Biomed Online 2005;10:473–477
11. Varasteh NN, Neuwirth RS, Levin B, Keltz MD. Pregnancy rates after hysteroscopic polypectomy and myomectomy in infertile women. Obstet Gynecol 1999;94:168–171
12. Jun SH, Ginsburg ES, Racowsky C, Wise LA, Hornstein MD. Uterine leiomyomas and their effect on in vitro fertilization outcome: a retrospective study. J Assist Reprod Genet 2001;18:139–143
13. Oliveira FG, Abdelmassih VG, Diamond MP, Dozortsev D, Melo NR, Abdelmassih R. Impact of subserosal and intramural uterine fibroids that do not distort the endometrial cavity on the outcome of in vitro fertilization-intracytoplasmic sperm injection. Fertil Steril 2004;81:582–587
14. Surrey ES, Minjarez DA, Stevens JM, Schoolcraft WB. Effect of myomectomy on the outcome of assisted reproductive technologies. Fertil Steril 2005;84:1473–1479
15. Ruiz-Velasco V, Alfani GG, Sanchez LP, Vera MA. Endometrial pathology and infertility. Fertil Steril 1997;67:687–692

16. Alborzi S, Dehbashi S, Khodaee R. Sonohysterosalpingographic screening for infertile patients. Int J Gynecol Obstet 2003;82: 57–62
17. Ayida G, Chamberlain P, Barlow D, Kennedy S. Uterine cavity assessment prior to in vitro fertilization: comparison of transvaginal scanning, saline contrast hysterosonography and hysteroscopy. Ultrasound Obstet Gynecol 1997;10:59–62
18. Ng EHY, Chan CCW, Tang OS, Yeung WSB, Ho PC. Endometrial and subendometrial blood flow measured during early luteal phase by three-dimensional power Doppler ultrasound in excessive ovarian responders. Hum Reprod 2004;19:924–931
19. Raine-Fenning NJ, Campbell BK, Kendall NR, Clewes JS, Johnson IR. Endometrial and subendometrial perfusion are impaired in women with unexplained subfertility. Hum Reprod 2004;19: 2605–2614
20. Edi-Osagie ECO, Seif MW, Aplin JD, Jones CJP, Wilson G, Leiberman BA. Characterizing the endometrium in unexplained and tubal factor infertility: a multiparametric investigation. Fertil Steril 2004; 82:1379–1389
21. Yalti S, Gurbuz B, Ficicioglu C, Canova H. Doppler evaluation of the uterine, intraovarian, stromal and spiral arteries on the day of human chorionic gonadotrophin administration in controlled ovarian hyperstimulation. J Obstet Gynaecol 2003;23:402–406
22. Ng EHY, Ajonuma LC, Lau EYL, Yeung WSB, Ho PC. Adverse effects of hydrosalpinx fluid on sperm motility. Hum Reprod 2000;15: 772–777
23. Strandell A, Lindhard A, Waldenstrom U, Thorburn J. Hydrosalpinx and IVF outcome: cumulative results after salpingectomy in a randomized controlled trial. Hum Reprod 2001;16:2403–2410
24. Bildirici I, Bukulmez O, Ensari A, Yarali H, Gurgan T. A prospective evaluation of the effect of salpingectomy on endometrial receptivity in cases of women with communicating hydrosalpinges. Hum Reprod 2001;16:2422–2426
25. Fleischer AC, Vasquez JM, Cullinan JA, Eisenberg E. Sonohysterography combined with sonosalpingography: correlation with endoscopic findings in infertility patients. J Ultrasound Med 1997;16: 381–384
26. Prefumo F, Serafini G, Martinoli C, Gandolfo N, Gandolfo NG, Derchi LE. The sonographic evaluation of tubal patency with stimulated acoustic emission imaging. Ultrasound Obstet Gynecol 2002;20: 386–389
27. Hauge K, Flo K, Riedhart M, Granberg S. Can ultrasound-based investigations replace laparoscopy and hysteroscopy in infertility? Eur J Obstet Gynecol Reprod Biol 2000;92:167–170
28. Sladkevicius P, Ojha K, Campbell S, Nargund G. Three-dimensional power Doppler imaging in the assessment of fallopian tube patency. Ultrasound Obstet Gynecol 2000;16:644–647
29. Johnson N, Vandekerckhove P, Watson A, Lilford R, Harada T, Hughes E. Tubal flushing for subfertility [review]. Cochrane Database Syst Rev 2005;Apr 18:1–45
30. Papaioannou S, Bourdrez P, Varma R, Afnan M, Mol BW, Coomarasamy A. Tubal evaluation in the investigation of subfertility: a structured comparison. BJOG 2004;111:1313–1321
31. Lane DE. Polycystic ovary syndrome and its differential diagnosis. Obstet Gynecol Surv 2006;61:125–135
32. The Rotterdam ESHRE/ASRM-Sponsored PCOS Consensus Workshop Group. Revised 2003 consensus on diagnostic criteria and long-term health risks related to polycystic ovary syndrome. Fertil Steril 2004;81:19–25
33. Pache TD, Wladimiroff JW, Hop WCJ, Fauser BCJM. How to discriminate between normal and polycystic ovaries: transvaginal US study. Radeology 1992;83:421–423
34. Dew JE, Don RA, Hughes GJ, Johnson TC, Steigrad SJ. The significance of pelvic ultrasound abnormalities detected on routine ultrasound scanning prior to assisted reproduction. J In Vitro Fert Emb 1998;43:150–154
35. Gonen Y, Casper R. Prediction of implantation by the sonographic appearance of the endometrium during controlled ovarian stimulation for in vitro fertilization (IVF). J In Vitro Fert Embryo Transf 1990;7:146–152
36. Basir GS, O WS, So WWK, Ng EHY, Ho PC. Evaluation of cycle-to-cycle variation of endometrial responsiveness using transvaginal sonography in women undergoing assisted reproduction. Ultrasound Obstet Gynecol 2002;19:484–489
37. De Geyter C, Schmitter M, De Geyter M, Nieschlag E, Holzgreve W, Schneider HPG. Prospective evaluation of the ultrasound appearance of the endometrium in a cohort of 1,186 infertile women. Fertil Steril 2000;73:106–113
38. Kolibianakis EM, Zikopoulos KA, Fatemi HM, et al. Endometrial thickness cannot predict ongoing pregnancy achievement in cycles stimulated with clomiphene citrate for intrauterine insemination. Reprod Biomed Online 2004;8:115–118
39. Yaman C, Ebner T, Sommergruber M, Polz W, Tews G. Role of three-dimensional ultrasonographic measurement of endometrium volume as a predictor of pregnancy outcome in an IVF-ET program: a preliminary study. Fertil Steril 2000;74:979–801
40. Quintero RB, Sharara FI, Milki AA. Successful pregnancies in the setting of exaggerated endometrial thickness. Fertil Steril 2004; 82:215–217
41. Chien LW, Au HK, Chen PL, Xiao J, Tzeng CR. Assessment of uterine receptivity by the endometrial–subendometrial blood flow distribution pattern in women undergoing in vitro fertilization–embryo transfer. Fertil Steril 2002;78:245–251
42. Klemetti R, Sevon R, Gissler M, Hemminki E. Complications of IVF and ovulation induction. Hum Reprod 2005;20:3293–3300
43. Budev MM, Arroliga AC, Falcone T. Ovarian hyperstimulation syndrome. Crit Care Med 2005;33:S301–S306
44. Papanikolaov, Pozzobon C, Kolibianakis EM, et al. Incidence and prediction of ovarian hyperstimulation syndrome in women undergoing gonadotropin-releasing hormone antagonist in vitro fertilization cycles. Fertil Steril 2006;85:112–120
45. Buckett WM. A meta-analysis of ultrasound-guided versus clinical touch embryo transfer. Fertil Steril 2003;80:1037–1041
46. Coroleu B, Carreras O, Veiga A, et al. Embryo transfer under ultrasound guidance improves pregnancy rates after in vitro fertilization. Hum Reprod 2000;15:616–620
47. Bennett SJ, Waterstone JJ, Cheng WL, Parsons J. Complications of transvaginal ultrasound directed follicle aspiration in a review of 2670 consecutive procedures. J Assist Reprod Genet 1993;10: 72–77
48. Dicker D, Ashkenaji J, Feldberg D, Levy T, Dekel A, Ben Raphael Z. Severe abdominal complication after transvaginal ultrasonographically guided retrieval of oocytes in vitro fertilization and embryo transfer. Fertil Steril 1993;59:1313–1315
49. Shalev J, Davidi O, Fisch B. Quantitative three dimensional sonographic assessment of pelvic blood after transvaginal ultrasound guided oocyte aspiration: factors predicting risk. Ultrasound Obstet Gynecol 2004;23:177–182
50. Goldstein SR, Wolfson R. Endovaginal ultrasonographic measurement of early embryonic sizes: a means for assessing gestational age. J Ultrasound Med 1994;13:27–31
51. Benson CB, Doubilet PM. Slow embryonic heart rate in early first trimester: indicator of poor pregnancy outcome. Radiology 1994; 192:343–344

52. Doubilet PM, Benson CB. Embryonic heart rate in the early first trimester: what rate is normal? J Ultrasound Med 1995;14:431–434
53. ACOG Technical Bulletin. Gynecologic ultrasonography. Number 215. Nov 1995. Int J Gynaecol Obstet 1996; 52:293–304
54. Rizk B, Tan SL, Morcos S, et al. Heterotopic pregnancies after in vitro fertilization and embryo transfer. Am J Obstet Gynecol 1991; 164:161–164
55. Goldman GA, Fisch B, Ovadia J, Tadir Y. Heterotopic pregnancy after assisted reproductive technologies. Obstet Gynecol Surv 1992;??: 217–221
56. Frates MC, Laing FC. Sonographic evaluation of ectopic pregnancy: an update. AJR Am J Roentgenol 1995;165:251–259
57. Brown DL, Doubilet PM. Transvaginal sonography for diagnosing ectopic pregnancy: positivity criteria and performance characteristics. J Ultrasound Med 1994;13:259–266
58. Dart R, McLean SA, Dart L. Isolated fluid in the cul-de-sac: how well does it predict ectopic pregnancy? Am J Emerg Med 2002;20: 1–4
59. Nyberg DA, Hughes MP, Mack LA, Wang KY. Extrauterine findings of ectopic pregnancy at transvaginal ultrasound: importance of echogenic fluid. Radiology 1991;178:823–826
60. Frates MC, Visweswaran A, Laing FC. Comparison of tubal ring and corpus luteum echogenicities: a useful differentiating characteristic. J Ultrasound Med 2001;20:27–31
61. Stein MW, Ricci ZJ, Novak L, Roberts JH, Koenigsberg M. Sonographic comparison of the tubal ring of ectopic pregnancy with the corpus luteum. J Ultrasound Med 2004;23:57–62
62. Korell M, Albrich W, Hepp H. Fertility after organ-preserving surgery of ectopic pregnancy: results of a multicenter study. Fertil Steril 1997;68:220–223

5 Amenorrhea in the Adolescent or Young Adult

Anna E. Nidecker, Harris L. Cohen, and Harry L. Zinn

Ultrasonography of the pelvis and reproductive organs is an essential diagnostic imaging technique for the patient who presents with amenorrhea. *Primary amenorrhea* is defined as a lack of menses by age 16. *Secondary amenorrhea* is the cessation of menses at any point in time after menarche and prior to menopause.[1] To establish a diagnosis and cause of amenorrhea, the referring physician and radiologist should understand the physiological mechanisms regulating normal menses and the abnormalities that may lead to its disruption. These abnormalities may be embryological, genetic, and/or endocrinologic.[2] Knowledge of the patient's history, physical findings, and laboratory values, as well as the spectrum of normal and abnormal ultrasound and other imaging findings for the patient's age, is also important for understanding and diagnosing the causes of amenorrhea.

Normal Structure, Function, and Development of Female Reproductive Organs

Menstrual Cycle

Menstruation is the periodic vaginal bleeding that is the end result of cyclical stimulation of ovarian follicles and the associated buildup and eventual shedding of uterine mucosa. In humans, the average time between one menses and the next is 28 days. Stages of the menstrual cycle are defined by the cyclical changes involving the ovary, the endometrium, and hormone levels. With regard to the ovary, the menstrual cycle is divided into follicular and luteal phases, with ovulation occurring 14 days before menses (menstrual bleeding). The first day of the cycle is defined as the first day of menstrual bleeding (menses).[1,3–5] With regard to the endometrium, the menstrual cycle is divided into the proliferative and secretory phases, with menses occurring after the secretory phase and before the proliferative phase begins again (**Fig. 5–1**).

The follicular phase of the normal cycle occurs between the first day of the menstrual cycle and ovulation. This phase is variable in length, and accounts for differences in cycle lengths among ovulating women.[5] During this phase, low levels of estrogen and progesterone as well as the pulsatile release of gonadotropin releasing hormone (GnRH) from the hypothalamus stimulate the secretion of follicle stimulating hormone (FSH) by the pituitary. This hormone stimulates a group of preselected primordial ovarian follicles (**Fig. 5–2**). By the sixth day of the cycle, one follicle becomes dominant. With the support of luteinizing hormone (LH) and FSH, this maturing ovarian (graafian) follicle continues to grow and produce estrogen. FSH stimulates an increase in the number of granulosa cells within the graafian follicle as well as the number of FSH receptors on these cells. It also induces production of aromatase, an enzyme necessary for the conversion of androgen precursors to estradiol. LH induces the ovarian theca cells to secrete androstenedione, testosterone, and estradiol into the bloodstream and into the follicle itself. By the midfollicular phase, FSH levels begin to decline and the secondary or nondominant follicles become atretic. Increasing levels of estrogen and the release of inhibin by ovarian granulosa cells contribute to the reduction in FSH production and release. However, the graafian follicle survives because of accumulation of FSH and estradiol in the follicular fluid as well as the earlier increased production of granulosa cells and FSH receptors, which amplify the effect of the available FSH.[2,4,5] The last half of the follicular phase coincides with the proliferative phase of the endometrial cycle. Estradiol induces hyperplasia and hypertrophy of the endometrium, with associated thickened mucosa and increased glandular length.

Ovulation occurs at midcycle, which is typically at 14 days, but can be anywhere from 9 to 21 days after menses in a normal population. The increasing estrogen and progesterone levels result in a surge of LH. This LH surge causes the distended graafian follicle to rupture and release the ovum (**Fig. 5–2**). The ovum enters the fallopian tube and either implants in the uterus after fertilization or passes through the uterus and out of the body through the vagina.

The length of the next step in the cycle, called the luteal phase, is remarkably constant, averaging 14 ± 2 days in most women and determined by the lifespan of the corpus luteum. During this phase, the ruptured graafian follicle becomes hemorrhagic (corpus hemorrhagicum). The clotted blood is then replaced by lipid-rich luteal cells, which form the corpus luteum. The luteal phase coincides with the secretory phase of the endometrium. After ovulation, estrogen and estradiol produced by the corpus luteum

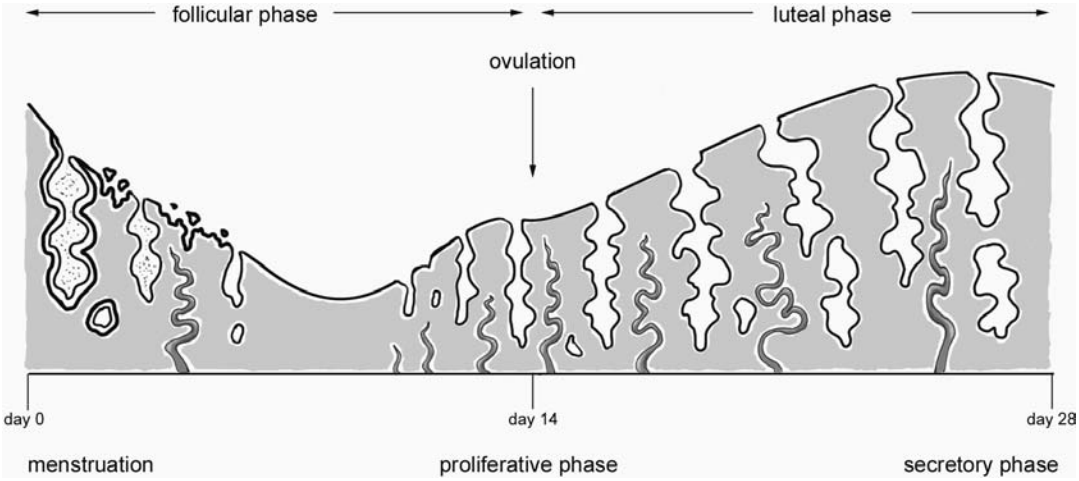

Figure 5–1 Cyclical changes in the endometrium during a normal 28 day menstrual cycle. The endometrium undergoes changes during a normal cycle. The beginning of menstruation is arbitrarily defined as day 0 of the endometrial cycle. During this phase, there is shedding of the superficial layers of the endometrium noted on the schematic as decreased height of the endometrial lining. Following this, in the proliferative phase, there is hyperplasia and hypertrophy of the endometrium with associated thickened mucosa and increased glandular length. Just after ovulation occurs, anywhere from day 9 to day 21 of the menstrual cycle, the secretory phase begins. It is during this time period that the endometrium becomes highly vascularized with spiral arteries and edematous in preparation for possible implantation by a fertilized egg. The corresponding time periods of the ovary's follicular and luteal phases are annotated at the top of the drawing, allowing one to note their relationship with the proliferative and secretory phases of the endometrium. (Drawing courtesy of Anna E. Nidecker, M.D.)

cause the endometrium to become highly vascularized and edematous in preparation for possible implantation by a fertilized egg.[5]

If pregnancy occurs, the corpus luteum persists and no menses occur until after delivery. If fertilization does not occur, the corpus luteum degenerates (**Fig. 5–2**), eventually becoming an area of scar tissue (corpus albicans). With corpus luteal degeneration, blood levels of estrogen and progesterone fall. Foci of necrosis appear in the endometrium and soon coalesce. With decreasing hormonal support, the endometrium begins to liberate proteolytic enzymes from lysosomes and increase prostaglandin production. This subsequently causes vasoconstriction and eventual rupture of the spiral arteries of the endometrium, leading to the initially spotty and then more confluent bleeding known as menstrual flow. The stratum functionale, the superficial two thirds of the endometrium fed by the long coiled spiral arteries, is shed. The stratum basale, the deepest third of the endometrium supplied by short straight basilar arteries, remains intact and serves as a regenerative layer for new endometrial proliferation in the next cycle.[1,2,4,5]

Physiology

Vaginal bleeding may be noted in the normal female in the immediate neonatal period. It is believed this occasional observation is secondary to withdrawal bleeding from exposure to high levels of maternal estrogen and

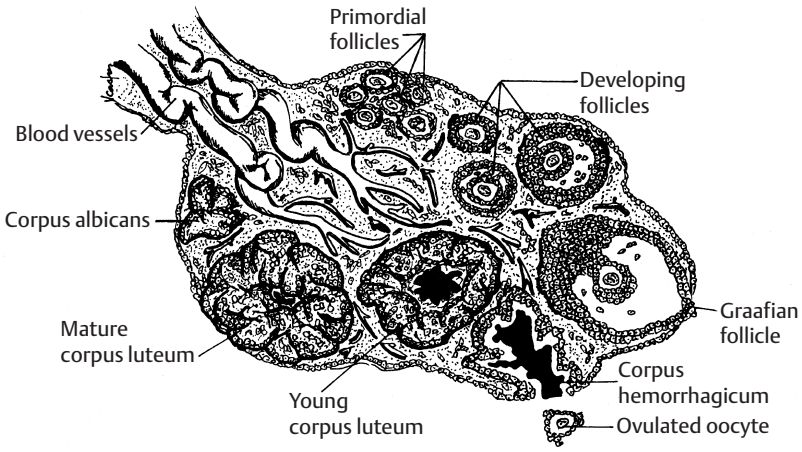

Figure 5–2 Cyclical changes in the postmenarchal ovary. The ovary undergoes various stages during the menstrual cycle. These include the follicular phase with formation of a dominant (graafian) follicle from among several stimulated primordial follicles; the ovulatory phase with formation of the corpus hemorrhagicum; and the secretory phase with formation of the corpus luteum, which produces estrogen and progesterone necessary for endometrial maturation. The corpus luteum degenerates, leaving scar tissue (corpus albicans), if no pregnancy occurs. (From Cohen HL. Evaluation of the Adolescent and Young Adult with Amenorrhea: Role of US. RSNA Special Course in Ultrasound. Radiological Society of North America; 1996: 171–183. Reprinted with permission from the Radiological Society of North America.)

progesterone in utero, which abruptly decrease after placental separation.[2,6]

Ordinarily, the final maturation of the reproductive system and subsequent menses do not begin until at least 8 years of age. A central inhibitory mechanism that prevents the pulsatile release of GnRH from the arcuate nucleus of the hypothalamus is thought to prevent menses in younger children. The inhibition of GnRH production in patients with Turner's syndrome who have no functioning gonadal tissue is evidence for this being due to a central control mechanism, rather than a negative feedback mechanism from ovarian hormone production.[7] However, the details of this mechanism remain a mystery.

At adolescence, most girls undergo ovarian folliculogenesis without ovulation with the start of the pulsatile release of GnRH.[2,8] Unopposed estrogen production leads to progressive uterine growth and endometrial proliferation, as well as physiological leukorrhea and accelerated linear long-bone growth. Thelarche, or breast budding, occurs. Soon afterwards, androgen production by the ovaries and adrenal glands stimulates pubarche, the development of axillary and pubic hair. Finally, menarche occurs, typically 2 to 5 years after breast bud development.[2,9] During this time, the hypothalamic–pituitary– ovarian–uterine axis continues to mature. Over an approximately 2-year span, anovulatory cycles with subnormal progesterone production and shortened intermenstrual intervals are gradually replaced by normal ovulatory menstrual cycles.[2]

The typical ovulatory cycle has a 24- to 35 day interval between menses.[10] Longer intervals are often associated with anovulation, although when bleeding occurs, it is often associated with some corpus luteal activity.[11] Improved nutrition and living conditions are thought responsible for the gradual decline in mean menarchal ages over the last century. In North America, it is currently 12.4 years, with a range of 9 to 17 years.[12]

Genital Embryology

The sex of the embryo is determined genetically at the time of fertilization, but the gonads do not develop sex-specific characteristics until the seventh week of gestation.[13,14] The mesodermal urogenital ridges give rise to parts of both the genital and the urinary systems. Because of the association of uterine and renal development, the concurrent presence of abnormalities in both systems is quite common. Thus, if a gynecologic anomaly is found in a patient, one should evaluate for a possible renal or urinary tract anomaly, such as complete renal agenesis (**Fig. 5–3**), and vice-versa.[1,13,15,16]

Both sexes develop two different pairs of genital ducts. Components of the wolffian (mesonephric) duct system develop into the epididymis, vas deferens, and seminal vesicles under the influence of testosterone in males. By 6 weeks, a mullerian (paramesonephric) duct has developed lateral to each ipsilateral wolffian duct. In the female fetus,

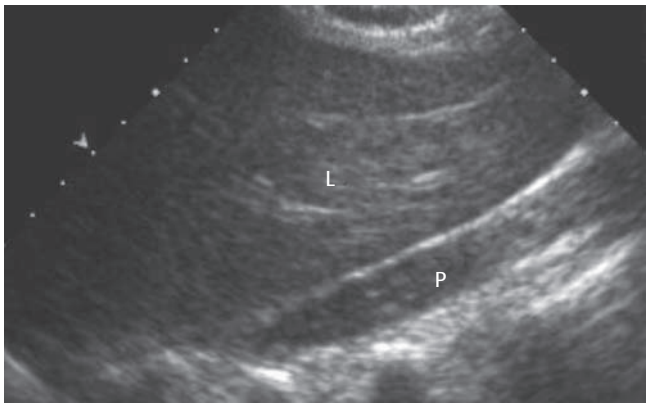

Figure 5–3 Renal agenesis associated with a congenital gynecologic anomaly. Right upper quadrant ultrasound. Longitudinal plane. The liver (L) and psoas muscle (P), but not the right kidney, are seen in the right upper quadrant of a 17-year-old with a mullerian duct system anomaly and right renal agenesis. If a kidney is not imaged in the renal bed it should be sought by nuclear medicine or other methods to rule out the possibility of an ectopic kidney rather than agenesis. (Image courtesy of SUNY Stony Brook Division of Body Imaging Teaching File.)

the mullerian duct system (MDS) develops into the fallopian tubes, uterus, and upper two thirds of the vagina, whereas the wolffian system degenerates. External genital development proceeds along female lines in an embryo unless androgens are present.[2,13,15] If the MDS is dysgenetic, as in Mayer-Rokitansky-Küster-Hauser syndrome, the uterus or vagina may be absent or rudimentary. Patients with this syndrome have normal karyotypes and normal secondary sex development, but have associated renal (50%) and skeletal (12%) anomalies.[2,13,16,17]

By 11-weeks gestational age, a Y-shaped uterovaginal primordium has developed into the two fallopian tubes, and fusion of a large portion of the MDS forms a single uterus and upper two thirds of the vagina. This event occurs with or without the presence of ovaries, as long as testes are not present and there are not high levels of androgens in the bloodstream.[15]

Lack of fusion or variably incomplete fusion of the mullerian duct system can lead to a wide spectrum of anomalies. A complete lack of fusion results in a didelphys uterus, which may consist of two vaginas, two cervices, and two uterine bodies. Partial fusion of only the caudal ends of the MDS results in a bicornuate uterus, characterized by variably separated uterine horns that communicate with a single uterine body, cervix, and vagina. The bicornuate uterus, which is often wider than normal, can be diagnosed on physical exam (usually when the patient is pregnant) by an anterior fundal depression, or sonographically when two endometrial cavities are imaged. The ultrasound diagnosis is most easily made when imaging is performed either during the secretory phase of the menstrual cycle or early in pregnancy, when the endometrial cavity or cavities are most easily seen (**Fig. 5–4**).[1,13,15]

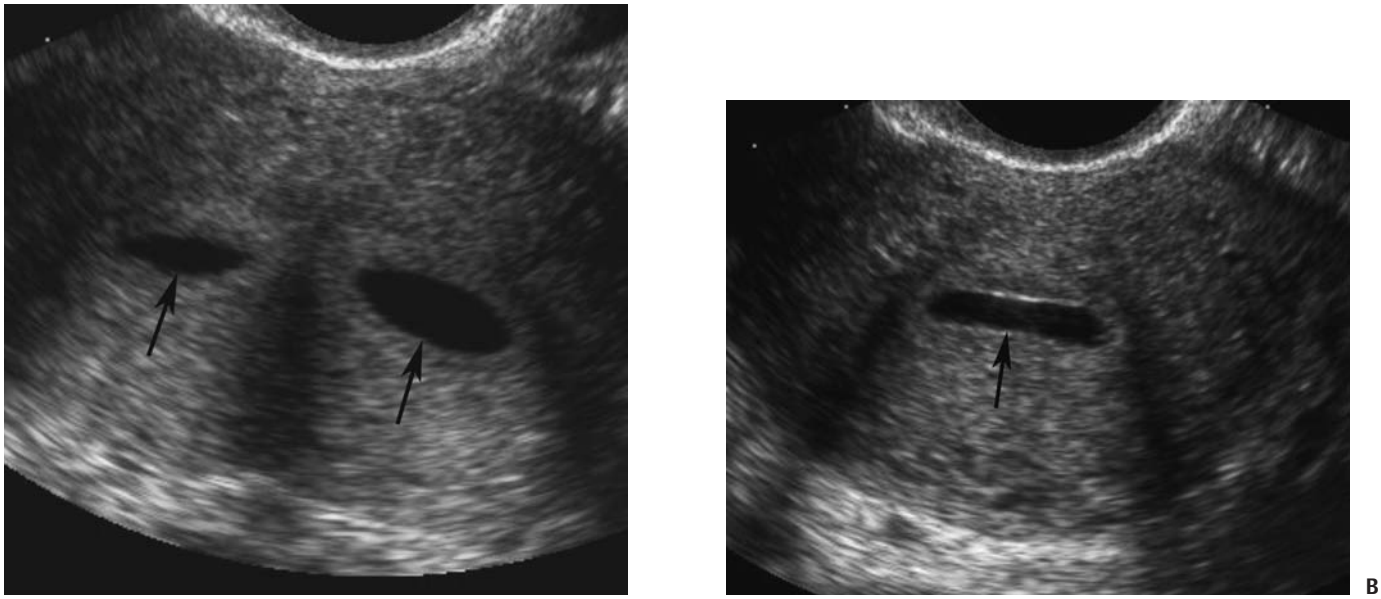

Figure 5–4 Bicornuate uterus. Transvaginal sonogram, transverse plane. **(A)** Two echogenic endometrial cavities (arrows) are noted in this patient whose uterus was imaged during a sonohystogram and whose diagnosis of a bicornuate uterus was an incidental finding. This image does not highlight the sometimes helpful associated finding of an anterior uterine depression where the uterine horns are separated. **(B)** An arrow points to a single endometrial cavity in the lower uterus. (Images courtesy of SUNY Stony Brook Division of Body Imaging Teaching File.)

At the point where the MDS joins the urogenital sinus, the lower third of the vagina develops by elongation of the primitive vaginal plate into a core of tissue that canalizes by week 20.[1,15,18] The lumen of the vagina is separated from the urogenital sinus vestibule by a hymenal membrane until late in fetal life. The hymen usually ruptures in the perinatal period, with only a thin fold of mucous membrane remaining around the vaginal entroitus.[15,19]

The Pediatric Uterus

Ultrasonography helps in the initial evaluation of patients with amenorrhea by determining whether uterine shape and size are premenarchal (infantile) or postmenarchal (adult). The shape and size of the uterus change during childhood. During the first few months of life, the uterus is influenced by transiently high levels of gonadotropins following placental separation. The typical newborn uterus is shaped like a spade, with the cervical anteroposterior (AP) measurement greater than that of the fundus, and the cervix twice as long as the fundus (**Fig. 5–5**). In a study of a group of neonates, Nussbaum et al found that the majority (58%) had a spade-shaped uterus. Of the remaining group, 32% had a tube-shaped uterus, with the AP measurement of the cervix equal to that of the fundus. They reported that 10% of their subjects showed the classic adult pear-shaped uterus with a fundus wider than the cervix (**Fig. 5–6**).[19] We have not found the pear-shaped uterus in the normal newborn group.

The neonatal uterus has a mean length of 3.5 cm. Transient hormonal stimulation of the neonatal uterus can result in some sonographic findings that are considered more typical of the adult uterus, including an echogenic central endometrial canal with a surrounding hypoechoic halo (seen in 29% of infant girls) and endometrial cavity fluid (seen in 23% of infant girls).[1,16] Under the lower gonadotropin levels found typically at ~3 months, the mean uterine length decreases to 2.6 to 3.0 cm.[19,20] After the first year of life, the uterus is typically tube-shaped (**Fig. 5–7**) and remains so through the next several years of childhood.[13,16,19]

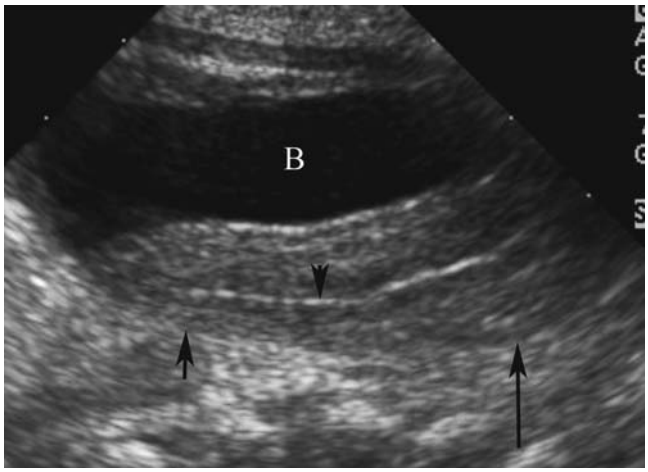

Figure 5–5 Neonatal uterus, longitudinal midline plane. A typical spade-shaped uterus of a newborn is seen posterior to the urinary bladder. The cervix (long arrow) is wider than the fundus (short arrow). A central echogenic endometrial stripe can be seen in the first few weeks of life (arrowhead).

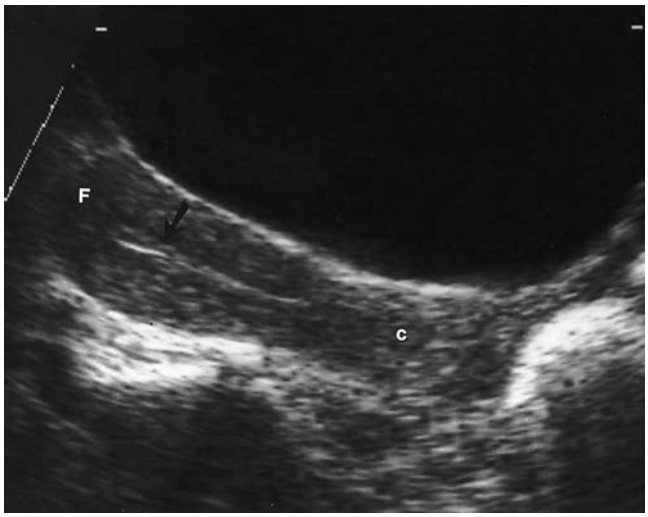

Figure 5–6 Normal postmenarchal adolescent uterus. Longitudinal midline plane. In the normal adult uterus, the anteroposterior dimension of the fundus (F) is greater than that of the cervix (c). The central endometrial echogenicity has a triple echogenic line appearance typical of the proliferative phase, rather than the single echogenic stripe typical of the secretory phase.

The length of the uterus increases gradually between 3 and 8 years of age, reaching an average measurement of 4.3 cm in the premenarchal child.[20–22] The increase in uterine length, its change to a pear shape, and the reversal of the ratio of corpus to cervical length are believed to be a consequence of increasing estradiol levels as well as two other independent variables: patient age and height.[20,21] There is a moderate correlation between uterine length and weight ($r = 0.69$).[21]

After puberty, the typical uterus measures 5 to 8 cm in length. It descends deeper into the pelvis and may become anteverted or retroverted.[1,23] In addition, cyclic endometrial changes can be seen on ultrasound. A well-defined "triple line," representing the echopenic functional layer and the central echogenic line of the coapted endometrial canal, is indicative of a proliferative endometrium. This triple line is replaced by a single echogenic stripe, representing the meeting of the thickening hyperechoic functional layers during the secretory phase of the endometrial cycle.[24]

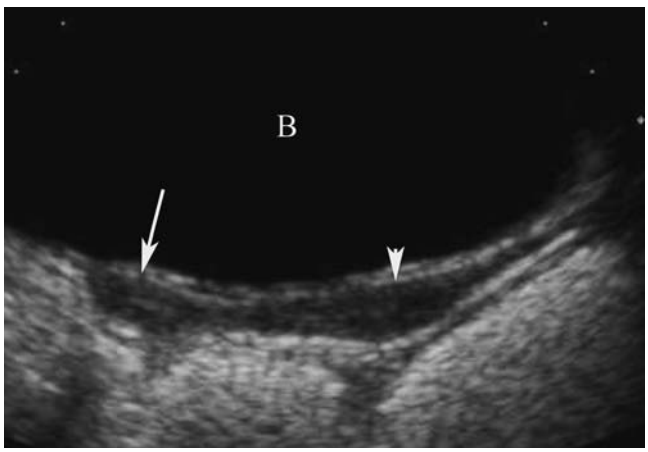

Figure 5–7 Tubular premenarchal uterus, longitudinal midline plane. A normal tubular premenarchal uterus in a 7-year-old girl. The large arrow points to the fundus and the arrowhead points to the cervix. A central endometrial stripe is seen. B, bladder.

Imaging Tests to Congenital Uterine Anomalies

The identification of the uterus and determination of its size are key pieces of diagnostic information in the evaluation of several pediatric and adolescent gynecologic disorders, including causes of amenorrhea.

Ultrasonography can aid in the diagnosis of anomalies of the mullerian duct system, particularly the bicornuate uterus and the uterus with partial or complete obstruction (**Fig. 5–8A**). Three-dimensional (3-D) ultrasound shows some further promise in the analysis of these anomalies.[25] Magnetic resonance imaging (MRI) with its multiplanar imaging has been successfully used to evaluate several of these anomalies (**Fig. 5–8B**). MRI, because of its accuracy and detail, is the study of choice for the further evaluation of MDS anomalies found on ultrasound, particularly in complex cases.[26] For example, MRI can identify the tissue composition of an intrauterine septum, helping to differentiate between a bicornuate uterus with a myometrium-containing septum and a septate uterus with a fibrous septum.[27–29]

The Pediatric Ovary

Premenarchal ovaries are best imaged sonographically. Normal premenarchal ovaries are almond shaped and typically found posterior and lateral to the uterus. They are often seen lateral to the uterus on transverse sonographic images while the transducer is angulated in a superior-inferior direction. On parasagittal scanning, ovaries appear medial and anterior to the iliac vessels. Although usually present at the level of the superior portion of the broad ligament, the ovaries may be found anywhere along their embryological course, from the inferior border of the kidneys to the broad ligament.[4] The true absence of an ovary is rare. If an ovary and its ipsilateral fallopian tube are found to be absent during surgery, it is more likely due to an antenatal torsion with secondary necrosis rather than ovarian agenesis.[1]

Concepts with regard to the sonographic analysis of the normal ovary for volume and echogenicity pattern have evolved over the past 15 years through the evaluation of both adults[30] and children.[31,32] The once classic adult ovary measurement of $3 \times 2 \times 1$ cm (3 cc volume) underestimates the normal mean ovarian volumes now reported in menstruating women, at 6 to 10 cc. At one time, the sonographic demonstration of pediatric ovaries was thought to be difficult and the normal mean ovarian volumes in patients under 10 years of age was reported to be as low as 0.7 cc.[32] However, Cohen et al imaged ovaries in 64% of 77

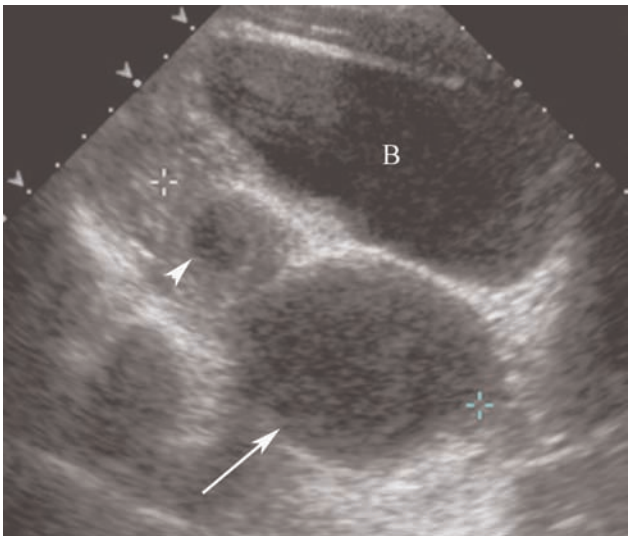

A

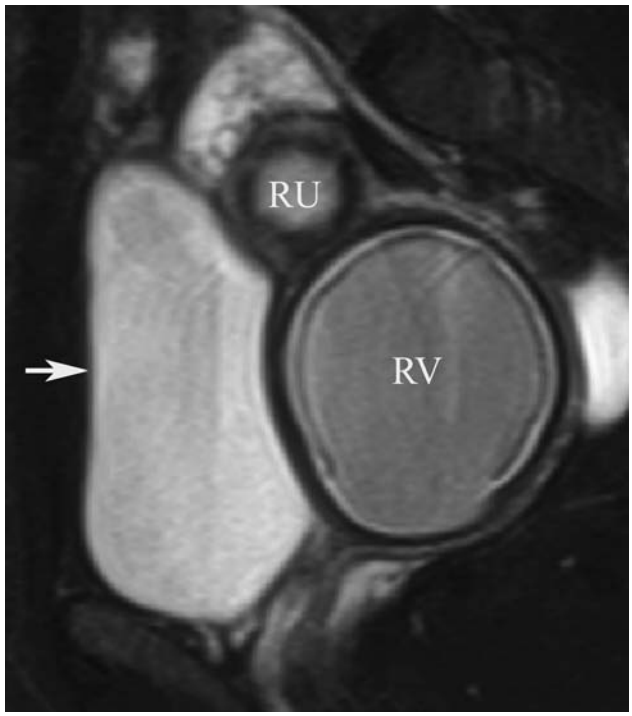

B

Figure 5–8 Vaginal obstruction in mullerian duct anomaly, didelphys uterus. **(A)** Transverse ultrasound showing the bladder (B) anterior to a fluid-filled obstructed right vagina (arrow) and uterus (arrowhead) of a teenager with two vaginas and two uteruses as part of a müllerian duct anomaly. **(B)** Sagittal T2-weighted magnetic resonance image to the right of midline shows a fluid-filled bladder (arrowhead) anterior to a fluid-filled obstructed right vagina (RV) in the same patient. RU, right uterus. (Images courtesy of SUNY Stony Brook Division of Body Imaging Teaching File.)

girls from birth to 2 years of age,[31] and in 78% of 101 girls between 2 and 12 years.[32]

Mean volumes for premenarchal girls range between 0.75 cc and 4.18 cc.[21,23] Salardi et al reported a statistically significant difference in ovarian size in children with Tanner 3 and higher stages of sexual development. These authors reported a volume of more than 3 cc for Tanner 3; 4 to 4.6 cc for Tanner 4; and 5 to 7.5 cc for Tanner 5.[33] Golden et al found the normal postpubertal ovarian volume in a series of teenagers to be 5.2 cc with a standard deviation of 2.7 cc.[34] Another study of women in their second decade found the mean ovarian volume to be 7.8 cc.[30]

The typical premenarchal ovary is no longer considered homogeneously solid in echogenicity, but heterogeneous, containing follicles/cysts (**Fig. 5–9**).[17,33] Microcysts (< 9 mm) can be demonstrated in as many as 72% of normal ovaries in children 2 to 6 years of age and in 68% of children 7 to 10 years of age. Even macrocysts (those > 9 mm) can be seen in premenarchal girls, although not as frequently as in postmenarchal girls.[32] Herter et al found that microcysts are common in prepubertal girls, but the presence of six or more follicles up to 10 mm in diameter in girls younger than 8 years of age may suggest central precocious puberty. Multicystic ovaries seemed to correlate with normal or premature pubertal stimuli.[35] The findings of cysts in the ovaries of premenarchal girls are consistent with reports in the pathology literature that have documented the presence of cystic follicles in the ovaries of fe-

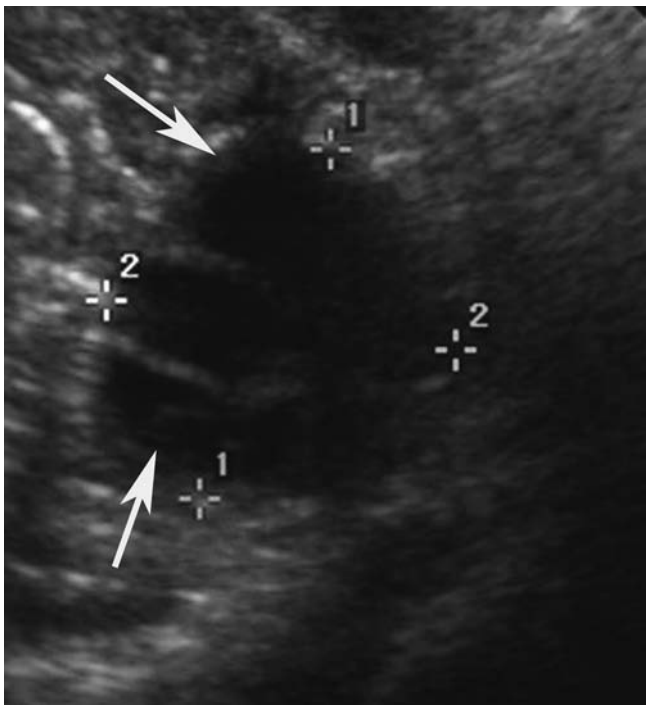

Figure 5–9 Normal premenarchal ovaries, transverse plane. Follicles and cysts are seen in the ovaries of a normal neonate, measuring up to 1.8 × 1.7 cm. Follicles and cysts can be a normal finding, rather than a rarity, in premenarchal children.

tuses, neonates, and children as far back as Rokitansky's report in 1861.[36] Therefore, the presence of a few follicles or cysts in a child cannot be used to conclude that the patient is in menarche or near menarche when evaluating for amenorrhea. In addition, the presence of such follicles/cysts cannot be used to differentiate between a normal child and a child with true isosexual precocious puberty. The pediatric ovary appears to be a dynamic organ undergoing constant internal change, with ovarian follicles beginning to mature at or even before birth.[17,23]

Ultrasound Imaging Techniques for Female Reproductive Organs

Technological advances in sonographic equipment over the last decade probably account for the more accurate imaging of premenarchal ovaries. The use of transvaginal (TV) imaging and, in virginal and other select patients who defer TV examination, transperineal or translabial scanning, as well as the now common availability of sensitive duplex and color Doppler imaging (CDI), have improved imaging of the female pelvis.[17] TV ultrasound has replaced the "water enema" technique in nonvirginal adults, although the latter technique is occasionally used for children. In the "water enema" technique, fluid is placed into the rectum by syringe injection through a Foley catheter. This displaces air and stool in the rectum, which can simulate a normal uterus. This technique can confirm the absence of a uterus, which is important information in the workup of very young patients with ambiguous genitalia and in older patients with amenorrhea. In TV ultrasound, a high-frequency transducer is placed into the upper vagina to evaluate adjacent pelvic structures. TV ultrasound has proven valuable in the identification of early intrauterine and ectopic pregnancies, and in the analysis of adnexal masses related to neoplasm or pelvic inflammatory disease (PID). Color Doppler imaging can be used as an adjunct in the evaluation of ectopic pregnancy by showing the high-velocity, low-impedance color flow that can be seen in the wall of a viable ectopic gestational sac. However, it should be noted that such flow can also be noted in a physiological corpus luteal cyst, making it less reliable for diagnosing an ectopic pregnancy. Color Doppler can be used for evaluation of ovarian and uterine vascular flow. However, the ability to image flow in ovaries, especially when the ovaries are small and when using a transabdominal (TA) approach, is limited.[17,37]

Transperineal or translabial sonography is performed by placing a transducer, covered by a glove or sheath containing gel, onto the introitus. This method has been used successfully to identify placenta previa in the late third trimester when TV ultrasound may be less desirable.[38] In children and adolescents, transperineal ultrasound has been used to image vaginal outflow obstruction, usually caused by an intact hymen.[39]

Table 5–1 Etiologies of Primary Amenorrhea35

Hypothalamus
Systemic illness
Chronic disease
Familial
Stress
Competitive athletics
Eating disorders
Obesity
Drugs
Pituitary
Idiopathic hypopituitarism
Tumor
Hemochromatosis
Thyroid Gland
Hypothyroidism
Hyperthyroidism
Adrenal Glands
Congenital adrenocortical hyperplasia
Adrenal tumor
Ovaries
Gonadal dysgenesis
Ovarian failure
Polycystic ovary syndrome
Ovarian tumor
Cervix
Agenesis
Vagina
Agenesis
Transverse Septum
Hymen
Imperforate

Source: From Emans S, Goldstein D. Pediatric Adolescent Gynecology. Boston: Little, Brown; 1990:149–242. Reprinted with permission.

Diagnostic Evaluation of Amenorrhea

Clinical Features, Testing, and Imaging

Indications for the ultrasound evaluation of the teenage pelvis include amenorrhea, delayed or retarded sexual development, lower abdominal pain, and pelvic mass.[1] Any of these individual complaints or a combination of them may be present in patients with amenorrhea, and the ultrasound findings, as well as the clinical presentation and causes, may overlap.[40] Conditions that may be responsible for pubertal delay in some patients may be responsible for primary or secondary amenorrhea in others. Primary amenorrhea has many causes and may involve several organ systems (**Table 5–1**). It may be seen in adolescents

with normal pubertal development as well as in those with delayed sexual development, with delayed menarche and some pubertal development, or with delayed menarche with virilization.[2,40]

Lack of pubertal development by 13 years of age is 2 standard deviations from the mean and should be evaluated. The workup for such a patient may be delayed for a year if there is a known debilitating illness as the cause or if the patient is involved in competitive or endurance sports such as running or ballet. Any interruption in sexual development is also a cause for concern and an endocrinologic workup should be performed. Only 0.03% of patients who fail to undergo menarche by 15.5 years will develop it later.[40]

Careful medical histories should be obtained from patients with amenorrhea. This should include a neonatal history, including information regarding maternal hormone ingestion or the presence of an androgen-producing tumor during pregnancy, which may account for virilization. A history of neonatal hypoglycemia may suggest hypopituitarism. Pertinent historical information also includes facts beyond the neonatal period, including growth data during childhood and any history of surgery, irradiation, or chemotherapy, eating disorders, and other psychological difficulties. Finally, a family history should be obtained, including the ages of menarche of family members and any possible genetic medical history, including endocrine or gynecologic abnormalities, such as congenital adrenocortical hyperplasia, thyroiditis, and ovarian tumors.

The patient should undergo a physical examination to determine whether she has a visual field disturbance or other neurological problem that may suggest a pituitary and/or other central nervous system cause of amenorrhea. A pelvic exam should include a vaginal smear and direct mucosal visualization. Red, thin vaginal mucosa is consistent with estrogen deficiency, whereas pink, moist vaginal mucosa is consistent with normal estrogenization. In pubertal patients, a pregnancy test should be done to rule out pregnancy as a cause of amenorrhea.[2,40]

Amenorrhea with Delayed Sexual Development

The age of onset of adolescence varies widely. Sexual development is considered delayed if there is a lack of breast budding by age 13 years. Patients whose sexual development is delayed typically have a small tubular (infantile) uterus rather than an adult uterus (**Fig. 5–10**). These hypoestrogenic patients can be divided into two major groups, depending on their levels of gonadotropin (i.e., FSH, LH) production.[1,2]

Hypogonadotropic Hypogonadism

Hypogonadotropic hypogonadism, characterized by low to normal LH and FSH levels, suggests pituitary or hypothalamic dysfunction as the cause of amenorrhea.[40] High prolactin levels suggest a pituitary cause of hypogonadotropic amenorrhea, whereas low prolactin levels suggest hypothalamic suppression of the pituitary.[2] Pituitary dysfunction may be the result of head trauma, including that caused by child abuse, leading to disruption of the pituitary stalk (usually with associated panhypopituitarism), tumors such as craniopharyngiomas (often presenting with visual field disturbances, headaches, and behavioral changes), pituitary microadenomas, infiltrative diseases, or prolactinomas. Causes of hypothalamic dysfunction include hypothalamic tumors and Kallman's disease (a lack of pulsatile release of gonadotropin-releasing hormone, associated with anosmia and midline craniofacial anomalies). Hypogonadotropic hypogonadism may also result from central causes such as systemic illness, constitutional growth delay, and extreme stress, which disrupt the endogenous release of GnRH. Systemic illnesses associated with such disruption include chronic diseases such as cystic fibrosis, sickle cell disease, and inflammatory bowel diseases (**Fig. 5–11**). Endocrinopathies associated with pubertal delay include hypothyroidism, Cushing's disease, and diabetes mellitus.[1,2,40,41]

Anorexia nervosa should also be included among these central causes of amenorrhea. Although typically this condition presents as a cause of secondary amenorrhea after the development of secondary sexual characteristics, it can and does occur in younger age groups and may therefore

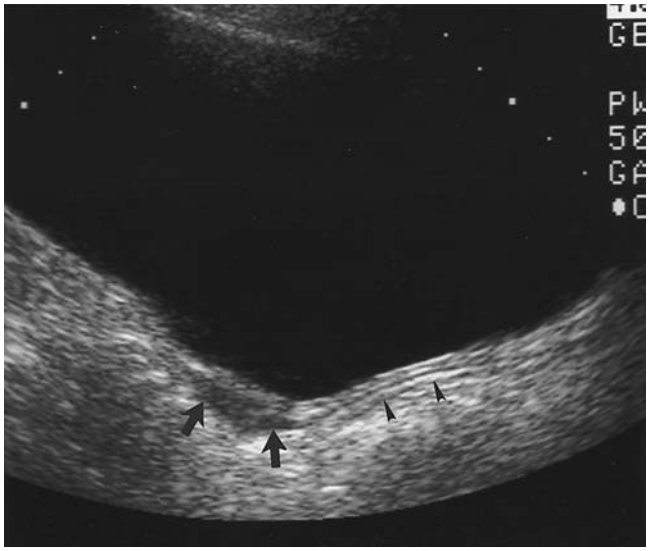

Figure 5–10 Infantile uterus in a 22-year-old woman with delayed puberty, longitudinal midline plane. A small, premenarchal- or infantile-appearing uterus with a tubular shape (arrows) is noted posterior to a large, fluid-filled bladder. Uterus length is 3.2 cm. Arrowheads outline the vagina. (From Cohen HL. Evaluation of the Adolescent and Young Adult with Amenorrhea: Role of US. RSNA Special Course in Ultrasound. Radiological Society of North America; 1996:171–183. Reprinted with permission from the Radiological Society of North America.)

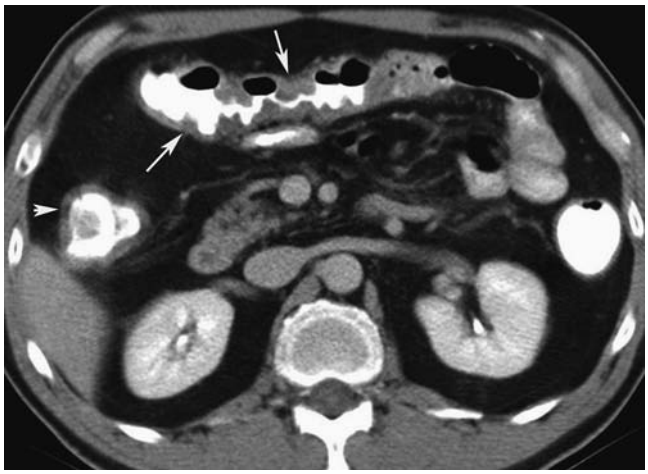

Figure 5–11 Amenorrhea in a patient with inflammatory bowel disease. Amenorrhea or delayed puberty may be due to many chronic diseases. Arrows point to intestinal wall thickening in a patient with Crohn's disease. (Images courtesy of SUNY Stony Brook Division of Body Imaging Teaching File.)

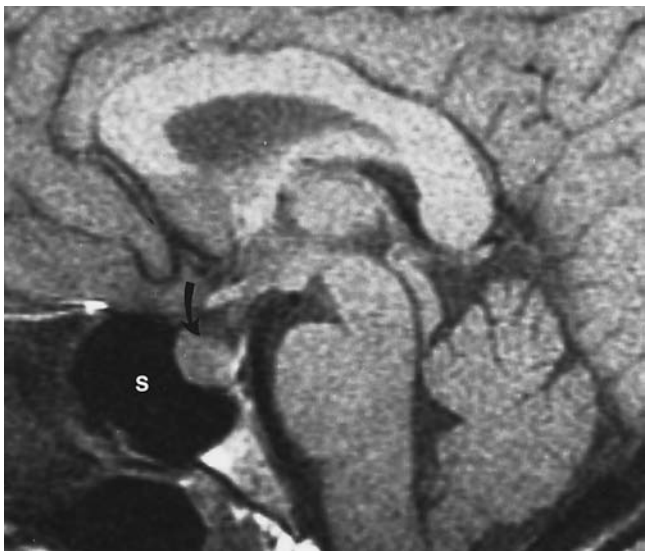

Figure 5–12 Pituitary adenoma. T1-weighted, midline sagittal image after gadolinium injection. A pituitary adenoma (arrow) is seen within the sella turcica of a young adult with headaches. The pituitary microadenoma is the most common pituitary tumor associated with amenorrhea. It is characteristically hypointense compared with the remainder of the pituitary on enhanced images. S, sphenoid sinus. (From Cohen HL. Evaluation of the Adolescent and Young Adult with Amenorrhea: Role of US. RSNA Special Course in Ultrasound. Radiological Society of North America; 1996:171–183. Reprinted with permission from the Radiological Society of North America.)

result in primary amenorrhea. Amenorrhea associated with anorexia nervosa usually occurs when weight loss is greater than 20% of normal body weight. Sobanski et al reported that all of a studied group of anorexic patients had ovaries that were significantly smaller than expected for their age. Those patients whom they reported as recovered with a "good outcome" had significantly greater ovarian volume measurements during follow-up examination than those patients who did not have a good outcome. Sobanski suggested that sonographic measurements of ovarian volumes may help determine recovery of ovarian function and predict a resumption of menses.[42]

Delayed sexual development can also be associated with anomalies, injuries, or infections of the central nervous system, including brain abscesses, tuberculosis, and prior cranial radiotherapy. Evaluation of amenorrhea caused by central nervous system pathology (usually pituitary or hypothalamic) is best done by computed tomography (CT) or MRI (**Fig. 5–12**). The role of sonography in these patients is the determination of the pelvic manifestations of these extrapelvic causes of delayed puberty or amenorrhea.

Hypergonadotropic Hypogonadism

Adolescents with hypergonadotropic hypogonadism, characterized by high FSH and high LH levels, have amenorrhea secondary to failure of the gonadal tissues to respond to endogenous gonadotropins. In pure forms, there is failure of development of secondary sexual characteristics as well as amenorrhea. Hypergonadotropic amenorrhea can be due to an abnormal karyotype such as Turner's syndrome or XY gonadal dysgenesis. Patients with normal karyotypes may have secondary ovarian failure due to radiation (usually 800 rads or greater to the pelvis), chemotherapy (transient amenorrhea occurs in 50% of women who undergo chemotherapy), or autoimmune oophoritis. Patients with these secondary causes of hypogonadotropic hypogonadism have varying degrees of pubertal development. Premature menopause, as a complication of chemotherapy or radiation therapy, is usually seen in those who are treated when 25 years of age or older. It is unusual in adolescents.[40,43,44]

Turner's syndrome, the most common human chromosomal abnormality, is also the most common example of gonadal dysgenesis associated with an abnormal karyotype. Half of these patients are isochromatous, 45X0. The remaining patients with Turner's syndrome may have a mosaic 45X or 46XX karyotype, or have a structural abnormality of their second X chromosome. These patients present with a spectrum of clinical manifestations ranging from normal development to the classic stigmata of the pure 45XO karyotype. Those patients with an isochromosome of the short arm of one of the X chromosomes may have associated Hashimoto's thyroiditis.[2,40]

Patients with classic Turner's syndrome are short in stature, have widely spaced nipples, a shield-shaped chest, low-set ears, cubitus valgus, lymphedema, a high-arched palate, a low hairline, short fourth and/or fifth metacarpals, large aortic roots, multiple pigmented nevi, and a webbed neck. One fourth of these patients have renal anomalies, usually horseshoe kidneys. Affected patients typically have a history of delayed onset of puberty and primary amenorrhea. In early adolescence, patients with

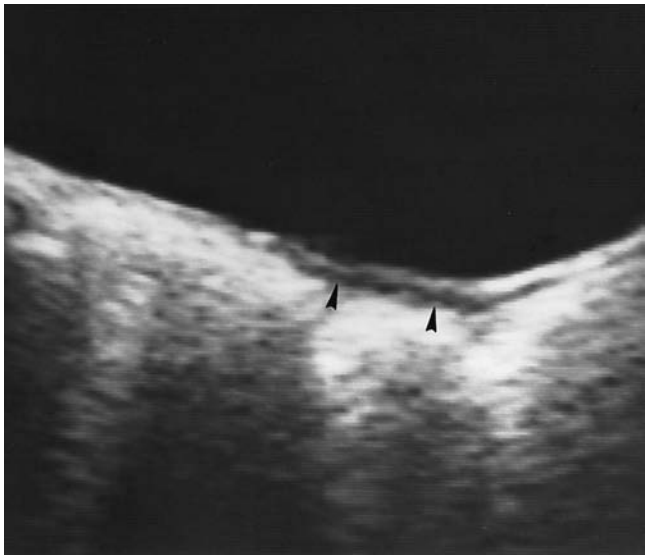

Figure 5–13 Turner's syndrome in a teenager with delayed puberty. Midline longitudinal plane. An infantile uterus (arrowheads) is seen in this 15½-year-old girl with a 45X0 karyotype. Her ovaries could not be definitively imaged. (From Cohen HL. Evaluation of the Adolescent and Young Adult with Amenorrhea: Role of US. RSNA Special Course in Ultrasound. Radiological Society of North America; 1996:171–183. Reprinted with permission from the Radiological Society of North America.)

Turner's syndrome have prepubertal genitalia, sparse axillary and pubic hair, and bilateral streak gonads. They have a normally formed uterus and vagina that will respond to exogenous hormones. In later adolescence, at around 15 to 16 years, many of these patients will develop pubic and axillary hair, but have no breast development or vaginal mucosal estrogenization.

Sonographic evaluation characteristically shows a prepubertal (infantile) uterus (**Fig. 5–13**). The typical dysgenetic or streak gonads are difficult to image. When imaged, the ovaries typically measure less than 1 cc and there is oocyte depletion seen upon pathological examination. Shawker et al[45] noted that some patients with Turner's syndrome, particularly those with mosaic karyotypes, have normal ovaries. Such patients may have only partial ovarian failure and consequently the ovaries may be able to produce estrogen. However, estrogen production in patients with Turner's syndrome can also be secondary to an associated theca lutein cyst or a germ cell tumor. If the karyotype of a patient with gonadal dysgenesis and ovaries includes a Y chromosome, there is an increased risk for the development of gonadoblastoma within the dysgenetic ovary. Evidence of an asymmetrically enlarged, solid adnexa on sonography should arouse suspicion for a gonadoblastoma.[1,2,40,45]

Pseudohermaphroditism

Sonography has been shown to be helpful in the evaluation of children whose karyotype, gonadal anatomy, and genital development are not in accord. This group of patients includes true hermaphrodites (a rare phenomenon), pseudohermaphrodites (also known as male and female intersex, as defined by the type of gonad present), and patients with mixed gonadal dysgenesis.[1]

Female pseudohermaphroditism (intersex) is a condition in which chromosomally normal females (46XX) have masculinized external genitalia. It is usually diagnosed in the neonatal period and is most often due to adrenal hyperplasia, which is often congenital. Occasionally, however, it results from maternal ingestion of androgens in early pregnancy or less frequently from endogenous production of androgens by a masculinizing ovarian tumor in the mother. Sonography can depict the enlarged adrenal glands as well the presence of a normal uterus in the affected newborn. These patients are potentially fertile after satisfactory genital reconstruction and female sex assignment.[1,19]

Male pseudohermaphrodites (intersex) may present with what appears to be hypergonadotropic amenorrhea. Some patients may have incomplete testosterone production, whereas others with early destruction or dysgenesis of the testes will have no production of testosterone. Decreased or lack of testosterone levels and a lack of production of mullerian inhibition factor result in a karyotypically normal male with a female phenotype (except for partial

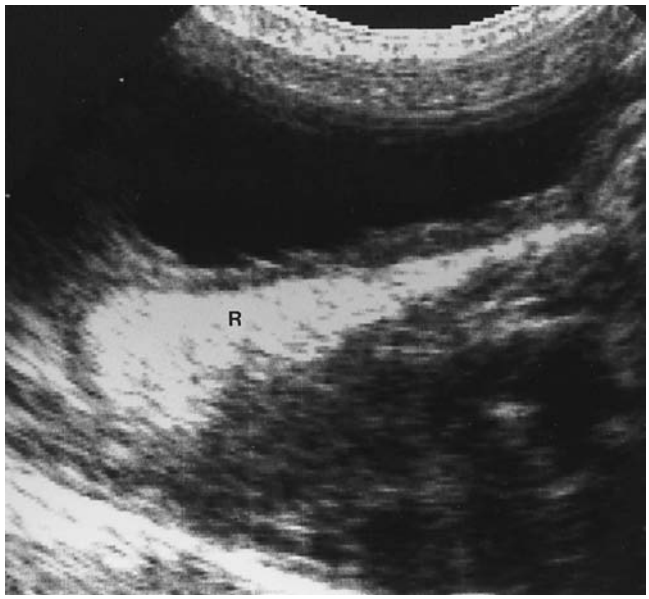

Figure 5–14 Testicular feminization syndrome. Midline longitudinal view. No uterus could be imaged in a phenotypically normal 17-year-old girl who was raised as such and presented with amenorrhea. She proved to have a 45 XY karyotype with complete androgen insensitivity (i.e., testicular feminization syndrome). Echogenic air in the rectosigmoid region (R) facilitates demonstration of the absence of a uterus, which normally should be seen between the bowel and the bladder wall (B). (From Cohen HL, Bober S, Bow S. Imaging the pediatric pelvis: the normal and abnormal genital system and simulators of its diseases. Urol Radiol 1992;14:273–283. Reprinted with permission from Springer Verlag, New York.)

masculinization of the external genitalia). There is variable development of the mullerian elements, such as the uterus, vagina, and fallopian tubes. These patients have no secondary sexual development at puberty and may have an infantile uterus on sonography.[1,14]

An unusual form of male intersex is the testicular feminization syndrome in which patients have 46XY karyotypes and well-formed testes (usually undescended within the abdomen or inguinal region) that produce androgens and mullerian inhibition factor. These patients, however, lack an end organ response to androgens. Mullerian system development is inhibited and therefore, affected patients do not develop a uterus, fallopian tubes, or upper two thirds of the vagina. Patients appear as phenotypically normal females, although they may have inguinal or labial masses due to the undescended testes. They have normal breast development (i.e., secondary female sexual characteristics) due to circulating estrogens (produced by the testes and adrenal gland) and a peculiar lack of body hair, as well as absence of acne. When these patients present, typically with amenorrhea, ultrasonography demonstrates the absence of either a uterus (**Fig. 5–14**) or ovaries.[1,46]

Female Adolescence with Virilization

Testosterone is the most potent of the circulating androgens. It is produced in normal females by the adrenal gland (25%), by the ovaries (25%), and by peripheral conversion of delta-4-androstenedione (50%). Only 1% of testosterone is typically free and biologically active. Virilization from excess androgens produces voice deepening, clitoromegaly, increased muscle mass, and temporal balding.

One in 20 ovarian tumors are hormonally active. Amenorrhea and virilization can occur in patients with hormonally active, androgen-producing tumors. Increased free testosterone may be seen in virilizing tumors of the adolescent ovary. These are usually Sertoli-Leydig cell tumors (once known as androblastomas or arrhenoblastomas) or hilar cell tumors. The marked androgen production of these rare, rapidly growing tumors results in amenorrhea, vaginal mucosal atrophy, decreased breast size, and virilization. Sonography will show a unilaterally enlarged solid ovary with abnormal echogenicity. Of interest is the fact that testosterone-producing *adrenal* tumors rarely result in amenorrhea in adolescent patients.[1,2,40,47]

There are also hormonally active ovarian tumors that produce estrogen. The most common such malignant tumor of the ovary is the granulosa cell tumor. These tumors grow rapidly and often disrupt the normal menstrual cycle, producing either amenorrhea or menorrhagia. Thecomas can also result in significant estrogen production.[2]

Polycystic Ovary Syndrome

Androgen excess may result from causes unrelated to tumors. It may occur in association with idiopathic hirsutism, late-onset congenital adrenal hyperplasia, exaggerated adrenarche, Cushing's disease, hyperprolactinemia, and acromegaly. However, most hyperandrogenic adolescents will have polycystic ovary syndrome (PCOS), also known as Stein-Leventhal syndrome.[48] Polycystic ovary syndrome is the most common cause of secondary amenorrhea associated with a hyperandrogenic state. Patients with this syndrome are usually 15 to 30 years of age and present with hirsutism (62%) and obesity (31%).[1] In a study of 466 women with PCOS, 80% had menstrual irregularities.[2,49] This is thought to be secondary to chronic anovulation.[50]

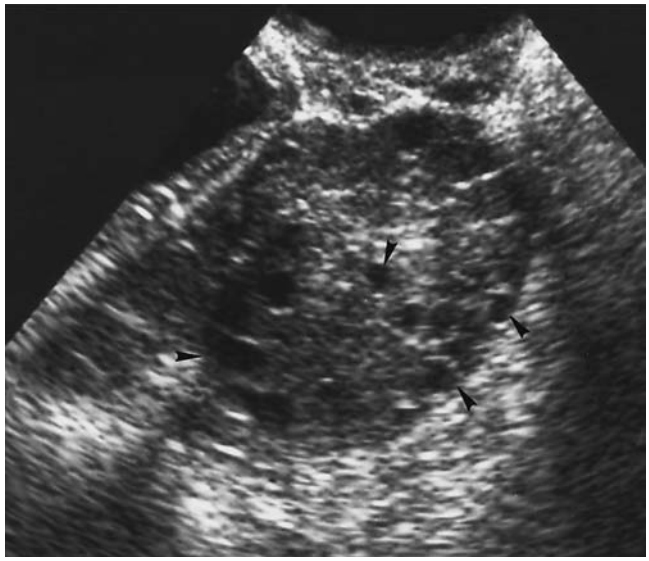

Figure 5–15 Polycystic ovary syndrome (PCOS) in a 20-year-old woman with hirsutism, obesity, and oligomenorrhea. Transvaginal ultrasound, transverse oblique plane. This right ovary is enlarged and contains more than 10 follicles that measure less than 8 mm in diameter. The left ovary had a similar appearance. Arrowheads point to a few of the follicles. The area of bright echogenicity (arrowhead) in the middle of the ovary may represent increased ovarian stroma found in patients with PCOS. (From Cohen HL. Evaluation of the Adolescent and Young Adult with Amenorrhea: Role of US. RSNA Special Course in Ultrasound. Radiological Society of North America; 1996:171–183. Reprinted with permission from the Radiological Society of North America, Oakbrook, IL.)

Laboratory confirmation of PCOS is based on the demonstration of an increased ratio of LH to FSH and elevated androgen levels.[45,50] The sonographic criteria for diagnosing PCOS remain confusing because of the variable criteria reported in the literature, whether patients are examined by transabdominal or TV ultrasonography.[51] In addition, normal ultrasound findings overlap with those considered to be evidence of PCOS in patients with known PCOS. Patients with PCOS often have an increased number of subcapsular follicles as well as enlarged, hyperechoic ovaries (**Fig. 5–15**).

Authors have suggested that PCOS may be diagnosed if patients have at least one of the following: two or more follicles measuring 2 to 9 mm (but no greater) in diameter,

or increased ovarian volume (> 10 cc).[52] This is problematic because many normal patients can have these findings. Herter et al reported that ovarian volumes of greater than 10 cc in adolescent girls with either or both menstrual disorders and hirsutism are suggestive of PCOS.[53,54] Takahashi et al noted mean ovarian volumes of 10.3 cc in 47 affected patients, a volume significantly greater than those of their control group. In that study, 94% of the patients with PCOS had either an ovarian volume greater than 6.2 cc or more than 10 follicles ranging between 2 and 8 mm in diameter. Only 6% of patients had what the authors defined as a normal number of follicles and ovarian volume.[51] Areas of increased intraovarian echogenicity have been attributed to ovarian stromal hypertrophy, which is thought to be secondary to hyperandrogenism in PCOS patients. Compared with normal ovaries, ovaries with stromal hypertrophy have larger volumes and demonstrate lower vascular resistance on Doppler evaluation.[45,52] High resistive indices are noted in the *uterine* arteries due to high androstenedione levels.[55,56]

Not all polycystic ovaries are due to hyperandrogenism. Unopposed estrogen stimulation from any source can result in polycystic ovaries. Genetic deficiencies of the enzymes 21-hydroxylase, 3-β-hydroxysteroid dehydrogenase, or 11-β hydroxylase are also associated with the development of polycystic ovaries.[1]

Eugonadism Estrogenization or Vaginal Obstruction

The absence of menses after development of secondary sexual characteristics suggests late disruption of the hypothalamic–pituitary–ovarian–uterine axis or outflow (uterine or vaginal) obstruction.[2] Ultrasound provides the best images for evaluation of such patients with primary amenorrhea and estrogenization because it depicts the genital anatomy, allowing the diagnosis of possible congenital anomalies or uterine outflow obstruction. This group also includes the myriad of causes of hypogonadotropic hypogonadism, in which estrogen levels are high enough to allow the normal follicular portion of the cycle but not high enough to allow normal menstrual cyclicity. Pelvic ultrasound findings in these patients may show abnormalities related to the vagina (imperforate hymen, vaginal atresia, or stenosis), the uterus (intersex-agenesis or testicular feminization syndrome), or the ovary (gonadal dysgenesis, Stein-Leventhal syndrome, or neoplasm).

If an ultrasound examination shows a solid midline mass in an adolescent girl with amenorrhea, the patient may have a distended uterus (metro) or vagina (colpos) or a combination of the two, which contains relatively echoless fluid or secretions (hydro) or variably echogenic blood (hemato) resulting from hormonal stimulation and obstructed menstrual outflow. Hematometrocolpos (**Fig. 5–16**) appears on ultrasound scans as a distended midline tubular structure between the bladder and the rectum that contains fluid with variable echogenicity. The peripheral wall is thick at the level of the uterus (due to the normal myometrial thickness) and thin at the level of the vagina. The scattered echoes in the fluid are due to cellular debris, mucoid material, and/or blood. Two thirds of cases are secondary to an imperforate hymen. In the remaining patients, the obstruction may be due to a complete vaginal

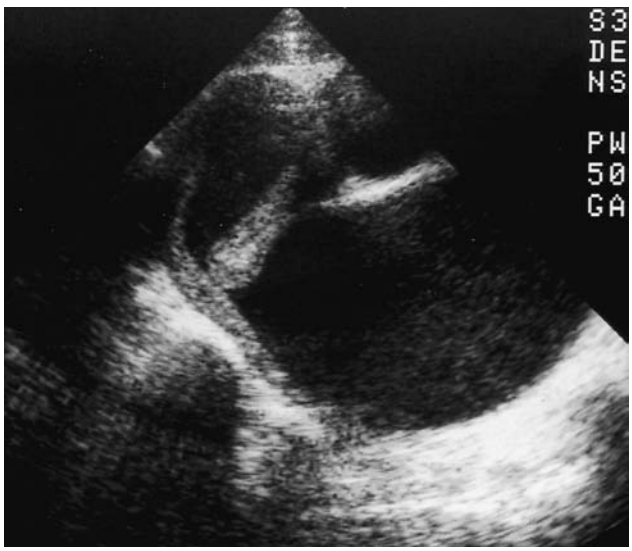

A

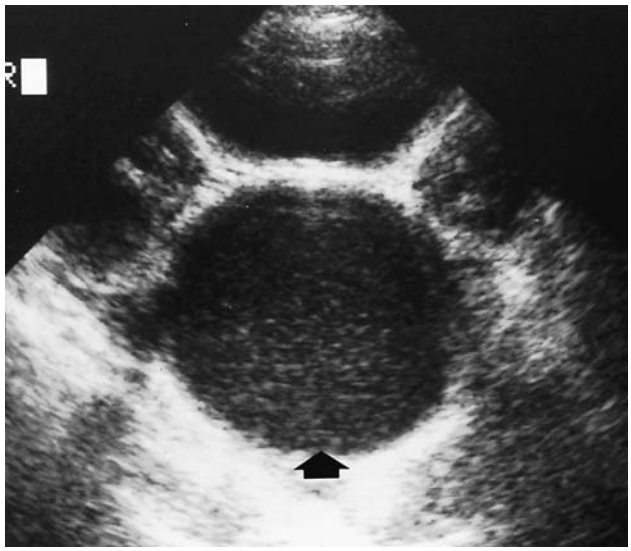

B

Figure 5–16 Hematometrocolpos. **(A)** Longitudinal midline plane. There is echogenic (hemorrhagic) debris within the fluid-filled and dilated vagina and uterus of this 14-year-old girl with hematometrocolpos due to an imperforate hymen. An open arrow points to the thick uterine wall; by comparison, the wall of the distended vagina is thin. (From Cohen HL, Bober S, Bow S. Imaging the pediatric pelvis: the normal and abnormal genital system and simulators of its diseases. Urol Radiol 1992;14:273–283. Reprinted with permission from Springer Verlag, New York.) **(B)** Pelvic ultrasound, transverse plane. An arrow points to the distended, debris-filled vagina of another teenager with hematometrocolpos due to an imperforate hymen. (From Cohen HL. Evaluation of the Adolescent and Young Adult with Amenorrhea: Role of US. RSNA Special Course in Ultrasound. Radiological Society of North America; 1996:171–183. Reprinted with permission from the Radiological Society of North America, Oakbrook, IL.)

membrane, vaginal stenosis, or vaginal atresia. Vaginal stenosis and atresia have been associated with anomalies of the gastrointestinal tract, genitourinary tract, and cardiovascular and skeletal systems.[1,17]

Postmenarchal females with vaginal or uterine obstruction can present with a history of intermittent monthly abdominal or pelvic pain and no history of menses or with an abdominal mass. The degree of distention of the uterus/vagina is related to the degree of obstruction and the time that has elapsed between menarche and presentation. The hematometrocolpos may be large enough to obstruct venous or lymphatic flow in the lower extremities or cause hydronephrosis due to obstruction of the ureters or bladder. Occasionally, patients have a history of difficulty with micturition. This condition is rare in neonatal life, but occurs in one of 1000 to 2000 teenagers.

When only hematometra is present, one must consider a more unusual abnormality such as cervical dysgenesis or obstruction of one horn of a bicornuate system. It can be more difficult to make a diagnosis when there is obstruction of only one uterine horn or one vagina in a duplicated genital system (**Fig. 5–8**). Urometrocolpos has been reported in patients with ectopic ureters implanting in the vagina proximal to the site of obstruction.[1,6,14,17]

Sonography or MRI of the vagina, cervix, and uterus helps provide important presurgical anatomical information.[1,6,14,17,26] For example, transverse perineal ultrasound may define the thickness of an imperforate hymen (**Fig. 5–17**).[39]

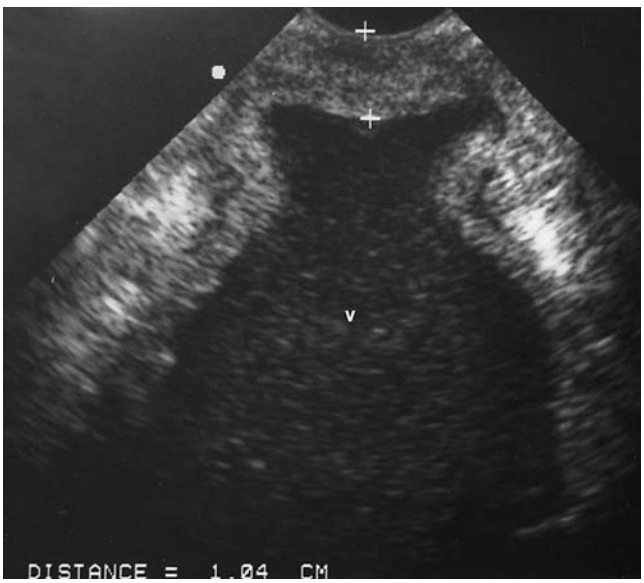

Figure 5–17 Hematometrocolpos, transperineal technique. A transducer placed on the perineum of a teenager with an imperforate hymen and hematometrocolpos shows a membrane (cursors) measuring 1.04 cm in thickness superficial to the distended, fluid-filled vagina. The vagina contains echogenic (hemorrhagic) debris. v, vagina. (From Cohen HL. Evaluation of the Adolescent and Young Adult with Amenorrhea: Role of US. RSNA Special Course in Ultrasound. Radiological Society of North America; 1996:171–183. Reprinted with permission from the Radiological Society of North America,Oakbrook, IL.)

Amenorrhea due to Uterine Aplasia or Hypoplasia

Fifteen percent of primary amenorrhea cases are thought to be due to absence or hypoplasia of the uterus. This diagnosis is suggested by a total absence of the uterus, but the presence of normal ovaries. Uterine agenesis is most often a result of testicular feminization or the Mayer–Rokitansky–Küster–Hauser syndrome. Mayer–Rokitansky–Küster–Hauser syndrome patients have amenorrhea due to vaginal atresia with variable uterine abnormalities. Despite an absent or severely atretic uterus and vagina, the ovaries and the fallopian tubes are normal. Approximately 50% of patients have unilateral renal anomalies and one eighth have skeletal abnormalities. They have a normal female karyotype and normal secondary sexual characteristics.[1,17,57]

Secondary Amenorrhea

Secondary amenorrhea is amenorrhea that occurs after menses has been established. The conditions that cause delayed puberty and primary amenorrhea may also cause secondary amenorrhea.

Pregnancy is the most common cause of secondary amenorrhea in girls older than 9 years of age. As little as a 2- to 3-week delay in menses should raise a clinical concern for pregnancy and the need to perform a pregnancy test.[40] Ultrasonography is most effective in the diagnosis of suspected pregnancy. TV sonography allows earlier and more accurate diagnosis of early pregnancy, whether intrauterine or extrauterine (ectopic) in location (**Fig. 5–18**).

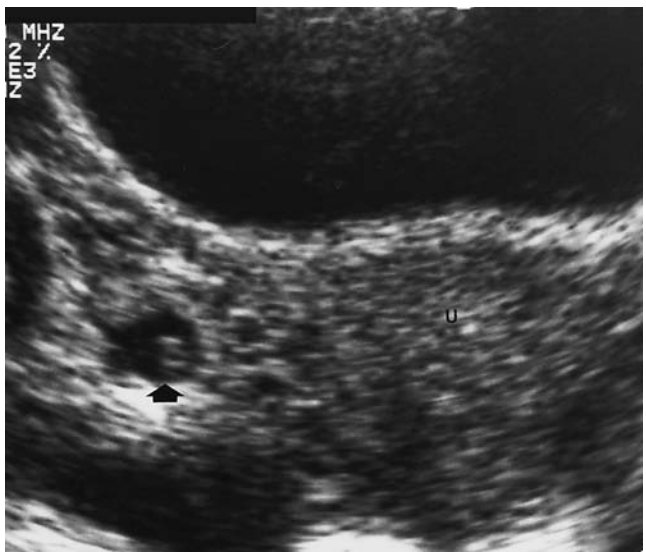

Figure 5–18 Ectopic pregnancy, transverse plane. An arrow points to the ectopic gestational sac in the right adnexa of a 16-year-old girl with amenorrhea. No intrauterine pregnancy was noted. U, uterus. (From Cohen HL. Evaluation of the Adolescent and Young Adult with Amenorrhea: Role of US. RSNA Special Course in Ultrasound. Radiological Society of North America; 1996:171–183. Reprinted with permission from the Radiological Society of North America, Oakbrook IL.)

An unusual cause of secondary amenorrhea is Asherman's syndrome. This disorder, which is unusual in adolescence, follows intrauterine instrumentation, such as endometrial curettage. Deep curettage with denudation of the basalis layer of the endometrium is thought to interfere with normal endometrial regeneration. The inability to regenerate endometrium allows the formation of adhesions in the endometrial cavity. Asherman's syndrome causes not only amenorrhea, but also hypomenorrhea, sterility, or habitual abortions.[58]

Conclusion

The normal menstrual cycle and female reproductive physiology are marvels of complexity that depend on the integrated actions of several body systems. The intricacies of menses are not completely understood. Multiple factors have a role in menarche and in regulating the menstrual cycle; these include embryological, genetic (karyotype), anatomical, and endocrinologic factors, along with psychological and other, as of yet, not clearly understood factors. Imaging is only one part of the workup of patients with amenorrhea, but the information provided by imaging is vital. Ultrasonography is the key tool for screening patients with amenorrhea and is often the only imaging tool necessary for the pelvic evaluation of such patients.

References

1. Cohen HL, Haller JO. Pediatric and adolescent genital abnormalities. Clin Diagn Ultrasound 1989;24:187–216
2. Reid R. Amenorrhea. In: Copeland L, ed. Textbook of Gynecology. Philadelphia: WB Saunders; 1993:367–387
3. Emans S, Goldstein D. The physiology of puberty. In: Emans S, Goldstein D, eds. Pediatric and Adolescent Gynecology. 3rd ed. Boston: Little, Brown; 1990:95–124
4. Ganong W. The gonads: development and function of the reproductive system. In: Ganong W. Review of Medical Physiology. 17th ed. Norwalk, CT: Appleton & Lange; 1995:399–402
5. Rhoades RA, Tanner GA. The female reproductive system. In: Medical Physiology. 1st ed. Baltimore: Lippincott Williams & Wilkins; 1995:757–776
6. Eldering J, Nay M, Hoberg L, Longcope C, McKracken J. Hormonal regulation of prostaglandin production by rhesus monkey endometrium. J Clin Endocrinol Metab 1990;71596–71604
7. Conte FA, Grumbach M, Kaplan S. A diphasic pattern of gonadotropin secretion in patients with the syndrome of gonadal dysgenesis. J Clin Endocrinol Metab 1975;40:670–674
8. Doring G. The incidence of anovular cycles in women. J Reprod Fertil Suppl 1967;6:77–81
9. Burstein S, Burstein R. Reply: pubertal data for growth velocity charts. J Pediatr 1986;109:564–565
10. Rosenfeld R, Garcia C. A comparison of endometrial histology with simultaneous plasma progesterone determinations in infertile women. Fertil Steril 1976;27:1256–1266
11. Sherman B, Korenman S. Hormonal characteristics of the human menstrual cycle throughout reproductive life. J Clin Invest 1975; 55:699–706
12. Bullough V. Age at menarche: a misunderstanding. Science 1981;213:365–366
13. Cohen HL, Bober S, Bow S. Imaging the pediatric pelvis: the normal and abnormal genital system and simulators of its diseases. Urol Radiol 1992;14:273–283
14. Grimes C, Rosenbaum D, Kirkpatrick J Jr. Semin Roentgenol 1982; 17:284–301
15. Moore K. Before We Are Born: Basic Embryology and Birth Defects. 3rd ed. Philadelphia: WB Saunders; 1989:180–120
16. Cohen HL. The female pelvis. In: Siebert J, ed. Syllabus: Current Concepts: A Categorical Course in Pediatric Radiology. Chicago: RSNA Publications; 1994:65–72
17. Rosenberg H, Sherman N, Tarry W, Duckett J, Snyder H. Mayer-Rokitansky- Küster-Hauser syndrome: US aid to diagnosis. Radiology 1986;161:815–819
18. Nussbaum AR, Sanders RC, Jones MD. Neonatal uterine morphology as seen on real-time US. Radiology 1986;160:641–643
19. Goldman H, Eaton D. Pediatric uroradiology. In: Elkin M, ed. Radiology of the Urinary System. Boston: Little, Brown; 1980: 1034–1109
20. Orsini L, Salardi S, Pilu G, Bovicelli L, Cacciari E. Pelvic organs in premenarchal girls: real-time ultrasonography. Radiology 1984; 153:113–116
21. Eisenberg P, Cohen HL, Mandel F, et al. US analysis of premenarchal gynecologic structures. J Ultrasound Med 1991;10:S30
22. Herter LD, Golendziner E, Flores JA, Becker E Jr, Spritzer PM. Ovarian and uterine sonography in healthy girls between 1 and 13 years old: correlation of findings with age and pubertal status. AJR Am J Roentgenol 2002;178:1531–1536
23. Deutsch A, Gosink B. Normal female pelvic anatomy. Semin Roentgenol 1982;17:241–250
24. Forrest T, Elyaderani M, Muilenburg M, Bewtra C, Kable W, Sullivan P. Cyclic endometrial changes: US assessment with histologic correlation. Radiology 1988;167:233–237
25. Kupesic S. Clinical implications of sonographic detection of uterine anomalies for reproductive outcome. Ultrasound Obstet Gynecol 2001;18:387–400
26. Troiano RN. Mullerian duct anomalies: imaging and clinical issues. Radiology 2004;233:19–34
27. Carrington B, Hricak H, Nuruddin R, Secaf E, Laros R Jr, Hill E. Mullerian duct anomalies: MR imaging evaluation. Radiology 1990; 176:715–720
28. Popovich M, Hricak H. Magnetic resonance imaging in the evaluation of gynecologic disease. In: Callen P, ed. Ultrasonography in Obstetrics and Gynecology. 3rd ed. Philadelphia: WB Saunders; 1994: 660–688
29. Fielding JR. MR imaging of the female pelvis. Radiol Clin North Am 2003;41:179–192
30. Cohen HL, Tice H, Mandel F. Ovarian volumes measured by US: bigger than we think. Radiology 1990;177:189–192
31. Cohen HL, Shapiro M, Mandel F, Shapiro M. Normal ovaries in neonates and infants: a sonographic study of 77 patients 1 day to 24 months old. AJR Am J Roentgenol 1993;160:583–586
32. Cohen HL, Eisenberg P, Mandel F, Haller J. Ovarian cysts are common in premenarchal girls: a sonographic study of 101 children 2–12 years old. AJR Am J Roentgenol 1992;159:89–91
33. Salardi S, Orsini L, Cacciari E, Bovicelli L, Tassoni P, Reggiani A. Pelvic ultrasonography in premenarchal girls: relation to puberty and sex hormone concentrations. Arch Dis Child 1985;60:120–125
34. Golden N, Cohen H, Gennari G, Neuhoff S. The use of ultrasonography in the evaluation of adolescents with pelvic inflammatory disease. Am J Dis Child 1987;141:1235–1238

35. Herter LD, Golendziner E, Flores JA, et al. Ovarian and uterine findings in pelvic sonography: comparison between prepubertal girls, girls with isolated thelarche, and girls with central precocious puberty. J Ultrasound Med 2002;21:1237–1238
36. Polhemus DW. Ovarian maturation and cyst formation in children. Pediatrics 1953;11:588–594
37. Pellerito J, Taylor K, Quedens-Case C, et al. Ectopic pregnancy: evaluation with endovaginal color imaging. Radiology 1992;183: 407–411
38. Hertzberg BS, Bowie J, Carroll BA, Kliewer M, Weber T. Diagnosis of placenta previa during the third trimester: Role of transperineal sonography. AJR Am J Roentgenol 1992;159:83–87
39. Scanlan K, Pozniak M, Fagerholm M, Shapiro S. Value of transperineal sonography in the assessment of vaginal atresia. AJR Am J Roentgenol 1990;154:545–548
40. Emans S, Goldstein D. Delayed puberty and menstrual irregularities. In: Emans S, Goldstein D, eds. Pediatric and Adolescent Gynecology. 3rd ed. Boston: Little, Brown; 1990:149–242
41. Falsetti L, Pasinetti E, Mazzani M, Gastaldi A. Weight loss and menstrual cycle: clinical and endocrinological evaluation. Gynecol Endocrinol 1992;6:49–56
42. Sobanski E, Hiltmann WD, Blanz B, Klein M, Schmidt MH. Pelvic ultrasound scanning of the ovaries in adolescent anorectic patients at low weight and after weight recovery. Eur Child Adolesc Psychiatry 1997;6:207–211
43. Stillman R, Schinfeld J, Schiff I, et al. Ovarian failure in long-term survivors of childhood malignancy. Am J Obstet Gynecol 1981;139: 62–66
44. Bookman M, Longo D, Young R. Late complications of curative treatment in Hodgkin's disease. JAMA 1988;260:680–683
45. Shawker T, Garra B, Loriaux, Cutler G, Ross J. Ultrasonography of Turner's syndrome. J Ultrasound Med 1986;5:125–129
46. Shah R, Woolley M, Costin G. Testicular feminization syndrome: the androgen insensitivity syndrome. J Ped Surg 1992;27:757–760
47. Larsen W, Felmar E, Wallace M, Frieder R. Sertoli-Leydig cell tumor of the ovary: a rare cause of amenorrhea. Obstet Gynecol 1992; 79:831–833
48. Goldzieher J, Green J. The polycystic ovary, I: Clinical and histologic features. J Clin Endocrinol Metab 1962;22:325–338
49. Rosenfield R. Hyperandrogenism in peripubertal girls. Pediatr Clin North Am 1990;37:1333–1358
50. Chang RJ. A practical approach to the diagnosis of polycystic ovary syndrome. Am J Obstet Gynecol 2004;191:713–717
51. Takahashi K, Okada M, Ozaki T, Uchida A, Yamasaki H, Kitao M. Transvaginal ultrasonographic morphology in polycystic ovarian syndrome. Gynecol Obstet Invest 1995;39:201–206
52. Balen AH, Laven JS, Tan SL, Dewailly D. Ultrasound assessment of the polycystic ovary: international consensus definitions. Hum Reprod Update 2003;9:505–514
53. Herter L, Magalnaes J, Spritzer P. Relevance of the determination of ovarian volumes in adolescent girls with menstrual disorders. J Clin Ultrasound 1996;24:243–248
54. Herter LD, Magalhaes JA, Spritzer PM. Association of ovarian volume and serum LH levels in adolescent patients with menstrual disorders and/or hirsutism. Braz J Med Biol Res 1993;26:1041–1046
55. Battaglia C, Artini PG, Genazzani AD, et al. Color Doppler analysis in olig- and amenorrheic women with polycystic ovary syndrome. Gynecol Endocrinol 1997;11:105–110
56. Battaglia C, Artini P, D'Ambrogio G, Genazzani AN, Genazzani AR. The role of color Doppler imaging in the diagnosis of polycystic ovary syndrome. Am J Obstet Gynecol 1995;172:108–113
57. Rosenblatt M, Rosenblatt R, Kutcher R, Coupey S, Kleinhaus S. Utero-vaginal hypoplasia: sonographic, embryologic and clinical considerations. Pediatr Radiol 1991;21:536–537
58. Daya S. Habitual abortion. In: Copeland L, ed. Textbook of Gynecology. Philadelphia: WB Saunders; 1993:204–230
59. Cohen HL. Evaluation of the Adolescent and Young Adult with Amenorrhea: Role of US. RSNA Special Course in Ultrasound. Oakbrook, IL: Radiological Society of North America; 1996: 171–183

6 Postmenopausal Vaginal Bleeding

Peter M. Doubilet

Postmenopausal vaginal bleeding is an important, and fairly common, problem in older women. It can be the presenting symptom of endometrial cancer, the fourth most common malignancy in women in the United States,[1] and the most common pelvic gynecologic malignancy.[2] Because of this, "unscheduled" postmenopausal bleeding (i.e., any bleeding other than that occurring at the expected time in the cycle of a woman on sequential hormone replacement therapy[3]) merits diagnostic evaluation. Henceforth, the term *postmenopausal bleeding* will refer to unscheduled bleeding.

Conventional teaching, until recently, has been that any woman with postmenopausal bleeding should undergo endometrial sampling (via one of the methods that will be described here).[2,3] With the advent of transvaginal sonography, done on its own or following the instillation of saline into the uterine cavity, the endometrium can be examined in exquisite detail in a minimally invasive fashion. This permits a more selective and directed approach to biopsying the endometrium in women with postmenopausal bleeding.

Differential Diagnosis

There are several etiologies of postmenopausal bleeding. The most common cause is endometrial atrophy.[4,5] The endometrium in a postmenopausal woman typically becomes thin and atrophic. This atrophic endometrium is prone to develop superficial ulcers that bleed. Bleeding can also be caused by several endometrial lesions, including endometrial carcinoma, which accounts for ~7 to 30% of cases of postmenopausal bleeding,[4–6] endometrial hyperplasia, and endometrial polyps. These lesions are somewhat interrelated, in that polyps may contain foci of malignancy or hyperplasia, and endometrial hyperplasia (especially in the presence of cytological atypia) may progress to carcinoma. In one series, 23% of women with atypical hyperplasia subsequently developed endometrial carcinoma, as did 1.6% of women with simple hyperplasia.[7] In addition to endometrial lesions, submucosal fibroids can be a cause of postmenopausal bleeding.

Diagnostic Evaluation

Nonimaging Tests

There are several ways to obtain an endometrial tissue specimen for pathological evaluation. Endometrial tissue can be obtained by dilation and curettage (D&C), usually performed in an operating room, or via an "office biopsy." The latter is substantially lower in cost and morbidity.[8,9] Both of these procedures obtain tissue from only a portion of the endometrium and so may miss lesions due to sampling error. In a study of 50 patients who had D&C immediately preceding hysterectomy, examination of the hysterectomy specimen revealed that in 16% of patients less than a quarter of the cavity had been sampled, and in 60% of patients less than half the endometrium had been sampled.[10] Office biopsies are likely to obtain even more limited samples.

Both D&C and office biopsy have been shown to have sensitivities below 100% for endometrial pathology, with polypoid lesions being missed most frequently. The false-negative rate of D&C is often found to be in the range of 2 to 6%, with somewhat higher rates for office biopsy.[11] Some studies have found even higher false-negative rates. Grimes estimated office biopsy to have a sensitivity of 96% for endometrial cancer and 80% for endometrial hyperplasia.[8] In 407 patients undergoing D&C prior to hysterectomy, Stovall et al found that D&C correctly diagnosed 28 of 30 cancers (93%) and 28 of 51 cases of hyperplasia (55%).[12] Although the reported sensitivity of office biopsy and D&C varies from study to study, it is clear that both of these sampling procedures miss some cases of endometrial pathology.

Another method of obtaining endometrial tissue for pathological examination is hysteroscopically guided biopsy. Because the biopsy is not performed blindly, but instead can be directed to sites of grossly visible abnormalities, this approach is less prone to sampling error. In particular, focal lesions such as polyps, or a small patch of malignant tissue, are less likely to be missed by hysteroscopically guided biopsy than by blind biopsy techniques (office biopsy or D&C). However, the cost of this procedure, and the skill required to carry it out expertly, limits its

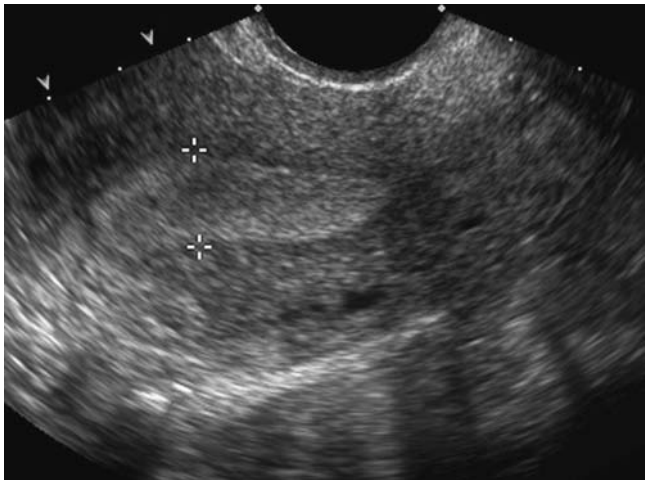

Figure 6–1 Endometrial thickness measurement technique. The measurement is done on a sagittal transvaginal image, measuring from the anterior endometrial–myometrial interface to the posterior endometrial–myometrial interface (calipers). This is a double-layer measurement because it includes both the anterior and the posterior layers of endometrium.

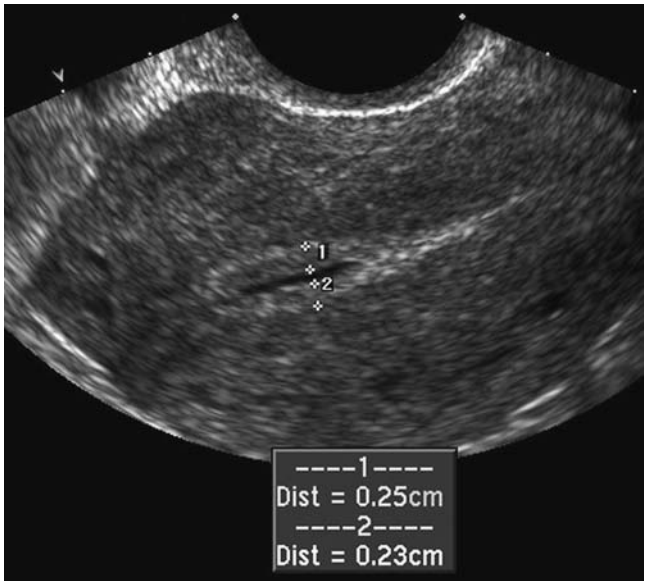

Figure 6–2 Endometrial thickness measurement with fluid in the endometrial cavity. The anterior endometrium (calipers #1) and posterior endometrium (calipers #2) are measured, and the values of 0.25 cm and 0.23 cm are summed to yield the endometrial thickness measurement of 0.48 cm (4.8 mm).

applicability to selected cases. Furthermore, some hysteroscopes do not have an operating channel through which biopsy can be performed, which necessitates removing the scope prior to biopsy.

Imaging Tests Other than Ultrasound

Hysterosalpingography and magnetic resonance imaging (MRI) can provide diagnostic information about the endometrium. The former can play a useful role in the workup of infertility,[13] but does not contribute to the evaluation of postmenopausal bleeding. Magnetic resonance imaging can occasionally be used for this purpose in patients with inadequate sonogram and sonohysterogram and who cannot undergo endometrial sampling due to cervical stenosis.[14] Its main role in endometrial evaluation, however, lies not in the workup of postmenopausal bleeding, but in the preoperative staging in cases of proven endometrial carcinoma.[15,16]

Ultrasound Imaging

The literature on ultrasound of the postmenopausal uterus is extensive and has focused on several questions. Is there an endometrial thickness below which significant endometrial pathology can be confidently excluded? How is endometrial thickness affected by various regimens of hormone replacement therapy? Besides endometrial thickness, can other sonographic features (e.g., echotexture of the endometrium, Doppler waveforms) identify pathology and distinguish among various pathological conditions? Can sonohysterography aid in the differential diagnosis of postmenopausal bleeding?

Postmenopausal endometrial thickness and its relationship to endometrial pathology have been extensively studied.[17–26] Although the technique for measuring endometrial thickness varies somewhat among different authors, most use double-layer endometrial measurements (anterior and posterior layers) obtained via transvaginal sonography. The endometrium is imaged sagittally and is measured at its thickest point from the anterior to the posterior endometrial–myometrial junction (**Fig. 6–1**). Each of these junctions is generally easy to identify because the endometrium is typically hyperechoic and the inner myometrium hypoechoic. If there is fluid in the endometrial cavity, the anterior and posterior layers of the endometrium are measured separately and the two values are summed (**Fig. 6–2**).

Table 6–1 summarizes the results of several studies examining whether there is a thickness cutoff below which significant endometrial pathology can be excluded in women with postmenopausal bleeding. In each study, patients underwent sonography shortly before endometrial tissue sampling, usually by D&C or hysterectomy. Most of the studies employ a cutoff of 4 or 5 mm. Although the findings vary somewhat among studies, the overall pattern of results suggests that postmenopausal bleeding is rarely due to significant endometrial pathology (carcinoma, hyperplasia, or polyp), and almost never due to carcinoma, when the endometrial thickness is

Table 6–1 Endometrial Pathology in Women with Postmenopausal Bleeding and Endometrial Thickness < 4 to 6 mm: Literature Review

Study	Endometrial Thickness Cutoff (mm)	# of Cases below Cutoff	Histological Findings	Minimal Thickness of Endometrial Carcinoma
Osmers et al[17]	≤ 6**	46	Negative**: 32 (70%)	
			Hyperplasia or polyps: 14 (30%)	
Goldstein et al[18]	≤ 5	11	Negative: 11 (100%)	
Nasri et al[19]	≤ 5	117	Negative: 117 (100%)	9 mm
Varner et al[20]	≤ 4	60	Negative: 60 (100%)	
Granberg et al[21]	≤ 5	150	Negative: 150 (100%)	9 mm
Karlsson et al[22]	≤ 5	58	Negative: 57 (98%)	
			Endometrial carcinoma: 1 (2%)	5 mm
Dorum et al[23]	≤ 4	54	Not malignant: 51 (94%)	
			Malignant: 3 (6%)	2 mm
Cacciatore et al[24]	< 5	11	Negative: 10 (91%)	
			Polyp: 1 (9%)	10 mm
Conoscenti et al[25]	< 4	46	Negative: 44 (96%)	
			Endometrial polyp: 1 (2%)	
			Endometrial carcinoma: 1 (2%)	3 mm
Karlsson et al[26]	≤ 4	518	Negative: 491 (95%)	
			Endometrial polyp: 6 (1%)	
			Endometrial hyperplasia: 6 (1%)	5 mm

*Was reported as a < 4 mm single-layer measurement.

**Negative histological findings include histological readings of "atrophic endometrium," "inactive endometrium," "tissue insufficient for diagnosis," and related findings.

≤ 4 to 5 mm. Using a conservative cutoff of ≤ 4 mm (**Fig. 6–3**), postmenopausal bleeding can be attributed to endometrial atrophy with a high degree of confidence when the endometrial thickness is below this cutoff.[27,28]

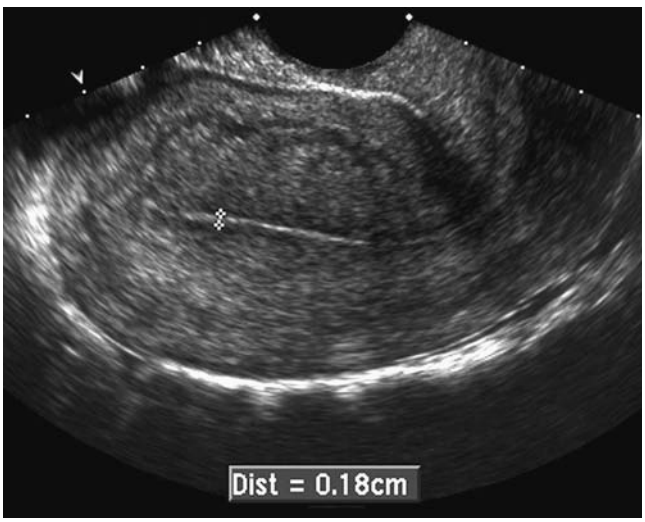

Figure 6–3 Thin endometrium. The endometrial thickness (calipers) is 0.18 cm (1.8 mm).

It should be noted that, although a thickness below 4 to 5 mm largely excludes significant pathology, a greater measurement does not exclude endometrial atrophy. In the 1995 Karlsson study, for example, among 245 women with endometrial thicknesses of 6 to 10 mm, 88 (36%) had endometrial atrophy.[26]

In a small fraction of cases the endometrial margins are obscure, so that the thickness cannot be measured. This is most likely to occur when there are uterine fibroids distorting the endometrium. In these cases, the sonogram provides no information about the presence or nature of endometrial pathology.[18]

Most studies have found that the endometrial thickness in cases of endometrial carcinoma is larger, on average, than it is with polyps or hyperplasia.[17,19,21,22,24–26] In the largest study, for example, the mean thickness with endometrial cancer was 21.1 mm, compared with 12.9 mm for polyps and 12.0 mm for hyperplasia.[26] However, there is considerable overlap in endometrial thickness among these three lesions, so that the degree of thickening cannot be used to make a specific diagnosis.

Endometrial thickness in postmenopausal women is somewhat affected by hormone replacement therapy, which some women take to counter the effects of menopause. Several treatment regimes are available, employing

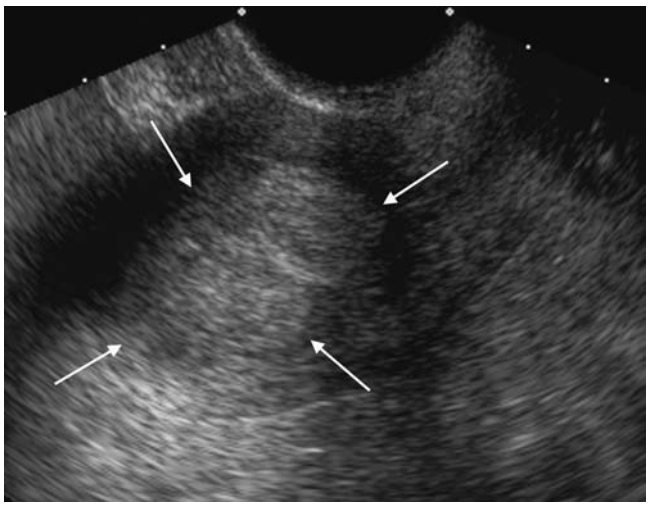

Figure 6–4 Endometrial carcinoma. The endometrium (arrows) is markedly thickened and has indistinct margins. Dilation and curettage revealed endometrial carcinoma.

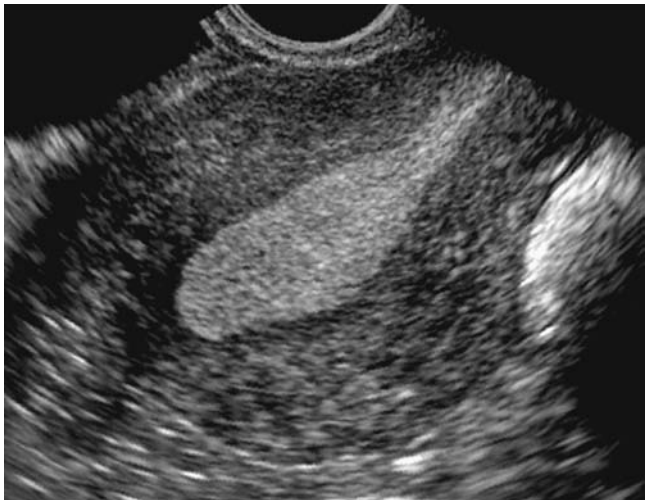

Figure 6–5 Endometrial hyperplasia. The endometrium is thick and homogeneous and has a distinct interface with the myometrium. Endometrial biopsy revealed hyperplasia.

estrogen with or without progesterone. Estrogen suppresses hot flashes and reduces the risk of osteoporosis and cardiovascular disease in postmenopausal women. It has the drawback of increasing the likelihood of endometrial hyperplasia or carcinoma and so is often given in combination with progesterone, which decreases the risk of endometrial pathology. Progesterone, when used, can be given either continuously or periodically (e.g., the first 10 to 14 days of each month), leading to three types of treatment regimen: estrogen only, continuous estrogen/progesterone, and sequential estrogen/progesterone. On the last of these regimens, "withdrawal" bleeding is expected each month and is not associated with endometrial pathology, so that bleeding in women on sequential therapy merits diagnostic workup only when unscheduled.[3,29]

Hormone replacement therapy tends to increase endometrial thickness, by ~1 to 1.5 mm for continuous estrogen or estrogen/progesterone, and by 3 mm for sequential therapy.[30] Women on sequential therapy also have more variation in thickness during each month than do those on continuous or no therapy, with the thinnest endometrium following progesterone withdrawal.

Several studies have examined whether sonographic features other than endometrial thickness, such as echotexture or Doppler indices, may be useful in the diagnosis of endometrial pathology. Several studies have found that the sonographic finding of cystic spaces in the postmenopausal endometrium suggests polyps, a heterogeneous appearance suggests malignancy (**Fig. 6–4**), and a homogeneously thickened endometrium suggests hyperplasia (**Fig. 6–5**).[31–33] There is too much overlap in the sonographic appearance of the various pathological entities, however, to allow a diagnosis to be made with confidence based on echotexture alone. Analysis of echotexture, therefore, has little or no practical impact on the diagnostic evaluation or management of patients with postmenopausal bleeding.

The data on Doppler for diagnosing endometrial pathology are mixed, at best. Bourne et al found that the uterine artery pulsatility index accurately distinguished between endometria with and without cancer,[34] but Aleem et al found no significant difference in uterine artery pulsatility index or resistive index in pathological versus control groups.[35] Sheth et al found that Doppler of endometrial vessels in postmenopausal women with thick ($\geq$ 8 mm) endometria was not helpful because there was no significant difference in mean pulsatility and resistive indices in benign versus malignant lesions.[36] It is noteworthy that the lead author of a favorable Doppler study in 1990[34] later wrote in a 1995 editorial, "Doppler has a relatively insignificant role to play in the context of evaluating the postmenopausal endometrium for the presence of carcinoma."[11]

Saline infusion sonohysterography (SIS)—transvaginal sonography immediately following saline instillation into the uterine cavity—provides excellent visualization of the endometrium and can be useful for diagnosing endometrial lesions.[37–42] To perform the procedure, a speculum is inserted into the vagina and a catheter is threaded through the cervix into the uterine cavity. The speculum is removed, taking care not to dislodge the catheter, a transvaginal ultrasound transducer is inserted, ~10 mL of saline is instilled, and the uterus is

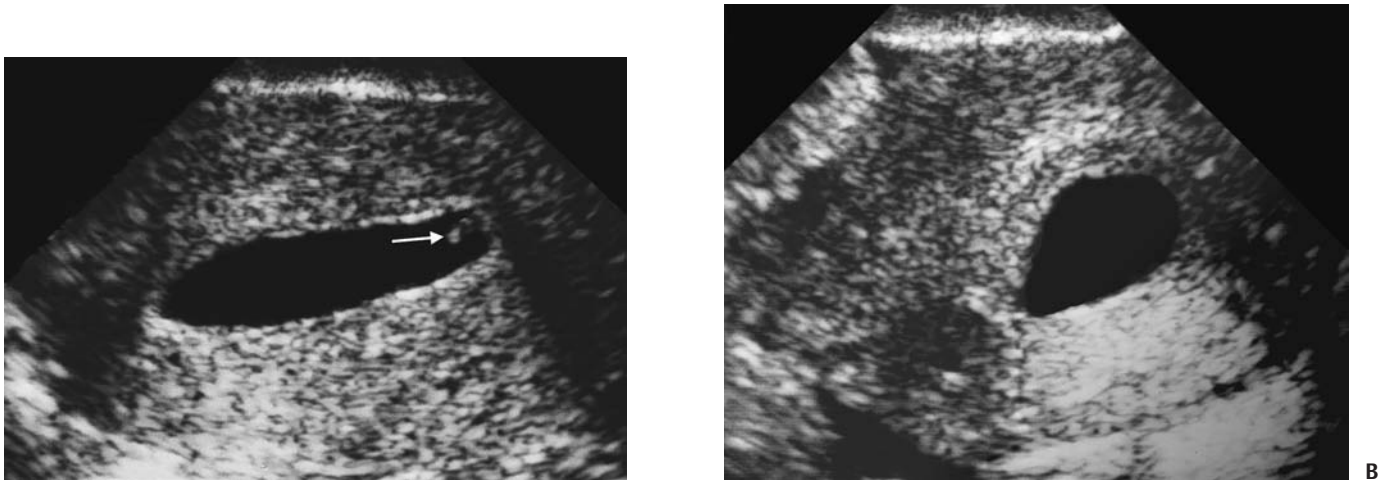

Figure 6–6 Normal sonohysterogram. Fluid in the uterine cavity delineates smooth, thin endometrium surrounding the entire cavity. **(A)** Sagittal view, with catheter tip (arrow) seen within the fluid-filled uterine cavity in the lower uterine segment. **(B)** Coronal view.

scanned thoroughly in sagittal and transverse planes (**Fig. 6–6**). Because fluid may leave the uterus through the cervix and fallopian tubes, several saline injections may be needed during the course of the examination. Some practitioners use a catheter with an inflatable balloon and place traction on the balloon-filled catheter to prevent fluid from escaping out of the cervix, especially in patients with a patulous cervix,[38] whereas others use a balloonless catheter.[39]

Sonohysterography can contribute useful diagnostic information in several clinical settings, including the workup of postmenopausal bleeding.[43] In a woman with postmenopausal bleeding in whom transvaginal sonography demonstrates endometrial thickening, an SIS can determine whether the thickening is diffuse (**Fig. 6–7**) or due to a focal lesion, such as a polyp (**Fig. 6–8**). This distinction can be used to help guide the selection of a biopsy approach.[38,39,41,42] In the presence of a submucosal fibroid,

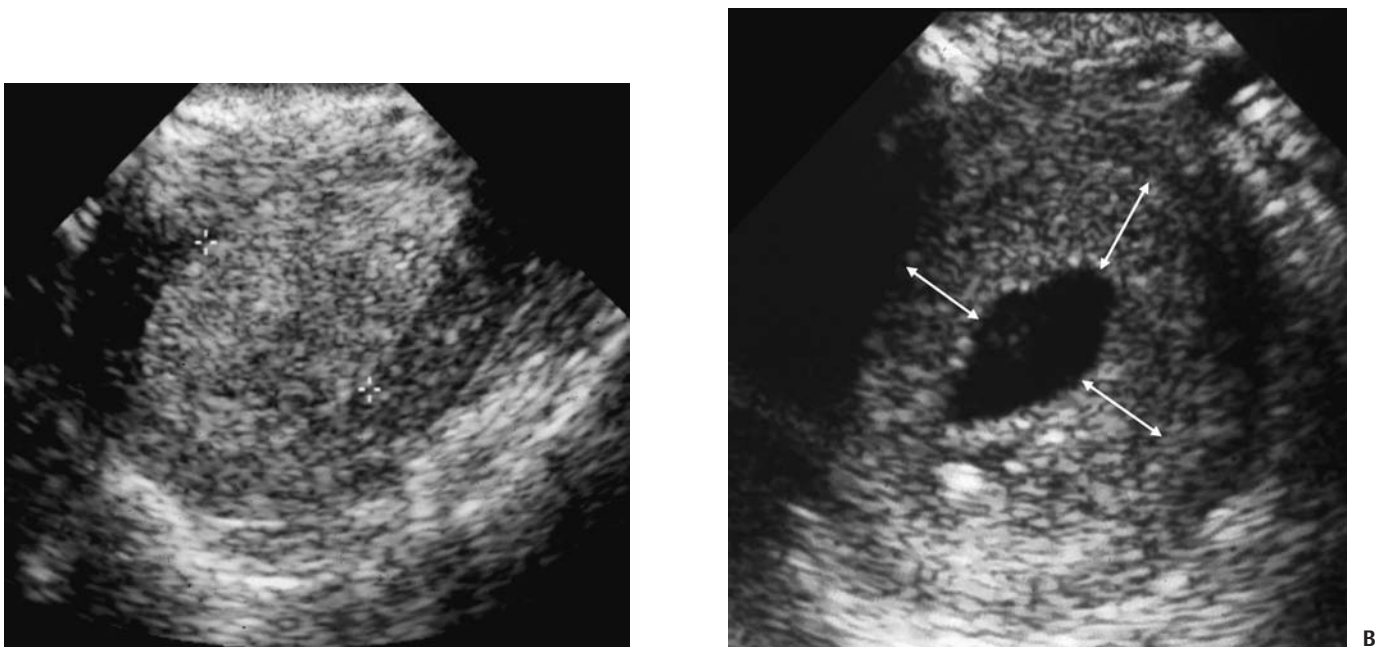

Figure 6–7 Diffuse endometrial thickening. **(A)** Sagittal sonogram demonstrates thickened endometrium (calipers). **(B)** Sonohysterogram demonstrates diffuse endometrial thickening (arrows).

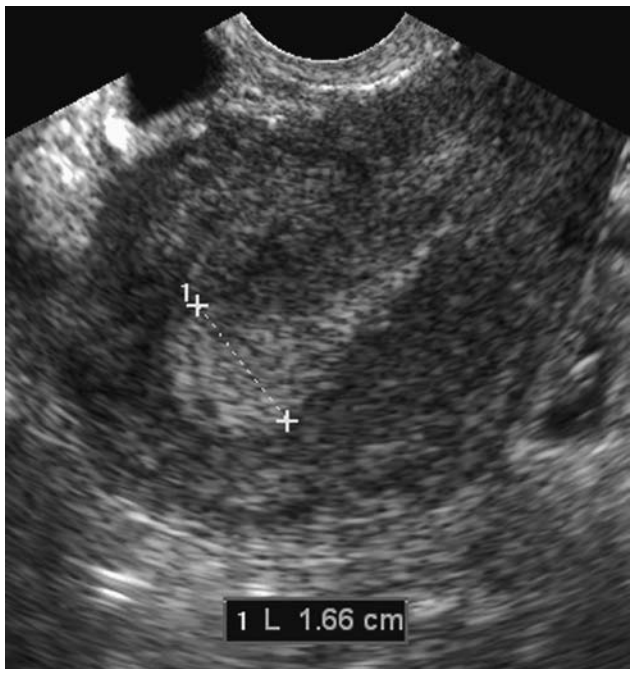

A

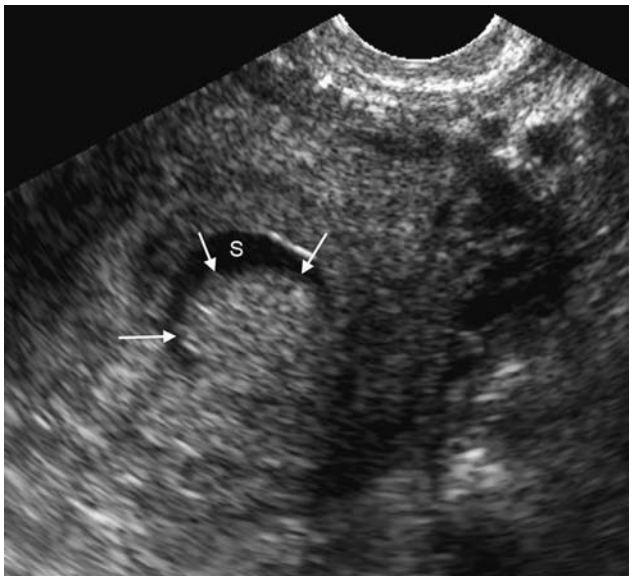

B

Figure 6–8 Endometrial polyp. **(A)** Sagittal sonogram demonstrates thickened endometrium (calipers) measuring 1.66 cm (16.6 mm). **(B)** Sonohysterogram demonstrates polyp (arrows) surrounded by saline (S).

SIS can aid in its diagnosis, and also assess whether it is pedunculated or superficial enough to permit transcervical resection via an operative hysteroscope.[38,39]

If the endometrial thickness cannot be measured on transvaginal sonography, SIS can clarify whether it appears normal (atrophic) or not, as well as identify one or more submucosal fibroids that may be distorting the endometrium.

Three-dimensional (3-D) sonography can be useful for evaluating the endometrium,[44] whether used with saline (3-D-SIS) or without saline. Three-dimensional ultrasound permits reconstruction in any plane, by allowing for the selection of the optimal plane for measuring endometrial thickness, or the plane that best depicts endometrial pathology (**Fig. 6–9**).

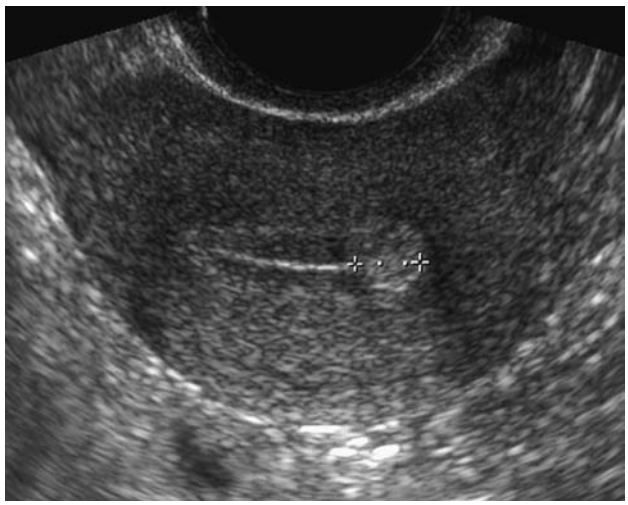

A

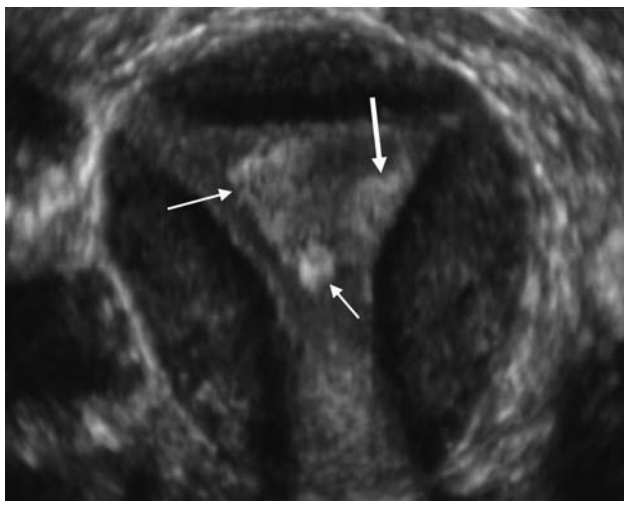

B

Figure 6–9 Endometrial polyps demonstrated by three-dimensional sonography. **(A)** Conventional coronal sonogram demonstrates a small echogenic mass in the left lateral aspect of the endometrium (calipers). **(B)** Planar reconstruction from a three-dimensional scan better demonstrates this polyp (thick arrow), and also identifies two other polyps (thin arrows).

Benefits of Ultrasound Imaging

Until recently, the conventional teaching had been that a woman with unscheduled postmenopausal bleeding should be biopsied, via either office biopsy or D&C.[2,3] The main benefits of ultrasound are twofold. First, ultrasound can identify a subset of women with postmenopausal bleeding in whom the risk of significant endometrial pathology is so low that biopsy may not be necessary. Second, in patients in whom biopsy is indicated, sonohysterography can help to select the optimal biopsy technique.

The ultrasound finding of an endometrial thickness ≤ 5 mm is near-definitive proof of endometrial atrophy[28] and excludes malignancy with very high confidence (**Table 6–1**). In fact, the false-negative rate associated with a sonographic thickness of ≤ 5 mm appears to be as low as, or lower than, that of office biopsy or D&C, so that a negative ultrasound may be at least as reliable as a negative biopsy or D&C. Transvaginal ultrasound can thus play a key role in the evaluation of postmenopausal bleeding in one of two ways. First, it can be performed prior to biopsy, and if the endometrial thickness is found to be ≤ 5 mm, it is reasonable to attribute the bleeding to endometrial atrophy and not perform a biopsy. In one study, this diagnostic strategy led to a 46% reduction in the number of biopsies performed, without loss of diagnostic accuracy.[26] Second, if endometrial biopsy has been performed (without prior ultrasound) and if there is "insufficient tissue for diagnosis," ultrasound can then help to decide whether to believe the result (i.e., attribute the bleeding to endometrial atrophy) or to proceed to D&C or hysteroscopy.[45,46] If the sonographically measured endometrial thickness is ≤ 5 mm, the biopsy result can be accepted, and if > 5 mm then further tissue sampling should be considered.

Ideally, diagnostic strategies for postmenopausal bleeding should involve a combination of sonography, SIS, and tissue sampling.[27] Sonography, using the ≤ 5 mm cutoff, can guide the decision concerning whom to biopsy or whether to accept the result of an office biopsy that yields scanty tissue. Sonohysterography can help to choose the best biopsy approach—office biopsy or D&C for diffuse endometrial thickening (**Fig. 6–7**) or hysteroscopically guided biopsy for focal or polypoid lesion (**Fig. 6–8**), as well as to clarify the significance of an unmeasurable endometrial thickness or to identify the best way to excise a submucosal fibroid. Tissue sampling yields a specific histopathologic diagnosis.

Two reasonable diagnostic algorithms that employ these tests are an ultrasound-first strategy (**Fig. 6–10A**) or a biopsy-first strategy (**Fig. 6–10B**). With the ultrasound-first strategy, the sonographically measured endometrial thickness is used to decide whether further workup is needed: no if ≤ 5 mm, yes if > 5 mm. If the thickness is > 5 mm or is unmeasurable, SIS is performed and the next step is based on the SIS findings. Using the biopsy-first approach, positive biopsy results end the diagnostic workup, whereas ultrasound (and, in some cases, SIS) is used following a negative biopsy. Both of these algorithms will lead to decreased cost and/or improved diagnostic accuracy, compared with relying on tissue sampling alone.

With either of these algorithms, if the evaluation is negative (i.e., negative biopsy and/or thin endometrium), the likelihood of endometrial carcinoma is very low, but not zero. In most cases, no additional testing is needed, but further evaluation should be considered if the patient has persistent bleeding. Long-term follow-up of women whose initial evaluation for postmenopausal bleeding is negative and who have persistent bleeding has demonstrated that there is a substantial chance that complex atypical hyperplasia or cancer will ultimately be diagnosed.[47]

These algorithms apply to any woman with postmenopausal bleeding, including those with unscheduled bleeding on hormone replacement therapy. For a woman with unscheduled bleeding on sequential therapy, the sonogram and SIS should be performed shortly after subsequent progesterone withdrawal bleeding, when the endometrium is expected to be at its thinnest. Although hormone therapy tends to increase endometrial thickness, the prudent and conservative approach in the face of unscheduled bleeding is to employ the same ≤ 5 mm cutoff for the decision concerning biopsy in women on hormones that is used in women who are not taking hormones.

It is important to recognize that these algorithms apply only to postmenopausal women who have vaginal bleeding, not to asymptomatic ones. The measurement of 5 mm is not a "normal" or "upper limit of normal" value for postmenopausal endometrial thickness, but instead is an "action threshold" for women with bleeding. In the absence of bleeding, the sonographic finding of an endometrial thickness > 5 mm in a postmenopausal woman does not necessarily indicate that she should be biopsied.[48] In this setting, the decision about whether to biopsy should take into account factors such as the degree of thickening, whether and what regimen of hormone replacement therapy she is on, the endometrial echotexture, as well as age and other risk factors for endometrial carcinoma.[49]

Summary

Postmenopausal bleeding, except that occurring at the expected time in certain hormone replacement regimens, may be a sign of malignant or premalignant endometrial lesions. Conventional teaching has been that any woman with unscheduled bleeding should undergo endometrial tissue sampling, via office biopsy or D&C. Because these

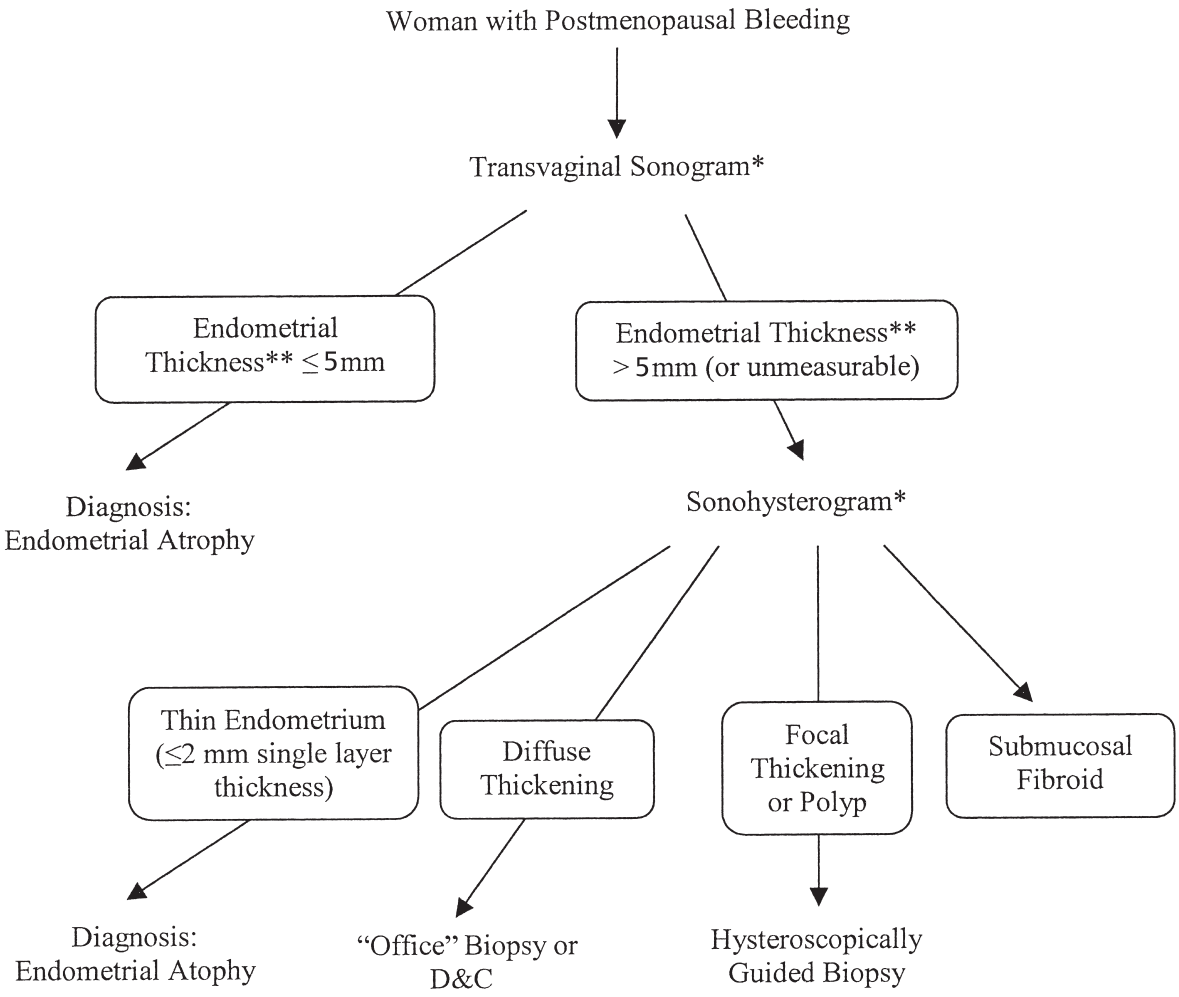

* If the woman has unscheduled bleeding on sequential hormone replacement therapy, sonogram and sonohysterogram should be done shortly after subsequent progesterone withdrawal bleeding.

** Double-layer thickness

*** Further evaluation may be needed if bleeding persists or patient has risk factors for endometrial carcinoma.

A

Figure 6–10 Algorithms for diagnostic workup of postmenopausal bleeding using sonography, sonohysterography, and endometrial sampling. **(A)** Ultrasound-first strategy. (*Continued*)

tests carry costs, risk, and a chance of false-negative results, sonography and sonohysterography can contribute to the diagnostic workup. A sonographically measured endometrial thickness of ≤ 5 mm indicates a high likelihood of endometrial atrophy being the cause of bleeding, and so may obviate the need for biopsy. When the endometrial thickness is > 5 mm, sonohysterography can determine whether the thickening is diffuse or due to a polyp or other focal lesion, and thus help guide the choice of biopsy technique. Incorporating sonography and sonohysterography into the diagnostic algorithm for postmenopausal bleeding can lead to decreased cost and morbidity with no loss of, or improvement in, diagnostic accuracy.

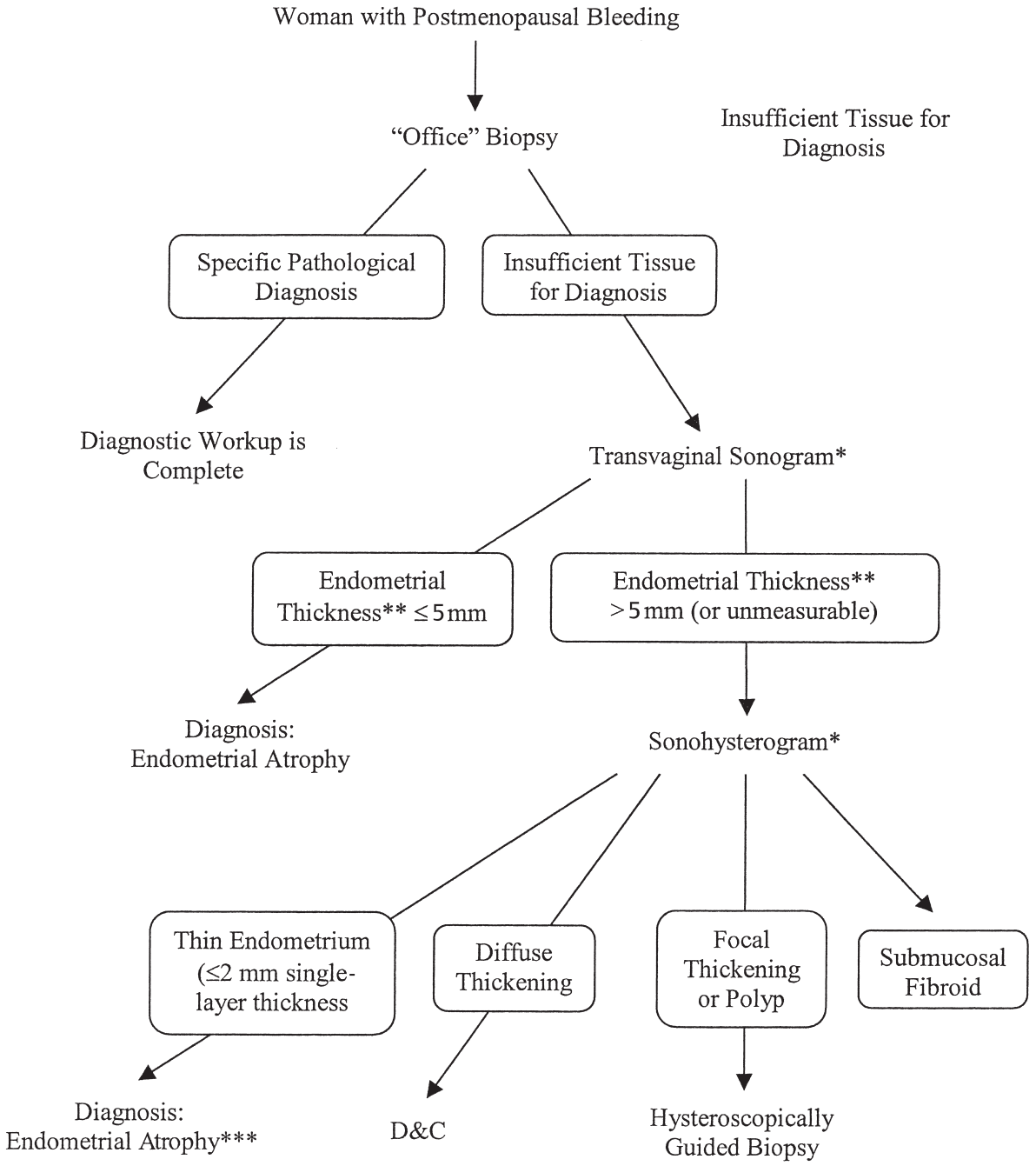

* If the woman has unscheduled bleeding on sequential hormone replacement therapy, sonogram and sonohysterogram should be done shortly after subsequent progesterone withdrawal bleeding.

** Double-layer thickness.

*** Further evaluation may be needed if bleeding persists or patient has risk factors for endometrial carcinoma.

B

Figure 6–10 *(Continued)* **(B)** Biopsy-first strategy. D&C, dilation and curettage.

References

1. Parker SL, Tong T, Bolden S, Wingo PA. Cancer statistics, 1996. CA 1996;46:5–27
2. American College of Obstetrics and Gynecology. Carcinoma of the Endometrium. Technical Bulletin 162. American College of Obstetrics and Gynecology; 1991
3. American College of Obstetrics and Gynecology. Hormone Replacement Therapy. Technical Bulletin 166. American College of Obstetrics and Gynecology; 1992
4. Choo YC, Mak KC, Hsu C, Wong TS, Ma HK. Postmenopausal uterine bleeding of nonorganic cause. Obstet Gynecol 1985;66:225–228
5. Lidor A, Ismajovic E, Confino E, David MP. Histopathological findings in 226 women with postmenopausal uterine bleeding. Acta Obstet Gynecol Scand 1986;65:41–43
6. Rosenwaks Z, Benjamin F, Stone ML. Gynecology: Principles and Practice. New York: Macmillan; 1987:515
7. Kurman RJ, Kaminski PF, Norris HJ. The behavior of endometrial hyperplasia: a long-term study of "untreated" hyperplasia in 170 patients. Cancer 1985;56:403–412
8. Grimes DA. Diagnostic dilation and curettage: a reappraisal. Am J Obstet Gynecol 1982;142:1–6
9. Feldman S, Berkowitz RS, Tosteson ANA. Cost-effectiveness of strategies to evaluate postmenopausal bleeding. Obstet Gynecol 1993;81:968–975
10. Stock RJ, Kanbour A. Prehysterectomy curettage. Obstet Gynecol 1975;45:537–541
11. Bourne TH. Evaluating the endometrium of postmenopausal women with transvaginal ultrasonography. Ultrasound Obstet Gynecol 1995;6:75–80
12. Stovall TG, Solomon SK, Ling FW. Endometrial sampling prior to hysterectomy. Obstet Gynecol 1989;73:405–409
13. Fagan CJ. Hysterosalpingography. In: Putman CE, Ravin CE, eds. Textbook of Diagnostic Imaging. Philadelphia: WB Saunders; 1988
14. Reinhold C, Khalili I. Postmenopausal bleeding: value of imaging. Radiol Clin North Am 2002;40:527–562
15. Yamashita Y, Mizutani H, Torashima M, et al. Assessment of myometrial invasion by endometrial carcinoma: transvaginal sonography vs contrast-enhanced MR imaging. AJR Am J Roentgenol 1993;161:595–599
16. Yamashita Y, Harada M, Sawada T, Takahashi M, Miyazaki K, Okamura H. Normal uterus and FIGO stage I endometrial carcinoma: dynamic gadolinium-enhanced MR imaging. Radiology 1993;186: 495–501
17. Osmers R, Volksen M, Schauer A. Vaginosonography for early detection of endometrial carcinoma? Lancet 1990;335:1569–1571
18. Goldstein SR, Nachtigall M, Snyder JR, Nachtigall L. Endometrial assessment by vaginal ultrasonography before endometrial sampling in patients with postmenopausal bleeding. Am J Obstet Gynecol 1990;163:119–123
19. Nasri MN, Shepherd JH, Setchell ME, Lowe DG, Chard T. Sonographic depiction of postmenopausal endometrium with transabdominal and transvaginal scanning. Ultrasound Obstet Gynecol 1991;1:279–283
20. Varner RE, Sparks JM, Cameron CD, Roberts LL, Soong SJ. Transvaginal sonography of the endometrium in postmenopausal women. Obstet Gynecol 1991;78:195–199
21. Granberg S, Wikland M, Karlsson B, Norstrom A, Friberg LG. Endometrial thickness as measured by endovaginal ultrasonography for identifying endometrial abnormality. Am J Obstet Gynecol 1991;164:47–52
22. Karlsson B, Granberg S, Wikland M, Ryd W, Norstrom A. Endovaginal scanning of the endometrium compared to cytology and histology in women with postmenopausal bleeding. Gynecol Oncol 1993;50:173–178
23. Dorum A, Kristensen B, Langebrekke B, Sornes T, Skaar O. Evaluation of endometrial thickness measured by endovaginal ultrasound in women with postmenopausal bleeding. Acta Obstet Gynecol Scand 1993;72:116–119
24. Cacciatore B, Ramsay T, Lehtovirta P, Ylostalo P. Transvaginal sonography and hysteroscopy in postmenopausal bleeding. Acta Obstet Gynecol Scand 1994;73:413–416
25. Conoscenti G, Meir YJ, Fischer-Tamaro L, et al. Endometrial assessment by transvaginal sonography and histological findings after D & C in women with postmenopausal bleeding. Ultrasound Obstet Gynecol 1995;6:108–115
26. Karlsson B, Granberg S, Wikland M, et al. Transvaginal ultrasonography of the endometrium in women with postmenopausal bleeding—a Nordic multicenter study. Am J Obstet Gynecol 1995;172: 1488–1494
27. Goldstein RB, Bree RL, Benson CB, et al. Consensus report: evaluation of the woman with postmenopausal bleeding. J Ultrasound Med 2001;20:1025–1036
28. Gull B, Carlsson SA, Karlsson B, Ylostalo P, Milsom I, Granberg S. Transvaginal ultrasonography of the endometrium in women with postmenopausal bleeding: is it always necessary to perform an endometrial biopsy? Am J Obstet Gynecol 2000;182:509–515
29. Padwick ML, Pryse-Davies J, Whitehead MI. A simple method for determining the optimal dosage of progestin in postmenopausal women receiving estrogens. N Engl J Med 1986;315:930–934
30. Levine D, Gosink BB, Johnson LA. Change in endometrial thickness in postmenopausal women undergoing hormone replacement therapy. Radiology 1995;197:603–608
31. Sheth S, Hamper UM, Kurman RJ. Thickened endometrium in the postmenopausal woman: sonographic-pathologic correlation. Radiology 1993;187:135–139
32. Hulka CA, Hall DA, McCarthy K, Simeone JF. Endometrial polyps, hyperplasia, and carcinoma in postmenopausal women: differentiation with endovaginal sonography. Radiology 1994;191:755–758
33. Atri M, Mazarnia S, Aldis AE, Reinhold C, Bret PM, Kintzen G. Transvaginal US appearance of endometrial abnormalities. Radiographics 1994;14:483–492
34. Bourne TH, Campbell S, Whitehead MI, Royston P, Steer CV, Collins WP. Detection of endometrial cancer in postmenopausal women by transvaginal ultrasonography and colour flow imaging. BMJ 1990;301:369
35. Aleem F, Predanic M, Calame R, Moukhtar M, Pennisi J. Transvaginal color and pulsed Doppler sonography of the endometrium: a possible role in reducing the number of dilatation and curettage procedures. J Ultrasound Med 1995;14:139–145
36. Sheth S, Hamper UM, McCollum ME, Caskey CI, Rosenshein NB, Kurman RJ. Endometrial blood flow analysis in postmenopausal women: can it help differentiate benign from malignant causes of endometrial thickening? Radiology 1995;195:661–665
37. Syrop CH, Sahakian V. Transvaginal sonographic detection of endometrial polyps with fluid contrast augmentation. Obstet Gynecol 1992;79:1041–1043
38. Parsons AK, Lense JJ. Sonohysterography for endometrial abnormalities: preliminary results. J Clin Ultrasound 1993;21:87–95
39. Goldstein SR. Use of ultrasonohysterography for triage of perimenopausal patients with unexplained uterine bleeding. Am J Obstet Gynecol 1994;170:565–570
40. Cohen JR, Luxman D, Sagi J, Yovel I, Wolman I, David MP. Sonohysterography for distinguishing endometrial thickening from en-

dometrial polyps in postmenopausal bleeding. Ultrasound Obstet Gynecol 1994;4:227–230
41. Dubinsky TJ, Parvey R, Gormaz G, Maklad N. Transvaginal hysterosonography in the evaluation of small endoluminal masses. J Ultrasound Med 1995;14:1–6
42. Cullinan JA, Fleischer AC, Kepple DM, Arnold AL. Sonohysterography: a technique for endometrial evaluation. Radiographics 1995; 15:501–514
43. Bree RL, Bowerman RA, Bohm-Velez M, Benson CB, DeDreu SR, Punch MR. Ultrasound evaluation of the uterus in patients with postmenopausal bleeding: a positive impact on diagnostic decision making. Radiology 2000;216:260–264
44. Bonilla-Musoles F, Raga F, Osborne NG, Blanes J, Coelho F. Three-dimensional hysterosonography for the study of endometrial tumors: comparison with transvaginal sonography, hysterosalpingography, and hysteroscopy. Gynecol Oncol 1997;65:245–252
45. Goldchmit R, Katz Z, Blickstein I, Caspi B, Dgani R. The accuracy of endometrial pipelle sampling with and without sonographic measurement of endometrial thickness. Obstet Gynecol 1993;82: 727–730
46. Van Den Bosch T, Vandendael A, Van Schoubroeck D, Wranz PAB, Lombard CJ. Combining vaginal ultrasonography and office endometrial sampling in the diagnosis of endometrial disease in postmenopausal women. Obstet Gynecol 1995;85:349–352
47. Feldman S, Shapter A, Welch WR, Berkowitz RS. Two-year follow-up of 263 patients with post/perimenopausal vaginal bleeding and negative initial biopsy. Gynecol Oncol 1994;55:56
48. Goldstein SR. The endometrial echo revisited: have we created a monster? Am J Obstet Gynecol 2004;191:1092–1096
49. Feldman S, Cook EF, Harlow BL, Berkowitz RS. Predicting endometrial cancer among older women who present with abnormal vaginal bleeding. Gynecol Oncol 1995;56:376–381

7 Family History of Ovarian Carcinoma

Andrew M. Fried and Carol B. Benson

The prevalence of ovarian carcinoma in the United States has been estimated at 30 to 50 cases per 100,000 women, translating into a lifetime incidence of one case per 70 women in the general population. With an anticipated 22,000 new cases and 16,000 deaths from the disease each year, ovarian cancer is the leading cause of death from gynecologic malignancies in this country.[1]

The preponderance (95%) of cases of ovarian carcinoma are sporadic in nature with no discernible pattern of inheritance. Some 5% occur in women considered at increased risk for the disease by virtue of first-degree relatives with ovarian cancer or a family history of one of three heritable syndromes discussed following here.

Because ovarian cancer in its early stages produces few if any symptoms, and those symptoms that do result are typically nonspecific, ~70% of these tumors are detected at advanced stages (stages III and IV), when the process has already spread beyond the ovaries. Only ~20% are discovered while still in stage I. Because the 5-year survival rate for stage III or IV disease is 15%, whereas that for stage I exceeds 90%, the impetus for early detection is obvious.[2–4]

Certain general factors contribute to an increased risk for ovarian cancer: advancing age, nulliparity, North American or Northern European descent, family members with documented ovarian cancers, and a personal history of cancer of the colon, endometrium, or breast. Forty-five percent of ovarian masses removed from postmenopausal patients proved to be malignant as opposed to 13% from premenopausal women in one large study.[5] In another report, 85% of all cases of ovarian cancer were found in women over 45 years of age.[6] Conditions that seem to impart a measure of protection against ovarian cancer include more than one full-term pregnancy, oral contraceptive use, and breast feeding. The physiological factor common to all these is the interruption of ovulation for some period of time.

A woman with one first- or second-degree relative with ovarian cancer faces a risk of developing the disease that is 3.1 times that of the general population (5% lifetime risk); the risk increases to 4.6-fold (7% lifetime risk) with two or three affected relatives[7]; some recommend annual screening to all women 25 years old and above with such a family history.[8] A very small number of women (0.05% of the population) are known to be at markedly increased risk for the development of ovarian cancer by virtue of a family history of one of three hereditary syndromes. Patients with a family history of hereditary nonpolyposis colorectal cancer (Lynch II syndrome), breast–ovarian cancer syndrome, or site-specific ovarian cancer incur a lifetime risk of developing ovarian cancer approaching 40%. In this small group of high-risk women, in addition to annual screening, comes the recommendation for prophylactic oophorectomy at age 35 or whenever childbearing is complete.[7–9] This is not applied to women who simply have a history of affected relatives without one of the defined syndromes.

Heritable Syndromes that Correlate with Increased Risk of Ovarian Cancer

Malignant ovarian neoplasms are found with much higher frequency in women with one of three heritable syndromes than in the general population. They also occur at significantly younger ages in this small group. Women with hereditary nonpolyposis colorectal cancer syndrome develop ovarian cancer at a mean age of 40 years; with hereditary breast–ovarian cancer syndrome at a mean age of 52 years. This is in contrast to the general population in whom sporadic cases of ovarian carcinoma occur at a mean age of 59 years.

Lynch II syndrome (hereditary nonpolyposis colorectal carcinoma syndrome) is an autosomal dominant trait with high penetrance. Affected women tend to develop colorectal cancers under the age of 45 years and have an increased risk for endometrial carcinoma. Women with this syndrome have an elevated risk of developing ovarian carcinoma.[10] Histologically, these tumors are most likely to be cystadenocarcinomas.

The recently identified *BRCA 1* gene (on the long arm of chromosome 17) is the marker for the hereditary breast–ovarian cancer syndrome, which carries with it a 50% lifetime risk of developing ovarian cancer.[11,12] *BRCA 2* is similarly implicated. The *BRCA 1* gene is characterized as a tumor-suppressor gene; it is considered responsible for disease in 45% of families with multiple cases of breast carcinoma and the preponderance of the families with both breast and ovarian malignancies.[13]

The site-specific ovarian cancer syndrome is much less common than either the Lynch II syndrome or the breast–ovarian cancer syndrome. Only an increased incidence of ovarian neoplasm is seen without involvement of breast, colon, or other organs.[12]

Screening for Women at Increased Risk of Ovarian Cancer

The decision to implement a screening program is based on estimates of prevalence of the disease, cost per case discovered, altered clinical outcomes, and availability of a practical, sensitive screening test, among other factors. Despite its obvious morbidity and mortality, ovarian cancer has a relatively low incidence and prevalence (as compared, for example, with breast cancer, whose prevalence and incidence unquestionably make mammographic screening worthwhile). Current recommendations, therefore, are for screening only a small subset of the population considered at increased risk for the disease by virtue of a family history of ovarian cancer or the presence of one of the syndromes known to confer a substantially increased risk of ovarian malignancy. Screening of the general population is not advocated by any authorities at this time.

Certain caveats with respect to screening bear mention. The detection of ovarian cancer by screening may still not be early enough in the evolution of the disease to affect ultimate outcome despite prompt intervention. The duration of preclinical disease has not been established; if it is short, screening at sufficiently close intervals to affect outcome may not be practically possible. There is also no assurance that tumors detected at an early stage by a screening program will exhibit the same biological behavior as those that are clinically manifested at the same stage.[8] That said, there is still a perceived benefit to be derived from screening a selected population.

Screening the high-risk patient is considered appropriate and advisable despite the current lack of definitive data to confirm improved outcomes from early detection. Logic dictates, however, that, because there is such a vast gap in 5-year survivals between early and advanced stages of the disease (90% vs. 15%, respectively), discovering and treating ovarian cancer in stage I will inevitably be of benefit. The goal in a screening program would understandably be the highest possible positive predictive value (PPV) for the process [i.e., (true-positive results/true-positive + false-negative) $\times$ 100]. Clinical investigators have suggested that a PPV of less than 10% (i.e., nine negative surgeries for the discovery of each ovarian cancer) would not be acceptable to either clinician or patient.[14]

Screening programs have used the combination of CA 125 and transvaginal ultrasound. CA 125 is a protein in the blood that is increased in the majority of women with ovarian cancer.[15] Screening using both CA 125 and transvaginal ultrasound has been studied in the general population[16–20] and in women with an increased risk for ovarian cancer due to family history.[21–23] Preliminary results suggest benefit of screening in the high-risk population with an overall specificity of 99.9% and a PPV of 26.8% in one study.[24] The PPVs in the general population, however, are not high enough to justify large screening programs.

History and Physical Examination

A targeted family history is a critical element in the evaluation of a woman to identify if she is at increased risk for ovarian cancer. Patients with a pertinent history for familial or syndromic predisposition to ovarian malignancy should undergo a careful bimanual rectovaginal examination yearly.[24] Unfortunately, the physical examination is relatively nonspecific and has limited sensitivity.[25] Limitations include examiner experience, patient body habitus, and a variety of pelvic pathologies that can produce masses or masslike effects on the physical examination. Nonetheless, physical examination continues to be viewed, rightly so, as the proper starting point in the screening process.

Serum CA 125 Levels

Serum CA 125, a tumor marker for ovarian cancer, does not have sufficiently high sensitivity and PPV to be used effectively for screening for ovarian malignancy. Although elevated in 85% of women diagnosed with ovarian cancer, it is also elevated in a variety of nonmalignant conditions, including pregnancy, liver failure, and endometriosis, and can be elevated from malignancies other than the ovary, such as breast cancer and colorectal cancer.[15] Serum levels greater than 35 U/mL are generally considered abnormal.[15,24,26,27] Overall, CA 125 is elevated in more than 90% of patients with epithelial cancers of the ovary of International Federation of Gynecology and Obstetrics (FIGO) stages II, III, and IV; unfortunately, fewer than 50% of women with stage I disease are found to have abnormal levels.[28,29] This latter group is the very one in which early detection might have a profound effect upon outcome.

Although other serum markers have been evaluated, none has been shown to have a sufficient PPV to be helpful in screening for ovarian cancer.[30,31] Although the combination of CA 125 and transvaginal ultrasound has shown promise,[25] the specificity of CA 125 levels is less useful in premenopausal women than in the postmenopausal group by virtue of a variety of physiological conditions (e.g., menstruation, pregnancy) and benign pathologies (e.g., endometriosis) associated with elevated CA 125 serum levels.[14,24,43]

Ultrasound

The basis for ultrasound screening by itself for ovarian neoplasm was established before the availability of transvaginal scanning using transabdominal techniques with transducer frequencies in the range of 3.5 MHz. Although these early studies form the basis for the current approach, it is universally recognized that transvaginal ultrasound is the only acceptable method of evaluating the ovary for

early-stage tumors.[33–36] Three parameters are considered in the sonographic assessment of the ovary: gray-scale morphology, spectral Doppler waveforms and quantification, and color Doppler imaging. These three have been studied for specificity, sensitivity, and predictive values in screening for ovarian cancer; each will be discussed and its overall contribution to effective screening outlined.

Gray-Scale Morphology

Essentially, all investigators attempting to define gray-scale characteristics of benign versus malignant ovarian neoplasms have established some form of morphological classification that assesses several parameters: size, wall thickness, number and thickness of septa, soft tissue excrescences (from walls or septa), and overall echogenicity.[29,37–47] Several authors have devised morphological classification systems that take into account sonographic characteristics, including size, wall characteristics, number and thickness of internal septa, and presence of internal debris. They assign numerical values to each factor and derive a composite score that reflects the likelihood of malignancy. This allows for at least a semiquantitative assessment of the likelihood a mass is malignant, although, admittedly, there is some measure of subjectivity to the interpretation of the transvaginal ultrasound. Most of the classification systems have considerable common ground; we have chosen that published by DePriest et al[47] by way of example (**Fig. 7–1**).

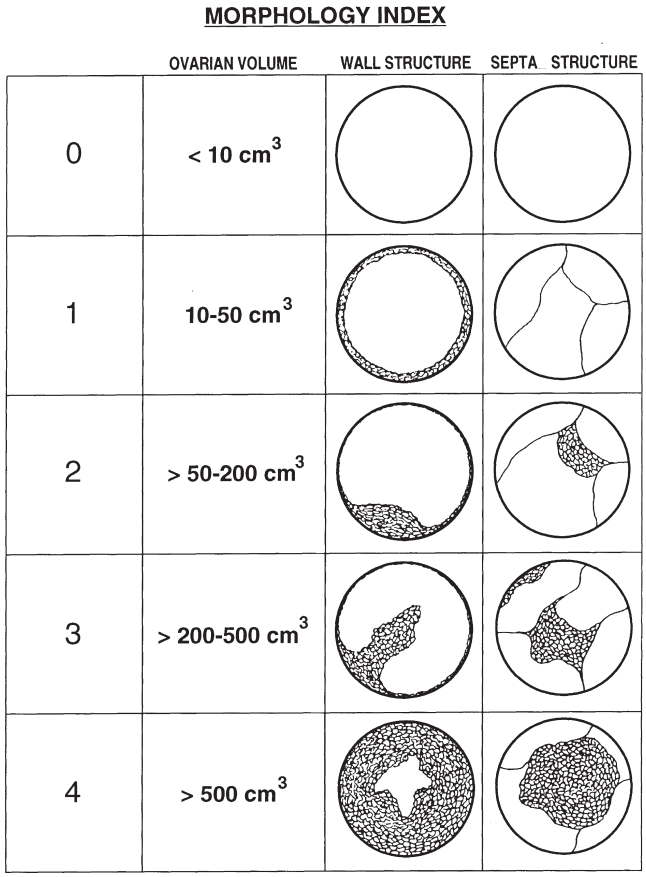

Figure 7–1 Morphology index for classifying ovarian tumors based on size, wall structure, and septa. (From Ueland FR, DePriest PD, Pavlik EJ, Kryscio RJ, van Nagell JR Jr. Preoperative differentiation of malignant from benign ovarian tumors: the efficacy of morphology indexing and Doppler flow sonography. Gynecol Oncol. 2003 Oct, 91: 47. Reprinted by permission.)

Size of Ovaries

Estimation of ovarian size is accomplished with the formula for the volume of a prolate ellipsoid (oval with flattened ends): volume = length × width × height × 0.5233 (or, by approximation, one half the product of the three dimensions). In premenopausal women, the normal ovary typically has a volume between 5 and 15 mL, decreasing in size with advancing age. In postmenopausal women, ovarian volume is usually less than 10 mL[41] (**Fig. 7–2**). Although larger ovaries, those greater than 5 cm in largest diameter, have a higher risk of malignancy than smaller ovaries, the parameter of overall ovarian size is not as useful for identifying ovarian cancer as is the sonographic evaluation of ovarian parenchyma.[38] The size of ovarian lesions does correlate somewhat with the risk of cancer because, in general, the larger the ovarian mass, the more likely it is to be malignant.[37,40]

Wall Features of Ovarian Mass

The thickness and contours of the walls of an ovarian mass are particularly important for predicting malignancy.[42,43] Solid tissue excrescences from the inner walls of a cystic mass and focal or diffuse thickening of the walls exceeding 3 mm are most worrisome for malignancy.[38,40,44–47] Overall, the greater the wall thickness and the more the number of soft tissue projections present, the higher the risk of malignancy (**Fig. 7–3, Fig. 7–4, Fig. 7–5**).

Septa within Ovarian Mass

Septa within an ovarian mass are evaluated with respect to number, thickness, and irregularity. Masses with many septa have a greater chance of malignancy than those with few. Those with thick septa, especially septa measuring more than 3 mm or septa with focal thickening, have an increased chance of malignancy. Although the number of septa does correlate somewhat with malignancy, it should be noted that mucinous ovarian tumors, whether benign or malignant, tend to have more septations than serous tumors. Thus, no specific number of septa nor any ratio of septations to tumor volume can be used to discriminate a benign ovarian cystic mass from a malignant one (**Fig. 7–6, Fig. 7–7, Fig. 7–8**).[38,40,44,48]

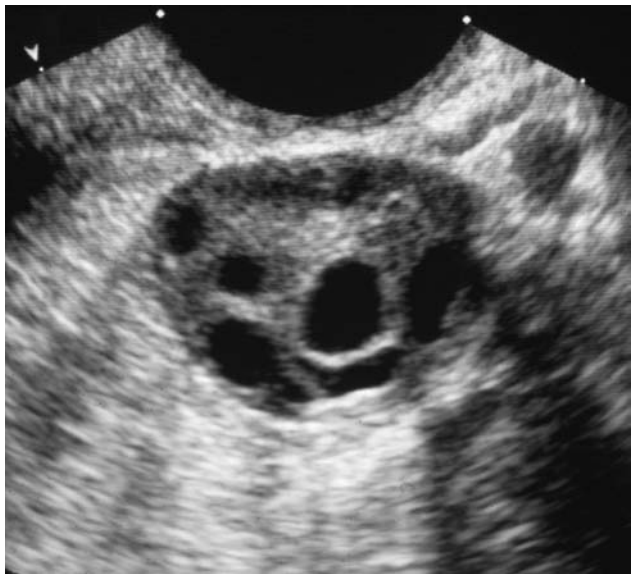

A

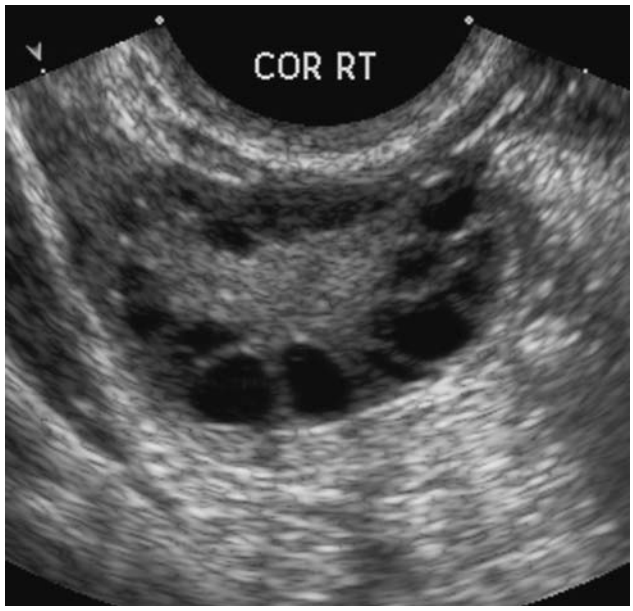

B

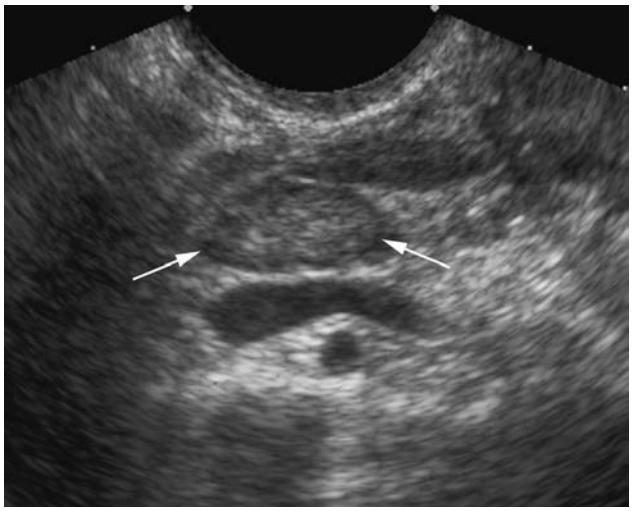

C

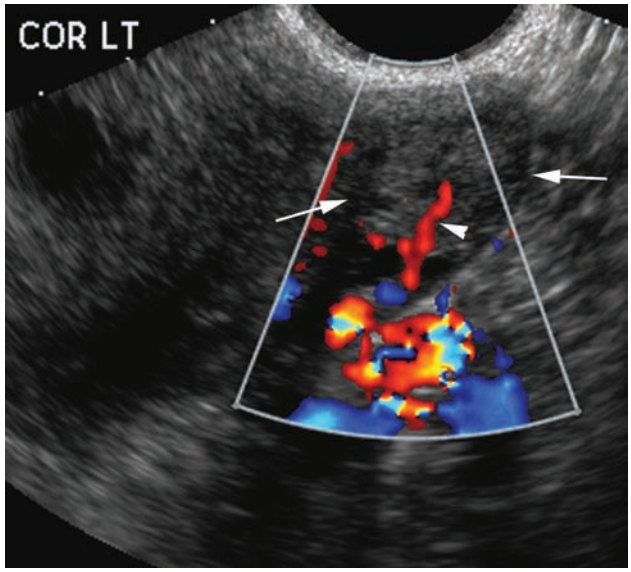

D

Figure 7–2 Normal ovaries. Sonographic images of ovaries from two different premenopausal patients. Multiple small follicles are seen in both. **(A)** Normal ovary; note multiple small follicles. **(B)** Normal ovary with radial arrangement of normal follicles. **(C)** Sonogram of ovary (arrows) in postmenopausal woman. The ovary contains no small follicles and is smaller than the ovaries in premenopausal women. **(D)** Normal ovary (arrows) with flow seen within it (arrowhead).

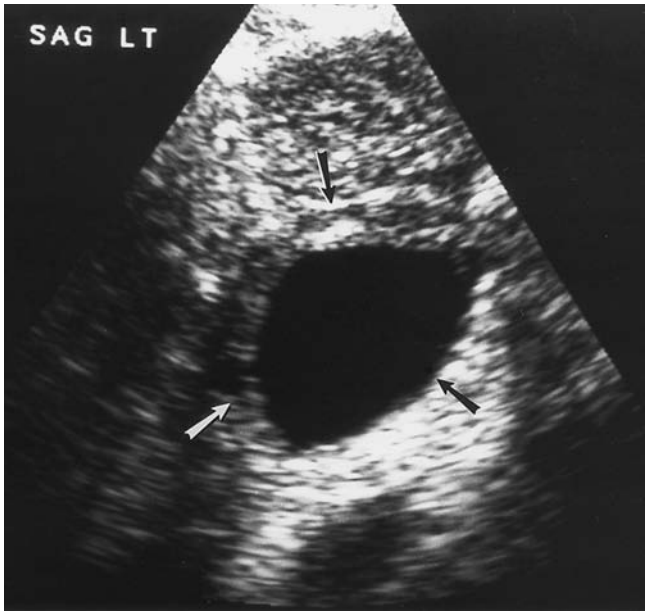

Figure 7–3 Simple cyst. Normal ovary (arrows) contains a simple cyst measuring ~33 mm in maximum diameter. This represents a functional (corpus luteum) cyst and will regress spontaneously. Follicles typically range up to 24 mm.

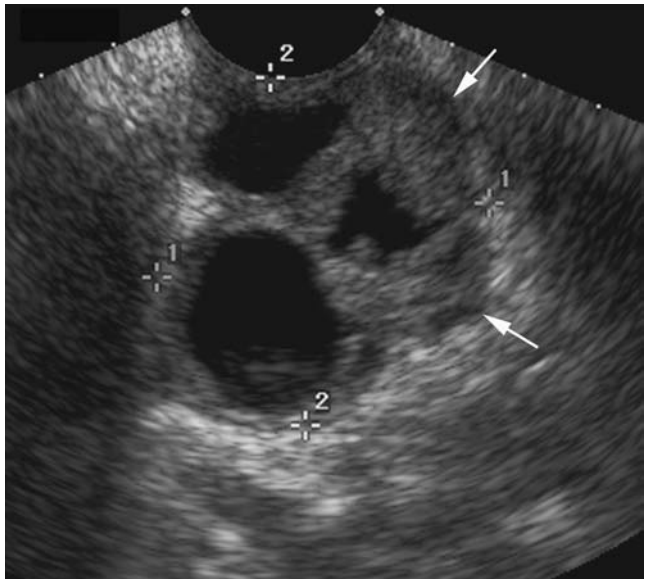

Figure 7–4 Thickening of cyst wall. Complex ovarian lesion (calipers) with thickening of some parts of the wall (arrows).

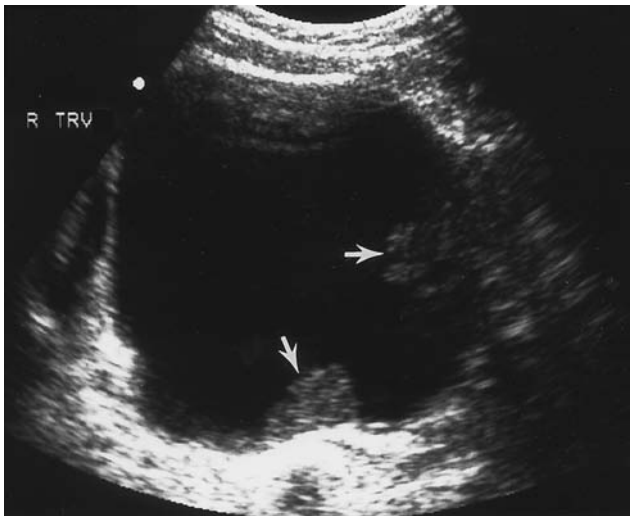

A

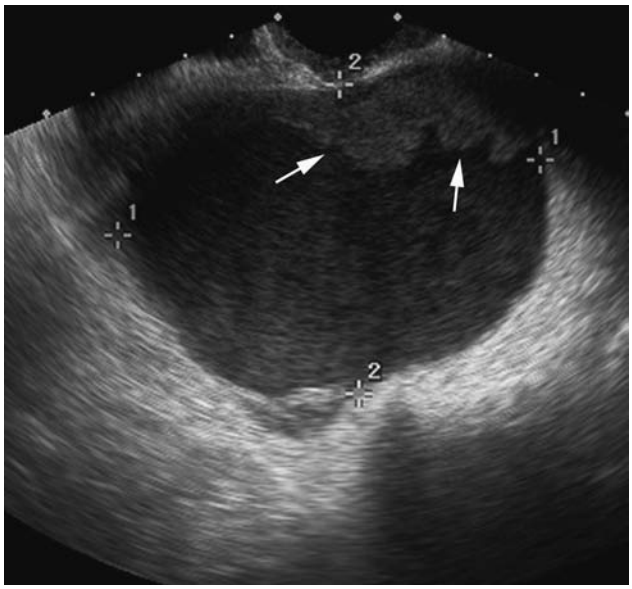

B

Figure 7–5 Mural nodules. **(A)** This histologically malignant ovarian neoplasm has at least two solid mural nodules (arrows), increasing its change of malignancy based on morphological criteria. **(B)** Another ovarian cystic neoplasm with solid tumor nodule (arrows) along one wall.

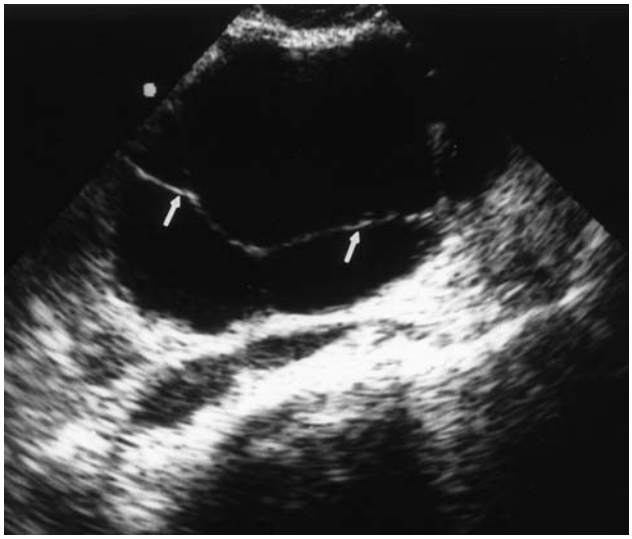

A

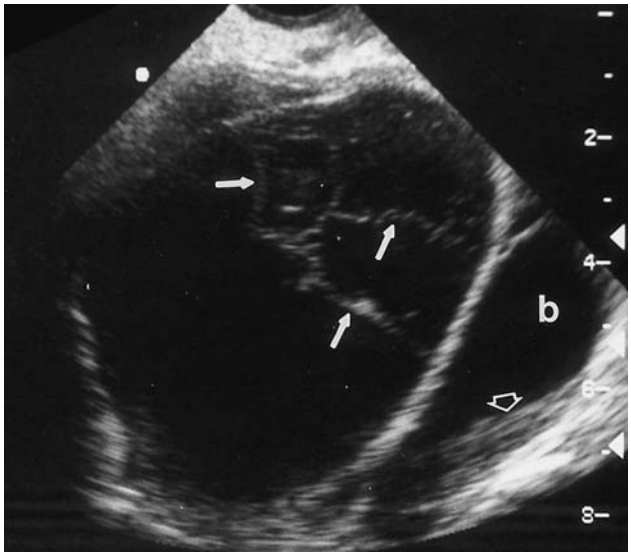

B

Figure 7–6 Serous cystadenoma. **(A)** This benign cystic mass contains a few thin septa (arrows) less than 3 mm thick, but is otherwise purely cystic. **(B)** Another benign serous cystadenoma, this cystic mass contains more septations (arrows), but they are still quite thin. b, urinary bladder with artifactual echoes (open arrowhead).

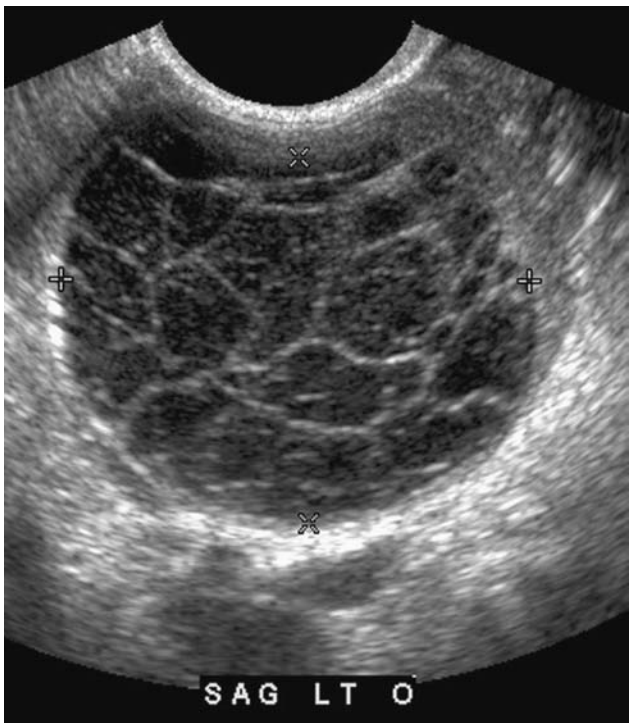

A

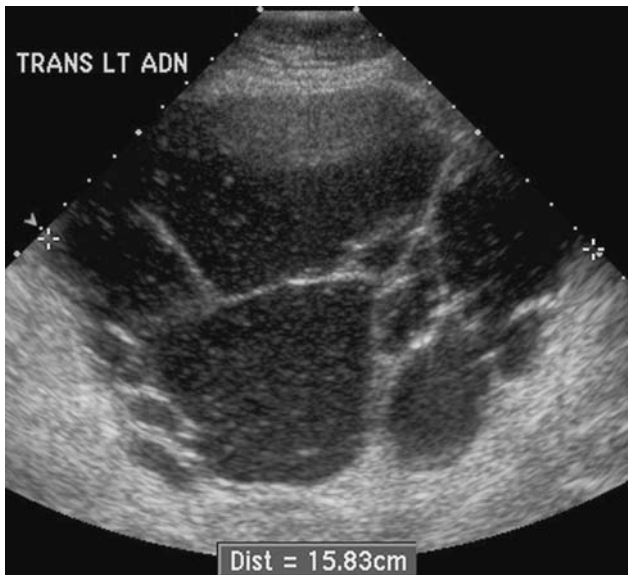

B

Figure 7–7 Thin septations. **(A)** Complex hemorrhagic ovarian cyst with many fine septations crisscrossing the cyst. **(B)** Mucinous cystadenoma with multiple fine septation and echoes within the cystic portion of the neoplasm.

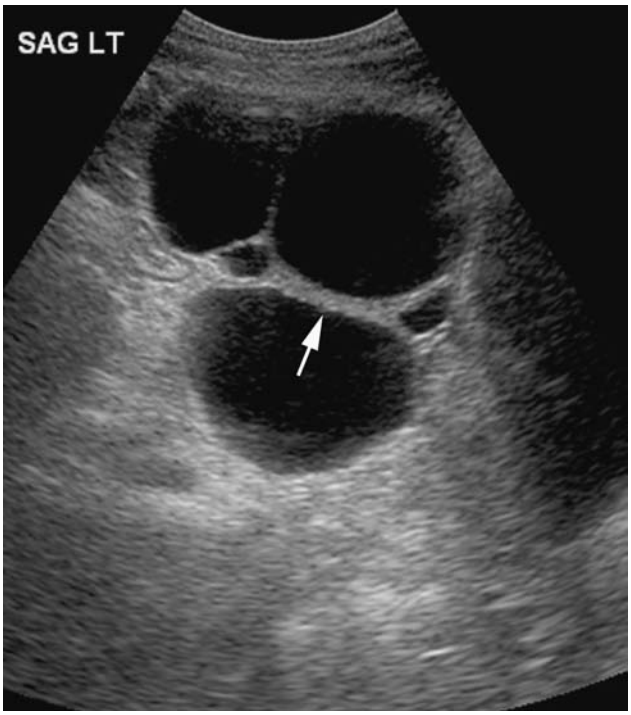

A

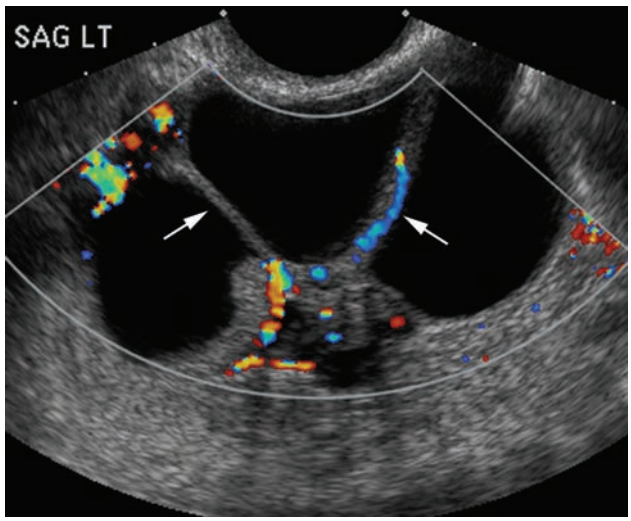

B

Figure 7–8 Thick septations. **(A)** Cystic ovarian benign neoplasm with thick septation (arrow) crossing it. **(B)** Cystic ovarian malignant neoplasm with several thick septations (arrows). Blood flow is seen with color Doppler within one of the septations on this image.

Echotexture of Ovarian Mass

The majority of primary neoplasms of the ovary are epithelial in origin; they are, to a greater or lesser degree, cystic. There is considerable variation in the amount of solid tissue within an epithelial tumor of the ovary and in the echotexture of the material within the mass. Tumors with a higher proportion of solid tissue admixed with the cystic components have a higher likelihood of malignancy than those with less solid tissue, as do those masses with substantial echogenic internal debris in the cystic components, when compared with those whose cystic components have few internal echoes. In general, the cystic components of mucin-producing tumors often demonstrate low-level internal echoes, sometimes with fluid/debris levels, presumed to represent the mildly echogenic mucin itself. Quantification of the amount of solid tissue present in any given tumor is subjective at best; and classification systems that assign numerical values to this factor do so on the basis of the subjective assessment.[38,44,49] Diagrammatic representation of the spectrum of solid tissue proportions is provided by charts such as the one in **Fig. 7–1** to serve as a reference guideline (**Fig. 7–9, Fig. 7–10, Fig. 7–11**).

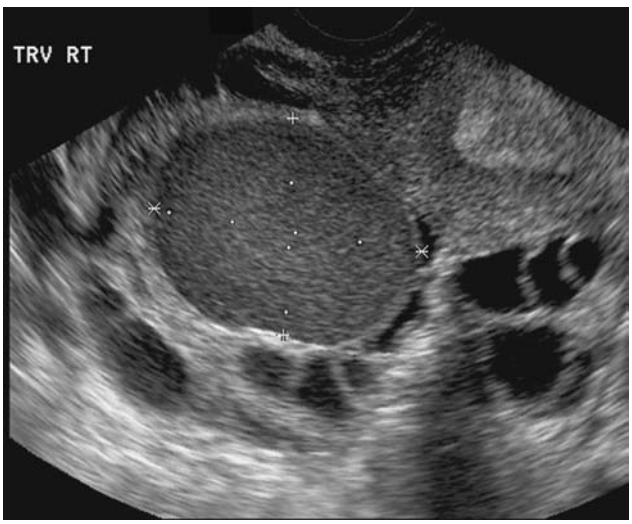

Figure 7–9 Ovarian cyst with internal echoes. Sonogram of right ovary containing a cyst (calipers) filled with homogeneous echoes. This proved to be a benign endometrioma.

Ovarian benign teratomas or dermoid tumors constitute a significant exception to the correlation between internal echogenicity of an ovarian mass and its risk of malignancy. Ovarian teratomas are usually benign tumors, although there are no reliable sonographic criteria for differentiating the benign from the malignant. Teratomas commonly have substantial internal echogenicity in the form of highly echogenic mural nodules of tissue (the "Rokitansky nodule" or "dermoid plug") or considerable amounts of highly echogenic material, representing fat or hair, often within a cystic area with fluid/debris levels.[50–53] It should be noted that the hair or fat found in a dermoid will be considerably more echogenic than the low-level reflectivity of mucin in an epithelial malignant neoplasm.

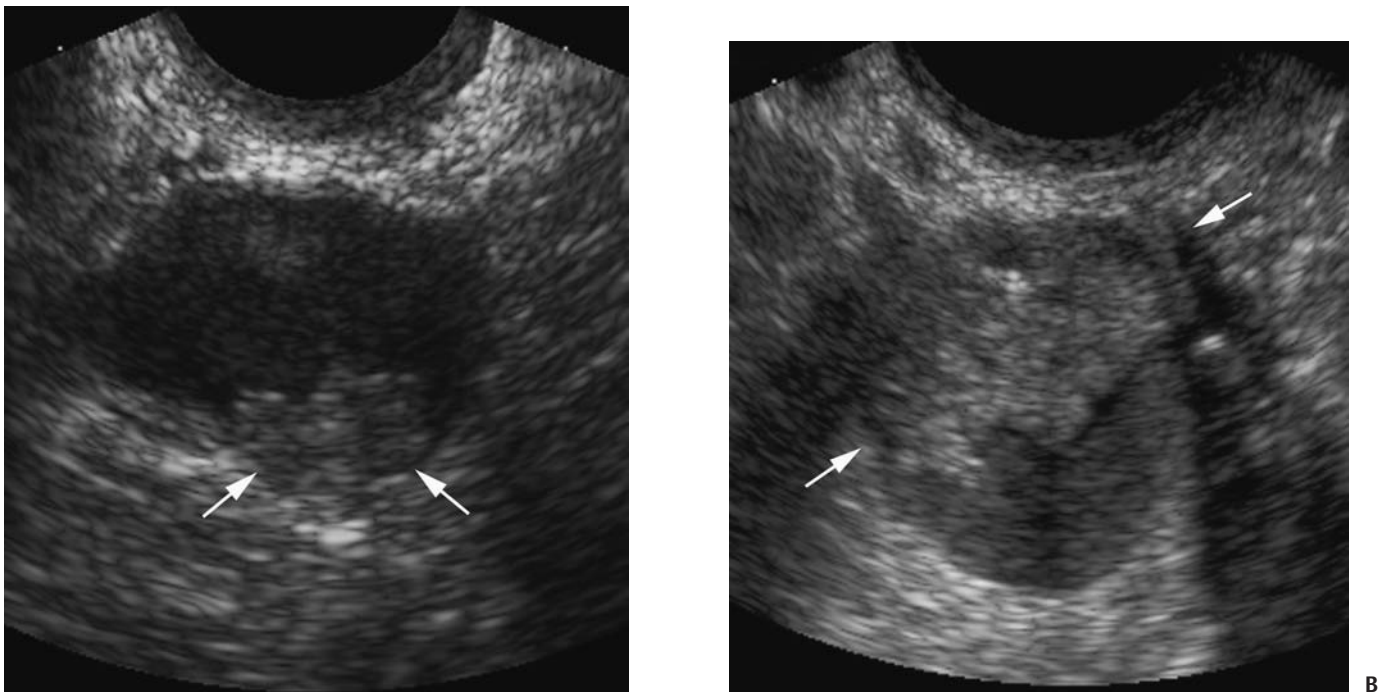

Figure 7–10 Mixed cystic and solid ovarian lesions. **(A)** Mucinous cystadenofibroma with solid component (arrows) and echoes in the cystic portion. **(B)** Mucinous cystadenoma with solid component (arrows) making up almost half the tumor.

The finding of a highly echogenic focus producing shadowing within a cystic mass strongly suggests calcification and reinforces the diagnosis of a dermoid tumor (**Fig. 7–12**).

The sonographic appearance of an ovarian mass can be used to predict whether it is benign versus malignant based on its composition (cystic versus solid) and internal echotexture. Morphologies that are typically benign, including anechoic simple cysts, cysts with smooth, thin septations less than 3 mm, complex cysts with homogeneous internal echoes, and typical dermoid tumors, have high negative predictive value of 99%.[48] Masses with sonographic findings worrisome for malignancy, including

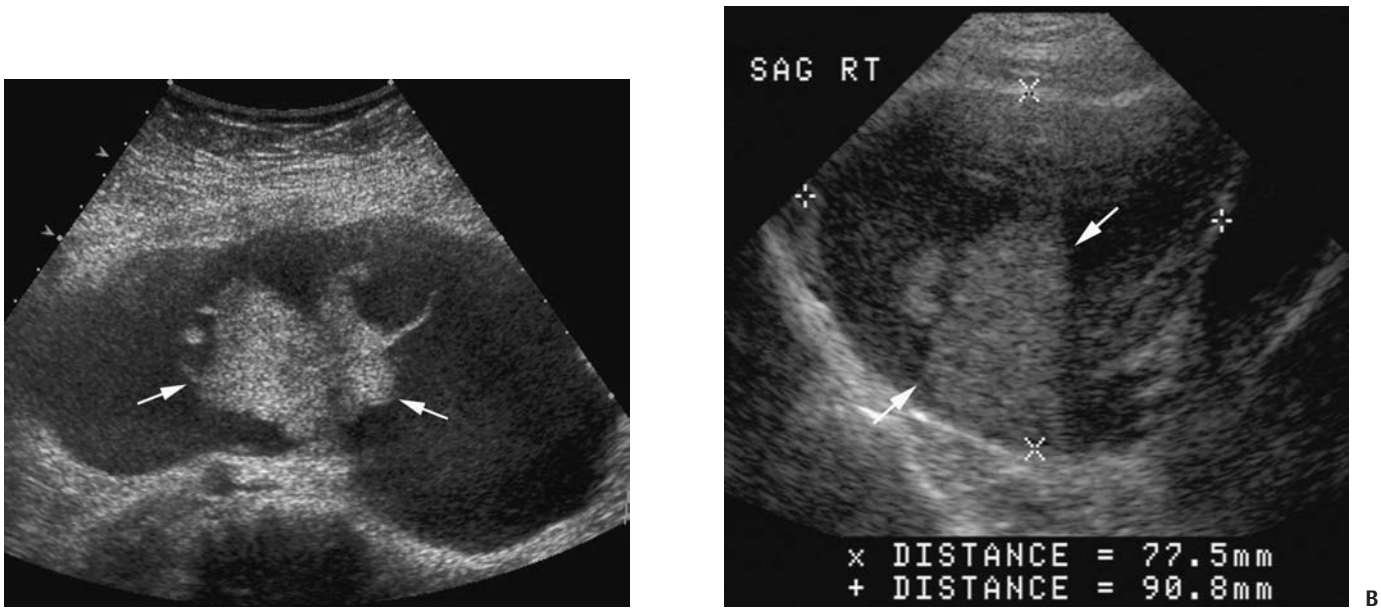

Figure 7–11 Ovarian cancer. **(A)** Large cystic ovarian carcinoma with irregular solid component (arrows) located centrally. **(B)** Another ovarian malignancy (calipers) with large solid component (arrows).

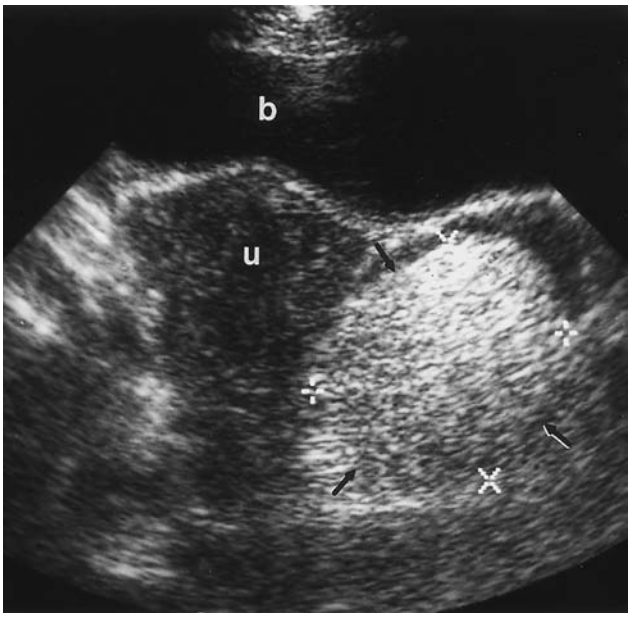

A

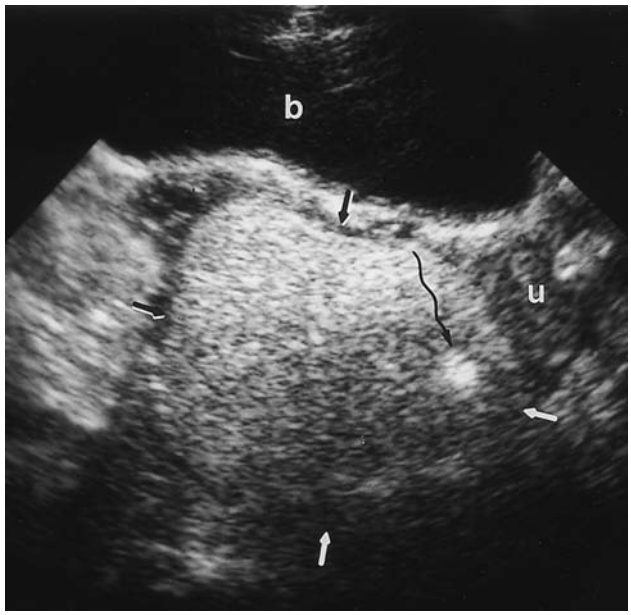

B

Figure 7–12 Dermoid. **(A)** Transverse image. **(B)** Left parasagittal image. In many cases, the echotexture of an ovarian mass will strongly suggest dermoid. This highly echogenic mass (arrows and calipers) containing mostly fat is seen to have an even more echogenic focus [wavy arrow in **(B)**] representing calcification. b, urinary bladder; u, uterus.

multiple septations, thick septations, solid components, and echogenic cystic areas, have a positive predictive value for malignancy of ~50%.

Most clinicians consider that a simple unilocular cyst less than 6 cm in a premenopausal woman has such a low chance of malignancy that it can be followed to resolution by ultrasound, rather than needing surgical removal. Likewise, a simple unilocular cyst less than 5 cm in a postmenopausal woman is considered safe to monitor with periodic ultrasound examinations.[54]

Several other neoplastic processes in the ovary (both primary and secondary) demonstrate high proportions of solid tissue. Endometrioid carcinoma of the ovary, metastatic tumors from several different primary malignancies (e.g., breast, lung, gastrointestinal tract) grouped under the broad heading of Krukenberg's tumors, germ cell tumors, and lymphoma all produce predominantly solid enlargement of the ovary or solid ovarian masses[55–60] (**Fig. 7–13**). It is uncommon for these processes to resemble epithelial carcinomas of the ovary sonographically.

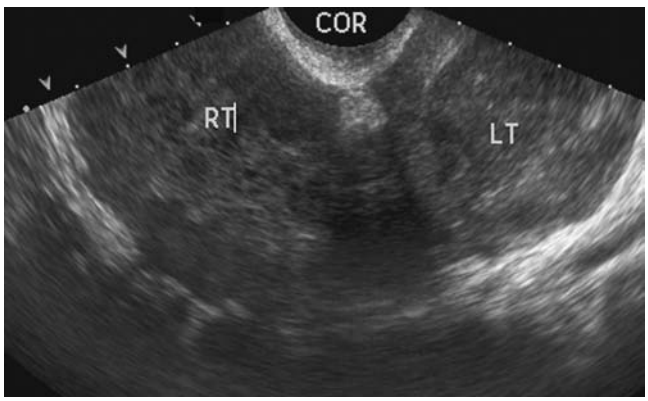

Figure 7–13 Lymphoma. Coronal image of both ovaries. Both the right (RT) and left (LT) ovaries are enlarged and solid due to lymphoma.

Spectral Doppler Imaging

The neovascularity produced by malignant neoplasms typically lacks both vasomotor control and muscular walls. As a result, the vascularity in a malignant tumor is usually high flow with a low-resistance perfusion pattern that translates into large passive forward diastolic flow. This effect is reflected in measurements of both the resistive index (RI) and the pulsatility index (PI). The RI [(peak systolic flow – end diastolic flow)/peak systolic flow] is calculated from the spectral Doppler waveform, as is the PI [(peak systolic flow – end diastolic flow)/mean Doppler shift]. Lower RI and PI values are associated with increased risk of malignancy, with acceptable cutoffs for RI of 0.40 and for PI of 1.0. Doppler waveforms yielding an RI or PI less than these values are indicative of increased diastolic flow and thus are suggestive of malignancy. Benign neoplasms, on the other hand, generally display little passive diastolic flow because they have high-resistance vascular

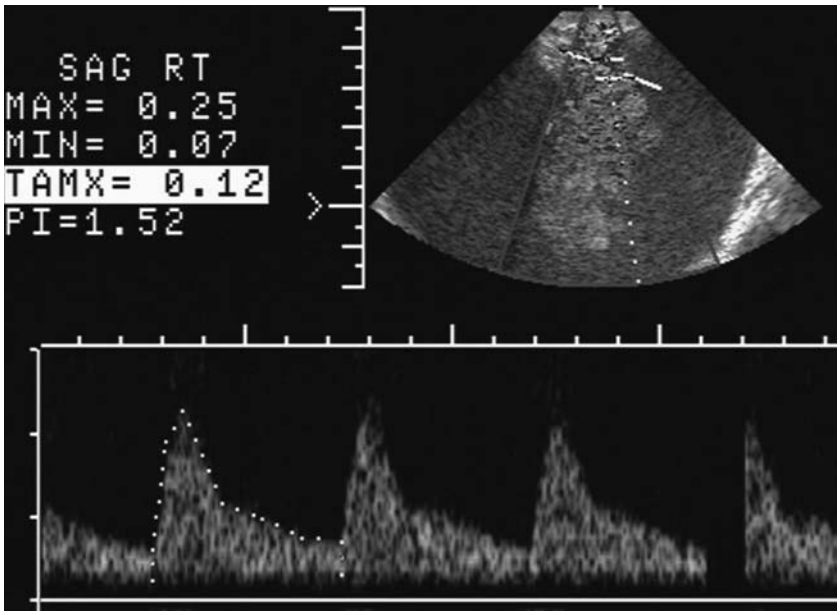

Figure 7–14 High-resistance flow. **(A)** Doppler waveform from a vessel in the solid component of an ovarian neoplasm. The pulsatility index (PI) of 1.52 indicates high-resistance flow, more often seen in benign than in malignant tumors.

beds and therefore, produce higher RI and PI values[42,44,45,61–67] (**Fig. 7–14** and **Fig. 7–15**).

Unfortunately, there is considerable overlap in RI and PI values from spectral Doppler waveforms of benign and malignant ovarian neoplasms, making these parameters on their own of little clinical utility for distinguishing between benign and malignant disease.[40,46,48,49,68–71] No cutoff value for RI or PI has acceptable sensitivity and specificity. Spectral Doppler on its own is, therefore, not considered a diagnostic parameter to distinguish between benign and malignant ovarian processes.

Color Doppler Imaging

Logic dictates that the neovascularity generated by a neoplasm would produce a significant increase in the color flow Doppler pattern. This premise has led several investigators to evaluate the presence, distribution, and prevalence of color flow signals in ovarian masses in an attempt to distinguish between benign and malignant processes.[48,61,71–73] Unfortunately, as with spectral Doppler in ovarian masses, there is considerable overlap in the color Doppler findings in benign and malignant ovarian masses,

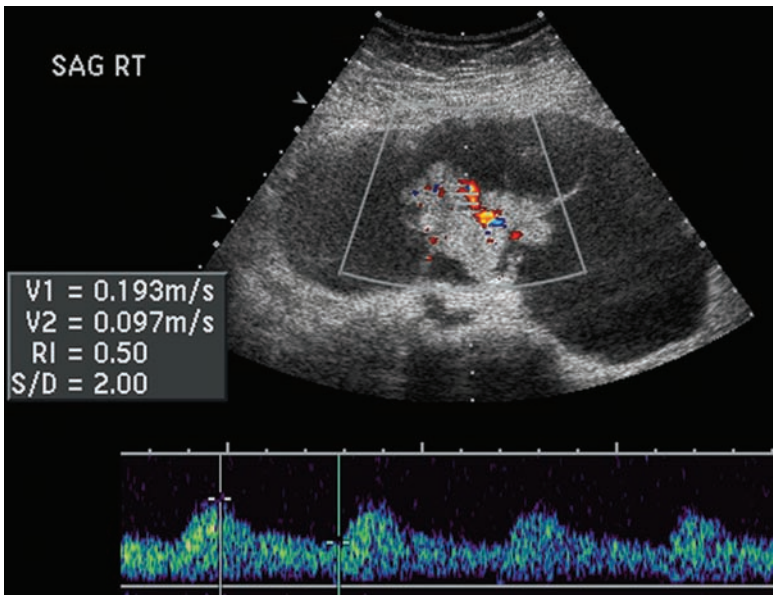

Figure 7–15 Doppler flow in ovarian cancer. **(A)** Doppler waveform from a vessel in the solid component of a malignant ovarian neoplasm. The resistive index (RI) of 0.50 is higher than the cutoff of 0.4 used to define low-resistance flow characteristic of malignancy.

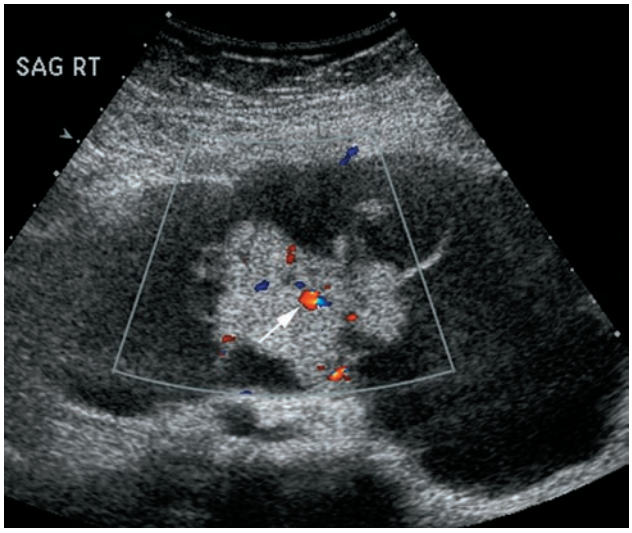

A

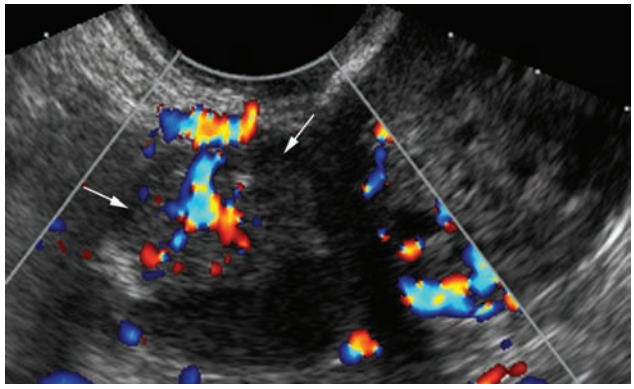

B

Figure 7–16 Color Doppler flow in an ovarian neoplasm. **(A)** Image of ovarian carcinoma with a central solid component in which blood flow is seen on color Doppler. **(B)** Extensive blood flow seen with color Doppler within the solid component (arrows) of another ovarian neoplasm.

making this parameter of limited value for distinguishing benign from malignant. In general, the less flow in a mass, the less likely it is to be malignant.[44,48] Flow within a nodule in the wall of a cystic mass or within a thick septation is suggestive of malignancy (**Fig. 7–16, Fig. 7–17**).[44] The presence of central flow is seen more often in malignant masses than in benign ones, and absence of central flow suggests a benign process[74,75]; however, complete absence of color flow still does not exclude malignancy.[48,69] Furthermore, these observations may not hold as color Doppler equipment improves and more sensitive equipment is able to detect scant and slower flow than could previously be detected.

In short, the basic premise that malignant tumors of the ovary will generally demonstrate more color flow, lower-resistance spectral tracings with higher passive diastolic flow, and lower RI (< 0.4) and PI (< 1.0) values compared with benign masses, appears to be valid. However, attempts thus far to establish discriminatory parameters that result in adequate sensitivity, specificity, and PPV have not been successful. Studies are ongoing, including those assessing ultrasound contrast agents,[76] and there is reason to believe that practical, applicable criteria will be developed to improve the ability of ultrasound and Doppler to distinguish benign from malignant ovarian masses. At present, findings of increased vascularity of low resistance by either spectral or color flow techniques will at least serve to raise suspicion of a malignant process and prompt further workup. It should be remembered that several nonmalignant processes (e.g., pelvic inflammatory

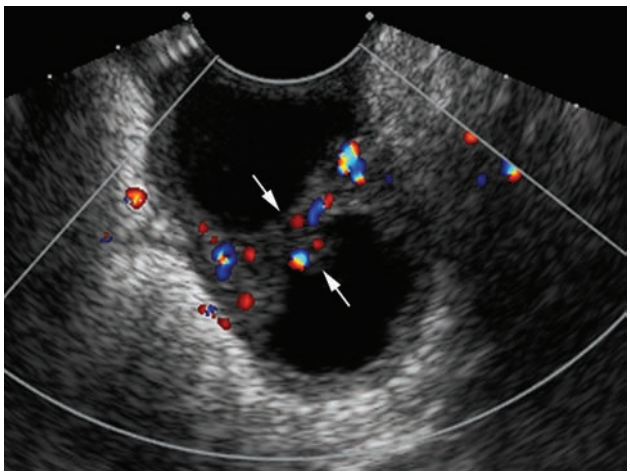

A

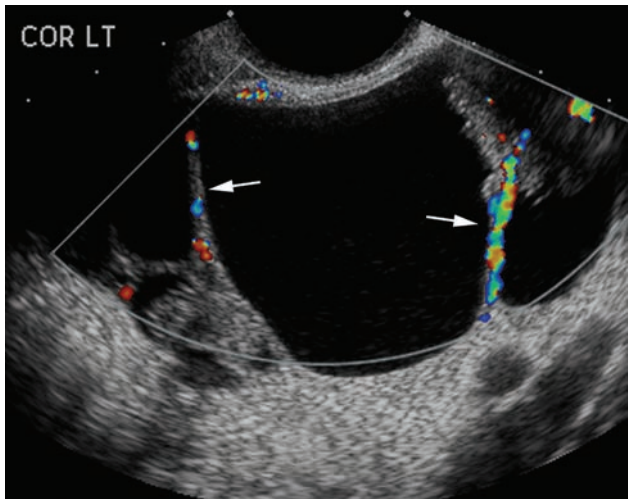

B

Figure 7–17 Color Doppler flow in a thick septation. **(A)** Flow identified with color Doppler within a thick septation (arrows) and **(B)** within two septations in two different ovarian neoplasms.

disease, ectopic pregnancy, corpus luteum of pregnancy) may also produce hypervascularity with relatively low-resistance flow patterns.

Summary

The role of ultrasound in screening for ovarian malignancy is still evolving with respect to technique, criteria, and application. Screening of the general population is not felt to be justified by virtue of the low prevalence of the disease and the unfavorable cost-per-case-discovered ratio. Extensive experimental screening protocols are ongoing and may yield strong objective data in the next several years by which our current approach can be reassessed.

A population considered at high risk by virtue of family history of ovarian malignancy (more than one first-degree relative) or the presence of a heritable syndrome that predisposes to the disease has been clearly identified and is considered appropriate for annual screening. Screening should begin at age 25 to 30 and include physical examination, serum CA 125, and transvaginal ultrasound. Women deemed to be at intermediate risk (single first-degree relative, several more distant relatives, or personal history of breast cancer) may be offered screening with CA 125 followed by ultrasound only if the serum CA 125 is elevated.[8]

The mainstay of sonographic evaluation of ovarian masses is currently their sonographic morphological characteristics. Enlargement of the ovary is generally considered abnormal and deserving of further evaluation.[8,36] Any patient with an abnormal volume at initial screening should be scheduled for repeat examination in 4 to 6 weeks. Any ovarian mass that exhibits wall thickening, focal or diffuse, of greater than 3 mm, or mural soft tissue excrescences of greater than 3 mm projecting into the cystic components is suspect. Likewise, the mass with multiple or thickened (greater than 3 mm, focal or diffuse) septa demands at least close follow-up, if not excision.

Several morphological classification systems are available, providing a means of summarizing and, to some extent, quantifying characteristics to arrive at a numerical scoring value; from this the level of suspicion with respect to malignancy is established. Although certain clinical situations allow for close follow-up of questionable lesions by rescanning in 6 to 8 weeks, cases in which the ultrasound morphology suggests malignancy should be recommended for surgical excision. Percutaneous biopsy is not considered an acceptable alternative because of the risk of tumor spread in the peritoneal cavity with rupture of malignant cystic mass. The tendency toward early surgery for suspicious lesions is justifiable on the basis of the excellent prognosis for early-stage ovarian malignancy (stage I and II) with greater than 90% five-year survival, and the discouraging outcomes (15 to 20% five-year survival) for those with advanced disease (stage III and IV). Several authors now advise prophylactic oophorectomy at age 35 or when childbearing is complete for women with two first-degree relatives with ovarian cancer or the inherited conditions discussed above.[7,13]

Both spectral and color flow Doppler are currently felt to be of adjunctive value in the assessment of ovarian masses; findings with these modalities influence levels of suspicion, but currently have insufficient discriminatory value to be used as stand-alone criteria to characterize a mass as benign or malignant.

References

1. American Cancer Society. Cancer facts & figures 2005. Atlanta: American Cancer Society; 2005
2. Young RC, Decker DG, Wharton TJ, et al. Staging laparotomy in early ovarian cancer. JAMA 1983;250:3072–3076
3. Ozols RF, Rubin SC, Dembo AJ, Robboy SJ. Epithelial ovarian cancer. In: Hoskins WJ, Perez CA, Young RC, eds. Principles and Practice of Gynecologic Oncology. Philadelphia: Lippincott; 1992:731–781
4. Morrow CP. Malignant and borderline epithelial tumors of the ovary: clinical features, staging, diagnosis, intraoperative assessment and review of management. In: Coppleson M, ed. Gynecologic Oncology. Edinburgh, Scotland: Churchill Livingstone, 1992:889–915
5. Koonings PP, Campbell K, Mishell D, et al. Relative frequency of primary ovarian neoplasms: a ten-year review. Obstet Gynecol 1989; 74:921–925
6. Westoff C, Randall MC. Ovarian cancer screening: potential effect on mortality. Am J Obstet Gynecol 1991;165:502–505
7. Kerlikowske K, Brown JS, Grady DG. Should women with familial ovarian cancer undergo prophylactic oophorectomy? Obstet Gynecol 1992;80:700–707
8. Jacobs I, van Nagell JR Jr, DePriest PD. Screening for epithelial ovarian cancer. In: Gershenson DM, McGuire WP, ed. Controversies in Management of Ovarian Cancer. New York: Churchill Livingstone; 1998:1–16
9. National Institute of Health. Ovarian cancer: screening, treatment and followup: Consensus Development Conference statement. Washington, DC: National Institute of Health, 1994, 1–29
10. Lynch HT, Kimberling WJ, Albano WA, et al. Hereditary non-polyposis colorectal cancer: Lynch syndrome I + II. Cancer 1985;56: 939–951
11. Lynch HT, Harris RE, Guirgis HA, et al. Familial association of breast/ovarian carcinoma. Cancer 1978;41:1543–1548
12. Lynch HT, Albano WA, Black L, et al. Familial excess of cancer of the ovary and anatomic sites. JAMA 1981;245:261–264
13. Gallion HH, Smith SA. Hereditary ovarian carcinoma. Semin Surg Oncol 1994;10:249–254
14. Jacobs I, Bridges J, Reynolds C, et al. Multimodal approach to screening for ovarian cancer. Lancet 1988;1:268–271
15. Ovarian Cancer. www.OncologyChannel.com/Ovarian Cancer. Healthcommunities.com, Inc. 1998–2006
16. Buys SS, Partridge E, Greene MH, et al. Ovarian cancer screening in the Prostate, Lung, Colorectal and Ovarian (PLCO) cancer screening trial: findings from the initial screen of a randomized trial. Am J Obstet Gynecol 2005;5:1630–1639
17. Menon U, Skates SJ, Lewis S, et al. Prospective study using the risk of ovarian cancer algorithm to screen for ovarian cancer. J Clin Oncol 2005;31:7919–7926

18. Fung MF, Bryson P, Johnston M, Chambers A. Cancer Care Ontario. Screening postmenopausal women for ovarian cancer: a systematic review. J Obstet Gynaecol Can 2004;8:717–728
19. Marchetti M, Zambon A, Lamaina V, Spadaro M, Marchiori S. Ultrasound as a possible screening method in ovarian cancer. Eur J Gynaecol Oncol 2002;2:123–126
20. Menon U, Jacobs IJ. Ovarian cancer screening in the general population. Curr Opin Obstet Gynecol 2001;13:61–64
21. Fishman DA, Cohen L, Blank SV, et al. The role of ultrasound evaluation in the detection of early-stage epithelialovarian cancer. Am J Obstet Gynecol 2005;192:1214–1221
22. Tailor A, Bourne TH, Campbell S, Okokon E, Dew T, Collins WP. Results from an ultrasound-based familial ovarian cancer screening clinic: a 10-year observational study. Ultrasound Obstet Gynecol 2003;21:378–385
23. Taylor KJ, Schwartz PE. Cancer screening in a high risk population: a clinical trial. Ultrasound Med Biol 2001;27:461–466
24. Jacobs I, Davies AP, Bridges J, et al. Prevalence screening for ovarian cancer in postmenopausal women by CA 125 measurement and ultrasonography. BMJ 1993;306:1030–1034
25. DePriest PD, van Nagell JR Jr. Transvaginal ultrasound screening for ovarian cancer. Clin Obstet Gynecol 1992;35:40–44
26. Helzlsouer KJ, Bush TL, Alberg AJ, et al. Prospective study of serum CA 125 levels as markers of ovarian cancers. JAMA 1993;269: 1123–1126
27. Zurawski VR Jr, Orjaseter H, Andersen A, Jellum E. Elevated serum CA 125 levels prior to diagnosis of ovarian neoplasia: relevance for early detection of ovarian cancer. Int J Cancer 1988;42:677–680
28. Jacobs I, Bast RC. The CA 125 tumour associated antigen: a review of the literature. Hum Reprod 1989;4:1–12
29. van Nagell JR Jr, Higgins RV, Donaldson ES, et al. Transvaginal sonography as a screening method for ovarian cancer: a report of the first 1000 cases screened. Cancer 1990;65:573–577
30. Woolas RP, Xu F-J, Jacobs IJ, et al. Elevation of multiple serum markers in patients with stage I ovarian cancer. J Natl Cancer Inst 1993;85:1748–1751
31. Garner EI. Advances in the early detection of ovarian carcinoma. J Reprod Med 2005;50:447–453
32. Jacobs IJ, Oram DH, Bast R Jr. Strategies for improving the specificity of screening for ovarian cancer with tumor-associated antigens CA 125, CA 15–3, and TAG 72.3. Obstet Gynecol 1992;80:396–399
33. Campbell S, Bhan V, Royston P, et al. Transabdominal ultrasound screening for early ovarian cancer. BMJ 1989;299:1363–1367
34. Davies AP, Jacobs I, Woolas R, Fish A, Oram D. The adnexal mass: benign or malignant? Evaluation of a risk of malignancy index. Br J Obstet Gynaecol 1993;100:927–931
35. DeLand M, Fried A, van Nagell JR, Donaldson ES. Ultrasonography in the diagnosis of tumors of the ovary. Surg Gynecol Obstet 1979;148:346–348
36. Goswamy RK, Campbell S, Whitehead MI. Screening for ovarian cancer. Clin Obstet Gynecol 1983;10:621–643
37. DePriest PD, van Nagell JR, Gallion HH, et al. Ovarian cancer screening in asymptomatic postmenopausal women. Gynecol Oncol 1993;51:205–209
38. Sassone AM, Timor-Tritsch IE, Artner A, et al. Transvaginal sonographic characterization of ovarian disease: evaluation of a new scoring system to predict ovarian malignancy. Obstet Gynecol 1991;78:70–76
39. Szpurek D, Moszynski R, Zietkowiak W, Spaczynski M, Sajdak S. An ultrasonographic morphological index for prediction of ovarian tumor malignancy. Eur J Gynaecol Oncol 2005;26:51–54
40. Jain KA. Prospective evaluation of adnexal masses with endovaginal gray-scale and duplex and color Doppler US: correlation with pathologic findings. Radiology 1994;191:63–67
41. Bruchim I, Aviram R, Halevy RS, Beyth Y, Tepper R. Contribution of sonographic measurement of ovarian volume to diagnosing ovarian tumors in postmenopausal women. J Clin Ultrasound 2004; 32:107–114
42. Kurjak A, Zalud I. Transvaginal colour Doppler in the differentiation between benign and malignant ovarian masses: In: Sharp F, Mason WP, Creasman W, eds. Ovarian Cancer. London: Chapman & Hall; 1992:249–264
43. Rottem S, Levit N, Thaler I, et al. Classification of ovarian lesions by high-frequency transvaginal sonography. J Clin Ultrasound 1990; 18:359–363
44. Buy JN, Ghossain MA, Hugol D, et al. Characterization of adnexal masses: combination of color Doppler and conventional sonography compared with spectral Doppler analysis alone and conventional sonography alone. Am J Roentgenol 1991;166: 385–393
45. Bourne TH, Campbell S, Reynolds KM, et al. Screening for early familial ovarian cancer with transvaginal ultrasonography and colour blood flow imaging. BMJ 1993;306:1025–1029
46. Bromley B, Goodman H, Benacerraf BR. Comparison between sonographic morphology and Doppler waveform for the diagnosis of ovarian malignancy. Obstet Gynecol 1994;83:434–437
47. DePriest PD, Shenson D, Fried A, et al. A morphology index based on sonographic findings in ovarian cancer. Gynecol Oncol 1993; 51:7–11
48. Stein SM, Laifer-Narin S, Johnson MB, et al. Differentiation of benign and malignant adnexal masses: relative value of gray-scale, color Doppler, and spectral Doppler sonography. AJR Am J Roentgenol 1995;164:381–386
49. Taylor KJW, Schwartz PE. Screening for early ovarian cancer. Radiology 1994;192:1–10
50. Quinn SF, Erickson S, Black WC. Cystic ovarian teratomas: the sonographic appearance of the dermoid plug. Radiology 1985;155: 477–478
51. Sisler CL, Siegel MJ. Ovarian teratomas: a comparison of the sonographic appearance in prepubertal and postpubertal girls. AJR Am J Roentgenol 1990;154:139–141
52. Guttman PH Jr. In search of the elusive benign cystic ovarian teratoma: application of the ultrasound "tip of the iceberg" sign. J Clin Ultrasound 1977;5:403–406
53. Sheth S, Fishman EK, Buck JL, et al. The variable sonographic appearance of ovarian teratomas: correlation with CT. AJR Am J Roentgenol 1988;151:331–334
54. Filly FA. Ovarian masses: what to look for; what to do. In: Callen PW, ed. Ultrasonography in Obstetrics and Gynecology. 3rd ed. Philadelphia: Saunders; 1994:625–640
55. Diakoumakis E, Vieux U, Seife B. Sonographic demonstration of thecoma: report of two cases. Am J Obstet Gynecol 1984;150:787–788
56. Yaghoobian J, Pinck RL. Ultrasound findings in thecoma in the ovary. J Clin Ultrasound 1983;11:91–93
57. Talerman A. Mesenchymal tumors and malignant lymphoma of the ovary. In: Blaustein A, ed. Pathology of the Female Genital Tract. 2nd ed. New York: Springer-Verlag; 1982:705–715
58. Athey PA, Malone RS. Sonography of ovarian fibromas/thecomas. J Ultrasound Med 1987;6:431–436
59. Athey PA, Siegel MF. Sonographic features of Brenner tumor of the ovary. J Ultrasound Med 1987;6:367–372

60. Young RH, Scully RE. Metastatic tumors of the ovary. In: Kurman RJ, eds. Blaustein's Pathology of the Female Genital Tract. 4th ed. New York: Springer-Verlag; 1994:939–974
61. Kurjak A, Shalan H, Kupesic S, et al. An attempt to screen asymptomatic women for ovarian and endometrial cancer with transvaginal color and pulsed Doppler sonography. J Ultrasound Med 1994; 13:295–301
62. Hata T, Hata K, Senoh D, et al. Doppler ultrasound assessment of tumor vascularity in gynecologic disorders. J Ultrasound Med 1989;8:309–314
63. Bourne T, Campbell S, Steer C, et al. Transvaginal colour flow imaging: a possible new screening technique for ovarian cancer. BMJ 1989;299:1367–1370
64. Fleischer AC, Rodgers WH, Kepple DM, et al. Color Doppler sonography of benign and malignant ovarian masses. Radiographics 1992;12:879–885
65. Hamper UM, Seth S, Abbas FM, et al. Transvaginal Doppler sonography of adnexal masses: differences in blood flow impedance in benign and malignant lesions. AJR Am J Roentgenol 1993;160: 1225–1228
66. Weiner Z, Thaler I, Beck D, et al. Differentiating malignant from benign ovarian tumors with transvaginal color flow imaging. Obstet Gynecol 1992;79:159–162
67. Bonilla-Musoles F, Ballester MJ, Simon C, et al. Is avoidance of surgery possible in patients with perimenopausal ovarian tumors using transvaginal ultrasound and duplex color Doppler sonography? J Ultrasound Med 1993;12:33–39
68. Levin D, Feldstein VA, Babcook CJ, Filly RA. Sonography of ovarian masses: poor sensitivity of resistive index for identifying malignant lesions. AJR Am J Roentgenol 1994;162:1355–1359
69. Brown DL, Frates MC, Laing FC, et al. Ovarian masses: can benign and malignant lesions be differentiated with color and pulsed Doppler US? Radiology 1994;190:333–336
70. Hata K, Hata T, Manabe A, et al. A critical evaluation of transvaginal Doppler studies, transvaginal sonography, magnetic resonance imaging, and CA 125 in detecting ovarian cancer. Obstet Gynecol 1992;80:922–926
71. Carter J, Saltzman Z, Hartenbach E, et al. Flow characteristics in benign and malignant gynecologic tumors using transvaginal color flow Doppler. Obstet Gynecol 1994;83:125–130
72. Guerriero S, Alcazar JL, Ajossa S, et al. Comparison of conventional color Doppler imaging and power Doppler imaging for the diagnosis of ovarian cancer: results of a European study. Gynecol Oncol 2001;83:299–304
73. Cohen LS, Escobar PF, Scharm C, Glimco B, Fishman DA. Three-dimensional power Doppler ultrasound improves the diagnostic accuracy for ovarian cancer prediction. Gynecol Oncol 2001;82: 40–48
74. Tekay A, Jouppila P. Validity of pulsatility and resistance indices in classification of adnexal tumors with transvaginal color Doppler ultrasound. Ultrasound Obstet Gynecol 1992;2:338–344
75. Fleischer AC, Rodgers WH, Kepple DM, et al. Color Doppler sonography of ovarian masses: a multiparameter analysis. J Ultrasound Med 1993;12:41–48
76. D'Arcy TJ, Jayaram V, Lynch M, et al. Ovarian cancer detected noninvasively by contrast-enhanced power Doppler ultrasound. BJOG 2004;111:619–622

8 Tamoxifen

Beverly G. Coleman

Although this chapter is somewhat unique in the sense that the title does not describe a particular clinical symptom, the subject matter is extremely relevant and important because tamoxifen remains the most widely prescribed endocrine therapy for breast cancer. Dramatic findings showed that tamoxifen reduced the rate of breast cancer by an estimated 45% for healthy women over the age of 34 at increased risk. This was reported by news agencies worldwide in 1998 when the Breast Cancer Prevention Trial was halted early.[1]

Tamoxifen is a member of a drug class called selective estrogen receptor modulators (SERMs). These drugs appear chemically similar to estrogen and function by blocking the action of estrogen in breast tissue. Tamoxifen was the first SERM to be investigated extensively for its anticancer properties and it remains the standard of care for early breast cancer today.

Breast cancer is the second leading cause of cancer deaths in women. It has long been a major public health problem for Americans, accounting for one of every three cancer diagnoses.[2] Currently, this disease cannot be prevented, and most risk factors cannot be modified. The high rate of morbidity and mortality associated with breast cancer has sparked renewed research efforts directed at the treatment and prevention of this dreaded disease. Therapeutic regimes currently include surgery, radiation, hormones, and/or chemotherapy.

Tamoxifen has been one of the most widely used, yet hotly debated treatments to date. Reported serious adverse effects, including an increased risk of endometrial cancer and venous thromboembolic events, initially raised the question of whether the net benefits outweigh the risks. There are now second-generation SERMs such as raloxifene. This drug was developed to avoid some of the undesirable estrogen agonist action of tamoxifen. Raloxifene is currently being used in the prevention and treatment of postmenopausal osteoporosis, with other potential indications still undergoing study. In the Multiple Outcomes of Raloxifene Evaluation (MORE) trial, raloxifene compared with placebo increased bone minimal density by 2 to 3% and reduced the incidence of new vertebral fractures by 30 to 50%.[3] Further studies have shown that raloxifene significantly decreases the incidence of breast cancer in selective populations; however, unlike Tamoxifen, any long-term use of raloxifene does not increase the risk of endometrial carcinoma.[4]

There is a new class of drugs challenging tamoxifen's status as a treatment of choice for advanced breast cancer. Aromatase inhibitors (AIs) have recently gained attention as a possible alternative therapy that can be taken instead of or as additional therapy after the completion of long-term tamoxifen. In several large, international clinical trials, AIs, drugs that block the synthesis of estrogen from precursor hormones, were shown to be very beneficial in that they delayed breast cancer longer than tamoxifen in women with advanced disease, who are sensitive to estrogen and progesterone. AIs had fewer side effects than tamoxifen, such as vaginal bleeding and deep venous thrombosis; however, unfortunately, some AIs were associated with increased bone loss with resultant higher fracture rates and musculoskeletal pain.[5]

Tamoxifen Effects and Mechanism of Action

Tamoxifen is a synthetic, nonsteroidal drug that acts primarily as an estrogen antagonist on breast tissue and as an estrogen agonist on the endometrium. It was introduced in the early 1970s and was found to be widely effective as palliative therapy for women with advanced or recurrent breast cancer. Tamoxifen competes for estrogen receptors when administered to women who produce estrogen, thereby decreasing the net estrogenic effect. It has been hypothesized that tamoxifen deprives estrogen receptor–positive tumor cells of one of their necessary growth stimulatory factors.[6] Another theory is that tamoxifen also interacts with estrogen receptors to induce synthesis of inhibitory substances that block the growth of mammary tumor cells and the cells of other organs as well.[7–9] Tamoxifen also has a weak estrogen effect in hypoestrogenic women.[10,11] About 50% of women with metastatic breast cancer benefit from tamoxifen.[12] The beneficial effects are most apparent for postmenopausal women with estrogen receptor–positive tumors and therefore, tamoxifen and other SERMs are not indicated in women with estrogen receptor–negative tumors, who are generally treated with chemotherapy.

By the 1980s, the success of tamoxifen in the management of advanced breast cancer provoked interest in its utility as adjuvant therapy in the treatment of surgically resected early-stage tumors. Overall survival statistics, as well as disease-free survival with reduced recurrence rates, have been documented for postmenopausal women when tamoxifen was added to other treatments. Several clinical trials also demonstrated prolonged disease-free survival for premenopausal women, as well as those with

estrogen receptor–negative disease.[12] The Scottish trial results suggested that postsurgical treatment with tamoxifen is more effective in prolonging survival than treatment at first signs of relapse. These data were used to support the rationale for preventative therapy in women at increased risk of developing breast cancer.[13] Large, randomized, controlled clinical trials of adjuvant therapy for early-stage breast cancer demonstrated a 35 to 40% decrease in contralateral breast tumors for women treated with tamoxifen compared with controls.[14,15]

Additional reported potential benefits derived from the estrogenic action of tamoxifen included the stabilization of bone mineral loss, which may prevent morbidity due to osteoporosis, and lowered circulating cholesterol levels, which may significantly reduce the risk of death from coronary artery disease.[16,17] Interestingly, tamoxifen is estrogenic on bones in postmenopausal women and antiestrogenic on bones in premenopausal women. It is antiestrogenic on certain parts of the brain, which can cause menopausal symptoms such as hot flashes, insomnia, and night sweats. Tamoxifen is estrogenic in the liver, producing an increase in blood clotting proteins, which slightly increases the risk of heart attacks and strokes, especially in those at high risk, such as cigarette smokers. Numerous studies report conflicting data on the effects of tamoxifen on total cholesterol.[18] Experts generally agree that tamoxifen provides very effective treatment for women with all stages of breast cancer. Evidence now supports the use of long-term adjuvant tamoxifen therapy for extended periods of up to 5 years to prevent the reemergence of tumors.[19] The benefits from 5 years of tamoxifen therapy, 20 mg daily, persists through 10 years of follow-up with no additional advantage to more prolonged treatment.[20]

Tamoxifen and the Endometrium

Tamoxifen's complex mode of action involves an estrogenic effect on the female genital tract. Estrogenic changes in the vaginal epithelium of postmenopausal women with breast cancer were first described in detail in the late 1970s.[21,22] Laboratory studies then demonstrated tamoxifen-stimulated growth of human endometrial carcinoma transplanted into athymic mice and breast cancer cells in culture medium.[23] Endometrial hyperplasia, polyps, uterine leiomyomas, uterine sarcomas, adenomyosis, and endometriosis were subsequently described in tamoxifen-treated patients by numerous researchers who implicated the prolonged estrogenic effects on the sensitive endometrium.[14,24,25] The endometrial response to tamoxifen may even vary according to the menopausal status of the patient. A small study of 46 patients described polyps mainly in younger women treated with tamoxifen compared with predominantly hyperplastic and neoplastic lesions among postmenopausal women.[26] The first case report of endometrial carcinoma associated with continuous postmenopausal tamoxifen exposure appeared in 1985 and many others soon followed.[14,24–27] Most experts agree that proliferation of the endometrium with tamoxifen is associated with a significantly increased risk of the development of endometrial carcinoma.

The relative risk of endometrial adenocarcinoma in patients with breast cancer has been reported as 1.72: 1.0 in women younger than 50 years, and almost 2.4 in women 70 years or older.[28] In asymptomatic postmenopausal women, the estimated prevalence of endometrial cancer approaches 7 per 1000.[29] In view of these statistics and the uncertain association between these two malignancies, a consideration is that a finite number of women will develop endometrial cancer, irrespective of their treatment protocol for breast cancer.

Some researchers also raise the issue of whether the increase in incidence of endometrial carcinoma was a true phenomenon or perhaps due to an improved detection rate of very early tumors.[7] A randomized Swedish trial of tamoxifen in 1846 postmenopausal patients undergoing primary surgery for early breast cancer with a median follow-up of 4 to 5 years reported a 6.5-fold higher occurrence of endometrial cancer in the tamoxifen group compared with that of controls. In addition, the cumulative frequency of endometrial cancer was significantly greater in those who continued on tamoxifen compared with those who stopped treatment at 2 years.[30]

Supporting data by others have shown relative risks for developing endometrial cancer ranging from 1.7 to 4.6.[31,32] Both the dose level and the duration of tamoxifen therapy are believed to be relevant to some degree. There may be a dose-dependency relationship associated with the proliferative effects of tamoxifen on endometrial tissue because the higher-dose Swedish trial had a more dramatic increase in endometrial cancer than other series using tamoxifen at lower doses of 20 mg daily.[13,33] However, endometrial cancers have developed in patients on daily dosages ranging from 20 to 60 mg. A higher frequency of endometrial cancer with increasing duration of therapy has also been reported by other investigators.[30] Endometrial cancer occurring after tamoxifen therapy is not of a different type with a worse prognosis than are such tumors in non–tamoxifen-treated patients.[19]

One study advocated pretreatment screening to identify patients at a higher risk of developing endometrial cancer. The authors reported a 17.4% incidence of asymptomatic endometrial lesions in 264 postmenopausal women who underwent pelvic sonography before starting tamoxifen at a daily dose of 20 mg. At 3 years of follow-up, the incidence of atypical endometrial lesions was significantly higher in women with initial lesions compared with those with a normal endometrium on pretreatment scans.[34] There is currently no general consensus as to whether it would be beneficial to perform pretreatment pelvic sonography before tamoxifen therapy.

Most researchers now concur that there is a definite increased risk of endometrial cancer, approximately two- to

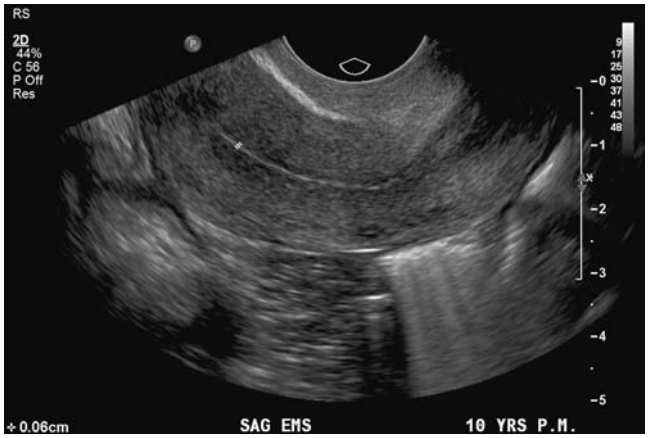

Figure 8–1 Normal postmenopausal uterus. Sagittal transvaginal sonography depicts the endometrium (cursors) as a 2 mm echogenic line in a patient on tamoxifen for 3 years, off therapy for 1 year, and then on Aromasin for the past year with numerous episodes of light spotting for 6 months.

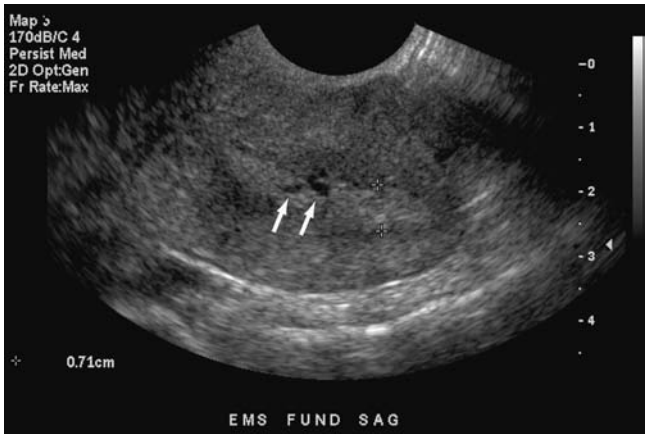

Figure 8–2 Mildly heterogeneous endometrium in retroverted uterus. Sagittal transvaginal sonography in a postmenopausal patient on tamoxifen for 5 years with elevated serum tumor markers, CA 125, and positive family history of ovarian carcinoma with 7 mm thick endometrium (cursors) containing tiny cysts (arrows).

threefold, following chronic tamoxifen therapy for invasive breast cancer. However, this increased risk does not necessarily translate to a very high absolute risk, which can be affected by other factors such as hypertension, diabetes, obesity, and prior hormone therapy. Although endometrial cancer and rarer uterine sarcoma are the worse complications of long-term tamoxifen use, the majority of tamoxifen-induced uterine pathology is benign. Many abnormal uterine growths associated with tamoxifen are endometrial polyps.

Although tamoxifen has proven valuable in the treatment of patients with various stages of breast cancer, some researchers object to its use as prophylaxis in healthy women until further information becomes available. A more stringent standard of safety is believed imperative for a primary prevention measure before it becomes acceptable for the general population.[18] Others report that the benefits of tamoxifen in saved lives exceed the incidence of endometrial cancer, which is predominantly a low-grade, well-differentiated disease.[35] However, the benefit:risk ratio must be assessed for each individual, especially when tamoxifen is being considered for prophylaxis. Regardless of how the drug is administered, informed consent should be obtained and patients should be counseled regarding its side effects. Gynecologic examination, PAP smears, endometrial biopsy, hysteroscopy, and pelvic ultrasound have been described as valuable methods of evaluating pelvic symptoms and complaints involving women on long-term tamoxifen therapy.[24–26]

Ultrasound Imaging

The imaging approach to evaluating the female pelvis includes both transabdominal (TAS) and transvaginal (TVS) sonography. TAS uses probes up to 5 MHz with scans over a distended urinary bladder to provide a general overview of the entire pelvis. TVS became an established tool in the investigation of obstetric and gynecologic pathology because it affords high-resolution scanning capability with multifocal 7 MHz or higher vaginal probes used in close proximity to the pelvic organs with an empty bladder. The many technological improvements have included the introduction of vaginal transducers with color/power Doppler and three-dimensional (3-D) imaging capability.

The vaginal technique is very well accepted by most premenopausal and postmenopausal women. TVS permits excellent visualization of the endometrium in the vast majority of patients and is far superior to TAS in this regard due to the improved resolution and near-field focusing. The endometrial–myometrial interface is much better depicted than was possible with full-bladder TAS (**Fig. 8–1**). The vaginal technique has been shown to consistently yield diagnostic information regarding subtle endometrial changes not detectable with transabdominal sonography.[36–38] Meticulous scanning techniques may be necessary to image the endometrium of the retroverted or retroflexed uterus, which sometimes is at odd angles to the incident sound beam (**Fig. 8–2**).

TVS can accurately measure endometrial thickness, which is the total measurement across the lumen of the endometrial cavity from one endometrial–myometrial interface to the other. This measurement should be performed with digital calipers in the sagittal plane at the site of maximal thickness, which is generally at or just below the uterine fundus. The value obtained actually represents two closely opposed endometrial layers. Endometrial fluid and the hypoechoic, inner compact layer of the myometrium should be excluded to avoid overestimation of endometrial thickness (**Fig. 8–3**). In experienced hands, sonographic measurements of the endometrium are usually

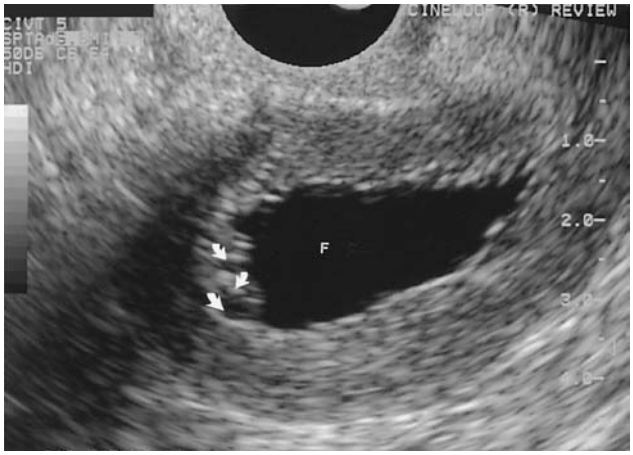

A

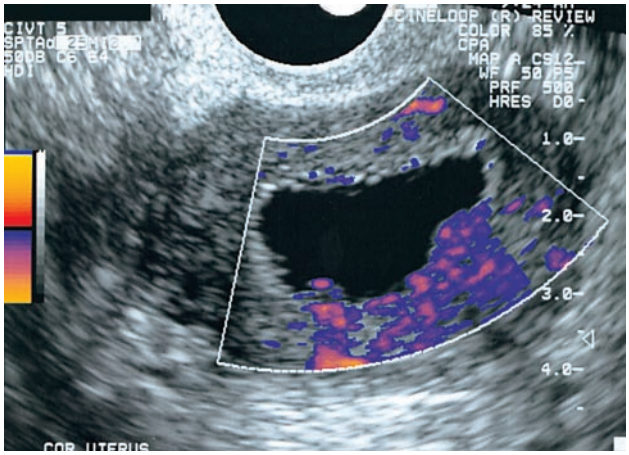

B

Figure 8–3 Endometrial fluid with tiny endometrial cysts. **(A)** Sagittal scan of the uterus in postmenopausal patient on tamoxifen for ~6 months demonstrates a large quantity of endometrial fluid (F) and numerous tiny cysts (arrows). **(B)** Coronal power Doppler scan demonstrates no areas of hypervascularity in this asymptomatic patient in whom the endometrial abnormalities were first noted incidentally on a renal sonogram.

in excellent agreement among observers and have been shown to correlate well with measurements from gross specimens.[39,40]

During the menstrual cycle in premenopausal women, the endometrium displays a wide range of appearances that can be correlated to the proliferative, secretory, or menstrual phase. Both the thickness and the texture of the endometrium are influenced by the amount of circulating estrogen and progesterone. In the early proliferative phase, the endometrium appears as a slightly irregular, thin echogenic interface. It progressively thickens and develops a multilayered appearance with the opposed endometrial surfaces constituting the central echogenic line, surrounded by the hypoechoic, developing functional layer with the basal endometrium as the outer echogenic layer. During the proliferative phase, the endometrium appears distinct and uniformly hyperechoic and ranges from 4 to 8 mm in thickness. The secretory phase of the endometrium begins after ovulation; during this time the maximum thickness and echogenicity is achieved. The secretory endometrium measures 10 to 15 mm or more in thickness. The endometrium has a variable appearance during menses, but once the functional layer has shed, it generally becomes thin with the degree of reflectivity based on the presence of blood or clots.

In postmenopausal patients, the endometrium becomes atrophic due to a lack of epithelial stimulation. It appears on sonography as a thin echogenic line that normally measures a few millimeters in thickness (**Fig. 8–1**). The relatively vascular and compact inner third of the myometrium appears as a surrounding hypoechoic halo.[41] It has been shown conclusively that endometrial thickness declines with age, yet measurements may increase to 6 to 10 mm following hormone replacement therapy (HRT). Most experts are advocating biopsy in asymptomatic postmenopausal patients only when the endometrial thickness exceeds 8 mm.

The Society of Radiologists in Ultrasound (SRU) consensus conference held in 2000, addressed the role of TVS in the evaluation of women with postmenopausal bleeding. All panelists agreed that TVS or endometrial biopsy (EMB) could be used safely and effectively as the first diagnostic step. The prevalence of benign endometrial abnormalities in postmenopausal women with bleeding was felt to be higher than previously thought. In addition, the panelists felt that further investigation into the clinical significance of benign endometrial abnormalities associated with postmenopausal bleeding is warranted.[42]

Clearly, some women may present for evaluation because of abnormal bleeding due to the friable nature of atrophic endometrial vessels.[43] However, numerous studies have consistently shown that regardless of symptoms, an endometrial thickness of $\leq$ 4 to 5 mm is associated with benign histopathology in the vast majority of cases.[44,45] The SRU consensus conference recommended a threshold level of 5 mm to serve as a useful guide for determining which patients should undergo endometrial biopsy.[42] Statistical analysis of the probability of endometrial pathology at a specific thickness indicates that the risk of missing an endometrial abnormality using a single measurement of 5 mm as a cutoff is ~5.5%, comparing favorably with the false-negative rate of 4 to 6% for dilation and curettage.[46]

Unfortunately, this cutoff value cannot be applied to patients on HRT, in whom abnormal bleeding occurs frequently due to breakdown of the atrophic endometrium. It is essential to ascertain which hormonal regimen a patient is actually taking. Commonly used sequential estrogen and progesterone induces cyclical endometrial changes similar to those occurring in premenopausal patients. Endometrial thickness is, therefore, significantly greater in these

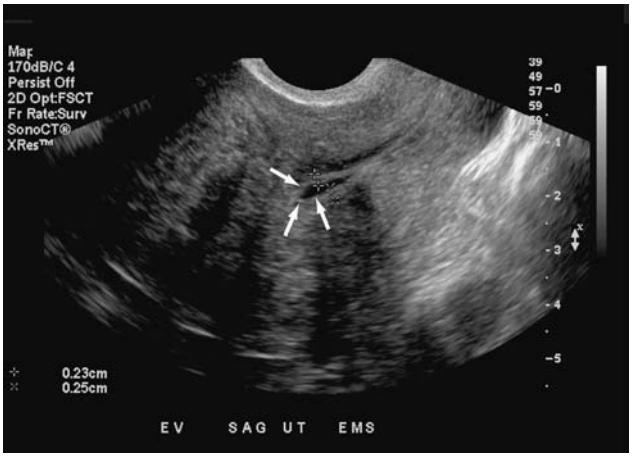

A

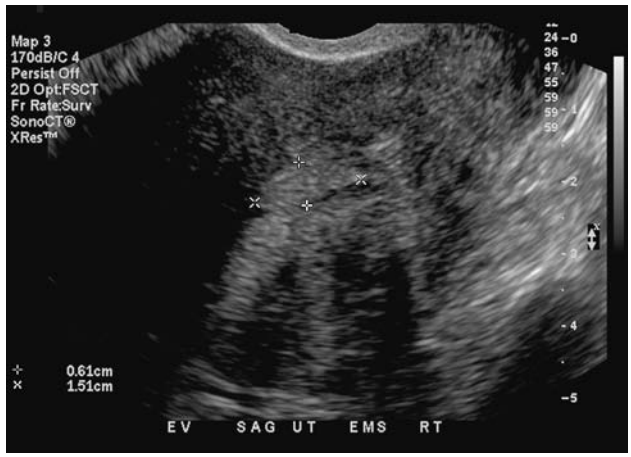

B

Figure 8–4 Endometrial polyp with trace fluid. **(A)** Sagittal transvaginal sonography (TVS) demonstrates a small amount of endometrial fluid (arrows) with a thin endometrium (cursors) in a 45-year-old patient on tamoxifen for 4 years with spotting. **(B)** Sagittal TVS of well-defined, echogenic polyp (cursors) in the right uterine fundus. TVS also showed findings of fibroids and adenomyosis.

women compared with controls, reaching maximum values on days 13 through 23.

Patients on sequential HRT should be scanned early in their cycle, 4 to 5 days after completion of cyclic bleeding, when the endometrium is most likely to be thin. Changes in endometrial thickness greater than 3 mm during a single cycle have been documented in patients on sequential hormones.[47] Scans can be performed anytime for patients on continuous HRT regimens, including unopposed estrogen and no HRT.

The use of continuous estrogen and progesterone regimens leads to endometrial atrophy, and, therefore, endometrial thickness in these patients usually measures within the normal range. Women on unopposed estrogen tend to have a greater percentage of endometrial thickening because of the cellular proliferation that occurs. Biopsy of endometria greater than 8 mm thick is required in these patients because of the known risk of endometrial cancer. Because of the accuracy of endometrial assessment with TVS, serial sonograms may be of value to closely monitor patients at high risk for malignancy.

The most important sign of carcinoma, endometrial thickening, unfortunately is not very specific. In symptomatic and asymptomatic patients, including those on tamoxifen or other SERMs, benign conditions such as hyperplasia, cystic atrophy, polyps, and proliferation occur more frequently than carcinoma. Nevertheless, a persistently thickened endometrium is worrisome even in patients on

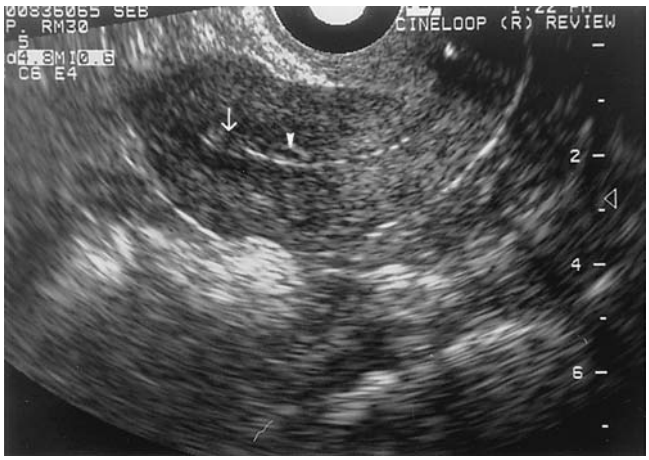

Figure 8–5 In situ cervical carcinoma. Sagittal transvaginal sonography of the endometrium demonstrates a slightly heterogeneous stripe (arrow) with a suggestion of a tiny amount of fluid (arrowhead). Histopathology in this tamoxifen-treated patient revealed inactive endometrium and squamous cell carcinoma of the cervix in situ.

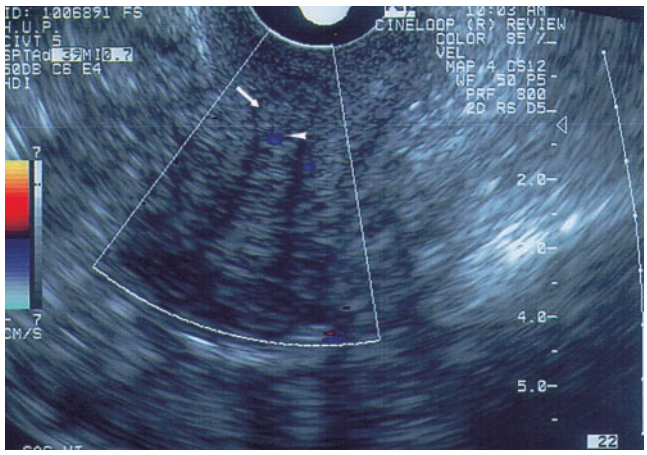

Figure 8–6 Retroverted uterus with endometrial venous flow. Sagittal transvaginal sonography was performed in this postmenopausal tamoxifen-treated patient with abnormal bleeding. The endometrium was thickened in the lower uterine segment (arrow) where venous flow was noted (arrowhead). Insufficient tissue for diagnosis was obtained on biopsy.

sequential therapy, and a change in hormonal regimen or biopsy is indicated. Endometrial fluid in postmenopausal patients is a more common finding than initially thought and is not unusual in women on HRT.[46] It is more often an indicator of benign rather than malignant disorders (**Fig. 8–4, Fig. 8–5**). The presence of a moderate degree of fluid helps in evaluating the appearance of the adjacent endometrium, which is the most important consideration (**Fig. 8–3**).

Although TVS is very sensitive in visualizing endometrial morphology, including abnormal thickening and small fluid collections, the differential diagnosis of such findings in postmenopausal patients includes so many benign disorders that the false-positive rate for malignancy is significant. In considering cost-effectiveness, the SRU consensus conference reported that the greater false-positive sonographic findings among hormone users seem considerably higher than those among patients who do not take HRT. The panel recommended that symptomatic women treated with tamoxifen or other SERMs be evaluated in a fashion similar to that of other postmenopausal women with vaginal bleeding, using a threshold thickness of 5 mm. The panelists acknowledged that tamoxifen-treated women are at an increased risk of endometrial cancer; however, they reported that there was insufficient evidence to warrant recommendation of routine evaluation of asymptomatic women on these therapies.

It is important to note that several researchers have documented that postmenopausal women taking tamoxifen, whether symptomatic or not, tend to have endometrial measurements that are frequently thicker than control subjects screened with TVS.[32] Color Doppler with TVS has been used to measure impedance to blood flow in the uterine arteries, which normally increases with years from menopause. Investigations have assessed uterine blood flow with color Doppler to determine if tumor neovascularity induces detectable arterial changes in endometrial cancer. Several researchers have reported alterations in uterine blood flow with endometrial cancer; one study suggests that the presence of malignant tissue decreases the impedance to blood flow in the main uterine artery.

It was thought that the observed changes were possibly due to neoangiogenesis in the endometrial cavity.[48] Other larger series compared color Doppler findings on TVS with endometrial biopsy, which was performed after the sonogram. The endometrium was significantly thicker in patients with cancer, compared with those with endometrial atrophy, and the PI value of the uterine vessels was significantly lower in endometrial cancer compared with atrophy.[49] More recent studies have shown that Doppler ultrasound, in contradistinction to saline infusion sonography, (SIS) does not add to the value of endometrial thickness measurements by TVS in the evaluation of endometrial pathology and tamoxifen-treated patients (**Fig. 8–6**). However, instead of reliance on specific spectral Doppler indices, we believe the various flow patterns of the endometrium seen on color Doppler may help in the differentiation of some pathological conditions involving the postmenopausal endometrium.

We have observed endometrial hypervascularity in numerous cases of endometrial polyps with the finding of a prominent feeding vessel supplying an area of endometrial thickening (**Fig. 8–7, Fig. 8–8**). Uterine leiomyomas have been reported to often display low-resistance, high-velocity flow patterns in the periphery of a hypoechoic, heterogeneous, sound-attenuating mass.[50] The concomitant occurrence of leiomyomas, adenomyosis, tamoxifen-induced

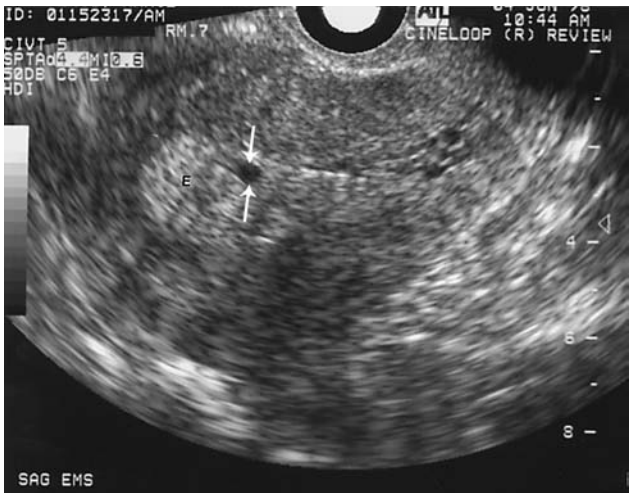

A

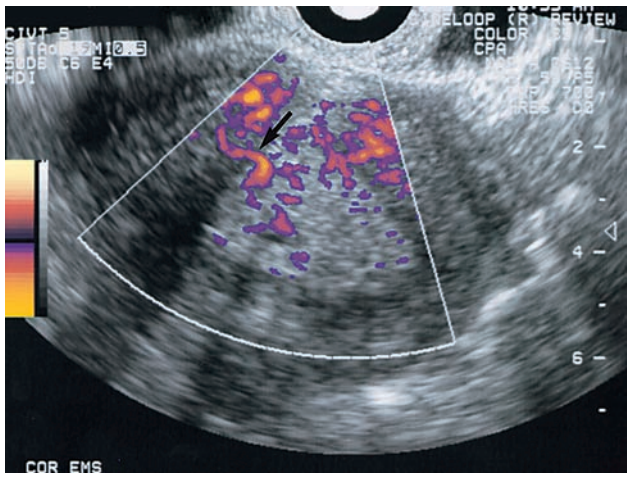

B

Figure 8–7 Endometrial polyp with large feeding vessel. **(A)** Sagittal scan in a postmenopausal patient whose endometrial stripe has doubled from 12 to 24 mm in the past 6 months. The patient has been on tamoxifen therapy for ~4 years. Endometrial polyps and cystic atrophy were noted at total abdominal hysterectomy and bilateral salpingo-oophorectomy. Endometrium (E) and tiny cysts (arrow). **(B)** Coronal power Doppler scan of large feeding vessel (arrows).

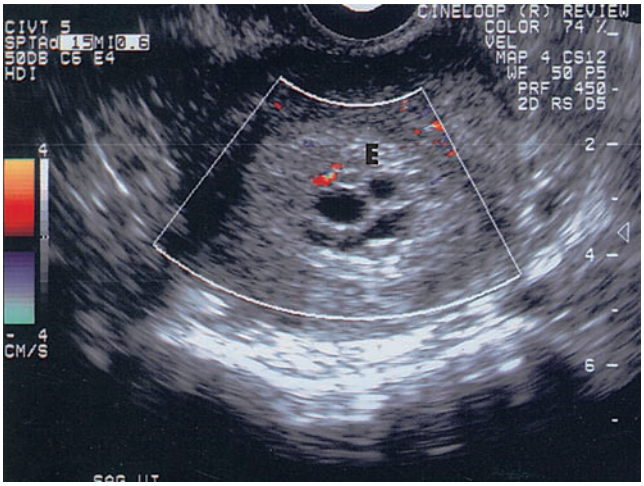

Figure 8–8 Endometrial polyp and atrophic endometrium. Sagittal transvaginal sonography in this patient with abnormal bleeding and a 4-year history of tamoxifen therapy demonstrates a markedly thickened endometrium (E), which had high-velocity, low-resistance flow.

cystic change, and endometrial cancer can pose a diagnostic dilemma when attempting to assess uterine blood flow (**Fig. 8–9, Fig. 8–10**). It is therefore unlikely that color Doppler will play any role other than that of a complementary tool, perhaps in some cases to increase diagnostic confidence. (**Fig. 8–11**).

Benefits of Ultrasound

The radiologist has a pivotal consulting role to play in the utilization of TVS in evaluating symptomatic and asymptomatic tamoxifen-treated patients. TVS is accepted as a screening tool because it affords excellent visualization of the endometrium and is less invasive than D&C, endometrial biopsy, and hysteroscopy. A normal appearance of the endometrium with TVS reliably excludes significant endometrial pathology. In tamoxifen-treated patients with an abnormally thickened endometrium, various sonographic patterns have been described, including hyperechoic, homogeneous endometrial thickening; hyperechoic, heterogeneous endometrial thickening; and hyperechoic endometrial thickening with cystic spaces that vary in size and number.[51] These endometrial changes are not specific for tamoxifen-treated patients and may actually be seen in asymptomatic postmenopausal patients without a contributory history.

In our experience, the extensive cystic changes that may occur in and around the endometrium are unique and more typical of tamoxifen stimulation. Careful inspection of the endometrial echotexture may be helpful in distinguishing between different endometrial processes. Although studies have correlated changes in the texture and thickness of the endometrium with histopathology, there is no particular distinguishing sonographic feature that permits a specific diagnosis (**Fig. 8–12**). It has been suggested that a well-defined, thickened, very echogenic endometrial cavity is likely due to hyperplasia, yet we have noted similar findings in polyps and other conditions.

Endometrial carcinoma, on the other hand, has been described as an irregular, thickened, hyperechoic area of the endometrium, with accompanying loss of the hypoechoic inner myometrial layer (**Fig. 8–11**).[52] However, in our experience, tamoxifen-treated patients not infrequently have mixed histology following biopsy, and we have seen poor definition of the subendometrial layer in various conditions (**Fig. 8–13, Fig. 8–14**).

Perhaps one of the most intriguing aspects of endometrial abnormalities in tamoxifen-treated patients has been

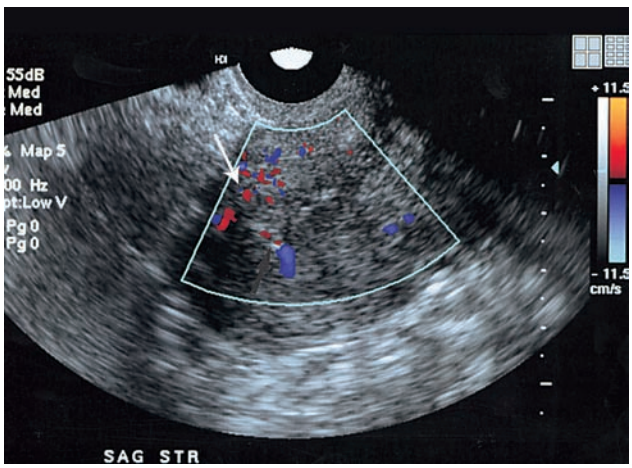

A

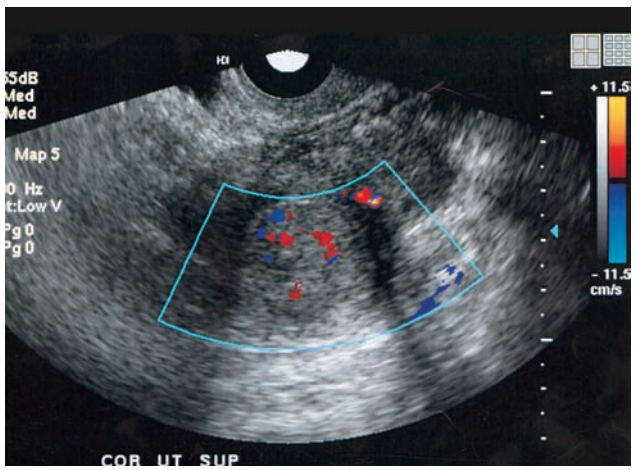

B

Figure 8–9 Endometrial carcinoma and leiomyomas. **(A)** Sagittal color Doppler scan in a postmenopausal patient on tamoxifen for 11 years in whom the endometrium (arrows) was not measured due to heterogeneity, poor marginal definition, and hypervascularity. **(B)** Coronal scan of myometrial hypervascularity probably arising in a leiomyoma.

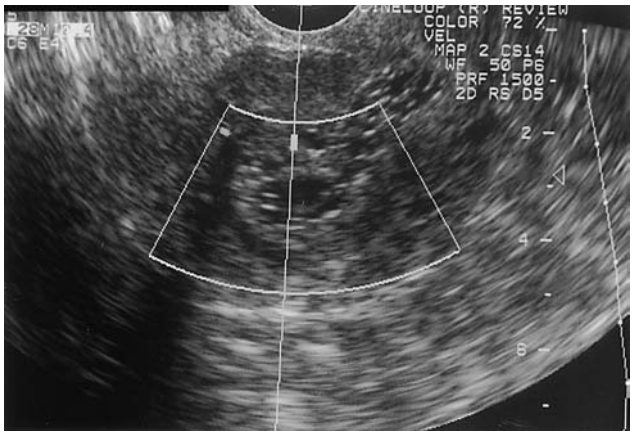

A

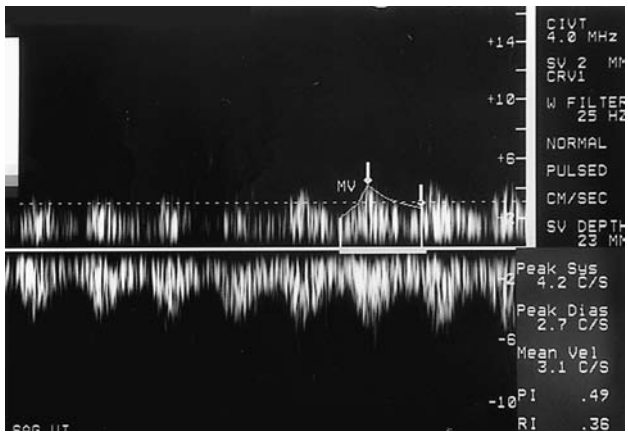

B

Figure 8–10 Endometrial carcinoma. **(A)** Sagittal transvaginal sonography in this patient on long-term tamoxifen therapy demonstrated extensive cysts and foci of hypervascularity (arrow). **(B)** Arterial waveform demonstrates low-resistance flow (arrow) with PI 0.49 and RI 0.36. Initial endometrial biopsy yielded benign tissue; however, poorly differentiated adenocarcinoma was subsequently diagnosed.

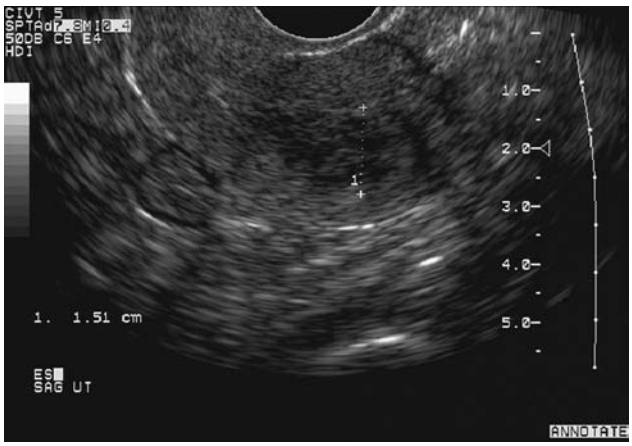

A

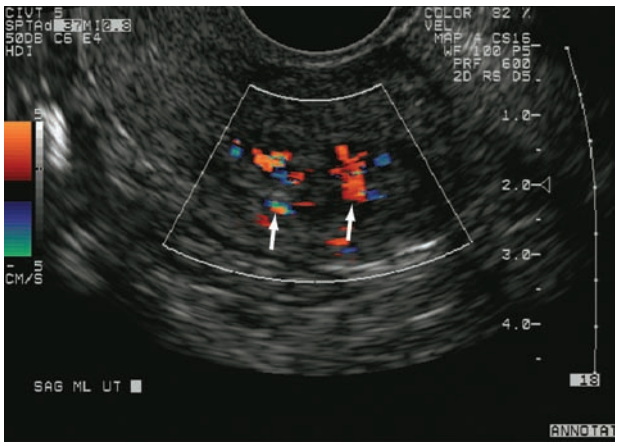

B

Figure 8–11 Endometrial carcinoma. **(A)** Sagittal transvaginal sonography of retroverted uterus with hypoechoic, thick endometrial stripe (cursors) referred for 5 days of vaginal bleeding. Patient had been on tamoxifen for 2 years, but this had been discontinued for 5 years. Attempted office biopsy was unsuccessful due to cervical stenosis. **(B)** Color Doppler demonstrates hypervascular endometrium with numerous foci of color flow (arrows).

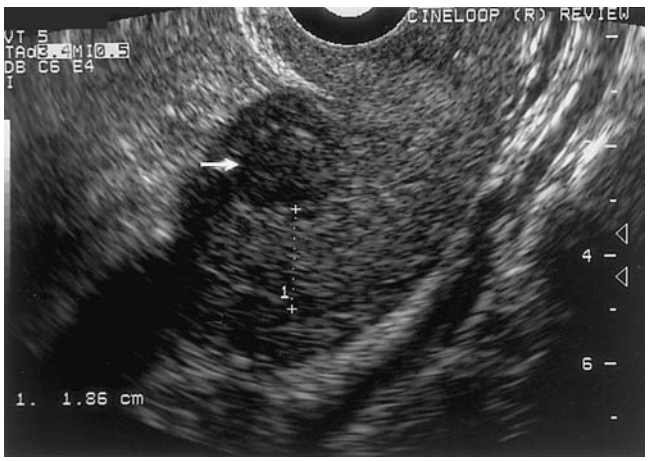

Figure 8–12 Chronic endometritis. Sagittal transvaginal sonography in this postmenopausal tamoxifen-treated patient demonstrates marked endometrial thickening (cursors) and fibroids (arrow).

the finding of atrophy and insufficient tissue for diagnosis following EMB of markedly thickened endometria with multiple small cysts (**Fig. 8–15, Fig. 8–16**). These findings were originally felt to be due to atypical, complex hyperplasia or endometrial polyps with cystically dilated glands.[53,54] SIS, in which sterile saline is instilled into the endometrial cavity, has been very helpful in improving the direct visualization of the endometrium.

In a high percentage of cases, the associated polyps with cystic change are well outlined by the adjacent fluid (**Fig. 8–17, Fig. 8–18**). In addition, researchers have found that the heterogeneous, bizarre appearance of the endometrium was actually due to subendometrial cystic change occurring in the inner myometrial layer.[55] The endometrium in these patients is actually quite thin, which explains the histological diagnosis of benign or atrophic endometrium, as well as the frequent lack of clinical signs such as abnormal bleeding, which often heralds endometrial

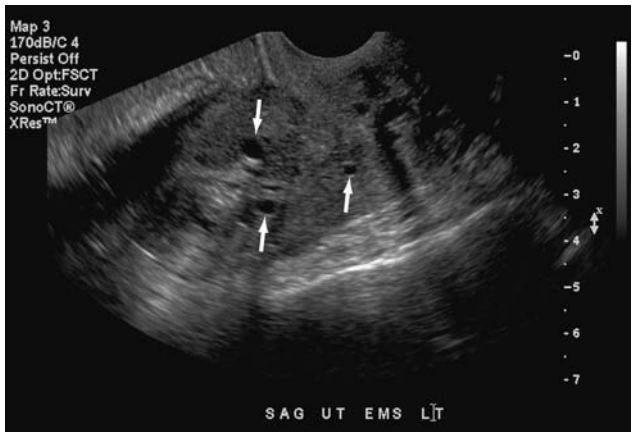

A

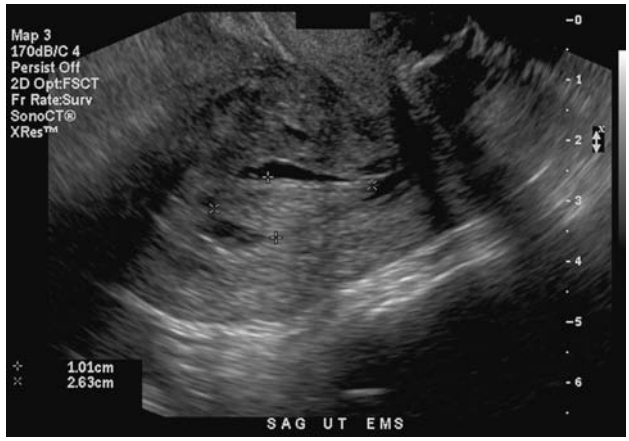

B

Figure 8–13 Recurrent endometrial polyps. Sagittal transvaginal sonography (TVS) in a postmenopausal patient on tamoxifen for 4 years with irregular vaginal bleeding. Endometrial polyp, which was diagnosed on TVS 7 months ago, was removed via dilation and curettage. **(A)** Thickened endometrium with multiple tiny cysts (arrows), endometrial and subendometrial. **(B)** Large polyp (cursors) on saline infusion sonography.

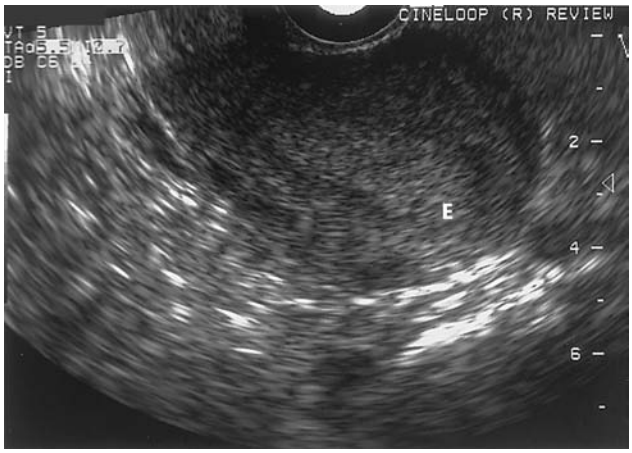

A

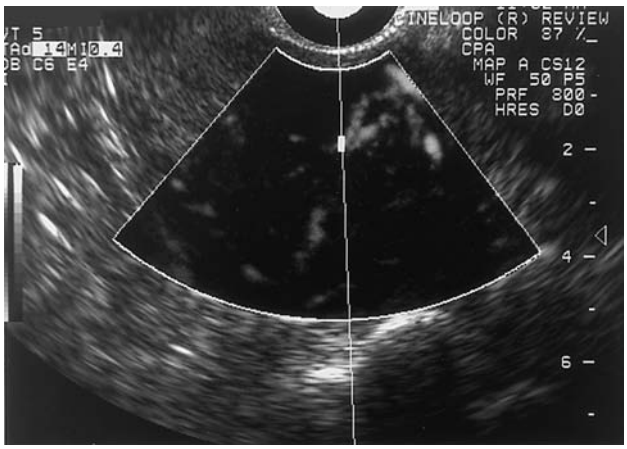

B

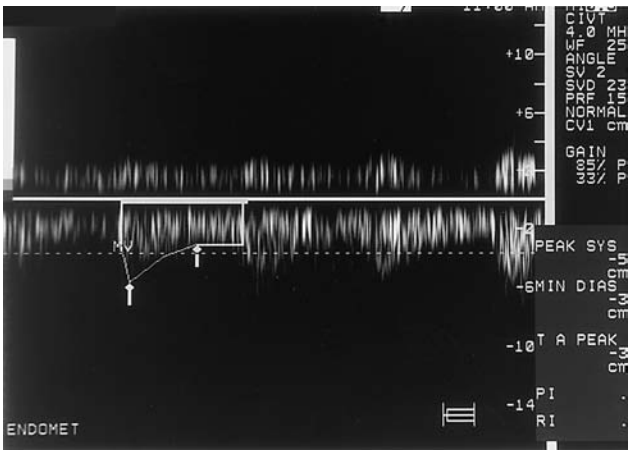

C

Figure 8–14 Endometrial polyp and complex hyperplasia. **(A)** Sagittal transvaginal sonography in patient on tamoxifen for 4 years shows a heterogeneous, markedly thickened endometrium (E). **(B)** Power Doppler scan of areas of endometrial hypervascularity. **(C)** Arterial waveform of low resistance flow (arrow) with PI 0.60 and RI 0.45.

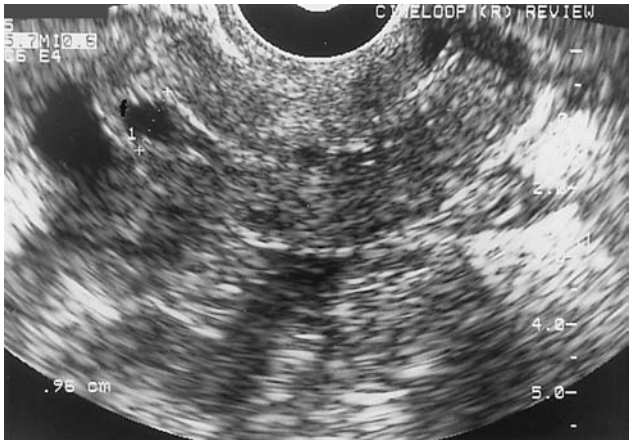

A

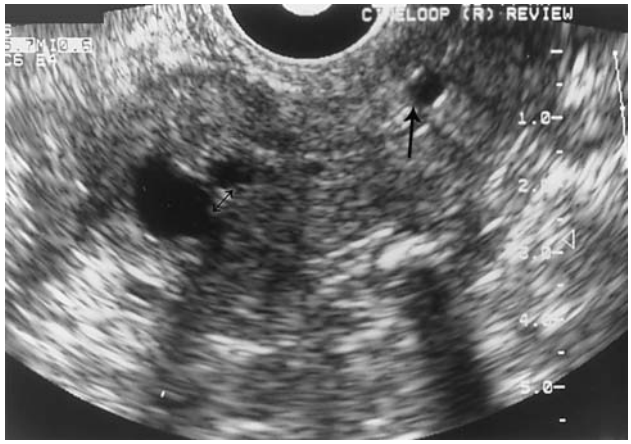

B

Figure 8–15 Endometrium with cystic atrophy. **(A)** Sagittal transvaginal sonography of thickened endometrium (cursors) with questionable fluid (f). **(B)** At total abdominal hysterectomy and bilateral salpingo-oophorectomy, multiple endometrial cysts (arrow) and endocervical cysts (arrowhead) were noted. The endometrial cavity actually measured 2.5 × 2 cm.

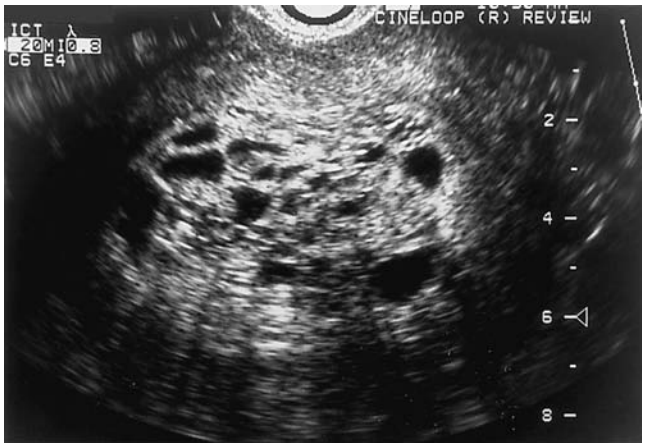

Figure 8–16 Cystic atrophy and endometrial polyp. Coronal transvaginal sonography of markedly thickened, highly reflective endometrium with numerous cysts of various sizes.

malignancy or hyperplasia. This type of extensive cystic change with marked thickening can also occur with single or multiple endometrial polyps (**Fig. 8–19**). In some cases, it may be virtually impossible to discern the exact site of diffuse cystic change (**Fig. 8–16**). Among panelists at the SRU consensus conference, it was uniformly felt that either SIS or hysteroscopy is appropriate when TVS suspects a focal abnormality in a symptomatic postmenopausal patient.

Hysteroscopy has the distinctive advantage of allowing one to perform a biopsy or a section of a focal mass at the time of the procedure. Interestingly, the panelists favored surgical hysteroscopy compared with office hysteroscopy, despite the requirement for operating room time, considerable anesthesia, and greater expense.[42] Radiologists who are comfortable with SIS find that this procedure can be performed safely and less expensively in an outpatient set-

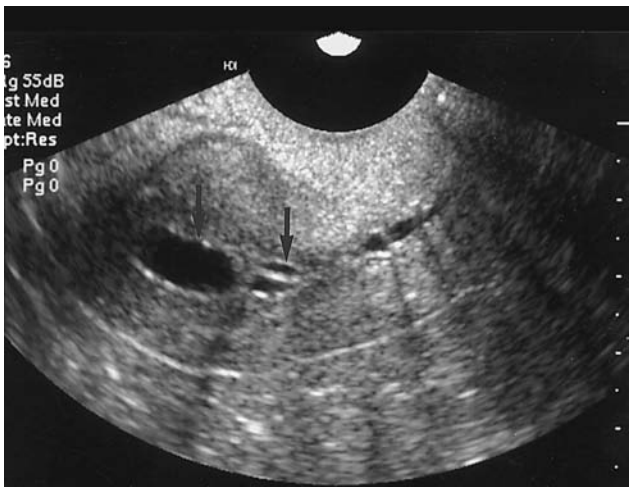

A

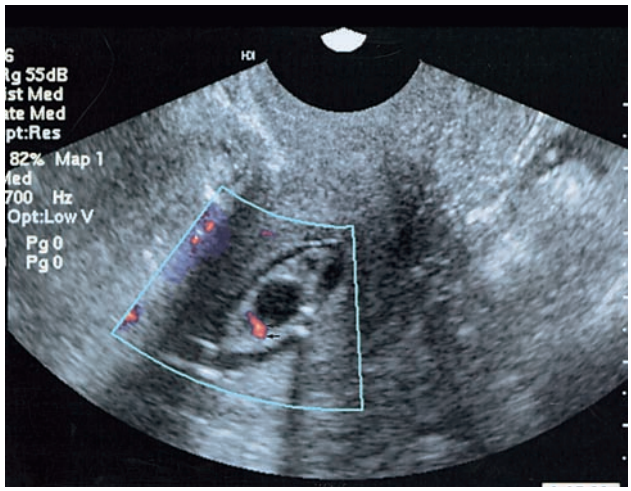

B

Figure 8–17 Endometrial polyp with cystic change. **(A)** Sagittal transvaginal sonography (TVS) of one large and several tiny central cysts (arrows), which obscure the endometrium in this patient, who was on tamoxifen for 3.5 years and exhibited a progressively thickened stripe on serial studies. **(B)** Sagittal TVS from sonohysterography (SHG) of large feeding vessel (arrow) within a solitary polyp with cystic change.

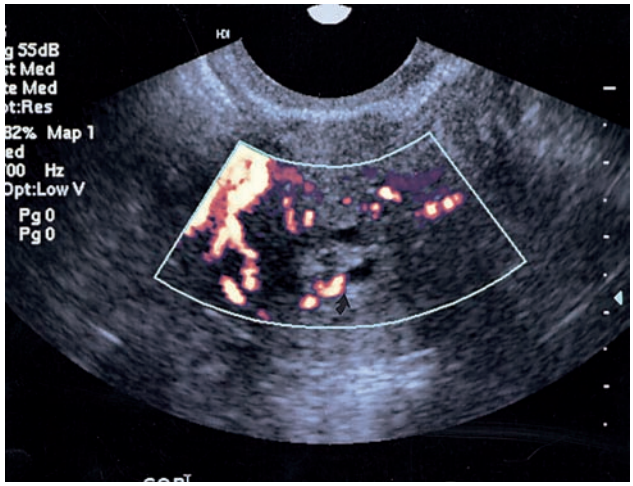

A

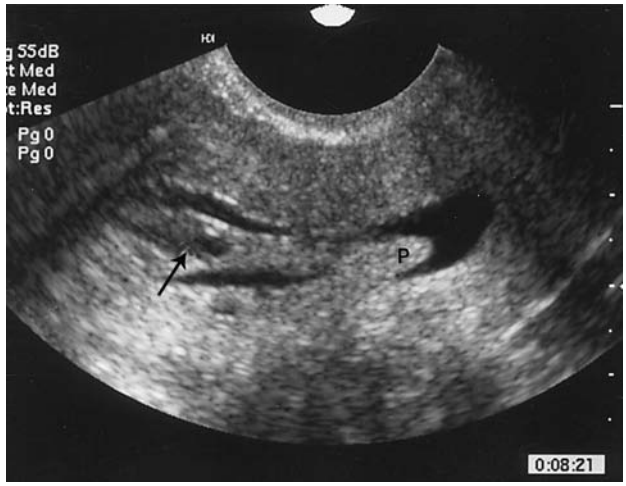

B

Figure 8–18 Endometrial polyp with cystic change. **(A)** Power Doppler scan of large feeding vessel (arrow) supplying a focal area of thickening in the uterine fundus in this patient who has been on tamoxifen for 4.5 years. **(B)** During saline infusion sonography, a large, broad-based, pedunculated polyp (arrows) originating from the fundus was noted with a tiny area of cystic change (arrow).

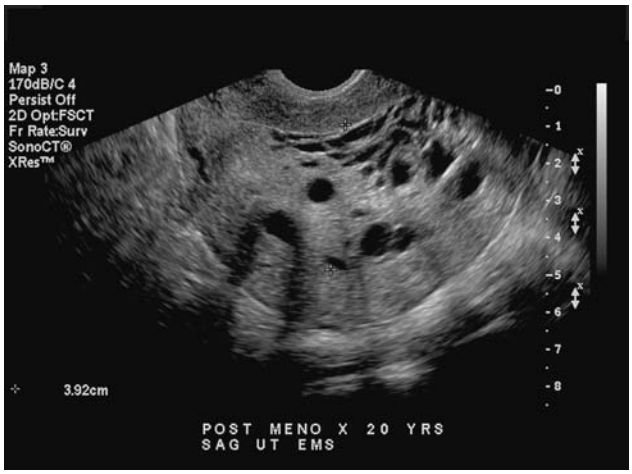

A

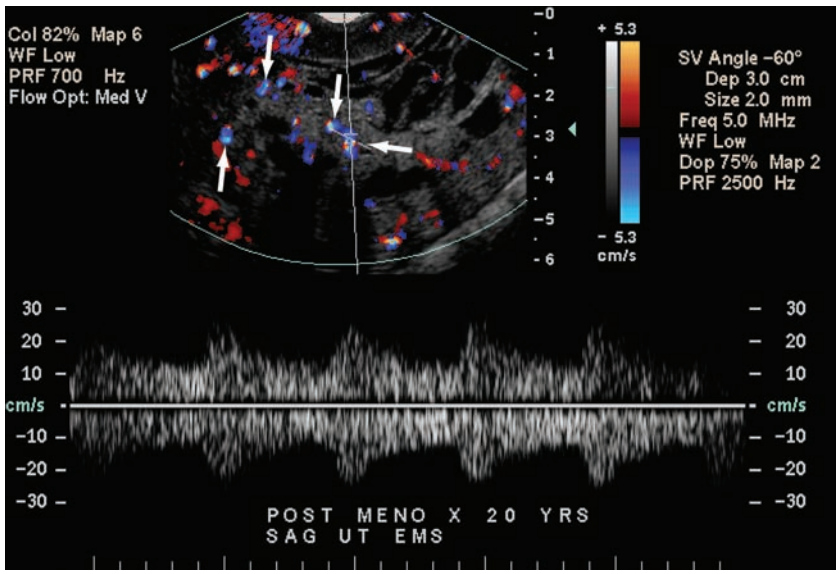

B

Figure 8–19 Multiple endometrial polyps with cystic change. Sagittal transvaginal sonography (TVS) in retroverted uterus in patient postmenopausal for 20 years, asymptomatic on tamoxifen therapy for the past 2 years. **(A)** Follow-up sagittal TVS of very thickened endometrial stripe (cursors), with progressive cystic change in a 1-year period. **(B)** Sagittal TVS of increased endometrial flow (arrows) with arterial waveform.

ting. It can be extremely useful when TVS suggests a possible focal endometrial abnormality, and it can be equally useful in effectively triaging patients to various sampling techniques such as office endometrial biopsy, office/surgical hysteroscopy or surgical D&C. SIS can also eliminate unnecessary, more invasive procedures when the endometrial lining is shown to be very thin but associated with endometrial tamoxifen-induced cystic changes. In inexperienced hands, SIS should clearly depict intracavitary lesions, characterize TVS-detected endometrial abnormalities as either focal or diffuse, and definitively localize cystic change as endometrial or subendometrial. SIS can be especially helpful when the endometrium is suboptimally visualized and cannot be accurately measured with TVS, regardless of etiology.

Summary

The long-term use of tamoxifen has been linked to a higher prevalence of proliferative endometrial lesions, including carcinoma, hyperplasia, uterine sarcoma, endometrial polyps, adenomyosis, submucosal fibroids, and cystic atrophy. Malignancies of the uterus are most concerning; however, it is important again to emphasize that the majority of tamoxifen-related changes are indeed benign. The risk of development of malignancy has been shown to increase with the duration of tamoxifen use and accumulative dose, prior estrogen replacement therapy, obesity, hypertension, diabetes, and the presence of preexisting endometrial pathology.

TVS is widely available, readily accepted by most postmenopausal patients, relatively inexpensive, and the least invasive method other than gynecologic examination for the evaluation of patients on long-term tamoxifen. Because tamoxifen and other SERMs will probably be increasingly used in more patients who will require evaluation of pelvic symptomatology, the radiologist will often be responsible for the actual triage of cases. TVS with the added benefits of SIS is simple and can be performed in the office setting. Patients who have a normal-appearing endometrium on TVS can be conservatively managed without follow-up sonograms unless symptoms change or progress. SIS is likely the preferred method of evaluating tamoxifen-treated patients with heterogeneous, markedly thickened endometria on TVS. This procedure affords excellent visualization of the endometrium and may actually obviate the need for more invasive and costly surgical procedures.

Endometrial sampling, if necessary, can be performed precisely at the site of the abnormality noted on SIS and can be directed by the radiologist as in the case of multiple, variably sized endometrial polyps. Increasing use of this procedure will perhaps decrease the frequency of unsuccessful, "blind" endometrial biopsies in which insufficient tissue for diagnosis is obtained.

References

1. McCullough M. Breast cancer breakthrough: drug cuts rates in study. Philadelphia Inquirer, April 5, 1998, PC1
2. Breast Cancer Facts and Figures. American Cancer Society Surveillance Research, 1995:1–12
3. Ettinger B, Black DM, Mitlak BH, et al. Reduction of vertebral fracture risk in postmenopausal women with osteoporosis treated with raloxifene: results from a three-year randomized clinical trial. JAMA 1999;282:637–645
4. Cohen FJ, Watts S, Shah A, et al. Uterine effects of three-year raloxifene therapy in postmenopausal women younger than age 60. Obstet Gynecol 2000;95:104–110
5. Baum M, Buzdor A, Cuzick J, et al. Anastrozole alone or in combination with tamoxifen versus tamoxifen alone for adjuvant treatment of postmenopausal women with early-stage breast cancer: results of the ATAC (Arimidex, tamoxifen alone or in combination) trial efficacy and safety update analyses. Cancer 2003;98:1802–1810
6. Rutqvist LE, Cedermark B, Fornander T. The relationship between hormone receptor content, and the effect of adjuvant tamoxifen in operable breast cancer. J Clin Oncol 1989;7:1474–1484
7. Wolf DM, Jordan VC. Gynecologic complications associated with long-term adjuvant tamoxifen therapy for breast cancer. Gynecol Oncol 1992;45:118–128
8. Jordan VC, Lababidi MK, Langan-Fahey S. Suppression of mouse mammary tumorigenesis by long-term tamoxifen therapy. J Natl Cancer Inst 1991;83:492–496
9. Osborne CK, Boldt DH, Clark GM, et al. Effects of tamoxifen on human breast cancer cell cycle kinetics: accumulation of cells in early G1 phase. Cancer Res 1983;43:3583–3585
10. Harper MJK, Walpole P. A new derivative of triphenylethelene: effect on implantation and mode of action in rats. J Reprod Fertil 1967;13:101–119
11. Jordan VC. Long-term adjuvant tamoxifen therapy for breast cancer. Breast Cancer Res Treat 1990;15:125–136
12. Early Breast Cancer Trialists' Collaborative Group. Effects of adjuvant tamoxifen and of cytotoxic therapy on mortality in early breast cancer: an overview of 61 randomized trials among 28,896 women. N Engl J Med 1988;319:1681–1692
13. Breast Cancer Trials Committee, Scottish Cancer Trials Office (MRC), Edinburgh. Adjuvant tamoxifen in the management of operable breast cancer: the Scottish trial. Lancet 1987;2:171–175
14. Nayfield SG, Karp JE, Ford LG, Dorr FA, Kramer BS. Potential role of tamoxifen in prevention of breast cancer. J Natl Cancer Inst 1991;83:1450–1459
15. Bonadonna G, Valagussa P, Brambilla C, et al. Adjuvant and neoadjuvant treatment of breast cancers with chemotherapy and endocrine therapy. Semin Oncol 1991;18:515–524
16. Prentice RL. Tamoxifen as a potential preventive agent in healthy postmenopausal women. J Natl Cancer Inst 1990;82:1310–1311
17. Turken S, Siris E, Seldin D, et al. Effects of tamoxifen on spinal bone density in women with breast cancer. J Natl Cancer Inst 1989; 81:1086–1088
18. Fugh-Berman A, Epstein S. Tamoxifen: disease prevention or disease substitution? Lancet 1992;340:1143–1145
19. Fisher B, Costantino J, Wickerman C, et al. Tamoxifen for prevention of breast cancer: report of the National Surgical Adjuvant Breast and Bowel Project P-1 Study. J Natl Cancer Inst 1998;90: 1371–1388

20. Fisher B, Dignam J, Bryant J, et al. Five vs. more than five years of tamoxifen therapy for breast cancer patients with negative lymph nodes in estrogen receptor positive tumors. J Natl Cancer Inst 1996;88:1529–1542
21. Ferrazzi E, Cortei G, Mattarazzo R, et al. Estrogen-like effect of tamoxifen on vaginal epithelium. BMJ 1977;1:1351–1352
22. Boccardo F, Bruzzi P, Rubagotti A, et al. Estrogen-like action of tamoxifen on vaginal epithelium in breast cancer patients. Oncology 1981;38:281–285
23. Satyaswaroop PG, Zaino RJ, Mortel R. Estrogen-like effects of tamoxifen on human endometrial carcinoma transplanted into nude mice. Cancer Res 1984;44:4006–4010
24. Cohen I, Altaras MM, Shapira J, Tepper R, Beyth Y. Postmenopausal tamoxifen treatment and endometrial pathology. Obstet Gynecol Surv 1994;49:823–829
25. Seoud, MA, Johnson J, Weed JC Jr. Gynecologic tumors in tamoxifen-treated women with breast cancer. Obstet Gynecol 1993; 82: 165–169
26. Muylder X, Neven P, DeSomer M, et al. Endometrial lesions in patients undergoing tamoxifen therapy. Int J Gynaecol Obstet 1991;36:127–130
27. Killackey MA, Hakes TB, Pierce VK, et al. Endometrial adenocarcinoma in breast cancer patients receiving antiestrogens. Cancer Treat Rep 1985;69:237–238
28. Adami HO, Kruesmo UB, Bergvist L, Person I, Pettersson B. On the age-dependent association between cancer of the breast and of the endometrium: a nationwide cohort study. Br J Cancer 1987;55: 77–80
29. Koss L, Schreiber K, Oberlander SG, et al. Detection of endometrial carcinoma and hyperplasia in asymptomatic women. Obstet Gynecol 1984;64:1–11
30. Fornander T, Cedermark B, Mattsson A, et al. Adjuvant tamoxifen in early breast cancer: occurrence of new primary cancers. Lancet 1989;1(8630) 21:117–120
31. Andersson M, Storm HH, Mouridsen HT. Incidence of new primary cancers after adjuvant therapy for early breast cancer. J Natl Cancer Inst 1991;83:1013–1017
32. Cohen I, Rosen DJD, Shapira J, et al. Endometrial changes with tamoxifen: comparison between tamoxifen-treated and nontreated asymptomatic, postmenopausal breast cancer patients. Gynecol Oncol 1994;52:185–190
33. Fisher B, Costantino JT, Redmond CK, et al. Endometrial cancer in tamoxifen-treated breast cancer patients: findings from the National Surgical Adjuvant Breast and Bowel Project (NSABP) B-14. J Natl Cancer Inst 1994;86:527–537
34. Berliere M, Charles A, Gallant C, Donnez J. Uterine side-effects of tamoxifen: a need for systematic pretreatment screening. Obstet Gynecol 1998;91:40–44
35. Assikis VJ, Jordan VC. Risks and benefits of tamoxifen therapy. Oncology 1997;11:21–23
36. Love RR. Tamoxifen prophylaxis in breast cancer. Oncology 1992; 6:33–43
37. Mendelson EB, Bohm-Velez M, Joseph N, Neiman HL. Endometrial abnormalities: evaluation with transvaginal sonography. AJR Am J Roentgenol 1988;150:139–142
38. Coleman BG, Arger PH, Grumbach K, et al. Transvaginal and transabdominal sonography: prospective comparison. Radiology 1988; 168:639–643
39. Tessler FN, Schiller VL, Perrella RR, Sutherland ML, Grant EG. Transabdominal vs. endovaginal pelvic sonography: prospective study. Radiology 1989;170:553–556
40. Karlsson B, Granberg S, Ridell B, Wikland M. Endometrial thickness as measured by transvaginal sonography: interobserver variation. Ultrasound Obstet Gynecol 1994;4:320–325
41. Fleischer AC, Kalemeris GC, Machin JE, Entman SS, James AE Jr. Sonographic depiction of normal and abnormal endometrium with histopathologic correlation. J Ultrasound Med 1986;5:445–452
42. Goldstein RB, Bree RL, Benson CB, et al. Evaluation of the woman with postmenopausal bleeding: Society of Radiologists in Ultrasound-Sponsored Consensus Conference Statement. J Ultrasound Med 2001;20:1025–1036
43. Goldstein SR, Nachtigall M, Snyder JR, Nachtigall L. Endometrial assessment by vaginal ultrasonography before endometrial sampling in patients with postmenopausal bleeding. Am J Obstet Gynecol 1990;163:119–123
44. Granberg S, Wikland M, Karlsson B, Norstrom A, Fribert L-G. Endometrial thickness as measured by endovaginal ultrasonography for identifying endometrial abnormality. Am J Obstet Gynecol 1991;164:47–52
45. Levine D. Postmenopausal pelvis. Ultrasound 1995;13:75–86
46. Granberg S, Bourne TH. Transvaginal ultrasonography of endometrial disorders in postmenopausal women. Ultrasound 1995;13: 61–74
47. Levine D, Gosink BB, Johnson LA. Change in endometrial thickness in postmenopausal women undergoing hormone replacement therapy. Radiology 1995;197:603–608
48. Bourne TH, Campbell S, Steer C, et al. Detection of endometrial cancer by transvaginal ultrasonography with color flow imaging and blood flow analysis: a preliminary report. Gynecol Oncol 1991;40: 253–259
49. Bourne TH, Crayford T, Hampson J, Collins WP, Campbell S. The detection of endometrial cancer by transvaginal ultrasonography with color Doppler. Ultrasound Obstet Gynecol 1992;2: 75–80
50. Creighton S, Bourne TH, Lawton F, et al. Use of transvaginal ultrasonography with color Doppler imaging to determine an appropriate treatment regimen for uterine fibroids with a GnRH agonist before surgery: a preliminary study. Ultrasound Obstet Gynecol 1994;4:494–498
51. Hulka CA, Hall DA. Endometrial abnormalities associated with tamoxifen therapy for breast cancer: sonographic and pathologic correlation. AJR Am J Roentgenol 1993;160:809–812
52. Nasri MN, Shepherd JH, Setchell ME, Lowe DG, Chard P. The role of vaginal scan in measurement of endometrial thickness in postmenopausal women. Br J Obstet Gynaecol 1991;98:470–475
53. Kedar RP, Bourne TH, Powles TJ, et al. Effects of tamoxifen on the uterus and ovaries of women involved in a randomized breast cancer prevention trial. Lancet 1994;343:1318–1321
54. Corley D, Rowe J, Curtis MT, et al. Postmenopausal bleeding from unusual endometrial polyps in women on chronic tamoxifen therapy. Obstet Gynecol 1992;79:111–116
55. Goldstein SR. Unusual ultrasonographic appearance of the uterus in patients receiving tamoxifen. Am J Obstet Gynecol 1994;170: 447–451

9 First-Trimester Pain or Bleeding or Both

Arthur C. Fleischer

Transvaginal sonography (TVS) has a pivotal role in the evaluation of the patient presenting with first-trimester pain or bleeding or both. Along with the pregnancy test, TVS is the most important diagnostic test used to determine the cause and proper treatment of the patient presenting with pain or bleeding in the first trimester.

The diagnostic entities that are considered in the patient who presents with first-trimester pain or bleeding include ectopic pregnancy, threatened abortion, gestational trophoblastic disease, and adnexal torsion. With the improved resolution afforded by TVS and the additional diagnostic information available through color Doppler sonography (CDS), these entities can be confidently distinguished from each other. This chapter emphasizes newly described sonographic signs, including CDS, which may enable more specific diagnosis in these patients.

Ultrasound Evaluation

Ectopic Pregnancy

The improved resolution afforded by TVS and CDS has greatly enhanced the ability to confidently diagnose ectopic pregnancy. These parameters are pivotal in determining the optimal management of patients with this condition.[1]

Fortunately, the fatality rate associated with this condition has been decreasing substantially, even though its incidence has increased significantly over the past 20 years. Many patients with ectopic pregnancy have a clinical history of pelvic inflammatory disease. The abnormal and irregular bleeding that occurs in ectopic pregnancies is associated with abnormal hormonal levels. The "classical" clinical triad for ectopic pregnancy, consisting of pain, abnormal vaginal bleeding, and an adnexal mass, occurs in fewer than half of patients. In fact, on pelvic examination in patients with ectopic pregnancy, only 50% of patients will have a palpable adnexal mass.

Pregnancy tests assist in establishing the presence of a pregnancy, but do not indicate whether it is intra- or extrauterine. The two major types of pregnancy tests available consist of maternal serum radioimmunoassay (RIA) and urinary enzyme-linked immunosorbent assay (ELISA) for the hormone β-human chorionic gonadotropin (β-hCG). The advantage of the serum test is that it is very sensitive, although it may not be available at the time of the patient's presentation. The urine pregnancy test is qualitative rather than quantitative, but now approaches the accuracy of the maternal serum test.

In general, most intrauterine pregnancies will exhibit an intrauterine gestational sac when the serum β-hCG is above 1500 mIU/mL. Thus, the lack of a sonographically apparent gestational sac in a patient whose β-hCG is greater than 1500 mIU/mL is considered suspicious of an ectopic pregnancy. Depending on the institution, β-hCG that ranges from 1000 to 2000 mIU/mL can help to discriminate between an intrauterine and an ectopic pregnancy ("discriminatory zone").

It is important to realize that in up to 20% of ectopic pregnancies examined transabdominally and 0 to 8% examined transvaginally, no apparent sonographic signs of an ectopic pregnancy are observed.[1] As a medicolegal precaution, it may be prudent to include a statement such as "although an ectopic pregnancy is considered unlikely, it cannot be totally excluded" in the official report in cases where no definite sonographic abnormality is seen.

Ultrasound Findings

TVS is clearly the most accurate means for documentating the presence or absence of an ectopic pregnancy. CDS can also be used as a means for detection and assessment of the vascularity of any adnexal masses detected. CDS can assist in the discrimination of intra- versus extraovarian masses as well as periuterine vessels versus tubal masses. Rarely, CDS may demonstrate a "ring of fire," representing the vascularity associated with an ectopic pregnancy that is not appreciated on TVS.[2]

The sonographic findings in ectopic pregnancy can be divided into consideration of uterine, adnexal, and cul-de-sac findings; however, in a single patient, any combination of findings may exist.

Uterine findings focus on the presence or absence of a gestational sac with intact choriodecidua. Typically, in early pregnancy the endometrium undergoes a decidualization, which is a microscopic change in the nuclei of the endometrial stromal cells. With ectopic pregnancy the endometrium may thicken and in some cases the cavity contains fluid or blood, having the appearance of a "pseudogestational sac." However, the decidua in ectopic pregnancies lacks the low-impedance flow seen on Doppler in normal early intrauterine pregnancy. In addition, the

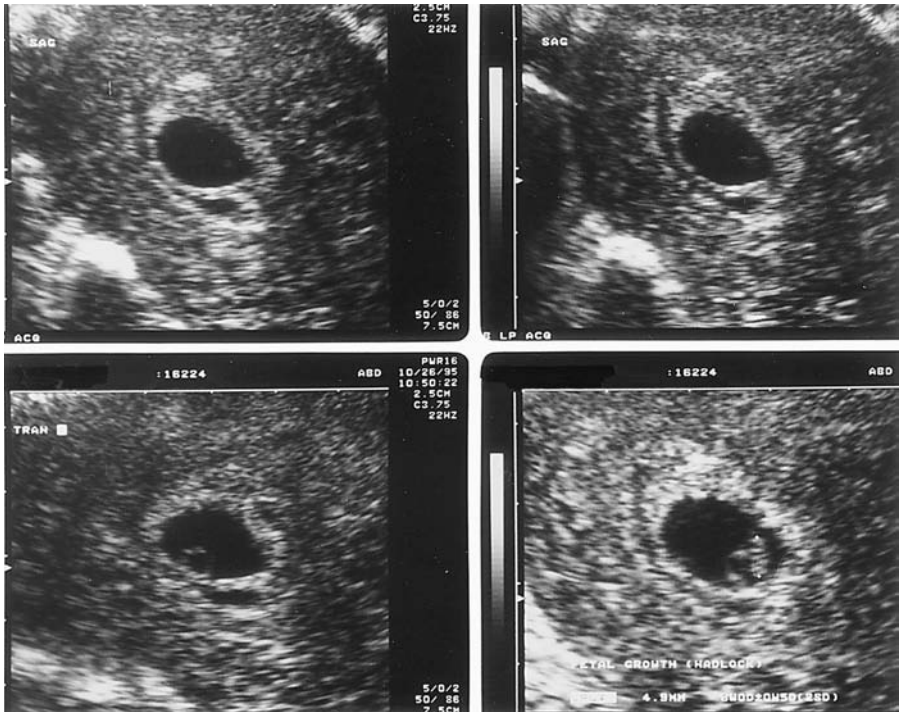

Figure 9–1 Composite transvaginal sonography of normal 6-week intrauterine pregnancy, showing decidua capsularis and vera. A yolk sac/embryo complex is also seen in the lower right-hand image.

decidualized endometrium in ectopic pregnancy lacks the focal thickening in the decidua basalis region seen in normal early pregnancies. In some cases of normal early (less than 6 weeks) intrauterine pregnancy, a double lining of decidua is present, representing decidua capsularis and opposing decidua vera. When this is documented sonographically, an intrauterine pregnancy is highly likely (**Fig. 9–1**).

In most cases of ectopic pregnancy, the endometrium is slightly thickened, similar to a secretory-phase endometrium. In more advanced ectopic pregnancies (8 weeks and more), there can be intraluminal blood and clotting due to sloughing of the endometrium secondary to poor corpus luteum support.

The adnexal findings in ectopic pregnancies form the basis for sonographic diagnosis of this entity. In most ec-

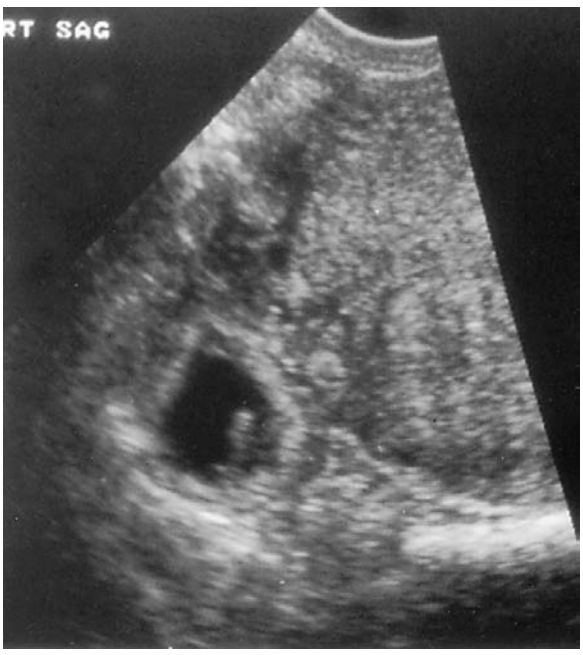

Figure 9–2 Transvaginal sonography of an unruptured tubal pregnancy showing a decidual ring containing an embryo.

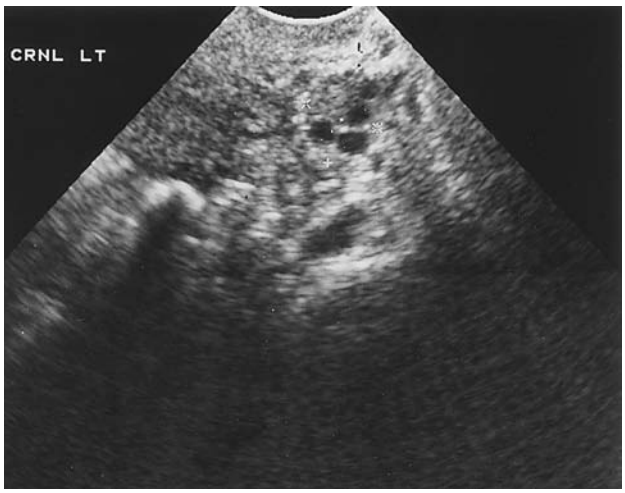

A

Figure 9–3 Enhanced visualization of an unruptured ectopic pregnancy adjacent to a corpus luteum with color Doppler sonography. **(A)** Transvaginal sonography showing a normal left ovary with tiny cystic areas. (*Continued*)

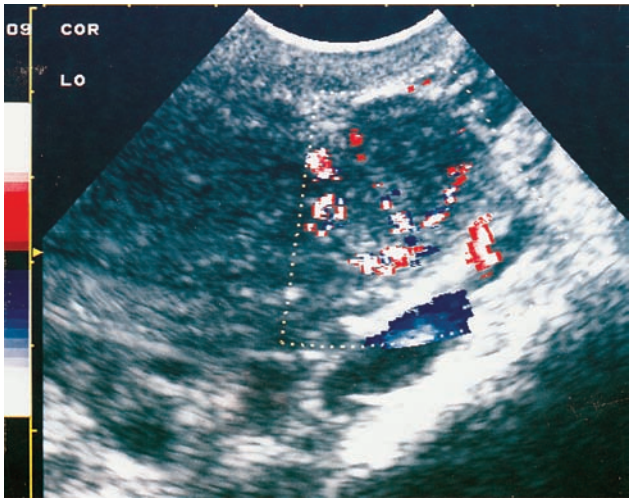

B

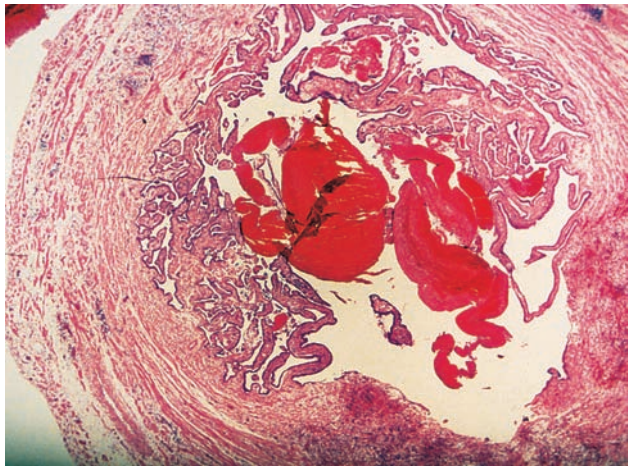

C

Figure 9–3 (*Continued*) **(B)** Transvaginal color Doppler sonography showing a vascular ring adjacent to the corpus luteum, suggesting the possibility of an unruptured ectopic pregnancy. **(C)** Histologic specimen showing a 3 × 4 mm unruptured ectopic pregnancy.

topic pregnancies, an adnexal ring of echogenic tissue with a hypoechoic center can be identified separate from the ovary (**Fig. 9–2**). One should be careful not to confuse a corpus luteum in the ovary with the presence of an ectopic pregnancy on TVS.

In some cases, CDS can be used as a "roadmap," outlining the presence of a corpus luteum as separate from the tubal mass itself (**Fig. 9–3**). The flow pattern seen in ectopic pregnancies can vary from absent diastolic flow to low-impedance, high-velocity flow, so this parameter is not accurate in determining whether an adnexal mass is a corpus luteum or an ectopic pregnancy (**Fig. 9–4,**

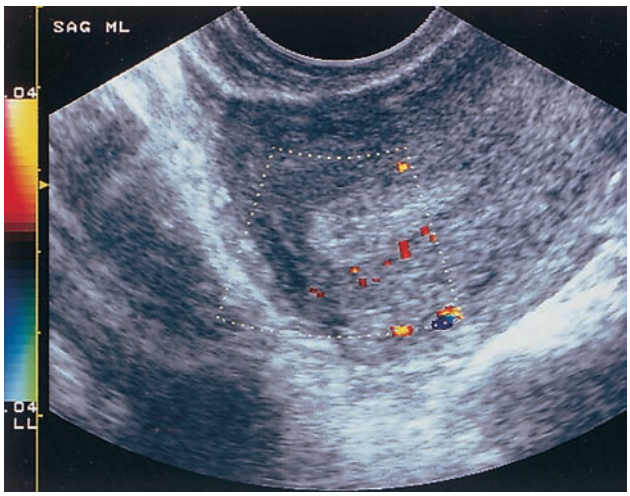

A

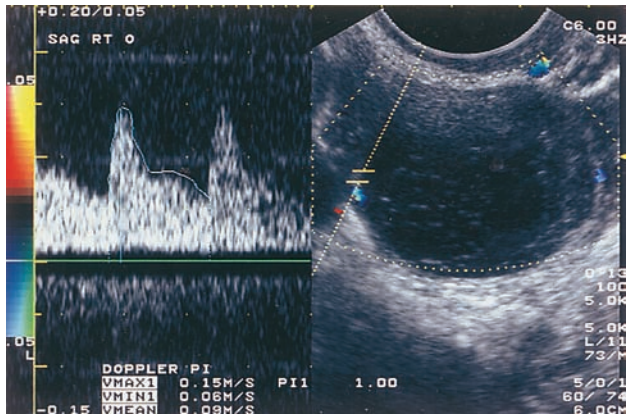

B

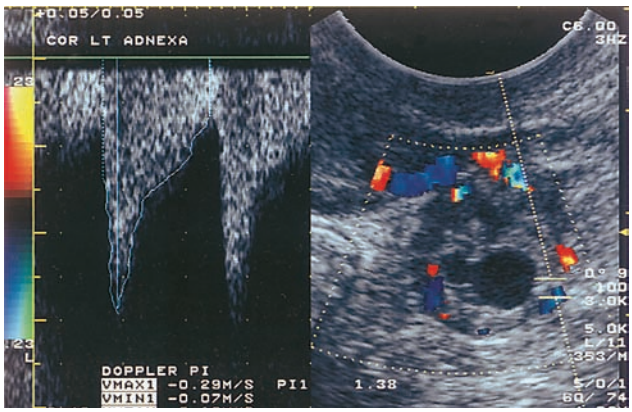

C

Figure 9–4 Transvaginal color Doppler sonography (TV-CDS) of an unruptured ectopic pregnancy. **(A)** TV-CDS of the uterus, showing mild endometrial thickening with sparse myometrial flow. **(B)** TV-CDS of the right ovary showing a mostly cystic mass with low-impedance flow within the wall. This represented a hemorrhagic corpus luteum. **(C)** In the left adnexa, a ringlike structure with relatively high-velocity and intermediate-impedance flow was seen. This was an unruptured ectopic pregnancy.

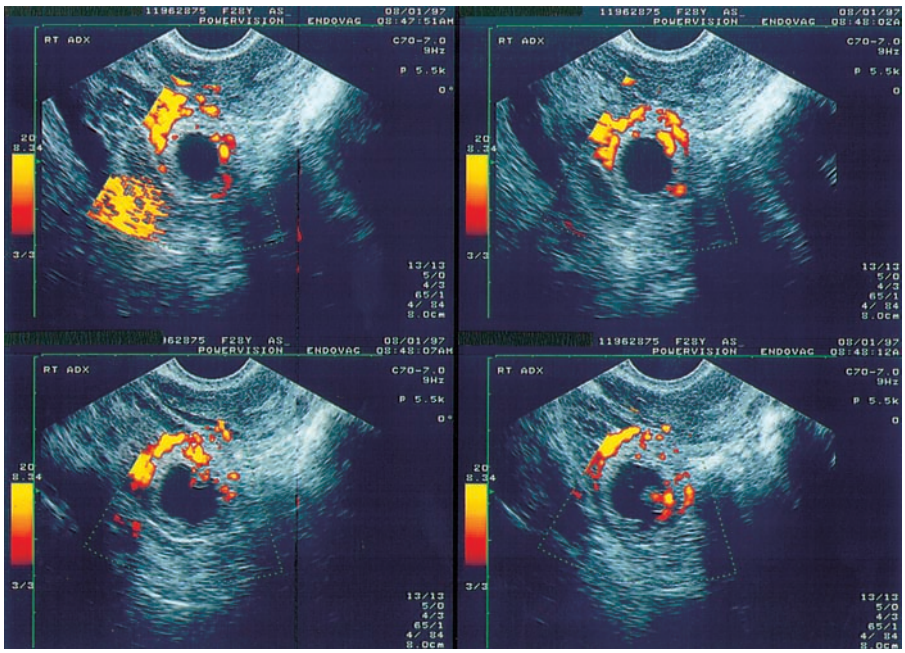

A

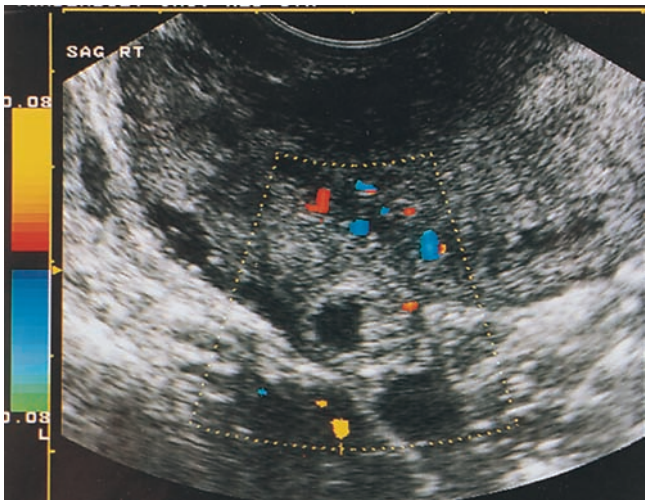

B

Figure 9–5 Vascularity of ectopic pregnancies. **(A)** Composite color Doppler sonography showing a hypervascular ectopic pregnancy, including flow to the embryo (lower left image). **(B)** In contrast to the patient shown in **(A)**, this ectopic is hypovascular, probably the result of sloughing.

Fig. 9–5, Fig. 9–6). However, using CDS, one can get a general approximation of the relative vascularity of the ectopic pregnancy (**Fig. 9–5**). Spontaneous resolution of an ectopic is more likely to occur when there is little or no adnexal ring flow than when there is an abundant flow. "Bizarre" waveforms that exhibit significant reversed diastolic flow have been described in ectopic pregnancies undergoing necrosis and resorption. If bleeding occurs surrounding an ectopic pregnancy within the tube, a fusiform adnexal mass can be seen, especially when associated with hemoperitoneum.

CDS can be used to assess the response of an ectopic pregnancy to methotrexate treatment.[3] In most cases, there is an initial increase in blood flow probably due to vasodilatation, as indicated by low-impedance diastolic flow, followed by a gradual increase in resistance to flow within the adnexal mass. Patients may experience additional pain when the decidualized endometrium begins to slough or if hemorrhage occurs.

Intraperitoneal or cul-de-sac fluid that has low-level echoes is highly indicative of a hemoperitoneum associated with an ectopic pregnancy. The presence of intraperitoneal fluid, however, does not always indicate that rupture is present because bleeding can occur as the gestational sac is being passed out the fimbriated end of the tube into the peritoneum.

Ultrasound can diagnose uncommon types of ectopic pregnancies, the most important of which include interstitial ectopic pregnancy, where the gestational sac is implanted at the end of the fallopian tube in the corner of the uterus.[4] One must be careful not to mistake a normal pregnancy implanted eccentrically within the uterine cavity for an interstitial pregnancy, which is implanted superolateral to and outside the cavity. However, when the gestational sac abuts the uterine serosa and is eccentric to the endometrium, this condition should be suspected—particularly if there is no myometrium or a very thin layer of myometrium surrounding the gestational sac.

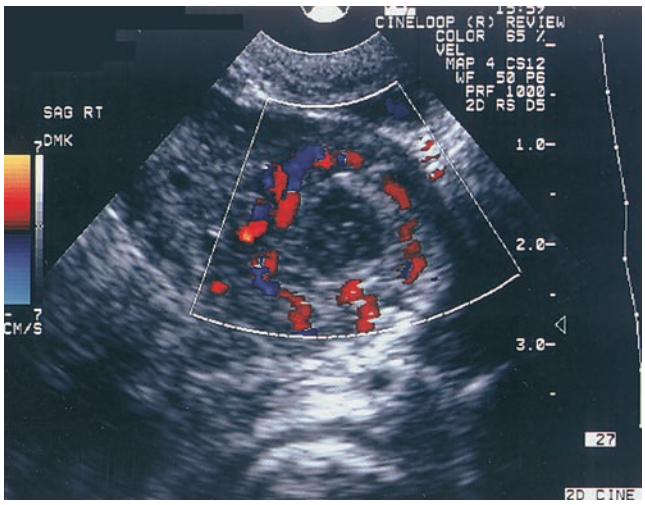

Figure 9–6 Transvaginal color Doppler sonography of a hemorrhagic corpus luteum that mimicked the appearance of an ectopic pregnancy except that it could be localized within the right ovary.

In abdominal ectopic pregnancies, the uterus can be seen as separate from the developing gestational sac. This condition may not be suspected until the second and third trimester, when the finding of a "pseudo placenta previa," abnormal amniotic fluid collection, or abnormal fetal position is seen on transabdominal sonography. It should be noted that over one quarter of abdominal ectopic pregnancies may be missed sonographically.[5]

Sonography has become a means for assessing proper management of patients with ectopic pregnancies. In some centers, systemic methotrexate is used for treatment of known ectopic pregnancies, whereas in others, local injection is performed utilizing TVS as a means for guidance.[3] In some cases, ectopic pregnancies are observed and followed sonographically for changes in blood flow, as well as abnormal increases in β-hCG.

Threatened Abortion

TVS plays a pivotal role in the evaluation of the patient presenting with pain or bleeding in the first trimester. Because bleeding can occur in up to 20% of normal pregnancies in the first trimester, TVS is used to distinguish conditions that are physiological from those that may require surgical intervention.

Subchorionic Hemorrhage

Subchorionic hemorrhage appears as a crescentic hypoechoic area adjacent to the choriodecidua in early pregnancy. Although there is significant controversy as to its importance, if it is localized to the placental edge and small (less than one quarter of the gestational sac size), it is usually not associated with adverse pregnancy outcome. However, if it extends behind the chorion and is large (over two thirds sac size), the prognosis for pregnancy completion is usually guarded (**Fig. 9–7**).[6–8] Other factors that

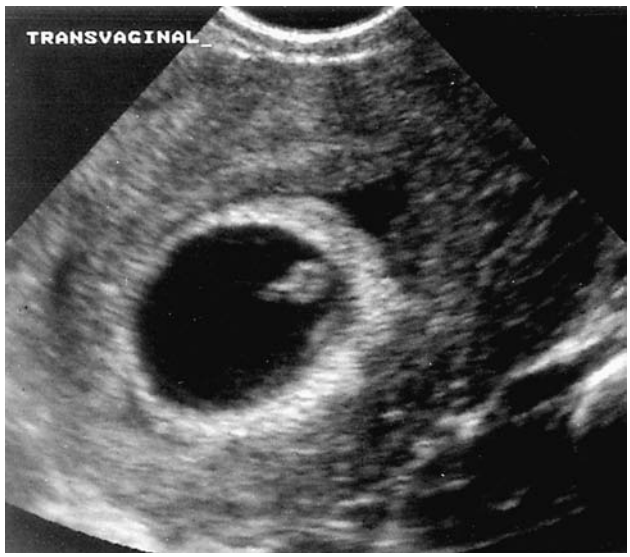

A

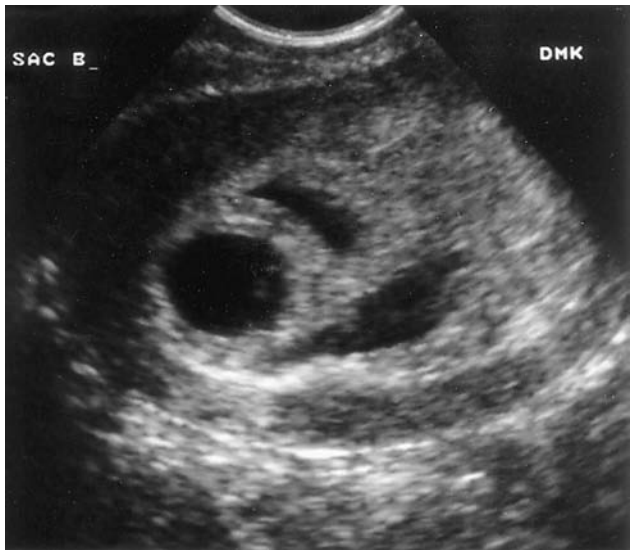

B

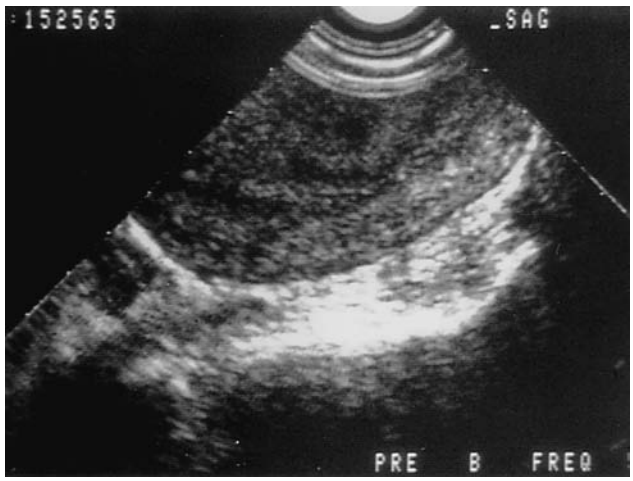

C

Figure 9–7 Hemorrhagic processes. **(A)** A hypoechoic space adjacent to choriodecidua. This is frequently seen in normal pregnancies. **(B)** Two areas of subchorionic hemorrhage adjacent to intact choriodecidua. This was associated with a spontaneous abortion. **(C)** Completed abortion with thin and closely opposed endometrial layers.

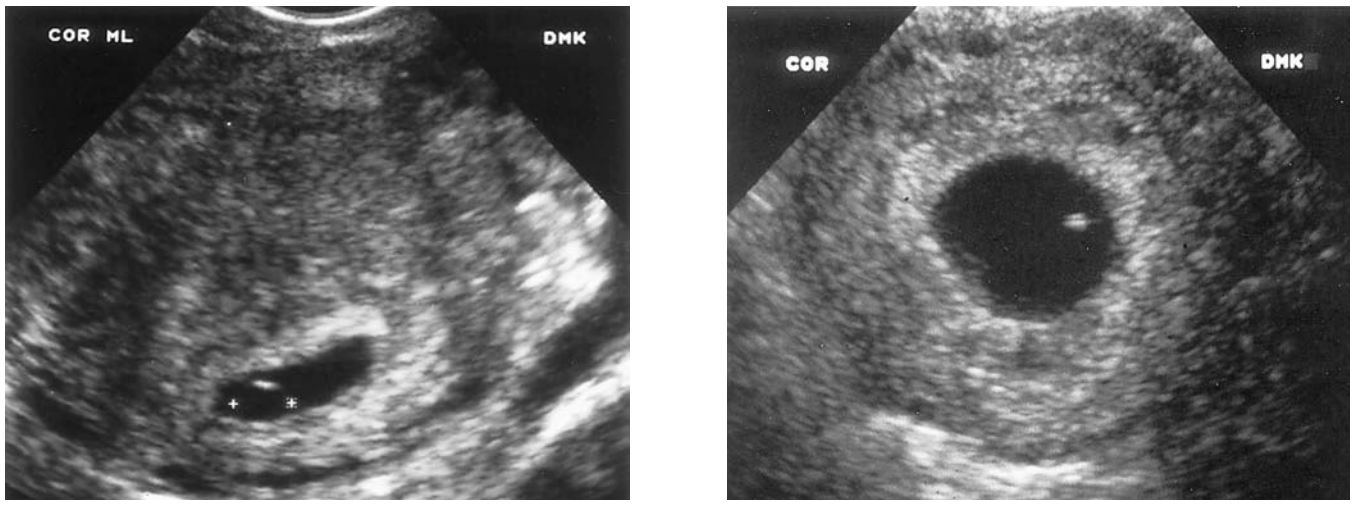

A B

Figure 9–8 Too large and too small yolk sacs. **(A)** Hydropic yolk sac (between cursors) associated with embryonic disease. **(B)** Tiny, deflated yolk sac associated with long-standing embryonic demise.

seem to indicate poor prognosis include weeks of gestation (less than 6 weeks) and more advanced maternal age (over 35 years).[9]

A similar sonographic finding involving a "blighted twin" can be encountered when two gestational sacs are observed with only one living embryo. In this condition, there is embryonic demise in one gestational sac with a living embryo or fetus in the second gestational sac. Usually, the gestational sac of the demised embryo deflates and is eventually absorbed.

Embryonic Demise

Embryonic heart activity can usually be identified as early as 6 weeks when the embryo is 3 to 4 mm in length. Heart rate analysis indicates that slow heart rates of 85 beats per minute or less are typically associated with spontaneous demise.[10] Embryonic demise may be associated with either a "deflated" yolk sac or an enlarged yolk sac (greater than 6 mm in size) (**Fig. 9–8**).[11]

Incomplete versus Complete Abortion

There are certain sonographic milestones that can be used to establish normalcy of pregnancy in the first trimester. In general, these include the presence of a yolk sac within a gestational sac and with a mean diameter of 10 mm or more, and/or the presence of an embryo at 15 mm mean gestational sac dimension with heart motion. In an incomplete abortion, there may be a small gestational sac, defined as less than a 5 mm difference between embryonic length and mean sac dimension, a nonvisible embryonic heart beat, or a very large gestational sac with no visible embryo.[12] The choriodecidua is typically irregular, and, on color Doppler, increased venous flow is seen within the choriodecidua.

In complete abortion, there is a thin and regular endometrium; and, on speculum examination, the cervix is closed. In these latter patients, conservative treatment might be indicated, with monitoring using serial β-HCG (**Fig. 9–7C**).[13]

Gestational Trophoblastic Disease

This rare condition occurs when there is fertilization of a chromosomally empty zygote. The typical morphological appearance of hydropic villi may not be seen in the first trimester. In fact, only echogenic irregular tissue may be seen in the uterus (**Fig. 9–9**). This condition is occasionally associated with ovarian theca lutein cysts and very high β-hCG levels.

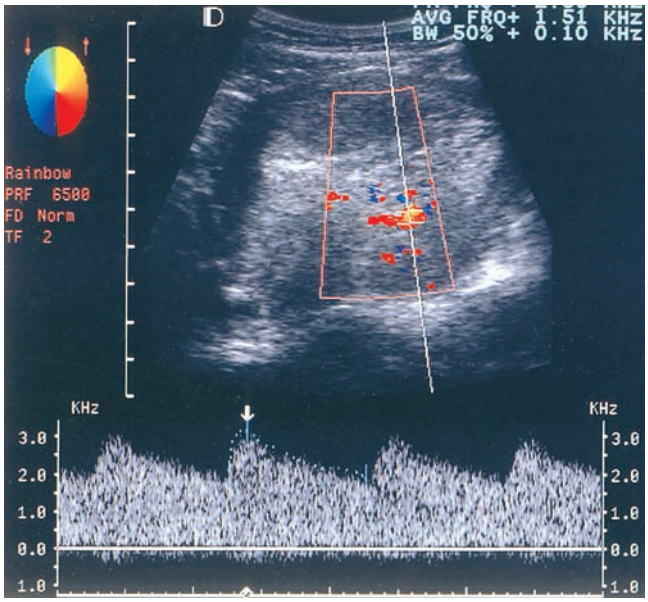

Figure 9–9 Transvaginal color Doppler sonography showing low-impedance flow within echogenic trophoblastic tissue.

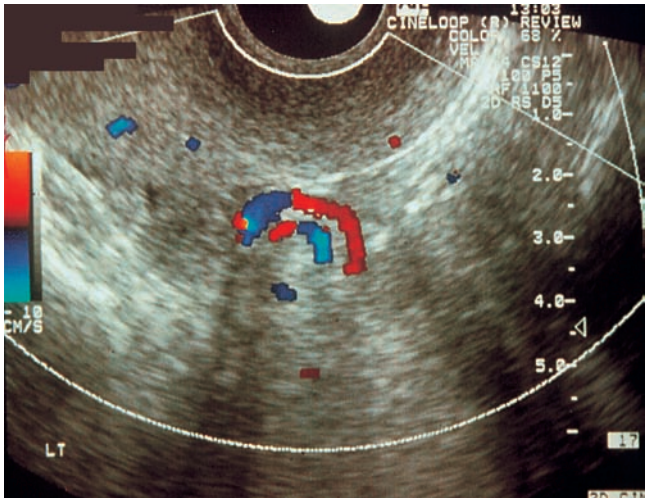

Figure 9–10 Transvaginal color Doppler sonography showing "twisted pedicle" sign associated with adnexal torsion. There is no flow within the enlarged ovary located in the cul-de-sac. (Courtesy of Dr. E. Lee)

Adnexal Torsion

Approximately 20% of ovarian torsion occurs in pregnant women. This may be related to enlargement of the ovary with a corpus luteum, with increased arterial flow to the ovary coupled with decreased venous return. This may result in diffuse ovarian edema and enlargement, thereby increasing susceptibility to torsion. Because intraovarian venous flow is most sensitive to interstitial pressure changes, venous flow is typically absent and arterial flow shows high impedance in most cases of adnexal torsion.[14] As the condition progresses, intraovarian arterial flow may cease. Sonographic depiction of the "twisted pedicle" may be diagnostic in some cases (**Fig. 9–10**).

Summary

TVS offers an accurate means not only for diagnosis, but also for establishing proper management of these patients with first-trimester pain and bleeding.[15]

References

1. Frates MC, Laing FC. Sonographic evaluation of ectopic pregnancy: an update. AJR Am J Roentgenol 1995;165:251–259
2. Emerson DS, Cartier MS, Altieri LA, et al. Diagnostic efficacy of endovaginal color Doppler flow imaging in an ectopic pregnancy screening program. Radiology 1992;183:413–420
3. Atri M, Bret PM, Tulandi T, Senterman MK. Ectopic pregnancy: evolution after treatment with transvaginal methotrexate. Radiology 1992;185:749–753
4. Ackerman T, Levic C, Dashefsky D. Interstitial line: sonographic findings in interstitial (cornual) ectopic pregnancy. Radiology 1993;189:83–86
5. Stanley R, Horger J, Fagon C, et al. Sonographic findings in abdominal pregnancies. AJR Am J Roentgenol 1986;147:1043
6. Pedersen JF, Mantoni M. Prevalence and significance of subchorionic hemorrhage in threatened abortion: a sonographic study. AJR Am J Roentgenol 1990;154:535–537
7. Jouppila P. Clinical consequences after ultrasonic diagnosis of intrauterine hematoma in threatened abortion. J Clin Ultrasound 1985;13:107–111
8. Sauerbrei EE, Pham DH. Placental abruption and subchorionic hemorrhage in the first half of pregnancy: US appearance and clinical outcome. Radiology 1986;160:109–112
9. Bennett G, Bromley B, Liebermans E, Bennaceraf B. Subchorionic hemorrhage in first trimester pregnancies: prediction of pregnancy outcome with sonography. Radiology 1996;199:447–451
10. Laboda LA, Estroff JA, Benacerraf BR. First trimester bradycardia: a sign of impending fetal loss. J Ultrasound Med 1989;8:561–563
11. Nyberg DA, Mack LA, Harvey D, Wang K. Value of the yolk sac in evaluating early pregnancies. J Ultrasound Med 1988;7:129–135
12. Bromley B, Harlow BKL, Laboda LA, et al. Small sac size in the first trimester: predictor of poor fetal outcome. Radiology 1991;178:375–377
13. Dillon EH, Case CQ, Ramos IM, Holland CK, Taylor KJW. Endovaginal US and Doppler findings after first-trimester abortion. Radiology 1993;186:887–891
14. Fleischer AC, Stein SM, Cullinan JC, Warner MA. Color Doppler sonography of adnexal torsion. J Ultrasound Med 1995;14:523–528
15. Arti M, Chow C-M, Kintzen G, et al. Expectant treatment of ectopic pregnancies: clinical and sonographic predictors. AJR Am J Roentgenol 2001;176:123–127

10 Second- and Third-Trimester Bleeding

Barbara S. Hertzberg

Ultrasound plays an important role in the workup of the patient who presents with vaginal bleeding. Bleeding is a common complication of pregnancy[1–4] and a frequent indication for sonography. Although the majority of patients who present with second- or third-trimester vaginal bleeding experience only slight blood loss, even minor bleeds can signal the presence of a life-threatening condition. Hemorrhage is a major source of perinatal morbidity and mortality: along with pulmonary embolism and pregnancy-induced hypertension, bleeding is one of the three leading causes of maternal death.[5]

Ultrasonography is a critical step in the evaluation for potentially life-threatening obstetric sources of hemorrhage. This discussion focuses on the role of ultrasonography in diagnosing serious obstetric causes of bleeding, including placenta previa, placental abruption, circumvallate placenta, vasa previa, and uterine rupture.

Diagnostic Considerations

The conditions causing second- and third-trimester hemorrhage fall into two main groups: obstetric and nonobstetric etiologies. Nonobstetric sources of hemorrhage are generally less hazardous and typically result in relatively little blood loss compared with the obstetric etiologies.[3] Among the nonobstetric causes of second- and third-trimester bleeding are benign vaginal and cervical lesions such as lacerations, varices, benign neoplasias, eversions, and polyps, and malignant lesions such as cervical carcinoma. Unusual nonobstetric etiologies of bleeding during pregnancy include urethral varices and condyloma acuminata.[2,6] In some patients, the source of bleeding is not found, and it is unclear whether the underlying etiology is obstetric or nonobstetric.[7]

Obstetric sources of hemorrhage tend to be more serious and can result in substantial blood loss. The most common serious obstetric causes of hemorrhage are placenta previa and placental abruption.[1,2] Other less frequent, but similarly important obstetric sources of third-trimester hemorrhage include vasa previa, circumvallate placenta, and uterine rupture.[1,3] Digital vaginal and rectal examinations are contraindicated in the patient with placenta previa, so a critical question guiding management of the patient who presents with vaginal bleeding is whether placental tissue overlies the cervix, a determination generally made by ultrasonography.

Near term, the most common cause of bleeding is a benign obstetric phenomenon termed the "bloody show." The bloody show occurs secondary to expulsion of the cervical plug and is a normal phenomenon that virtually never requires medical intervention.[3,7] Despite this, it can result in sufficient blood loss that the mother seeks medical attention and should, therefore, be considered in the differential diagnosis of bleeding late in the third trimester.

Diagnostic Evaluation

Nonobstetric sources of hemorrhage are assessed with nonimaging tests such as pap smear, speculum examination, and culture. Speculum examination is helpful in evaluating for a vaginal or cervical lesion such as a vaginal laceration or a cervical eversion, but should be done only after placenta previa has been excluded.

Depending on the source and severity of the hemorrhage, a variety of other laboratory and clinical tests may be needed. With large bleeds, a complete blood count, type and cross match, serial vital signs, and serial hematocrit levels may be necessary.[2] Tests for nucleated blood cells or fetal hemoglobin in the expelled blood may be indicated if vasa previa is suspected because it is the only source of pure fetal blood.[2,3] When heavy bleeding is due to placental abruption, continuous electronic fetal monitoring may be required to determine if emergent intervention is indicated for fetal distress. Additionally, coagulation profiles are followed in patients with severe degrees of placental abruption to assess for the development of disseminated intravascular coagulation.

Ultrasound is the primary imaging test used to assess the patient with vaginal bleeding. Although angiography, radiography, and radioisotope scanning were performed in the past to assess for placenta previa because of the potential risks of ionizing radiation and contrast, such tests are now of only historical interest in this assessment.[8] Magnetic resonance imaging may be helpful in selected cases when sonography is not diagnostic, but it is not generally used as the initial imaging technique in patients with vaginal bleeding.[9,10]

Ultrasound and Clinical Features of Obstetric Sources

Placental Abruption

Placental abruption is defined as a premature separation of a normally implanted placenta prior to the birth of the fetus. A common and serious disorder, placental abruption complicates ~1% of pregnancies.[11] Abruption is the most common cause of intrapartum fetal death and accounts for up to 15 to 25% of perinatal mortality.[12–15] Other complications can include preterm delivery,[12] and neurological impairment in surviving infants.[2]

The clinical diagnosis of placental abruption can be surprisingly difficult.[2] Placental abruptions present a wide variety of clinical symptomatology that overlaps with symptoms accompanying other disorders, such as placenta previa and uterine rupture. The constellation of clinical signs in severe cases may include vaginal bleeding, abdominal pain and uterine tenderness, painful uterine contractions, fetal distress or demise, and coagulopathy, but the full complement of clinical signs occurs in only a small proportion of patients.

The variability in clinical presentation is partly attributable to the wide range of severity of placental abruption. Placental separation can be complete, partial, or involve only the margin of the placenta. Minor degrees of abruption can be self-limited events with little impact on maternal and fetal outcome, even though they can be accompanied by alarming amounts of vaginal bleeding.[15–17] Some patients have signs and symptoms that are so mild that the diagnosis is only established retrospectively after delivery of a placenta with a retroplacental clot.[2]

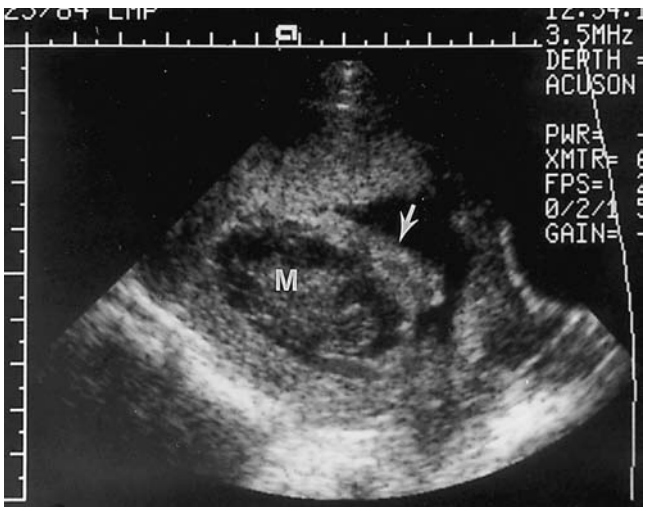

Figure 10–1 Retroplacental hematoma due to placental abruption. Longitudinal transabdominal sonogram demonstrates a heterogeneous mass (M) posterior to the placenta (arrow), which corresponded to a retroplacental hematoma at delivery.

The sensitivity and specificity of ultrasound for diagnosing placental abruption is not well established. The wide range of clinical presentations makes such an assessment difficult, and most ultrasound reports of abruption consist of case reports and retrospective reviews.[12–14,16,18–21] Histopathologic confirmation of placental abruption is likewise complicated by the wide spectrum of pathological findings, which include placental infarction, decidual necrosis, marginal thrombosis, and retroplacental blood clot.[12] Confirmation cannot always be obtained, even in cases strongly suspected by clinical and sonographic findings.[21,22]

There is likewise a wide range of sonographic findings attributable to placental abruption,[12,13] and ultrasonography is considered a relatively insensitive test for diagnosing placental abruption.[19,21,23] This is partly because the ultrasound evaluation previously focused on identification of a retroplacental hematoma: the retroplacental hematoma is not the most common sonographic presentation of placental abruption. Additionally, in some cases, imaging findings are not seen because the bleeding is predominantly external.

At ultrasonography, retroplacental hemorrhage typically results in focal elevation of the placenta by a hematoma which is less echogenic than the overlying placental tissue (**Fig. 10–1**). Several processes can potentially be confused with a retroplacental hematoma at ultrasound.[13] For example, because the normal subplacental vascular region is less echogenic than placenta,[14] it can mimic a retroplacental hematoma. Distinguishing features are that the normal subplacental vascular complex does not exert a mass effect on the placenta,[22,24,25] and that high-resolution gray-scale ultrasound or color Doppler evaluation may reveal discrete vascular spaces in the normal retroplacental space.

A retroplacental myometrial contraction can also resemble a retroplacental hematoma because it can cause a rounded soft-tissue thickening posterior to the placenta.[25] Like the retroplacental hematoma, a contraction will exert mass effect on the placenta. A contraction will, however, be transient and is typically more homogeneous in echopattern than a retroplacental hematoma. In contrast, a hematoma exhibits a range of appearances, dependent on the time interval since the bleed.

Finally, a retroplacental mass such as a leiomyoma should also be considered in the differential diagnosis of retroplacental hematoma (**Fig. 10–2**).[25] A leiomyoma will not exhibit the typical evolution a retroplacental hemorrhage demonstrates on follow-up sonography and may also have other characteristic findings, such as calcifications, posterior sound attenuation, and shadowing.

The acute retroplacental hemorrhage can be particularly difficult to diagnose because if it is echogenic it can resemble the overlying placenta. The placenta may then spuriously appear to be thickened because the hematoma

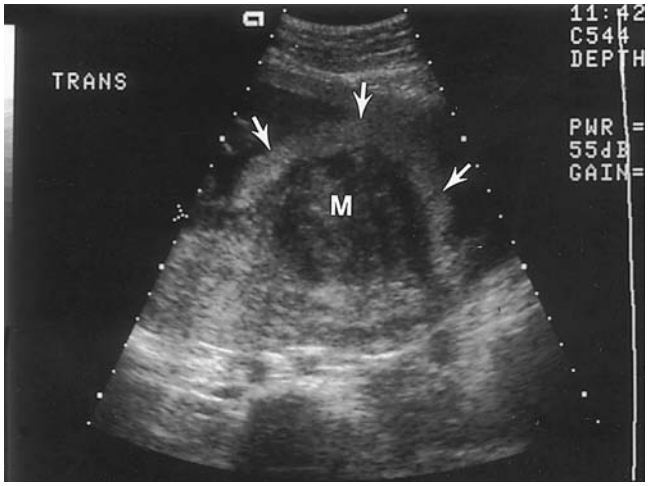

Figure 10–2 Retroplacental leiomyoma. The mass (M) elevating the placenta (arrows) is a leiomyoma. Note the similarity in appearance of this mass to the retroplacental hematoma in **Fig. 10–1**.

is not perceived as being distinct from placenta.[13,18,22,26,27] Demonstration of an apparently thick placenta in a patient suspected clinically of having placental abruption should therefore suggest the possibility of a retroplacental hematoma secondary to placental abruption. If definitive diagnosis is not possible at the time of the initial scan, then follow-up sonography should confirm the diagnosis by depicting interval evolution of the hematoma.[13,27]

Although the retroplacental region would intuitively seem to be a logical place to search for sonographic signs of placental abruption, in fact, it is not the most common location for detecting an intrauterine hematoma. Rather, a subchorionic hematoma is more frequently seen. The subchorionic hematoma is thought to be a consequence of detachment of the placental margin. At ultrasonography, it typically presents as a region of variable echogenicity, which elevates the overlying amniochorionic membrane and is usually contiguous with the edge of the placenta.[1] Subchorionic hematomas also exhibit a variety of other sonographic presentations, which include an intrauterine membrane, an intrauterine mass, and an apparently elongated placenta.

The intrauterine membrane is the most common sonographic presentation of a subchorionic hematoma (**Fig. 10–3**). Sonography will depict a membrane projecting into the amniotic cavity when a chronic subchorionic hematoma has an echopattern similar in echogenicity to that of the amniotic fluid. With the hematoma nearly identical in appearance to amniotic fluid, only the elevated amniochorionic membrane is perceived by sonography. Increasing ultrasound gain settings can occasionally corroborate the diagnosis by depicting low-level echoes within the hematoma.

A subchorionic hematoma can mimic an intrauterine mass if it is echogenic and bulges into the amniotic cavity (**Fig. 10–4**).[13,16,20,22] This sonographic pattern could potentially be mistaken for a uterine contraction, a fibroid, an accessory lobe of the placenta, a chorioangioma, or other placental mass. When these diagnoses are contemplated in a patient clinically suspected of placental abruption, the competing diagnosis of subchorionic hematoma resembling the intrauterine mass should also be considered. Typically, a subchorionic hematoma is soft, gelatinous, and impressionable when kicked by the fetus.[16,20] When the

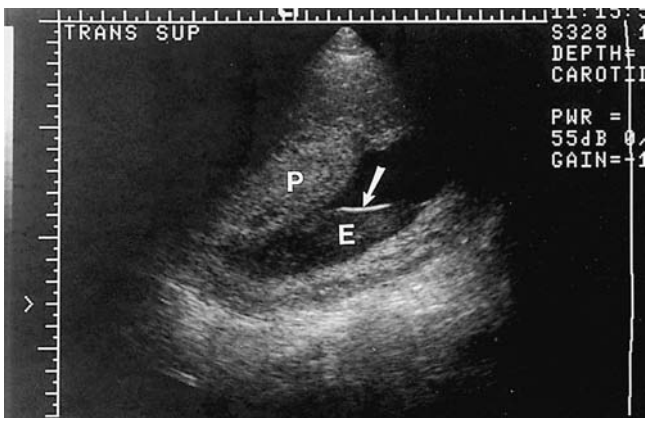

Figure 10–3 Intrauterine membrane due to subchorionic hematoma. Transabdominal sonogram demonstrates a highly echogenic membrane (arrow), which has been elevated by a chronic subchorionic hematoma. Although the hematoma is predominantly echopenic in sonographic pattern, note that low-level echoes (E) are seen within. The intrauterine membrane presentation of a subchorionic hematoma tends to occur in patients with chronic hematomas. P, placenta.

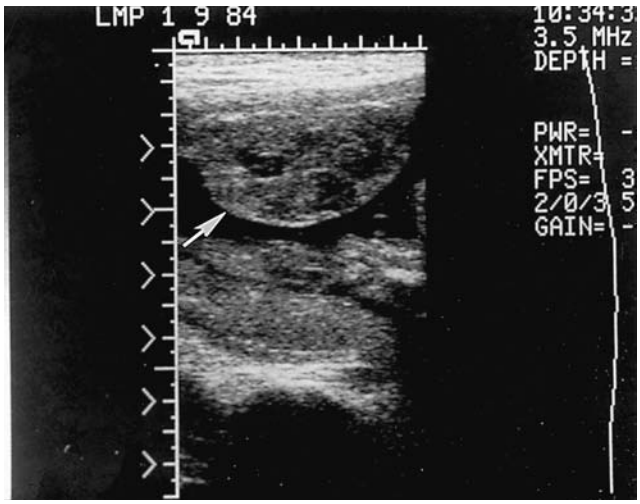

Figure 10–4 Subchorionic hematoma simulating intrauterine mass. The heterogeneous mass (arrow) bulging into the uterine cavity corresponds to a subchorionic hematoma. This sonographic presentation can mimic the ultrasound pattern produced by a uterine contraction, a fibroid, an accessory lobe of the placenta, or a placental mass such as a chorioangioma.

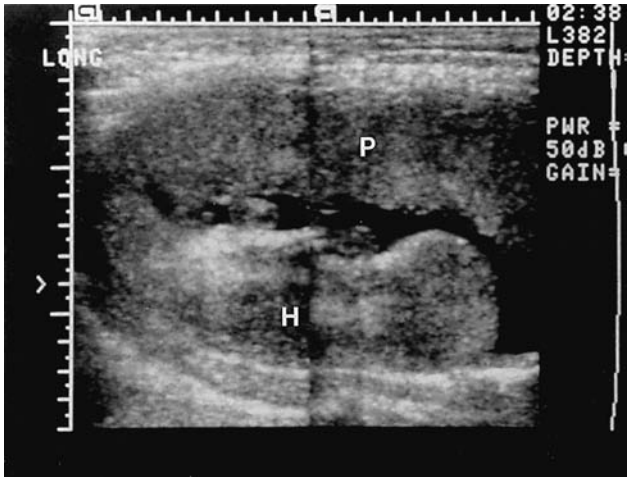

A

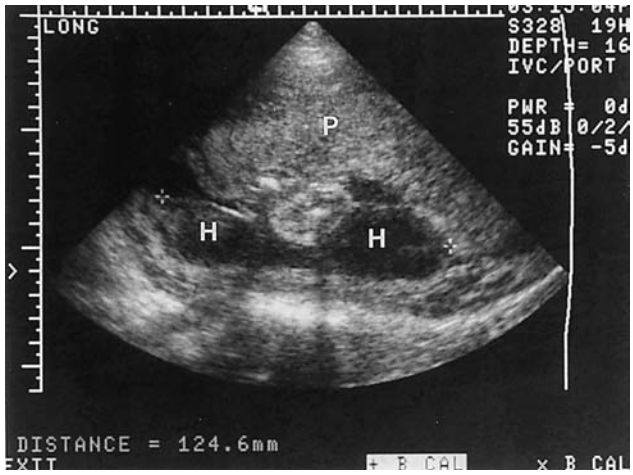

B

Figure 10–5 Subchorionic hematoma resembling elongated placenta. **(A)** An echogenic subchorionic hematoma (H) is seen along the posterior surface of the uterus. Normal placental tissue (P) is imaged along the anterior surface of the uterus. The overall appearance is similar to that of an elongated placenta, although the edge of the subchorionic hematoma has a more rounded appearance than is typical of normal placenta. **(B)** Sonogram obtained 2.5 weeks after the image in **(A)** demonstrates interval evolution of the subchorionic hematoma (H), which is now considerably less echogenic than on the initial scan. P, placenta.

diagnosis is in question, serial sonography may be helpful because it can demonstrate evolution in the echo pattern of the hematoma. With time, the hematoma should become progressively less echogenic in appearance. Color Doppler or power Doppler imaging may also prove helpful in making this distinction.

Because a subchorionic hematoma originates near the edge of the placenta, the hematoma may not be perceived as distinct from the placenta if it is scanned at a stage in which its overall echogenicity is similar to that of the placenta. The overall sonographic pattern can then simulate that of an elongated placenta (**Fig. 10–5A**). In the appropriate clinical setting, detection of an apparently elongated placenta should be considered corroborative evidence supporting the possibility of a subchorionic hematoma. A subtle distinction in echo pattern between the true placenta and the hematoma should be sought. If the diagnosis is still not clear, serial sonography may clarify the question by showing evolution in appearance of the hematoma (**Fig. 10–5B**).

Placental abruptions can also cause other sonographic findings, including an intraplacental fluid-fluid level, a preplacental clot, or intraamniotic echoes owing to intraamniotic hemorrhage.[20,28] A hemorrhage in the "preplacental" location can be in either the subamniotic or the subchorionic space. Clinical symptoms include vaginal bleeding and can be remarkably similar to those arising from other sites of placental abruption. Even though such preplacental hematomas may not be associated with actual placental separation, they can be just as serious as the classic placental abruption. A preplacental hematoma can cause preterm delivery due to stimulation of uterine contractions or fetal demise from compression of the umbilical cord.[12]

Retroplacental hematomas tend to have a poorer outcome than subchorionic hematomas. In general, the greater the percentage of placental involvement, the worse the outcome tends to be.[12]

In conclusion, ultrasound can strengthen the case for a clinically suspected placental abruption. Negative findings at ultrasonography do not, however, exclude placental abruption. Indeed, in the setting of severe fetal distress or unstable maternal condition and suspected placental abruption, it may not be in the patient's best interest to perform ultrasonography, potentially losing valuable time and delaying emergent delivery. Nevertheless, in the more common case in which symptomatology is less extreme, ultrasound can provide valuable information and definitively distinguish placental abruption from placenta previa.

Placenta Previa

Placenta previa is an abnormality of placental location in which placental tissue is implanted on the cervix. Patients with placenta previa typically present with painless third-trimester vaginal bleeding. Fewer than half of patients who experience painless vaginal bleeding, however, have placenta previa.[2] Ultrasound has long been considered a critical step in the assessment of patients with third-trimester bleeding because a vaginal or rectal examination should not be performed until placenta previa has been excluded. Indeed, ultrasound is so useful in excluding placenta previa that it has for the most part replaced the potentially dangerous "double setup examination" traditionally used for assessing patients with third-trimester bleeding.[3]

The sensitivity of ultrasonography for detecting placenta previa approaches 100%. Even the earliest reports of placental

localization by ultrasound describe an accuracy between 93 and 97%.[29–33] To optimize sensitivity, it is necessary to image both the lower edge of the placenta and the cervix. Evaluation of the cervix is needed to exclude the rare but potentially dangerous coincidence of an accessory (succenturiate) lobe of the placenta implanted over the cervical os.[34]

Reported specificities of ultrasound for placenta previa vary widely.[35–37] The specificity depends on the severity of the condition (a complete placenta previa is less likely to resolve with advancing gestation than an incomplete placenta previa), the time in gestation at which placenta previa is detected, and whether a concerted effort was made to avoid sources of false-positives and false-negatives.[38–41] The reported incidence of sonographically detected placenta previa during the second trimester varies from 6 to 49%, but the incidence of placenta previa at term is much lower.[35–37]

Ultrasound can be used to classify the severity of placenta previa. Grading systems vary slightly from institution to institution,[8] but variations in grading systems are relatively unimportant provided the clinicians involved understand the terminology used. A typical classification defines complete placenta previa as comprising placental tissue overlying the entire internal cervical os, and a marginal or partial previa as indicating placental tissue that covers only part of either or both the cervix and the os. Measuring the distance from the lower edge of the cervix to the internal cervical os is helpful in predicting outcome. Vaginal delivery is more likely to be successful if this distance is greater than 2 cm.[42,43] The configuration of the edge of a low-lying placenta also appears to influence outcome: complications are more likely if the placental edge is thick than if it is thin.[44]

The severity of vaginal bleeding tends to be proportional to the severity of placenta previa. Complete placenta previa is associated with earlier, more severe bleeding, and virtually always requires cesarean section. In contrast, less severe degrees of placenta previa have variable outcomes. Some patients can have a vaginal delivery, but others have such severe hemorrhage that blood transfusion or cesarean section or both must be performed.[36,37] A true centrally implanted complete placenta previa (**Fig. 10–6**) will virtually never resolve, but many marginal and partial previas detected in the second trimester resolve later in pregnancy. In patients with an apparent placenta previa during the second trimester, the degree of symmetry of the placenta with regard to the internal os is helpful in predicting the likelihood that placenta previa will persist or resolve. A symmetrical, centrally located placenta previa predicts a much higher likelihood of persistence to delivery than an asymmetric or a marginal placenta previa.[45]

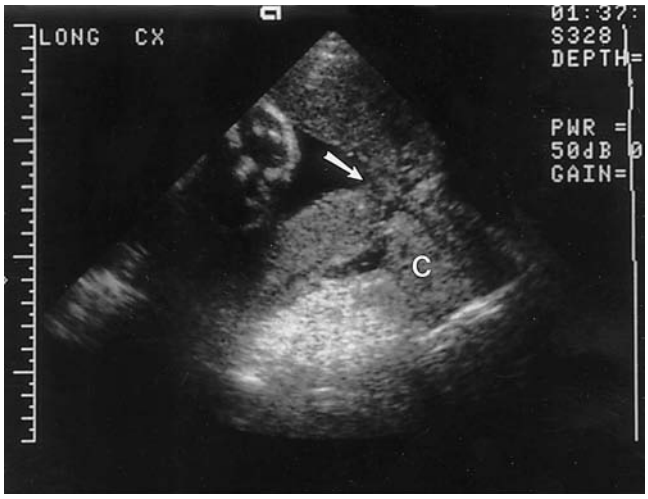

Figure 10–6 Complete central placenta previa. Transabdominal sonogram of the lower uterus reveals placental tissue (arrow) centrally implanted on the cervix (C).

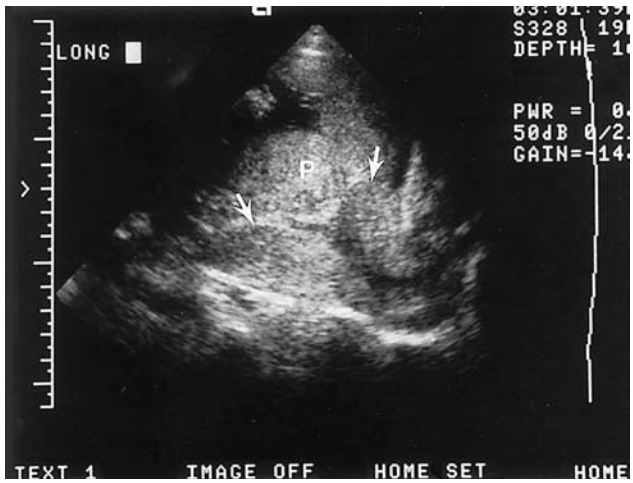

A

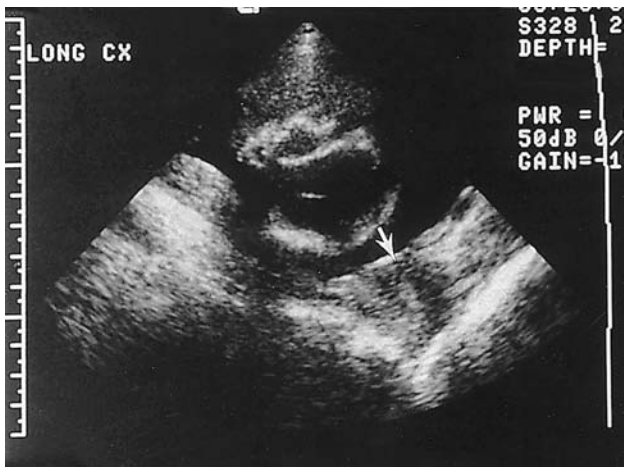

B

Figure 10–7 Lower uterine contraction simulating placenta previa. **(A)** Longitudinal transabdominal sonogram of the lower uterus demonstrates placental tissue (P) apparently overlying the region of the cervix. Closer scrutiny of the image, however, reveals rounding and bulging of the upper margin of the cervix (arrows), suggesting a lower uterine contraction. **(B)** Image obtained 22 minutes after the scan in **(A)** after resolution of the lower uterine contraction reveals a normal-appearing cervix (arrow) without overlying placental tissue.

Several potential sources of a false-positive diagnosis of placenta previa have been described. An important but avoidable explanation for a false-positive result is an overdistended urinary bladder. The bladder can cause a spurious impression of placenta previa because it compresses and distorts the lower uterine segment. If placenta previa is suspected after scans are performed with a full urinary bladder, then imaging should be repeated after the bladder has been emptied.

Another common source of false-positives is a contraction in the lower uterine segment. Like the overdistended urinary bladder, a uterine contraction can distort the appearance of the lower uterus and produce a spurious appearance of placental tissue overlying the cervix (**Fig. 10–7A**). A contraction is recognized as a focal thickening of the myometrium with a distorted appearance to the region of the cervix and lower uterine segment. The cervix may spuriously appear to be elongated: a cervical length of 5 cm or more with an empty urinary bladder suggests that not only the cervix, but also a lower uterine contraction was imaged. A rounding or bulging of the upper margin of the cervix may also be seen: in the absence of a contraction, the normal cervix, is shaped like a cylinder with a flat upper surface. When a contraction is suspected, images obtained after the contraction subsides will reveal the true relationship of the placental edge to the cervix (**Fig. 10–7B**).

A subchorionic hematoma overlying the cervix is another source of a false-positive diagnosis of placenta previa. This is most likely to occur if imaging is performed soon after the bleed, when the hemorrhage may be similar in echogenicity to the adjacent placental tissue. Distinction between subchorionic hematoma overlying the cervix and placenta previa can be difficult, particularly because both disorders may present with similar symptomatology (i.e., vaginal bleeding). Color Doppler may help distinguish a hematoma from a previa because it will demonstrate blood flow in a placenta previa, whereas a hematoma will be avascular. Follow-up ultrasound should show interval evolution in the echo pattern of a subchorionic hematoma, but little change in appearance of a placenta previa.

Transabdominal sonography alone may not be sufficient to accomplish the dual goals of imaging both the lower edge of the placenta as well as the cervix. The lower edge of the placenta may be difficult to see by transabdominal sonography during the third trimester of pregnancy, particularly if it is located in the midline, directly posterior to the fetus. Moreover, though transabdominal ultrasound is usually successful in depicting the cervix during the second trimester of pregnancy, it becomes increasingly difficult to image the cervix with advancing pregnancy, largely due to attenuation of sound by the presenting part of the fetus. Consequently, a variety of techniques have been developed in an attempt to improve transabdominal visualization of the cervix. Such maneuvers include Trendelenburg positioning, overdistention of the urinary bladder, and the application of traction to the presenting part of the fetus in an attempt to elevate it out of the pelvis.[46–48] These techniques, however, can be uncomfortable for the patient, can distort the appearance of the cervix and lower uterus, and frequently are ineffective late in pregnancy.[46]

Transperineal and endovaginal sonography have both been used to circumvent this problem. These ultrasound approaches effectively bypass the shadowing from the presenting part of the fetus, thereby permitting cervical visualization in the vast majority of patients.[49–55] Placenta previa has the same overall appearance by transabdominal, transperineal, and endovaginal sonography, except that the orientation of the cervix varies depending on the approach used (**Fig. 10–8A,B**). Both the transperineal and

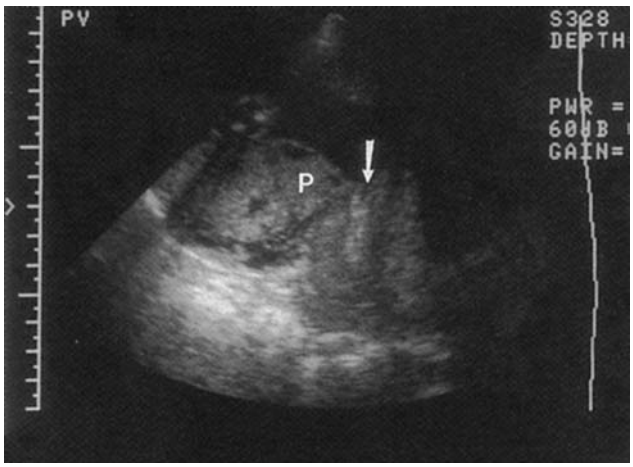

A

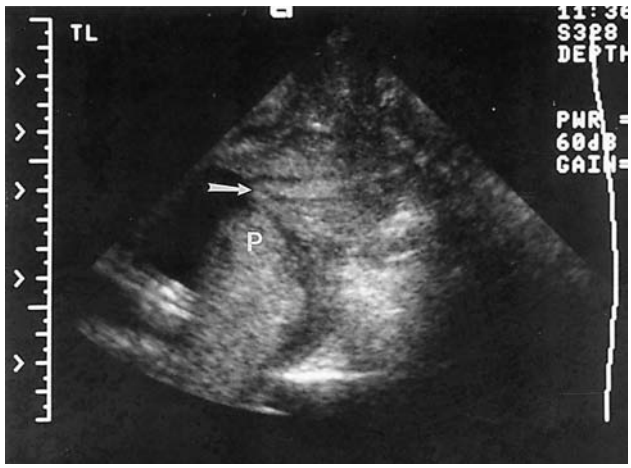

B

Figure 10–8 Marginal placenta previa at transabdominal and transperineal ultrasound. **(A)** Transabdominal ultrasound reveals placental tissue (P) overlying a portion of the cervix (arrow), but not implanted on the os, consistent with marginal placenta previa. **(B)** Transperineal ultrasound reveals a similar appearance, with placental tissue (P) overlying a portion of the cervix (arrow). Note that the transabdominal and transperineal images are depicted in different orientations: the cervix is in an approximately vertical orientation by transabdominal ultrasound, and approximately horizontal orientation by transperineal ultrasound.

the endovaginal techniques are highly successful in visualizing the cervix and establishing the presence or absence of placenta previa.[49–56] Transperineal sonography has the relative advantage of not requiring vaginal penetration, but endovaginal images of the cervix are frequently superior to transperineal images.[57] Endovaginal ultrasound has been shown to be safe in patients with placenta previa, with the caveat that it should be performed cautiously.[53–55,58]

The patient with placenta previa is at increased risk for aberrant placental attachment.[36] Therefore, once an ultrasound diagnosis of placenta previa has been established, the sonologist should consider the question of whether there is ancillary evidence to suggest a concurrent abnormality of placental attachment. The grades of abnormal placental attachment include placenta accreta, placenta increta, and placenta percreta. Placenta accreta refers to extension of chorionic villi into the myometrium, placenta increta indicates extension of villi through the myometrium, and placenta percreta denotes penetration of villi through the uterine serosa. These complications are most likely in the multigravid woman with a prior history of cesarean section and placenta previa during the current pregnancy. The risk of placenta accreta rises progressively as the number of prior cesarean sections increases.

Sonographic features predicting an increased likelihood of abnormal placental attachment in patients with placenta previa have been described. Recognition of these signs can alert the obstetrician to the possibility of placenta accreta and thereby facilitate advance preparation for the possibility of severe hemorrhage and the possible need for cesarean hysterectomy at the time of delivery. Detection of large and irregular placental vascular lacunar spaces, with flow by color Doppler interrogation (**Fig. 10–9**)[59–66] has been associated with an increased likelihood of placenta accreta and has been shown to be the ultrasound finding with the highest positive predictive value.[64] Although vascular spaces can also be seen in the placentas of patients without placenta accreta, there is a tendency for them to be more numerous, larger, and more irregular in configuration in the setting of placenta accreta.[67] Other sonographic findings may include loss of the normal hypoechoic retroplacental area, thinning or disruption of the hyperechoic uterine serosa–bladder interface, and the presence of focal mass-like elevations of tissue (similar in echogenicity to the placenta) projecting beyond the uterine serosa, into or adjacent to the bladder.[67,68] Loss of the normal hypoechoic retroplacental area is a relatively nonspecific finding that accounts for many false-positive diagnoses of placenta accreta.[64] During the first trimester, identification of the gestational sac in the lower uterine segment of a patient with a history of prior C-section has recently been shown to correlate with an increased likelihood of placenta accreta.[69] Magnetic resonance imaging may be helpful in assessing for placenta accreta if the placenta is suboptimally seen by ultrasound.[59]

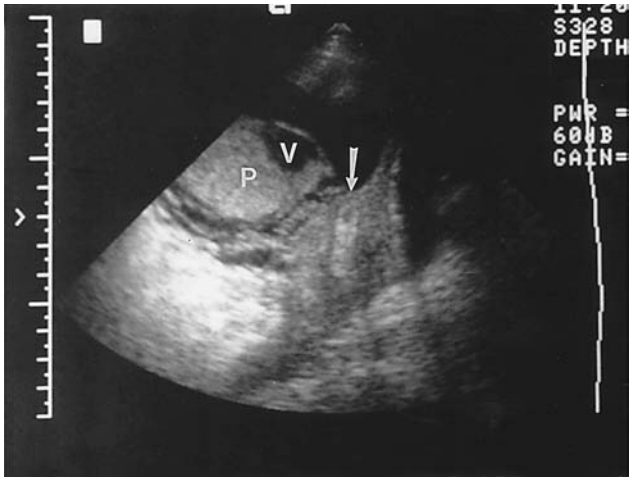

Figure 10–9 Placenta previa with placenta accreta. Transabdominal ultrasound reveals placental tissue (P) partially overlying the cervix (straight arrow), consistent with a marginal placenta previa. In addition, a large hypoechoic vascular space (V) is seen in the lower placenta. Similar spaces were seen throughout the inferior portion of the placenta, suggesting the possibility of placenta accreta. This diagnosis was confirmed histopathologically, and the patient required emergency cesarean hysterectomy due to profuse bleeding.

Circumvallate Placenta

The normal placenta is completely covered by villus chorion. Circumvallate or circummarginate placenta occurs when the villus chorion ends short of the placental margin so that some villi are unprotected by membranes. Placenta circummarginate is characterized by a narrow band of exposed villi, with the transition from villus to membranous chorion marked by a flat ring of membranes.[70] Circummarginate placenta generally does not cause symptoms and is considered a variant of normal. Circumvallate placenta, in contrast, is characterized by a raised, rolled edge of tissue with a larger volume of unexposed villi. Circumvallate placenta can cause bleeding, most commonly during the second trimester of pregnancy.[70] The etiology for the bleeding is postulated to be that the exposed placental tissue is more friable so it bleeds more easily than the normal placenta. Other potential complications include inflammation, infection, and preterm delivery.

At ultrasonography, circumvallate placenta is characterized by an elevated shelf of placental tissue at the placental edge, projecting into the amniotic fluid[70–72] (**Fig. 10–10**). The shelf can involve the entire perimeter of the placental margin, but frequently is only partial.[70] The elevated shelf of placental tissue can be difficult to image if it is obscured by a uterine contraction or closely apposed to the placenta.[70] Indeed, a recent study showed that the

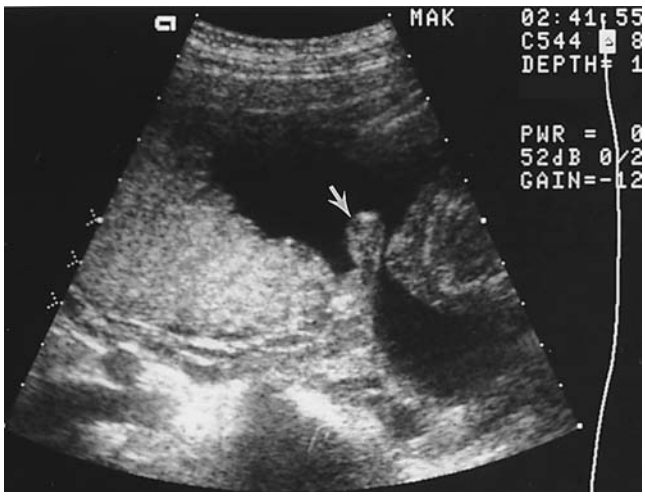

Figure 10–10 Circumvallate placenta. An elevated shelf of tissue (arrow) projects into the amniotic fluid at the inferior margin of the placenta. This is a typical appearance for circumvallate placenta.

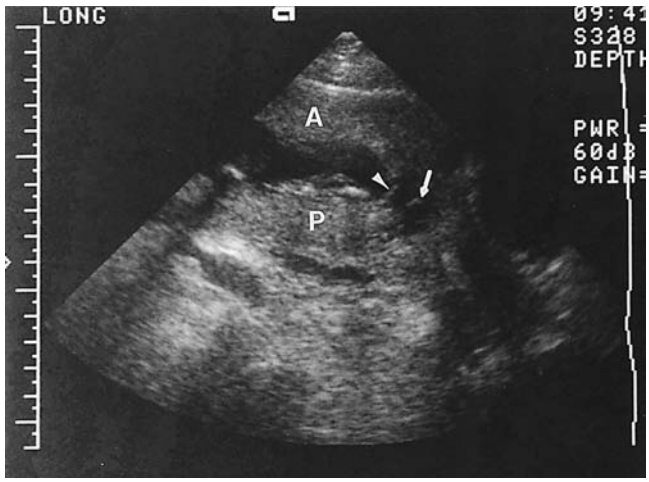

Figure 10–11 Vasa previa. Transabdominal sonogram of the lower uterus reveals anterior (A) and posterior (P) lobes of the placenta, connected by a membrane (arrowhead), containing blood vessels (closed arrow) overlying the cervix (arrows). The diagnosis of succenturiate lobes of the placenta with vasa previa was confirmed at delivery.

sensitivity and specificity of ultrasonography in identifying circumvallate placenta are limited.[73]

Vasa Previa

Vasa previa is a rare but dangerous condition in which fetal placental vessels within the membranes cross the internal cervical os in advance of the presenting part of the fetus, unprotected by placenta or umbilical cord. Vasa previa occurs in patients with a bilobate or succenturiate lobe of the placenta or a velamentous insertion of the umbilical cord. The only known source of vaginal bleeding comprising pure fetal blood, it is an extremely important diagnosis to make because fetal complications are potentially catastrophic. The vessels crossing the internal cervical os are prone to rupture at the time of rupture of the membranes, potentially leading to rapid fetal exsanguination and death. Vasa previa is therefore considered an absolute indication for cesarean section. Despite the high incidence of fetal mortality, vasa previa poses little or no risk to the mother.

Clinically, the diagnosis of vasa previa should be suspected in the patient with the classic clinical presentation of bright red vaginal bleeding beginning around the time of membrane rupture. At ultrasound, a high level of suspicion is indicated in patients with a velamentous insertion of the umbilical cord, a bilobate placenta, or succenturiate placental lobes, particularly when an accessory placental lobe is implanted low in the uterus. Gray-scale ultrasound may depict circular or linear hypoechoic structures typical of vessels traversing the cervical os (**Fig. 10–11**).[74] Color Doppler should be performed to confirm the presence of blood vessels over the cervix when the possibility of vasa previa is considered.[74–84]

The blood vessels comprising a vasa previa must be distinguished from prominent, but normal cervical and lower uterine blood vessels. Cervical varices and myometrial vessels can be distinguished from vasa previa based on their location lateral to the lower uterine segment and around the periphery of the cervix. Umbilical cord presentation or umbilical cord prolapse can also present a sonographic picture resembling that of vasa previa, with blood vessels overlying the cervix but contained within the umbilical cord structure. Recently, three-dimensional ultrasound has been shown to provide useful ancillary information when the diagnosis of vasa previa is uncertain.[85]

The accuracy of ultrasound for vasa previa is unknown because the literature has been predominantly case reports. There are well-documented cases in which antenatal ultrasonography failed to detect a vasa previa that was subsequently documented at delivery.[79,86] Antenatal ultrasound diagnosis seems to require a high level of suspicion and is more likely to be made in the patient with suggestive clinical signs such as bright red vaginal bleeding at the time of membrane rupture, or ultrasonographic evidence of a high risk of vasa previa based on the presence of succenturiate lobes of the placenta, a bilobate placenta, or a velamentous umbilical cord insertion.

Uterine Rupture and Uterine Dehiscence

Uterine rupture is a rare, but clinically important etiology for third-trimester bleeding. This potentially catastrophic event poses an extremely high risk both to the fetus and to the mother. Maternal death rates have been reported to be as high as 2 to 20%, with fetal mortality in the 10 to 60% range.[87] The classic clinical presentation of uterine rupture includes uterine pain, vaginal bleeding, and shock. Often, however, the clinical picture is less dramatic. Clinical

symptomatology can be surprisingly elusive, and signs or symptoms may be absent in up to 50% of patients, with symptoms mimicking other conditions.[88–90] For example, the pain that accompanies uterine rupture may closely resemble the pain occurring due to placental abruption. Not surprisingly then, in some cases uterine rupture is not discovered until the time of delivery.[88]

The terms *uterine rupture* and *uterine dehiscence* have been used interchangeably in the literature.[89] Strictly speaking, *uterine rupture* is defined as disruption of all the layers surrounding the fetus, including the membranes, myometrium, and serosa, and results in direct communication between the uterine cavity and peritoneal cavity.[87] In contrast, *uterine dehiscence* refers to rupture of the myometrium, but does not imply rupture of fetal membranes.[87] Dehiscence tends to be a gradual process, often with few if any symptoms, whereas rupture tends to be acute in nature and is more likely to be fatal.[89]

The possibility of uterine rupture should be considered in the symptomatic pregnant patient who has undergone prior uterine surgery or a complicated curettage procedure. The majority of ruptures occur in patients who have had a prior cesarean section, but other predisposing conditions include myomectomy, curettage, resection of cornual ectopic pregnancy, and other uterine surgeries.[67,91,92] Rupture of a low transverse cesarean section scar tends to occur during labor[93] and should be considered in patients with prior cesarean sections who experience vaginal bleeding during labor. The classic cesarean section scar, on the other hand, tends to rupture explosively, usually before the onset of labor.[87,93] Uterine rupture can also occur secondary to intense labor induction or excessively long or difficult labor, or following blunt abdominal trauma.

Several cases of preoperative sonographic diagnosis of uterine rupture or dehiscence have been reported. Diagnosis has typically relied on nonspecific ultrasound findings, such as progressive myometrial thinning,[94] intraperitoneal or extraperitoneal hematomas, or intraamniotic blood clots[88,95] detected in the appropriate clinical setting. A more specific diagnosis has been rendered based on sonographic depiction of a defect in the uterine wall, in conjunction with free or loculated abdominal fluid, a hematoma, or protrusion of the amniotic sac and/or fetal parts through the defect.[89,90,92,93,96] In one of the more extreme examples reported, ultrasound revealed an empty uterus in conjunction with hemoperitoneum and an intraabdominal placenta and fetus, creating an ultrasound picture similar to that of abdominal pregnancy.[97]

Summary

Second- and third-trimester bleeding occurs due to a range of obstetric and nonobstetric disorders. Obstetric sources of bleeding tend to be more serious and can pose grave risks to the health and welfare of mother and fetus. Ultrasonography plays a critical role in evaluating serious obstetric sources of hemorrhage, but is of less importance in assessing nonobstetric etiologies. Important obstetric conditions to be considered in the differential diagnosis of second- and third-trimester bleeding include placenta previa, placental abruption, circumvallate placenta, vasa previa, and uterine rupture.

Acknowledgment
The author wishes to thank Susan Murray for assistance with manuscript preparation.

References

1. Tucker SM. Perinatal protocol. Second or third trimester bleeding. J Perinatol 1988;8:174–177
2. Scott JR. Placenta previa and placental abruption. In: Scott JR, DiSaia PJ, Hammond CB, Spellacy WN, eds. Danforth's Obstetrics and Gynecology. 7th ed. Philadelphia: JB Lippincott; 1994:489–500
3. Pernoll ML. Third-trimester hemorrhage. In: Pernoll ML, ed. Current Obstetric and Gynecologic Diagnosis and Treatment. 7th ed. Norwalk, CT: Appleton & Lange; 1991:388–400
4. Spinillo A, Fazzi E, Stronati M, et al. Early morbidity and neurodevelopmental outcome in low-birthweight infants born after third trimester bleeding. Am J Perinatol 1994;11:85–90
5. Third-trimester bleeding. In: Dunnihoo DR, ed. Fundamentals of Gynecology and Obstetrics. 2nd ed. Philadelphia: JB Lippincott; 1992:535–538
6. Prater JM, Warrington P. Urethral varices as an unusual cause of third-trimester bleeding: a case report. J Reprod Med 1988;33: 664–666
7. Obstetrical hemorrhage. In: Cunningham FG, MacDonald PC, Gant NF, eds. William's Obstetrics. Norwalk, CT: Appleton & Lange; 1989:695–725
8. Langlois SLP, Miller AG. Placenta praevia: a review with emphasis on the role of ultrasound. Aust N Z J Obstet Gynaecol 1989;29:110–116
9. Powell MD, Buckley J, Price H, Worthington BS, Symonds EM. Magnetic resonance imaging and placenta previa. Am J Obstet Gynecol 1986;154:565–569
10. Verswijvel G, Grieten M, Gyselaers W, et al. MRI in the assessment of pregnancy related intrauterine bleeding: a valuable adjunct to ultrasound? JBR-BTR 2002;85:189–192
11. Toivonen S, Heinonen S, Anttila M, et al. Reproductive risk factors, Doppler findings, and outcome of affected births in placental abruption: a population-based analysis. Am J Perinatol 2002;19: 451–460
12. Nyberg DA, Mack LA, Benedetti TJ, Cyr DR, Schuman WP. Placental abruption and placental hemorrhage: correlation of sonographic findings with fetal outcome. Radiology 1987;164:357–361
13. Nyberg DA, Cyr RD, Mack LA, Wilson DA, Shuman WP. Sonographic spectrum of placental abruption. Am J Roentgenol 1987;148: 161–164
14. Jouppila P, Kirkinen P. Problems associated with the ultrasonic diagnosis of abruptio placentae. Int J Gynaecol Obstet 1982;20:5–11
15. Combs CA, Nyberg DA, Mack LA, Smith JR, Benedetti TH. Expectant management after sonographic diagnosis of placental abruption. Am J Perinatol 1992;9:170–174
16. Metzger DA, Bowie JD, Killam AP. Expectant management of partial placental abruption in previable pregnancies-a report of two cases. J Reprod Med 1987;32:789–792

17. Sholl JS. Abruptio placentae: clinical management in nonacute cases. Am J Obstet Gynecol 1987;156:40–51
18. Mintz MC, Kurtz AB, Arenson R, et al. Abruptio placentae: apparent thickening of the placenta caused by hyperechoic retroplacental clot. J Ultrasound Med 1986;5:411–413
19. Ito M, Kawasaki N, Matsui K, Fujisaki S. Fetal heart monitoring and ultrasound in the management of placental abruption. Int J Gynaecol Obstet 1986;24:269–273
20. Hill LM, Breckle R. Fetal outcome after intraamniotic hemorrhage with placental abruption: a report of three cases. J Reprod Med 1986;31:1065–1070
21. Jaffe MH, Schoen WC, Silver TM, Bowerman RA, Stuck KJ. Sonography of abruptio placentae. Am J Roentgenol 1981;137:1049–1054
22. McGahan JP, Phillips HE, Reid MH, Oi RH. Sonographic spectrum of retroplacental hemorrhage. Radiology 1982;142:481–485
23. Glantz C, Purnell L. Clinical utility of sonography in the diagnosis and treatment of placental abruption. J Ultrasound Med 2002; 21:837–840
24. McGahan JP, Phillips HE, Reid MH. The anechoic retroplacental area. Radiology 1980;134:475–478
25. Gottesfeld KR. The clinical role of placental imaging. Clin Obstet Gynecol 1984;27:327–341
26. Kuhn W, Ulbrich R, Rath W. Changes of the clinical presentation of abruptio placentae. Eur J Obstet Gynecol Reprod Biol 1984;17:131–140
27. Fleming AD. Abruptio placentae. Crit Care Clin 1991;7:865–875
28. Nishijima K, Shukunami K, Tsuyoshi H, et al. Massive subchorionic hematoma: peculiar prenatal images and review of the literature. Fetal Diagn Ther 2005;20:23–26
29. Gottsfeld KR, Thompson HE, Holmes JH, Taylor ES. Ultrasonic placentography: a new method for placental localization. Am J Obstet Gynecol 1966;96:538–547
30. Donald I, Abdulla U. Placentography by sonar. J Obstet Gynaecol Br Commonw 1968;75:993–1006
31. Campbell S, Kohorn EI. Placental localization by ultrasonic compound scanning. J Obstet Gynaecol Br Commonw 1968;75:1007–1013
32. Sunden B. Placentography by ultrasound. Acta Obstet Gynecol Scand 1970;49:179–184
33. Bowie JD, Rochester D, Cadkin AV, Cooke WT, Kunzmann A. Accuracy of placental localization by ultrasound. Radiology 1978;128: 177–180
34. Shukunami K, Tsunezawa W, Hosokawa K, et al. Placenta previa of a succenturiate lobe: a report of two cases. Eur J Obstet Gynecol Reprod Biol 2001;99:276–277
35. Townsend RR, Laing FC, Nyberg DA, et al. Technical factors responsible for "placental migration": sonographic assessment. Radiology 1986;160:105–108
36. Mabie WC. Placenta previa. Clin Perinatol 1992;19:425–435
37. Lavery JP. Placenta previa. Clin Obstet Gynecol 1990;33:414–421
38. Dola CP, Garite TJ, Dowling DD, et al. Placenta previa: does its type affect pregnancy outcome? Am J Perinatol 2003;20:353–360
39. Chama CM, Wanonyi IK, Usman JD. From low-lying implantation to placenta praevia: a longitudinal ultrasonic assessment. J Obstet Gynaecol 2004;24:516–518
40. Mustafa SA, Briozot ML, Carvalho MH, et al. Transvaginal ultrasonography in predicting placenta previa at delivery: a longitudinal study. Ultrasound Obstet Gynecol 2002;20:356–359
41. Dashe JS, McIntire DD, Ramus RM, et al. Persistence of placenta previa according to gestational age at ultrasound detection. Obstet Gynecol 2002;99:692–697
42. Bhide A, Thilaganathan B. Recent advances in the management of placenta previa. Curr Opin Obstet Gynecol 2004;16:447–451
43. Bhide A, Prefumo F, Moore J, et al. Placental edge to internal os distance in the late third trimester and mode of delivery in placenta praevia. BJOG 2003;110:860–864
44. Ghourab S. Third-trimester transvaginal ultrasonography in placenta previa: does the shape of the lower placental edge predict clinical outcome? Ultrasound Obstet Gynecol 2001;18:103–108
45. Zelop CC, Bromley B, Frigoletto FD Jr, Benacerraf BR. Second trimester sonographically diagnosed placenta previa: prediction of persistent previa at birth. Int J Gynaecol Obstet 1994;44:207–210
46. Wells SW, Anderson NG, Allan RB. Efficacy of fetal part elevation to visualise internal cervical os. Australas Radiol 1992;36:110–111
47. Jeffrey RB, Laing FC. Sonography of the low-lying placenta: value of Trendelenburg and traction scans. Am J Roentgenol 1981;137: 547–549
48. Lee TG, Knochel JQ, Melendez MG, Henderson SC. Fetal elevation: a new technique for placental localization in the diagnosis of previa. J Ultrasound Med 1981;9:467–471
49. Hertzberg BS, Bowie JD, Carroll BA, Kliewer MA, Weber TM. Diagnosis of placenta previa during the third trimester: role of transperineal sonography. Am J Roentgenol 1992;159:83–87
50. Zilianti M, Azuaga A, Calderon F, Redondo C. Transperineal sonography in second trimester to term pregnancy and early labor. J Ultrasound Med 1991;10:481–485
51. Farine D, Fox HE, Jakobson S, Timor-Tritsch IE. Vaginal ultrasound for diagnosis of placenta previa. Am J Obstet Gynecol 1988;159: 566–569
52. Timor-Tritsch IE, Monteagudo A. Diagnosis of placenta previa by transvaginal sonography. Ann Intern Med 1993;25:279–283
53. Timor-Tritsch IE, Yunis RA. Confirming the safety of transvaginal sonography in patients suspected of placenta previa. Obstet Gynecol 1993;81:742–744
54. Leerentveld RA, Gilberts ECAM, Arnold MJCWJ, Wladimiroff JW. Accuracy and safety of transvaginal sonographic placental localization. Obstet Gynecol 1990;76:759–762
55. Tan NH, Abu M, Woo JLS, Tahir HM. The role of transvaginal sonography in the diagnosis of placenta praevia. Aust N Z J Obstet Gynaecol 1995;35:42–45
56. Farine D, Peisner DB, Timor-Tritsch IE. Placenta previa: is the traditional diagnostic approach satisfactory? J Clin Ultrasound 1990; 18:328–330
57. Hertzberg BS, Livingston E, DeLong DM, et al. Ultrasonogarphhic evaluation of the cervix: transperineal versus endovaginal imaging. J Ultrasound Med 2001;20:1071–1080
58. Hilpert PL, Kurtz AB. The role of transvaginal ultrasound in the second and third trimesters. Semin Ultrasound CT MR 1990;11:59–70
59. Levine D, Hulka CA, Ludmir J, Li W, Edelman RR. Placenta accreta: evaluation with color Doppler US, power Doppler US, and MR imaging. Radiology 1997;205:773–776
60. Silver LE, Hobel CJ, Lagasse L, Luttrull JW, Platt LD. Placenta previa percreta with bladder involvement: new considerations and review of the literature. Ultrasound Obstet Gynecol 1997;9:131–138
61. Lerner JP, Deane S, Timor-Tritsch IE. Characterization of placenta accreta using transvaginal sonography and color Doppler imaging. Ultrasound Obstet Gynecol 1995;5:198–201
62. Craigo S. Placenta previa with suspected accreta. Curr Opin Obstet Gynecol 1997;9:71–75
63. Guy GP, Peisner DB, Timor-Tritsch IE. Ultrasonographic evaluation of uteroplacental blood flow patterns of abnormally located and adherent placentas. Am J Obstet Gynecol 1990;163:723–727
64. Comstock CH, Love JJ Jr, Bronsteen RA, et al. Sonographic detection of placenta accreta in the second and third trimesters of pregnancy. Am J Obstet Gynecol 2004;190:1135–1140

65. Chou MM, Ho ES, Lee YH. Prenatal diagnosis of placenta previa accreta by transabdominal color Doppler ultrasound. Ultrasound Obstet Gynecol 2000;15:28–35
66. Moodley J, Ngambu NF, Corr P. Imaging techniques to identify morbidly adherent placenta praevia: a prospective study. J Obstet Gynaecol 2004;24:742–744
67. Finberg HJ, Williams JW. Placenta accreta: prospective sonographic diagnosis in patients with placenta previa and prior cesarean section. J Ultrasound Med 1992;11:333–343
68. Hoffman-Tretin JC, Koenigsberg M, Rabin A, Anyaegbunam A. Placenta accreta-additional sonographic observations. J Ultrasound Med 1992;11:29–34
69. Comstock CH, Lee W, Vettraino IM, Bronsteen RA. The early sonographic appearance of placenta accreta. J Ultrasound Med 2003; 22:19–23
70. McCarthy J, Thurmond AS, Jones MK, et al. Circumvallate placenta: sonographic diagnosis. J Ultrasound Med 1995;14:21–26
71. Cutillo DP, Swayne LC, Schwartz JR, Dise CA, Faux RG. Intra-amniotic hemorrhage secondary to placenta circumvallate. J Ultrasound Med 1989;8:399–401
72. Bey M, Dott A, Miller JM Jr. The sonographic diagnosis of circumvallate placenta. Obstet Gynecol 1991;78:515–517
73. Harris RD, Wells WA, Black WC, et al. Accuracy of prenatal sonography for detecting circumvallate placenta. AJR Am J Roentgenol 1997;168:1603–1608
74. Reuter KL, Davidoff A, Hunter T. Vasa previa. J Clin Ultrasound 1988;16:346–348
75. Gianopoulos J, Carver T, Tomich PG, Karlman R, Gadwood K. Diagnosis of vasa previa with ultrasonography. Obstet Gynecol 1987;69:488–491
76. Hsieh FJ, Chen HF, Ko TM, Hsieh CY, Chen HY. Antenatal diagnosis of vasa previa by color-flow mapping. J Ultrasound Med 1991;10: 397–399
77. Meyer WJ, Blumenthal L, Cadkin A, Gauthier DW, Rotmensch S. Vasa previa: prenatal diagnosis with transvaginal color Doppler flow imaging. Am J Obstet Gynecol 1993;169:1627–1629
78. Hata K, Hata T, Fujiwaki R, et al. An accurate antenatal diagnosis of vasa previa with transvaginal color Doppler ultrasonography. Am J Obstet Gynecol 1994;171:265–267
79. Hurley VA. The antenatal diagnosis of vasa praevia: the role of ultrasound. Aust N Z J Obstet Gynaecol 1988;28:177–179
80. Harding JA, Lewis DF, Major CA, et al. Color flow Doppler: a useful instrument in the diagnosis of vasa previa. Am J Obstet Gynecol 1990;163:1566–1568
81. Nelson LH, Melone PJ, King M. Diagnosis of vasa previa with transvaginal and color flow Doppler ultrasound. Obstet Gynecol 1990;76:506–509
82. Lee W, Lee VL, Kirk JS, et al. Vasa previa: prenatal diagnosis, natural evolution, and clinical outcome. Obstet Gynecol 2000;95:572–576
83. Catanzarite V, Maida C, Thomas W, et al. Prenatal sonographic diagnosis of vasa previa: ultrasound findings and obstetric outcome in ten cases. Ultrasound Obstet Gynecol 2001;18:109–115
84. Hertzberg BS, Kliewer MA. Vasa previa: prenatal diagnosis by transperineal sonography with Doppler evaluation. J Clin Ultrasound 1998;26:405–408
85. Lee W, Kirk JS, Comstock CH, Romero R. Vasa previa: prenatal detection by three-dimensional ultrasonography. Ultrasound Obstet Gynecol 2000;16:384–387
86. Eddleman KA, Lockwood CJ, Berkowit GS, Lapinski RH, Berkowitz RL. Clinical significance and sonographic diagnosis of velamentous umbilical cord insertion. Am J Perinatol 1992;9:123–126
87. Rooholamini SA, Au AH, Hansen GC, et al. Imaging of pregnancy-related complications. Radiographics 1993;13:753–770
88. Gale JT, Mahony BS, Bowie JD. Sonographic features of rupture of the pregnant uterus. J Ultrasound Med 1986;5:713–714
89. Shrout AB, Kopelman JN. Ultrasonographic diagnosis of uterine dehiscence during pregnancy. J Ultrasound Med 1995;14:399–402
90. Osmers R, Ulbrich R, Schauer A, Kuhn W. Sonographic detection of an asymptomatic rupture of the uterus due to necrosis during the third trimester. Int J Gynaecol Obstet 1988;26:279–284
91. Acton CM, Long PA. The ultrasonic appearance of a ruptured uterus. Australas Radiol 1978;22:254–256
92. van Alphen M, van Vugt JMG, Hummel P, van Geijn HP. Recurrent uterine rupture diagnosed by ultrasound. Ultrasound Obstet Gynecol 1995;5:419–421
93. Suonio S, Saarikoski S, Kääriäinen J, Virtanen R. Intrapartum rupture of uterus diagnosed by ultrasound: a case report. Int J Gynaecol Obstet 1984;22:411–413
94. Chapman K, Meire H, Chapman R. The value of serial ultrasounds in the management of recurrent uterine scar rupture. Br J Obstet Gynaecol 1994;101:549–551
95. Bedi DG, Salmon A, Winsett MZ, Fagan CJ, Kumar R. Ruptured uterus: sonographic diagnosis. J Clin Ultrasound 1986;14:529–533
96. Kushnir O, Tamarkin M, Barkai G, et al. Extrauterine amniotic sac (amniocele): clinical workup in a case of silent uterine rupture. J Ultrasound Med 1990;9:367–369
97. Harrison SD, Nghiem HV, Shy K. Uterine rupture with fetal death following blunt trauma. Am J Roentgenol 1995;165:1452

11 Premature Labor

Geoffrey Wong and Deborah Levine

Premature delivery (delivery before 37 weeks gestational age) is a major cause of perinatal morbidity and mortality, being responsible for 70% of perinatal deaths.[1,2] The rate of premature delivery in the United States increased from 9.4% in 1981 to 11.9% in 2001.[3] This change is attributed to an increase in the population at high risk for premature delivery. The number of twin births increased by 32% between 1989 and 2000. In the same time period, the number of triplet births almost tripled and the number of quadruplet births more than doubled. These changes are, in part, attributable to the increased use of assisted reproductive technology.[4] In addition, patients with either or both medical and reproductive risk factors previously advised not to conceive are now attempting pregnancy under the supervision of high-risk obstetrical teams. These patients often deliver before full term for medical reasons. Indicated premature delivery presently accounts for 15 to 25% of premature births.[3]

However, there are some encouraging trends in preterm morbidity and mortality. Advances in prenatal and neonatal care have reduced perinatal mortality from premature deliveries. The lower limit of infant viability has been extended: presently over 50% of infants born at 24 to 25 weeks survive to be discharged home from the hospital.[3,5] However, the cost of providing care to an extremely premature infant in the immediate neonatal period is 50 times more than that of an infant born at term, and the health care cost for the rest of the first year of life is 20 times more expensive.[6] There are frequently significant physical and neurological sequelae in children born very prematurely as well.[7] Although the total number of premature births in the last decade has not decreased, there has been a decrease in the proportion of infants born very prematurely: 1.57% of singleton births occurred before 32 weeks in 2001, compared with 1.69% in 1990. The proportion of singleton births between 32 to 36 weeks increased from 8.01% in 1990 to 8.81% in 2001.[3] These infants are technically considered as premature births but have fewer morbidities than those delivered at an earlier gestational age. This shift to a less vulnerable stage of the pregnancy may in part be the result of advances in the diagnosis of premature labor so that intervention can be instituted earlier and more effectively.

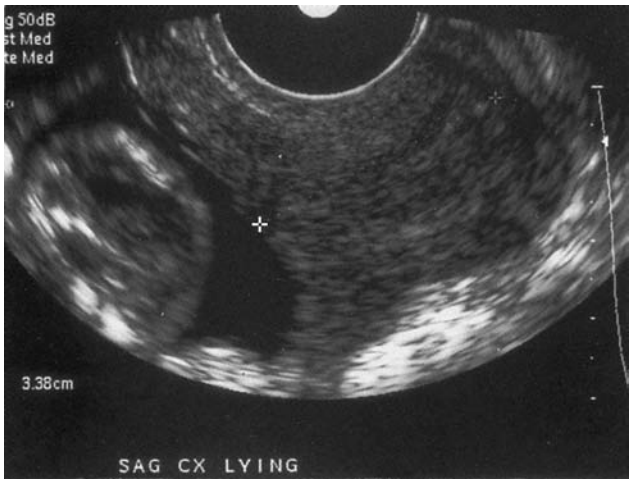

Figure 11–1 Normal transvaginal view of the cervix. The endocervical canal is indicated with calipers.

Obstetrical ultrasound plays an important role in the evaluation of patients in spontaneous premature labor, not only in the determination of gestational age and fetal well-being, but also in the assessment of the cervix. Sonography, using a transvaginal (**Fig. 11–1**) or transperineal (**Fig. 11–2**) approach, provides an additional method beyond the traditional digital examination for the study of the uterine cervix during pregnancy.

The cervix plays a unique role in pregnancy. The closed and uneffaced cervix physically maintains the fetus in utero, and secretions from the cervix form the mucous plug that is partly responsible for preventing ascending infection. The cervix can be the cause of premature delivery in cases of incompetent cervix. An incompetent cervix, which may be congenital or acquired, is associated with a silent decrease in cervical length and painless dilatation of the cervix that may result in premature labor recognized only at an advanced stage. Changes in cervical length, dilatation, and effacement can reflect the progression of premature labor. Recognizing these changes can help identify patients that are heading toward premature delivery. This chapter reviews the use of sonography in the assessment of the cervix in premature labor and delivery.

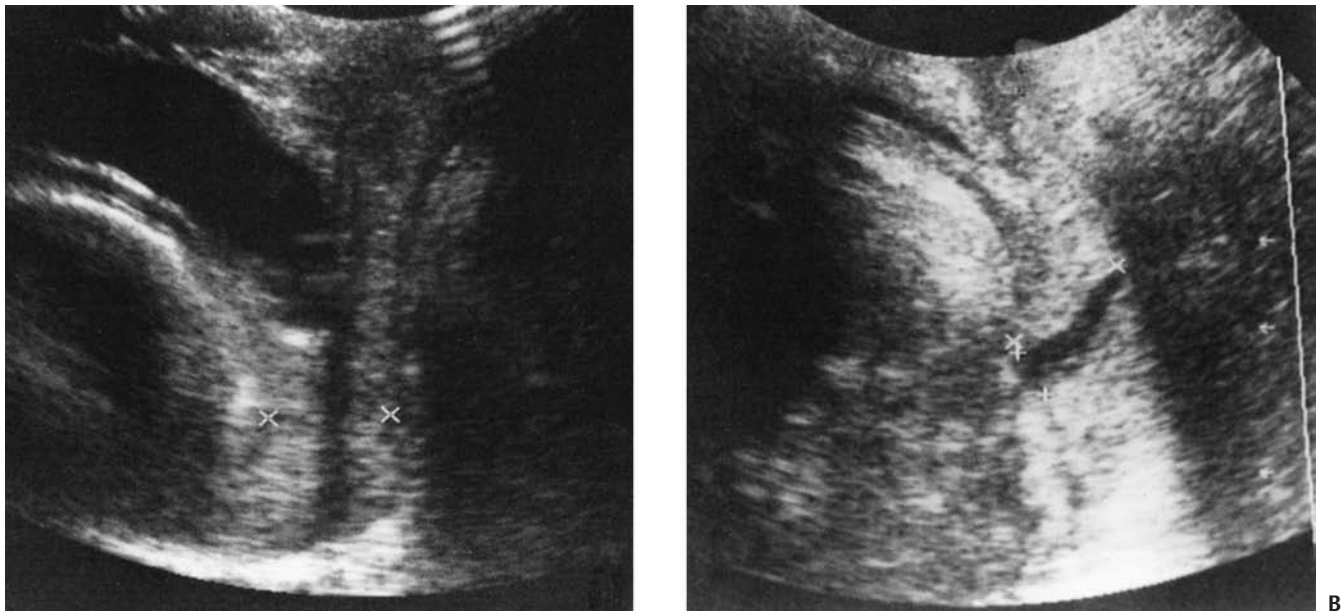

A B

Figure 11–2 Transperineal scan. **(A)** Calipers mark the internal and external os in a normal-appearing cervix. **(B)** In a different patient, ballooning membranes are present × measures length of open cervix; + meaures dilation.

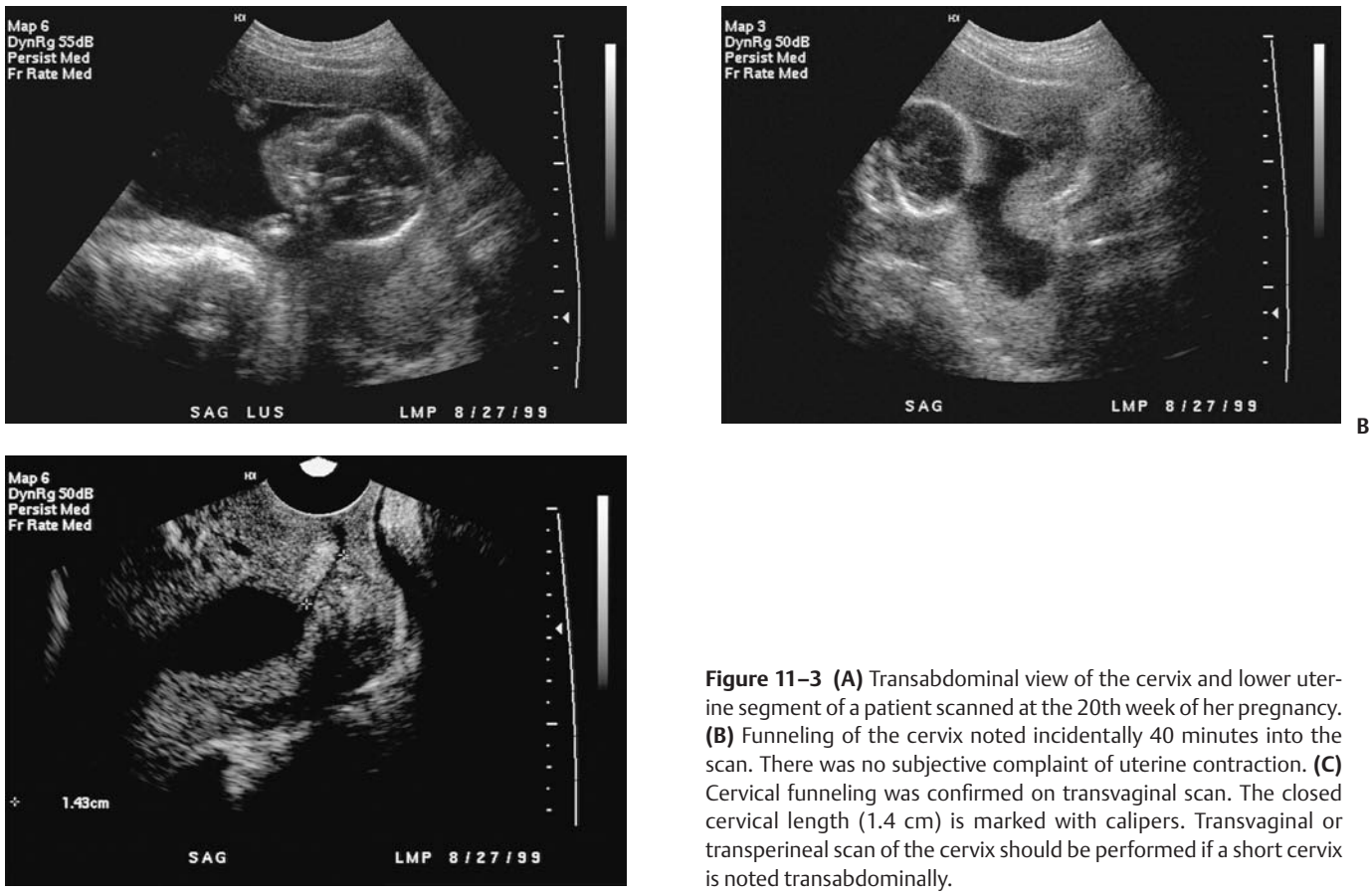

A B C

Figure 11–3 **(A)** Transabdominal view of the cervix and lower uterine segment of a patient scanned at the 20th week of her pregnancy. **(B)** Funneling of the cervix noted incidentally 40 minutes into the scan. There was no subjective complaint of uterine contraction. **(C)** Cervical funneling was confirmed on transvaginal scan. The closed cervical length (1.4 cm) is marked with calipers. Transvaginal or transperineal scan of the cervix should be performed if a short cervix is noted transabdominally.

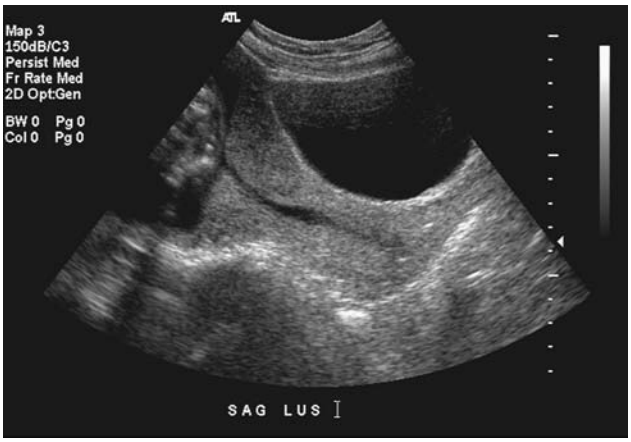

A

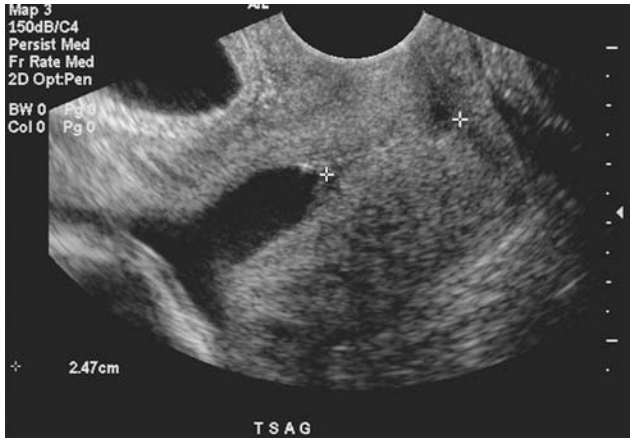

B

Figure 11–4 Pitfalls of overfull bladder and contraction at the lower uterine segment. **(A)** Compression of the cervix by a full bladder may give the impression of a long cervix. In this image there is also a contraction at the lower uterine segment that adds to the impression of a long cervix. The contraction can be recognized by the thickness of the myometrium in the anterior and posterior lower uterine segment. This can give the false appearance of funneling above a long closed cervix. **(B)** Cervical funneling was demonstrated by transvaginal scan with an emptied bladder a few minutes after the image in **(A)** was taken.

Ultrasound Evaluation

Technical Aspects

The transabdominal approach to scanning the cervix is less accurate than the transvaginal or transperineal approach because the cervix is poorly visualized when the maternal bladder is empty (**Fig. 11–3**).[8] However, overdistention of the bladder artificially increases the length of the cervix and can obscure the presence of a dilated cervix (**Fig. 11–4**). Maternal body habitus or a low fetal presenting part can also limit visualization of the cervix transabdominally. Because of the problems inherent with transabdominal scanning, imaging of the cervix is best performed with either a transperineal or a transvaginal approach.[9–11]

Transperineal scanning (**Fig. 11–2**) is performed with a 3.5 to 5 MHz sector probe. The probe should be covered by a condom or plastic wrap for hygienic reasons and infection control.[12] The probe is placed on the perineum, over the labia minora, and is aimed in the direction of the vaginal canal toward the cervix. Transperineal scanning is very operator-dependent. Pitfalls include obscuration of the cervix by rectal gas, shadowing by the pelvic bones, and inadequate visualization of the external os due to direct contact of the vaginal wall with the cervix. Hertzberg et al have shown that elevating the patient's hips and buttocks off the scanning table can improve cervical visualization in cases where routine transperineal views are inadequate.[13] Transperineal sonography has an advantage over transvaginal sonography in that the probe is not introduced into the vagina. Therefore, in patients with active bleeding or in whom ruptured membranes are suspected, transperineal scanning is our recommended approach. Additional benefits are that transperineal scanning is more comfortable for the patient than is transvaginal scanning and no artifact is produced by pressure exerted on the cervix.

A 5 to 10 MHz vaginal probe is used in transvaginal scanning of the cervix (**Fig. 11–1**). The probe should be disinfected prior to use and covered by a condom or probe cover. Latex allergy is present in some patients, and in those cases, a nonlatex condom or a nonlatex glove can be used to cover the probe. When using the transvaginal approach, care should be taken not to insert the probe abruptly or too deeply. The ultrasound monitor should be viewed in real time during insertion of the probe to avoid traumatizing prolapsed fetal membranes or a low placenta (**Fig. 11–5**).

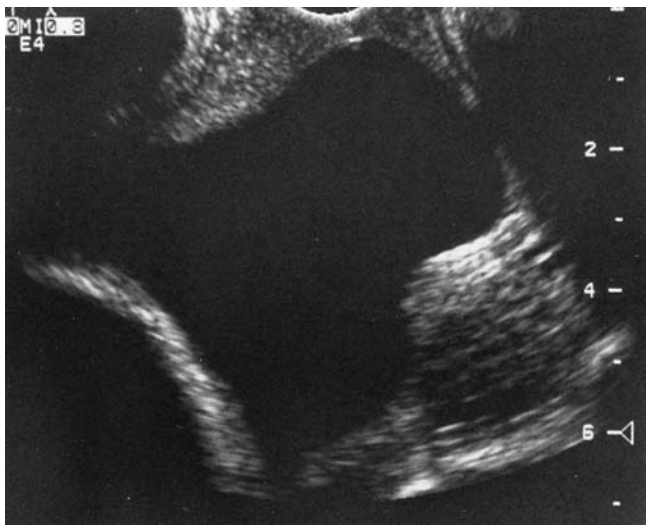

Figure 11–5 Ballooning membranes. When ballooning membranes are seen, the probe should not be inserted further into the vagina, but should be removed. The patient should be placed in Trendelenburg's position and transferred to labor and delivery.

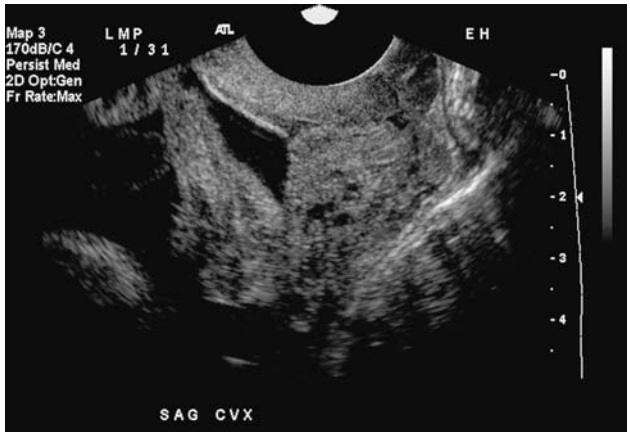

A

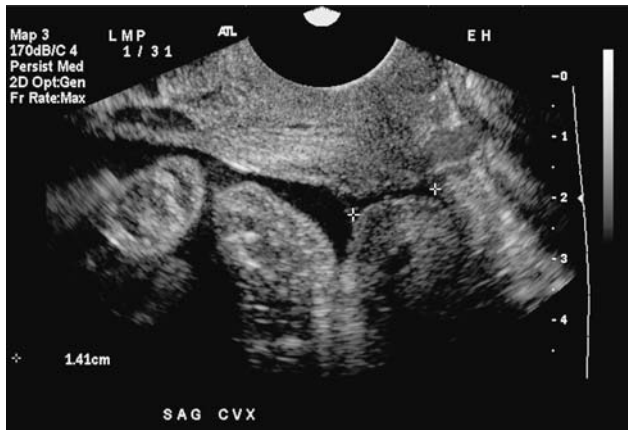

B

Figure 11–6 Pitfall in measuring cervical length. **(A)** Pressure was exerted on the cervix by the vaginal probe. Note the relatively thin anterior cervical lip when compared with the posterior lip. **(B)** Funneling of the internal os and a short cervix (calipers) were noted after the probe was withdrawn slightly to eliminate the pressure artifact.

The cervix should be identified and then the probe should be slightly withdrawn to obtain an accurate image of the internal os, external os, and cervical length (**Fig. 11–6**). The image of the cervix should meet the following criteria: (1) the internal os appears either flat or as an isosceles triangle, (2) the whole length of the cervical canal can be visualized, (3) a symmetric image of the external os can be obtained, and (4) the distance from the surface of the posterior lip to the cervical canal is equal to the distance from the anterior lip to the cervical canal.[14] The cervix should be observed for several minutes to detect dynamic change of the internal os and cervical length. Even patients with known placenta previa can be safely scanned with a transvaginal probe, although for patients with active bleeding we recommend the transperineal approach.

The cervical length is measured from the internal os to the external os. When the internal os is open, with funneling, only the closed portion of the cervix is measured. When funneling is present, the anteroposterior diameter (at the region of the presumed internal os) and length of the funnel (from the presumed internal os to the closed portion of the cervix) are also measured. A cervix that has prolapsing membranes into the cervical canal on ultrasound may still feel long and closed on clinical examination. The technical success of placing a cervical cerclage when there are prolapsing fetal membranes into the cervical canal is influenced by the clinical length of the cervix and the width and length of the canal dilation, and not just the functional length of the cervix. In addition, it is not clear how a 2-cm long cervix with a closed cervical canal behaves when compared with a 4-cm cervix with prolapsing membranes and a functional length of 2 cm. A complete description of the sonographic picture of the cervix, including the total length, the width of dilation of the internal os and along the cervical canal, and the remaining closed (functional) length conveys the entire appearance.[15]

The Cervix in Normal Pregnancy

It is difficult to distinguish the cervix from the lower uterine segment in the nonpregnant state and in the first trimester. By the second trimester, the growing amniotic sac provides a clear landmark for the internal cervical os. Cervical length measurements (defined as the distance between the internal and the external cervical os) have been shown to correlate well with digital examination of the cervix. Many authors suggest cervical sonography is superior to digital examination because the measurements are reproducible, the intraabdominal portion of the cervix can be measured, and the internal cervical os, where early changes from incompetent cervix and premature labor occur, can be assessed.[16–20] Sonography also has the theoretical advantage of less risk of infection and irritation of the cervix than digital examination.

Cervical length often measures over 5 cm in the first trimester,[21] but some of this length may reflect the inability to define clearly the upper cervix from the lower uterine segment. Most studies define a normal cervical length as 3 to 4 cm in midpregnancy.[22–24] In a study sponsored by the National Institute of Child Health and Human Development Network (NICHD), 2915 women with singleton pregnancies were studied by transvaginal cervical ultrasound examination at 22 to 24 weeks with follow-up examinations in 2531 patients at 26 to 28 weeks gestation. The mean cervical length was 3.52 cm in the first group and 3.37 cm in the second group.[25] The distribution of cervical lengths in the population followed a normal bell curve. At 24 weeks gestation, the 10th and 90th percentiles are 25 mm and 45 mm, respectively. Normal cervical length appears to be the same in nulliparous and multiparous women, and both exhibit shortening of the cervix as pregnancy progresses. Such normal shortening of the cervix

does not result in premature delivery.[26–29] It is therefore important to distinguish between the normal, expected rate of cervical shortening as compared with an accelerated rate of change that may result in premature delivery.

Patients carrying multiple gestations have significantly shorter cervical lengths than singleton pregnancies when matched for gestational age. Normograms of cervical length have been developed for twins.[30,31] In singleton pregnancies, cervical length usually remains above 4 cm through 37 weeks, whereas in twin pregnancies it is often less than 3 cm by 32 weeks.

The Role of Cervical Sonography in Premature Labor

The most commonly used sonographic parameters in the assessment of premature labor are cervical length, dilation of the cervix, and the appearance of the internal cervical os. The length of the cervix of patients who have a history of premature delivery might not be different from the general population when measured in the first trimester.[32–34] It is important to follow patients who are at risk for premature delivery. There is an inverse relationship between the sonographically measured length of the cervix at midpregnancy and the risk of preterm delivery. Most studies place the at-risk threshold at 2 to 3 cm.[35–38] The NICHD study demonstrated that a sonographically measured cervical length of less than 3.2 cm at 24 weeks gestation is associated with a sixfold increased risk of premature delivery before 35 weeks, and a cervical length of 1.2 cm at 24 weeks has a 14-fold risk of premature delivery. A transvaginally measured cervical length of less than 2 cm at 24 weeks has a sensitivity of 23% and a specificity of 97% for the prediction of preterm delivery. Cervical lengths measured sonographically at 24 weeks gestation of 3, 2.5, and 2 cm are associated with premature delivery in 9.3, 18, and 25%, respectively, of cases.[25] Combining the patients' obstetrical history and the cervical length measurement may increase the predictive value of the cervical sonography.

Some authors have proposed using a single transvaginal measurement of cervical length at midpregnancy to detect patients at risk for premature delivery.[39,40] However, the cost-effectiveness of such a program for the general population is questionable given the low prevalence of premature birth in the low–risk population.[41–43]

The inverse relationship between cervical length and the risk for premature labor also holds for multiple gestations.[43–50] Imseis et al in their study of twin pregnancies noted that a cervical length of 3.5 cm at 24 to 26 weeks predicts delivery at term in the majority of cases, whereas a mean cervical length of 2.7 cm is associated with either premature delivery or necessity for obstetrical intervention.[44]

In addition to cervical length, the appearance of the internal os is important in the assessment of preterm labor. The presence of funneling or wedging (dilation of the internal os with prolapse of fetal membranes into the cervical canal) is associated with preterm delivery. Ominous signs predicting preterm delivery include a funnel length of greater than 1.5 cm, a funnel width of greater than 1.4 cm, a residual cervical length of less than 2 cm, and funneling over 40% of the cervical length.[15] There are still controversies as to which of these is most important. Guzman et al maintain that cervical length has the highest predictive value.[52] Other studies, however, find that the internal cervical os dilation and the extent of the cervical funneling are equally important in predicting the group at risk for premature delivery.[53–55] Further research with standardized criteria for the description of cervical change will help evaluate the importance of these markers.

Recently, there has been interest in the use of fetal fibronectin,[56–59] prostaglandin,[60] and interleukin-6 and 8 assays[61] on swab specimens in combination with cervical sonography to identify patients at risk for premature labor and delivery. The most promising of such combined protocols found that a negative fetal fibronectin test on the vaginal swab and a cervical length of over 3 cm on ultrasound examination have a 97% negative predictive value for premature delivery in the subsequent 14 days.[59]

In addition to predicting preterm delivery, cervical sonography can be used to select patients who would benefit from the treatment of preterm contractions.[62–68] Premature labor is associated with a heavy economic cost and is one of the most overdiagnosed and overtreated medical conditions. Yet, it is important to diagnose and treat true premature labor to gain time to administer antenatal steroid treatment to promote fetal lung maturation and transport the pregnant woman to a tertiary care facility when necessary.

In patients with premature contractions, sonography of the cervix can be used to direct management. Rageth reported that patients require hospitalization and tocolytic therapy only when the cervical length measures less than 3 cm.[68] Fuchs et al studied 87 twin pregnancies that presented with premature labor and found that cervical length measurement helped in identifying patients at risk for premature delivery within 7 days.[68] He found that the shorter the cervical length, the higher the risk of premature delivery. None of a group of 21 patients with a cervical length of over 25 mm delivered within 7 days of observation.

Ultrasound and Other Findings for Causes of Premature Labor

Incompetent Cervix

Cervical incompetence is suspected if cervical shortening, cervical os dilation, and prolapsing fetal membranes into the cervical canal are found in a pregnant patient in the absence

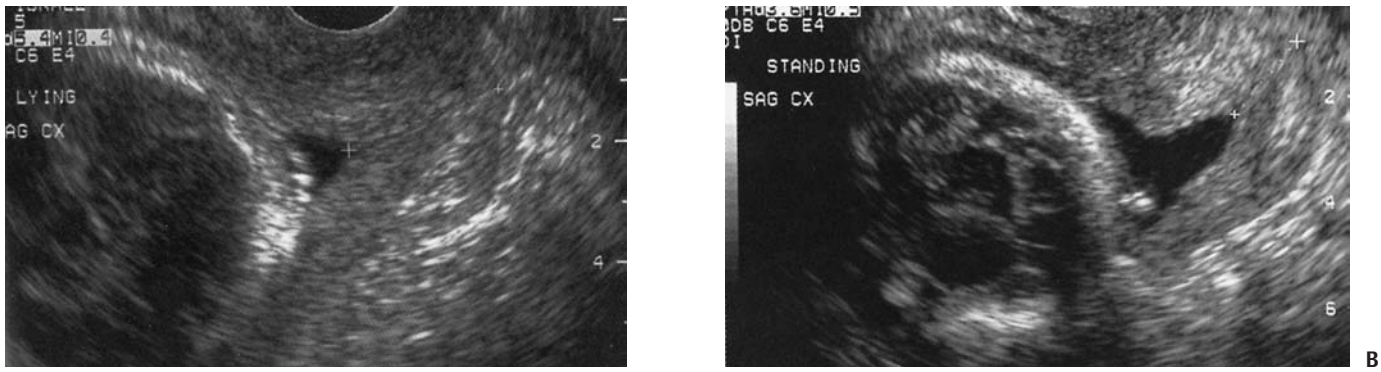

A B

Figure 11–7 Changing cervix in a patient with a history of second-trimester pregnancy loss. **(A)** In the supine exam, the closed cervical length was 2.9 cm with 7 mm of wedging of the internal os. **(B)** After standing for 15 minutes and being scanned upright, the patient's closed cervical length was 1.8 cm. The patient delivered at 33 weeks gestational age. (Reproduced with permission from Wong G, Levine D, Ludmir J. Maternal postural challenge as a functional test for cervical incompetence. J Ultrasound Med 1997;16:169–175.)

of uterine contractions. The findings can be made clinically or by ultrasound examination, but cervical sonography can detect those changes earlier.[69–73] Although the etiology of premature delivery is often multifactorial, incompetent cervix is felt to be the primary cause in 16% of premature births.[2] Risk factors such as diethylstilbestrol exposure in utero, cone biopsy of the cervix, and prior cervical laceration identify some of the patients at risk, but the diagnosis of cervical incompetence is often made on the basis of a history of midtrimester pregnancy loss associated with painless dilatation of the cervix. Often the patient cannot give an accurate description of the events surrounding a prior pregnancy loss. It is difficult to determine the initiating cause of preterm delivery when the patient has already embarked upon the final common pathway of premature labor, premature rupture of membranes, and chorioamnionitis. The identification of patients at risk for incompetent cervix is further made difficult because some patients with an incompetent cervix are nulliparous with no identifiable risk factors.

In the past, it was believed that the cervix was either competent or incompetent. However, recent studies have shown the cervical changes occur on a continuum.[73,74] The rate of cervical change may differ according to the underlying cause, but the change is often gradual and takes place over weeks. The initial site of change is at the internal cervical os. Iams reported that cervical length in the current pregnancy can be predicted by the gestational age at delivery of the previous preterm birth.[74] For women who previously had preterm delivery before 32 weeks, the association between cervical length and preterm birth holds true in subsequent pregnancies.[74] This leads to the hope that when cervical sonography detects either or both shortening of the cervix and development of membranes funneling at the internal os, timely intervention can be performed with improved perinatal outcome.

The timing of the initial examination and the frequency of follow-up examinations in patients with possible incompetent cervix have not been established. In patients

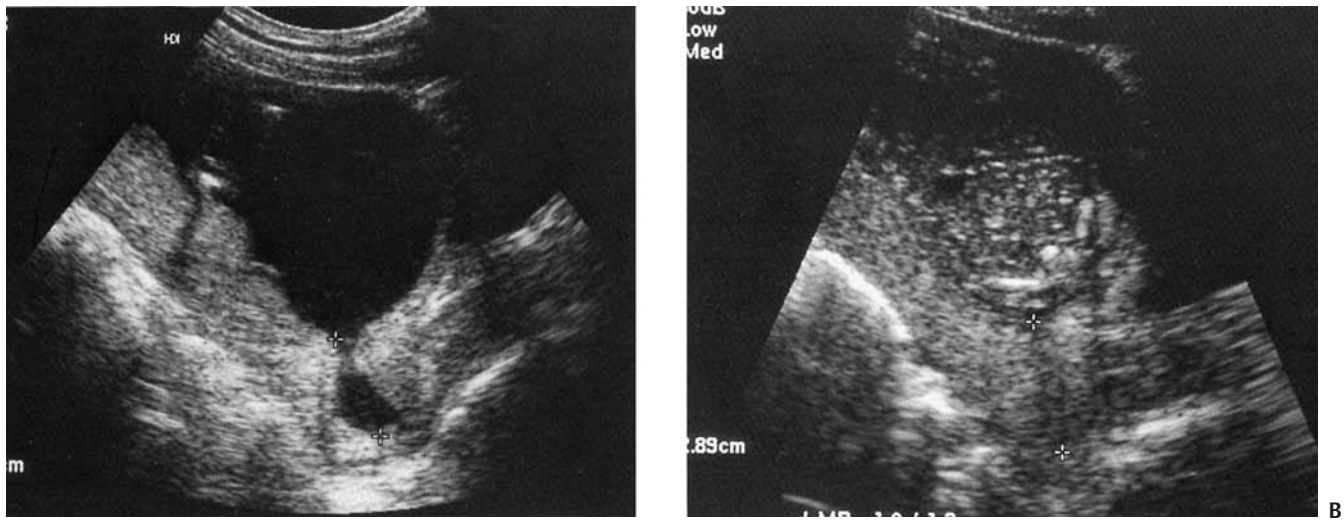

A B

Figure 11–8 Incompetent cervix. Transabdominal view of the cervix at 19 weeks gestational age in an otherwise asymptomatic patient. **(A)** The initial image demonstrates ballooning membranes. Calipers measure the open portion of the cervix. **(B)** Later in the examination, the cervix appeared normal. Calipers measure the apparent closed cervical length. We recommend that the initial image taken during routine obstetric sonography be the view of the cervix. This will help to identify cases of cervical incompetence that would otherwise escape detection.

with a history of pregnancy loss from an incompetent cervix, repeated loss usually occurs at the same gestational age or at an earlier gestational age. Therefore, in subsequent pregnancies, it is prudent to get an initial cervical scan to establish the baseline cervical length at a time before the gestational age at which the previous loss occurred. We recommend follow-up examinations every 1 to 2 weeks, depending on the findings of examinations and the clinical symptoms.

Conventional vaginal sonography to diagnose incompetent cervix will only detect a short cervix if cervical changes have taken place before the examination. Functional maneuvers, such as transfundal pressure,[75] straining,[76] or scanning the cervix with the patient standing[77,78] can elicit early cervical changes and identify patients at risk for incompetent cervix who otherwise would go undiagnosed. After a positive response is elicited from transfundal pressure, many patients have progressive cervical change 1 to 3 weeks later.[79] In a study by Wong et al, pregnant patients at 20 to 24 weeks gestation were examined in a standing position to study the effect of posture on the cervix, which may represent a more physiological reproduction of daily activity than transfundal pressure.[78] The standing position had no effect on the normal cervix, but patients with greater than 33% shortening in cervical length measured in the standing position after standing for 15 minutes were likely to deliver prematurely (**Fig. 11–7**). Patients who have a positive test on functional challenge may benefit from close follow up, reduced physical activity, and possibly cervical cerclage.

Because up to one third of patients with cervical incompetence are nulliparous with no identifiable risk factors, when routine obstetrical sonography is performed during the second trimester, it may be beneficial to obtain the view of the cervix at the beginning of the study rather than at the end (**Fig. 11–8**). This will be a transabdominal view with the limitations mentioned earlier; however, it can identify an unsuspected short cervix or dilated internal os in those low-risk patients. These early cervical views, obtained just after the patient has attained the supine position, may identify a short cervix that would no longer be apparent after the patient had been lying supine for 30 or more minutes during a routine obstetric scan.

A dynamic or spontaneously changing cervix has been noted during transvaginal scanning of the cervix (**Fig. 11–3**). Transient, but striking dilation of the internal cervical os and cervical canal occurs in the absence of subjective symptoms and objective signs of uterine contractions.[80,81] The etiology and mechanism of the dynamically changing cervix are not known. Because many patients with this finding deliver preterm, most patients with a changing cervix are advised to reduce their physical activities. The shorter the measurement of the cervix, the more likely the patient is to deliver preterm.

The treatment of patients at risk for premature delivery from incompetent cervix is controversial. While cervical cerclage is still a frequently performed obstetrical procedure, recent studies do not show significant benefit of prophylactic cerclage.[82,83] Because cerclage is a surgical procedure that can have iatrogenic complications, the currently suggested management approach for patients with an obstetrical history suspicious for cervical incompetence is to follow them closely with serial cervical sonography instead of placing a prophylactic cerclage.[84–86] It is also unclear at present what treatment is most effective when ultrasound examination detects changes in the cervix.[87–93] The length of prolongation of pregnancy in patients after cervical change is detected on ultrasound examination is similar between those getting cerclage placement versus those getting bed rest.[93] Sonography will continue to be important to monitor for progressive change in the cervix. If premature delivery becomes a distinct probability, the premature neonates would benefit by antenatal steroid treatment and receiving perinatal care at the appropriate clinical facilities. If cerclage placement is chosen as treatment, scans performed after the procedure are useful in assessing the result of the cerclage placement and in monitoring the cervical length and canal dilatation the portion of cervix above the cerclage (**Fig. 11–9, Fig. 11–10**).[94–98] Shortening of the

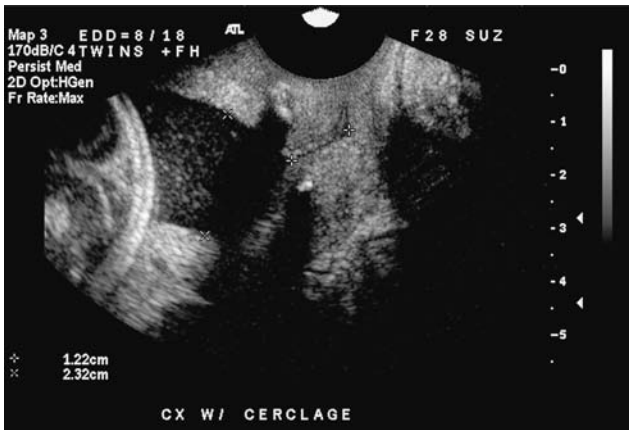

A

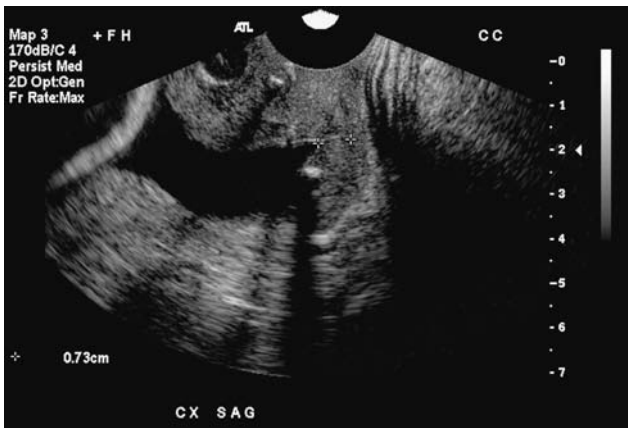

B

Figure 11–9 Cervical ultrasound is useful for following patients who have cerclage placement. **(A)** The cervix is funneled to and **(B)** through the cerclage. These changes in the cervix proximal to the cerclage may not be recognizable by clinical examination alone. Calipers low closed cervical length.

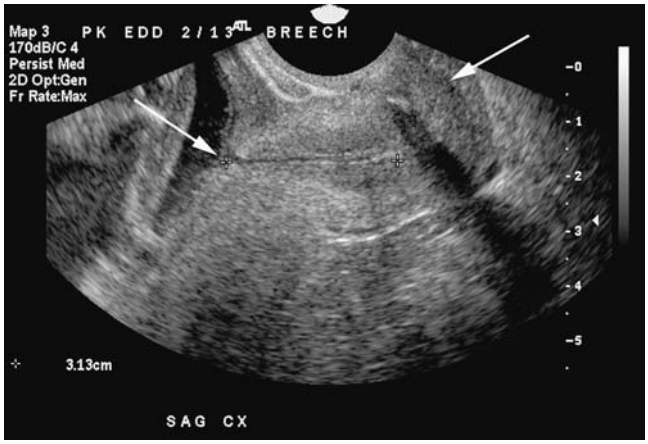

Figure 11–10 Pitfall in measuring cervical length. The suture used in cervical cerclage can create a shadow and obscure landmarks located beneath the suture. Note the true cervical length (arrows). The distal caliper was placed incorrectly at the time of the study because shadowing from the cerclage obscured the location of the external os, leading to undermeasurement of the cervical length.

proximal cervical length (less than 1 cm) is associated with an increased risk of preterm delivery.[98] Additional therapeutic maneuvers, such as bed rest or reduced physical activity, are important if there is either significant funneling above the cerclage or only a short portion of closed cervix remaining.

False-Positive Incompetent Cervix

False-positive findings of incompetent cervix can be caused by uterine contractions, improper probe placement, and overdistended bladder.[99–101] The narrowed lower uterine segment during a uterine contraction can mimic funneling of the cervix (**Fig. 11–3A**). The artifact can be recognized by the abnormally long cervix if measured from the purported internal os, and by the fact that the functional length is close to the length of a normal cervix. Often, the thickened myometrium associated with uterine contractions can also be visualized. This condition can be clarified by extending the period of observation until the contraction disappears, usually within 20 minutes. Compression of the lower uterine segment to produce an impression of funneling can also result from an overdistended urinary bladder (**Fig. 11–3A**). A transvaginal scan of the cervix largely eliminates this artifact. Nabothian cysts (**Fig. 11–11**) and vaginal cysts located near the internal cervical os can create the false impression of a dilated internal os.

Premature Rupture of Membranes

When premature rupture of fetal membranes occurs, expectant management is often pursued to gain time for further fetal maturation. Digital examination of the cervix is contraindicated because of the risk of infection. Speculum examination is often used to help make the diagnosis of rupture of membranes, but visualization of the cervix is not accurate in determining dilatation or effacement of the cervix. Cervical sonography is helpful in assessing cervical dilation and effacement when there is premature rupture of membranes.[102] It is also useful in excluding the presence of umbilical cord in the lower uterine segment or near the cervical opening. Transvaginal sonography has not been associated with increased risk of infection when used to assess the cervix after premature rupture of membranes.[103,104] However, until more studies are available to substantiate

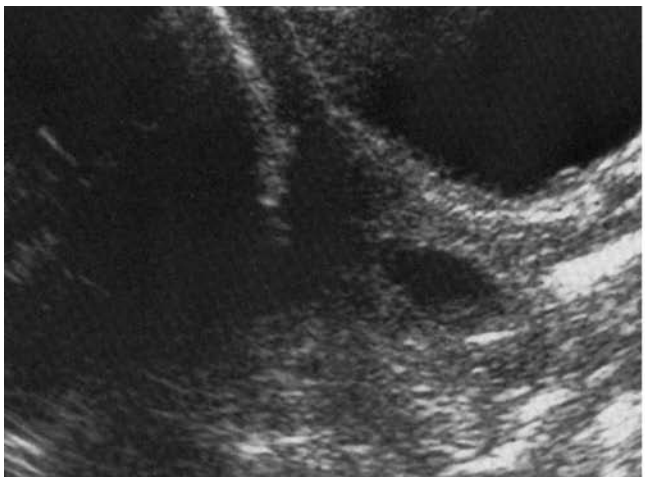
A

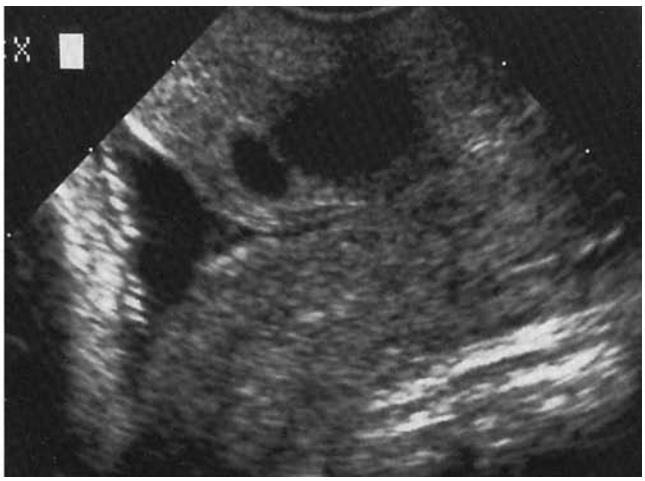
B

Figure 11–11 Nabothian cyst masquerading as funneling of the internal os. **(A)** Transabdominal view of the cervix shows an anechoic region suggestive of funneling of the internal os. This region is eccentric to the cervical canal. **(B)** Transvaginal scan shows two Nabothian cysts in the anterior cervix. A small amount of funneling of the internal os is present; however, this is not the region in question on the transabdominal scan. (Reproduced with permission from Wong G, Levine D. Sonographic assessment of the cervix in pregnancy. Semin Ultrasound CT MR 1998;19:370–380.)

the safety of the transvaginal approach, we prefer to use transperineal sonography to assess the cervix in such a setting.

Summary

Ultrasonography is an important diagnostic tool in assessment of the cervix during pregnancy. Cervical length, cervical dilation, and the status of the internal cervical os are all important prognosticators in premature labor and can be safely and accurately assessed by transvaginal and transperineal sonography. A short cervical length (less than 2 cm) and funneling of 40 to 50% of the length of the cervix places patients at high risk of premature delivery. Transvaginal sonography can also be used to diagnose and manage patients with incompetent cervix. Tests to provoke an incompetent cervix (such as transfundal pressure or scanning with the patient upright) help detect incompetent cervix even earlier in asymptomatic patients. It is hoped that early identification of these at-risk patients will lead to more effective treatment, resulting in a decrease in perinatal morbidity and mortality.

References

1. Berkowitz G, Papiernik K. Epidemiology or preterm birth. Epidemiol Res 1993;15:141–143
2. Roberts WE, Morrison JC, Hamer C, Wiser WL. The incidence of preterm labor and specific risk factors. Obstet Gynecol 1990;76 (Suppl 1):85S–89S
3. Martin JA, Hamilton BE, Ventura SJ, Menacker F, Park MM, Sutton PD. Births: final data for 2001. Natl Vital Stat Rep 2002;51:1–102
4. Centers for Disease Control and Prevention. Contribution of assisted reproductive technology and ovulation-inducing drugs to triplet and higher-order multiple births–United States, 1980–1997. MMWR Morb Mortal Wkly Rep 2000;49:535– 538
5. Effer SB, Moutquin JM, Farine D, et al. Neonatal survival rates in 860 singleton live births at 24 and 25 weeks gestational age: a Canadian multicentre study. BJOG 2002;109:740–745
6. Rogowski J. The economics of preterm deliveries. Prenat Neonat Med 1998;3:16–20
7. Wood NS, Marlow N, Costeloe K, Gibson AT, Wilkinson AR. Neurologic and developmental disability after extremely preterm birth. EPICure Study Group. N Engl J Med 2000;343:378–384
8. Wong G, Levine D. Sonographic assessment of the cervix in pregnancy. Semin Ultrasound CT MR 1998;19:370–380
9. Kurtzman JT, Goldsmith LJ, Gall SA, Spinnato JA. Transvaginal versus transperineal ultrasonography: a blinded comparison in the assessment of cervical length at midgestation. Am J Obstet Gynecol 1998;179:852–857
10. Cicero S, Skentou C, Souka A, To MS, Nicolaides KH. Cervical length at 22–24 weeks of gestation: comparison of transvaginal and transperineal-translabial ultrasonography. Ultrasound Obstet Gynecol 2001;17:335–340
11. Yazici G, Yildiz A, Tiras MB, Arslan M, Kanik A, Oz U. Comparison of transperineal and transvaginal sonography in predicting preterm delivery. J Clin Ultrasound 2004;32:225–230
12. Laing FC, Ryan T, Hadley K, Jeffrey RB, Wing VW. Plastic wrap for US transducer sterility or sanitization. Radiology 1986;160: 846
13. Hertzberg BS, Kliewer MA, Baumeister LA, McNally PB, Fazekas CK. Optimizing transperineal sonographic imaging of the cervix: the hip elevation technique. J Ultrasound Med 1994;13:933–936; quiz 1009–1010
14. Burger M, Weber-Rossler T, Willmann M. Measurement of the pregnant cervix by transvaginal sonography: an interobserver study and new standards to improve the interobserver variability. Ultrasound Obstet Gynecol 1997;9:188–193
15. Berghella V, Kuhlman K, Weiner S, Texeira L, Wapner RJ. Cervical funneling: sonographic criteria predictive of preterm delivery. Ultrasound Obstet Gynecol 1997;10:161–166
16. Sonek JD, Iams JD, Blumenfeld M, Johnson F, Landon M, Gabbe S. Measurement of cervical length in pregnancy: comparison between vaginal ultrasonography and digital examination. Obstet Gynecol 1990;76:172–175
17. Mahony BS, Nyberg DA, Luthy DA, Hirsch JH, Hickok DE, Petty CN. Translabial ultrasound of the third-trimester uterine cervix: correlation with digital examination. J Ultrasound Med 1990;9:717–723
18. Gomez R, Galasso M, Romero R, et al. Ultrasonographic examination of the uterine cervix is better than cervical digital examination as a predictor of the likelihood of premature delivery in patients with preterm labor and intact membranes. Am J Obstet Gynecol 1994;171:956–964
19. Berghella V, Tolosa JE, Kuhlman K, Weiner S, Bolognese RJ, Wapner RJ. Cervical ultrasonography compared with manual examination as a predictor of preterm delivery. Am J Obstet Gynecol 1997;177:723–730
20. Goldberg J, Newman RB, Rust PF. Interobserver reliability of digital and endovaginal ultrasonographic cervical length measurements. Am J Obstet Gynecol 1997;177:853–858
21. Ayers JW, DeGrood RM, Compton AA, Barclay M, Ansbacher R. Sonographic evaluation of cervical length in pregnancy: diagnosis and management of preterm cervical effacement in patients at risk for premature delivery. Obstet Gynecol 1988;71(6 Pt 1):939–944
22. Andersen HF. Transvaginal and transabdominal ultrasonography of the uterine cervix during pregnancy. J Clin Ultrasound 1991; 19:77–83
23. Brown JE, Thieme GA, Shah DM, Fleischer AC, Boehm FH. Transabdominal and transvaginal endosonography: evaluation of the cervix and lower uterine segment in pregnancy. Am J Obstet Gynecol 1986;155:721–726
24. Smith CV, Anderson JC, Matamoros A, Rayburn WF. Transvaginal sonography of cervical width and length during pregnancy. J Ultrasound Med 1992;11:465–467
25. Iams JD, Goldenberg RL, Meis PJ, et al. The length of the cervix and the risk of spontaneous premature delivery. National Institute of Child Health and Human Development Maternal Fetal Medicine Unit Network. N Engl J Med 1996;334:567–572
26. Zorzoli A, Soliani A, Perra M, Caravelli E, Galimberti A, Nicolini U. Cervical changes throughout pregnancy as assessed by transvaginal sonography. Obstet Gynecol 1994;84:960–964
27. Cook CM, Ellwood DA. A longitudinal study of the cervix in pregnancy using transvaginal ultrasound. Br J Obstet Gynaecol 1996; 103:16–18
28. Kushnir O, Vigil DA, Izquierdo L, Schiff M, Curet LB. Vaginal ultrasonographic assessment of cervical length changes during normal pregnancy. Am J Obstet Gynecol 1990;162:991–993
29. Gramellini D, Fieni S, Molina E, Berretta R, Vadora E. Transvaginal sonographic cervical length changes during normal pregnancy. J Ultrasound Med 2002;21:227–232; quiz 234–225

30. Kushnir O, Izquierdo LA, Smith JF, Blankstein J, Curet LB. Transvaginal sonographic measurement of cervical length: evaluation of twin pregnancies. J Reprod Med 1995;40:380–382
31. Eppel W, Schurz B, Frigo P, et al. Vaginal sonography of the cervix in twin pregnancies [in German]. Geburtshilfe Frauenheilkd 1994;54:20–26
32. Carvalho MH, Bittar RE, Brizot ML, Maganha PP, Borges da Fonseca ES, Zugaib M. Cervical length at 11–14 weeks' and 22–24 weeks' gestation evaluated by transvaginal sonography, and gestational age at delivery. Ultrasound Obstet Gynecol 2003;21:135–139
33. Conoscenti G, Meir YJ, D'Ottavio G, et al. Does cervical length at 13–15 weeks' gestation predict preterm delivery in an unselected population? Ultrasound Obstet Gynecol 2003;21:128–134
34. Yost NP, Owen J, Berghella V, et al. Number and gestational age of prior preterm births does not modify the predictive value of a short cervix. Am J Obstet Gynecol 2004;191:241–246
35. Andersen HF, Nugent CE, Wanty SD, Hayashi RH. Prediction of risk for preterm delivery by ultrasonographic measurement of cervical length. Am J Obstet Gynecol 1990;163:859–867
36. Okitsu O, Mimura T, Nakayama T, Aono T. Early prediction of preterm delivery by transvaginal ultrasonography. Ultrasound Obstet Gynecol 1992;2:402–409
37. Tongsong T, Kamprapanth P, Srisomboon J, Wanapirak C, Piyamongkol W, Sirichotiyakul S. Single transvaginal sonographic measurement of cervical length early in the third trimester as a predictor of preterm delivery. Obstet Gynecol 1995;86:184–187
38. Timor-Tritsch IE, Boozarjomehri F, Masakowski Y, Monteagudo A, Chao CR. Can a "snapshot" sagittal view of the cervix by transvaginal ultrasonography predict active preterm labor? Am J Obstet Gynecol 1996;174:990–995
39. Owen J, Yost N, Berghella V, et al. Mid-trimester endovaginal sonography in women at high risk for spontaneous preterm birth. JAMA 2001;286:1340–1348
40. Owen J, Yost N, Berghella V, et al. Can shortened midtrimester cervical length predict very early spontaneous preterm birth? Am J Obstet Gynecol 2004;191:298–303
41. To MS, Skentou C, Cicero S, Nicolaides KH. Cervical assessment at the routine 23-weeks' scan: problems with transabdominal sonography. Ultrasound Obstet Gynecol 2000;15:292–296
42. Rozenberg P, Gillet A, Ville Y. Transvaginal sonographic examination of the cervix in asymptomatic pregnant women: review of the literature. Ultrasound Obstet Gynecol 2002;19:302–311
43. Hoesli I, Tercanli S, Holzgreve W. Cervical length assessment by ultrasound as a predictor of preterm labour: is there a role for routine screening? BJOG 2003;110(Suppl 20):61–65
44. Imseis HM, Albert TA, Iams JD. Identifying twin gestations at low risk for preterm birth with a transvaginal ultrasonographic cervical measurement at 24 to 26 weeks' gestation. Am J Obstet Gynecol 1997;177:1149–1155
45. Crane JM, Van den Hof M, Armson BA, Liston R. Transvaginal ultrasound in the prediction of preterm delivery: singleton and twin gestations. Obstet Gynecol 1997;90:357–363
46. To MS, Skentou C, Cicero S, Liao AW, Nicolaides KH. Cervical length at 23 weeks in triplets: prediction of spontaneous preterm delivery. Ultrasound Obstet Gynecol 2000;16:515–518
47. Ramin KD, Ogburn PL Jr, Mulholland TA, Breckle RJ, Ramsey PS. Ultrasonographic assessment of cervical length in triplet pregnancies. Am J Obstet Gynecol 1999;180(6 Pt 1):1442–1445
48. Guzman ER, Walters C, O'Reilly-Green C, et al. Use of cervical ultrasonography in prediction of spontaneous preterm birth in twin gestations. Am J Obstet Gynecol 2000;183:1103–1107
49. Guzman ER, Walters C, O'Reilly-Green C, et al. Use of cervical ultrasonography in prediction of spontaneous preterm birth in triplet gestations. Am J Obstet Gynecol 2000;183:1108–1113
50. Skentou C, Souka AP, To MS, Liao AW, Nicolaides KH. Prediction of preterm delivery in twins by cervical assessment at 23 weeks. Ultrasound Obstet Gynecol 2001;17:7–10
51. Souka AP, Heath V, Flint S, Sevastopoulou I, Nicolaides KH. Cervical length at 23 weeks in twins in predicting spontaneous preterm delivery. Obstet Gynecol 1999;94:450–454
52. Guzman ER, Walters C, Ananth CV, et al. A comparison of sonographic cervical parameters in predicting spontaneous preterm birth in high-risk singleton gestations. Ultrasound Obstet Gynecol 2001;18:204–210
53. Benham BN, Balducci J, Atlas RO, Rust OA. Risk factors for preterm delivery in patients demonstrating sonographic evidence of premature dilation of the internal os, prolapse of the membranes in the endocervical canal and shortening of the distal cervical segment by second trimester ultrasound. Aust N Z J Obstet Gynaecol 2002;42:46–50
54. Honest H, Bachmann LM, Coomarasamy A, Gupta JK, Kleijnen J, Khan KS. Accuracy of cervical transvaginal sonography in predicting preterm birth: a systematic review. Ultrasound Obstet Gynecol 2003;22:305–322
55. Yost NP, Owen J, Berghella V, et al. Second-trimester cervical sonography: features other than cervical length to predict spontaneous preterm birth. Obstet Gynecol 2004;103:457–462
56. Rizzo G, Capponi A, Arduini D, Lorido C, Romanini C. The value of fetal fibronectin in cervical and vaginal secretions and of ultrasonographic examination of the uterine cervix in predicting premature delivery for patients with preterm labor and intact membranes. Am J Obstet Gynecol 1996;175:1146–1151
57. Rozenberg P, Goffinet F, Malagrida L, et al. Evaluating the risk of preterm delivery: a comparison of fetal fibronectin and transvaginal ultrasonographic measurement of cervical length. Am J Obstet Gynecol 1997;176(1 Pt 1):196–199
58. Iams JD, Casal D, McGregor JA, et al. Fetal fibronectin improves the accuracy of diagnosis of preterm labor. Am J Obstet Gynecol 1995;173:141–145
59. Iams JD. Prediction and early detection of preterm labor. Obstet Gynecol 2003;101:402–412
60. Vavra N, Eppel W, Sevelda P, et al. Serum prostaglandin F2 alpha (PGFM) and oxytocin levels correlate with sonographic changes in the cervix in patients with preterm labor. Arch Gynecol Obstet 1993;253:33–36
61. Kurkinen-Raty M, Ruokonen A, Vuopala S, et al. Combination of cervical interleukin-6 and -8, phosphorylated insulin-like growth factor-binding protein-1 and transvaginal cervical ultrasonography in assessment of the risk of preterm birth. BJOG 2001;108:875–881
62. Bartolucci L, Hill WC, Katz M, Gill PJ, Kitzmiller JL. Ultrasonography in preterm labor. Am J Obstet Gynecol 1984;149:52–56
63. Iams JD, Paraskos J, Landon MB, Teteris JN, Johnson FF. Cervical sonography in preterm labor. Obstet Gynecol 1994;84:40–46
64. Murakawa H, Utumi T, Hasegawa I, Tanaka K, Fuzimori R. Evaluation of threatened preterm delivery by transvaginal ultrasonographic measurement of cervical length. Obstet Gynecol 1993;82:829–832
65. Rageth JC, Kernen B, Saurenmann E, Unger C. Premature contractions: possible influence of sonographic measurement of cervical

length on clinical management. Ultrasound Obstet Gynecol 1997; 9:183–187
66. Tsoi E, Akmal S, Rane S, Otigbah C, Nicolaides KH. Ultrasound assessment of cervical length in threatened preterm labor. Ultrasound Obstet Gynecol 2003;21:552–555
67. Fuchs IB, Henrich W, Osthues K, Dudenhausen JW. Sonographic cervical length in singleton pregnancies with intact membranes presenting with threatened preterm labor. Ultrasound Obstet Gynecol 2004;24:554–557
68. Fuchs I, Tsoi E, Henrich W, Dudenhausen JW, Nicolaides KH. Sonographic measurement of cervical length in twin pregnancies in threatened preterm labor. Ultrasound Obstet Gynecol 2004;23: 42–45
69. Brook I, Feingold M, Schwartz A, Zakut H. Ultrasonography in the diagnosis of cervical incompetence in pregnancy: a new diagnostic approach. Br J Obstet Gynaecol 1981;88:640–643
70. Jackson G, Pendleton HJ, Nichol B, Wittmann BK. Diagnostic ultrasound in the assessment of patients with incompetent cervix. Br J Obstet Gynaecol 1984;91:232–236
71. Michaels WH, Schreiber FR, Padgett RJ, Ager J, Pieper D. Ultrasound surveillance of the cervix in twin gestations: management of cervical incompetency. Obstet Gynecol 1991;78(5 Pt 1): 739–744
72. Macdonald R, Smith P, Vyas S. Cervical incompetence: the use of transvaginal sonography to provide an objective diagnosis. Ultrasound Obstet Gynecol 2001;18:211–216
73. Owen J, Iams JD, Hauth JC. Vaginal sonography and cervical incompetence. Am J Obstet Gynecol 2003;188:586–596
74. Iams JD, Johnson FF, Sonek J, Sachs L, Gebauer C, Samuels P. Cervical competence as a continuum: a study of ultrasonographic cervical length and obstetric performance. Am J Obstet Gynecol 1995;172(4 Pt 1):1097–1103 discussion 1104–1096
75. Althuisius SM, Dekker GA, van Geijn HP. Cervical incompetence: a reappraisal of an obstetric controversy. Obstet Gynecol Surv 2002;57:377–387
76. Guzman ER, Rosenberg JC, Houlihan C, Ivan J, Waldron R, Knuppel R. A new method using vaginal ultrasound and transfundal pressure to evaluate the asymptomatic incompetent cervix. Obstet Gynecol 1994;83:248–252
77. Sherif LS, Shalan HM. Detection of pregnant women at risk of cervical incompetence by transvaginal sonography during straining. J Obstet Gynaecol Res 1997;23:353–357
78. Wong G, Levine D, Ludmir J. Maternal postural challenge as a functional test for cervical incompetence. J Ultrasound Med 1997;16:169–175
79. Guzman ER, Vintzileos AM, McLean DA, Martins ME, Benito CW, Hanley ML. The natural history of a positive response to transfundal pressure in women at risk for cervical incompetence. Am J Obstet Gynecol 1997;176:634–638
80. Parulekar SG, Kiwi R. Dynamic incompetent cervix uteri: sonographic observations. J Ultrasound Med 1988;7:481–485
81. Hertzberg BS, Kliewer MA, Farrell TA, DeLong DM. Spontaneously changing gravid cervix: clinical implications and prognostic features. Radiology 1995;196:721–724
82. Althuisius SM, Dekker GA, van Geijn HP, Bekedam DJ, Hummel P. Cervical incompetence prevention randomized cerclage trial (CIPRACT): study design and preliminary results. Am J Obstet Gynecol 2000;183:823–829
83. Drakeley AJ, Roberts D, Alfirevic Z. Cervical cerclage for prevention of preterm delivery: meta-analysis of randomized trials. Obstet Gynecol 2003;102:621–627
84. Kelly S, Pollock M, Maas B, Lefebvre C, Manley J, Sciscione A. Early transvaginal ultrasonography versus early cerclage in women with an unclear history of incompetent cervix. Am J Obstet Gynecol 2001;184:1097–1099
85. Berghella V, Haas S, Chervoneva I, Hyslop T. Patients with prior second-trimester loss: prophylactic cerclage or serial transvaginal sonograms? Am J Obstet Gynecol 2002;187:747–751
86. Groom KM, Bennett PR, Golara M, Thalon A, Shennan AH. Elective cervical cerclage versus serial ultrasound surveillance of cervical length in a population at high risk for preterm delivery. Eur J Obstet Gynecol Reprod Biol 2004;112:158–161
87. To MS, Alfirevic Z, Heath VC, et al. Cervical cerclage for prevention of preterm delivery in women with short cervix: randomised controlled trial. Lancet 2004;363:1849–1853
88. Berghella V, Daly SF, Tolosa JE, et al. Prediction of preterm delivery with transvaginal ultrasonography of the cervix in patients with high-risk pregnancies: does cerclage prevent prematurity? Am J Obstet Gynecol 1999;181:809–815
89. Rust OA, Atlas RO, Reed J, van Gaalen J, Balducci J. Revisiting the short cervix detected by transvaginal ultrasound in the second trimester: why cerclage therapy may not help. Am J Obstet Gynecol 2001;185:1098–1105
90. Berghella V, Odibo AO, Tolosa JE. Cerclage for prevention of preterm birth in women with a short cervix found on transvaginal ultrasound examination: a randomized trial. Am J Obstet Gynecol 2004;191:1311–1317
91. Belej-Rak T, Okun N, Windrim R, Ross S, Hannah ME. Effectiveness of cervical cerclage for a sonographically shortened cervix: a systematic review and meta-analysis. Am J Obstet Gynecol 2003;189:1679–1687
92. Rust OA, Atlas RO, Jones KJ, Benham BN, Balducci J. A randomized trial of cerclage versus no cerclage among patients with ultrasonographically detected second-trimester preterm dilatation of the internal os. Am J Obstet Gynecol 2000;183:830–835
93. Althuisius SM, Dekker GA, Hummel P, Bekedam DJ, van Geijn HP. Final results of the Cervical Incompetence Prevention Randomized Cerclage Trial (CIPRACT): therapeutic cerclage with bed rest versus bed rest alone. Am J Obstet Gynecol 2001;185:1106–1112
94. Andersen HF, Karimi A, Sakala EP, Kalugdan R. Prediction of cervical cerclage outcome by endovaginal ultrasonography. Am J Obstet Gynecol 1994;171:1102–1106
95. Fox R, Holmes R, James M, Tuohy J, Wardle P. Serial transvaginal ultrasonography following McDonald cerclage and repeat suture insertion. Aust N Z J Obstet Gynaecol 1998;38:27–30
96. Parulekar SG, Kiwi R. Ultrasound evaluation of sutures following cervical cerclage for incompetent cervix uteri. J Ultrasound Med 1982;1:223–228
97. Rana J, Davis SE, Harrigan JT. Improving the outcome of cervical cerclage by sonographic follow-up. J Ultrasound Med 1990;9: 275–278
98. O'Brien JM, Hill AL, Barton JR. Funneling to the stitch: an informative ultrasonographic finding after cervical cerclage. Ultrasound Obstet Gynecol 2002;20:252–255
99. Confino E, Mayden KL, Giglia RV, Vermesh M, Gleicher N. Pitfalls in sonographic imaging of the incompetent uterine cervix. Acta Obstet Gynecol Scand 1986;65:593–597
100. Karis JP, Hertzberg BS, Bowie JD. Sonographic diagnosis of premature cervical dilatation: potential pitfall due to lower uterine segment contractions. J Ultrasound Med 1991;10:83–87
101. Yost NP, Bloom SL, Twickler DM, Leveno KJ. Pitfalls in ultrasonic cervical length measurement for predicting preterm birth. Obstet Gynecol 1999;93:510–516

102. Rizzo G, Capponi A, Angelini E, Vlachopoulou A, Grassi C, Romanini C. The value of transvaginal ultrasonographic examination of the uterine cervix in predicting preterm delivery in patients with preterm premature rupture of membranes. Ultrasound Obstet Gynecol 1998;11:23–29
103. Krebs-Jimenez J, Neubert AG. The microbiological effects of endovaginal sonographic assessment of cervical length. J Ultrasound Med 2002;21:727–729
104. Carlan SJ, Richmond LB, O'Brien WF. Randomized trial of endovaginal ultrasound in preterm premature rupture of membranes. Obstet Gynecol 1997;89:458–461

12 Estimating Fetal Gestational Age

Chaitali Shah and Ashok Bhanushali

The gestational age assignment to a pregnancy is needed subsequent to evaluation to assess the fetal anatomy and growth, interpret the various screening tests, and predict the expected delivery date.

There are various ways of calculating the fetal gestational age, including menstrual history, clinical examination, and ultrasound.[1–3] Of these three, ultrasound is superior for dating a pregnancy.[3] The menstrual age is calculated from the first day of the last menstrual period. The conceptual age is calculated from ovulation. The gestational age is calculated from the theoretical time of ovulation, plus 2 weeks. In addition to estimating fetal gestational age, fetal biometry is used to detect problems related to growth disturbances, such as intrauterine growth retardation, macrosomia, and microcephaly. The other advantages of fetal biometry are the early diagnosis of malformations (e.g., the measurement of long bones in skeletal dysplasias)[4] and detection of patients at risk for aneuploidy (fetal nuchal translucency).[5]

Calculations based on fetal measurements are also used to determine growth and weight. Ultimately, assessment of fetal biometry is important for decreasing the perinatal morbidity and mortality.

Perameters Used in Fetal Biometry to Determine Gestational Age

The assessment of gestational age and fetal growth is based on different parameters, which are described in this chapter. In all the tables outlined, the gestational age is expressed in weeks and days from the (theoretical) onset of the last menstrual period (conception date minus 14 days).[2]

There are many well-established charts that have been in use for a long time; however, marked differences between populations sometimes force researchers to build new nomograms for the different races.[6]

Mean Gestational Sac Diameter

This parameter is useful in the early stages of pregnancy when the fetal pole or the embryo is still not identifiable on ultrasound. This can be as early as 5 weeks by transvaginal examination and 6 weeks by transabdominal exam. In the setting of an ectopic gestation, a pseudogestational sac may mimic a true sac. Therefore, in the absence of a definite fetal pole or yolk sac, caution should be taken in labeling a true sac as such. A normal gestational sac can be confidently diagnosed when its hyperechoic rim is thick (> 2 mm) and its shape is round or oval without unusual angulation. The mean gestational sac diameter is measured inside its hyperechoic rim. If the sac is round, only one measurement is needed. More commonly, when it is oval, three orthogonal (perpendicular) measurements of the sac are taken and averaged. Gestational age is estimated based on the mean sac diameter (**Table 12–1**). According to one study by Muller et al, three-dimensional volumetric scans

Table 12–1 Mean Diameter of Gestational Sac and Corresponding Estimate of Gestational Age

Mean Sac Diameter (mm)	Gestation in Weeks (Mean)
2	5.0
3	5.1
4	5.2
5	5.4
6	5.5
7	5.6
8	5.7
9	5.9
10	6.0
11	6.1
12	6.2
13	6.4
14	6.5
15	6.6
16	6.7
17	6.9
18	7.0
19	7.1
20	7.3
21	7.4
22	7.5
23	7.6
24	7.8
25	7.9
26	8.0
27	8.1
28	8.3
29	8.4
30	8.5

The mean gestational age was calculated from a regression equation. Reported range: ± 0.1 week at 2 SD.

From Alfred B. Kurtz. Estimating gestational age. In: Bluth EI, Arger PH, Benson CB, Ralls PW, and Siegel MJ, eds. *Ultrasound: A Practical Approach to Clinical Problems*. New York: Thieme Medical Publishers; 2000. Reproduced with permission.

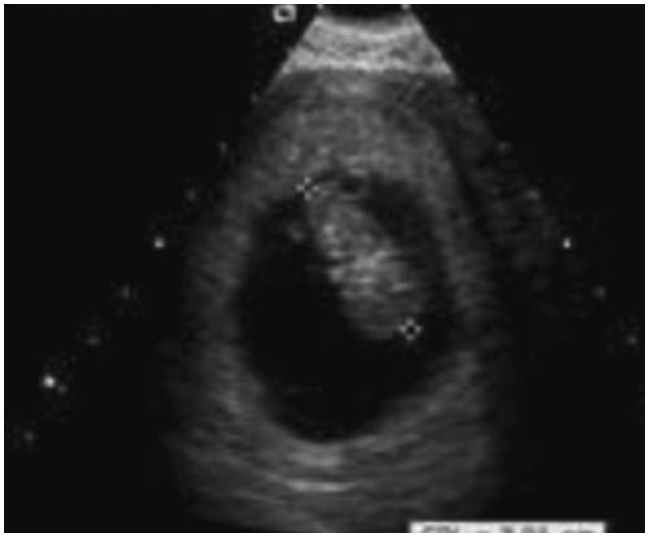

Figure 12–1 Scan demonstrating the crown–rump length measurement.

are more accurate than two-dimensional scans in obtaining the gestational sac volume, but have shown to be of no prognostic significance for gestational outcome.[7]

Crown–Rump Length

The crown–rump length (CRL) is the longest demonstrable length of the embryo, excluding the limbs and yolk sac.[8] The CRL is the most accurate indicator of the gestational age throughout the first trimester because, early in the pregnancy, the CRL has a rapid linear growth acceleration curve, and, at this stage, the growth of the embryo is minimally affected by various pathologies.

The CRL is measured from the outer edge of the cephalic pole to the outer edge of the fetal rump. One must be careful not to include the yolk sac in the measurement[9] (**Fig. 12–1**).

The CRL can be used to assess the gestational age between 6 and 14 weeks (**Table 12–2**). Its best accuracy is

Table 12–2 Assessment of the Gestational Age from the Crown–Rump Length

Mean Sac Diameter (mm)	Mean	Mean Sac Diameter (mm)	Mean	Mean Sac Diameter (mm)	Mean
2	5.7	29	9.7	56	12.2
3	5.9	30	9.9	57	12.3
4	6.1	31	10.0	58	12.3
5	6.2	32	10.1	59	12.4
6	6.4	33	10.2	60	12.5
7	6.6	34	10.3	61	12.6
8	6.7	35	10.4	62	12.6
9	6.9	36	10.5	63	12.7
10	7.1	37	10.6	64	12.8
11	7.2	38	10.7	65	12.8
12	7.4	39	10.8	66	12.9
13	7.5	40	10.9	67	13.0
14	7.7	41	11.0	68	13.1
15	7.9	42	11.1	69	13.1
16	8.0	43	11.2	70	13.2
17	8.1	44	11.2	71	13.3
18	8.3	45	11.3	72	13.4
19	8.4	46	11.4	73	13.4
20	8.6	47	11.5	74	13.5
21	8.7	48	11.6	75	13.6
22	9.0	49	11.7	76	13.7
23	9.1	50	11.7	77	13.8
24	9.2	51	11.8	78	13.8
25	9.2	52	11.9	79	13.9
26	9.4	53	12.0	80	14.0
27	9.5	54	12.0		
28	9.6	55	12.1		

The 95% confidence interval is ± 8% of the predicted age.

From Alfred B. Kurtz. Estimating gestational age. In: Bluth EI, Arger PH, Benson CB, Ralls PW, and Siegel MJ, eds. *Ultrasound: A Practical Approach to Clinical Problems*. New York: Thieme Medical Publishers; 2000. Reproduced with permission.

Table 12–3 Assessment of the Gestational Age from the Biparoetal Diameter

Gestational Age in Weeks					
Biparietal Diameter (mm)	Meana	Range 90% Variationb	Biparietal Diameter (mm)	Meana	Range 90% Variationb
22	12.7	12.2–13.2	61	24.2	22.6–25.8
23	13.0	12.4–13.6	62	24.6	23.1–26.1
24	13.2	12.6–13.8	63	24.9	23.4–26.4
25	13.5	12.9–14.1	64	25.3	23.8–26.8
26	13.7	13.1–14.3	65	25.6	24.1–27.1
27	14.0	13.4–14.6	66	26.0	24.5–27.5
28	14.3	13.6–15.0	67	26.4	25.0–27.8
29	14.5	13.9–15.2	68	26.7	25.3–28.1
30	14.8	14.1–15.5	69	27.1	25.8–28.4
31	15.1	14.3–15.9	70	27.5	26.3–28.7
32	15.3	14.5–16.1	71	27.9	26.7–29.1
33	15.6	14.7–16.5	72	28.3	27.2–29.4
34	15.9	15.0–16.8	73	28.7	27.6–29.8
35	16.2	15.2–17.2	74	29.1	28.1–30.1
36	16.4	15.4–17.4	75	29.5	28.5–30.5
37	16.7	15.6–17.8	76	30.0	29.0–31.0
38	17.0	15.9–18.1	77	30.3	29.2–31.4
39	17.3	16.1–18.5	78	30.8	29.6–32.0
40	17.6	16.4–18.8	79	31.1	29.9–32.5
41	17.9	16.5–19.3	80	31.6	30.2–33.0
42	18.1	16.6–19.8	81	32.1	30.7–33.5
43	18.4	16.8–20.2	82	32.6	31.2–34.0
44	18.8	16.9–20.7	83	33.0	31.5–34.5
45	19.1	17.0–21.2	84	33.4	31.9–35.1
46	19.4	17.4–21.4	85	34.0	32.3–35.7
47	19.7	17.8–21.6	86	34.3	32.836.2
48	20.0	18.2–21.8	87	35.0	33.4–36.6
49	20.3	18.6–22.0	88	35.4	33.9–37.1
50	20.6	19.0–22.2	89	36.1	34.6–37.6
51	20.9	19.3–22.5	90	36.6	35.1–38.1
52	21.2	19.5–22.9	91	37.2	35.9–38.5
53	21.5	19.8–23.2	92	37.8	36.7–38.9
54	21.9	20.1–23.7	93	38.8	37.3–39.3
55	22.2	20.4–24.0	94	39.0	37.9–40.1
56	22.5	20.7–24.3	95	39.7	38.5–40.9
57	22.8	21.1–24.5	96	40.6	39.1–41.5
58	23.2	21.5–24.9	97	41.0	39.9–42.1
59	23.5	21.9–25.1	98	41.8	40.5–43.1
60	23.8	22.3–25.5			

Abbreviations: BPD, biparietal diameter; GA, mean gestational age.

[a]Weighted least mean square fit equation: BPD (mm) = -34 5701 + 5.0157GA - 0.00441 GA.

[b]For each biparietal diameter, 90% of gestational age data points fell within this range.

From Alfred B. Kurtz. Estimating gestational age. In: Bluth EI, Arger PH, Benson CB, Ralls PW, and Siegel MJ, eds. *Ultrasound: A Practical Approach to Clinical Problems*. New York: Thieme Medical Publishers; 2000. Reproduced with permission.

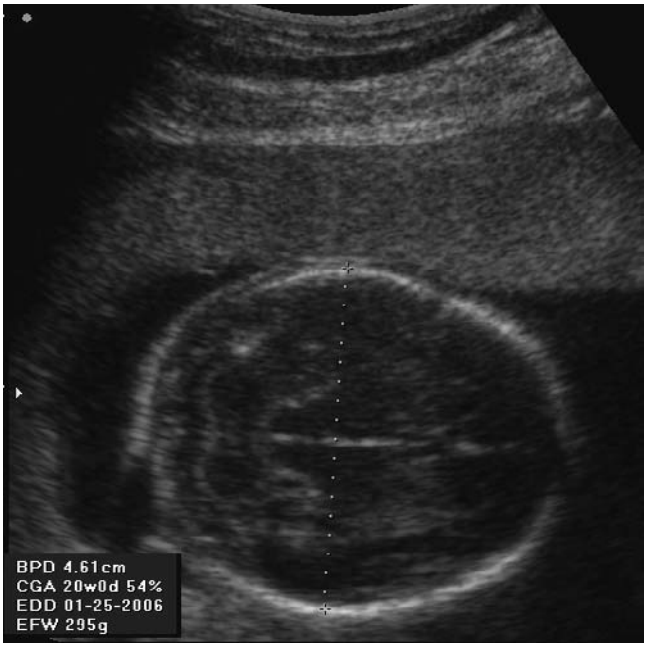

Figure 12–2 Scan demonstrating the biparietal diameter measurement, which is measured from the outer table of the skull to the inner table at the level of the thalami.

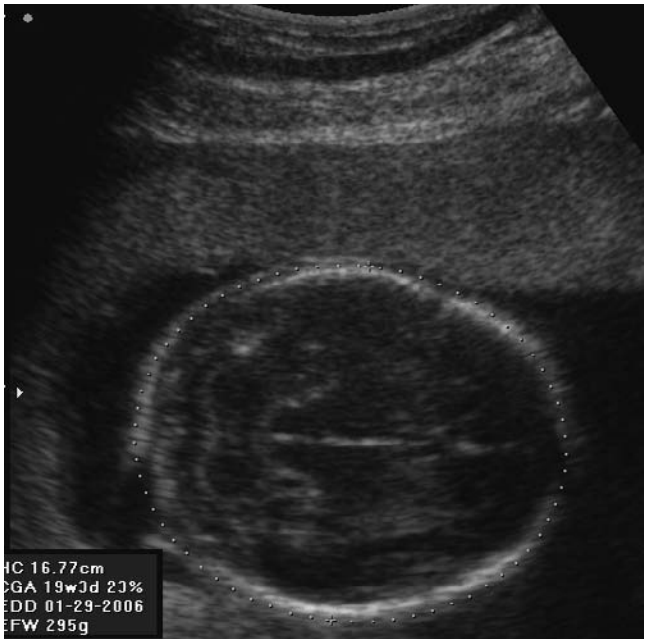

Figure 12–3 Scan demonstrating the measurement of the head circumference.

from 6 to 10 weeks, during which time it has an error of ± 3 to 4 days (95% confidence interval). However, as the gestation advances, there are methodological issues because the fetus may flex and extend, making reproducible linear measurements difficult. The error increases to ± 5 days between 10 and 14 weeks of gestation.

The CRL parameter in the first trimester is as accurate as or more accurate than any second-trimester fetal measurement for estimating gestational age.[10] There are no well-established measurement tables of fetal parts for gestational ages below 12 weeks.

Biparietal Diameter

The biparietal diameter (BPD) is one of the first parameters that was used to estimate gestational age and has been extensively researched in the literature. BPD is the most widely accepted parameter in estimating fetal gestational age[11,12] (**Table 12–3**). It is measured in a transverse plane at the level of the thalami from the outer table of the proximal skull to the inner table of the distal skull, corresponding to the "leading edge to leading edge" measurement (**Fig. 12–2**).

Measurements rostral to the thalami (i.e., below the level of the cerebral peduncles) may result in underestimation of the BPD and consequently the fetal gestational age. For accurate serial assessment, the biparietal diameter should be measured using the same landmarks (i.e., level of the thalami). If the BPD is measured at different levels, erroneous readings can result.

The biparietal diameter is most accurate between 12 and 28 weeks of gestation. After 28 weeks of gestation, head shape, intrauterine crowding, and individual variations affect the size of the head; hence, BPD must be used with caution.[2]

Difficulties Accurately Measuring the Biparietal Perimeter

Occasionally, the fetal head may be dolichocephalic (flattened and elongated) or brachycephalic (broadened and shortened), resulting in inaccurate estimation of gestational age based on BPD measurements.[13] The presence of an abnormal skull shape can be determined using the cephalic index. The index is the ratio between the BPD and the occipital-frontal diameter (OFD); its normal range is 75 to 85%. A value of 0.75 or less indicates dolichocephaly, whereas a value of 0.85 or higher indicates brachycephaly. In the presence of an abnormal cephalic index an alternative parameter (such as the head circumference) or a corrected BPD measurement should be used to estimate the gestational age.[14]

Doubilet and Greenes have suggested an alternative means of calculating the true BPD if the head is deformed.[15] They have a twofold approach: either calculate the area of the head and then derive the BPD from it, or use a circumference to "correct" the BPD.

According to studies conducted by Wolfson et al[16] and by O'Keeffe et al,[17] both BPD as well as cephalic index (which can predict an abnormal BPD) have a limited role in estimating the gestational age in preterm pregnancies that are complicated by the premature rupture of membranes.

Table 12–4 Assessment of the Gestational Age from the Head Circumference

Gestational Age in Weeks					
Head Circumference (mm)	Predicted Mean Values	95% Confidence Limits	Head Circumference (mm)	Predicted Mean Values	95% Confidence Limits
80	13.4	12.1–14.7	225	24.4	22.1–26.7
85	13.7	12.4–15.0	230	24.9	22.6–27.2
90	14.0	12.7–15.3	235	25.4	23.1–27.7
95	14.3	13.0–15.6	240	25.9	23.6–28.2
100	14.6	13.3–15.9	245	26.4	24.1–28.7
105	15.0	13.7–16.3	250	26.9	24.6–29.2
110	15.3	14.0–16.6	255	27.5	25.2–29.8
115	15.6	14.3–16.9	260	28.0	25.7–30.3
120	15.9	14.6–17.2	265	28.1	25.8–30.4
125	16.3	15.0–17.6	270	29.2	26.9–31.5
130	16.6	15.3–17.9	275	29.8	27.5–32.1
135	17.0	15.7–18.3	280	30.3	27.6–33.1
140	17.3	16.0–18.6	285	31.0	28.3–33.7
145	17.7	16.4–19.0	290	31.6	28.9–34.3
150	18.1	16.5–19.7	295	32.2	29.5–34.8
155	18.4	16.8–20.0	300	32.8	30.1–35.5
160	18.8	17.2–20.4	305	33.5	30.7–36.2
165	19.2	17.6–20.8	310	32.4	31.5–36.9
170	19.6	18.0–21.2	315	34.9	32.2–37.6
175	20.0	18.4–21.6	320	35.5	32.8–38.2
180	20.4	18.8–22.0	325	36.3	32.9–39.7
185	20.8	19.2–22.4	330	37.0	33.6–40.4
190	21.2	19.8–22.8	335	37.7	34.3–41.1
195	21.6	20.0–23.2	340	38.5	35.1–41.9
200	22.1	20.5–23.7	345	39.2	35.8–42.6
205	22.5	20.9–24.1	350	40.0	36.6–43.4
210	23.0	21.4–24.6	355	40.8	37.4–44.2
215	23.4	21.8–25.0	360	41.6	38.2–45.0
220	23.9	22.3–25.5			

From Alfred B. Kurtz. Estimating gestational age. In: Bluth EI, Arger PH, Benson CB, Ralls PW, and Siegel MJ, eds. *Ultrasound: A Practical Approach to Clinical Problems*. New York: Thieme Medical Publishers; 2000. Reproduced with permission.

In preterm gestations that present for the first time and require accurate dating, head circumference, corrected-BPD, and femur and humerus length are better parameters for assessing the gestational age. O'Keeffe et al suggested the use of abdominal circumference as an additional parameter for estimating the fetal age. However, given that the premature fetuses could be growth retarded, the use of abdominal circumference is not recommended because there might be an underestimation of the fetal age.

Head Circumference

The head circumference is measured in the same plane as the BPD and is used to estimate gestational age (**Table 12–4**). A study by Ott concluded that the fetal head circumference has a statistically significant lower mean error as compared with the BPD.[18] Growth disorders affect the head circumference to a lesser extent than the BPD. Also, the head circumference is useful in cases of dolichocephaly or brachycephaly. The head circumference can be measured via electronic calipers or computed using Jeanty's formula: (BPD + OFD) × 1.62.[2] The longest (anteroposterior) length should be obtained while measuring the head circumference, which means that the cavum pellucidum or the roof of the posterior fossa is included in the scan (**Fig. 12–3**).

Femur and Other Long Bone Lengths

Femur length is an excellent parameter to determine fetal age (**Table 12–5**). The length is measured from the most proximal

Table 12–5 Assessment of the Gestational Age from the Femur Length

Predicted Gestational Age in Weeks					
Femur Length (mm)	**Predicted Mean Values**	**2 SD Range**	**Femur Length (mm)**	**Predicted Mean Values**	**2 SD Range**
10	13.7	12.5–14.9	45	24.5	22.6–26.4
11	13.9	12.7–15.1	46	24.9	23.0–26.8
12	14.2	13.0–15.4	47	25.3	23.4–27.2
13	14.4	13.2–15.6	48	25.7	23.8–27.6
14	14.6	13.4–15.8	49	26.2	23.5–28.9
15	14.9	13.7–16.1	50	26.2	23.9–29.3
16	15.1	13.9–16.3	51	27.0	24.3–29.7
17	15.4	14.2–16.6	52	27.5	24.8–30.2
18	15.6	14.4–16.8	53	28.0	25.3–30.7
19	15.9	14.7–17.1	54	28.4	25.7–31.1
20	16.2	15.0–17.4	55	28.9	26.2–31.6
21	16.4	15.2–17.6	56	29.4	26.7–32.1
22	16.7	15.5–17.9	57	29.9	27.2–32.6
23	17.0	15.8–18.2	58	30.4	27.7–33.1
24	17.3	16.1–18.5	59	30.9	28.2–33.6
25	17.6	16.4–18.8	60	31.4	28.7–34.1
26	17.9	16.7–19.1	61	31.9	29.2–34.6
27	18.2	17.0–19.4	62	32.5	28.5–36.5
28	18.5	17.3–19.7	63	33.0	29.0–37.0
29	18.8	17.6–20.0	64	33.6	29.6–37.6
30	19.1	17.9–20.3	65	34.1	30.1–38.1
31	19.4	18.2–20.6	66	34.7	30.7–38.7
32	19.7	18.5–20.9	67	35.3	31.3–39.3
33	20.1	18.2–22.0	68	35.9	31.9–39.9
34	20.4	18.5–22.3	69	36.5	32.5–40.5
35	20.7	18.8–22.6	70	37.1	33.1–41.1
36	21.1	19.2–23.0	71	37.7	33.7–41.7
37	21.4	19.5–23.3	72	38.3	35.1–41.5
38	21.8	19.9–23.7	73	39.0	35.8–42.2
39	22.2	20.3–24.1	74	39.6	36.4–42.8
40	22.5	20.6–24.4	75	40.3	37.1–43.5
41	22.9	21.0–24.8	76	40.9	37.7–44.1
42	23.3	21.4–25.2	77	41.6	38.4–44.8
43	23.7	21.8–25.6	≥78	42.0	38.8–45.2
44	24.1	22.2–26.0			

Abbreviation: SD, standard deviation

From Alfred B. Kurtz. Estimating gestational age. In: Bluth EI, Arger PH, Benson CB, Ralls PW, and Siegel MJ, eds. *Ultrasound: A Practical Approach to Clinical Problems*. New York: Thieme Medical Publishers; 2000. Reproduced with permission.

portion of the ossified shaft to the distal end. The nonossified femoral head and distal epiphysis are not included. Femur length can be measured from 14 to 42 weeks.[19–21] A recent study by Dare et al concluded that the femur length was a more reliable indicator than the BPD in estimating the gestational age in late third trimester[22] (**Fig. 12–4**).

The length of the humerus can also be used to estimate the gestational age (**Fig. 12–5**). The other long bones that are used for gestational age estimation, in decreasing order of frequency, are the tibia, radius, and ulna. According to Jeanty, in clinical practice, the bone-derived gestational age is averaged and compared with the BPD-derived gestational age. If the difference is greater than 11 days, bone-derived gestational age should be preferentially used.[2]

Abdominal Circumference

The abdominal circumference is largely determined by the size of the liver, which, in turn, reflects the amount of glycogen that is stored in the liver. Any condition that

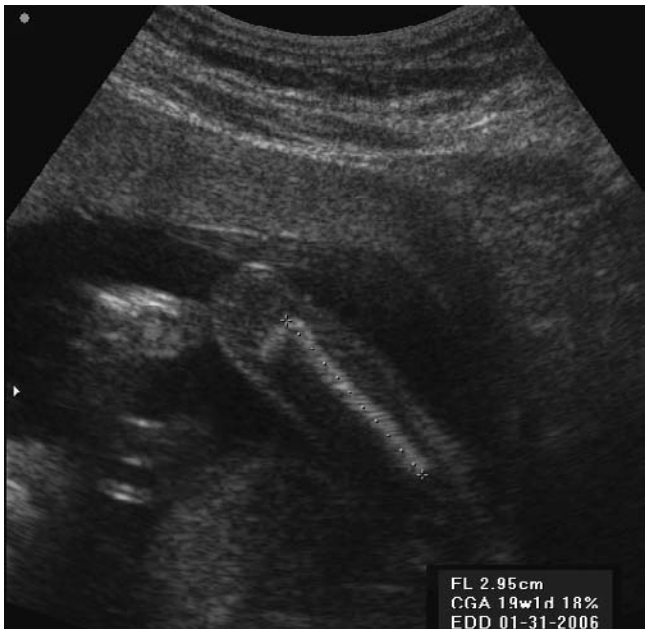

Figure 12–4 Scan demonstrating the femur length, which is measured from the proximal end to the distal end of the shaft.

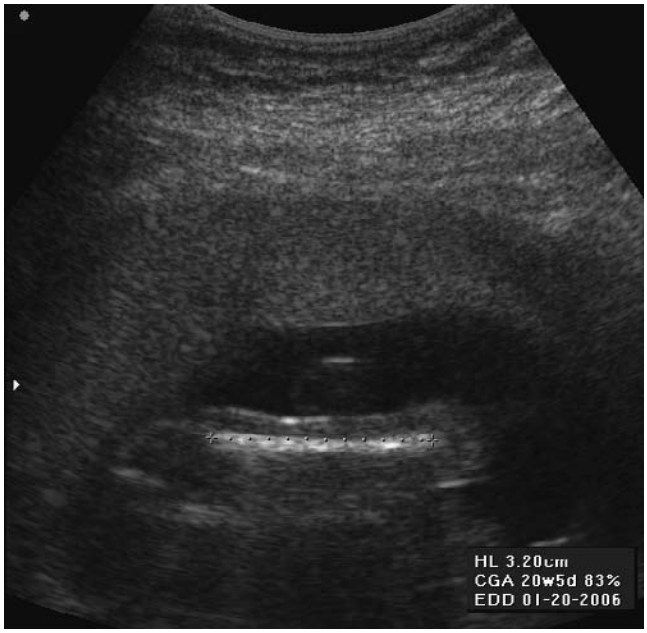

Figure 12–5 Scan demonstrating the humeral length, which is obtained in the same way as the femur.

causes nutritional growth retardation will cause the abdominal circumference to be small for gestational age. Conversely, conditions such as maternal diabetes that can cause increased glycogen deposition in the liver can result in abdominal circumferences that are large for gestational age. In both these situations, the abdominal circumference will not accurately represent the gestational age. It is therefore not very commonly used.[2] However, it may be used in conjunction with other fetal parameters and is helpful in calculating the interval fetal growth and the estimated fetal weight. The abdominal circumference is measured in the transverse plane at the level of the stomach and junction of the umbilical vein and portal sinus (outer line including the spine). It can be measured from 14 to 42 weeks.

Clavicular Length

This parameter is occasionally used to estimate the gestational age in fetuses with chondrodysplasias. Because the clavicle has an intramembranous ossification pattern (and not an endochondral ossification) it is less affected than the femur and humerus in those fetuses. Remember that in achondroplasia the skull is deformed too. The length of the clavicle is measured in its long axis. The clavicular length expressed in millimeters is close to the gestational age expressed in weeks.[23] It can be measured from 14 to 42 weeks. The measurement of the clavicular length is also helpful in certain congenital skeletal anomalies that affect the clavicle, such as cleidocranial dysplasia.

Transverse Cerebellar Diameter

The transverse cerebellar diameter (TCD) parameter proposed by Reece and colleagues is not affected much by growth retardation and correlates well with the gestational age.[24] The maximum width of the cerebellum is measured in the transverse plane and can be measured from 16 to 42 weeks. The transverse cerebellar diameter expressed in millimeters correlates well with the gestational age in weeks and hence can serve as a quick check of gestational age in both the normally grown as well as the growth-retarded fetus[25,26] (**Fig. 12–6**).

Nuchal Translucency

Although not a gestational age parameter, the nuchal translucency is important and mentioned here because it

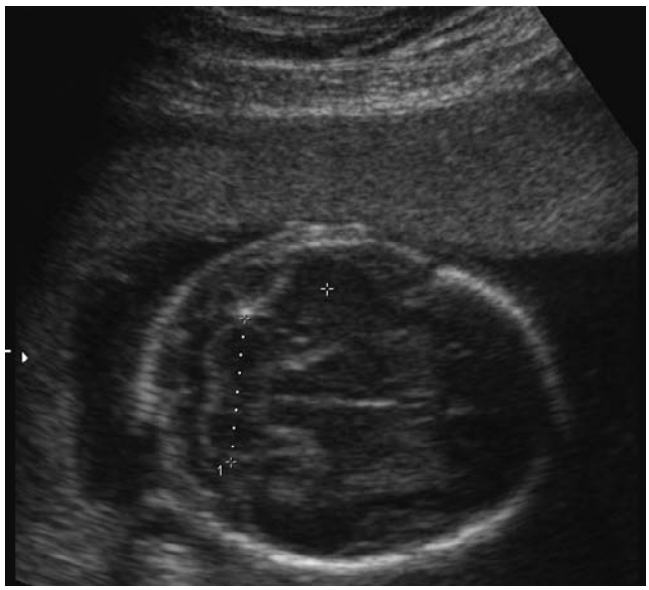

Figure 12–6 Scan demonstrating the measurement of the transcerebellar diameter. This is obtained in its longest plane.

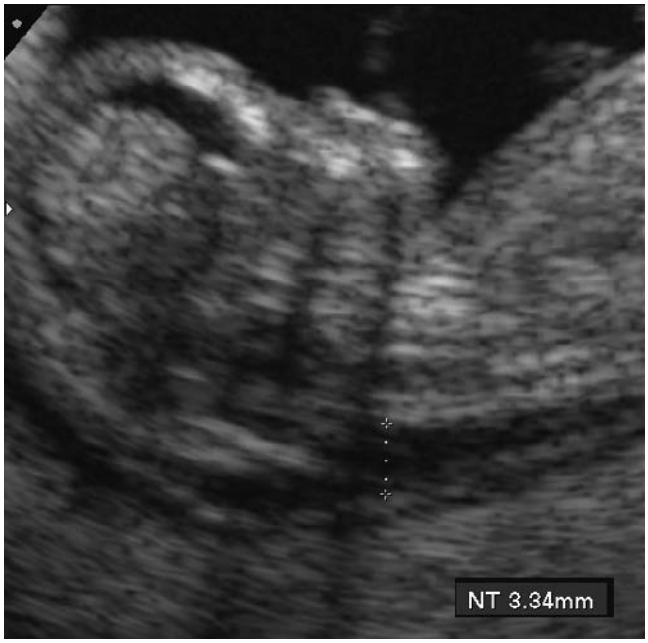

Figure 12–7 Scan demonstrating nuchal translucency.

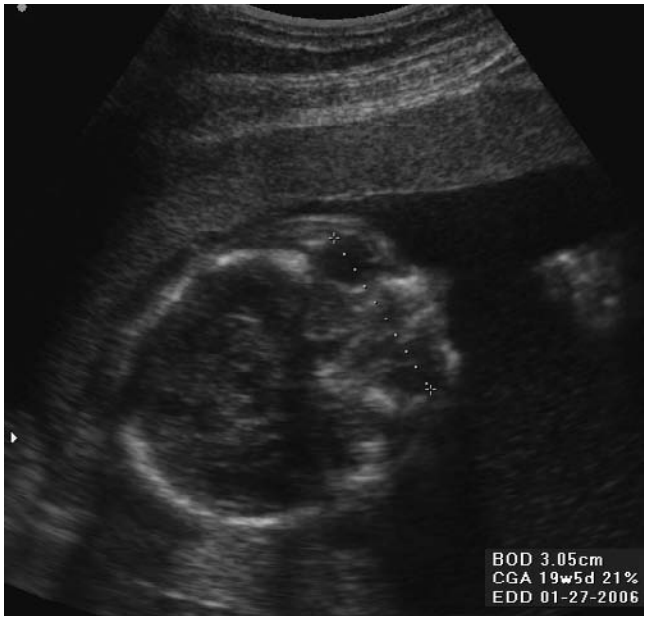

Figure 12–8 Scan demonstrating the binocular distance. Both the orbits should be symmetrical and the longest diameter of the orbit must be used.

is used for the early detection of aneuploidy. An enlarged nuchal translucency in the late first trimester is associated with aneuploidy and a few structural anomalies such as cardiac defects and congenital diaphragmatic hernia. It is measured in the midsagittal plane of the fetal neck, from the inner skin outline echo to the inner border of the soft tissue (**Fig. 12–7**).

A measurement of > 2.5 mm is considered abnormal and needs further evaluation by karyotype analysis.[27] It is measured from 11w1d to 13w6d. Flexion of the fetal neck may result in erroneous measurement.

Binocular Distance

This parameter is occasionally useful in assessing the gestational age.[28,29] The correct plane of measurement is obtained by starting from the plane of the biparietal diameter and proceeding caudally until the orbits are visualized. The measurement should be made in a plane where the orbits appear symmetrical and the interocular distance is the smallest. The largest diameter of the orbit should be used. It is useful from 7 to 42 weeks (**Fig. 12–8, Fig. 12–9**).

Other Parameters that May Be Measured

Several other uncommonly used parameters have been researched and mentioned in the literature. Renal length may be used to compute the gestational age between 24 and 38 weeks of gestation.[30] Some authors have proposed the presence of ossification centers as a means to calculate the gestational age. Several charts are available that assess the gestational age or fetal growth using the earlobe length, nasal length, scapular length, cavum septum pellucidi, foot length, orbital diameters, chin length, and upper lip width, lungs, heart diameter, liver, and iliac angle.[31–39] Placental thickness has also been used as a sonographic parameter to estimate the gestational age of the fetus. According to one study, the placental thickness corresponds to the gestational age between 22 and 35 weeks.[40] However, these parameters are of pure academic interest and have limited practical utility.

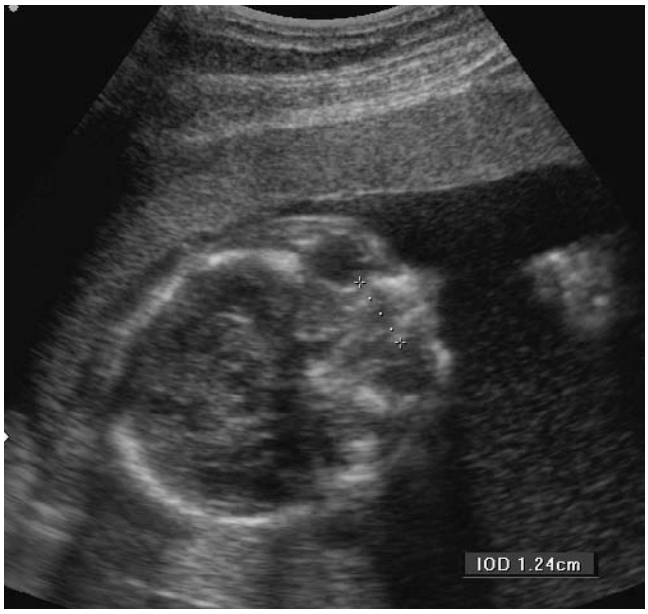

Figure 12–9 Scan demonstrating the interocular distance. This distance should be the smallest while measuring the binocular distance.

For a parameter to be useful the error on the measurement has to be small compared with the measurement. The error on the measurement is dependent on the equipment and human aptitude. It is, for instance, hard to be consistently more precise than a millimeter. Thus, the error on the measurement is largely fixed. If the object being measured is small (a nasal bone, for instance) the contribution of the error in the measurement is large compared with a larger object such as the femur. Furthermore, large errors in the measurement can easily mask anomalies. Thus, the ideal parameters that are used for measurement have to be large, with clear boundaries and little biological variation. This is the reason why the femur and humerus are among the most reliable parameters.

Estimating Gestational Age in Cases Where Parameters Suggest Different Ages

Sometimes, different fetal parameters provide different estimates of gestational ages. The general rule is that the earlier the estimation of the age, the more accurate it is. Therefore, gestational age should be assigned at the time of the first ultrasound. Gestational age at the time of all subsequent ultrasound examinations should be based on the first ultrasound, calculated as the gestational age at the first ultrasound plus the number of weeks that have elapsed since that ultrasound. For example, if an earlier scan has been performed at 15 weeks, and a follow-up scan is done 7 weeks later, the gestational age for that examination is 22 weeks. If fetal measurements are not consistent with 22 weeks gestational age, then the fetus should be evaluated for a growth disturbance.

Problems Raised in Fetal Biometry by Introduction of PACS and Their Reporting Programs

Some unexpected problems were reported with the introduction of reporting programs and PACS. Previously, measurements were provided by the ultrasound machine, and in some cases the machine would also use user-selected equations to provide derived values such as the gestational age or the estimated fetal weight. The values were then transferred into the report, either by dictation or by capturing the reporting program.

When reporting programs and PACs are added to the equation it is critical that the equations selected in the ultrasound machine, the PACs, and the reporting program are matched. It is usually simple to use a well-recognized equation, such as Robinson's CRL, and have all three systems matched. However, for more complicated formulas, such as the estimated fetal weight, there are many sources of possible deviations. Not only do all the formulas have to be set to be the same (which assumes that the ultrasound machine, the PACs, and the reporting system have the same equations or the ability to "add" equations), but the growth curves of the estimated fetal weight have to be the same as well. Otherwise, the same estimated fetal weight will fall at different levels in different growth curves. What would appear as an "appropriate for gestational age" fetus on the ultrasound scanner could be considered "low growth" on the reporting system, if the same growth curves are not selected. Furthermore, it is clear that the patient's dates have to match. Often the ultrasound scanner will assign a date to the pregnancy, either from a previous scan or from the current examination. If the reporting system contains a different gestational age (for whatever reason) there can be a difference in the gestational age between the ultrasound machine and the reporting software. Thus, this can be another source of discrepancy, even if the same equations are in use.

Therefore, although it appears to be a simple matter to synchronize the ultrasound machine, the reporting system, and the PACs, in practice, this can be a frustrating experience, given the limitations present in all the components of the equation. A careful review of the values and result is important before using the calculated values in clinical settings.

The Best Measurement to Use to Assess Gestational Age

The selection of appropriate measurement to assess the gestational age is relative because the growth pattern changes during pregnancy and the accuracy of each parameter changes with gestational age. The following parameters are recommended in decreasing order of preference (when two or more parameters are close to the same gestational age, it improves the accuracy of each):

- 7 to 12 weeks: CRL
- 10 to 14 weeks: CRL, BPD, FL, HL
- 15 to 26 weeks: HC, BPD, FL, HL
- 27 to term: FL, HL, BPD (corrected BPD value using the cephalic index)

This order was established based on the reliability, confidence limits, and ease of measurement of the various parameters. This order should be adapted to suit specific circumstances.

Acknowledgment
The authors express their appreciation to Philippe Jeanty for reviewing this manuscript, and to the TheFetus.net for allowing reproduction in print.

References

1. Kurtz A. Estimating fetal gestational age. In: Ultrasound: A Practical Approach to Clinical Problems. 2nd ed.
2. Jeanty P. Fetal biometry. In: The Principles and Practice of Ultrasonography in Obstetrics and Gynecology. 4th ed.
3. Taipale P, Hiilesmaa V. Predicting delivery date by ultrasound and last menstrual period in early gestation. Obstet Gynecol 2001; 97:189–194

4. Goncalves L, Jeanty PJ. Fetal biometry of skeletal dysplasias. J Ultrasound Med 1994;13:977–985
5. Nicolaides KH, Azar G, Byrne D, et al. Fetal nuchal translucency: ultrasound screening for chromosomal defects in the first trimester of pregnancy. BMJ 1992;304:867
6. Davis RO, Cutter GR, Goldenberg RL, Hoffman HJ, Cliver SP, Brumfield CG. Fetal biparietal diameter, head circumference, abdominal circumference and femur length: a comparison by race and sex. J Reprod Med 1993;38:201–206
7. Muller T, Sutterlin M, Pohls U, Dietl J. Transvaginal volumetry of first trimester gestational sac: a comparison of conventional with three-dimensional ultrasound. J Perinat Med 2000;28:214–220
8. Robinson HP, Fleming JEE. A critical evaluation of sonar crown–rump length measurements. Br J Obstet Gynaecol 1975;82: 702–710
9. Goldstein SR, Wolfson R. Endovaginal ultrasonographic measurement of early embryonic size as a means of assessing gestational age. J Ultrasound Med 1994;13:27–31
10. Hadlock FP, Shah YP, Kanon DJ, Math B, Lindsey JV. Fetal crown–rump length: reevaluation of relation to menstrual age (5–18 weeks) with high-resolution real-time US. Radiology 1992; 182:501–505
11. Hadlock FP, Deter RL, Harrist RB, Park SK. Fetal biparietal diameter: a critical reevaluation of the relation to menstrual age by means of real-time ultrasound. J Ultrasound Med 1982;1:97–104
12. Hadlock FP, Deter RL, Harrist RB, Park SK. Fetal biparietal diameter: rational choice of plane of section for sonographic measurement. Am J Roentgenol 1982;138:871–874
13. Hadlock FP, Deter RL, Carpenter RJ, Park SK. Estimating fetal age: effect of head shape on BPD. AJR Am J Roentgenol 1981;137:83–85
14. Kurtz AB, Kurtz RJ. The ideal fetal head circumference calculation. J Ultrasound Med 1989;8:25–29
15. Doubilet PM, Greenes RA. Improved prediction of gestational age from fetal head measurements. Am J Roentgenol 1984;142: 797–800
16. Wolfson RN, Zador IE, Halvorsen P, Andrews B, Sokol RJ. Biparietal diameter in premature rupture of membranes: errors in estimating gestational age. J Clin Ultrasound 1983;11:371–374
17. O'Keeffe DF, Garite TJ, Elliott JP, Burns PE. The accuracy of estimated gestational age based on ultrasound measurement of biparietal diameter in preterm premature rupture of the membranes. Am J Obstet Gynecol 1985;151:309–312
18. Ott WJ. The use of ultrasonic fetal head circumference for predicting expected date of confinement. J Clin Ultrasound 1984;12:411–415
19. Jeanty P, Romero R. Obstetrical Ultrasound. New York: McGraw-Hill; 1984
20. Jeanty P, Rodesch F, Delbeke D, Dumont JE. Estimation of gestational age from measurements of fetal long bones. J Ultrasound Med 1984;3:75–79
21. Johnsen SL, Rasmussen S, Sollien R, Kiserud T. Fetal age assessment based on femur length at 10–25 weeks of gestation, and reference ranges for femur length to head circumference ratios. Acta Obstet Gynecol Scand 2005;84:725–733
22. Dare FO, Smith NC, Smith P. Ultrasonic measurement of biparietal diameter and femur in fetal age determination. West Afr J Med 2004;23:24–26
23. Yarkoni S, Schmidt W, Jeanty P, Reece EA, Hobbins JC. Clavicular measurement: a new biometric parameter for fetal evaluation. J Ultrasound Med 1985;4:467–470
24. Reece EA, Goldstein I, Pilu G, Hobbins JC. Fetal cerebellar growth unaffected by intrauterine growth retardation: a new parameter for prenatal diagnosis. Am J Obstet Gynecol 1987;157:632–638
25. Makhoul IR, Goldstein I, Epelman M, Tamir A, Reece EA, Sujov P. Neonatal transverse cerebellar diameter in normal and growth-restricted infants. J Matern Fetal Med 2000;9:155–160
26. Chavez MR, Ananth CV, Smulian JC, Yeo L, Oyelese Y, Vintzileos AM. Fetal transcerebellar diameter measurement with particular emphasis in the third trimester: a reliable predictor of gestational age. Am J Obstet Gynecol 2004;191:979–984
27. Acacio GL, Barini R, Pinto Junior W, Ximenes RL, Pettersen H, Faria M. Nuchal translucency: an ultrasound marker for fetal chromosomal abnormalities. Sao Paulo Med J 2001;119:19–23
28. Mayden KL, Tortora M, Berkowitz RL. Orbital diameters: a new parameter for prenatal diagnosis and dating. Am J Obstet Gynecol 1982;144:289
29. Jeanty P, Cantraine F, Cousaert E, Romero R, Hobbins JC. The binocular distance: a new way to estimate fetal age. J Ultrasound Med 1984;3:241–243
30. Konje JC, Abrams KR, Bell SC, Taylor DJ. Determination of gestational age after the 24th week of gestation from fetal kidney length measurements. Ultrasound Obstet Gynecol 2002;19:592–597
31. Chitkara U, Lee L, El-Sayed YY, et al. Ultrasonographic ear length measurement in normal second- and third-trimester fetuses. Am J Obstet Gynecol 2000;183:230–234
32. Sherer DM, Plessinger MA, Allen TA. Fetal scapular length in the ultrasonographic assessment of gestational age. J Ultrasound Med 1994;13:523–528
33. Jou HJ, Shyu MK, Wu SC, Chen SM, Su CH, Hsieh FJ. Ultrasound measurement of the fetal cavum septi pellucidi. Ultrasound Obstet Gynecol 1998;12:419–421
34. Mercer BM, Sklar S, Shariatmadar A, Gillieson M, Dalton M. Fetal foot length as a predictor of gestational age. Am J Obstet Gynecol 1987;156:350–355
35. Sivan E, Chan L, Mallozi-Eberle A, et al. Sonographic imaging of the fetal face and the establishment of normative decisions for chin length and upper lip width. Am J Perinatol 1997;14:191
36. Heiling KS, Kalache K, Chaoui R, et al. Ultrasound biometry of the fetal lung-measurement planes and reference values. Zentralbl Gynakol 1997;119:625
37. Hata T, Senoh D, Hata K, et al. Intrauterine sonographic assessment of embryonic heart diameter. Hum Reprod 1997;12:2286
38. Hata T, Fujiwaki R, Senoh D, et al. Intrauterine sonographic assessment of the fetal liver length. Hum Reprod 1996;11:2758
39. Bork MD, Egan JF, Cusick W, et al. Iliac wing angle as a marker for trisomy 21 in the second trimester. Obstet Gynecol 1997;89(5 Pt 1):734
40. P Mital, N Hooja, K Mehndiratta. Placental thickness: a sonographic parameter for estimating gestational age of the fetus. Ind J Radiol Imag 2002;12:553–554
41. Chervenak FA, Skupski DW, Romero R, Myers MK, Smith-Levytin M, Rosenwaks Z, Thaler HT. How accurate is fetal biometry in the assessment of fetal age? Am J Obstet Gynecol 1998;178:678–687

13 Uterine Size Greater than Dates

Beryl Benacerraf

Ultrasound Evaluation

Sonography is very helpful in evaluating pregnancies that are larger than expected based on menstrual dates. Possible explanations for a large uterine size include incorrect dates, macrosomia, multiple fetuses, as well as complications of twinning such as twin/twin transfusion syndrome or acardia. The pregnancy can be complicated by polyhydramnios, which can be idiopathic or a result of fetal growth acceleration, maternal diabetes, or fetal malformations. The fetal anomalies most often associated with polyhydramnios include those involving the gastrointestinal tract, central nervous system, thoracic and cardiac anomalies, fetal hydrops (isoimmune and nonimmune etiologies), some skeletal defects, chromosomal anomalies, and fetal tumors. When a fetus in the presence of polyhydramnios appears structurally normal sonographically, the outcome is generally excellent.

Masses unrelated to the fetus may also be responsible for the clinical impression that the uterus is larger than expected for the patient's dates. These masses include uterine fibroids and adnexal enlargement such as an ovarian cyst. The evaluation of the patient whose uterine size is larger than dates includes a complete structural survey of the fetus, including an echocardiogram, fetal biometry, and estimated weight assessment, as well as an evaluation of the myometrium and adnexae for possible masses.

Size/date discrepancy is one of the most common indications for obtaining an obstetrical ultrasound. Obstetricians can measure the uterus externally and compare its overall size to what is expected from the patient's dates. It is common to find that the size is either too large or too small, thus prompting further evaluation of the pregnancy. When the uterus is larger than anticipated based on the patient's dates, a sonogram will most often find the explanation.

Incorrect Dating of Pregnancy

Most commonly, the dates are incorrect. The patient may have had some spotting within the first month after she conceived. If she mistook the spotting for a true menstrual period, she would have estimated her dates at 4 weeks less than the actual gestation. It is not uncommon to find that the gestational age is 4 weeks ahead of what was expected, based on the final menstrual period prior to conception. If the fetal biometry measures several weeks ahead of what the menstrual dates would predict, the fetus may have macrosomia or growth acceleration. Although in the first trimester the fetal size is normally within 3 to 5 days of the menstrual age, by the third trimester the fetal size can be as much as a month ahead of dates due to accelerated growth. It is important not to rely on sonographic biometry for dating pregnancies in the third trimester due to differential growth rates.

Multiple Pregnancy

Nowadays, it is extremely rare to make the discovery of twins at the time of delivery. In the vast majority of cases, the size of the uterus will have exceeded the expectation by dates sometime during the pregnancy, thus prompting an ultrasound to discover multiple fetuses. Once an ultrasound shows that there is more than one fetus (in most cases, twins), the pregnancy is considered at higher risk. Although multiple gestations account for only 1 to 2% of all births, they represent 10 to 15% of perinatal mortality and more than 15% of the low birth weight incidence. Higher-order multiple fetal pregnancies than twins are more common than ever before due to assisted reproduction treatments. The more fetuses present, the higher the risk of prematurity and other complications (**Fig. 13–1**).

Once a twin pregnancy is identified, its chorionicity must be determined because monochorionic twins have yet a higher morbidity and mortality than dichorionic twins.[1] The prenatal death rate has been reported as 9% for dichorionic/diamniotic twins and 26% for monochorionic/diamniotic twins. When twins are monochorionic/ monoamniotic with no membrane separating them into two sacs, the incidence of nonsurvival is 50% (**Fig. 13–1**).[1] It is crucial to search for the dividing membrane and to evaluate its morphology. Determining whether the membrane is monochorionic/diamniotic (thin) versus dichorionic/diamniotic (thick) is easier in the first trimester, when the difference in thickness is more obvious. It may be difficult to distinguish between the two types of chorionicity in the third trimester. When monozygotic twins split late in the second week after conception, conjoined twins may result (**Fig. 13–2**).

Monochorionic/diamniotic twins are at risk for complications based on the shared placenta, such as twin-to-twin transfusion syndrome (**Fig. 13–3**).[1–3] Deep vascular anastomoses within the placenta can result in an uneven distribution of blood flow to the two fetuses, with one fetus essentially transfusing the other. This results in one anemic fetus and one plethoric fetus. The anemic fetus is usually associated with severe oligohydramnios, whereas the fetus who has received too much blood flow tends to have

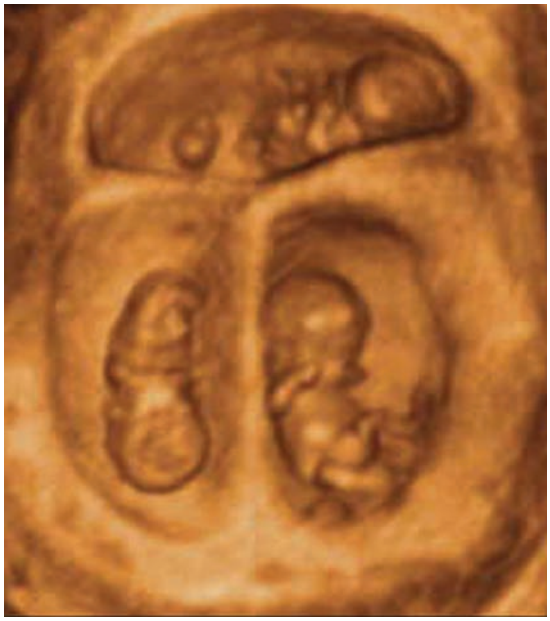

A

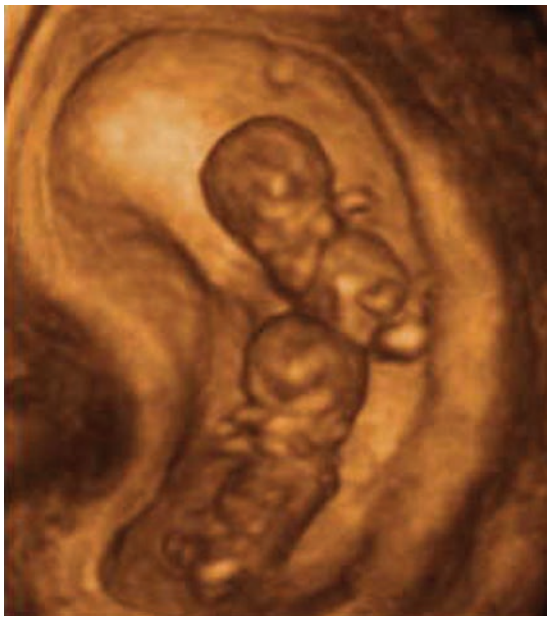

B

Figure 13–1 (A) Trichorionic triamniotic triplet pregnancy at 9 weeks with three live embryos in a three-dimensional (3-D) image. **(B)** A 3-D image of a monochorionic twin pregnancy at 10 weeks showing the twins in the same chorionic sac.

severe polyhydramnios. Acute enlargement of the uterus, secondary to the development of polyhydramnios, is typical of severe twin-to-twin transfusion syndrome. When discovered at less than 22 weeks, there is a 90 to 100% chance of complete loss of the pregnancy. And in most cases, this is due to premature labor before viability.[2,3] Attempts at treating the polyhydramnios by serial removal of large quantities of amniotic fluid by amniocentesis have been helpful in some cases, although the mortality of the polyhydramnios/oligohydramnios sequence in monochorionic twins remains very high. More recently, investigators

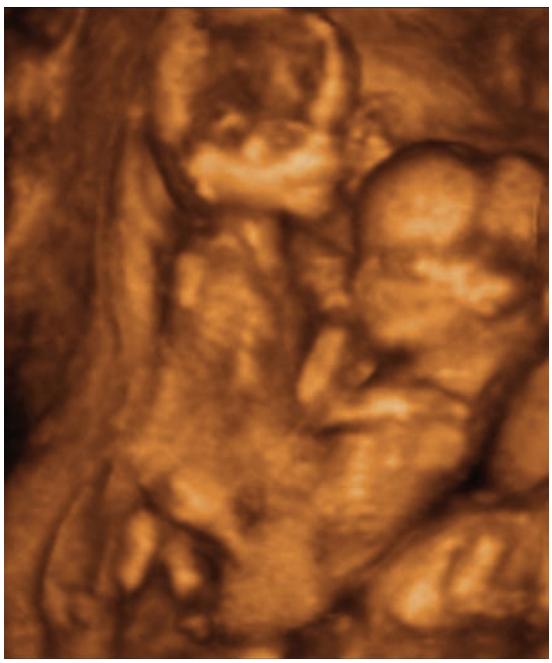

Figure 13–2 A three-dimensional image of a set of thoracopagus conjoined twins sharing a liver and facing each other in the amniotic sac.

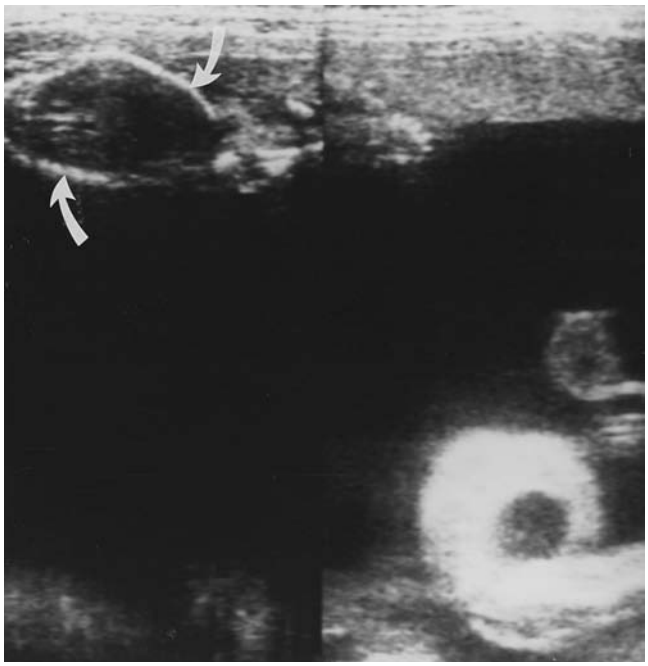

Figure 13–3 Composite image of the uterus in a monochorionic-diamniotic twin pregnancy, complicated by twin-to-twin transfusion syndrome. Note the tremendous amount of polyhydramnios associated with the twin in the dependent portion of the uterus. The twin associated with the polyhydramnios has an enlarged bladder, indicating increased perfusion (arrows). The stuck twin's head is noted in a superior aspect of the uterus, as indicated by curved arrows. It is suspended by its membrane, due to the severe oligohydramnios in its sac.

have used laser ablation of the artery to vein anastomoses in the placenta to arrest the transfusion process and better divide the vascular communications between the twins. This technique is more promising than serial amniocentesis, and improves the outcome for severe twin-to-twin transfusion.[4]

Another complication of the monochorionic twinning process is the development of an acardiac twin that is kept alive by its co-twin. This phenomenon results from artery-to-artery shunts in the placenta, and reversal of the arterial blood flow in one twin due to the overpowering arterial pressure of its co-twin (pump twin). With blood flowing in reverse through its arterial system, the acardiac twin's heart fails to develop and, in most cases, the head and upper body regress, leaving an isolated, malformed lower body with edema. These acardiac twins can grow very large, often larger than the pump twin, and thus threaten the well-being of the pump twin.

Polyhydramnios

The volume of amniotic fluid normally increases throughout gestation until ~24 weeks, after which it declines until term. During pregnancy, the fetus swallows and excretes fluid in the form of urine. The swallowed fluid is resorbed through the gastrointestinal tract and recirculated through the fetal kidneys. Although in the early second trimester fetal urine only represents ~10% of the total volume of amniotic fluid, during the second half of pregnancy the portion of amniotic fluid resulting from fetal urine increases until it is largely dependent upon fetal urination. Amniotic fluid is constantly being used and replenished, not unlike keeping a bathtub filled by constantly running the water with the drain open. Sonographic determination of the amniotic fluid volume has been attempted using various means, including the largest single pocket measurement as well as the four-quadrant measurement of amniotic fluid volume. Many experienced practitioners use subjective assessments of amniotic fluid volume rather than an actual measurement.[5] The best accepted measurement, however, is the Amniotic Fluid Index, which is based on the four-quadrant technique.[6]

The presence or absence of fetal malformations associated with polyhydramnios is largely related to the degree of excess amniotic fluid present. In pregnancies complicated by mild polyhydramnios, the risk of fetal malformation ranges between 20 and 40%.[7–9] Most of the malformations, however, are visible sonographically.

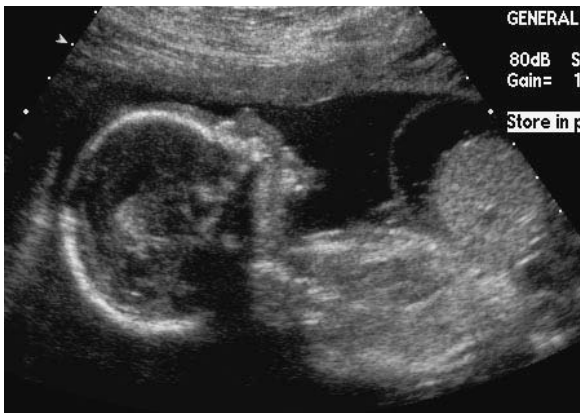

A

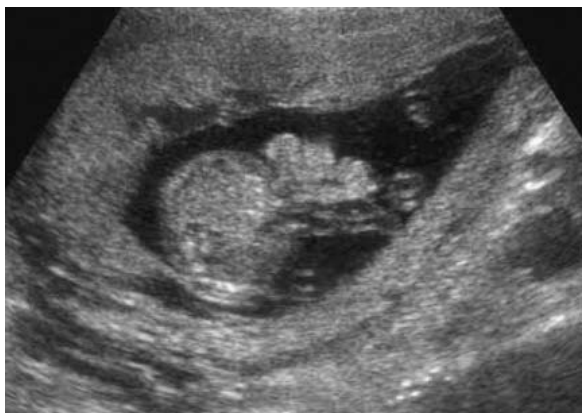

B

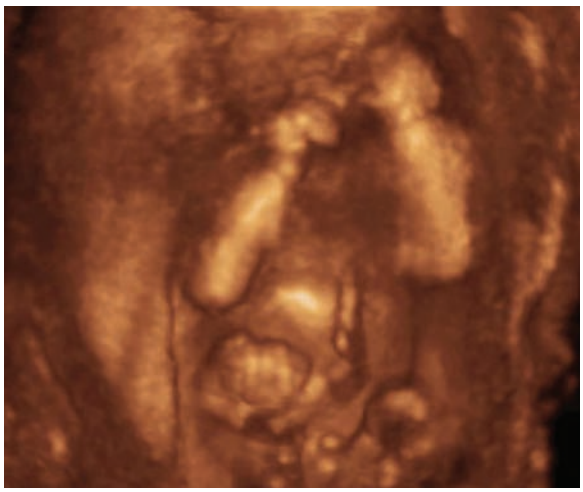

C

Figure 13–4 (A) Anterior abdominal wall defects. Longitudinal view of the fetal upper body, showing a mass coming off the anterior abdominal wall with the liver protruding out into an anterior abdominal wall defect (omphalocele). **(B)** Transverse view through the fetal lower abdomen at the level of the umbilical cord insertion, showing a gastroschisis adjacent to the insertion of the cord. **(C)** Three-dimensional surface rendering image of the gastroschisis defect next to the umbilical cord insertion on the fetal belly.

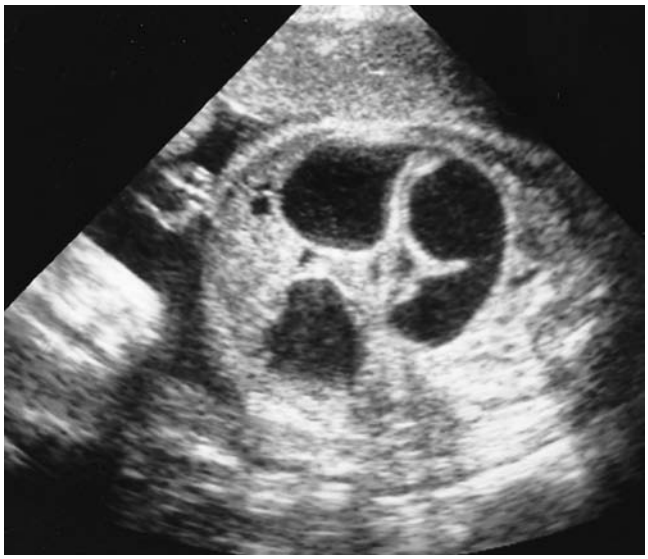

Figure 13–5 Transverse view through the fetal abdomen, directly caudad to the fetal liver. Note the marked dilatation of several loops of bowel, indicating small bowel obstruction.

In the absence of any sonographic finding, mild polyhydramnios is usually idiopathic or associated with macrosomia.[10–12] Several studies have shown that, when compared with pregnancies with normal amniotic fluid volumes, sonographically unexplained mild polyhydramnios was associated with a significantly higher incidence of birth weights greater than 4000 g. Birth weights were in the 90th percentile or more in 28% of fetuses with mild polyhydramnios versus 9% of normal controls.[10–12]

Diabetic women are at an increased risk for having macrosomic fetuses as well as for having their pregnancies complicated by polyhydramnios. When polyhydramnios associated with growth acceleration is detected by a prenatal sonogram, a glucose tolerance test is indicated to detect possible diabetes.

The incidence of malformations is considerably higher when the polyhydramnios is severe versus when it is mild. Fetuses associated with severe polyhydramnios have a prevalence of fetal anomalies of 75% versus 29% when the polyhydramnios is mild.[7,8]

The most common malformations associated with polyhydramnios are those involving the gastrointestinal tract.[8] Gastrointestinal obstructions, such as duodenal atresia, jejunal atresia, or esophageal atresia, invariably cause polyhydramnios as early as the mid–second trimester.[8,13,14] Other gastrointestinal conditions sometimes associated with polyhydramnios include meconium peritonitis, anterior abdominal wall defects, and intraluminal masses such as intraoral teratomas or other obstructions to the swallowing mechanism (**Fig. 13–4**).[8] The sonographic manifestation of gastrointestinal obstruction includes marked dilatation of the bowel

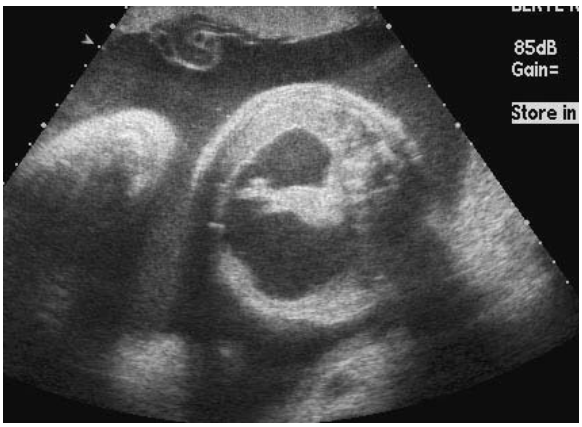

A

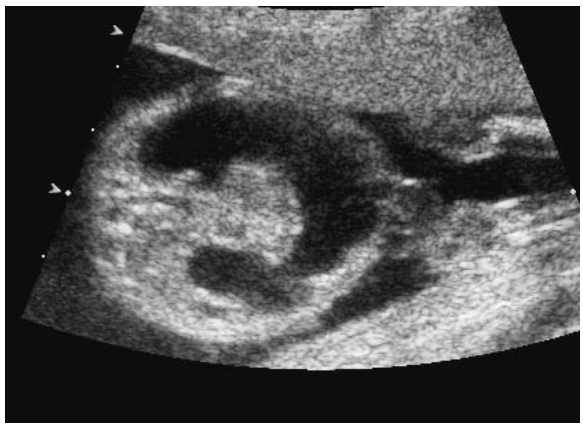

B

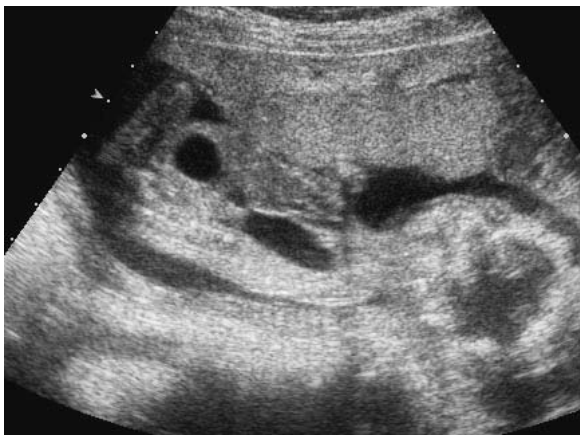

C

Figure 13–6 (A) Transverse view through the fetal abdomen in the third trimester, directly caudal to the fetal liver. Note the double bubble appearance of the bowel, consistent with duodenal atresia. **(B)** Second-trimester fetus with both duodenal and esophageal atresia. The transverse view through the abdomen shows a large C-shaped fluid collection typical of a distended stomach and duodenum in cases with duodenal atresia. **(C)** Longitudinal view of the same fetus with both duodenal and esophageal atresia showing the dilated esophagus.

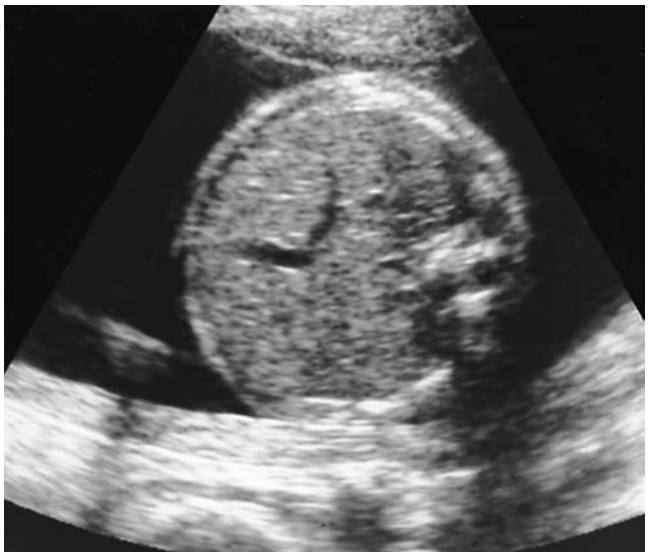

Figure 13–7 Transverse view through the fetal abdomen at the level of the stomach bubble. Note the absence of the stomach bubble in this image. This pregnancy was complicated by polyhydramnios, and the fetus had esophageal atresia at birth.

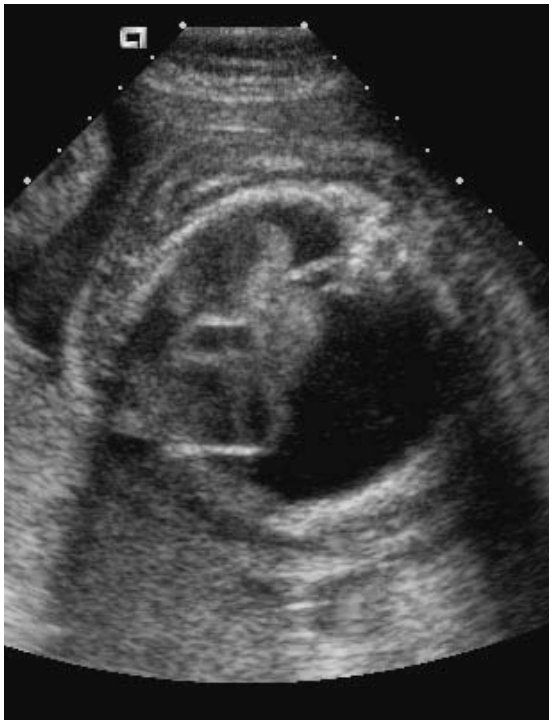

Figure 13–8 Longitudinal view of the fetal chest showing a bilateral pleural effusion, greater on the left. Note that the lungs appear very small.

proximal to the obstruction, such as proximal duodenum in duodenal atresia or the duodenum and stomach as well as proximal jejunum in jejunal atresia (**Fig. 13–5, Fig. 13–6**). More distal obstructions, such as anal atresia, may not be associated with polyhydramnios or marked bowel dilatation. Absence of the stomach bubble associated with polyhydramnios may be the result of a tracheoesophageal fistula, in particular, associated with esophageal atresia (**Fig. 13–7**).

Nonimmune hydrops is a condition almost always associated with polyhydramnios.[15] It is easily detected sonographically by a marked accumulation of fluid in various body cavities, such as ascites and pleural effusions, as well as marked skin edema (**Fig. 13–8, Fig. 13–9, Fig. 13–10, Fig. 13–11, Fig. 13–12**). There is a large number of etiologies for nonimmune hydrops, including heart abnormalities such as arrhythmias and cardiomyopathies, as well as chromosomal anomalies, infectious processes such as TORCH syndromes, fetal tumors, and so on. Nonimmune hydrops can be present

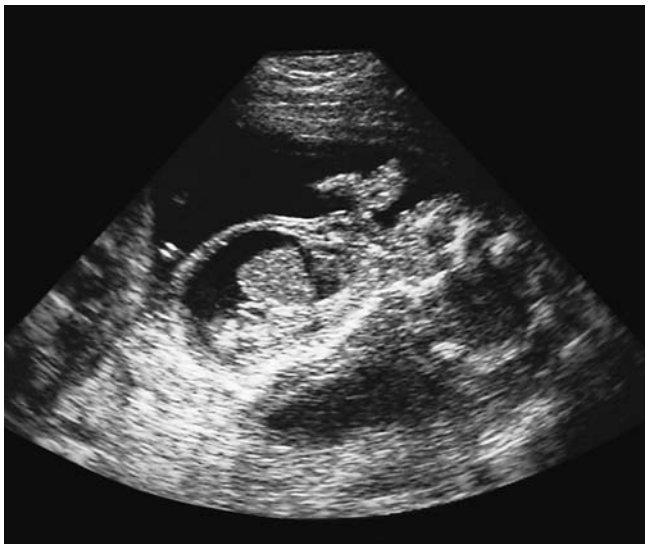

Figure 13–9 Longitudinal view of the fetal body showing marked ascites.

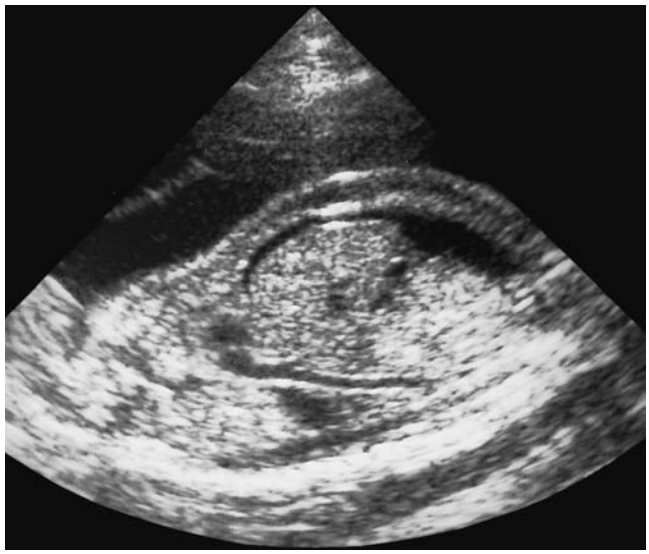

Figure 13–10 Longitudinal view of the fetal abdomen showing ascites in a fetus with hydrops. Note the skin edema.

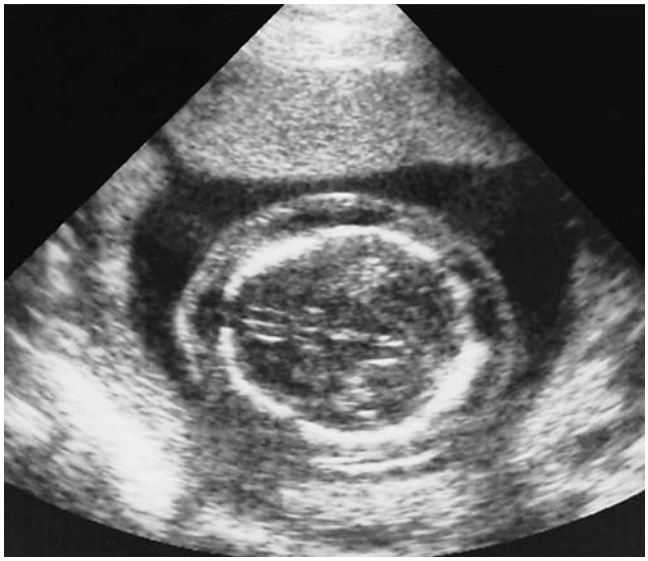

Figure 13–11 Transverse view through the fetal head, showing marked scalp edema throughout the entire scalp in a fetus with hydrops. Note the difference between the circumference of the head and the circumference of the outer aspect of the skin, caused by the edema.

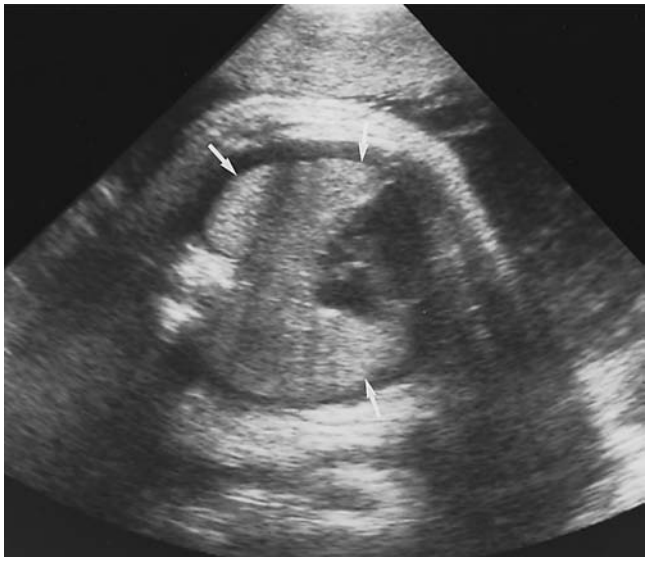

Figure 13–12 Transverse view through the fetal chest in a fetus with nonimmune hydrops. There are bilateral pleural effusions surrounding the fetal lungs (arrows), as well as marked soft tissue edema of the torso.

in twin pregnancies, particularly when associated with either twin-to-twin transfusion syndrome or acardiac twinning (where one twin is responsible for pumping blood throughout the entire placenta as well as through its abnormal co-twin, which does not have cardiac function). A detailed sonogram, including a fetal echocardiogram, is indicated when hydrops fetalis is detected. When hydrops is present, the fetus is considered very ill and the prognosis is guarded.[15] Workup includes umbilical blood sampling to aid in establishing a cause for the hydrops as well as to determine whether an early delivery is necessary if in utero treatment is not possible.

Hydrops may be secondary to fetal anemia, as in the patient whose exposure to the parvo virus has resulted in a reversible but profound fetal anemia, and in cases of isoimmune hydrops due to Rh or Kell incompatibility of the mother and fetus.[16] Massive fetal-to-maternal hemorrhage can also cause nonimmune hydrops. If fetal anemia is suspected clinically, Doppler of the middle cerebral artery to measure the blood flow velocity is the most effective noninvasive method of detecting anemia.[17] Once the middle cerebral artery Doppler is abnormal, umbilical blood sampling is necessary to determine the actual fetal hematocrit. Treatment, in the form of intrauterine transfusion, is indicated for those fetuses and can be completely lifesaving.

Central nervous system abnormalities are a common group of malformations that cause polyhydramnios.[8,18] Specific anomalies, most often associated with excess amniotic fluid, include open neural tube defects such as anencephaly, encephaloceles, and meningomyeloceles (**Fig. 13–13, Fig. 13–14**). Other central nervous system abnormalities, such as hydrocephalus, holoprosencephaly, and agenesis of the corpus callosum, have been associated with polyhydramnios, although these abnormalities may be secondary to the specific etiologies of the intracranial malformations, as in chromosomal abnormalities such as trisomy.[18]

Thoracic abnormalities, including diaphragmatic hernia and adenomatoid cystic malformation of the lung, invariably cause polyhydramnios, as do tracheal atresia and intrathoracic tumors such as teratomas (**Fig. 13–15, Fig. 13–16, Fig. 13–17**).[8] Isolated pleural effusions may be associated with polyhydramnios, although when polyhydramnios exists in association with pleural effusions, this is often an early stage of nonimmune hydrops.

Skeletal dysplasias may lead to nonimmune hydrops, thus to polyhydramnios as well.[19,20] This includes bone dysplasias such as spondyloepitheseal dysplasia congenita, camptomyelic dysplasia, thanatophoric dwarfism, and achondrogenesis (**Fig. 13–18**). Although the cause of the polyhydramnios in fetuses with dwarf syndromes is unclear, the enhanced acoustic window provided by the excess amniotic fluid improves our capability of studying the fetal limbs by ultrasound.

Chromosomal abnormalities such as trisomies 21, 18, and 13 are associated with polyhydramnios.[21] Fetuses with trisomy 21 may develop polyhydramnios because of duodenal atresia and/or congenital heart defects. Those with trisomy 18 are well known to develop the combination of intrauterine growth retardation and

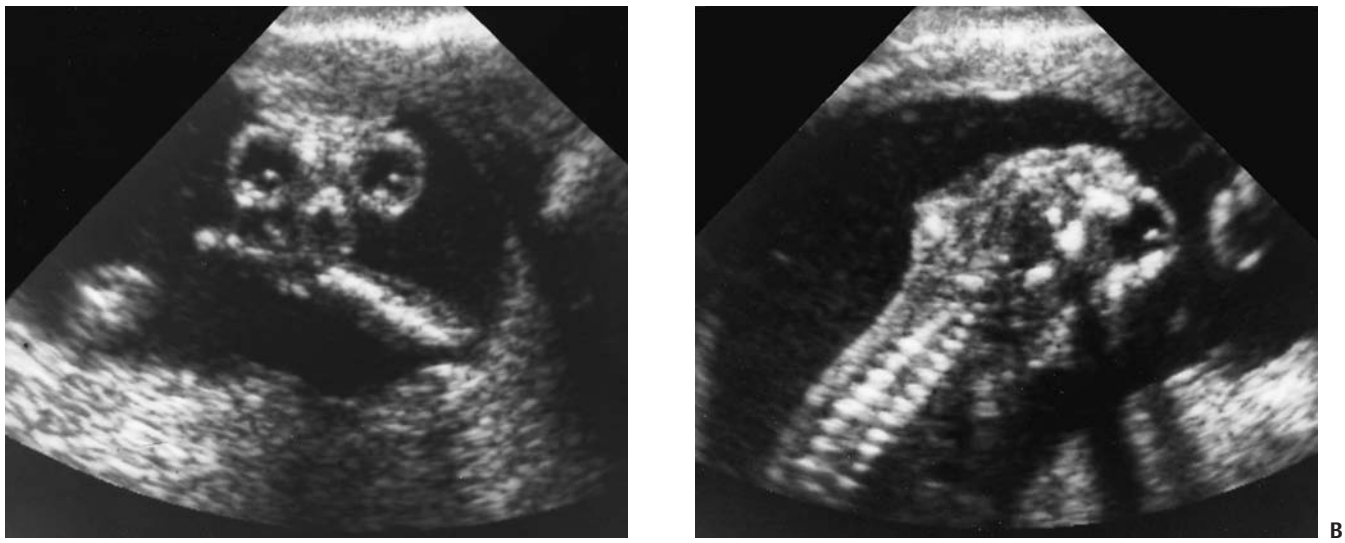

Figure 13–13 (A) Transvaginal view of the head of a fetus with anencephaly. Note the prominent orbits without any evidence of skull formation. **(B)** Longitudinal view of the same fetus, showing the relationship between the orbit and the cervical spine. Note the absence of the cranium.

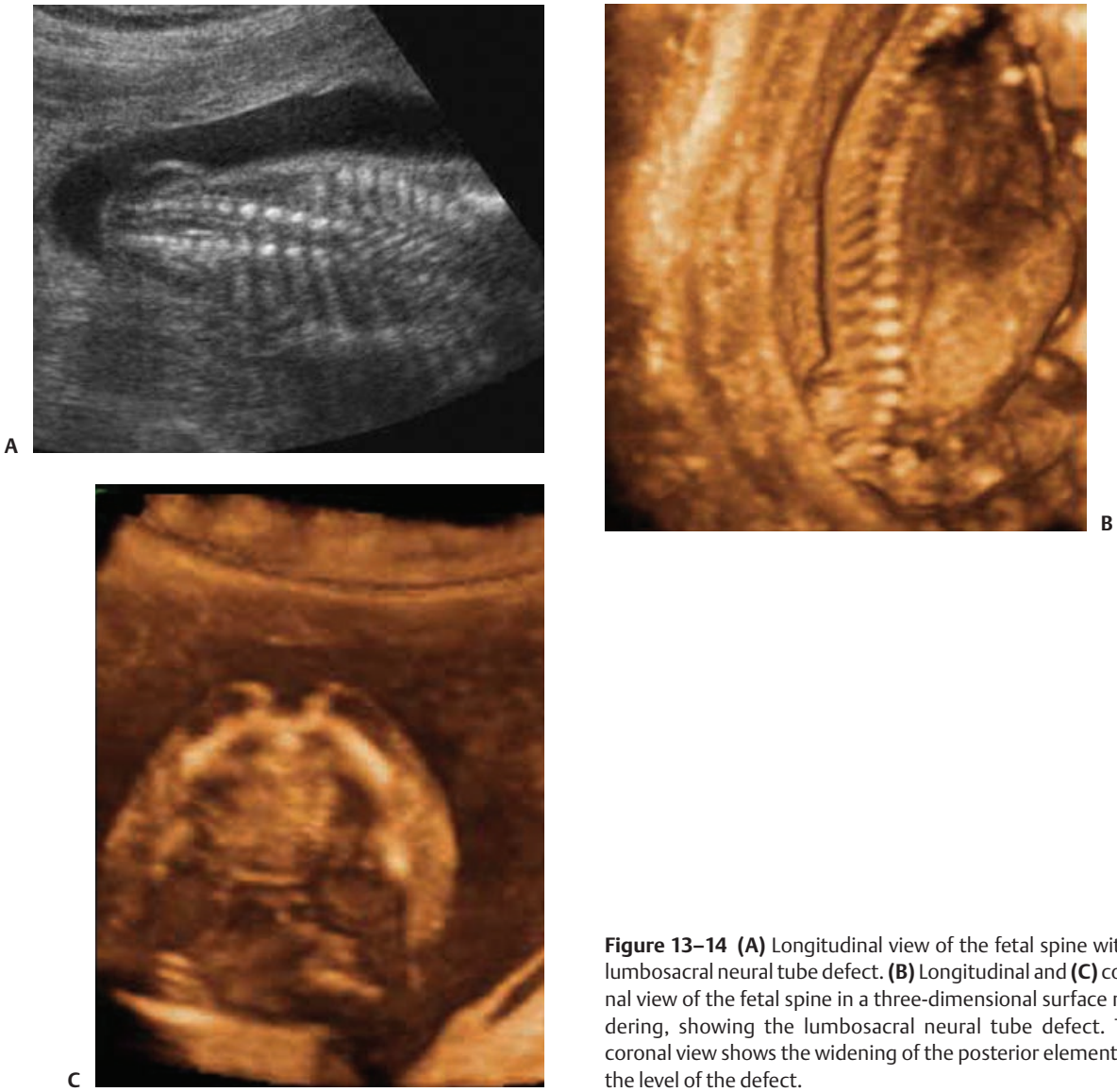

Figure 13–14 (A) Longitudinal view of the fetal spine with a lumbosacral neural tube defect. **(B)** Longitudinal and **(C)** coronal view of the fetal spine in a three-dimensional surface rendering, showing the lumbosacral neural tube defect. The coronal view shows the widening of the posterior elements at the level of the defect.

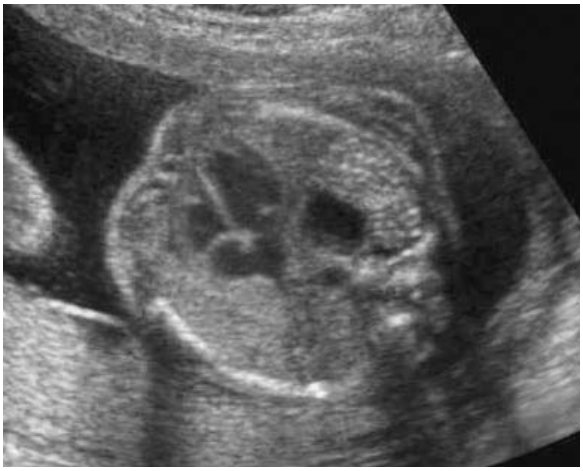

Figure 13–15 Transverse view through the fetal thorax of a late second-trimester fetus, showing a left diaphragmatic hernia. Note that the stomach is at the same level as the fetal heart, and small bowel is also noted in the left hemithorax.

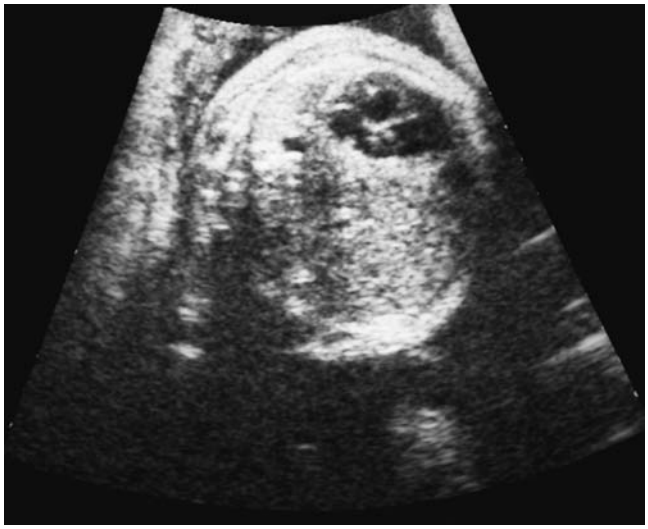

Figure 13–16 Transverse view through the fetal thorax showing a right diaphragmatic hernia. Note that the heart is displaced to the left by a part of the liver (arrows) in the right hemithorax.

polyhydramnios, which is often an indication for increased risk of a lethal trisomy. Fetuses with trisomy 13 and 9 are prone to having neural tube defects as well as major intracranial, facial, and multiorgan abnormalities, often leading to excess amniotic fluid volume (**Fig. 13–19, Fig. 13–20**). Even when these defects are discovered after 24 weeks' gestation, rapid karyotyping is required to aid in obstetrical management, particularly in cases of lethal trisomies (trisomies 13 and 18) so as to avoid unnecessary monitoring and operative delivery of nonviable fetuses.

Cardiac abnormalities have been associated with polyhydramnios, although most isolated cardiac malformations have normal amniotic fluid volumes (**Fig. 13–21**). The presence of polyhydramnios may be secondary to nonimmune hydrops in cases of arrhythmia or to congestive heart failure in cases of left heart outflow obstruction such as critical aortic stenosis.[22]

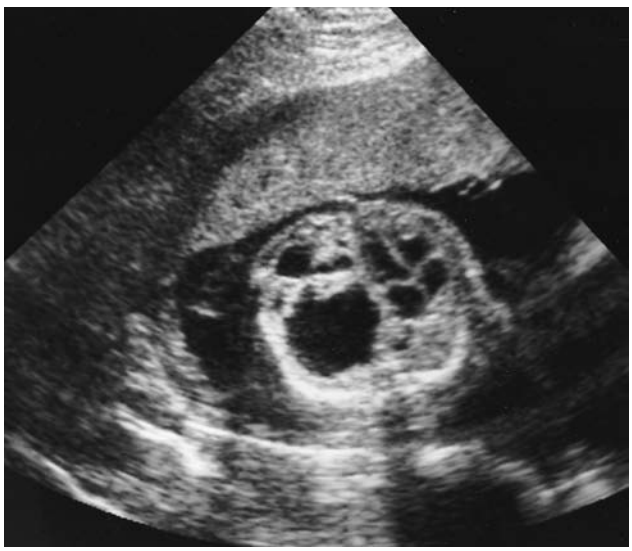

A

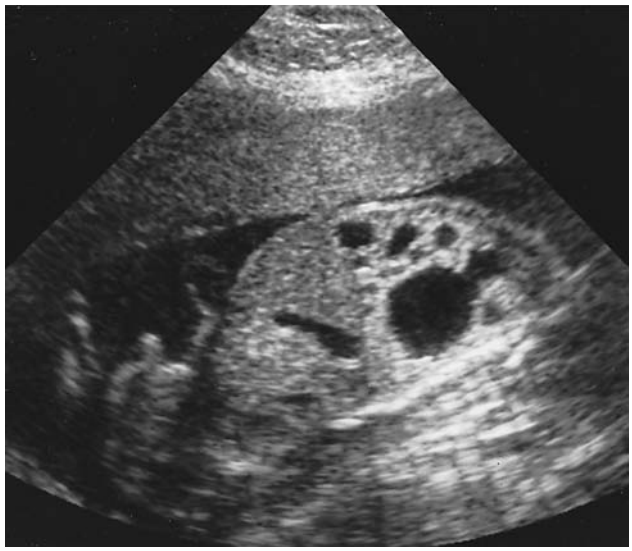

B

Figure 13–17 (A) Transverse and **(B)** longitudinal view of the thorax of a fetus with a type I cystic adenomatoid malformation of the lung. Note the cysts of different sizes, located in the left hemithorax and deviating the heart and mediastinum to the right.

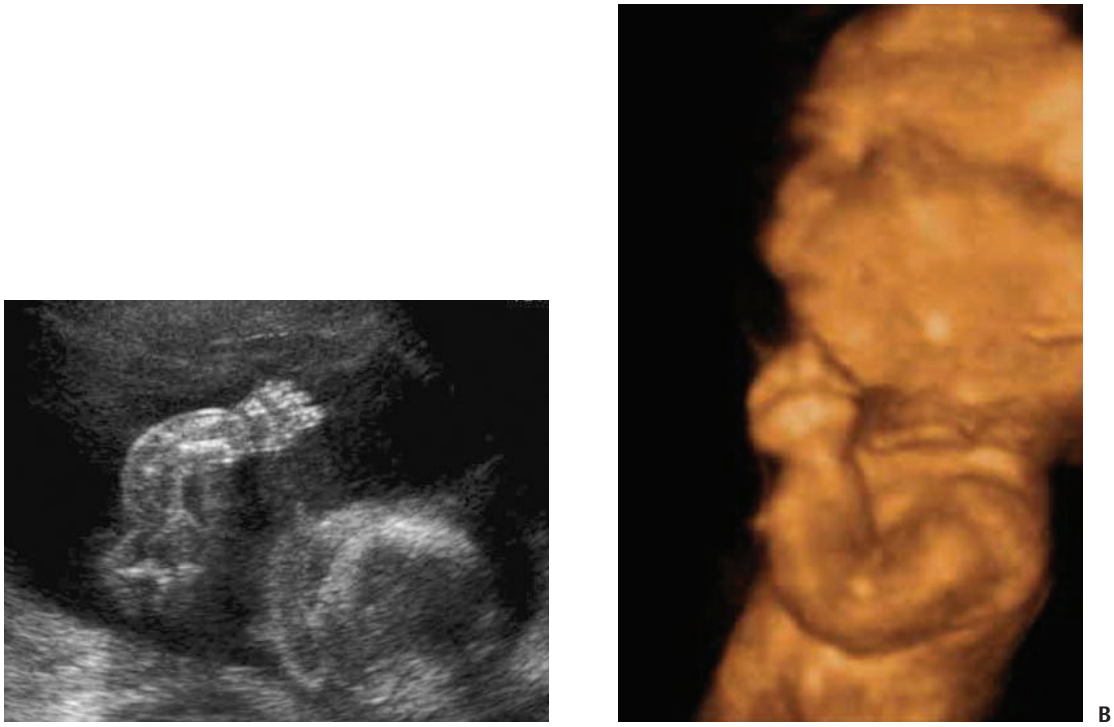

A B

Figure 13–18 (A) Fetal arm and side of the head in a fetus with thanatophoric dysplasia. **(B)** A three-dimensional surface reconstruction of the same fetus.

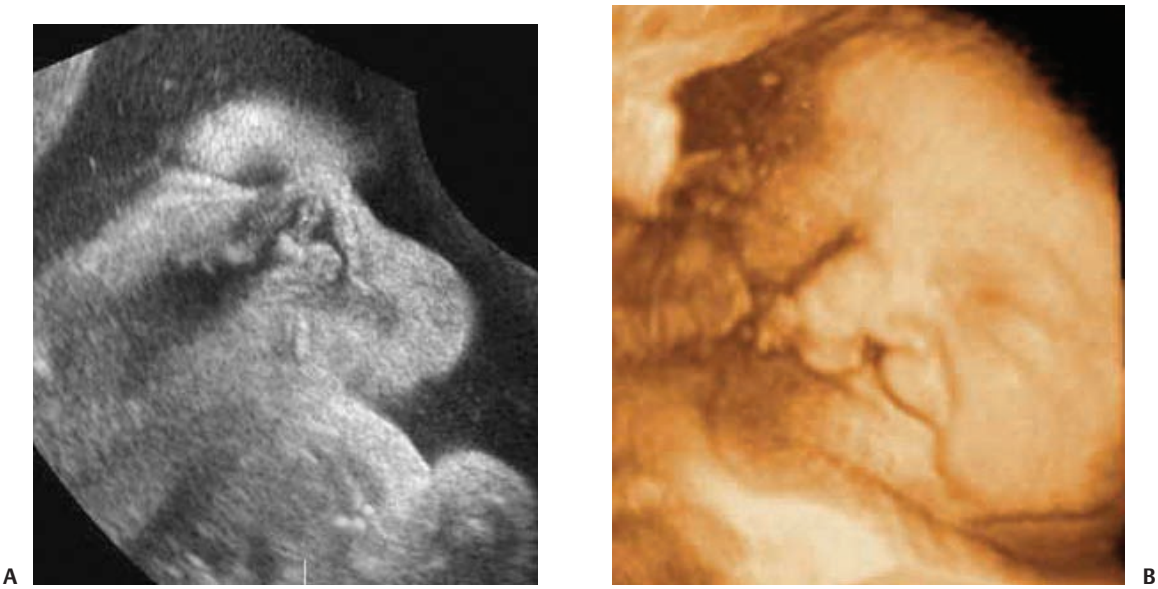

A B

Figure 13–19 (A) Coronal view of the fetal lower face in a fetus with a bilateral complete cleft lip and palate. **(B)** Same fetus with the facial cleft shown using three-dimensional surface reconstruction.

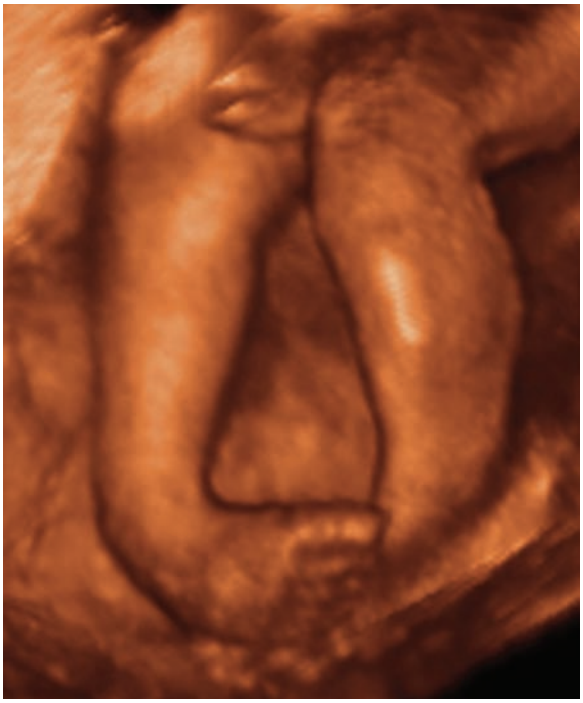

Figure 13–20 Longitudinal view of the fetal lower leg, using three-dimensional surface rendering, showing bilateral congenital clubbed foot.

Fetal tumors are rare, but can be a cause for an enlarged uterus and excess amniotic fluid volume (**Fig. 13–22, Fig. 13–23**). These tumors include sacrococcygeal teratomas, intracranial teratomas, large fetal liver hemangiomas, renal hamartomas, and even placental tumors such as chorioangiomas.[21–33] These can, in turn, lead to severe polyhydramnios associated with fetal hydrops and fetal vascular compromise. Cystic hygromas, lymphangiomas, as well as hemangiomas will also cause polyhydramnios. Any mass in the cervical region of the fetus is associated with polyhydramnios. The survival of such fetuses depends upon the location and type of tumor and the possibility of successful surgical resection. Other miscellaneous conditions sometimes associated with polyhydramnios include amniotic band syndrome, lethal multiple pterygium syndrome, facial clefts, and dysmorphia.[8]

The outcomes of fetuses who have malformations associated with polyhydramnios vary greatly, according to the types of lesions. In one study, the survival rate of all fetuses with polyhydramnios was 58%.[7] However, when idiopathic polyhydramnios was noted where no fetal abnormality could be seen sonographically, all fetuses survived. Several authors suggest that ultrasound is an excellent modality for the detection of malformations associated with polyhydramnios.[7–9,25] If no anomalies are found sonographically, the prognosis is good.[7–9,25] This is not surprising because the presence of excess amniotic fluid enhances the acoustic window for viewing fetal anatomy.

Large Masses in the Uterus

Other than polyhydramnios and multiple fetuses, large masses in the uterus can lead the clinician to detect a uterus that is larger than anticipated by gestational age. These masses include tumors such as molar pregnancies or partial moles with markedly enlarged and hydropic placentas or large chorioangiomas (**Fig. 13–24**). Tumors, such as large sacrococcygeal teratomas, will cause the uterus to enlarge because of both the tumor's size and the associated polyhydramnios (**Fig. 13–23**). Fetuses with nonimmune hydrops are also subject to having enlarged

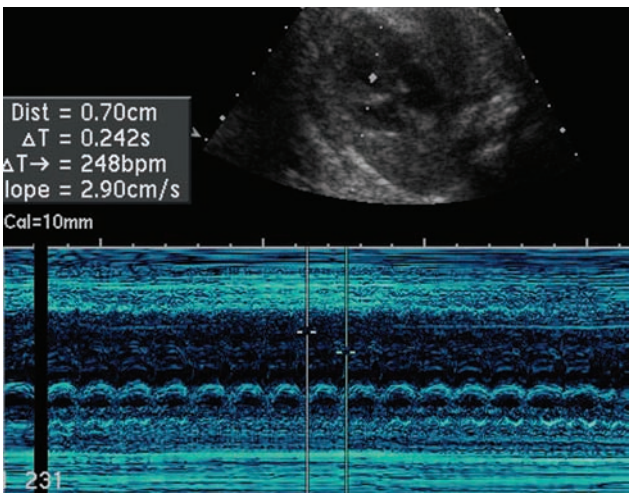

A

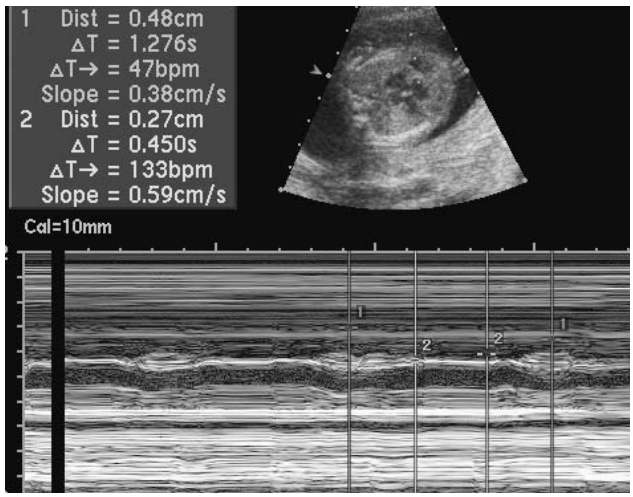

B

Figure 13–21 **(A)** M-Mode showing fetal tachycardia at 248 beats per minute. The diagnosis was supraventricular tachycardia. **(B)** M-mode showing complete heart block. Note that the atrial rate is 133, whereas the ventricular rate is 47. Both of these arrythmias can lead to heart failure and hydrops.

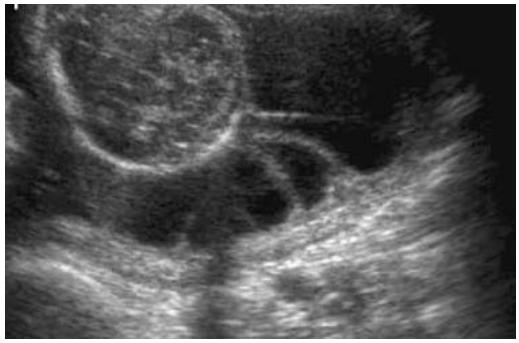

A

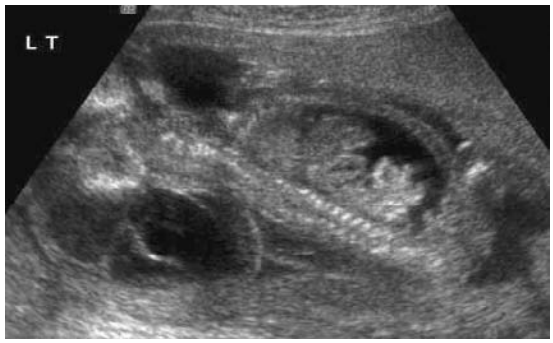

B

Figure 13–22 (A) Transverse view through the fetal head, showing large septated cystic hygromas of the nuchal region in a fetus with Turner's syndrome. **(B)** Longitudinal view of the same fetus showing the cystic hygromas as well as ascites and skin thickening consistent with lymphangiectasia.

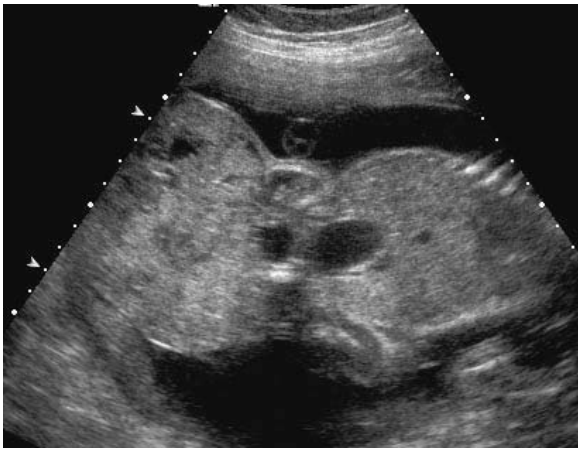

A

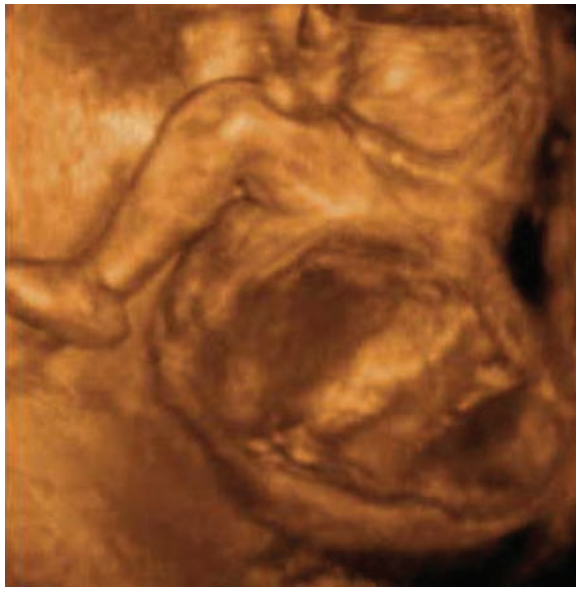

B

Figure 13–23 (A) Longitudinal view of the fetal body in the second trimester showing a large sacrococcygeal teratoma. The fetus is at risk for hydrops and polyhydramnios. **(B)** Same fetus seen using three-dimensional surface reconstruction showing the fetus sitting on the large sacral tumor.

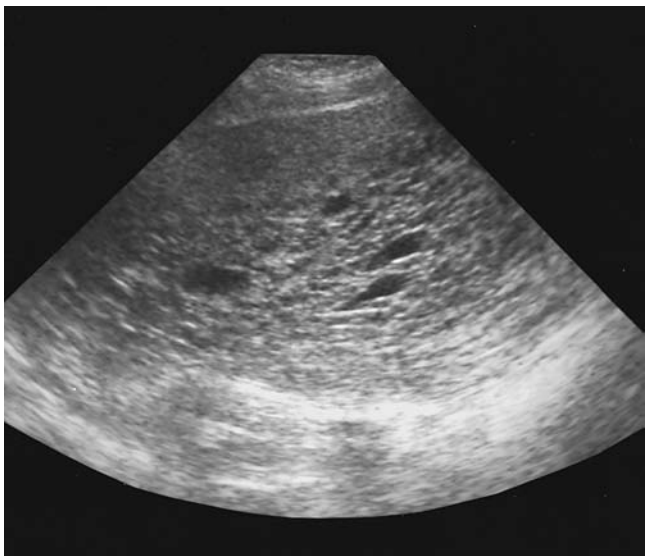

Figure 13–24 View of the uterus early in the second trimester showing no visible fetus. The uterus is filled with a solid mass with many small cystic spaces, typical of a complete mole.

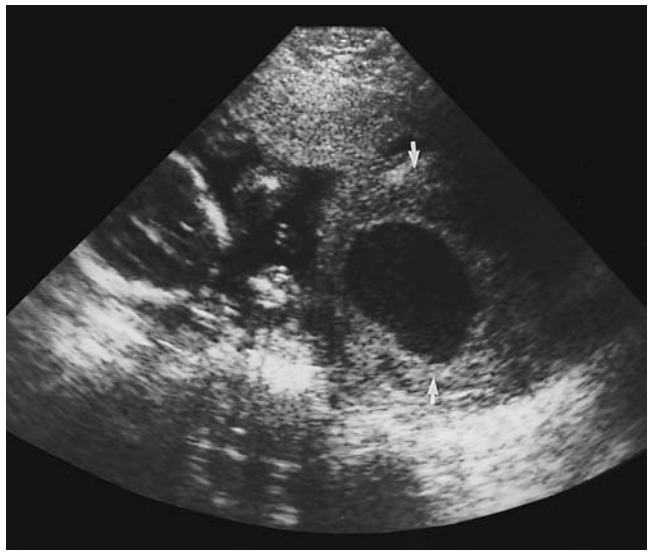

Figure 13–25 The uterus is larger than dates because of a cystic mass (arrows) in the wall of the uterus, typical of a degenerating fibroid.

placentas, which can contribute to the enlargement of the uterus. Pelvic masses not associated with the pregnancy may also lead to the clinical finding of an enlarged uterus. These include fibroid tumors, which can enlarge dramatically in the first part of pregnancy (**Fig. 13–25**). Also, adnexal masses such as ovarian cysts, dermoids, and other adnexal enlargements can result in the perception of an enlarged uterus by the clinician. Part of the evaluation of the pregnant uterus includes the assessment of the adnexa as well as the surrounding myometrium and cervix.

Summary

In conclusion, ultrasound is very successful at evaluating the pregnancy that is thought to be large for dates. In many cases, an explanation can be found (incorrect dates, multiple pregnancies, or a uterine fibroid). When polyhydramnios is detected, fetal biometry can be helpful to detect any growth acceleration leading to macrosomia, perhaps in a diabetic mother. A careful structural survey is necessary, however, when evaluating a fetus associated with polyhydramnios. When abnormalities are detected, it may be necessary to proceed with an amniocentesis or a percutaneous blood sampling for evaluation or treatment. In most cases, a normal structural survey, even in association with significant polyhydramnios, results in a good outcome.

References

1. Benirschke K, Kim CK. Multiple pregnancy part one. N Engl J Med 1973;288:1276–1284
2. Blickstein I. Review: the twin–twin transfusion syndrome. Obstet Gynecol 1990;76:714–722
3. Bromley B, Frigoletto FD, Estroff JA, Benacerraf BR. The natural history of oligohydramnios/polyhydramnios sequence in monochorionic diamniotic twins. Ultrasound Obstet Gynecol 1992;2:317–320
4. Hecher K, Plath H, Bregenzer T, Hansmann M, Hackeloer BJ. Endoscopic laser surgery versus serial amniocenteses in the treatment of severe twin–twin transfusion syndrome. Am J Obstet Gynecol 1999;180:717–724
5. Goldstein RB, Frilly RA. Sonographic estimation of amniotic fluid volume: subjective assessment versus pocket measurements. J Ultrasound Med 1988;7:363–367
6. Phelan JP, Ahn MO, Smith CV, Rutherford SE, Anderson E. Amniotic fluid index measurements during pregnancy. J Repro Med 1987; 32:601–604
7. Barkin SZ, Pretorius DH, Beckett MK, et al. Severe polyhydramnios: incidence of anomalies. AJR Am J Roentgenol 1987; 148:155–159
8. Damato N, Filly RA, Goldstein RB, et al. Frequency of fetal anomalies in sonographically detected polyhydramnios. J Ultrasound Med 1993;12:11–15
9. Stoll CG, Alembik Y, Dott B. Study of 156 cases of polyhydramnios and congenital malformations in a series of 118,265 consecutive births. Am J Obstet Gynecol 1991;165:586–590
10. Benson CB, Coughlin BF, Doubilet PM. Amniotic fluid volume in large-for-gestational-age fetuses of nondiabetic mothers. J Ultrasound Med 1991;10:149–151
11. Sohaey R, Nyberg DA, Sickler GK, Williams MA. Idiopathic polyhydramnios: association with fetal macrosomia. Radiology 1994; 190:393–396
12. Smith CV, Plambeck RD, Rayburn WF, Albaugh KJ. Relation of mild idiopathic polyhydramnios to perinatal outcome. Obstet Gynecol 1992;79:387–389
13. Pretorius DH, Drose JA, Dennis MA, Manchester DK, Manco-Johnson ML. Tracheoesophageal fistula in utero: 22 cases. J Ultrasound Med 1987;6:509–513
14. Heydanus R, Spaargaren MC, Wladimiroff JW. Prenatal ultrasonic diagnosis of obstructive bowel disease: a retrospective analysis. Prenat Diagn 1994;14:1035–1041
15. Hutchison AA, Drew JH, Yu VYH, et al. Nonimmunologic hydrops fetalis: a review of 61 cases. Obstet Gynecol 1982; 59:347–352
16. Chitkara U, Wilkins, Lynch L, Mehalek K, Berkowitz RL. The role of sonography in assessing severity of fetal anemia in Rh and Kell isoimmunized pregnancies. J Obstet Gynecol 1988;71:393–397
17. Mari G, Deter RL, Carpenter RL, et al. Noninvasive diagnosis by Doppler ultrasonography of fetal anemia due to maternal red-cell alloimmunization. Collaborative Group for Doppler Assessment of the Blood Velocity in Anemic Fetuses. N Engl J Med 2000;342: 9–14
18. Goldstein RB, Filly RA. Prenatal diagnosis of anencephaly: spectrum of sonographic appearances and distinction from the amniotic band syndrome. AJR Am J Roentgenol 1988;151:547–550
19. Pretorius DH, Rumack CM, Manco-Johnson ML, et al. Specific skeletal dysplasias in utero: sonographic diagnosis. Radiology 1986; 195:237–242
20. Wong WS, Filly RA. Polyhydramnios associated with fetal limb abnormalities. AJR Am J Roentgenol 1983;140:1001–1003
21. Brady K, Polzin WJ, Kopelman JN, Read JA. Risk of chromosomal abnormalities in patients with idiopathic polyhydramnios. Obstet Gynecol 1992;79:234–238
22. Jouppila P, Makarainen L, Rasanen J, Valkama M, Paavilainen T. Aggressive direct treatment of a fetus with supraventricular tachycardia and hydrops fetalis. Ultrasound Obstet Gynecol 1993;3: 279–283
23. Hubinont C, Bernard P, Khalil N, et al. Fetal liver hemangioma and chorioangioma: two unusual cases of severe fetal anemia detected by ultrasonography and its perinatal management. Ultrasound Obstet Gynecol 1994;4:330–331
24. Williams FL, Williams RA. Placental teratoma: prenatal ultrasonographic diagnosis. J Ultrasound Med 1994;13:587–589
25. Sivit CJ, Hill MC, Larsen JW, Lande IM. Second-trimester polyhydramnios: evaluation with US. Radiology 1987;165: 467–469
26. Tonkin IL, Setzer ES, Ermocilla R. Placental chorioangioma: a rare cause of congestive heart failure and hydrops fetalis in the newborn. AJR Am J Roentgenol 1980;134:181–183
27. Treadwell MC, Sepulveda W, LeBlanc LL, Romero R. Prenatal diagnosis of fetal cutaneous hemangioma: case report and review of the literature. J Ultrasound Med 1993;12:683–687
28. Kangarloo H, Diament MJ. Diagnostic oncology case study: cervical mass in a fetus associated with maternal hydramnios. AJR Am J Roentgenol 1983;140:507–509
29. Chervanak FA, Isaacson G, Blakemore KJ, et al. Fetal cystic hygroma: cause and natural history. N Engl J Med 1983;309: 822–825

30. Perez-Aytes A, Sanchis N, Barbal A, et al. Short communication: non-immunological hydrops fetalis and intrapericardial teratoma: case report and review. Prenat Diagn 1995;15:859–863
31. Chervenak FA, Tortora M, Moya FR, Hobbins JC. Antenatal sonographic diagnosis of epignathus. J Ultrasound Med 1984;3:235–237
32. Benacerraf BR, Frigoletto FD. Prenatal sonographic diagnosis of isolated congenital cystic hygroma, unassociated with lymphedema or other morphologic abnormality. J Ultrasound Med 1987;6:63–66
33. Gross SJ, Benzi RJ, Sermer M, Skidmore MB, Wilson SR. Sacrococcygeal teratoma: prenatal diagnosis and management. Am J Obstet Gynecol 1987;156:393–396

14 Uterine Size Less than Dates: A Clinical Dilemma

Alfred Abuhamad

Accurate pregnancy dating is the most important step in prenatal management. Precise knowledge of gestational age is essential for the management of high-risk pregnancies and, in particular, fetal growth restriction. Although uterine size, as measured by the fundal height, provides a subjective assessment of the fetal size, ultrasound plays an integral and more precise role in confirming gestational age and has been shown to have an accuracy of 3 to 4 days when performed between 14 and 22 weeks of gestation.[1]

Several definitions exist in the literature for the diagnosis of intrauterine growth restriction (IUGR). The definition that is most commonly used in clinical practice is an estimated fetal weight at less than the 10th percentile for gestational age. At this diagnostic threshold, ~70% of fetuses will be small for gestational age (constitutionally small) and have no increase in perinatal morbidity or mortality.[2] Using the fifth percentile as a cutoff for the diagnosis of IUGR may be more clinically applicable, given that perinatal morbidity and mortality have been shown to increase beyond this threshold.[3] Of all the ultrasound-derived biometric parameters, the abdominal circumference is the most sensitive indicator for growth restriction in the fetus. An abdominal circumference of less than the 2.5th percentile for gestational age carries a sensitivity of greater than 95% for the diagnosis of IUGR.[4,5] The growth profile of the abdominal circumference should therefore be monitored closely in fetuses at risk for growth abnormalities. Furthermore, when estimating fetal weights by ultrasound, the appropriate growth curves should be used. Curves generated at high altitudes will underestimate IUGR by ~50% for sea-level populations.[6]

When compared with appropriately grown fetuses matched for gestational age, IUGR fetuses have an increased risk of perinatal morbidity and mortality.[7] Long-term follow-up studies have shown an increased incidence of physical handicap and neurodevelopmental delay in growth-restricted fetuses.[8,9] The presence of chronic metabolic acidemia in utero, rather than actual birth weight, appears to be the best predictor of long-term neurodevelopmental delay.[10] In pregnancies with growth-restricted fetuses, timing of the delivery is the most critical step in clinical management. Balancing the risk of prematurity with the risk of long-term neurodevelopmental delay is a serious challenge facing physicians involved in the care of these pregnancies.

Traditionally, the management of pregnancies with fetal growth restriction relied on cardiotocography for fetal surveillance. During cardiotocography, the physician looks for heart rate variability as a sign of fetal well-being. Heart rate variability is the final result of the rhythmic, integrated activity of autonomic neurons generated by organized cardiorespiratory reflexes.[11] In growth-restricted fetuses, higher baseline rates, decreased long- and short-term variability, and delayed maturation of reactivity are seen in heart rate tracings.[12,13] These studies have relied on computer-generated analyses of fetal heart rate tracings in their evaluation. Unaided visual analyses of fetal heart rate records show limited reliability and reproducibility.[14,15] Furthermore, the presence of overtly abnormal patterns of fetal heart rate tracings represents late signs of fetal deterioration.[16,17] Relying on unaided visual analysis of cardiotocography as the only test of fetal surveillance in growth-restricted fetuses has come under criticism recently because it represents late signs of fetal deterioration and thus its sole use may not optimize long-term outcome of these pregnancies.

Doppler ultrasound has been shown to improve outcome in high-risk pregnancies.[18] The use of Doppler ultrasound in the management of pregnancies with fetal growth restriction has received significant attention in the recent literature. Several cross-sectional and longitudinal studies have highlighted the fetal cardiovascular adaptation to hypoxemia and the progressive stages of such adaptation.[19–24] Findings from these studies and the use of Doppler ultrasound in the management of the growth-restricted fetus are discussed in the following section.

Ultrasound Evaluation

Fetal Arterial Doppler Ultrasound of the Umbilical Circulation

The umbilical arterial circulation is normally a low impedance circulation (**Fig. 14–1**) with an increase in the amount of end diastolic flow with advancing gestation.[25] Umbilical arterial Doppler waveforms reflect the status of the pla-

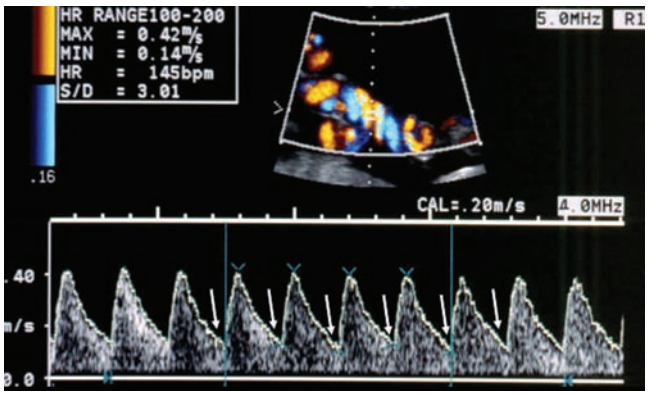

Figure 14–1 Normal Doppler waveforms obtained from the umbilical artery in the third trimester. In the third trimester of pregnancy, the umbilical circulation is a low impedance circulation. Note the increased amount of flow at end diastole (white arrows).

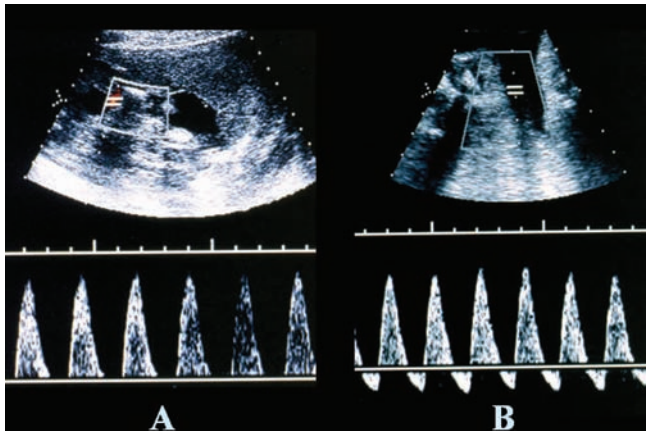

Figure 14–2 (A) Absent end-diastolic velocity and **(B)** reversed end-diastolic velocity are noted in the umbilical circulation when the downstream impedance is increased. These Doppler waveforms are associated with significant fetal compromise.

cental circulation, and the increase in end diastolic flow that is seen with advancing gestation is a direct result of an increase in the number of tertiary stem villi that takes place with placental maturation.[26] Diseases that obliterate small muscular arteries in placental tertiary stem villi result in a progressive decrease in end-diastolic flow in the umbilical arterial Doppler waveforms until absent and then reverse flow during diastole is noted[27] (**Fig. 14–2**). Reversed diastolic flow in the umbilical arterial circulation represents an advanced stage of placental compromise and is associated with more than 70% of placental arterial obliteration.[28,29] The presence of absent or reversed end diastolic flow in the umbilical artery is commonly associated with severe intrauterine growth restriction and oligohydramnios.[30]

Doppler waveforms of the umbilical arteries can be obtained from any segment along the umbilical cord. Waveforms obtained from the placental end of the cord show more end diastolic flow than waveforms obtained from the abdominal cord insertion.[31] Differences in Doppler indices of arterial waveforms obtained from different anatomical locations of the same umbilical cord are generally minor and have no significance on clinical practice.[25]

Fetal Arterial Doppler Ultrasound of the Middle Cerebral Circulation

The cerebral circulation is normally a high impedance circulation with continuous forward flow throughout the cardiac cycle.[32] The middle cerebral artery is the most accessible cerebral vessel to ultrasound imaging in the fetus and it carries more than 80% of cerebral blood flow.[33] In the presence of fetal hypoxemia, central redistribution of blood flow occurs, resulting in increased blood flow to the brain, heart, and adrenals and a reduction in flow to the peripheral and placental circulations. This blood flow redistribution is known as the brain-sparing reflex and plays a major role in fetal adaptation to oxygen deprivation.[32,34]

The right and left middle cerebral arteries represent major branches of the circle of Willis in the fetal brain. The circle of Willis, which is supplied by the internal carotids and vertebral arteries, can be imaged with color flow Doppler ultrasound in a transverse plane of the fetal head obtained at the base of the skull. In this transverse plane, the proximal and distal middle cerebral arteries are seen in their longitudinal view, with their course almost parallel to the ultrasound beam (**Fig. 14–3**). Middle cerebral artery Doppler waveforms, obtained from the proximal portion of

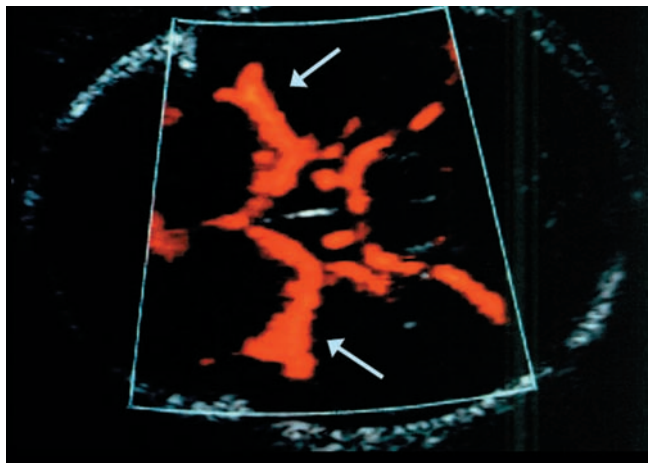

Figure 14–3 Axial view of the fetal head in the second trimester with color Doppler showing the circulation at the level of the circle of Willis. Note the course of the middle cerebral arteries, almost parallel to the ultrasound beam (white arrows).

the vessel, immediately after its origin from the circle of Willis, have shown the best reproducibility.[35]

Fetal Arterial Doppler Ultrasound and Fetal Growth Restriction

Central redistribution of blood flow to the brain, known as the brain-sparing reflex, represents an early stage in fetal adaptation to hypoxemia[21–24] and follows the lag in fetal growth.[36] At this early stage, the brain-sparing reflex is clinically evident by increased end-diastolic flow in the middle cerebral artery (lower middle cerebral artery pulsatility or resistance index) and decreased end-diastolic flow in the umbilical artery (higher umbilical artery resistance index or systolic:diastolic ratio). The cerebroplacental ratio, derived by dividing the cerebral resistance index by the umbilical resistance index, defines the brain-sparing reflex and has been shown to predict outcome in IUGR fetuses at less than 34 weeks of gestation.[19,37–39]

In the presence of IUGR, Doppler changes in the umbilical artery precede the decrease in cerebroplacental ratio and middle cerebral artery pulsatility or resistance index.[21,36] Furthermore, middle cerebral artery Doppler waveforms are of clinical value in differentiating a growth restricted/hypoxemic fetus from a constitutionally small/normoxemic fetus. In the clinical setting of a small for gestational age fetus, the presence of normal middle cerebral artery Doppler waveforms, obtained at less than 32 weeks of gestation, has a 97% negative predictive value for major adverse perinatal outcomes.[41]

Several studies have shown that this early stage of arterial redistribution is not associated with the presence of fetal metabolic acidemia.[21–24] It is therefore inferred that infants delivered at this early stage of fetal adaptation are expected to have no adverse long-term neurodevelopmental complications.

Fetal Venus Doppler Ultrasound and Fetal Growth Restriction

Chronic fetal hypoxemia results in decreased preload, decreased cardiac compliance, and elevated end-diastolic pressure in the right ventricle.[20,41–44] These changes are evidenced by an elevated central venous pressure in the chronically hypoxemic fetus, which is manifested by increased reverse flow in Doppler waveforms of the inferior vena cava and the ductus venosus during late diastole (**Fig. 14–4**). Changes in the fetal central venous circulation are associated with an advanced stage of fetal hypoxemia. At this late stage of fetal adaptation to hypoxemia, cardiac decompensation is often noted with myocardial dysfunction.[43] Furthermore, fetal metabolic acidemia is often present in association with Doppler waveform abnormalities of the inferior vena cava and ductus venosus.[16,20,21]

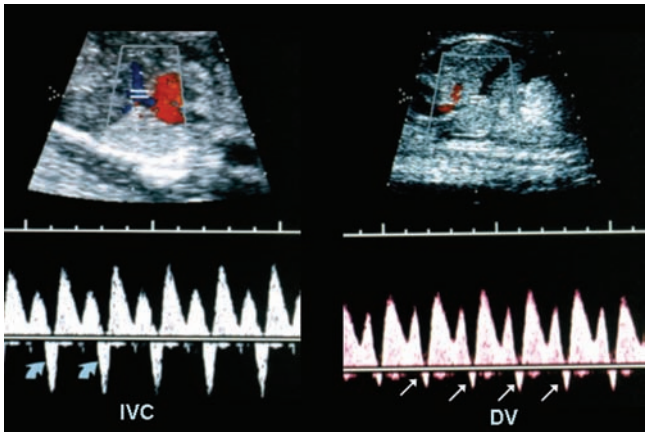

Figure 14–4 Doppler velocimetric waveforms of the inferior vena cava (IVC) and the ductus venosus (DV) in a fetus with severe growth restriction. Note the increased amount of reverse flow during the atrial kick in the IVC and the DV (arrows).

Fetal Doppler Ultrasound Findings in Intrauterine Growth-Restricted Fetuses

In clinical practice, Doppler ultrasound provides important information on the extent of fetal compromise and thus may aid in the timing of delivery in IUGR fetuses. Arterial Doppler abnormalities, at the level of the umbilical and middle cerebral arteries (brain-sparing reflex), confirm the presence of hypoxemia in the growth-restricted fetus and present early warning signs. Once arterial centralization occurs, however, no clear trend is noted in the observational period and thus arterial redistribution may not be helpful for the timing of the delivery.[45–47] On the other hand, the presence of reversed diastolic flow in the umbilical arteries is a sign of advanced fetal compromise, and strong consideration should be given for delivery except for extreme prematurity. Cesarean section should be given preference in this setting because labor may cause further fetal compromise.

The current literature is suggestive that venous Doppler abnormalities in the inferior vena cava and ductus venosus and abnormal fetal heart rate monitoring, even in its computerized version, follow arterial Doppler abnormalities and are thus associated with a more advanced stage of fetal compromise.[21–24,48]

Furthermore, in the majority of severely growth restricted fetuses, sequential deterioration of arterial and venous Doppler precedes biophysical profile score deterioration.[22] At least one third of fetuses show early signs of circulatory deregulation 1 week before biophysical profile deterioration and that, in most cases, Doppler deterioration preceded biophysical profile deterioration by 1 day.[22]

The occurrence of such abnormal late-stage changes of vascular adaptation by the IUGR fetus appears to be the best predictor of perinatal death, independent of

gestational age and weight.[24] In a longitudinal study on Doppler and IUGR fetuses, all intrauterine deaths and all neonatal deaths, with the exception of one case, had late Doppler changes at the time of delivery, whereas only a few of the surviving fetuses showed such changes.[24]

This sequential deterioration of the hypoxemic, growth-restricted fetus is rarely seen at gestations beyond 34 weeks.[36,49] Indeed, normal umbilical artery Doppler is common in growth-restricted fetuses in late gestations, and cerebroplacental ratios have poor correlation with outcome of IUGR fetuses at greater than 34 weeks of gestation.[19] Caution should therefore be exercised when Doppler is used in the clinical management of IUGR fetuses beyond 34 weeks of gestation.

The pathophysiology of fetal growth restriction has not been fully described because recent studies have highlighted the presence of significant variation in fetal adaptation to hypoxemia. The pattern of incremental deterioration of arterial Doppler abnormalities, followed by venous Doppler abnormalities, then followed by fetal heart tracings and biophysical profile abnormalities, is not seen by ~20% of preterm fetuses.[21] Furthermore, only 70% of IUGR fetuses show significant deterioration of all vascular beds by the time they are delivered and ~10% show no significant circulatory change by delivery time.[22] In a recent prospective, observational study, more than 50% of IUGR fetuses delivered because of abnormal fetal heart rate tracings that did not have venous Doppler abnormalities.[24] In view of these findings, the universal introduction of venous Doppler in the clinical management of the growth-restricted fetus should await the results of randomized trials on this subject.

It is currently evident that fetal growth restriction is a complex disorder involving multiple fetal organs and systems.[50] Although fetal biometry and arterial Doppler provide information on the early compensatory phase of this disorder, venous Doppler, fetal heart rate analysis, and the biophysical profile provide information on the later stages commonly associated with fetal cardiovascular collapse. It is hoped that future studies will shed more light on the pathophysiology of this disease and on the various interactions of diagnostic tools in fetal surveillance.

References

1. Chervenak FA, Skupski DW, Romero R, et al. How accurate is fetal biometry in the assessment of fetal age? Am J Obstet Gynecol 1998;178:228–237
2. Ott WJ. The diagnosis of altered fetal growth. Obstet Gynecol Clin North Am 1988;15:237–263
3. Manning FA. Intrauterine growth restriction: diagnosis, prognostication, and management based on ultrasound methods. In: Manning FA, ed. Fetal Medicine: Principles and Practice. Norwalk, CT: Appleton & Lange; 1995:87–94
4. Hadlock FP, Deter RL, Harrist RB, Roecker E, Park SK. A date-independent predictor of intrauterine growth retardation: femur length/abdominal circumference ration. AJR Am J Roentgenol 1993;141:979–984
5. Brown HL, Miller JM Jr, Gabert HA, Kissling G. Ultrasonic recognition of the small-for-gestational-age fetus. Obstet Gynecol 1987;69:631–635
6. Creasy RK, Resnick R. Intrauterine growth retardation. In: Creasy RK, Resnick R, eds. Maternal Fetal Medicine: Principles and Practice. Philadelphia: Saunders; 1984:491ff
7. Bernstein IM, Horbar JD, Badger GJ, Ohlsson A, Golan A. Morbidity and mortality among very-low-birth weight neonates with intrauterine growth restriction. Am J Obstet Gynecol 2000;182; 198–202
8. Kok JH, den Ouden AL, Verloove-Vanhorick SP, Brand R. Outcome of very preterm small for gestational age infants: the first nine years of life. Br J Obstet Gynaecol 1998;105:162–168
9. Fattal-Valevski A, Leitner Y, Kutai M, et al. Neurodevelopmental outcome in children with intrauterine growth retardation: a 3-year follow-up [abstract]. J Child Neurol 1999;14:724–727
10. Soothill PW, Ajayi RA, Campbell S, et al. Relationship between fetal academia at cordocentesis and subsequent neurodevelopment. Ultrasound Obstet Gynecol 1992;2:80–83
11. Hanna BD, Nelson MN, White-Traut RC, et al. Heart rate variability in preterm brain-injured and very-low-birth-weight infants. Biol Neonate 2000;77:147–155
12. Nijhuis IJ, ten Hof J, Mulder EJ, et al. Fetal heart rate in relation to its variation in normal and growth retarded fetuses. Eur J Obstet Gynecol Rep Biol 2000;89:27–33
13. Vindla S, James D, Sahota D. Computerised analysis of unstimulated and stimulated behaviour in fetuses with intrauterine growth restriction. Eur J Obstet Gynecol Rep Biol 1999;83:37–45
14. Devoe L, Golde S, Kilman Y, Morton D, Shea K, Waller J. A comparison of visual analyses of intrapartum fetal heart rate tracings according to the new National Institute of Child Health and Human Development guidelines with computer analyses by an automated fetal heart rate monitoring system. Am J Obstet Gynecol 2000;183:361–366
15. Bracero LA, Roshanfekr D, Byrne DW. Analysis of antepartum fetal heart rate tracing by physician and computer. J Matern Fetal Med 2000;9:181–185
16. Hecher K, Hackelöer B. Cardiotocogram compared to Doppler investigation of the fetal circulation in the premature growth-retarded fetus: longitudinal observations. Ultrasound Obstet Gynecol 1997;9:152–160
17. Ribbert LS, Visser GH, Mulder EJ, Zonneveld MF, Morssink LP. Changes with time in fetal heart rate variation, movement incidences and haemodynamics in intrauterine growth retarded fetuses: a longitudinal approach to the assessment of fetal well being. Early Hum Dev 1993;31:195–208
18. Zarko A, Neilson JP. Doppler ultrasonography in high-risk pregnancies: systematic review with meta-analysis. Am J Obstet Gynecol 1995;172:1379–1387
19. Bahado-Singh RO, Kovanci E, Jeffres A, et al. The Doppler cerebroplacental ratio and perinatal outcome in intrauterine growth restriction. Am J Obstet Gynecol 1999;180:750–756
20. Rizzo G, Capponi A, Talone PE, Arduini D, Romanini C. Doppler indices from inferior vena cava and ductus venosus in predicting pH and oxygen tension in umbilical blood at cordocentesis in growth-retarded fetuses. Ultrasound Obstet Gynecol 1996;7:401–410
21. Baschat AA, Gembruch U, Reiss I, Gortner L, Weiner CP, Harman CR. Relationship between arterial and venous Doppler and perinatal outcome in fetal growth restriction. Ultrasound Obstet Gynecol 2000;16:407–413
22. Baschat AA, Gembruch U, Harman CR. The sequence of changes in Doppler and biophysical parameters as severe fetal growth restriction worsens. Ultrasound Obstet Gynecol 2001;18:571–577

23. Hecher K, Bilardo CM, Stigter RH, et al. Monitoring of fetuses with intrauterine growth restriction: a longitudinal study. Ultrasound Obstet Gynecol 2001;18:564–570
24. Ferrazzi E, Bozzo M, Rigano S, et al. Temporal sequence of abnormal Doppler changes in the peripheral and central circulatory systems of the severely growth-restricted fetus. Ultrasound Obstet Gynecol 2002;19:140–146
25. Fleischer A, Schulman H, Farmakides G, Bracero L, Blattner P, Randolph G. Umbilical artery waveforms and intrauterine growth retardation. Am J Obstet Gynecol 1985;151:502–505
26. Giles WB, Trudinger BJ, Baird PJ. Fetal umbilical artery flow velocity waveforms and placental resistance: pathological correlation. Br J Obstet Gynaecol 1987;157:900–902
27. Trudinger BJ, Stevens D, Connelly A, et al. Umbilical artery flow velocity waveforms and placental resistance: the effect of embolizations of the umbilical circulation. Am J Obstet Gynecol 1987; 157:1443–1448
28. Kingdom JC, Burrell SJ, Kaufmann P. Pathology and clinical implications of abnormal umbilical artery Doppler waveforms. Ultrasound Obstet Gynecol 1997;9:271–286
29. Morrow RJ, Adamson SL, Bull SB, Ritchie JW. Effect of placental embolization on the umbilical arterial velocity waveform in fetal sheep. Am J Obstet Gynecol 1989;161:1055–1060
30. Copel JA, Reed KL. Doppler Ultrasound in Obstetrics and Gynecology. New York: Raven Press; 1995:187–198
31. Trudinger BJ. Doppler ultrasonography and fetal well-being. In: Reece EA, Hobbins JC, Mahoney M, Petrie RH, eds. Medicine of the Fetus and Mother. Philadelphia: JB Lippincott; 1992:701–723
32. Mari G, Deter RL. Middle cerebral artery flow velocity waveforms in normal and small-for-gestational age fetuses. Am J Obstet Gynecol 1992;166:1262–1270
33. Veille JC, Hanson R, Tatum K. Longitudinal quantitation of middle cerebral artery blood flow in normal human fetuses. Am J Obstet Gynecol 1993;169:1393–1398
34. Berman RE, Less MH, Peterson EN, Delannoy CW. Distribution of the circulation in the normal and asphyxiated fetal primate. Am J Obstet Gynecol 1970;108:956–969
35. Mari G, Abuhamad AZ, Brumfield J, Ferguson JE III. Doppler ultrasonography of the middle cerebral artery peak systolic velocity in the fetus: reproducibility of measurement [abstract #669]. Am J Obstet Gynecol 2001;185:261
36. Harrington K, Thompson MO, Carpenter RG, et al. Doppler fetal circulation in pregnancies complicated by pre-eclampsia or delivery of a small for gestational age baby, II: Longitudinal analysis. Br J Obstet Gynaecol 1999;106:453–466
37. Wladimoroff JW, van den Wijingaard JAGN, Degani S, Noordam MJ, van Eyck J, Tonge HM. Cerebral and umbilical arterial blood flow velocity waveforms in normal and growth retarded pregnancies: a comparative study. Obstet Gynecol 1987;69:705–709
38. Gramellini D, Folli MC, Raboni S, Vadora E, Marialdi A. Cerebral-umbilical Doppler ratio as a predictor of adverse perinatal outcome. Obstet Gynecol 1992;74:416–420
39. Arduini D, Rizzo G. Prediction of fetal outcome in small for gestational age fetuses: comparison of Doppler measurements obtained from different fetal vessels. J Perinat Med 1992;20:29–38
40. Fong KW, Ohlsson A, Hannah ME, et al. Prediction of perinatal outcomes in fetuses suspected to have intrauterine growth restriction: Doppler US study of fetal cerebral, renal and umbilical arteries. Radiology 1999;213:681–689
41. Rizzo G, Arduini D. Fetal cardiac function in intrauterine growth retardation. Am J Obstet Gynecol 1991;165:876–882
42. Chang CH, Chang FM, Yu CH, Liang RI, Ko HC, Chen HY. Systemic assessment of fetal hemodynamics by Doppler ultrasound. Ultrasound Med Biol 2000;26:777–785
43. Mäkikallio K, Vuolteenaho O, Jouppila P, Räsänen J. Ultrasonographic and biochemical markers of human fetal cardiac dysfunction in placental insufficiency. Circulation 2002;:2058–2062
44. Tsyvian P, Malkin K, Wladimiroff JY. Assessment of mitral a-wave transit time to cardiac outflow tract and isovolumic relaxation time of left ventricle in the appropriate and small-for-gestational-age human fetus. Ultrasound Med Biol 1997;23:187–190
45. Baschat AA, Gembruch U, Gortner L, et al. Coronary artery blood flow visualization signifies hemodynamic deterioration in growth restricted fetuses. Ultrasound Obstet Gynecol 2000;16 :425–431
46. Senat MV, Schwarzler P, Alcais A, et al. Longitudinal changes in the ductus venosus, cerebral transverse sinus and cardiotocogram in fetal growth restriction. Ultrasound Obstet Gynecol 2000;16: 19–24
47. Baschat AA, Gembruch U, Weiner CP, et al. Longitudinal changes of arterial and venous Doppler in fetuses with intrauterine growth restriction [abstract]. Am J Obstet Gynecol 2001;184:103
48. Pardi G, Cetin I, Marconi AM, et al. Diagnostic value of blood sampling in fetuses with growth retardation. N Engl J Med 1993; 328:692–696
49. Hecher K, Campbell S, Doyle P, Harrington K, Nicolaides K. Assessment of fetal compromise by Doppler ultrasound investigation of the fetal circulation: arterial, intracardiac, and venous blood flow velocity studies. Circulation 1995;91:129–138
50. Romero R, Kalache KD, Kadar N. Timing the delivery of the preterm severely growth-restricted fetus: venous Doppler, cardiotocography or the biophysical profile? Ultrasound Obstet Gynecol 2002; 19:118–121

15 Ruling Out Fetal Anomalies

Carol B. Benson

In the first few weeks after conception, the embryo undergoes growth, morphogenesis, and differentiation of tissues and organs. This is termed the embryonic period and lasts until about 8 weeks gestational (menstrual) age. The remaining weeks of gestation are termed the fetal period, during which rapid growth occurs.[1] Fetal anomalies most often result from abnormal morphogenesis or differentiation during the embryonic period.

Ultrasound is the imaging modality of choice for evaluation of the fetal anatomy to assess for fetal anomalies. The fetus can be assessed from multiple angles in multiple planes to obtain the images required. The real-time capabilities of ultrasound permit evaluation even while the fetus is moving. In addition, real-time scanning allows identification of fetal cardiac activity before other means of assessment can document fetal life. Real-time is essential when assessing the fetal heart for structural or rhythmic abnormalities.

Fetal anomalies occur in ~2.5% of newborn infants,[2,3] and, in most cases, no prior history of a fetal malformation is present. There are, however, some conditions associated with increased risk of fetal anomaly, including a prior family history of congenital anomaly, maternal diabetes, advanced maternal age, and exposure to certain teratogens, drugs, or infections during pregnancy. Upon conception, signs associated with increased risk of fetal malformation include abnormal amniotic fluid volume, either polyhydramnios or oligohydramnios, abnormal maternal serum α-fetoprotein levels, and multiple gestations. Given any of these conditions, ultrasound is used to evaluate the developing fetus for an anomaly.

The American College of Radiology, American College of Obstetrics and Gynecology, and the American Institute of Ultrasound in Medicine have published joint standards for antepartum obstetrical ultrasound that include a list of the fetal anatomical structures that should be evaluated when performing ultrasound during the second and third trimesters (**Table 15–1**).[4] Although it is not possible to detect all fetal anomalies prenatally, if these standards are used for fetal evaluation, most major congenital malformations will be detected. In some cases, more specialized examinations may be required, whereas in other cases, a fetal anomaly may not be visible on prenatal ultrasound.

Table15–1 Fetal Anatomical Survey: Structures to Be Assessed[a]

Head
Lateral ventricles and choroid plexus
Midline falx and cavum septum pellucidum
Posterior fossa to include cerebellum and cisterna magna
Heart
Four-chamber view including its position in thorax
Spine
Cervical, thoracic, lumbar, and sacral
Stomach
Urinary bladder
Umbilical cord insertion at anterior abdominal wall
Kidneys
Extremities
Images taken for fetal measurements
Biparietal diameter/head circumference
Abdominal diameter/circumference
Femur length

[a]From: AIUM Practice Guideline for the Performance of an Antepartum Obstetric Ultrasound Examination. American Institute of Ultrasound in Medicine; 2003. Published in conjunction with the American College of Obstetricians and Gynecologists (ACOG) and the American College of Radiology (ACR).

Ultrasound Evaluation

The Fetal Head

During an obstetrical ultrasound examination, three views of the fetal head are routinely obtained: the biparietal diameter, the cerebral ventricles, and the posterior fossa. The biparietal diameter view is an axial view of the fetal head at the level of the paired thalami and cavum septum pellucidum (**Fig. 15–1**). On this view, the presence of the head is confirmed and the cranial contour is assessed. The midline falx and cavum septum pellucidum are typically visible. The normal fetal head is oval in shape with a smooth contour.

Anencephaly (**Fig. 15–2**) is a neural tube defect where the cranium and brain tissue are absent. The lower face is

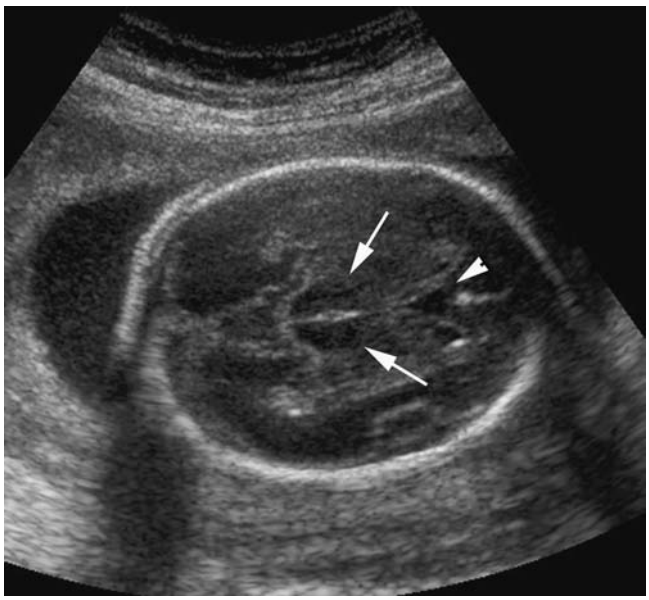

Figure 15–1 Image of the fetal head for the biparietal diameter measurement. Axial image at the level of the paired thalami (arrows) and the cavum septum pellucidum (arrowhead) is used for measurement of the biparietal diameter.

usually normally formed, but the forehead above the orbits and the cranium above the cervical spine are absent.

An encephalocele (**Fig. 15–3**) is a neural tube defect involving the cranium. These lesions are often identified on the biparietal diameter view. A defect in the skull is present, through which intracranial contents herniate outside

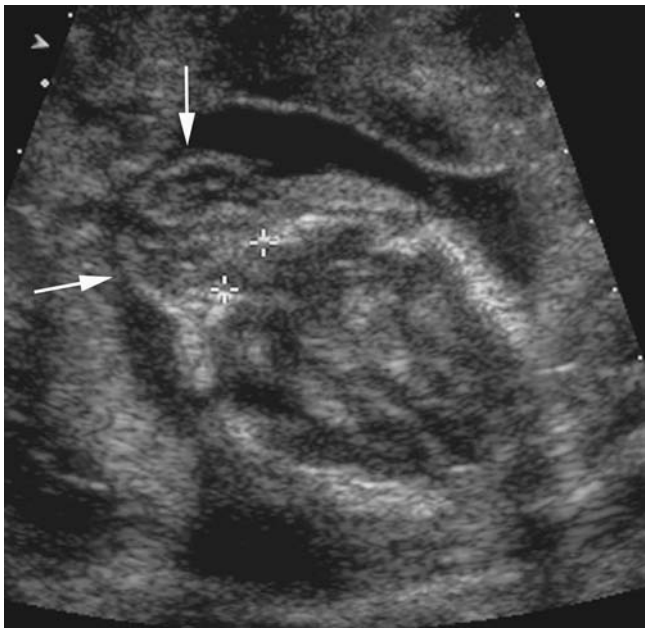

Figure 15–3 Encephalocele. Axial sonogram of fetal head demonstrating occipital defect (calipers) with brain tissue and meninges protruding outside the skull into the encephalocele (arrows).

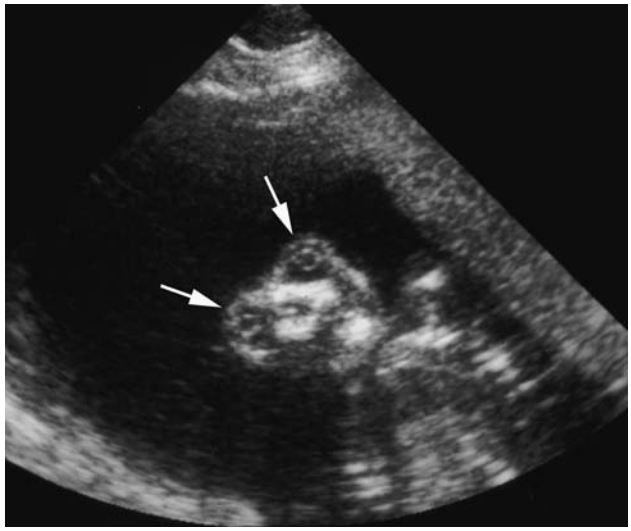

A

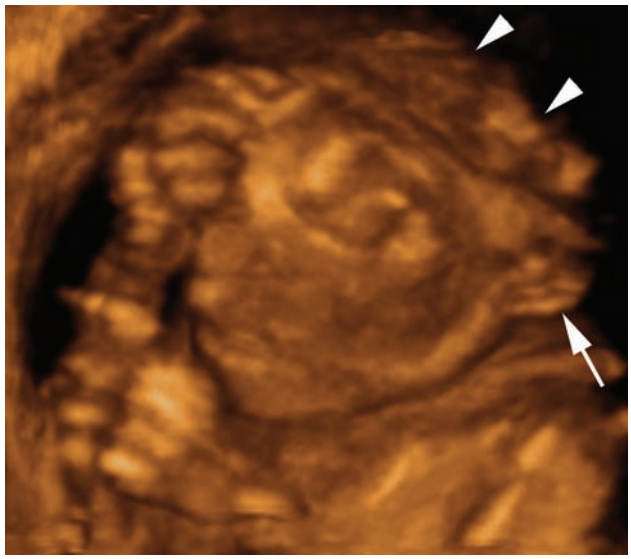

B

Figure 15–2 Anencephaly. **(A)** Sonogram of fetal face with absence of forehead above the orbits (arrows). **(B)** Three-dimensional image of a fetal head demonstrating absence of the cranium above the ear (arrow). Dysplastic brain tissue is seen posterior to the face (arrowheads).

the skull. Most encephaloceles are midline and posterior involving the occipital bone. Less common are frontal and parietal encephaloceles. Sonographically, the encephalocele defect appears as an interruption in the calvarium with a sac containing soft tissue and sometimes fluid protruding outside the skull.

Flattening of the frontal bones in the second trimester, giving the appearance of a "lemon"-shaped head (**Fig. 15–4**) on the biparietal diameter view, is associated with meningomyeloceles. When this finding is present, the posterior fossa should be evaluated carefully for a Chiari II malformation, and the spine should be examined for spina bifida.[5]

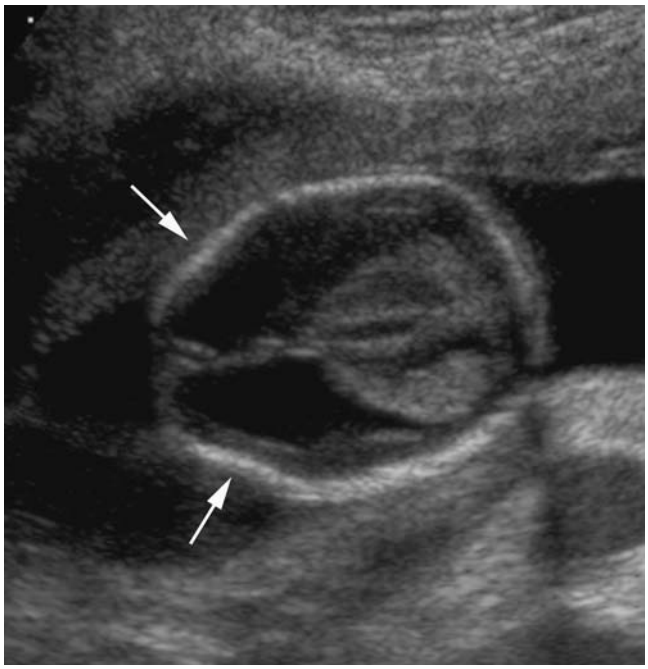

Figure 15–4 "Lemon" sign. Axial view of the fetal head in a fetus with a meningomyelocele demonstrating flattening of the frontal bones (arrows) giving the head a lemon shape. There is associated hydrocephalus.

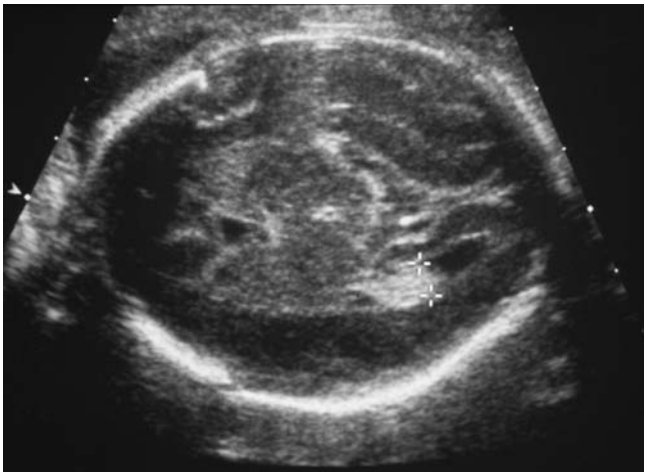

Figure 15–5 Lateral ventricular measurement. Axial view of the fetal head demonstrating measurement of a normal lateral ventricle. The measurement is taken at the level of the atrium of the lateral ventricle (calipers).

Evaluation of intracranial contents should include assessment of the lateral ventricles, the choroid plexus, and the posterior fossa. The lateral ventricles are evaluated on axial view to assess both the size and the shape of the ventricles. The width of the lateral ventricle is measured at the atrium of the lateral ventricle, perpendicular to the axis of the ventricle (**Fig. 15–5**), and should not exceed 10 mm. Excess cerebral spinal fluid in the head can be seen with dilatation of the lateral ventricles in such anomalies as hydrocephalus or agenesis of the corpus callosum. Excess fluid may also be a sign of an abnormal configuration of the ventricles, as in anomalies such as holoprosencephaly or porencephaly.

Hydrocephalus is defined as dilatation of the lateral ventricles. It may be an isolated anomaly, or it may result from in utero exposure to infection or a toxic agent, or it may be part of a syndrome or other complex congenital malformation. Hydrocephalus is commonly seen in association with meningomyeloceles and Dandy-Walker malformations. On ultrasound the diagnosis of hydrocephalus is made when the width of the lateral ventricle at the atrium measures more than 10 mm on axial view (**Fig. 15–6**),[6] and the choroid plexus appears to dangle away from its midline attachment.[7] If the lateral ventricles are dilated, then the third ventricle, located between the thalami on axial view, should be examined to look for dilatation. Aqueductal stenosis is a cause of hydrocephalus that leads to dilatation of the lateral and third ventricles with a normal fourth ventricle and posterior fossa.

An abnormal configuration of the cerebral ventricles is seen with holoprosencephaly (**Fig. 15–7**), a developmental anomaly in which there is absence or incomplete cleavage of the prosencephalon. This malformation is characterized by fusion of the lateral ventricles into a single ventricle that communicates across the midline. The cerebral hemi-

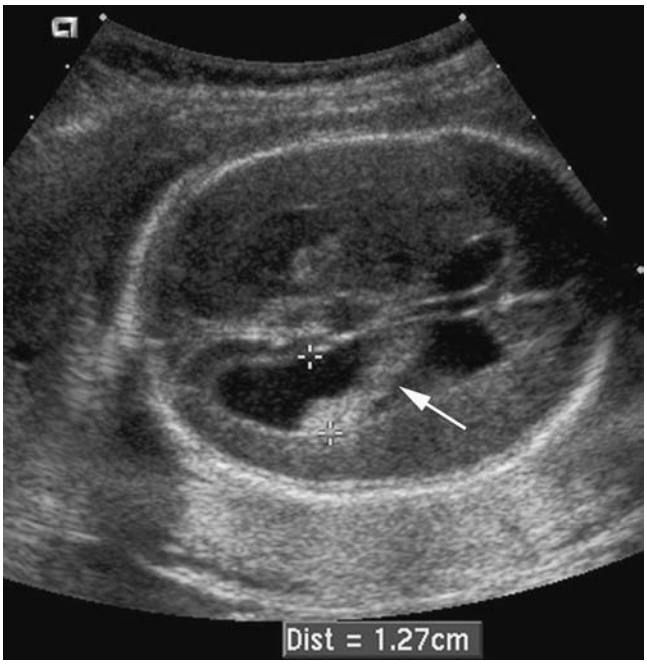

Figure 15–6 Hydrocephalus. Axial sonogram of the fetal head showing a dilated lateral ventricle (calipers) with the choroid plexus dangling from its medial attachment (arrow).

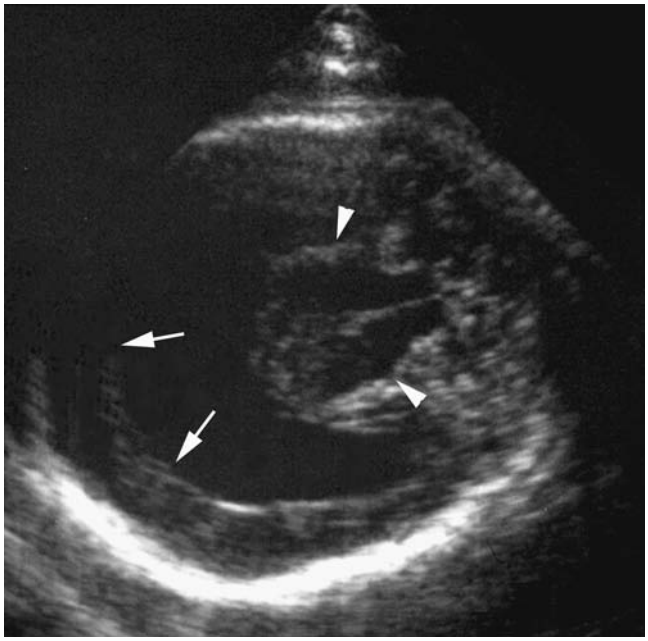

Figure 15–7 Holoprosencephaly. Vaginal sonogram of the fetal head demonstrating a single cerebral ventricle between fused cerebral cortex (arrows) and fused thalami (arrowheads).

spheres are fused as well, and the falx is absent or rudimentary. This anomaly is often associated with abnormalities of the fetal face, including midline facial clefts, hypotelorism, a proboscis, and cyclops.[3]

The choroid plexus is examined for its position in the lateral ventricle and for cysts. This is best done on the same view used to assess the cerebral ventricles. A dangling choroid plexus, where the posterior end of the choroid plexus is abnormally separated from the medial wall of the lateral ventricle, is seen with hydrocephalus. Choroid plexus cysts (**Fig. 15–8**) may be seen in the second trimester and are associated with increased risk for chromosomal abnormalities, especially trisomy 18.[8] These cysts are round, anechoic, with thin, smooth walls. Sometimes in the early second trimester, the choroid plexus has a

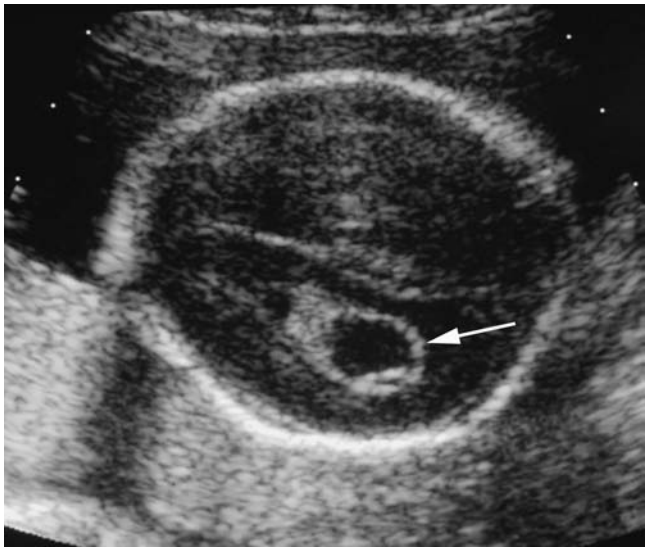

Figure 15–8 Choroid plexus cyst. Axial image of the fetal head demonstrating a cyst (arrow) in the choroid plexus.

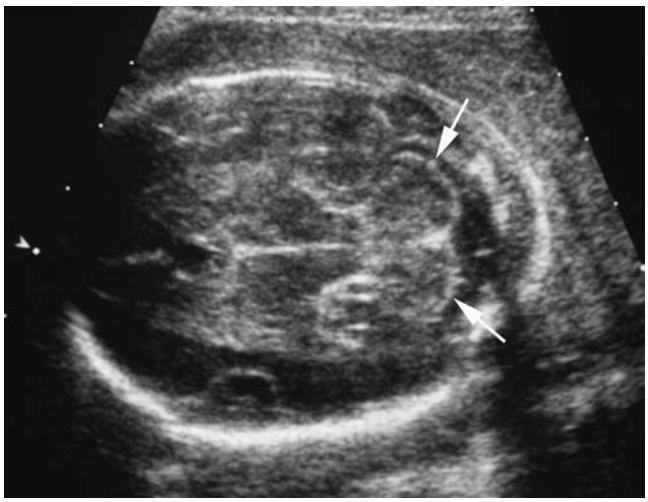

Figure 15–9 Normal posterior fossa. Angled axial view of the fetal head demonstrating a normal posterior fossa with the rounded cerebellar hemispheres (arrows) separated by echogenic vermis and fluid in the cisterna magna posterior to the vermis.

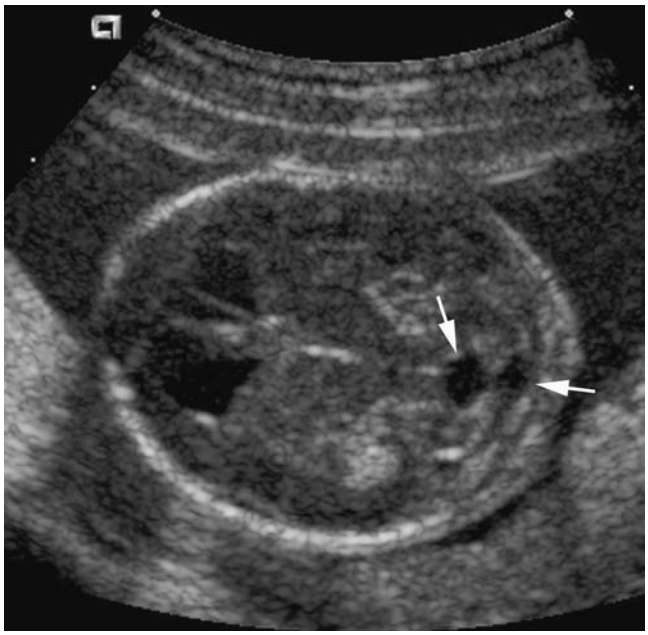

Figure 15–10 Dandy-Walker malformation. Image of posterior fossa demonstrating absence of the vermis between the cerebellar hemisphere, replaced by a cystic structure (arrows) connecting the fourth ventricle to the cisterna magna.

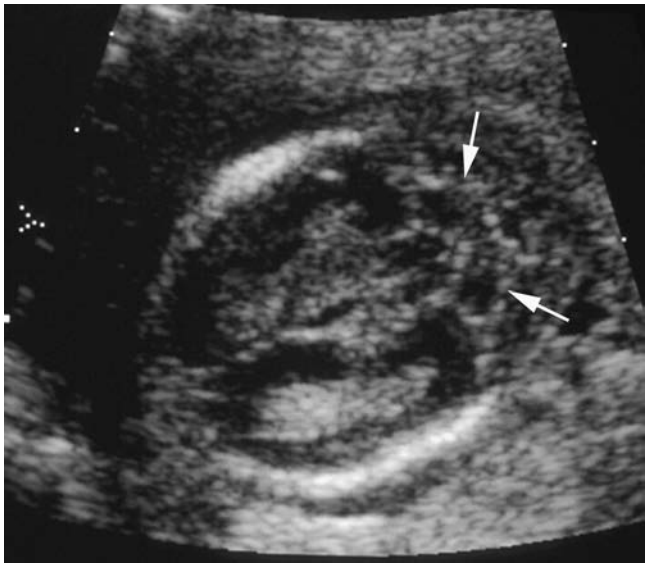

Figure 15–11 Chiari II malformation of the cerebellum, the "banana" sign. Sonogram of the posterior fossa showing small curved cerebellum (arrows) and no cisterna magna.

"spongy" appearance, containing lobular, hypoechoic areas. This is a normal finding that should not be confused with choroid plexus cysts.

Evaluation of the posterior fossa includes careful assessment of the cerebellum and the cisterna magna (**Fig. 15–9**). The normal cerebellum is made up of two rounded cerebellar hemispheres, separated by the echogenic vermis. The cisterna magna is a fluid space between the posterior aspect of the cerebellar vermis and the occipital bone. When a Dandy-Walker malformation is present, the vermis is hypoplastic or absent, replaced by a cystic space connecting the fourth ventricle with the cisterna magna (**Fig. 15–10**). In such cases, the cerebellar hemispheres often have an abnormal appearance as well.[3]

Chiari II malformations are associated with meningomyeloceles and are characterized by a small posterior fossa with loss of the cisterna magna and compression of the cerebellum against the occiput. The cerebellum appears curved and flattened posteriorly against the occipital bone.[9,10] In the second trimester, the appearance of the cerebellum has been termed the "banana" sign (**Fig. 15–11**). When a Chiari II malformation is identified at sonography, careful examination of the spine is warranted to locate the spinal defect.

Examination of the fetal face is not listed in the published standards as a component of the fetal anatomical survey. However, when performing a thorough examination of the fetus, evaluation of the face will permit diagnosis of abnormalities, such as cleft lip or hypoplastic mandible, that would otherwise be missed. The two best views for examining the fetal face are a coronal view of the lower face demonstrating the nose and upper lip (**Fig. 15–12**), and a sagittal or profile view demonstrating the

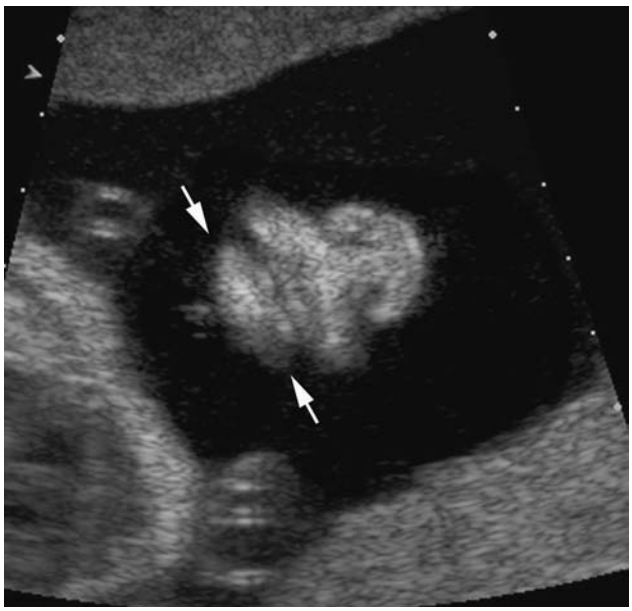

A

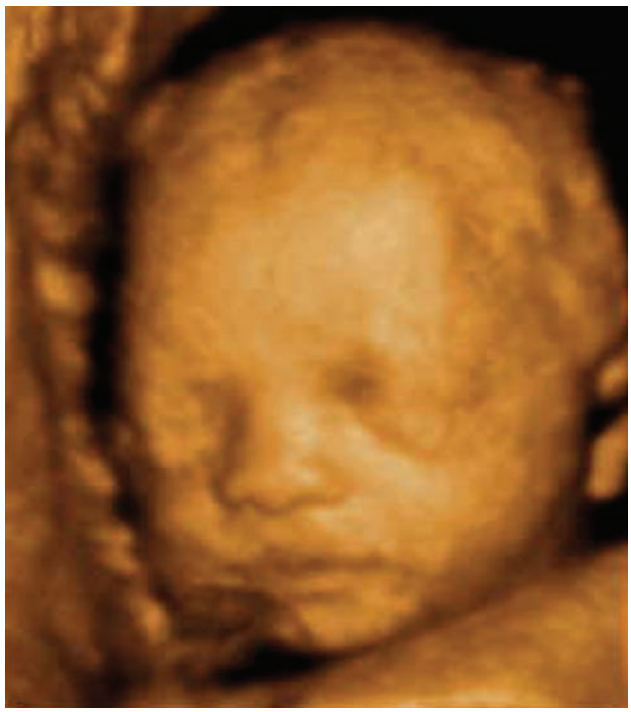

B

Figure 15–12 Fetal face. **(A)** Coronal image of the lower face demonstrating the two nostrils and upper and lower lips (arrows). **(B)** Three-dimensional image of the fetal face.

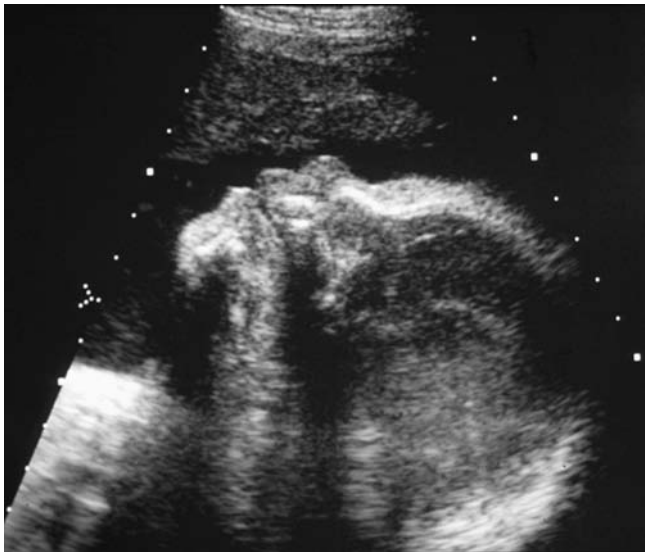

Figure 15–13 Fetal face in profile. Sagittal image of the fetal face demonstrating a normal profile of the forehead, nose, lips, and chin.

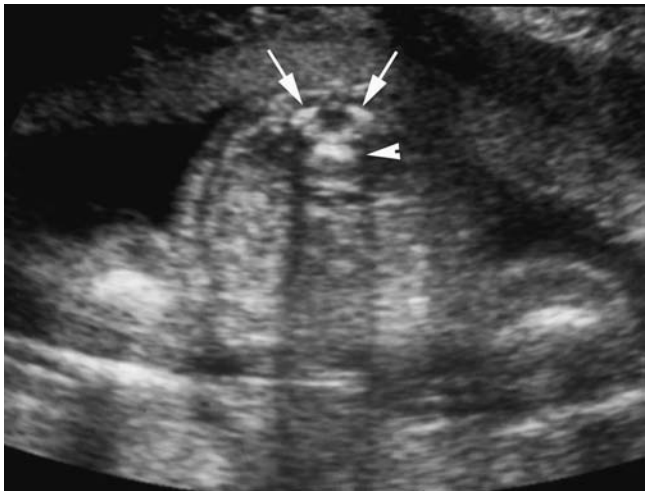

Figure 15–14 Fetal spine. Transverse view of the fetal spine demonstrating three ossification centers, two posterior (arrows) and one anterior (arrowhead), forming a C-shape or closed ring.

forehead, nose, lips, and chin (**Fig. 15–13**). Midline facial defects are associated with intracranial anomalies, such as holoprosencephaly. Lateral cleft lip and hypoplastic mandible are also often associated with other anomalies.

The Fetal Spine

Each vertebra of the fetal spine develops with three ossification centers, two posterior that form the pedicles and posterior elements and one anterior that forms the vertebral body. On transverse view, the three ossification centers form a C-shape, with the two posterior ossification centers pointing toward each other (**Fig. 15–14**). On longitudinal view, the spine appears as parallel ossification centers that converge in the distal sacrum (**Fig. 15–15**). During an obstetrical ultrasound examination, the entire spine should be assessed both longitudinally and transversely.

Neural tube defects involving the spine are characterized by disruption and splaying of the posterior elements, with protrusion of meninges and nerve tissue

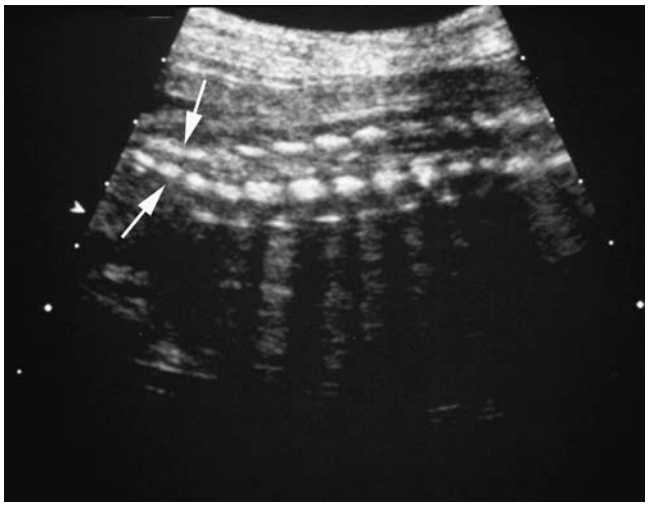

Figure 15–15 Lumbosacral spine. Longitudinal image of the lower spine demonstrating converging posterior ossification centers in the lower sacrum (arrows).

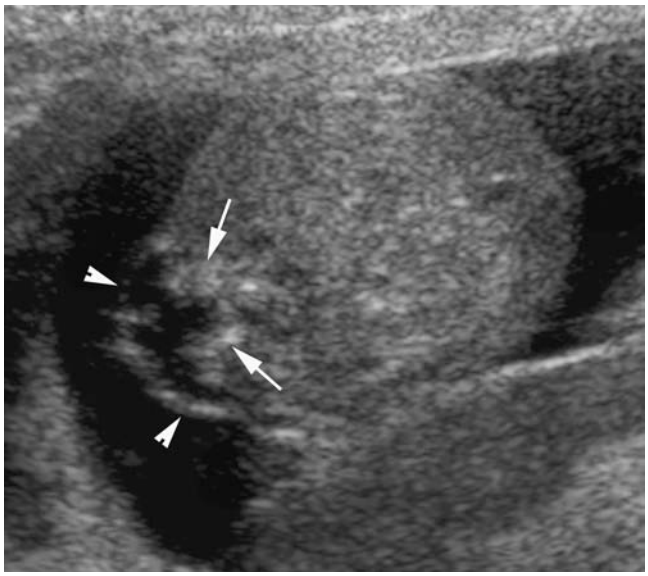

Figure 15–16 Meningomyelocele. Transverse sonogram of the fetal spine demonstrating splaying of the posterior elements of the vertebral body (arrows) and a dorsal sac of the meningomyelocele (arrowheads).

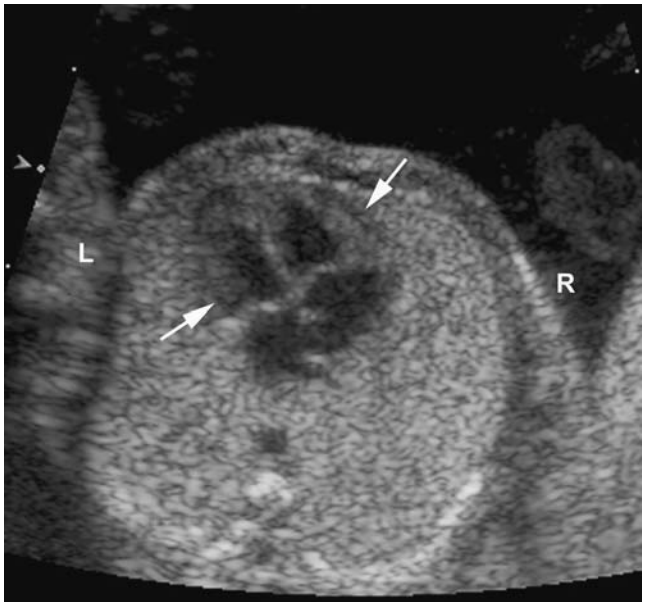

Figure 15–17 Fetal heart in the thorax. Transverse view of the fetal thorax demonstrating a normal heart (arrows) located in the left thorax, with the apex pointing to the left. R, right; L, left.

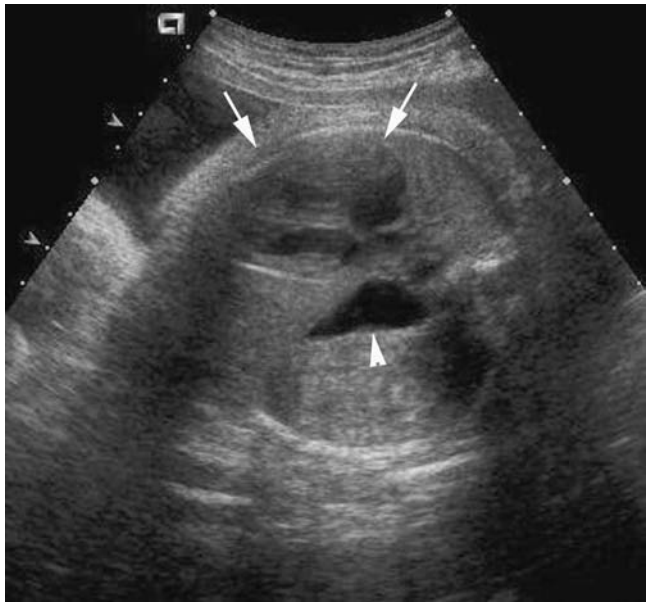

Figure 15–18 Left diaphragmatic hernia displacing the heart to the right. Transverse sonogram of the fetal thorax demonstrating the heart (arrows) displaced to the right by abdominal contents, including the fetal stomach (arrowhead) herniated into the left thorax.

outside the spinal canal. These bony defects are visible sonographically as splaying of the posterior ossification centers. The protruding tissue forms a dorsal sac that extends posteriorly (**Fig. 15–16**). Meningomyeloceles are most commonly located in the lower lumbar spine and sacrum, but they can also occur in the thoracic and cervical spine.

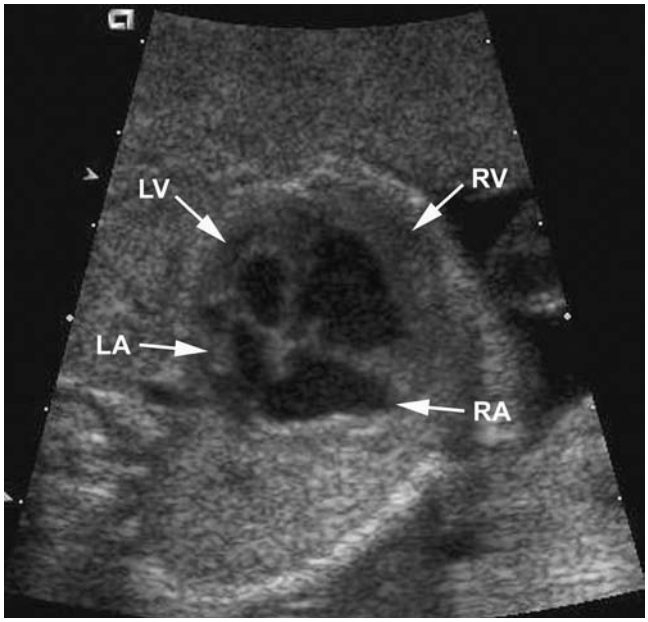

Figure 15–19 Hypoplastic left ventricle. Four-chamber view of an abnormal heart with an enlarged right atrium (RA, arrow) and right ventricle (RV, arrow) and small left atrium (LA, arrow) and left ventricle (LV, arrow).

The Fetal Heart

The normal fetal heart is positioned in the thorax slightly to the left of midline with the apex pointing to the left (**Fig. 15–17**). Homogeneous lung tissue fills the rest of the thorax. When an intrathoracic mass is present, such as a diaphragmatic hernia or cystic adenomatoid malformation, the heart is displaced to the contralateral side (**Fig. 15–18**). Intrathoracic masses may arise from the lung, as with cystic adenomatoid malformation and bronchial atresia, or they may arise in the mediastinum, as with a teratoma, or they may result from a diaphragmatic hernia.[11,12] Secondary signs of an intrathoracic mass include polyhydramnios and hydrops.

The four-chamber view of the heart, demonstrating both ventricles and both atria, is obtained in an axial plane of the thorax. The right and left chambers should be symmetric. Asymmetry of the ventricles is usually a sign of a cardiac anomaly. Absence of one ventricle suggests hypoplastic left or right heart (**Fig. 15–19**). Enlargement of the right atrium suggests Ebstein's anomaly. Ventricular septal defects may also be diagnosed on the four-chamber view of the heart.[3,13]

Anomalies of the great vessels can be detected if, in addition to the four-chamber view, images of the right

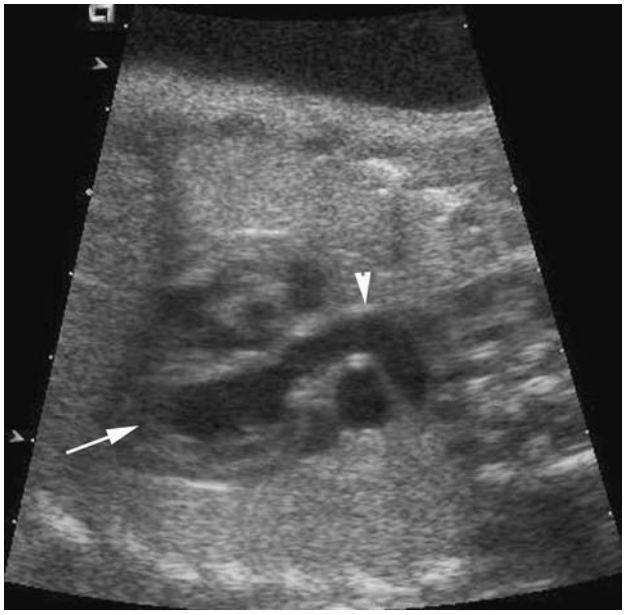

A

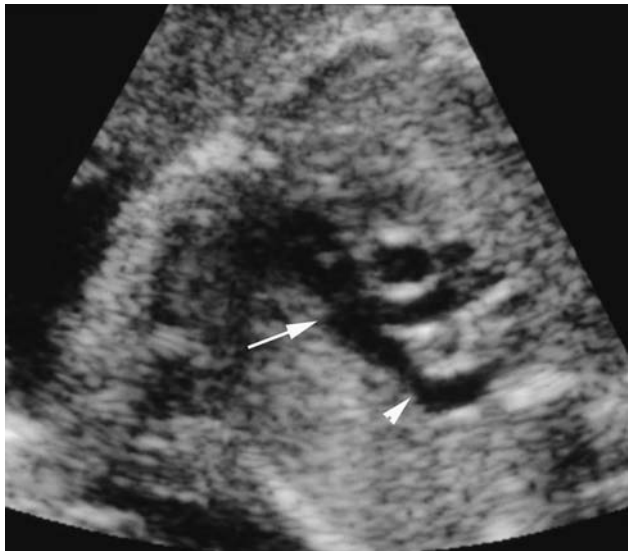

B

Figure 15–20 Cardiac outflow tracts. **(A)** Long axis image of the left ventricular outflow tract demonstrating the aorta (arrowhead) arising from the left ventricle (arrow). The ventricular septum is continuous with the anterior aortic wall. **(B)** Transverse image of the right ventricular outflow tract, demonstrating the pulmonary artery (arrow) bifurcating into the ductus arteriosus (arrowhead) and the right pulmonary artery.

and left ventricular outflow tracts are obtained (**Fig. 15–20**). With these views, tetralogy of Fallot, truncus arteriosus, and transposition of the great vessels can be diagnosed.

The Fetal Abdomen

Four views of the fetal abdomen are routinely obtained during the obstetrical ultrasound examination. These include images of (1) the abdomen for measurement of the abdominal diameter or circumference, (2) the kidneys, (3) the bladder, and (4) the anterior abdominal wall at the umbilical cord insertion.

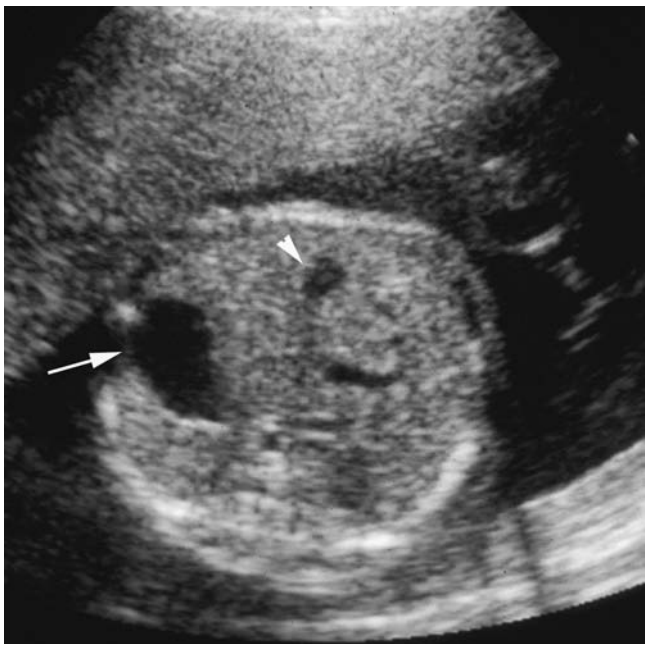

Figure 15–21 Abdomen. Transverse view of the fetal abdomen at the level of the stomach (arrow) and intrahepatic portion of the umbilical vein (arrowhead). This is the level used to measure the abdominal diameter or circumference.

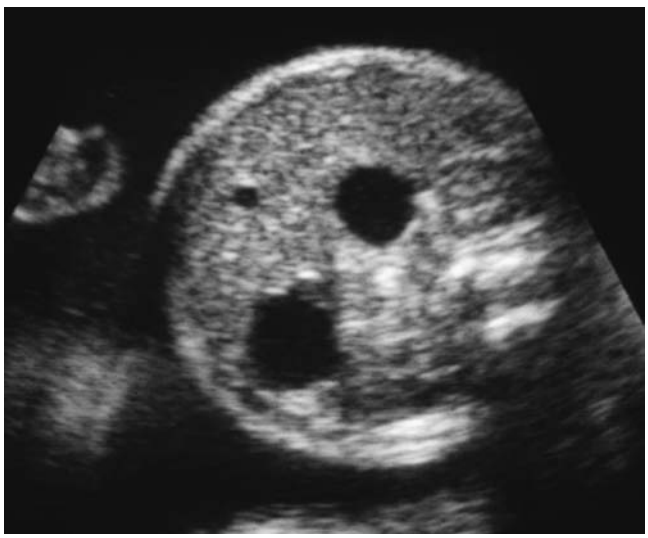

Figure 15–22 Duodenal atresia. Transverse sonogram of the fetal abdomen demonstrating two fluid collections in the upper abdomen, the dilated stomach and the duodenal bulb.

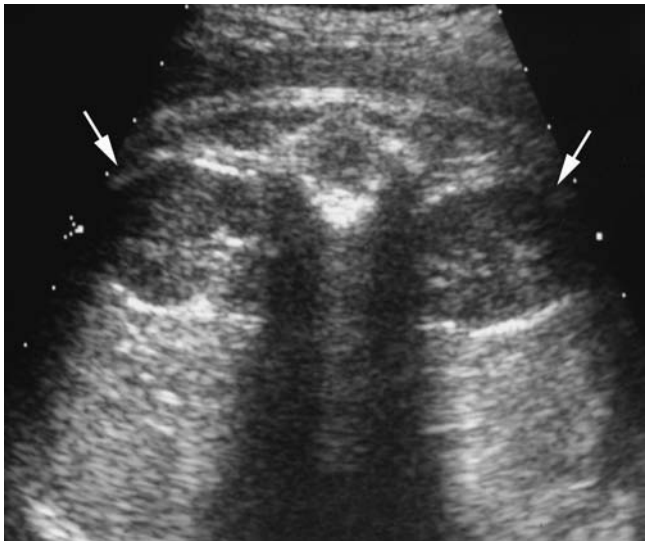

Figure 15–23 Kidneys. Transverse view of the posterior fetal abdomen at the level of the kidneys. The kidneys (arrows) are seen on either side of the spine, which casts an acoustic shadow.

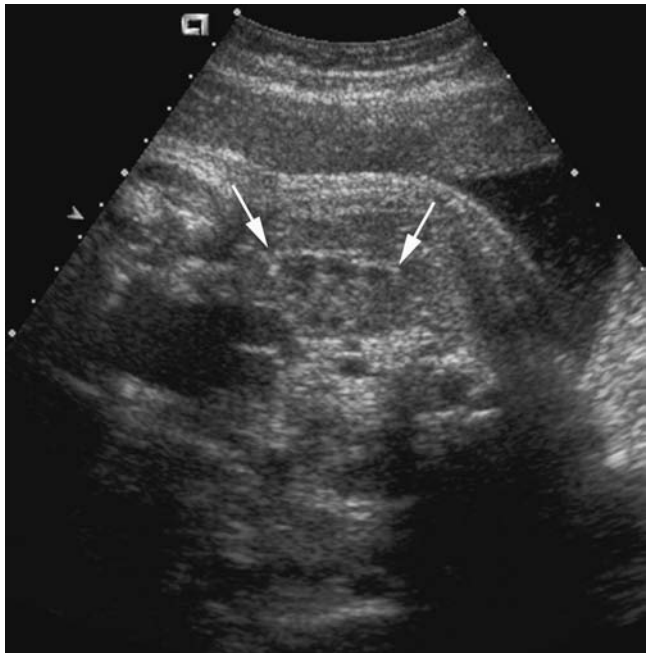

Figure 15–24 Pelvic kidney. Sonogram through the fetal pelvis demonstrating a pelvic kidney (arrows) adjacent to the fluid-filled bladder.

The image used to measure the fetal abdomen is a transverse view at the level of the fetal stomach and the umbilical vein in the liver (**Fig. 15–21**). The fetal stomach should be identified in the left upper quadrant in all normal fetuses by the beginning of the second trimester. Persistent absence of the stomach is a sign of a fetal abnormality, the most common being esophageal atresia. Severe polyhydramnios is usually associated with this abnormality. In syndromes associated with situs inversus or situs ambiguous, the stomach may be seen in the midline or in the right upper quadrant.[14] A dilated stomach accompanied by a second round fluid collection in the upper abdomen is seen with duodenal obstruction from duodenal atresia or an annular pancreas (**Fig. 15–22**). As with esophageal atresia, polyhydramnios is usually severe in these cases.

If other dilated loops of bowel are present in the fetal abdomen, the diagnosis of a gastrointestinal obstruction is made. The obstruction may be at any level and result from a variety of causes, including atresia, volvulus, or meconium plug. Polyhydramnios is usually associated with the gastrointestinal obstruction.

The fetal kidneys can usually be seen in the renal fossas (**Fig. 15–23**), adjacent to the spine on each side, by the beginning of the second trimester. Failure to see one or both kidneys in their usual location should prompt a thorough examination of the fetal abdomen in search of an ectopic kidney, such as a pelvic kidney (**Fig. 15–24**) or cross-fused ectopic kidney or horseshoe kidney. Unilateral or bilateral renal agenesis may also occur. When agenesis is bilateral, there is absence of renal function, leading to severe oligohydramnios and pulmonary hypoplasia. The prognosis is usually fatal.[15]

Dilatation of the fetal renal collecting system can occur due to obstruction at the ureteropelvic junction, in the distal ureter at the ureterovesical junction, or at the bladder outlet. Dilatation or the renal collecting system may also occur as a result of vesicoureteral reflux. The diagnosis of hydronephrosis (**Fig. 15–25**) is made when there is intrarenal calyceal dilatation or when the renal pelvis meas-

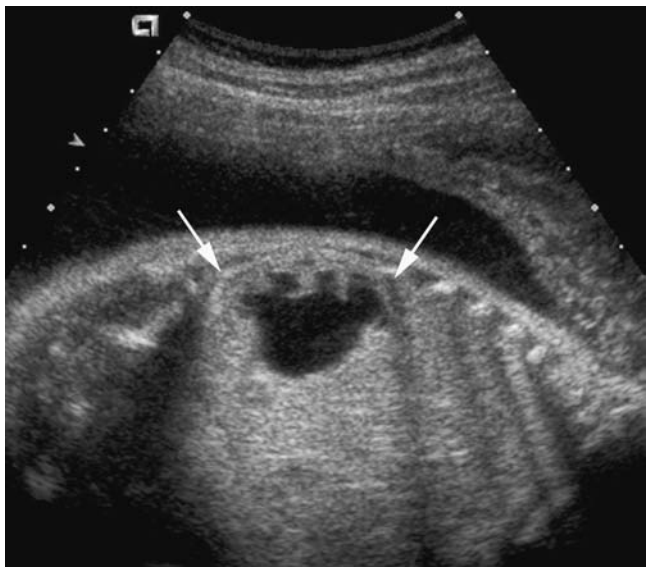

Figure 15–25 Hydronephrosis. Sonogram of the fetal kidney (arrows) demonstrating calyceal dilatation and dilated renal pelvis.

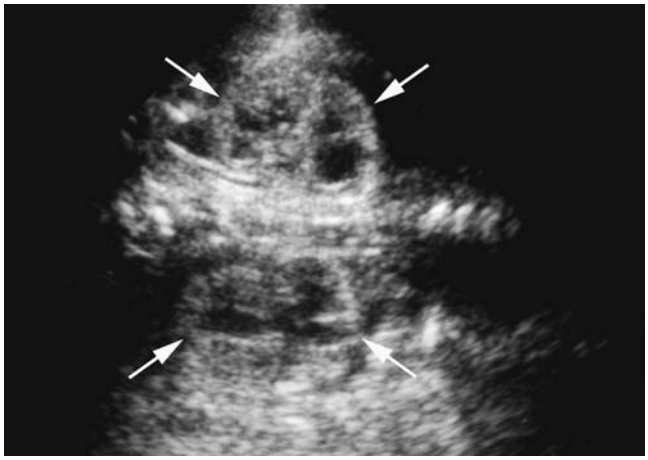

Figure 15–26 Dysplastic kidney. The kidneys (arrows) are both echogenic, with thinned cortices and hydronephrosis due to dysplasia from bladder outlet obstruction.

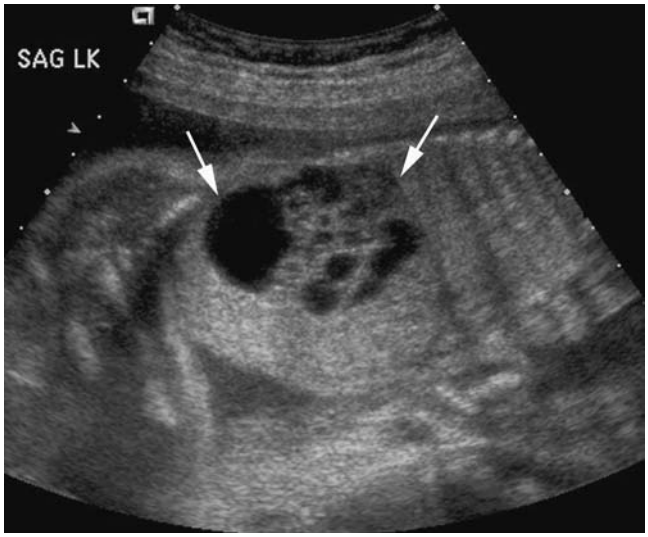

Figure 15–27 Multicystic dysplastic kidney. Longitudinal sonogram of the fetal abdomen showing dysplastic kidney with multiple cysts (arrows) in the renal fossa.

ures in anteroposterior dimension at least 7 mm before 20 weeks gestation and at least 10 mm after 20 weeks. When the measurement of the renal pelvis is 4 to 6 mm before 20 weeks gestation or 5 to 9 mm after 20 weeks, hydronephrosis may be present, although the diagnosis is less certain. Dilatation of the ureters is seen when the obstruction is below the ureteropelvic junction or in cases of vesicoureteral reflux.[15]

Severe urinary obstruction that occurs after ~10 weeks gestation or that is incomplete, such as with posterior urethral valves, causes renal dysplasia. The resulting kidneys appear small, with a thin, echogenic cortex (**Fig. 15–26**). Dilated calyces may remain visible in some cases. Complete urinary obstruction beginning early in the embryonic period causes a multicystic dysplastic kidney (**Fig. 15–27**). The kidney is replaced by multiple cysts of varying sizes that do not communicate with each other. The overall size of the kidney is typically larger than a normal kidney.[15]

Autosomal recessive polycystic kidney disease is an inherited disorder that leads to enlarged, echogenic kidneys with poor function and an absent urinary bladder (**Fig. 15–28**). In most cases, the prognosis is dismal due to severe oligohydramnios.[15]

The fetal urinary bladder is usually visible sonographically by the end of the first trimester (**Fig. 15–29**). Absence of the bladder is seen when renal function is se-

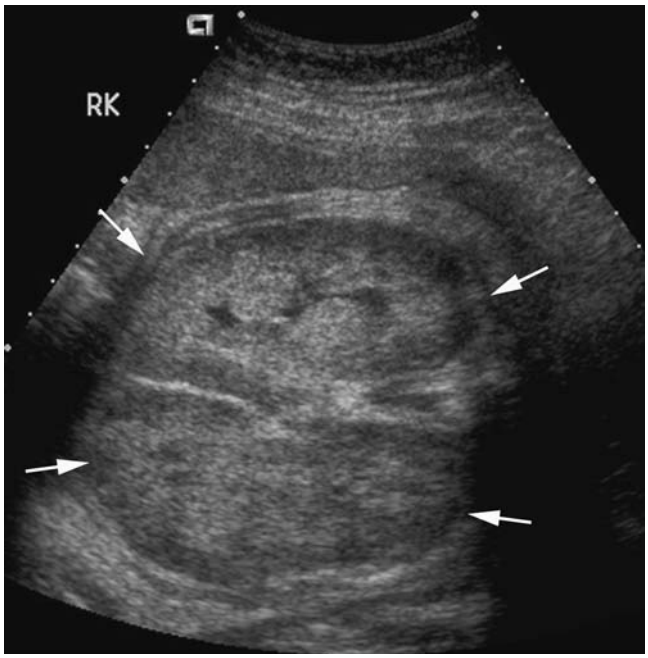

Figure 15–28 Autosomal recessive polycystic kidneys. Longitudinal sonogram of both fetal kidneys (arrows), which are enlarged and echogenic. The fetus is surrounded by severe oligohydramnios.

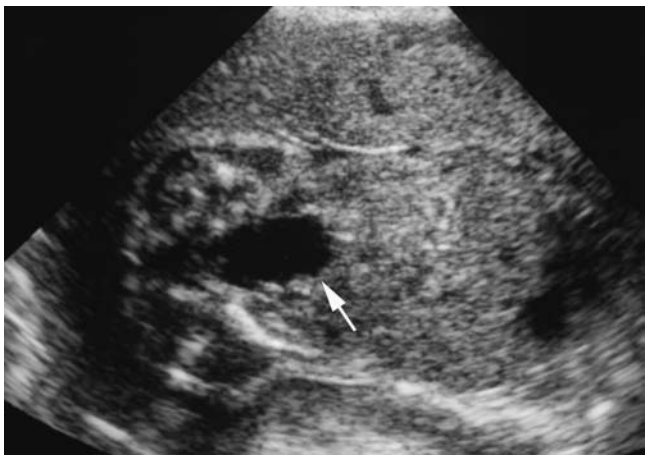

Figure 15–29 Bladder. Longitudinal view of the fetus demonstrating the fluid-filled bladder (arrow) in the pelvis.

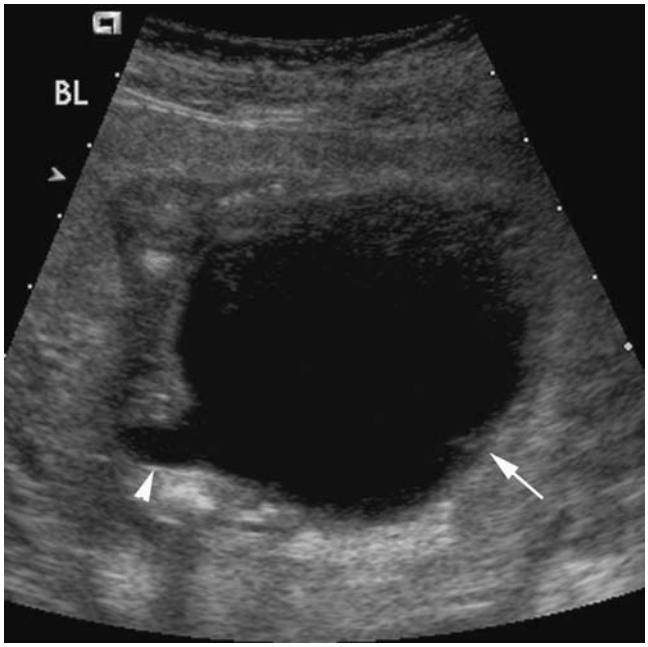

Figure 15–30 Posterior urethral valves. Sonogram of the pelvis of a fetus with posterior urethral valves. The bladder is dilated (arrow) and the dilated posterior urethra (arrowhead) is seen inferiorly.

verely impaired or absent, such as with bilateral renal agenesis or autosomal recessive polycystic kidney disease. These conditions are associated with severe oligohydramnios. With posterior urethral valves, the bladder is very dilated and the dilated posterior urethra may be visible inferiorly (**Fig. 15–30**). Both kidneys usually show changes of long-standing obstruction, including hydronephrosis and renal dysplasia. Hydroureters can be seen in the fetal abdomen.[15]

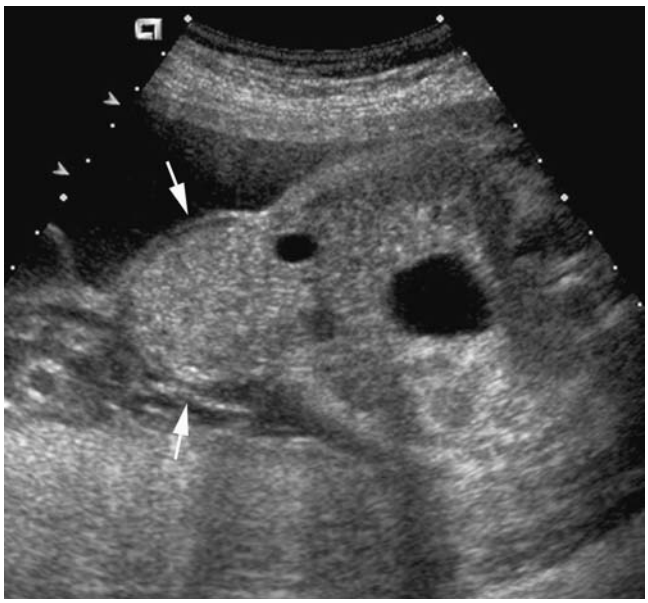

Figure 15–32 Omphalocele. Transverse sonogram of the fetal abdomen at the level of the umbilical cord insertion, showing the omphalocele (arrows) extending anterior to the anterior abdominal wall.

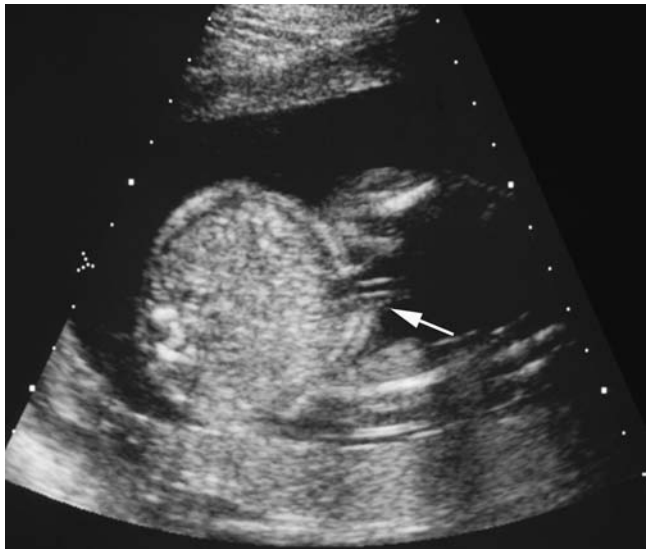

Figure 15–31 Normal umbilical cord insertion. Transverse view of the fetal abdomen at the umbilical cord insertion demonstrates the vessels of the umbilical cord (arrow) entering the abdomen.

The normal fetal anterior abdominal wall is intact except for the three vessels of the umbilical cord that enter the abdomen at the umbilicus (**Fig. 15–31**). Omphaloceles (**Fig. 15–32**) are abdominal wall defects at the umbilicus through which abdominal contents, contained by a peritoneal membrane, herniate. Omphaloceles are commonly associated with other anomalies and with chromosomal abnormalities and thus have a poor prognosis.[16] Gastroschisis (**Fig. 15–33**) is an abdominal wall defect that is

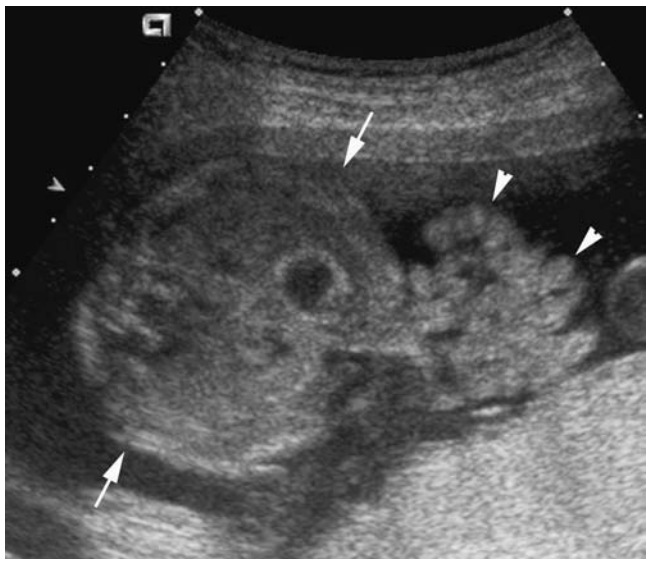

Figure 15–33 Gastroschisis. Transverse sonogram of the fetal abdomen (arrows) demonstrating herniated loops of bowel freely floating in the amniotic cavity (arrowheads).

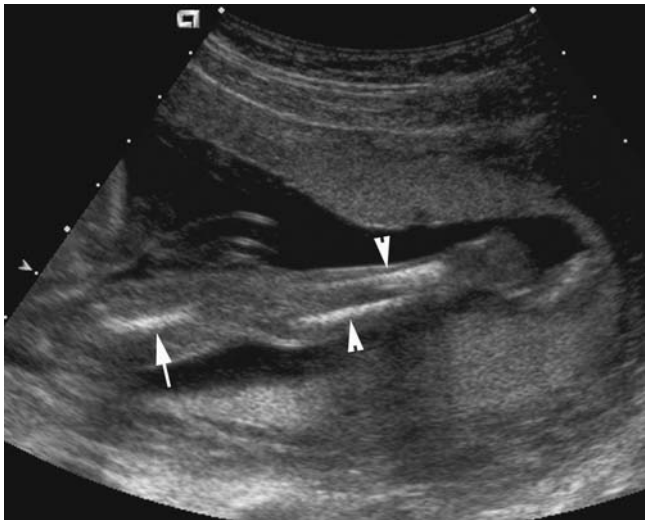

Figure 15–34 Normal lower extremity. Sonogram of a fetal leg demonstrating one bone in the thigh (arrow) and two bones in the lower leg (arrowheads).

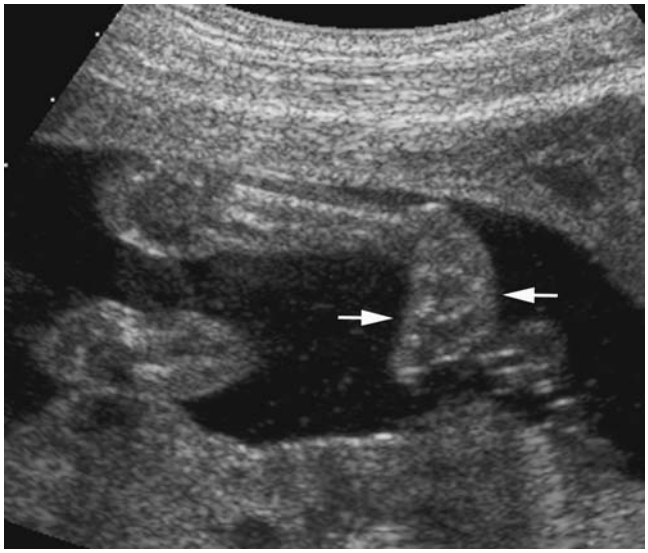

Figure 15–35 Clubfoot. Sonogram of the lower leg demonstrating the foot (arrows) turned such that the bones of the feet are in the same plane as the tibia and fibula in the lower leg.

paraumbilical. Herniated abdominal contents are not contained by a membrane, but are seen floating freely in the amniotic cavity. The prognosis is good because this defect is not usually associated with other anomalies.[17]

The Fetal Extremities

Evaluation of the fetal extremities, to be certain all four are present, is a component of the obstetrical sonogram. In addition, the femur length is measured routinely to assess gestational age and growth of the long bones.[4] The fetal extremities can be followed with real-time scanning to be certain they are present and normally formed (**Fig. 15–34**). In particular, a single long bone should be identified in the upper arm and thigh, whereas two long bones should be seen in the forearm and lower leg. Careful examination of the feet will permit diagnosis of clubfoot, where the bones of the feet lie in parallel with the bones of the lower leg (**Fig. 15–35**).

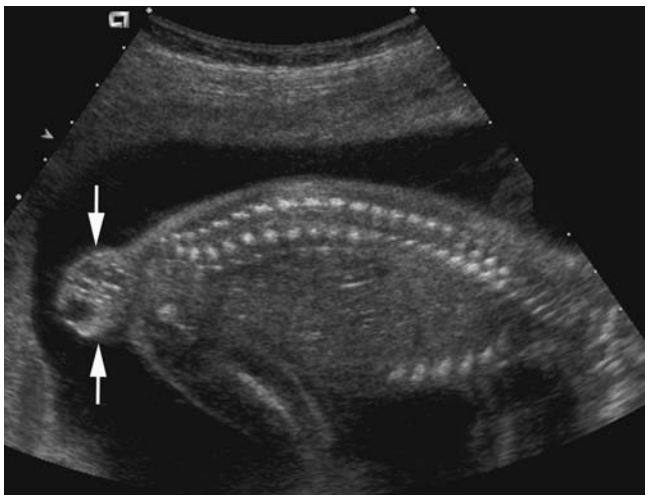

Figure 15–36 Sacrococcygeal teratoma. Longitudinal image of the lower fetus including the lower spine demonstrating a complex solid and cystic mass (arrows) protruding from the fetus posteriorly, caudal to the sacral spine.

Other Fetal Structures

Although other fetal anatomical structures, such as the gallbladder, are not listed specifically in the published standards, a thorough examination of the fetus should include scanning the fetus from head to toe. In this way, abnormalities, such as intraabdominal cysts or sacrococcygeal teratomas (**Fig. 15–36**), will be identified.

References

1. Moore KL, Persaud TVN. The Developing Human, 5th ed. Philadelphia: WB Saunders; 1993:1–13
2. Ewigman BG, Crane JP, Frigoletto RD, et al. Effect of prenatal ultrasound screening on perinatal outcome. N Engl J Med 1993;329: 821–827
3. Nyberg DA, Mahony BS, Pretorius DH. Diagnostic Ultrasound of Fetal Anomalies. Chicago: Year Book Medical Publishers; 1990:21–31
4. AIUM Practice Guideline for the Performance of an Antepartum Obstetric Ultrasound Examination. Laurel, MD: American Institute of Ultrasound in Medicine; 2003
5. Nyberg DA, Mack LA, Hirsch J, Mahony BS. Abnormalities of fetal cranial contour in sonographic detection of spina bifida: evaluation of the "lemon" sign. Radiology 1988;167:387–392
6. Cardoza JD, Goldstein RB, Filly RA. Exclusion of fetal ventriculomegaly with a single measurement: the width of lateral ventricular atrium. Radiology 1988;169:711–714

7. Cardoza JD, Filly RA, Podrasky AE. The dangling choroid plexus: a sonographic observation of value in excluding ventriculomegaly. Am J Roentgenol 1988;151:767–770
8. Nadel AS, Bromley BS, Frigoletto FD, Estroff JA, Benacerraf BR. Isolated choroid plexus cysts in the second-trimester fetus: is amniocentesis really indicated? Radiology 1992;185:545–548
9. Benacerraf BR, Stryker J, Frigoletto FD. Abnormal US appearance of the cerebellum (banana sign): indirect sign of spina bifida. Radiology 1989;171:151–153
10. Goldstein RB, Podrasky AE, Filly RA, Callen PW. Effacement of the fetal cisterna magna in association with myelomeningocele. Radiology 1989;172:409–413
11. Bromley B, Parad R, Estroff JA, Benacerraf BR. Fetal lung masses: prenatal course and outcome. J Ultrasound Med 1995;14:927–936
12. Guibaud L, Filiatrault D, Garel L, et al. Fetal congenital diaphragmatic hernia: accuracy of sonography in diagnosis and prediction of the outcome after birth. Am J Roentgenol 1996;166:1195–1202
13. Benacerraf BR, Pober BR, Sanders SP. Accuracy of fetal echocardiography. Radiology 1987;165:847–849
14. Silverman NH, Schmidt KG. Ultrasound evaluation of the fetal heart. In: Callen PW, ed. Ultrasonography in Obstetrics and Gynecology. 3rd ed. Philadelphia: WB Saunders; 1994:291–332
15. Benson CB, Doubilet PM. Fetal genitourinary anomalies. In: Fleischer AC, Manning FA, Jeanty P, Romero R, eds. Sonography in Obstetrics and Gynecology: Principles and Practice. 5th ed. Stamford: Appleton and Lange; 1996:433–446
16. Nyberg DA, Fitzsimmons J, Mack LA, et al. Chromosomal abnormalities in fetuses with omphalocele, significance of omphalocele contents. J Ultrasound Med 1989;8:299–308
17. Langer JC, Khanna J, Caco C, Dykes EH, Nicolaides KH. Prenatal diagnosis of gastroschisis: development of objective sonographic criteria for predicting outcome. Obstet Gynecol 1993;81:53–56

16 Family History of Congenital Heart Disease

Douglas L. Brown

Risk Factors and Hereditary Issues for Congenital Heart Disease

Congenital heart disease (CHD) is estimated to occur in 0.4 to 0.8% of live births.[1,2] Because the majority of fetuses with CHD do not have a known risk factor,[3–5] it is important to evaluate the heart of each fetus who has a sonogram. However, there are fetal and maternal factors that increase the risk of CHD. Fetal risk factors include a thick nuchal translucency, hydrops, extracardiac anomalies, complete heart block, and single umbilical artery. Maternal risk factors include metabolic disorders, teratogens, and a family history of CHD.[6] Diabetes mellitus and phenylketonuria are metabolic disorders that predispose to CHD. Teratogens that are associated with CHD include lithium, anticonvulsants (such as phenytoin, trimethadione, and valproic acid), ethanol, and retinoic acid.

Although ~10 to 15% of CHD is considered to be due to chromosomal abnormalities (such as trisomy 21, 18, and 13, or Turner's syndrome), genetic syndromes (such as Noonan's or Williams syndrome), or teratogens,[6] the cause of the majority of cases of CHD is not well understood[7,8] and is believed to be multifactorial.[9] A family history of CHD will generate concerns for recurrence and typically prompts evaluation of the fetal heart in subsequent pregnancies. It is useful to know as much information as possible about the previous affected family member and the full family history, however, because this will influence the recurrence risk. CHD that is isolated carries a different significance than if the affected family member had a chromosomal abnormality, a syndrome associated with CHD, or knowledge that the CHD previously was related to teratogen exposure.

In the absence of any of these other associations, there are some general risk estimates available. Most of the available data relates to affected first-degree relatives. The recurrence risk in a particular family is not always clear, but in general there is an increased risk for recurrence of CHD when either parent or a previous child has CHD. The recurrence risk when one previous child has CHD is estimated at 2 to 5%,[1,7,8] suggesting a 3- to 10-fold increase over the baseline population risk of CHD. If two previous children have had CHD, the risk increases slightly to 3 to 10%.[7,8] If a parent has CHD, the recurrence risk for the fetus has been variably reported, ranging from 1.5 to 17.8%.[2,10–12] Many of the prior studies did not have a control group and could not estimate relative risk. A more recent study with a control group found a 3.1% prevalence of CHD when a parent had CHD, with an adjusted odds ratio of 1.73 (95% CI 0.89 to 2.44).[10] The risk of recurrence also appears to be higher when the mother, rather than the father, is the parent affected with CHD.[10,11,13] It is important that a full family history be taken, however. If there have been multiple affected individuals in a family, the recurrence risk may be higher than what is predicted by population-based studies.[1] The recurrence risk for second- and third-degree relatives of a single-index case with isolated congenital heart disease is probably not much different than the general population risk.[9]

When cardiac anomalies are considered in terms of their developmental mechanism rather than by anatomy,[14] there seems to be a higher recurrence risk for lesions due to abnormal flow patterns, which includes hypoplastic left heart syndrome, coarctation of the aorta, aortic valve stenosis, pulmonary valve stenosis, and membranous ventricular septal defects.[1,2,7,9,13] When CHD does recur, it is not necessarily the same anatomical defect. The concordance rate (i.e., whether recurrences were the same abnormality as in the first affected family member) varies widely. In one study, 37% of cases were reported to have exact concordance, though the rates ranged from 0 to 80% depending on the type of CHD.[15] Isolated atrioventricular septal defect (with normal cardiac situs) had a concordance rate of 80%, whereas atrial septal defects had a 0% concordance rate for the same abnormality.[15] When considered in broadly defined groups of CHD, the concordance rates are higher than for the exact abnormality recurrence.[15] Ventricular septal defects had an exact concordance of 55%, but the nonconcordant cases varied widely and included some severe forms of CHD. Thus a minor form of CHD in the index case does not exclude more severe CHD in recurring cases.[15] Also, severe CHD in the index case does not necessarily mean severe CHD when there is recurrence.[15]

It is of some interest that aortic valvular stenosis seems to be one of the lesions with a higher recurrence risk.[1,9] When the mother has aortic stenosis, the recurrence risk to the fetus may be as high as 18%.[13] When recurring, an exact concordance rate of 38% has been reported for aortic stenosis.[15] Severe aortic valve stenosis is one of the few cardiac structural lesions for which prenatal intervention has

been attempted. In utero balloon valvuloplasty has been attempted at 21 to 33 weeks in fetuses with severe aortic stenosis, with the hope of preventing progression to hypoplastic left heart syndrome.[16,17] Initial results have been variable. Whether closer scrutiny and earlier diagnosis of fetuses at higher risk for aortic stenosis would contribute to improved outcome is not clear.

The association of cardiac anomalies with deletions in the long arm (q) of chromosome 22 has been increasingly recognized over the past several years. It is important to be aware of this particular association because other than trisomy 21, deletions in 22q11 are believed to be the most important chromosomal cause of heart malformations.[18] The majority of patients with DiGeorge syndrome and velocardiofacial (Shprintzen's) syndrome have deletions in chromosome 22q11.[18] The clinical features of these two syndromes overlap, but the majority of patients with either syndrome have cardiac defects. Although many types of CHD have been reported in patients with deletions in 22q11, the most common cardiac defects associated with 22q11 deletions include tetralogy of Fallot (TOF), pulmonary atresia, truncus arteriosus, and type B interrupted aortic arch.[19–21] Renal abnormalities, which may also be identified prenatally, have been reported in association with 22q11 deletions.[20,22] About three fourths of cases of 22q11 deletions arise de novo, and the other one fourth are inherited in an autosomal dominant manner.[18,20] Individuals who have a 22q11 deletion have a 50% risk of transmitting the deletion to their offspring.[18]

The pregnant patient with an increased risk for fetal cardiac anomalies, such as a family history of congenital heart disease, is understandably anxious. The parents' level of anxiety will likely vary with their past experience. Parents whose child has had serious heart disease with numerous hospitalizations and surgery are likely to be more anxious than those whose child had a minor defect such as a small, isolated ventricular septal defect. With a properly performed obstetric sonogram, one can identify the majority of fetuses with cardiac anomalies. In the following sections, I discuss when and how to perform the sonographic exam, reasonable expectations of sonography for identifying CHD, and the sonographic features of the more common structural cardiac anomalies.

Timing of the Ultrasound Exam of the Fetal Heart

At what gestational age should one examine the fetal heart by sonography? It is important to identify CHD as early as possible, but also to perform the exam at a gestational age when the heart can be adequately evaluated. Although the push is generally for an earlier diagnosis, one should realize that, though uncommon, a few cardiac lesions (such as cardiomyopathies, some cases of valvular stenosis, and tumors) may not develop until later in gestation.[23] Not surprisingly, the ability to obtain the four-chamber (4C) view in normal second-trimester fetuses increases with gestational age. In a prior study of fetuses at 16 to 17 weeks gestational age, the 4C view was obtained in ~80% of normal fetuses, increasing to 95% or greater after 18 weeks.[22] Adequate views of the aortic and pulmonary outflow tracts were also obtained in more than 95% of fetuses after 18 weeks.[24–26] In general, the fetal heart tends to be best seen between ~20 and 30 weeks. It has been suggested that in a low-risk pregnancy, around 25 to 30 weeks would probably be the ideal time to scan if one just considers the goals of obtaining the best ultrasound images and not missing late-developing lesions.[23] However, one would generally want to scan earlier if termination of pregnancy is an option, and around 20 weeks would probably be a reasonable time in a low-risk pregnancy.[23] However, many so-called routine second-trimester obstetric sonograms in the United States are performed at around 16 to 18 weeks, and the fetal heart can usually be adequately evaluated at that time.

For the fetus with an increased risk of CHD, a targeted evaluation of the heart would traditionally be done around 18 to 22 weeks gestational age. There will be a small minority of patients at increased risk for fetal CHD who will need follow-up sonograms due to an inability to fully evaluate the heart for such technical reasons as maternal obesity or poor fetal position.

There is another option for earlier diagnosis in some centers now. Evaluation of the fetal heart, using both transabdominal and transvaginal transducers, can be attempted at around 12 to 14 weeks. The expertise to perform such exams is not available at all centers, but will probably become more widely available with time. The majority of anomalies diagnosed at this earlier gestational age are severe, complex anomalies.[27] With transvaginal sonography the 4C and outflow tract views can be obtained in 70 to 100% of fetuses at 13 to 14 weeks gestational age.[27]

Transvaginal sonography is limited by restricted angles of imaging, decreased penetration, and the small size of the fetal heart.[27] Not surprisingly, a complete exam is more likely to be obtained closer to 14 weeks than at 12 weeks. In experienced hands, this early scanning in the late first trimester seems to be able to identify, or at least suspect, the majority of CHD.[28,29] A normal scan at 12 to 14 weeks can offer preliminary reassurance to the patient, but should be followed up with another ultrasound later in pregnancy, probably around 20 to 22 weeks.[23]

Sensitivity of Ultrasound for Identifying Congenital Heart Disease

A wide range (4 to 96%) has been reported for the sensitivity of the 4C view for identifying CHD in the second trimester.[5] Although several factors may help explain the

variable sensitivity in different studies, a large part of the variable sensitivity probably has to do with how well the heart is seen and what criteria are used to consider the 4C view as normal. There is more to the 4C view than just seeing four chambers. In the next section, what constitutes an adequate 4C view is discussed. In the Routine Antenatal Diagnostic Imaging Ultrasound Study (RADIUS), the sensitivity for "complex" CHD using the 4C view was 43%.[30] A reasonable estimate of the sensitivity of the 4C view for CHD is probably around 50 to 60%, increasing to about 80 to 85% when the outflow tracts are also evaluated.[25,31,32] The variably reported sensitivity, however, should reinforce the notion that more consistent and complete sonographic examinations are needed to achieve optimal sensitivity.[5]

There are several cardiac anomalies that are particularly difficult to detect even with an optimal sonographic exam. These include patent ductus arteriosus (PDA), secundum atrial septal defect (ASD), small ventricular septal defect (VSD), mild degrees of aortic or pulmonary valve stenosis, anomalous pulmonary venous return, and coarctation of the aorta. PDA and secundum ASD (the most frequent type of ASD) are rarely, if ever, diagnosed prenatally because the ductus arteriosus and foramen ovale are normally patent in the fetus. Small VSDs, mild degrees of aortic or pulmonary valve stenoses, anomalous pulmonary venous return, and coarctation of the aorta are sometimes difficult to diagnose because the lesion is small or produces only minor changes in the appearance of the 4C or outflow tract views. It is important for parents to be aware of these limitations of fetal cardiac sonography. Because ASDs and small VSDs are relatively common lesions, it is particularly important for parents who have a previous child with one of these lesions to understand the limitations of sonography.

Although the prenatal diagnosis of a specific cardiac lesion may not always be exactly correct, false-positive diagnoses of CHD are uncommon. Small VSDs and coarctation of the aorta are probably the most frequent false-positive diagnoses and will be discussed subsequently.

Ultrasound Evaluation

General Aspects

Different approaches and views have been suggested to evaluate the fetal heart, although the 4C view is the basic view used by most sonographers and sonologists. The 4C view is taken on a transverse view through the fetal thorax (**Fig. 16–1**). For the 4C view to be considered normal, one should be able to determine that (1) the four chambers are normal in size, (2) the ventricular septum is intact, (3) the "crux" region of the heart is intact, and (4) the general appearance (i.e., size, position, and axis) of the heart is normal.[33–35] The two atria are generally of the same width, as are the two ventricles, although the right-sided chambers of the heart may be minimally larger than the left-sided chambers later in gestation. The ventricular septum should be continuous, with no defect in it. The membranous portion of the ventricular septum is normally thin and, as will be discussed subsequently, may be difficult to image well. The "crux" of the heart refers to the area where the ventricular and atrial septa meet the atrioventricular valves.[33] At the crux, the septa should be intact, and the tricuspid valve should appear to attach to the septum just slightly more toward the apex of the heart than does the mitral valve.

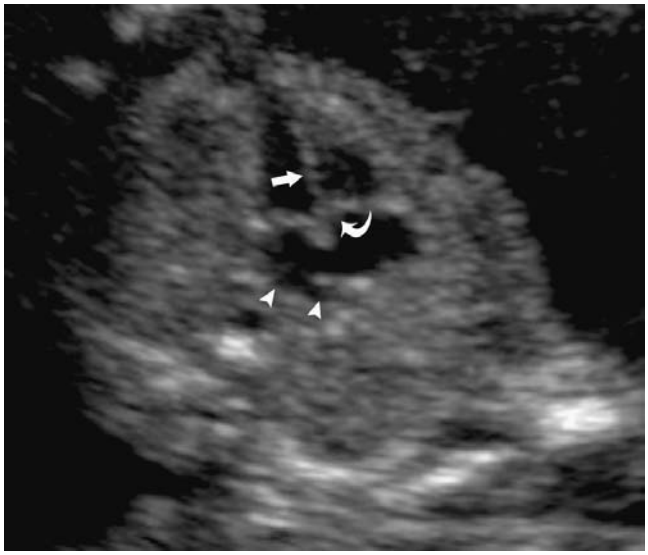

Figure 16–1 Four-chamber (4C) view. The ventricles are approximately equal in size as are the atria in this normal 4C view. The ventricular septum is intact (arrow is within left ventricle and points to ventricular septum). The crux region (curved arrow is within the right atrium and points to the crux where the tricuspid valve is attached) is intact, with the tricuspid valve slightly more toward the apex than the mitral valve at this level. Two of the pulmonary veins (arrowheads) can be seen entering the left atrium. (Image courtesy of William J. Watson, M.D., Rochester, MN)

Overall assessment of the heart reveals that it normally occupies about one third of the cross-sectional area of the thorax. The heart is basically midline, but with the cardiac apex to the left, and the ventricular septum is usually oriented at about a 45-degree angle to the midline sagittal plane.[36,37] The normal range of the cardiac axis is reported as 20 to 55 degrees in one study[37] and 22 to 75 degrees in another study.[36] Although fetuses with CHD may have a normal cardiac axis, an abnormal cardiac axis is frequently associated with CHD.[36–38] Ideally, one should also determine if the abdominal situs (position of abdominal organs) is normal. The stomach should be on the left side of the fetus, and, particularly if one suspects a situs abnormality, the inferior vena cava should be assessed for

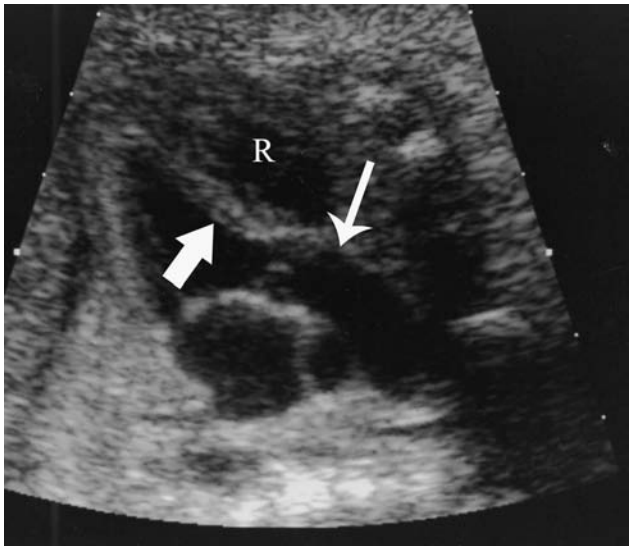

A

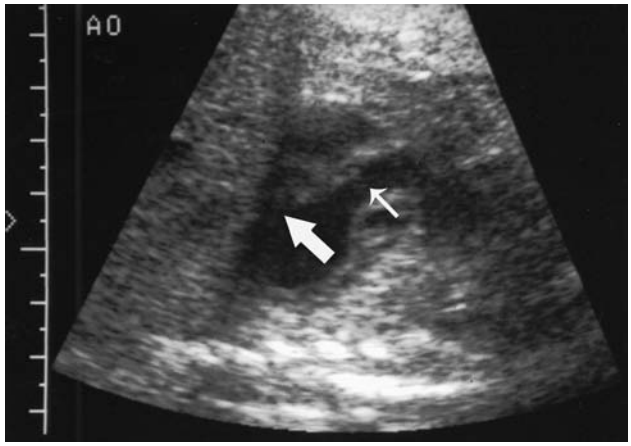

B

Figure 16–2 Left ventricular outflow tract views. **(A)** This view from a normal fetus demonstrates continuity of the ventricular septum (thick arrow within the left ventricle that points to the septum) and the wall of the aorta (thin arrow). A portion of the right ventricle (R) is seen on the other side of the ventricular septum. This view is used to assess for an overriding aorta, and one may not recognize an overriding aorta if the view does not include at least a small portion of the right ventricular lumen. (Reprinted with permission from Brown DL, Hornberger LK. Problems and pitfalls in the sonographic diagnosis of fetal cardiac anomalies. Ultrasound Q 1995;13:221–227.) **(B)** This view from a different fetus illustrates an inadequate left ventricular outflow tract view. It may be tempting to accept a view like this as normal because it seems to show a normal aorta, but it is not adequate to exclude overriding of the aorta. Although it does show the aorta (thin arrow) arising from the left ventricle, it does not adequately demonstrate continuity of the ventricular septum and aorta (thick arrow is within the left ventricle and points to part of the ventricular septum). Other views showed overriding of the aorta in this fetus who had tetralogy of Fallot. One should be able to see a portion of the right ventricular lumen, as in **(A),** on the other side of the ventricular septum before continuity of the ventricular septum and aorta can be adequately evaluated.

abnormal location or for interruption of its hepatic segment, which may occur with polysplenia or asplenia.

New guidelines for obstetric ultrasound were jointly developed by the American Institute of Ultrasound in Medicine (AIUM), the American College of Radiology (ACR), and the American College of Obstetricians and Gynecologists (ACOG); they were published in 2003.[39] The guidelines state that the basic cardiac exam includes a 4C view of the fetal heart. It further states that, if technically feasible, an extended basic cardiac examination can also be attempted to evaluate both outflow tracts.[39] Including the right and left ventricular outflow tracts will help identify abnormalities of the great arteries that are likely to be missed on the 4C view alone.[26,34] We find a long-axis view most helpful for evaluating the left ventricular outflow tract (**Fig. 16–2**). It is attained by slight cranial angulation (with respect to the fetus) of the transducer from the 4C view and slight rotation of the transducer toward the fetal right shoulder.[6,40] The key feature to note on 4C view is that the ventricular septum is continuous with the anterior wall of the aorta. The right ventricular outflow tract can be imaged with slightly more cranial angulation and rotation of the transducer in the opposite direction. This gives a short-axis view, which shows bifurcation of the main pulmonary artery (PA) into the right PA and ductus arteriosus (**Fig. 16–3**). The left PA is not seen in this plane. A key feature to note in obtaining the two outflow tract views is that the great arteries cross at right angles to each other as they exit the heart. The PA is usually slightly larger than the aorta.[41]

One could argue that, although color Doppler is sometimes helpful,[42–44] it is not generally needed for evaluation of the normal fetal heart.[42] Color Doppler is most helpful when an abnormality is suspected, particularly abnormalities of the great arteries or pulmonary veins, and to assess for valvular regurgitation. Some investigators, however, feel that color Doppler does result in increased detection of cardiac abnormalities, at least in patients at increased risk for trisomy 21.[45]

From the foregoing discussion, there are six key features (four features on the 4C view and two features on the two outflow tract views) that will allow one to decide if the fetal heart is normal or abnormal. The six features, posed as questions, are listed here. If all six questions can confidently be answered "yes," then the heart is very likely to be normal.

Regarding the 4C view, the following are important:

1. Are four chambers present and symmetric in size?
2. Is the ventricular septum intact?
3. Is the crux region of the heart normal?
4. Are the size, position, and axis of the heart in the chest normal?

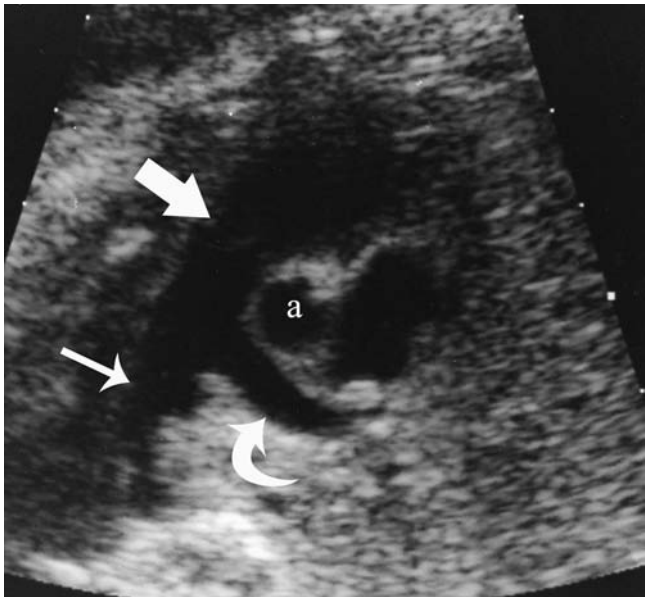

Figure 16–3 Right ventricular outflow tract view. The pulmonary artery appears to "wrap around" the aorta (a) which is seen in cross-section. The pulmonary artery (thick arrow) appears to bifurcate into the ductus arteriosus (thin arrow) and the right pulmonary artery (curved arrow). The left pulmonary artery is not seen in this view. In the course of obtaining the two outflow tract views, one observes that the aorta and pulmonary artery criss-cross at right angles to one another as they exit the heart. This is shown indirectly in this view where one sees the aorta in cross-section and a longitudinal segment of the pulmonary artery. (Reprinted with permission from Brown DL, Hornberger LK. Problems and pitfalls in the sonographic diagnosis of fetal cardiac anomalies. Ultrasound Q 1995;13:221–227.)

Table 16–1 Summary of Abnormalities to Consider on Each View

I. Four-Chamber View
- A. Septal defect
  - 1. Ventricular septal defect
  - 2. Atrioventricular canal defect
- B. Left ventricle relatively smaller than right ventricle
  - 1. Hypoplastic left heart syndrome
  - 2. Coarctation
  - 3. Severe intrauterine growth restriction
  - 4. Total anomalous pulmonary venous return
- C. Right ventricle relatively smaller than left ventricle
  - 1. Pulmonary atresia/severe pulmonary stenosis
  - 2. Critical aortic stenosis
  - 3. Tricuspid atresia
- D. Enlarged right atrium
  - 1. Ebstein's anomaly
  - 2. Other tricuspid valve anomalies: dysplasia, absent leaflets, Uhl's anomaly
  - 3. Pulmonary atresia/severe pulmonary stenosis
- E. Mass within cardiac chamber
  - 1. Tumor
  - 2. Distinguish from echogenic foci, prominent moderator band

II. Outflow tract evaluation
- A. Overriding of the aorta
  - 1. Tetralogy of Fallot
  - 2. Truncus arteriosus
  - 3. Pulmonary atresia with ventricular septal defect
- B. Absence of "criss-crossing" of aorta and pulmonary artery
  - 1. Complete transposition
  - 2. Double-outlet right ventricle
  - 3. Corrected transposition

On the two outflow tract views, the following are important:

5. Is the wall of the aorta continuous with the ventricular septum?
6. Do the aorta and pulmonary artery criss-cross as they exit the heart?

In the following sections, the more common abnormalities of the fetal heart that one may identify are considered, first on the 4C view and then on the outflow tract views (**Table 16–1**). Possible abnormal findings that may be seen on each view will be reviewed and their differential diagnosis discussed. Several sources provide further examples of abnormalities that can be seen on the 4C view and outflow tract views, and also normal variants.[26,34,35,46,47]

The question is sometimes asked as to whether the pregnant patient with an increased risk of CHD should have a more detailed fetal echocardiogram performed by a pediatric cardiologist. This is a debatable issue without a clear, universal answer. The ability of obstetric sonographers and sonologists to evaluate the fetal heart varies considerably, and different approaches to evaluate the fetal heart are probably reasonable in different locales. The wide range of reported sensitivities of prenatal sonography for CHD suggests that to achieve high sensitivity, one should evaluate the heart in a careful and consistent manner. If the sonographer and sonologist performing the obstetric sonogram are adequately trained and capable of evaluating the heart as discussed in this CHAPTER, it is unlikely that major CHD will be missed. If one is not comfortable evaluating the heart in such a manner, then the exam should be performed by someone who is, which in some locales may be the pediatric cardiologist.

In our practice, we value the expertise of our pediatric cardiologists who have experience in fetal cardiology, and we refer patients to them for a more detailed study if we identify a cardiac anomaly or if we encounter an uncertain finding in the fetal heart. We feel that in such cases, it is important for the fetus to have a more detailed sonographic evaluation so that the most accurate diagnosis can

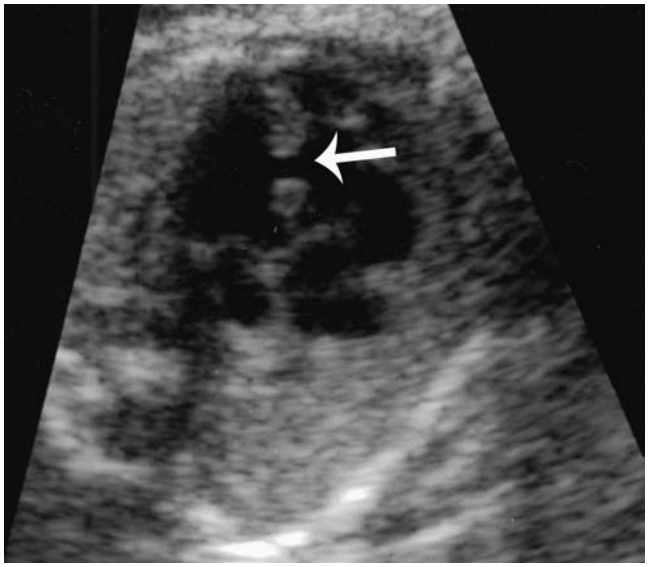

Figure 16–4 Ventricular septal defect. The four-chamber view shows a distinct defect (arrow) in the muscular portion of the ventricular septum. Defects in this portion of the septum tend to be easier to recognize than those in the membranous septum. (Reprinted with permission from Brown DL, Hornberger LK. Problems and pitfalls in the sonographic diagnosis of fetal cardiac anomalies. Ultrasound Q 1995;13:221–227.)

be made. The patient can then receive appropriate counseling from the cardiologist about the prognosis.

The Four-Chamber View: Abnormal Findings

Defects in the Septum

A VSD is identified as a gap in the ventricular septum (**Fig. 16–4**). It is often seen on the 4C view, but because a single 4C image only evaluates part of the septum, one needs to sweep through the entire septum. A VSD can be both over- and underdiagnosed. A potential pitfall can occur with an apical 4C view (where the sound beam is parallel to the septum); there may appear to be a defect in the membranous septum (**Fig. 16–5**). This is probably due to the limitations of lateral resolution and the relative thinness of the membranous portion of the septum. This artifact can usually be recognized by its characteristic location, sometimes by a gradual fading of the septum as opposed to the more abrupt termination of the septum with a true VSD, and probably and most importantly, by the absence of a defect when imaging more perpendicular to the septum.[33,46]

Although a VSD is the most frequent cardiac anomaly seen postnatally, it seems to be a difficult lesion to diagnose prenatally. The sensitivity of prenatal ultrasound for VSDs has been reported from 0 to 71%, with most of these

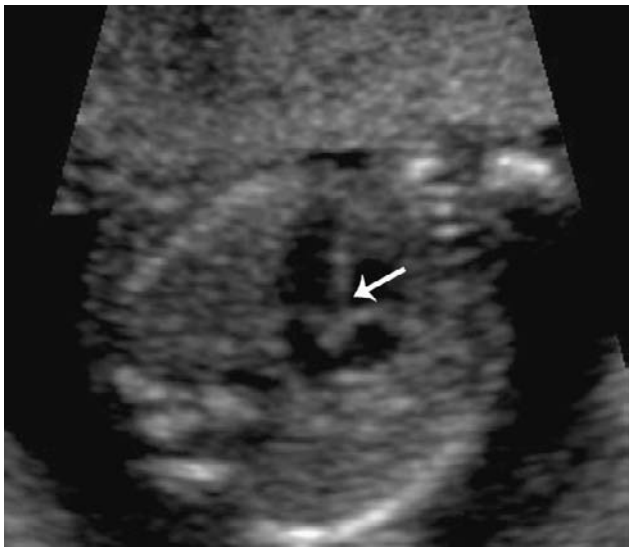

A

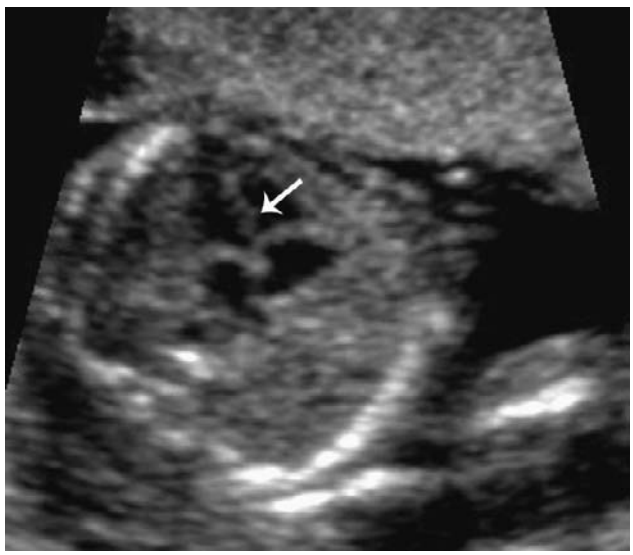

B

Figure 16–5 Pseudoventricular septal defect. **(A)** In this apical four-chamber view (referred to as apical because the cardiac apex points toward the transducer), the ventricular septum is essentially parallel to the ultrasound beam. In such a view, one may question if there is a small defect in the thin, membranous portion of the ventricular septum (arrow). This can be a difficult area in which to diagnose small ventricular septal defects (VSDs), and both false-positive and false-negative sonographic diagnoses are possible. One should be cautious about diagnosing an isolated VSD in this location, based on just one view such as this. **(B)** The most helpful feature before diagnosing such a small VSD is that one should also be able to see the VSD in a view where the ultrasound beam is more perpendicular to the septum. In this view, though the change in angle is small, the ultrasound beam is further away from parallel to the ventricular septum and shows an intact ventricular septum (arrow).

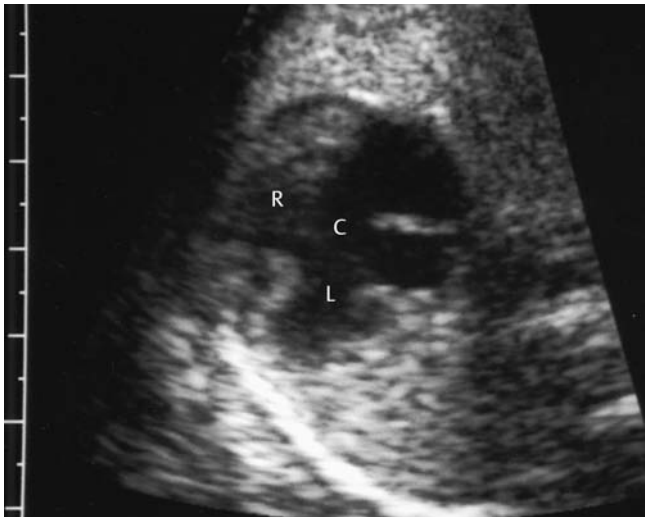

Figure 16–6 Atrioventricular canal defect. This four-chamber view shows the characteristic defect at the crux (C) of the heart. The defect includes the upper portion of the ventricular septum and lower portion of the atrial septum. R, right ventricle; L, left ventricle.

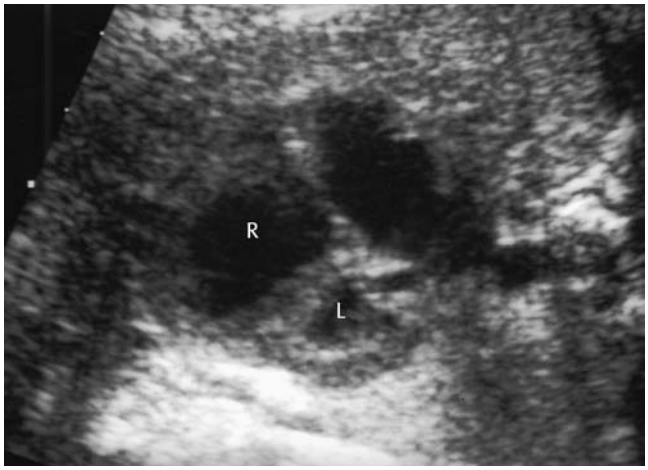

Figure 16–7 Hypoplastic left heart syndrome (HLHS). The left ventricle (L) is very small relative to the right ventricle (R). In some cases of HLHS, the left ventricle is even smaller than this and may be difficult to identify. Other views in this fetus demonstrated a very small aorta.

studies reporting well under 50% sensitivity.[25,30,48–53] Small, isolated VSDs are most likely to escape detection. About 70% of isolated small VSDs will close spontaneously, either before birth or generally within the first year of life.[54,55] Although VSDs are common lesions and often isolated, they also occur commonly in fetuses with trisomy 21 and trisomy 18. Thus, one should look carefully for other cardiac anomalies and for extracardiac anomalies.

Atrioventricular canal defect (AVCD) is identified as a defect in the lower portion of the atrial septum and upper portion of the ventricular septum and is an important reason to evaluate the "crux" of the heart (**Fig. 16–6**). The normal slight differential insertion of the atrioventricular (AV) valves is lost and a common AV valve may be present. AVCD is associated with Down syndrome and also with polysplenia and asplenia. About 30 to 40% of patients with AVCD will have trisomy 21. Complete heart block may be present due to distortion of the conduction tissue. Heart block or AV valve regurgitation may lead to congestive heart failure and hydrops. One should be aware that the entrance of the coronary sinus into the right atrium can simulate a defect in the lower atrial septum, which might raise concern for an ostium primum atrial septal defect that may be a component of AVCD.[56]

Left Ventricle Smaller than Right Ventricle

We will consider ventricular size discrepancy in relative, rather than absolute, terms. The ventricles are normally the same size or the right ventricle (RV) may be slightly larger than the left ventricle (LV). Care must be taken not to oblique the plane of imaging, thus falsely producing an image of one ventricle being small. When the LV is very small, hypoplastic left heart syndrome (HLHS) is the most likely lesion. When the LV is only slightly small, coarctation of the aorta is the main lesion to consider, but the differential diagnosis also includes total anomalous pulmonary venous return, changes secondary to intrauterine growth restriction (IUGR), and some forms of pulmonary atresia.

In HLHS, the LV is usually severely underdeveloped (**Fig. 16–7**), but there is a spectrum of severity. Typically, the mitral valve is hypoplastic, whereas the aortic valve is an imperforate membrane. The ascending aorta and arch are usually very small. In utero, there may be no hemodynamic consequence because the RV supplies both the pulmonary and the systemic circulations. The ascending aorta fills retrograde via the ductus arteriosus.[57]

Coarctation of the aorta produces a less marked decrease in left ventricular size than does HLHS (**Fig. 16–8**). It is unlikely to cause significant hemodynamic disturbance in the fetus. The sonographic diagnosis is challenging, but should be suspected when the LV is relatively smaller than the RV.[58–62] The sensitivity of prenatal sonography for coarctation remains only moderate, however, around 50 to 62%.[53,60] A relatively small LV is usually first detected with subjective evaluation. Norms for ventricular size can be used for more objective evaluation.[63] However, not all fetuses with a slightly small LV will have coarctation and some will be normal at birth. The RV normally becomes larger, relative to the LV with increasing gestational age. Thus the LV:RV ratio (ratio of LV to RV width) decreases with increasing gestational age, and at term the mean LV:RV ratio is 0.78.[63]

False-positive diagnoses of coarctation, based on ventricular disproportion, are more likely in the third trimester.[60,62] Accurate prenatal diagnosis remains difficult in many cases. Evaluation of the size of the aortic arch (typically small with coarctation) may help improve the

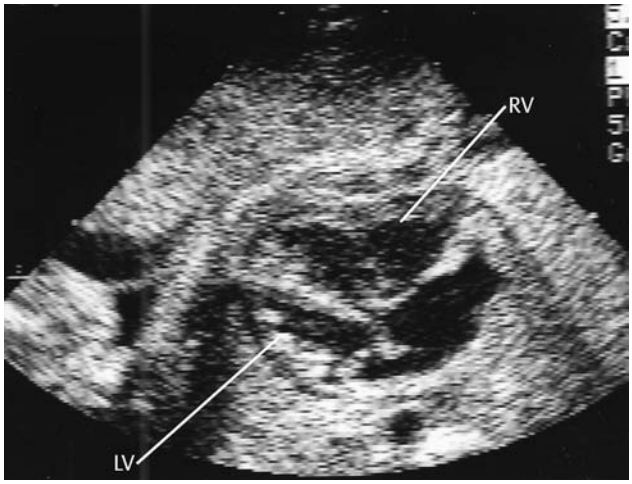

A

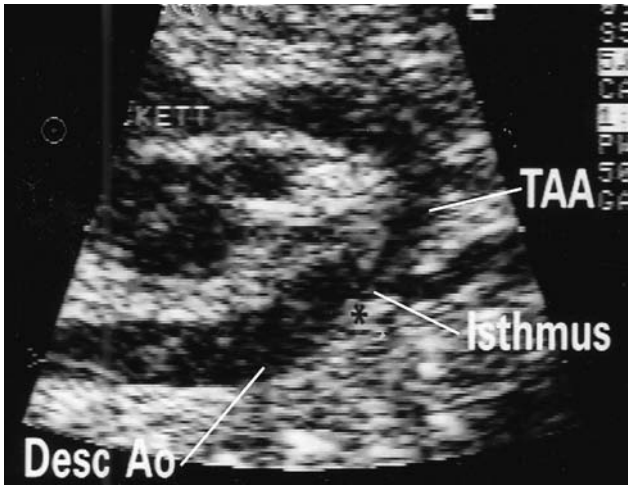

B

Figure 16–8 Coarctation of the aorta. **(A)** In this four-chamber view, the left ventricle (LV) is slightly smaller than the right ventricle (RV). Such ventricular size discrepancy is an indirect finding that may be seen with coarctation, but can be problematic because some fetuses with mild discrepancy will have a normal heart. When we identify such a finding, we generally refer patients to our pediatric cardiology colleagues for more detailed assessment, particularly of the aortic arch. **(B)** An image of the aortic arch in this same fetus revealed a small transverse aortic arch (TAA) and isthmus, which is supportive evidence of a coarctation. Desc Ao, descending aorta. (From Brown DL, Hornberger LK. Problems and pitfalls in the sonographic diagnosis of fetal cardiac anomalies. Ultrasound Q 1995;13:221–227. Reprinted by permission.)

accuracy of prenatal diagnosis.[64,65] The actual narrowing in the aortic arch is often difficult to image directly, and conversely, slight narrowing in the isthmus of the aorta can be seen in some normal fetuses. Coarctation of the aorta seems to be the most common cardiac lesion seen prenatally in fetuses with Turner's syndrome.[66] Thus, this diagnosis should be carefully evaluated for in fetuses with known Turner's syndrome or those with risk factors for Turner's syndrome, such as nuchal cystic hygroma.

Some fetuses with severe IUGR may have ventricular disproportion due to an enlarged RV.[67,68] This is postulated to be secondary to the increased placental vascular resistance that the RV pumps against or to myocardial dysfunction related to hypoxemia.[67]

Total anomalous pulmonary venous return (TAPVR) may produce a slightly small LV compared with the RV.[33] One should suspect TAPVR if no pulmonary veins are seen to enter the left atrium, if there is a common pulmonary venous chamber posterior to the left atrium, or if the anomalous draining vein is seen. Though TAPVR is uncommon, it remains one of the more frequently missed cardiac anomalies by prenatal sonography.

Fetuses with pulmonary atresia can have variable RV size. Although the RV may be large and thus considered in this differential diagnosis, it more frequently is small. The RV will be discussed in the next section.

Right Ventricle Smaller than Left Ventricle

Pulmonary atresia is considered in this section, although the RV can be either small, normal, or slightly large.[33] This variability may be related to two types of pulmonary atresia.[69] Pulmonary atresia with an intact ventricular septum (PA-IVS) may be an "acquired" congenital lesion. The valve typically has minimal to no abnormality. The PA is often large and the RV, although variable in size, is usually small (**Fig. 16–9**). Pulmonary atresia with a VSD (PA-VSD) is considered by some to be a severe form of TOF. The valve is

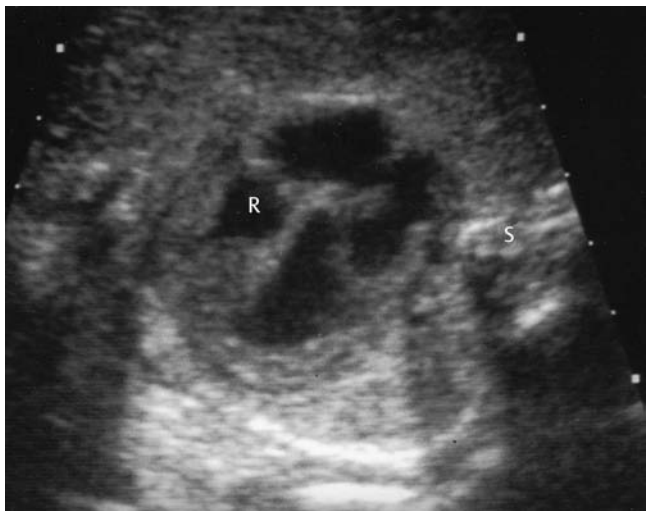

Figure 16–9 Pulmonary atresia, with intact ventricular septum. In this four-chamber view, the right ventricle (R) is small and has a slightly thick wall. Other views demonstrated a relatively normal-sized pulmonary artery, and more detailed assessment showed no flow through the pulmonary valve. Severe pulmonary stenosis may have a similar appearance prenatally. This view also shows an abnormal cardiac axis. The ventricular septum is oriented at nearly 90 degrees to the midline sagittal plane. S, spine.

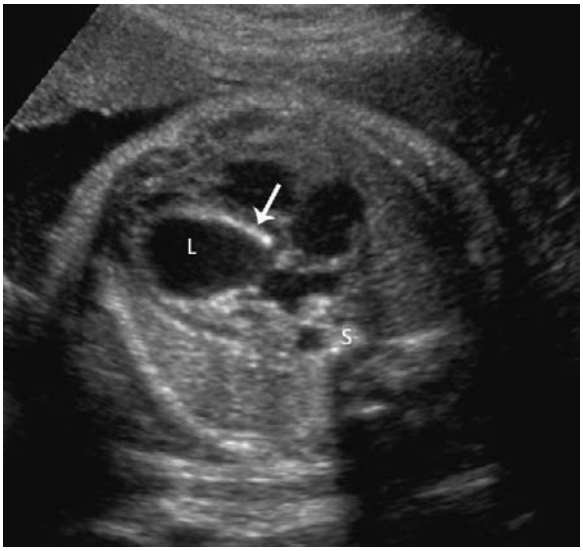

Figure 16–10 Critical aortic stenosis. Four-chamber view shows a dilated left ventricle (L). At real-time scanning, there was poor contractility of the left ventricle. The increased echogenicity along the ventricular wall (arrow) is typically due to secondary endocardial fibroelastosis. S, spine. (Image courtesy of William J. Watson, M.D., Rochester, MN)

usually abnormally formed and the PA is generally small. The RV is usually normal in size. Right atrial enlargement may be present due to tricuspid regurgitation, and can be so severe that pulmonary hypoplasia results. Pulmonary atresia and severe pulmonic valvular stenosis may appear similar prenatally, and one may not be able to distinguish them unless antegrade flow through the pulmonic valve is detected by Doppler ultrasound (thereby excluding pulmonary atresia).[70] Obstructive lesions of the pulmonary (or aortic) valve may evolve in utero, sometimes progressing from valve stenosis to atresia (at least functional atresia).

Critical aortic stenosis generally causes an enlarged, poorly contractile LV (**Fig. 16–10**). The endocardium may be very echogenic due to associated endocardial fibroelastosis. The aortic valve is often small. The left atrium may be enlarged due to mitral regurgitation. This lesion can progress in utero to HLHS.

Tricuspid atresia is an uncommon lesion in which the RV may be small. The tricuspid valve is absent and one may see a thick band of tissue in its expected location. Doppler helps confirm absence of flow from the right atrium to the RV. Transposition of the great arteries coexists in some cases.

Enlarged Right Atrium

Abnormalities of both the pulmonic valve and the tricuspid valve need to be considered when the right atrium is enlarged. Pulmonary atresia/severe stenosis has been discussed previously. This section considers tricuspid valve abnormalities.

Ebstein's anomaly is due to downward displacement, to varying degrees, of the septal and posterior leaflets of the tricuspid valve. The valve may also be dysplastic. The tricuspid valve is usually insufficient, leading to further right atrial enlargement. Ultrasound demonstrates variable degrees of downward displacement of the tricuspid valve into the RV and variable degrees of right atrial enlargement[71–73] (**Fig. 16–11**). The resulting RV cavity may be small, as may the PA. There is a wide spectrum of clinical severity of Ebstein's anomaly. Other cardiac anomalies, such as pulmonary atresia/stenosis or transposition anomalies, may coexist with Ebstein's anomaly. Maternal lithium use has been reported to be a risk factor for Ebstein's anomaly, though the risk may not be as high as once thought.[74]

Ebstein's anomaly is part of a spectrum of malformations that has variable degrees of dysplasia of the tricuspid valve and/or RV.[75] Any of the anomalies in this spectrum may cause a large right atrium. Also in this spectrum is dysplasia of the tricuspid valve, where the valve is abnormally thickened, but normally attached.[71–73] Other rare anomalies in this spectrum of malformations are Uhl's anomaly and a congenital absence of tricuspid valve leaflets.

Masses within the Cardiac Chambers

Cardiac tumors are the primary consideration here. One should be aware that the apex of the RV is normally

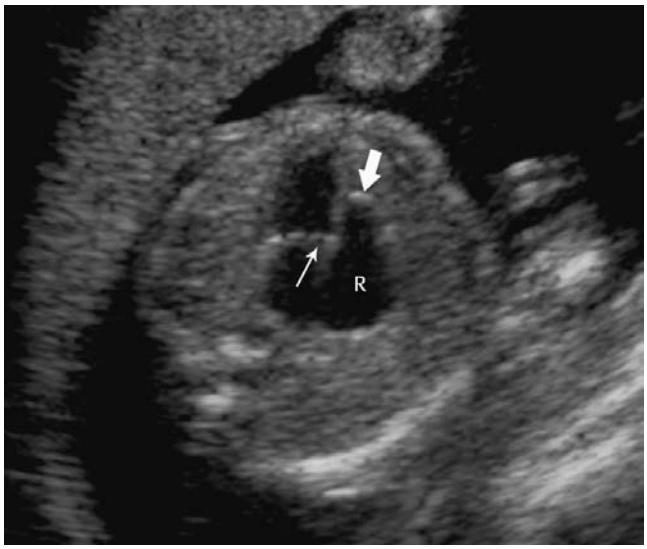

Figure 16–11 Ebstein's anomaly. In this four-chamber view, the right atrium (R) is enlarged and the tricuspid valve (thick arrow) inserts lower on the ventricular septum than normal. Although the tricuspid valve attachment to the ventricular septum is normally slightly more toward the cardiac apex than is the mitral valve attachment (thin arrow), the difference in insertion levels in this fetus is much more than normal. In this view the right ventricle is even difficult to discern due to the marked downward displacement of tricuspid valve leaflets. (Image courtesy of Roger W. Harms M.D., Rochester, MN)

blunted, due to the moderator band, and should not be mistaken for a mass.

Rhabdomyomas are the most common type of fetal cardiac tumor.[76] Tuberous sclerosis is frequently present when a cardiac tumor is seen, although the diagnosis of tuberous sclerosis may not be made for several months, or sometimes years, after birth. Aside from this association, cardiac tumors are generally isolated anomalies. Size and location of tumors vary considerably. Although most are benign, they should be followed during pregnancy because congestive heart failure may occur if the tumor is positioned such that there is obstruction of blood flow. Arrhythmias have been reported—most frequently, supraventricular tachycardia,[33] but also bradycardia[77]—and can also cause congestive failure. Sonographically, one observes a hyperechoic mass within the heart (**Fig. 16–12**). Postnatally, most cardiac rhabdomyomas undergo total or partial regression.[78,79]

Most tumors can be distinguished from the more frequent echogenic foci within the cardiac ventricles by assessment of their echogenicity and size. The echogenic foci are generally due to papillary muscle mineralization[80] and are more brightly echogenic than tumors. These echogenic foci are small (generally less than 3 mm), whereas tumors are more variable, and often larger, in size.

Outflow Tract Views: Abnormal Findings

The most important points to note when evaluating the great arteries are that there normally is continuity between the ventricular septum and the anterior wall of the aorta, and that the great arteries cross at right angles to each other as they exit the heart. The aorta crosses from left to right, and the PA from right to left. Demonstration of these two normal relationships helps exclude abnormalities of the great arteries such as TOF, truncus arteriosus, and transposition anomalies.

Overriding Aorta

Although the aorta normally courses over the plane of the ventricular septum as it leaves the heart, the septum is intact. With an overriding aorta, one observes a VSD and the aorta displaced toward the right side. This disrupts the normal continuity of the ventricular septum and the wall of the aorta. It is possible, however, to falsely produce an image of aortic overriding. The origin of this artifact is uncertain, although it may be due to partial volume artifact of the more superior PA or of a sinus of Valsalva. If overriding is seen, then it needs to be confirmed with slightly different angulation of the transducer.[46] At least in some cases of pseudooverriding, close observation of the site of apparent discontinuity will show that it is actually distal to the aortic valve, whereas with true overriding, the discontinuity is proximal to the aortic valve.

TOF is the primary diagnosis to consider when overriding of the aorta is seen (**Fig. 16–13**). The VSD and overrid-

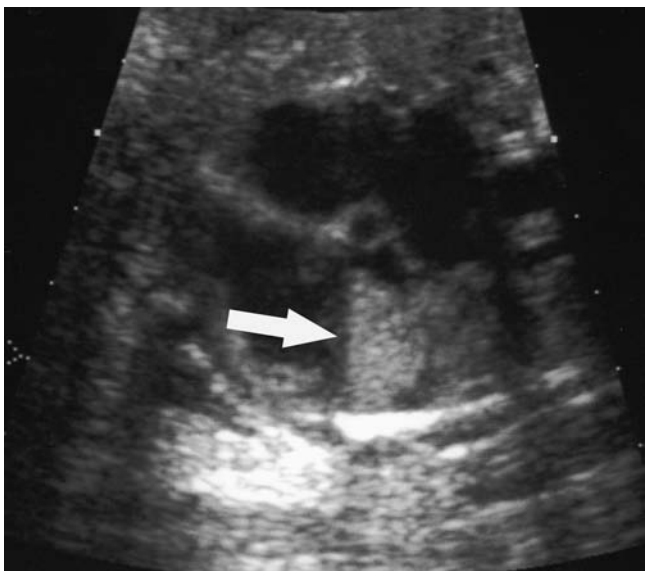

Figure 16–12 Cardiac tumor. A moderate-sized hyperechoic mass (arrow) fills much of the left ventricle in this four-chamber view. Additional cardiac tumors were also seen in this fetus. The pregnancy progressed uneventfully, and no hydrops or arrhythmias occurred.

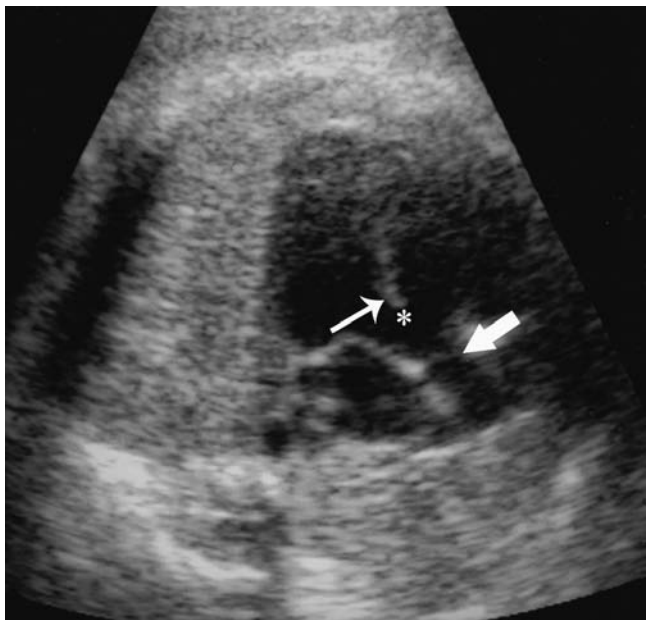

Figure 16–13 Tetralogy of Fallot. Left ventricular outflow tract views shows a ventricular septal defect (asterisk) and overriding of the aorta. The overriding appears as a lack of continuity between the ventricular septum (thin arrow points to upper end of ventricular septum) and wall of the aorta (thick arrow). The aorta is shifted toward the right ventricle and appears to "straddle" the ventricular septum. Additional views showed the pulmonary artery arising normally from the right ventricle, helping to confirm tetralogy of Fallot.

ing of the aorta are the two features that generally suggest the diagnosis prenatally. The PA may be small, but infundibular pulmonary stenosis may not be apparent, particularly early in pregnancy.[33] Right ventricular hypertrophy is not typically seen in the fetus.[81] If the pulmonary valve is absent, there is usually dilatation of the PA and its more peripheral branches.

When one observes an overriding aorta, the PA is a key structure to evaluate[33] to help distinguish TOF from other lesions that may have apparent overriding of the aorta. In TOF, the PA arises from the RV. Truncus arteriosus, although a less common lesion, is the likely diagnosis if the PA (or arteries) arises from the aorta. The PA may arise as a single vessel from the truncus arteriosus, or the right and left PAs may arise separately from the truncus arteriosus. If the PA is not present or is very small, pulmonary atresia with a VSD (probably a severe form of TOF) should be considered.

Parallel Aorta and Pulmonary Artery

The normal "criss-crossing" of these two arteries occurs in their initial course, as they exit the heart. Slightly more distally in their course (e.g., near the aortic arch level) one normally observes a segment of parallel orientation of the aorta and PA/ductus arteriosus. When the great arteries exit the ventricles in parallel, some type of transposition abnormality is probably present.

In complete transposition of the great arteries, the aorta arises from the RV, and the PA from the LV. Usually there is no hemodynamic consequence in utero, although if pulmonary stenosis is present, congestive heart failure can occur. Sonographically, one observes parallel orientation of the aorta and the PA as they exit the heart (**Fig. 16–14**). The aorta can be correctly identified by noting the head and neck arteries originating from it.

Double-outlet right ventricle (DORV) is a type of transposition abnormality. It occurs when the PA and most of the aorta arise from the RV. As in complete transposition, the normal criss-crossing of the aorta and PA is lost, but one observes both great arteries arising predominantly from the RV. A VSD is usually also present. Accurate diagnosis may be difficult at times because the abnormality may appear similar to either complete transposition of the great arteries or TOF. DOVR may coexist with other anomalies such as HLHS.

Corrected transposition is an uncommon anomaly, but may also produce an initial parallel course of the great arteries. The blunted appearance of the ventricular apex due to the moderator band may help one identify the morphologic RV, which is now the more posterior ventricle and gives rise to the aorta. The morphologic LV, with its pointed apex, is now the more anterior ventricle, and gives rise to the PA. This anomaly may be associated with situs abnormalities. Other lesions such as pulmonic stenosis or a VSD may be present. Atrioventricular block may occur due to distortion of the conducting tissue.

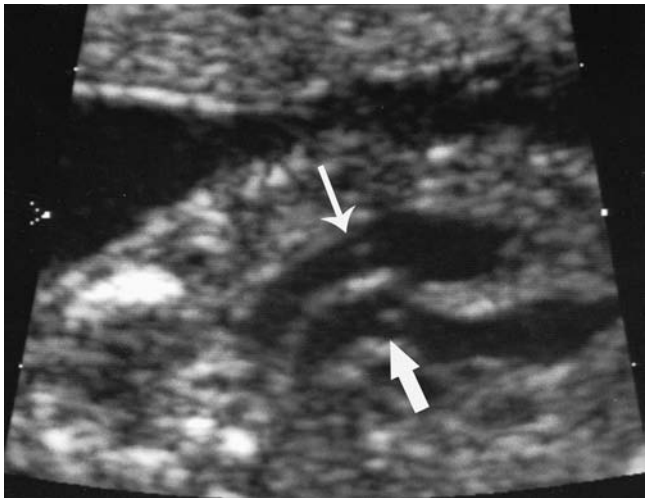

Figure 16–14 Transposition of the great arteries. A normal right and left ventricular outflow tract view could not be obtained in this fetus. Instead, the aorta (thin arrow) and the pulmonary artery (thick arrow) are in a parallel orientation as they exit the heart. Additional views confirmed which great artery was the aorta by demonstrating the head and neck arteries arising from it. (Image courtesy of Peter M. Doubilet, M.D., Ph.D., Boston, MA)

Summary

Although the 4C view is the basic view for evaluating the fetal heart, further evaluation of both outflow tracts will improve the sensitivity of obstetric ultrasound for CHD. If the sonographer and sonologist can adequately evaluate the six key features discussed here, four on the 4C view and two on the outflow tract views, then the majority of congenital heart anomalies can be diagnosed before birth, both in patients at higher risk for CHD and in those at lower risk.

In the future, more widespread use of late first trimester ultrasound to evaluate the heart in patients at higher risk for CHD will likely contribute to earlier diagnosis of CHD. Newer techniques such as three-dimensional and four-dimensional ultrasound may also play a role.[82,83]

References

1. Ardinger RH. Genetic counseling in congenital heart disease. Pediatr Ann 1997;26:99–104
2. Boughman JA, Berg KA, Astemborski JA, et al. Familial risks of congenital heart defect assessed in a population-based epidemiologic study. Am J Med Genet 1987;26:839–849
3. Cooper MJ, Enderlein ME, Dyson DC, Roge CL, Tarnoff H. Fetal echocardiography: retrospective review of clinical experience and an evaluation of indications. Obstet Gynecol 1995;86:577–582
4. Allan L. Fetal cardiology [editorial]. Ultrasound Obstet Gynecol 1994;4:441–444
5. Spevak PJ. New developments in fetal echocardiography. Curr Opin Cardiol 1997;12:78–83
6. Abuhamad A. A Practical Guide to Fetal Echocardiography. Philadelphia: Lippincott-Raven; 1997

7. Rice MJ, McDonald RW, Pilu G, Chaoui R. Cardiac malformations. In: Nyberg DA, McGahan JP, Pretorius D, Pilu G, eds. Diagnostic Imaging of Fetal Anomalies. Philadelphia: Lippincott Williams and Wilkins; 2003:451–506
8. Nora JJ, Nora AH. Update on counseling the family with a first-degree relative with a congenital heart defect. Am J Med Genet 1988; 29:137–142
9. Genetics of disorders with complex inheritance. In: Nussbaum RL, McInnes RR, Willard HF. Thompson and Thompson Genetics in Medicine. 6th ed., rev. reprint ed. Philadelphia: Saunders; 2004: 289–310
10. Romano-Zelekha O, Hirsh R, Blieden L, Green M, Shohat T. The risk for congenital heart defects in offspring of individuals with congenital heart defects. Clin Genet 2001;59:325–329
11. Burn J, Brennan P, Little J, et al. Recurrence risks in offspring of adults with major heart defects: results from first cohort of British collaborative study. Lancet 1998;351:311–316
12. Whittemore R, Wells JA, Castellsague X. A second-generation study of 427 probands with congenital heart defects and their 837 children. J Am Coll Cardiol 1994;23:1459–1467
13. Nora JJ, Nora AH. Maternal transmission of congenital heart diseases: new recurrence risk figures and question of cytoplasmic inheritance and vulnerability to teratogens. Am J Cardiol 1987;59: 459–463
14. Clark EB. Pathogenetic mechanisms of congenital cardiovascular malformations revisited. Semin Perinatol 1996;20:465–472
15. Gill HK, Splitt M, Sharland GK, Simpson JM. Patterns of recurrence of congenital heart disease: an analysis of 6,640 consecutive pregnancies evaluated by detailed fetal echocardiography. J Am Coll Cardiol 2003;42:923–929
16. Kohl T, Sharland G, Allan LD, et al. World experience of percutaneous ultrasound-guided balloon valvuloplasty in human fetuses with severe aortic valve obstruction. Am J Cardiol 2000;85:1230–1233
17. Tworetzky W, Wilkins-Haug L, Jennings RW, et al. Balloon dilation of severe aortic stenosis in the fetus: potential for prevention of hypoplastic left heart syndrome: candidate selection, technique, and results of successful intervention. Circulation 2004;110:2125–2131
18. Thomas JA, Graham JM. Chromosome 22q11 deletion syndrome: an update and review for the primary pediatrician. Clin Pediatr (Phila) 1997;36:253–266
19. Strauss AW, Johnson MC. The genetic basis of pediatric cardiovascular disease. Semin Perinatol 1996;20:564–576
20. Ryan AK, Goodship JA, Wilson DI, et al. Spectrum of clinical features associated with interstitial chromosome 22q11 deletions: a European collaborative study. J Med Genet 1997;34:798–804
21. Johnson MC, Hing A, Wood MK, Watson MS. Chromosome abnormalities in congenital heart disease. J Med Genet 1997;70:292–298
22. Shultz SM, Pretorius DH, Budorick NE. Four-chamber view of the fetal heart: demonstration related to menstrual age. J Ultrasound Med 1994;13:285–289
23. Allan LD. Cardiac anatomy screening: what is the best time for screening in pregnancy? Curr Opin Obstet Gynecol 2003;15:143–146
24. DeVore GR. The aortic and pulmonary outflow tract screening examination in the human fetus. J Ultrasound Med 1992;11:345–348
25. Bromley B, Estroff JA, Sanders SP, et al. Fetal echocardiography: accuracy and limitations in a population at high and low risk for heart defects. Am J Obstet Gynecol 1992;166:1473–1481
26. Benacerraf BR. Sonographic detection of fetal anomalies of the aortic and pulmonary arteries: value of four-chamber view vs direct images. AJR Am J Roentgenol 1994;163:1483–1489
27. Gembruch U, Baschat AA, Knopfle G, Hansmann M. First- and early second-trimester diagnosis of fetal cardiac anomalies. In: Wladimiroff JW, Pilu G, eds. Ultrasound and the Fetal Heart. New York: Parthenon Publishing Group; 1996:39–46
28. Huggon IC, Ghi T, Cook AC, Zosmer N, Allan LD, Nicolaides KH. Fetal cardiac abnormalities identified prior to 14 weeks' gestation. Ultrasound Obstet Gynecol 2002;20:22–29
29. Haak MC, Twisk JW, Van Vugt JM. How successful is fetal echocardiographic examination in the first trimester of pregnancy? Ultrasound Obstet Gynecol 2002;20:9–13
30. Crane JP, LeFevre ML, Winborn RC, et al. A randomized trial of prenatal ultrasonographic screening: impact on the detection, management, and outcome of anomalous fetuses. Am J Obstet Gynecol 1994;171:392–399
31. Achiron R, Glaser J, Gelernter I, Hegesh J, Yagel S. Extended fetal echocardiographic examination for detecting cardiac malformations in low risk pregnancies. BMJ 1992;304:671–674
32. Kirk JS, Riggs TW, Comstock CH, Lee W, Yang SS, Weinhouse E. Prenatal screening for cardiac anomalies: the value of routine addition of the aortic root to the four-chamber view. Obstet Gynecol 1994;84:427–431
33. Allan LD. Manual of Fetal Echocardiography. Lancaster, England: MTP Press Limited; 1986
34. Brown DL, Emerson DS, Cartier MS, Felker RE, DiSessa TG, Smith WC. Congenital cardiac anomalies: prenatal sonographic diagnosis. AJR Am J Roentgenol 1989;153:109–114
35. McGahan JP. Sonography of the fetal heart: findings on the four-chamber view. AJR Am J Roentgenol 1991;156:547–553
36. Comstock CH, Smith R, Lee W, Kirk JS. Right fetal cardiac axis: clinical significance and associated findings. Obstet Gynecol 1998;91:495–499
37. Shipp TD, Bromley B, Hornberger LK, Nadel A, Benacerraf BR. Levorotation of the fetal cardiac axis: a clue for the presence of congenital heart disease. Obstet Gynecol 1995;85:97–102
38. Smith RS, Comstock CH, Kirk JS, Lee W. Ultrasonographic left cardiac axis deviation: a marker for fetal anomalies. Obstet Gynecol 1995;85:187–191
39. Practice AIUM. Guideline for the performance of an antepartum obstetric ultrasound examination. J Ultrasound Med 2003;22: 1116–1125
40. Frates M. Sonography of the normal fetal heart: a practical approach. AJR Am J Roentgenol 1999;173:1363–1370
41. Cartier MS, Davidoff A, Warneke LA, et al. The normal diameter of the fetal aorta and pulmonary artery: Echocardiographic evaluation in utero. AJR Am J Roentgenol 1987;149:1003–1007
42. Copel JA, Morotti R, Hobbins JC, Kleinman CS. The antenatal diagnosis of congenital heart disease using fetal echocardiography: is color flow mapping necessary? Obstet Gynecol 1991;78:1–8
43. Sharland GK, Chita SK, Allan LD. The use of colour Doppler in fetal echocardiography. Int J Cardiol 1990;28:229–236
44. Rice MJ, McDonald RW, Sahn DJ. Contributions of color Doppler to the evaluation of cardiovascular abnormalities in the fetus. Semin Ultrasound CT and MRI 1993;14:277–285
45. DeVore GR, Alfi O. The use of color Doppler ultrasound to identify fetuses at increased risk for trisomy 21: an alternative for high-risk patients who decline genetic amniocentesis. Obstet Gynecol 1995; 85:378–386
46. Brown DL, DiSalvo DN, Frates FC, et al. Sonography of the fetal heart: normal variants and pitfalls. AJR Am J Roentgenol 1993;160: 1251–1255
47. Silverman NH. Pediatric Echocardiography. Baltimore: Williams and Wilkins; 1993

48. Tegnander E, Eik-Nes SH, Johansen OJ, Linker DT. Prenatal detection of heart defects at the routine fetal examination at 18 weeks in a non-selected population. Ultrasound Obstet Gynecol 1995;5: 372–380
49. Stoll C, Alembik Y, Dott B, Roth PM, De Getter B. Evaluation of prenatal diagnosis of congenital heart disease. Prenat Diagn 1993;13: 453–461
50. Wigton TR, Sabbagha RE, Tamura RK, Cohen L, Minogue JP, Strasburger JF. Sonographic diagnosis of congenital heart disease: comparison between the four-chamber view and multiple cardiac views. Obstet Gynecol 1993;82:219–224
51. Benacerraf BR, Pober BR, Sanders SP. Accuracy of fetal echocardiography. Radiology 1987;165:847–849
52. Copel JA, Pilu G, Green J, Hobbins JC, Kleinman CS. Fetal echocardiographic screening for congenital heart disease: the importance of the four-chamber view. Am J Obstet Gynecol 1987;157:648–655
53. Kirk JS, Comstock CH, Lee W, Smith RS, Riggs TW, Weinhouse E. Sonographic screening to detect fetal cardiac anomalies: a 5-year experience with 111 abnormal cases. Obstet Gynecol 1997;89: 227–232
54. Paladini D, Palmieri S, Lamberti A, Teodoro A, Martinelli P, Nappi C. Characterization and natural history of ventricular septal defects in the fetus. Ultrasound Obstet Gynecol 2000;16:118–122
55. Orie J, Flotta D, Sherman FS. To be or not to be a VSD. Am J Cardiol 1994;74:1284–1285
56. Brown DL, Hornberger LK. Problems and pitfalls in the sonographic diagnosis of fetal cardiac anomalies. Ultrasound Q 1995;13:221–227
57. Cartier MS, Emerson DS, Plappert T, St. John Sutton M. Hypoplastic left heart with absence of the aortic valve: prenatal diagnosis using two-dimensional and pulsed Doppler echocardiography. J Clin Ultrasound 1987;15:463–468
58. Allan LD, Chita SK, Anderson RH, Fagg N, Crawford DC, Tynan MJ. Coarctation of the aorta in prenatal life: an echocardiographic, anatomical, and functional study. Br Heart J 1988;59:356–360
59. Benacerraf BR, Saltzman DH, Sanders SP. Sonographic sign suggesting the prenatal diagnosis of coarctation of the aorta. J Ultrasound Med 1989;8:65–69
60. Brown DL, Durfee SM, Hornberger LK. Ventricular discrepancy as a sonographic sign of coarctation of the fetal aorta: how reliable is it? J Ultrasound Med 1997;16:95–99
61. Emerson D, Cartier M, DiSessa T, Brown D, Felker R. Prenatal sonographic identification of coarctation of the aorta. J Ultrasound Med 1988;7:S271
62. Sharland GK, Chan K, Allan LD. Coarctation of the aorta: difficulties in prenatal diagnosis. Br Heart J 1994;71:70–75
63. Sharland GK, Allan LD. Normal fetal cardiac measurements derived by cross-sectional echocardiography. Ultrasound Obstet Gynecol 1992;2:175–181
64. Hornberger LK, Weintraub RG, Pesonen E, et al. Echocardiographic study of the morphology and growth of the aortic arch in the human fetus: observations related to the prenatal diagnosis of coarctation. Circulation 1992;86:741–747
65. Hornberger LK, Sahn DJ, Kleinman CS, Copel J, Silverman NH. Antenatal diagnosis of coarctation of the aorta: a multicenter experience. J Am Coll Cardiol 1994;23:417–423
66. Surerus E, Huggon IC, Allan LD. Turner's syndrome in fetal life. Ultrasound Obstet Gynecol 2003;22:264–267
67. Siassi B. Normal and abnormal transitional circulation in the IUGR infant. Semin Perinatol 1988;12:80–83
68. DeVore GR. Examination of the fetal heart in the fetus with intrauterine growth retardation using M-mode echocardiography. Semin Perinatol 1988;12:66–79
69. Kutsche LM, Van Mierop LHS. Pulmonary atresia with and without ventricular septal defect: a different etiology and pathogenesis for the artesia in the 2 types. Am J Cardiol 1983;51:932–935
70. Hornberger LK, Benacerraf BR, Bromley BS, Spevak PJ, Sanders SP. Prenatal detection of severe right ventricular outflow tract obstruction. J Ultrasound Med 1994;13:743–750
71. Hornberger LK, Sahn DJ, Kleinman CS, Copel JA, Reed KL. Tricuspid valve disease with significant tricuspid insufficiency in the fetus: diagnosis and outcome. J Am Coll Cardiol 1991;17:167–173
72. Roberson DA, Silverman NH. Ebstein's anomaly: echocardiographic and clinical features in the fetus and neonate. J Am Coll Cardiol 1989;14:1300–1307
73. Sharland GK, Chita SK, Allan LD. Tricuspid valve dysplasia or displacement in intrauterine life. J Am Coll Cardiol 1991;17:944–949
74. Cohen LS, Friedman JM, Jefferson JW, Johnson EM, Weiner ML. A reevaluation of risk of in utero exposure to lithium. JAMA 1994;271:146–150
75. Kumar AE, Gilbert G, Aerichide N, Van Praagh R. Ebstein's anomaly, Uhl's disease and absence of tricuspid valve leaflets: a new spectrum [abstract]. Am J Cardiol 1970;25:111–112
76. Groves AMM, Fagg NLK, Cook AC, Allan LD. Cardiac tumors in intrauterine life. Arch Dis Child 1992;67:1189–1192
77. Gresser CD, Shime J, Rakowski H, Smallhorn JF, Hui A, Berg JJ. Fetal cardiac tumor: a prenatal echocardiographic marker for tuberous sclerosis. Am J Obstet Gynecol 1987;156:689–690
78. Pipitone S, Mongiovi M, Grillo R, Gagliano S, Sperandeo V. Cardiac rhabdomyoma in intrauterine life: clinical features and natural history: a case series and review of published reports. Ital Heart J 2002;3:48–52
79. Fesslova V, Villa L, Rizzuti T, Mastrangelo M, Mosca F. Natural history and long-term outcome of cardiac rhabdomyomas detected prenatally. Prenat Diagn 2004;24:241–248
80. Brown DL, Roberts DJ, Miller WA. Left ventricular echogenic focus in the fetal heart: pathologic correlation. J Ultrasound Med 1994;13:613–616
81. Allan LD, Sharland GK. Prognosis in fetal tetralogy of Fallot. Pediatr Cardiol 1992;13:1–4
82. Chaoui R, Hoffman J, Heling KS. Three-dimensional (3D) and 4D color Doppler fetal echocardiography using spatio-temporal image correlation. Ultrasound Obstet Gynecol 2003;23:535–545
83. DeVore GR, Falkensammer P, Sklansky MS, Platt LD. Spatio-temporal image correlation (STIC): new technology for evaluation of the fetal heart. Ultrasound Obstet Gynecol 2003;22:380–387

17 Pregnant Women with High Maternal Serum–Alpha-Fetoprotein

Andrea L. Fick and Ruth B. Goldstein

Maternal Serum–Alpha-Fetoprotein Screening

Alpha-fetoprotein (AFP) screening was shown to be effective for detecting neural tube defects (NTDs) in the 1970s.[1] In 1991, the American College of Obstetrics and Gynecology (ACOG) endorsed offering maternal serum (MS)-AFP testing to all pregnant women. Since then, screening in the United States has become more widespread, and experience in this country and others has demonstrated considerable benefits from AFP screening, not only for the detection of NTDs, but also for several other fetal abnormalities (i.e., twins, ventral abdominal wall defects, and chromosomal abnormalities). In one study, either high or low MS-AFP was associated with 34% of all major congenital defects.[2] Further, even in the absence of multiple gestations and discrete fetal defects, earlier studies suggested that women with high MS-AFP had a much higher rate of adverse pregnancy outcomes.[3,4] More recent publications indicate that this association holds true for fetal death and premature birth, but an elevated AFP may not be a risk factor for fetal growth restriction and preeclampsia.[5–8]

It is estimated that as many as 20 to 38% of women with unexplained high MS-AFP will suffer adverse pregnancy outcomes[9,10]; this information is another important benefit of MS-AFP screening. These fetal deaths occur mainly in the second trimester, and the risk appears to be directly related to the degree of MS-AFP elevation.[4]

California implemented a statewide screening program in 1986. It is now required by California state law that women who begin prenatal care before 20 weeks be offered MS-AFP screening. Currently, over 300,000 pregnant women in California are tested annually. Among the first 1.1 million women screened through the California AFP Screening Program, 1390 fetal anomalies (morphological and chromosomal) were detected (prevalence of 1.3/1000). These included 710 NTDs (417 anencephaly, 247 spina bifida, and 46 encephalocele), 286 ventral abdominal wall defects, 163 fetuses with Down syndrome, and 231 cases of other chromosomal anomalies. Impressively, of all anomalies detected in this program, nearly three quarters involved two organ systems: the neural axis (51%) and the ventral abdominal wall (21%). This distribution of "likely" fetal anomalies is especially germane to the sonologist examining women with elevated MS-AFP. These two groups of fetal defects (and many others) can now be accurately detected on targeted prenatal sonograms performed by experienced examiners.

Sources of Maternal Serum–Alpha-Fetoprotein

AFP is a glycoprotein produced initially by the yolk sac and fetal gut, and later predominantly by the fetal liver. At the end of the first trimester, it is present in the fetal serum in milligram quantities, and in the amniotic fluid in microgram quantities, and in the maternal serum in quantities measured in nanograms. In the fetus, serum AFP level increases until ~14 to 15 weeks and then falls progressively. In normal pregnancies, AFP from fetal serum enters the amniotic fluid through fetal urination, fetal gastrointestinal secretions, and transudation across fetal membranes (amnion and placenta) and immature epithelium. Detectable quantities of AFP in the MS gradually increase during gestation, peaking at 30 to 32 weeks and declining thereafter. MS levels are usually reported in multiples of the median (MoM) to standardize interpretation among laboratories.

There are several potential ways that fetal AFP can enter the MS in abnormal quantities. Among fetal defects, the most common mechanism is through fetal cutaneous defects. These defects result in leakage of fetal serum proteins into the amniotic fluid, and secondarily into MS. Other abnormalities, including intrinsic placental abnormalities and maternal–fetal hemorrhage, also allow fetal AFP to mix with MS. In some cases, the precise mechanism for the fetomaternal transfer is not known (proximal gut obstruction, renal agenesis), and may be secondary to diminished fetal gut degradation or elevated fetal serum concentrations of AFP.

It would be ideal if a single MS-AFP level could completely segregate normal from abnormal fetuses. Unfortunately, this is impossible owing to considerable overlap in MS-AFP levels between normal and abnormal pregnancies. Thus, the choice of a judicious cutoff value that maximizes detection of anomalies and minimizes the number of false-positive results is necessary for this screening program to be effective. Most screening programs in the United States have settled on a serum value of ≥ 2.5 MoM. Using this cutoff, ~90% of anencephalic fetuses, 75 to 80% of fetuses with an open spinal defect, 98% of fetuses with gastroschisis, and ~70% of fetuses with omphaloceles will be detected.[11] Further, using 2.5 MoM as the cutoff has resulted in a reasonably low screen-positive rate (~4 to 5%).

How Patients Are Triaged in Maternal Serum Screening Programs

It is optimal to test MS between 16 and 18 weeks. Accurate dating is critical for AFP screening because serum AFP levels rise ~15% per week during the 16 to 18 week window. MS-AFP values are also corrected for maternal age, maternal weight, race, and the presence of diabetes (diabetes has a depressing effect on MS-AFP, so lower levels may be found in association with NTDs).[12] In California, ~2% of screened women have elevated MS-AFP levels (≥ 2.5 MoM), and ~3% have MS-AFP levels ≤ 0.5 MoM. The latter group is discussed elsewhere. Roughly 6 to 15% of women with high MS-AFP have some type of major congenital defect, and this risk increases with the magnitude of MS-AFP elevation.[2,13,14]

If MS-AFP is elevated, then a nontargeted, standard antepartum obstetrical sonogram (level 1) is performed for the purpose of identifying easily recognized causes of "false-positives" (gestational age ≥ 2 weeks more advanced than estimated clinically, multiple gestations, fetal death, and obvious fetal defects). The intent of a standard antepartum obstetrical sonogram is to provide a general assessment of fetal/pregnancy health; it is performed according to the published guidelines endorsed by the American Institute of Ultrasound in Medicine (AIUM), ACOG, and American College of Radiology (ACR).[15] The standard antepartum obstetrical sonogram is an important step in the triage of patients with high MS-AFP; impressively, approximately 20 to 50% of the elevated MS-AFP levels will be explained by findings on this preliminary sonogram (including the detection of a number of neural tube and abdominal wall defects).[16,17] If the elevated MS-AFP is not explained by findings of the standard antepartum obstetrical sonogram, traditionally, the next step has been to counsel patients and offer amniocentesis for measurement of amniotic fluid (AF)-AFP. Among women who choose to undergo amniocentesis following an "unrevealing" sonogram, > 90% will have normal AF-AFP (< 2.0 MoM), and no further diagnostic evaluation is done.[18] If the AF-AFP is elevated (≥ 2.0 MoM), then acetylcholinesterase (an isoenzyme important in neurotransmission) is tested on the amniotic fluid sample. Acetylcholinesterase is present in association with exposed neural tissue (and occasionally with abdominal wall defects). High AF-AFP plus positive acetylcholinesterase is quite specific for a fetal defect. In most screening programs, karyotype testing is also routinely performed on the amniotic fluid specimen.

If the AF-AFP is elevated (≥ 2.0 MoM), a targeted fetal sonogram (level 2) is offered. Among women with elevated AF-AFP, approximately one third of fetuses are anomalous.[18] Similar to MS-AFP, the likelihood of a neural tube or other defect increases proportionately with the degree of AF-AFP elevation, but clearly not all of these fetuses will be abnormal. The targeted sonogram is performed to determine (1) whether any fetal anomaly is present (AF-AFP may be false-positive); (2) if the fetus is abnormal, what the nature of the anomaly is (e.g., NTD versus omphalocele); and (3) if present, the severity of the anomaly and presence/absence of associated malformations (e.g., spinal level of myelomeningocele).

AF-AFP testing is a highly sensitive method for detecting or excluding NTDs. The negative predictive value of a normal AF-AFP is ~97 to 99%, and elevated AF-AFP plus acetylcholinesterase allows > 99% accurate detection of NTDs.[19,20] The specificity is 94.9%.[20] High-resolution, targeted ultrasonography performed in conjunction with abnormal AF-AFP is also highly accurate in identifying anomalous fetuses (i.e., > 99% accurate).[18,21]

Nevertheless, there is a small, but important procedural fetal loss rate, 1/200 (0.5%), associated with amniocentesis. As a result, women with elevated MS-AFP have, in increasing numbers, opted to go directly from the serum AFP test to a targeted fetal sonogram, skipping the amniocentesis. The latter approach has become more popular in the last few years for two major reasons. First, sonographic detection of the "likely" anomalies associated with high MS-AFP has improved over the last 10 to 15 years. Expected rates of sonographic detection for neural tube and abdominal wall defects are currently > 90%.[21–27] It is estimated that a complete, detailed, normal sonogram can now reduce the MS-AFP-based risk of a neural tube or ventral abdominal wall defect by 95%.[28,29] Second, going directly to a targeted sonogram circumvents the small, but important procedural risk of fetal loss from amniocentesis. Indeed, the United Kingdom has adopted this paradigm and detailed, targeted sonograms are now routinely performed as the second diagnostic step in women with high MS-AFP.

Some have cautioned against adopting a routine policy of circumventing the amniocentesis because (1) this approach will require a much larger number of targeted sonograms (i.e., 10 times as many), and the larger number of experienced examiners may not be available, or patients may be required to travel a long distance for the targeted sonogram; (2) even experienced examiners, especially as the prevalence of defects falls in the population scanned,

may not detect as many defects as AF-AFP testing; and (3) skipping amniocentesis will cause potentially detectable chromosomal abnormalities to be missed.[23,30] The last issue remains controversial, and multicenter consensus has not been reached.

Some favor a paradigm in which targeted sonography follows a high MS-AFP, arguing that there is only a very small risk of an abnormal karyotype in a fetus without morphological defects. Recall that most of the unsuspected autosomal trisomies detected with AFP screening will occur in the low MS-AFP group, and that autosomal trisomies represent the minority of abnormal karyotypes found in women with high MS-AFP. These include mosaic trisomy 8 and trisomy 9.[31,32] For example, trisomies 13, 18, and 21 account for only 28% of abnormal karyotypes in women with high MS-AFP, compared with 75% of abnormal karyotypes in women ≥ of age. Further, fetuses with autosomal trisomies 13, 18, 21 detected as a result of high MS-AFP often have sonographically detectable structural abnormalities.[25,33] If the targeted sonographic fetal survey in a woman with elevated MS-AFP is normal, it has been estimated that the risk of a fetal chromosomal abnormality is only 0.6 to 1.1%, and sex chromosome aberrations (other than 45X) account for many (30 to 50%) of the chromosomal abnormalities in these fetuses.[24–28]

There is no right or wrong choice, all women facing the choice of targeted sonography versus amniocentesis should be fully informed of these controversies during their counseling. Decisions to perform an amniocentesis versus a targeted sonogram will vary according to patient (maternal age, other serologic markers, e.g., HCG and estriol, and personal choice) and institution (depending on availability of experienced sonologists). Although many patients will elect to have a targeted sonogram instead of amniocentesis, amniotic fluid testing should still be strongly considered in the following patients: (1) fetal position or maternal body habitus precludes an adequate sonographic fetal anatomical survey; (2) equivocal sonographic findings (e.g., abnormal posterior fossa, but spinal defect not seen); (3) experienced sonographic examiner not available; and (4) nonlethal anomaly detected on standard antepartum obstetrical sonogram for which karyotype testing is appropriate.[33–35]

Ultrasound Evaluation

Increased Maternal Serum-Alpha-Fetoprotein: What Should You Look For?

Accurate sonographic diagnosis has become extremely important in light of AFP screening in pregnancy. If the preliminary, standard antepartum sonogram is unrevealing or an amniocentesis shows an elevated AF-AFP, a targeted fetal survey is performed. Because the most commonly encountered defects are those of the neural tube and ventral abdominal wall, the neural axis and ventral abdominal wall will be the most critical regions for scrutiny during the targeted sonogram.

A focused examination of the neural axis in each fetus should include an assessment of overall cranial size and contour, ventricular size (transaxial diameter of ventricular atrium > 10 mm is abnormal), and posterior fossa, including cerebellar morphology and cisterna magna.[36–39] At the University of California–San Francisco, we also include images of the cavum septum pellucidum as a check for forebrain malformations. The spine should be carefully examined in each fetus, including segment by segment images in the transaxial and sagittal planes from the craniocervical junction through the sacrum. Sagittal and transaxial images of the spine should demonstrate an intact dorsal skin line. The normal curvature of the spine should be documented, and the ossified posterior elements examined for abnormal splaying. The ventral abdominal wall of the fetus is examined, with focused attention on the umbilical cord insertion. The examiner should maintain a heightened sensitivity to the presence of bowel loops within the umbilical cord or floating in the amniotic fluid distant from the cord insertion/abdominal wall.

Several other important fetal anomalies are associated with elevated AFP, and these potential defects should also be sought on the targeted sonogram (**Table 17–1**). Less common defects include fetal teratoma (pharyngeal,

Table 17–1 Differential Diagnosis of High Maternal Serum–Alpha-Fetoprotein

Common
A. Neural tube defects
Anencephaly
Myelomeningocele (Chiari II)
Cephalocele
B. Abdominal wall defects
Omphalocele
Gastroschisis
Gastropleuralschisis associated with abdominal band syndrome or limb–body wall
C. Multiple gestations
Uncommon
A. Cystic hygroma
B. Renal abnormalities
Finnish nephrosis (no defect observed sonographically)
Pelviectasis
C. Chorioangioma
D. Teratoma (oropharyngeal or sacrococcygeal)
E. Esophageal/duodenal atresia
F. Placental subchorionic hematoma
G. Maternal hepatoma

sacral), defects caused by the amniotic band syndrome (asymmetric cephaloceles, gastropleuralschisis), cystic hygroma, lesions that alter the placentomaternal barrier (e.g., placental chorioangioma, lakes, and abruption/hemorrhage), proximal fetal gut obstructions (e.g., esophageal and duodenal atresias), some renal abnormalities, and oligohydramnios.[39] Thus, careful examination of the face, posterior neck, oropharynx, thorax, abdomen (including a normally filled stomach) should be performed.[40] The limbs and digits should be assessed for abnormalities suggesting the amniotic band syndrome or the vertebral, anorectal, cardiac, tracheoesophageal fistula, renal, and limb (VACTERL) anomalies association. Amniotic fluid volume should be qualitatively or semiquantitatively assessed in addition to careful examination of the placenta. The most commonly encountered individual defects are discussed in the following section.

Anencephaly

Anencephaly accounts for approximately half of all NTDs (**Fig. 17–1**). On average, anencephaly is associated with the highest AF-AFP and MS-AFP values of all NTDs, and ~90% will be detected by an MS-AFP ≥ 2.5 MoM. This is a lethal anomaly in which the bony calvarium is absent above the orbits. Normal cerebral cortex is absent. Some dysplastic "brain tissue," representing angiomatous stroma, may be observed above the orbits, apparently floating freely in the amniotic fluid. Eighty-nine percent of fetuses with acrania had echogenic amniotic fluid on ultrasound performed between 11 and 13 weeks.[41] Owing to its irregular shape and absence of recognizable normal morphology, it is unlikely to be confused for normal brain. One should be cautious, however, not to confuse an engaged fetal head (in which the convexity may not be well visualized) for anencephaly. This distinction is accomplished by the observation of amniotic fluid above the orbits and the calvarial defect. It is critical that this be diagnosed accurately because most patients will electively terminate their pregnancies following this diagnosis. Anencephaly can be diagnosed in virtually all affected fetuses after 14 weeks gestation.[42]

Myelomeningocele

Since the 1960s, the number of infants born with neural tube defects has been declining.[43–45] The birth prevalence of myelomeningocele in 1970 was 1.3 per 1000 live births.[43] This contrasts with a birth prevalence of 0.6 per 1000 live births after serum screening became available in the 1980s.[43,44] This decrease is likely due to termination of pregnancies with a fetal neural tube defect. There has been a further decrease in birth prevalence to 0.41 per 1000 due to the Folic Acid Mandate of 1992 by the U.S. Public Health Service, which required fortification of foods with folic acid and encouraging daily folate supplements in women of child-bearing age.[46]

The myelomeningocele sac can be detected on sagittal or transverse views, but the sensitivity for detection of the spinal dysraphism is especially important if a sac is not seen or has ruptured. A myelomeningocele is suggested by a defect in the normal smooth dorsal skin line and splayed posterior ossification centers on the transaxial image (**Fig. 17–2**). Widening of the posterior ossification centers can

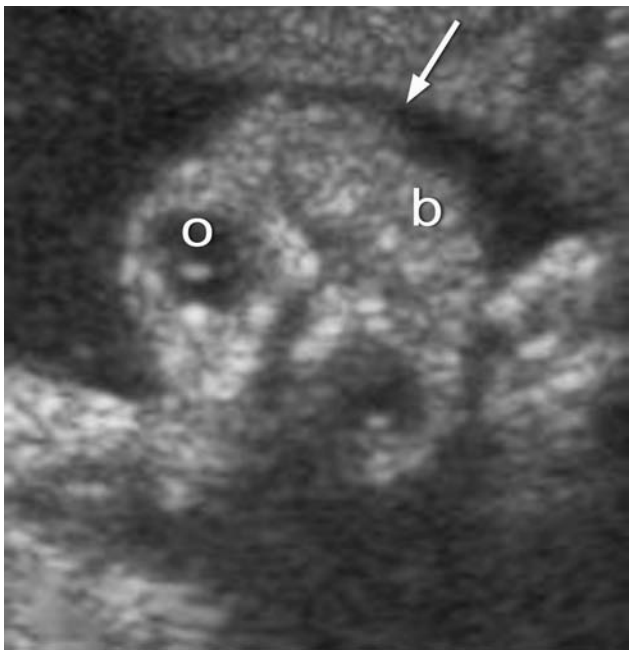

A

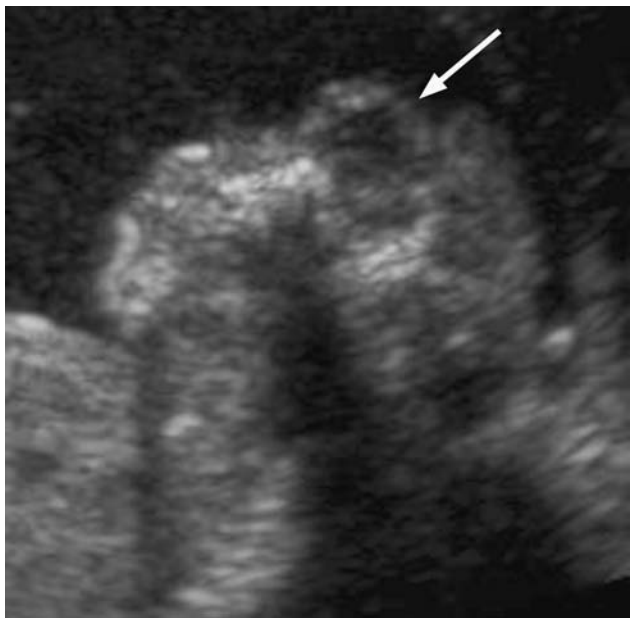

B

Figure 17–1 Anencephaly. **(A)** The cranial bones are absent and a small amount of angiomatous stroma (arrow) is seen floating in the expected location of the brain (b) above the orbits (o). **(B)** Sagittal view of the head of an anencephalic fetus with absent cranium above the orbits (arrow).

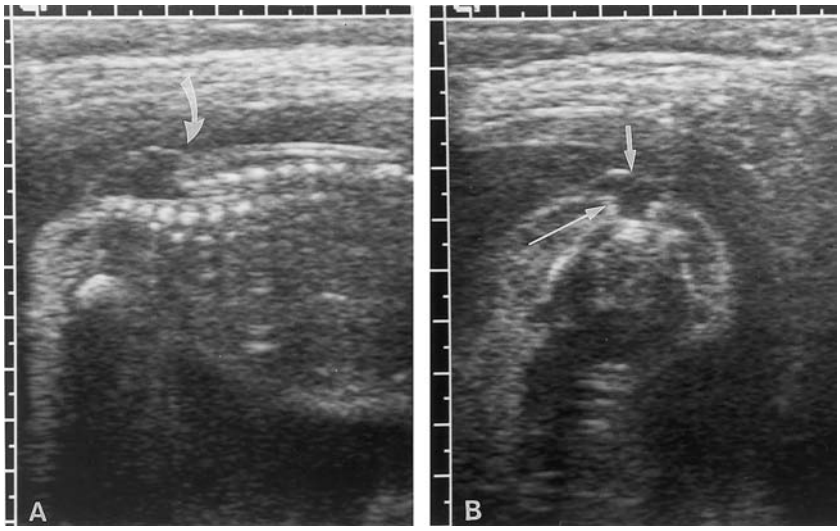

Figure 17–2 Myelomeningocele, **(A)** Sagittal image demonstrates the break in the skin line (curved arrow). The top of the lesion is L5. **(B)** Transaxial image shows the myelomeningocele sac (short arrow) and divergent posterior ossification centers (long arrow).

also be seen on coronal images of the spine. The majority of spinal dysraphisms occur in the lumbosacral region, so this area should be scrutinized with extra care. Very abnormal spine curvature may be associated with the amniotic band syndrome or limb–body wall complex (**Fig. 17–3**). If the fetus is persistently in breech presentation and the distal spine is not well visualized with transabdominal imaging, then endovaginal scanning should be performed.

Spinal defects in some fetuses with spina bifida can be very difficult to observe owing to their small size, absence of a discrete myelomeningocele sac, and relatively inconspicuous bony defects. This is undoubtedly the reason that sonographic detection was only mediocre (50 to 80%) in reports from the early 1980s.[13,47,48] Descriptions of several important cranial findings associated with "open" spinal bifida have been tremendously beneficial and have dramatically improved our ability not only to sensitively detect fetal myelomeningocele, but also to confidently exclude it. Cranial findings associated with open (non–skin covered) fetal myelomeningoceles include the "lemon sign," "banana sign," effaced cisterna magna, ventriculomegaly, and small biparietal diameter.[28,37,38,49–53] At least one of these findings is present in > 99% of affected fetuses.[28]

The lemon sign (**Fig. 17–4**) describes an inward scalloping of the frontal cranial bones seen in nearly all second-

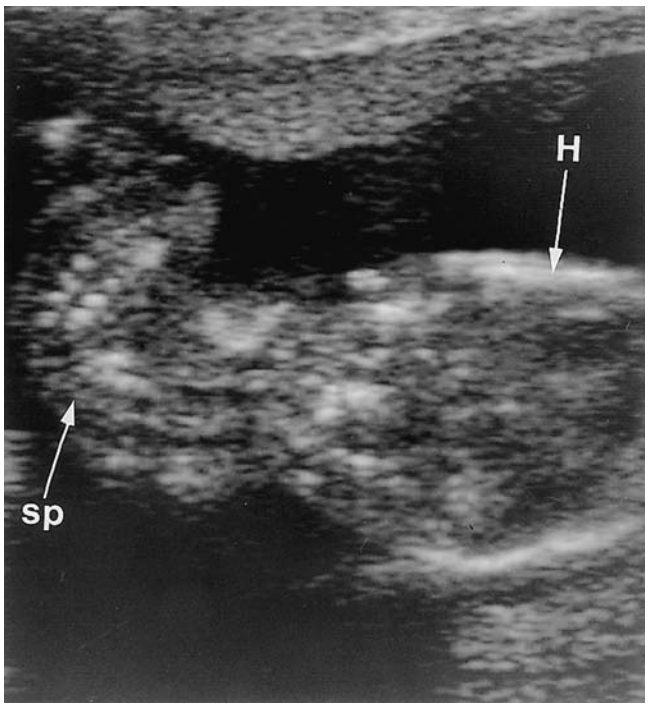

Figure 17–3 Limb–body wall complex. A ventral abdominal wall defect (not shown) was seen in association with a dramatic fixed angulation of the spine (sp). H, head.

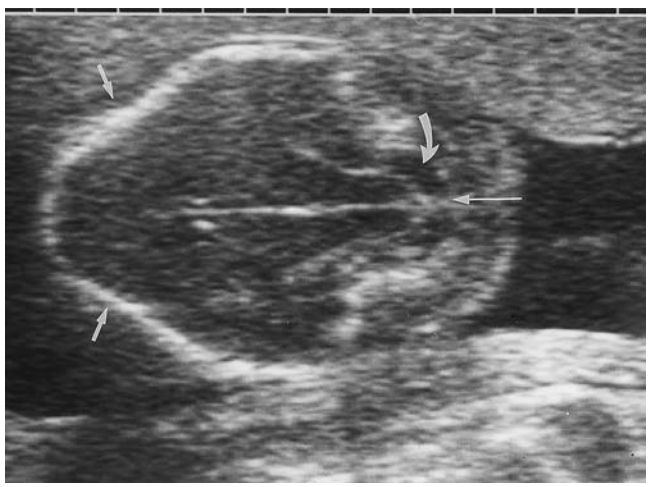

Figure 17–4 Cranial findings associated with "open" spina bifida and the Chiari II malformation: inward scalloping of the frontal bones (short arrows), also known as the "lemon sign," small posterior fossa and banana-shaped cerebellum ("banana sign") (curved arrow), and effaced cisterna magna (long arrow).

trimester fetuses with open spina bifida, but tends to disappear in affected fetuses in the third trimester. Importantly, the lemon sign may also be seen in as many as 1% of normal fetuses in addition to several other neural axis anomalies, diminishing its positive predictive value for spina bifida.[50,54,55] Thus, sonographic diagnosis of spina bifida should never be based solely on the observation of a lemon sign.

The banana sign and the effaced cisterna magna occur secondary to the hindbrain malformation known as the Chiari II malformation, which is present in almost all (> 95%) fetuses who have open spinal lesions.[2] The posterior fossa is small in the Chiari II malformation, and the developing cerebellum is cramped. As a result, the cerebellum often herniates superiorly through the tentorium or inferiorly through the foramen magnum. Neither of these potential herniations are seen sonographically, but the deformation of the cerebellum can be easily recognized. The crowded cerebellum appears to wrap around the brain stem (creating a transaxial cerebellar configuration akin to the shape of a banana) or, at a minimum, the cisterna magna is completely or nearly obliterated. These are extremely important observations and have enhanced the sensitivity of sonographic detection of fetal spinal bifida.

The banana sign is highly specific for the Chiari II malformation, but not quite as sensitive as effacement of the cisterna magna (some of the posterior fossa deformities of the Chiari II malformation are not severe enough to produce a banana cerebellum). Effacement of the cisterna is more sensitive for detection of the Chiari II malformation, but less specific (and can be seen in association with hydrocephalus and also in normals). The cisterna magna (3 to 10 mm) can be visualized in 97% of normal fetuses at 15 to 25 weeks gestation. Because the Chiari II malformation (and myelomeningocele) is nearly always associated with an abnormal-appearing posterior fossa, a small or absent cisterna should raise suspicion for a spinal lesion. As a corollary, the presence of a normal-appearing cerebellum and cisterna magna has a negative predictive value for the Chiari II malformation of > 98%. Thus, especially if the distal spine is somewhat obscured, it should be reassuring to the examiner that a normal-appearing posterior fossa reduces the risk of an open spinal lesion by > 98%.

Other cranial findings associated with spina bifida include a biparietal diameter that is small for dates (second trimester) and ventricular enlargement. The degree of ventricular dilatation in fetuses with myelomeningoceles tends to increase with gestational age.[52] In a series of 51 fetuses with spina bifida aperta (non–skin covered), we found ventriculomegaly (atrium > 10 mm) present in only 44% of myelomeningocele fetuses examined before 24 weeks, but present in 94% of fetuses scanned in the third trimester.[52] The degree of ventriculomegaly is also related to the degree of visualized posterior fossa deformity but not to the spinal level of the lesion.[52,56] It should be emphasized that, even though the cranial findings have so greatly improved the sensitivity with which we can detect myelomeningocele (currently reported to be > 90% and > 95% in many centers), the final diagnosis of a myelomeningocele should be made only after direct observation of the spinal defect.[2,18,29] The Chiari II malformation is usually not associated with skin-covered (closed) spinal abnormalities (skin-covered myelomeningocele, lipomeningocele, or midline spinal hematoma). Therefore, the banana sign and effaced cisterna magna will not appreciably improve sonographic detection of these fetal abnormalities.

Other Defects Accompanying Myelomeningocele

Outcome of fetuses with myelomeningocele is influenced by the presence of associated malformations, chromosomal abnormalities, the level of the spinal lesion (children with higher lesions have more severe motor handicaps), and childhood shunt infections.[57] Prenatal sonography has little to offer in estimating the number and severity of shunt infections, but we can offer important and accurate information regarding the presence of ventriculomegaly, the level of the spinal lesion, and the presence of associated malformations.

The bony level of the defect can be accurately estimated (± one spinal level) sonographically in 79% of fetuses.[58] This is accomplished in most cases by counting up from the last sacral ossification center (assumed to be S4 in the second trimester and S5 in the third) (**Fig. 17–2**). Associated malformations, in addition to the Chiari malformation and hydrocephalus, are rare in childhood series, but present in 13 to 24% of fetuses with myelomeningocele.[22,52,59] Multiple malformations increase the likelihood of fetal karyotype abnormalities, but chromosomal abnormalities are reported in 10 to 15% of fetuses with isolated myelomeningocele.[60–63] Thus, if the parents plan to carry the pregnancy, it is prudent not only to perform a complete, detailed, fetal anatomical survey, but also to offer fetal karyotype testing.

Cephalocele

Cephaloceles are relatively rare (1.2/10,000 births) midline cranial defects that contain meninges, and cerebrospinal fluid (meningocele) in neural tissue (encephalocele).[64] These lesions account for only ~3% of fetal anomalies detected with MS-AFP screening and 6% of detected NTDs.[30,65] In the United States, most (80 to 85%) of these occur in the occipital location, and a small percentage occur in the frontal (10 to 15%) or parietal (10 to 15%) area.[66] Because encephaloceles occur in the midline, off-midline

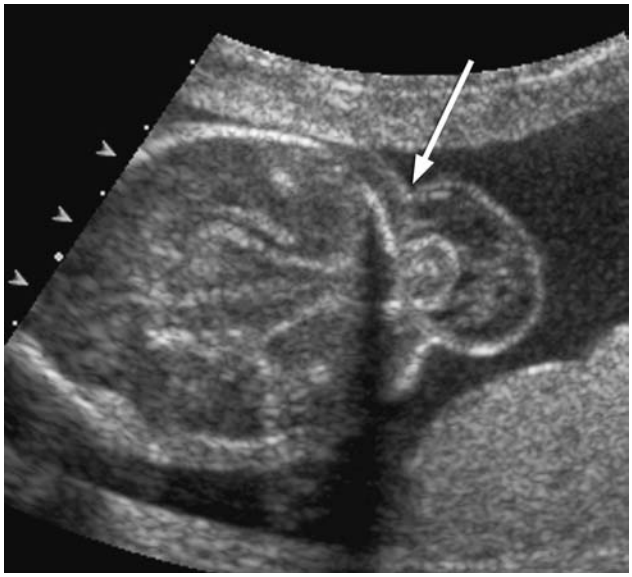

Figure 17–5 Encephalocele. The sac forms acute angles with the scalp (arrow). Note a small amount of brain herniated into the sac.

cranial defects should suggest the presence of the amniotic band syndrome.

Occipital cephaloceles are usually easily recognized, particularly on images of the posterior fossa and cisterna magna (**Fig. 17–5**). Small frontal and parietal lesions, however, may be difficult to detect because these regions of the cranium do not usually receive focused attention. Most occipital lesions are associated with abnormalities of the posterior fossa, and parietal lesions may also be associated with the Chiari malformation. The face and orbits should be carefully examined. The interorbital distance is usually widened in association with a frontal encephalocele.

Prognosis of fetuses with cephaloceles is generally poor (only 21% liveborn in our series) and outcome is related to the presence of associated neural and nonneural malformations (common), as well as the size and content of the lesion; poorer outcome is associated with a large volume of herniated brain.[66] Associated brain malformations include the Dandy-Walker malformation, agenesis of the corpus callosum, cerebellar hypoplasia, and migrational abnormalities. Karyotype abnormalities are common, found in 44% of tested fetuses in one report.[66] It is important to remember that many encephaloceles are skin-covered (60% in one series) and, therefore, may elude detection with MS-AFP screening.[1,64,67] Occipital cephaloceles may occur as part of the heritable (autosomal recessive) Meckel's syndrome (encephalocele, cystic dysplastic kidneys, and polydactyly).[68] Affected pregnancies may be terminated without adequate pathological diagnosis. Therefore, prenatal recognition of this potential syndromic association is important for counseling regarding future pregnancies because the 25% risk of recurrence associated with Meckel's syndrome greatly exceeds the recurrence risk of other cephaloceles (3%).[19]

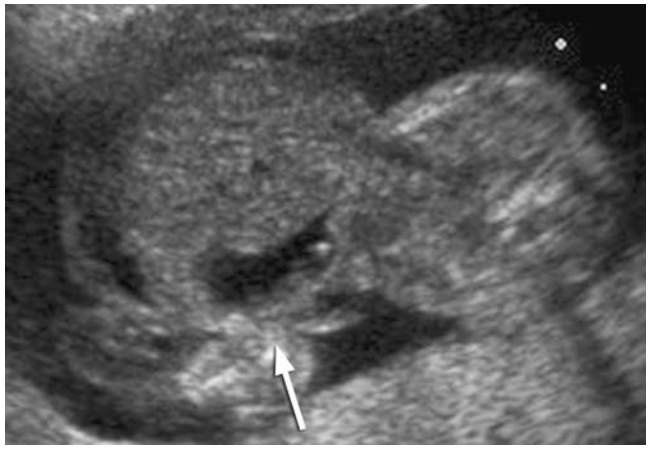

Figure 17–6 Omphalocele containing liver. The umbilical cord (arrow) inserts centrally into the sac.

Ventral Abdominal Wall Defects

Ventral abdominal wall defects include omphalocele, gastroschisis, and those defects associated with the amniotic band syndrome or limb–body wall complex. Scrutiny of the fetal umbilical cord insertion and ventral abdominal wall allows sonographic detection of omphalocele and gastroschisis in > 90% of fetuses.[18,29] Omphaloceles occur in ~1:4,000 livebirths and include a spectrum of midline defects that range from large (usually containing liver and bowel) (**Fig. 17–6**) to small (which may contain only one or two bowel loops). The exteriorized viscera are contained by an amnioperitoneal membrane, and the umbilical cord inserts midline into the sac. Very large lesions can be difficult to repair postnatally, but features most predictive of prognosis are other serious malformations (expected in 50 to 75% of affected fetuses), including cardiac (in 30 to 35%) and chromosomal abnormalities (~10 to 20%), mainly trisomies 18 and 13. Although "bowel only" omphaloceles are generally smaller, sonographically less conspicuous, and often easier to repair postnatally, the rate of chromosomal abnormalities (perhaps 70 to 80%) is eight to10 times higher than that found in fetuses in whom the omphaloceles contain liver within a herniated sac.[49,69] Be aware that small bowel–only omphaloceles may contain only one or two loops of bowel that have migrated into the cord so that the abnormality may not be recognized solely by examination of the cord insertion into the fetal abdomen. Thus, examination of the umbilical cord beyond the fetal abdomen for several centimeters is prudent.

Gastroschisis is a full-thickness, paramedian, abdominal wall defect, usually occurring to the right of the fetal umbilical cord insertion, through which bowel is exteriorized. Importantly, there is no covering membrane

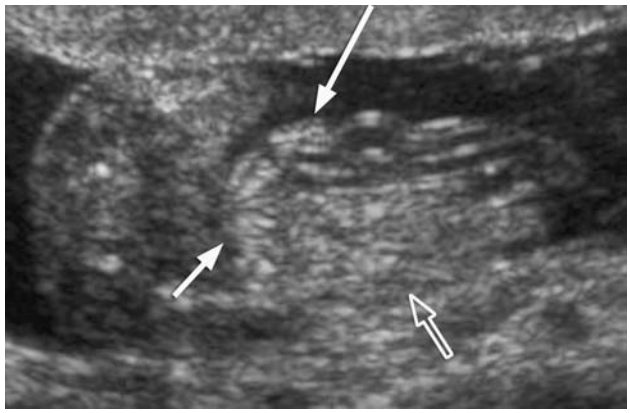

A

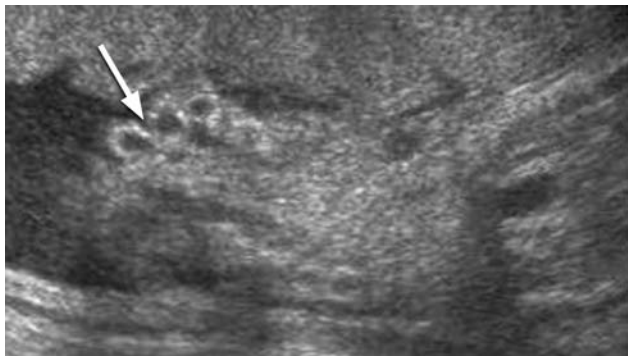

B

Figure 17–7 Gastroschisis. **(A)** Umbilical cord inserts normally into the fetal abdomen (long white arrow). A small defect (short white arrow) is seen to the right of the cord insertion, and exteriorized bowel is not covered by a membrane (hollow arrow). **(B)** Because the bowel loops are not confined by a membrane, amniotic fluid can be seen separating the loops (arrow).

(**Fig. 17–7**). Associated malformations other than gut malrotation and atresia are rare, and the prevalence of chromosomal abnormalities is not increased. Fetal growth retardation is seen in up to 40%[69] Bowel dilatation and mild thickening are common as gestation progresses. The degree of bowel dilation and wall thickening loosely correlates with seriously damaged bowel requiring resection postnatally.[70] Early in the second trimester (< 20 weeks), gastroschisis may be difficult to observe. The defect in the abdominal wall is small (1 to 3 cm) (**Fig. 17–7**) and, early on, the bowel is usually nondilated. As mentioned earlier, sensitivity to the presence of tubular structures other than cord floating in the amniotic fluid will allow detection of most cases.

A large, population-based study involving 72,782 consecutively screened pregnancies was used to establish distributions of AFP in pregnancies with gastroschisis and omphalocele.[11] Based on a cutoff of 2.5 MoM, all fetuses (20/20) with gastroschisis and ~70% (10/18) with omphaloceles were detected during MS-AFP screening.

Less Commonly Observed Fetal Defects Associated with Elevated Maternal Serum–Alpha-Fetoprotein

The AF- and MS-AFP may be elevated in fetuses with cystic hygroma (CH) (**Fig. 17–8**). Although the precise mechanism is not known, it is speculated that fetal serum proteins may leak through the membrane/integument covering the CH, or perhaps enter the maternal blood through an intrinsic, placental abnormality associated with an abnormal karyotype (present in 60 to 80% of second- and third-trimester fetuses with CH).

Teratomas, most commonly sacral (**Fig. 17–9**), but also oropharyngeal and lingual, can grow to a very large size in fetal life. These tumors often ulcerate, allowing leakage of fetal protein into the amniotic fluid and secondarily into

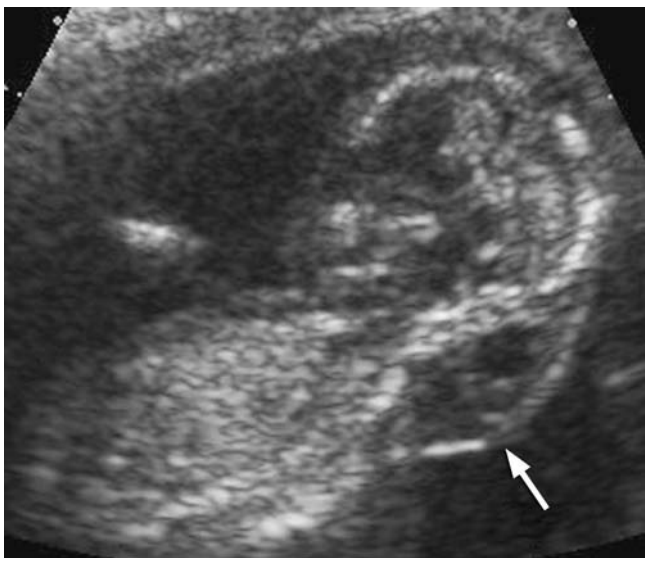

Figure 17–8 Sagittal image of a cystic hygroma.

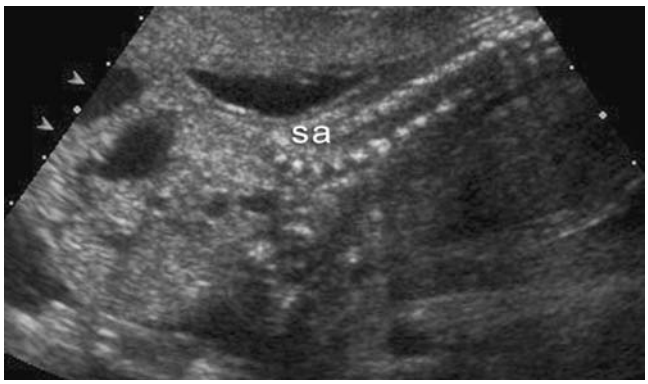

Figure 17–9 Solid sacrococcygeal teratoma growing from the sacrum (sa).

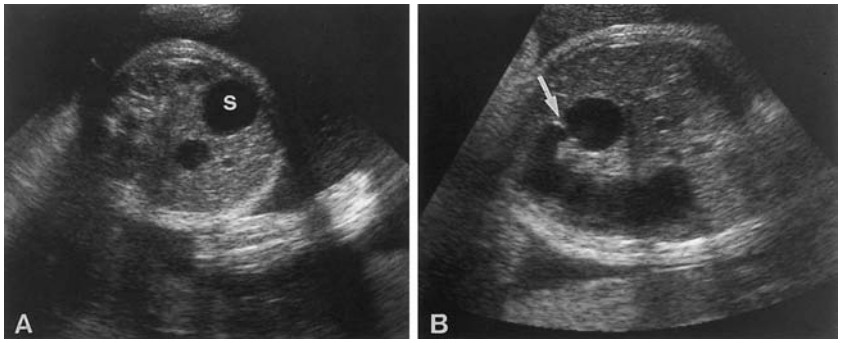

Figure 17–10 Duodenal atresia. **(A)** Double bubble dilated stomach (s) and duodenum. **(B)** Care should be taken to demonstrate that the stomach and duodenum are connected (arrow).

MS. In many cases, they are not completely skin covered. Transverse axial views of the oropharynx, coronal, and axial views of the face (to exclude oropharyngeal and lingual teratomas), and transverse and longitudinal views of the sacral area (sacrococcygeal teratomas are most common) should be obtained in patients referred for elevated MS-AFP. The sensitivity of MS-AFP screening for teratomas is not known.

Esophageal atresia and duodenal atresia have been associated with elevated AFP. Anal atresia is associated with a low AFP.[71] Some have speculated that a smaller than average degradation of swallowed AFP might account for the AFP elevation. A normally filled fetal stomach and the absence of a persistently filled or dilated duodenum should be sought. The normal fetal duodenum empties immediately, and a persistently filled duodenum (even if it does not appear "overdistended") is always abnormal. The presence of a fetal "double bubble" (**Fig. 17–10**) suggests duodenal obstruction (usually atresia, but can be due to stenosis, Ladd's bands, or annular pancreas). Importantly, nearly one third of fetuses with duodenal atresia have Down syndrome. Thus, if a double bubble is detected, a focused examination of the fetal heart is performed and karyotype testing is offered to the parents. Fifty-five percent of fetuses with a gastrointestinal obstruction will have other congenital anomalies.[71]

Esophageal atresia is suggested by an absent/unfilled stomach (**Fig. 17–11**) and polyhydramnios, but this constellation of observations is insensitive (< 50%) for the sonographic detection of fetal esophageal atresia before the third trimester. This is due to the fact that the proximal esophageal pouch is only rarely seen in fetuses, and a fistula exists between the lower esophagus and bronchial tree in > 90%, allowing passage of some fluid into the fetal stomach. A small, not absent, stomach was observed in 5 of 12 fetuses with proven esophageal atresia by McKenna et al.[40] In addition, frank polyhydramnios is typically not seen before 20 to 24 weeks gestation.

Renal abnormalities, including congenital (Finnish) nephrosis, multicystic dysplastic kidney, renal agenesis, and pelviectasis, have been associated with elevated MS-AFP.[31,58] In some cases the AFP is elevated secondary to abnormal leakage of proteins into fetal urine. Congenital nephrosis results in a dramatic fetal proteinuria in utero and, because there are no renal morphological features, this is a very difficult diagnosis to make with certainty antenatally. The clue to the diagnosis is that both the MS- and AF-AFP levels are extremely high (i.e., typically ≥ 10 MoM), with negative amniotic fluid acetylcholinesterase and without evidence of maternal–fetal hemorrhage or other fetal morphological defects.[72] Prenatal genetic testing is available for patients with a family history of congenital Finnish nephrosis and an established mutation.[73] A subset of congenital nephrosis cases are associated with mild ventriculomegaly, echogenic kidneys, and pericardial effusion on ultrasound, but have negative testing for congenital Finnish nephrosis.[74] In cases of renal agenesis, the mechanism for MS-AFP elevation is not known, but it is speculated that these fetuses may have higher serum protein levels owing to diminished excretion.

Finally, placental abnormalities, including chorioangioma, placental abruption, periplacental hemorrhages

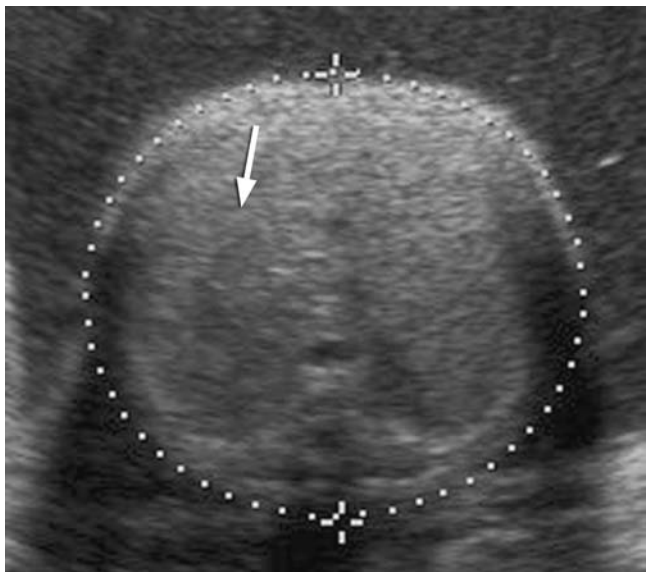

Figure 17–11 Absent stomach. No stomach bubble is observed (arrow). Diagnosis is esophageal atresia.

(i.e., subchorionic hemorrhage), molar pregnancies, and placental lakes, may result in elevated MS-AFP.[75] A careful examination of the placenta should be performed.[76–78] Relatively minor placental abnormalities (e.g., placental lakes, large marginal veins) are seen commonly in pregnancy patients. Although the placenta should be carefully examined in all women referred for high AFP, a placental lesion should only be the diagnosis of exclusion (after morphological defects have been excluded), as the cause of increased MS-AFP.

Comment

Recall that amniocentesis performed following an elevated MS-AFP eliminates almost 90% of women with elevated MS-AFP from further testing. If we do not have AF-AFP levels to help us in triaging patients, 10 times as many targeted sonograms will be required to find the same number of fetal defects. Further, the likelihood of finding an anomaly during each targeted sonogram referred for high MS-AFP will be considerably lower than it is in the population scanned for high AF-AFP. Therefore, the examiner must "work harder" to remain vigilant while searching for fetal defects in this low-prevalence population. The level of MS-AFP elevation may provide guiding information. The likelihood of finding a fetal defect increases with MS-AFP levels. Minor elevations of MS-AFP (i.e., 2.5 to 3 MoM), are associated with fetal defects in only 3 to 4%.[63] Whereas if the MS-AFP is > 5 MoM, the prevalence of fetuses with defects may be as high as 20 to 30%,[5] and if the MS-AFP is > 7 MoM, the prevalence of abnormal fetuses may be as high as 30 to 40%.[79,80] Thus, the risk of a neural tube defect is almost 10 times (13%) greater among women with MS-AFP > 7 MoM, compared with those having elevations 2.5 to 2.9 MoM (1.4%).[80] This MS-AFP-related risk also parallels the rate of neural tube and ventral wall defects reported with increasing levels of AF-AFP.[18]

This information may be useful to the examiner and counselor of women with elevated MS-AFP. If a woman chooses to circumvent the amniocentesis, the degree to which her MS-AFP is elevated not only helps to adjust the index of suspicion for an anomaly, but also helps to prepare and counsel the pregnant patient.

References

1. Wald NJ, Cuckle H, Brock JH, et al. Maternal serum-alpha-fetoprotein measurement in antenatal screening for anencephaly and spina bifida in early pregnancy. Report of U.K. collaborative study on alpha-fetoprotein in relation to neural-tube defects. Lancet 1977;i:1323–1332
2. Milunsky A, Jick SS, Bruell CL, et al. Predictive values, relative risks, and overall benefits of high and low maternal serum alpha-fetoprotein screening in singleton pregnancies: new epidemiologic data. Am J Obstet Gynecol 1989;161:291–297
3. Davis RO, Goldenberg RL, Boots L, et al. Elevated levels of midtrimester maternal serum alpha-fetoprotein are associated with preterm delivery but not with fetal growth retardation. Am J Obstet Gynecol 1992;167:596–601
4. Maher JE, Davis RO, Goldenberg RL, et al. Unexplained elevation in maternal serum alpha-fetoprotein and subsequent fetal loss. Obstet Gynecol 1994;83:138–141
5. Moawad AH, Goldenberg RL, Mercer B, et al. NICHD MFMU Network. The Preterm Prediction Study: the value of serum alkaline phosphatase, alpha-fetoprotein, plasma corticotropin-releasing hormone, and other serum markers for the prediction of spontaneous preterm birth. Am J Obstet Gynecol 2002;186:990–996
6. Chandra S, Scott H, Dodds L, et al. Unexplained elevated maternal serum alpha-fetoprotein and/or human chorionic gonadotropin and the risk of adverse outcomes. Am J Obstet Gynecol 2003; 189:775–781
7. Davidson EJ, Riley SC, Roberts SA, et al. Maternal serum activin, inhibin, human chorionic gonadotrophin and alpha-fetoprotein as second trimester predictors of pre-eclampsia. Br J Obstet Gynaecol 2003;110:46–52
8. Ilagan JG, Stamilio DM, Ural SH, et al. Abnormal multiple marker screens are associated with adverse perinatal outcomes in cases of intrauterine growth restriction. Am J Obstet Gynecol 2004;191: 1465–1469
9. Crandall BF, Robinson L, Grau P. Risks associated with an elevated maternal serum alpha-fetoprotein. Am J Obstet Gynecol 1991;165: 581–586
10. Robinson L, Grau P, Crandall BF. Pregnancy outcomes after increasing maternal serum alpha-fetoprotein levels. Obstet Gynecol 1989; 74:17–20
11. Palomaki GE, Hill LE, Knight GJ, et al. Second-trimester maternal serum alpha-fetoprotein levels in pregnancies associated with gastroschisis and omphalocele. Obstet Gynecol 1988;71:906–909
12. Macri JN. Critical issues in prenatal maternal serum alpha-fetoprotein screening for genetic anomalies. Am J Obstet Gynecol 1986; 155:240–246
13. Robinson HP, Hood VD, Adam AH, et al. Diagnostic ultrasound: early detection of fetal neural tube defects. Obstet Gynecol 1980; 56:705–710
14. Haddow JE, Kloza EM, Smith DE, et al. Data from an alpha-fetoprotein pilot screening program in Maine. Obstet Gynecol 1983;62: 556–560
15. American Institute of Ultrasound in Medicine (AIUM). Guidelines for performance of the antepartum obstetrical ultrasound examination. J Ultrasound Med 2003;22:1116–1125
16. Burton BK, Sowers SG, Nelson LH. Maternal serum alpha-fetoprotein screening in North Carolina: experience with more than twelve thousand pregnancies. Am J Obstet Gynecol 1983;146:439–444
17. Lindfors KR, Gorczycz DP, Hanson FW, et al. The roles of ultrasonography and amniocentesis in evaluation of elevated maternal serum alpha-fetoprotein. Am J Obstet Gynecol 1991;164:1571–1576
18. Robbin M, Filly RA, Fell S, et al. Elevated levels of amniotic fluid alpha-fetoprotein: sonographic evaluation. Radiology 1993;188: 165–169
19. Main DM, Mennuti MT. Neural tube defects: issues in prenatal diagnosis and counselling. Obstet Gynecol 1986;67:1–16
20. Gonzalez D, Barrett T, Apuzzio J. Is routine fetal karyotyping necessary for patients undergoing amniocentesis for elevated maternal serum alpha-fetoprotein? J Matern Fetal Med 2001;10:376–379

21. Sepulveda W, Domalson A, Johnson RD, et al. Are routine alpha-fetoprotein and acetylcholinesterase determinations still necessary at second-trimester amniocentesis? Impact of high-resolution ultrasonography. Obstet Gynecol 1995;85:107–112
22. Hogge WA, Thiagarajah S, Ferguson JE II, et al. The role of ultrasonography and amniocentesis in the evaluation of pregnancies at risk for NTD. Am J Obstet Gynecol 1989;161:520–524
23. Platt LD, Feuchtbaum L, Filly R, et al. The California maternal serum alpha-fetoprotein screening program: the role of ultrasonography in the detection of spina bifida. Am J Obstet Gynecol 1992;166: 1328–1329
24. Morrow RJ, McNay MB, Whittle MJ. Ultrasound detection of neural tube defects in patients with elevated maternal serum alpha-fetoprotein. Obstet Gynecol 1991;78:1055–1057
25. Benacerraf BR. Should patients with elevated levels of maternal serum alpha-fetoprotein always undergo amniocentesis? Radiology 1993;188:17–18
26. Lennon CA, Gray DL. Sensitivity and specificity of ultrasound for the detection of neural tube and ventral wall defects in a high risk population. Obstet Gynecol 1999;94:562–566
27. Watson WJ, Chescheir NC, Katz VL, et al. The role of ultrasound in evaluation of patients with elevated maternal serum alpha-fetoprotein: a review. Obstet Gynecol 1991;78:123–128
28. Nadel AS, Green JK, Holmes LB, et al. Absence of need for amniocentesis in patients with elevated levels of maternal serum alpha-fetoprotein and normal ultrasonographic examinations. N Engl J Med 1990;323:557–561
29. Filly RA, Callen PW, Goldstein RB. Alpha-fetoprotein screening programs: what every obstetric sonologist should know. Radiology 1993;188:1–9
30. Megerian G, Godmilow L, Donnenfeld AE. Ultrasound-adjusted risk and spectrum of fetal chromosomal abnormality in women with elevated maternal serum alpha-fetoprotein. Obstet Gynecol 1995; 85:952–956
31. Miller R, Stephan MJ, Hume RF, et al. Extreme elevation of maternal serum alpha-fetoprotein associated with mosaid trisomy 8 in a liveborn. Fetal Diagn Ther 2001;16:120–122
32. Chen CP, Chern SR, Cheng SJ, et al. Second-trimester diagnosis of complete trisomy 9 associated with abnormal maternal serum screen results, open sacral spina bifida and congenital diaphragmatic hernia. Prenat Diagn 2004;24:455–462
33. Feuchtbaum LB, Cunningham G, Waller DK, et al. Fetal karyotyping for chromosome abnormalities after an unexplained elevated maternal serum alpha-fetoprotein screening. Obstet Gynecol 1995; 86:248–254
34. Thiagarajah S, Stroud CB, Vavelidis F, et al. Elevated maternal serum alpha-fetoprotein levels: what is the risk of fetal aneuploidy? Am J Obstet Gynecol 1995;173:388–392
35. Barth WH, Frigoletto FD Jr, Krauss CM, et al. Ultrasound detection of fetal aneuploidy in patients with elevated maternal serum alpha-fetoprotein. Obstet Gynecol 1991;77:897–900
36. Filly RA, Goldstein RB, Callen PW. Fetal ventricle: importance in routine obstetrical sonography. Radiology 1991;181:1–7
37. Goldstein RB, Podrasky AE, Filly RA, et al. Effacement of the fetal cisterna magna in association with myelomeningocele. Radiology 1989;172:409–413
38. Cardoza JD, Goldstein RB, Filly RA. Exclusion of fetal ventriculomegaly with a single measurement: the width of the lateral ventricular atrium. Radiology 1988;169:711–714
39. Townsend RR, Goldstein RB, Filly RA, et al. Sonographic identification of autosomal recessive polycystic kidney disease associated with increased maternal serum/amniotic fluid alpha-fetoprotein. Obstet Gynecol 1988;71:1008–1012
40. McKenna KM, Goldstein RB, Stringer MD. Prognostic significance of a small or absent fetal stomach. Radiology 1995;197:729–733
41. Cafici D, Sepulveda W. First-trimester echogenic amniotic fluid in the acrania-anencephaly sequence. J Ultrasound Med 2003;22: 1075–1079
42. Goldstein RB, Filly RA, Callen PW. Sonography of anencephaly: pitfalls in early diagnosis. J Clin Ultrasound 1989;17:397–402
43. Yen IH, Khoury MJ, Erickson JD, et al. The changing epidemiology of neural tube defects: United States, 1968–1989. Am J Dis Child 1992;146:857–861
44. Centers for Disease Control and Prevention (CDC). Surveillance for anencephaly and spina bifida and the impact of prenatal diagnosis: United States, 1985–1994. MMWR 1995;44:1–13
45. Centers for Disease Control and Prevention (CDC). Spina bifida and anencephaly before and after the folic acid mandate: United States, 1995–1996 and 1999–2000. MMWR 2004;53:362–365
46. Persson PH, Kullander S, Gennser G, et al. Screening for fetal malformations using ultrasound and measurements of alpha-fetoprotein in maternal serum. BMJ 1983;286:747–749
47. Roberts CJ, Evans KT, Hibbard BM, et al. Diagnostic effectiveness of ultrasound in detection of neural tube defects: the South Wales experience of 2509 scans (1977–1982) in high-risk mothers. Lancet 1983;ii:1068–1069
48. Nyberg DA, Mack LA, Hirsch J, et al. Abnormalities of fetal cranial contour in sonographic detection of spina bifida: evaluation of the "lemon" sign. Radiology 1988;167:387–392
49. Van den Hof MC, Nicolaides KH, Campbell J, et al. Evaluation of the lemon and banana signs in one hundred thirty fetuses with open spina bifida. Am J Obstet Gynecol 1990;162:322–327
50. Nicolaides KH, Campbell S, Gabbe SG, et al. Ultrasound screening for spina bifida: cranial and cerebellar signs. Lancet 1986;ii:72–74
51. Babcook CJ, Goldstein RB, Barth RA, et al. Prevalence of ventriculomegaly in association with myelomeningocele: correlation with gestational age and severity of posterior fossa deformity. Radiology 1994;190:703–707
52. Wald N, Cuckle H, Boreham J, et al. Small biparietal diameter of fetuses with spina bifida: implications for antenatal screening. Br J Obstet Gynaecol 1980;87:219–221
53. Campbell J, Gilbert WM, Nicolaides KH, et al. Ultrasound screening for spina bifida: cranial and cerebellar signs in a high-risk population. Obstet Gynecol 1987;70:247–250
54. Ball R, Filly RA, Goldstein RB. The "lemon sign": not a specific indicator of myelomeningoceles. J Ultrasound Med 1993;12:131–134
55. Babcook CJ, Goldstein RB, Filly RA. Spinal level of fetal myelomeningocele: does it influence ventricular size or severity of the posterior fossa deformity? (Abstr) American Roentgen Ray Society, Boston, March
56. Sturgiss S, Robson S. Prognosis for fetuses with antenatally detected myelomeningocele. Fetal Matern Med Rev 1995;7:235–249
57. Kollias SS, Goldstein RB, Cogen PH, et al. Prenatally detected myelomeningoceles: sonographic accuracy in estimation of the spinal level. Radiology 1992;185:109–112
58. Luthy DA, Wardinsky T, Shurtleff DB, et al. Cesarean section before the onset of labor and subsequent motor function in infants with meningomyelocele diagnosed antenatally. N Engl J Med 1991; 324:662–666
59. Babcook CJ, Goldstein RB, Filly RA. Prenatally detected fetal myelomeningocele: is karyotype analysis warranted. Radiology 1995;194:491–494

60. Drugan A, Johnson MP, Dvorin E, et al. Aneuploidy with neural tube defects: another reason for complete evaluation in patients with suspected ultrasound anomalies or elevated maternal serum alpha-fetoprotein. Fetal Ther 1989;4:88–92
61. Lindfors KK, McGahan JP, Tennant FP, et al. Midtrimester screening for open neural tube defects: correlation of sonography with amniocentesis results. AJR Am J Roentgenol 1987;149:141–145
62. Harmon JP, Hiett AK, Palmer CG, et al. Prenatal ultrasound detection of isolated neural tube defects: is cytogenetic evaluation warranted? Obstet Gynecol 1995;86:595–599
63. Lorber J. The prognosis of occipital encephalocele. Dev Med Child Neurol 1967;??:75
64. Chan A, Robertson EF, Haan EA, et al. The sensitivity of ultrasound and serum alpha-fetoprotein in population-based antenatal screening for neural tube defects, South Australia 1986–1991. Br J Obstet Gynaecol 1995;102:370–376
65. Goldstein RB, LaPidus AS, Filly RA. Fetal cephaloceles: diagnosis with US. Radiology 1991;180:803–808
66. Simpson JL, Palomaki GE, Mercer B, et al. Associations between adverse perinatal outcome and serially obtained second- and third-trimester maternal serum alpha-fetoprotein measurements. Am J Obstet Gynecol 1995;173:1742–1748
67. Johnson VP, Holzwarth DR. Prenatal diagnosis of Meckel syndrome: case reports and literature review. Am J Med Genet 1984;18:699–711
68. Getachew MM, Goldstein RB, Edge V, et al. Correlation between omphalocele contents and karyotype abnormality: sonographic study in 37 cases. AJR Am J Roentgenol 1992;158:133–136
69. Babcook CJ, Hendrick MH, Goldstein RB, et al. Gastroschisis: can sonography of the fetal bowel accurately predict postnatal outcome? J Ultrasound Med 1994;13:701–706
70. Petrikovsky BM, Nardi DA, Rodis JF, et al. Elevated maternal serum alpha-fetoprotein and mild fetal uropathy. Obstet Gynecol 1991;78:262–264
71. Van Rijn M, Christaens GC, Hagenaars AM, et al. Maternal serum alpha-fetoprotein in fetal anal atresia and other gastrointestinal obstructions. Prenat Diagn 1998;18:914–921
72. Albright SG, Warner AA, Seeds JW, et al. Congenital nephrosis as a cause of elevated alpha-fetoprotein. Obstet Gynecol 1990;76:969–971
73. Kestila M, Jarvela I. Prenatal diagnosis of congenital nephrotic syndrome (CNF, NPHS1). Prenat Diagn 2003;23:323–324
74. Jolly M, Goodburn S, Cox P, et al. Congenital nephropathy and ventriculomegaly: a report of cases. Prenat Diagn 2003;23:48–51
75. Billieux MH, Petignat P, Fior A, et al. Pre-eclampsia and peripartum cardiomyopathy: clinical implications for maternally imprinted genes. Ultrasound Obstet Gynecol 2004;23:398–401
76. Williams MA, Hickok DE, Zingheim RW, et al. Elevated maternal serum alpha-fetoprotein levels and midtrimester placental abnormalities in relation to subsequent adverse pregnancy outcomes. Am J Obstet Gynecol 1992;167:1032–1037
77. Salafia CM, Silberman L, Herrera NE, et al. Placental pathology at term associated with elevated midtrimester maternal serum alpha-fetoprotein concentration. Am J Obstet Gynecol 1988;158:1064–1066
78. Fleischer AC, Kurtz AB, Wapner RJ, et al. Elevated alpha-fetoprotein and a normal fetal sonogram: association with placental abnormalities. AJR Am J Roentgenol 1988;150:881–883
79. Reichler A, Hume RF Jr, Drugan A, et al. Risk of anomalies as a function of level of elevated maternal serum alpha-fetoprotein. Am J Obstet Gynecol 1994;171:1052–1055
80. Killam Wm P, Miller RC, Seeds JW. Extremely high maternal serum alpha-fetoprotein levels at second-trimester screening. Obstet Gynecol 1991;78:257–260

18 Maternal Serum Screening Test Positive for Down Syndrome

Thomas D. Shipp

Down syndrome is the most common karyotypic abnormality among liveborns.[1] Over the past few decades, much research has concentrated on screening for fetal Down syndrome and the prenatal diagnosis of this condition. The primary factor associated with fetal Down syndrome is maternal age. The rate of fetal Down syndrome increases with increasing maternal age. Because most women who are delivering babies are younger, the majority of fetuses with Down syndrome occur in younger mothers. Therefore, using maternal age alone would be an inefficient approach for prenatal Down syndrome screening. Given the desire of many pregnant women for the knowledge of whether their fetus has Down syndrome, a relatively safe and more effective screening technique is necessary.

Screening tests give us a risk estimate for fetal Down syndrome and do not diagnose a fetus as having Down syndrome. Invasive testing, such as amniocentesis or chorionic villus sampling, is currently the only method for definitively determining the fetal karyotype. As ineffective as maternal age is as a screen for fetal Down syndrome, universal invasive testing for fetal Down syndrome also has its drawbacks. The rate of loss of normal fetuses would be excessive. A more effective screening strategy has become commonplace; namely, using maternal serum analytes to determine the risk for fetal Down syndrome. Because many varied screening strategies will be discussed, it is important to remember that there is not one best screening model.[2] Further, a particular screening test may fit the needs of a patient when she is young, but it might not be optimal for her and her family as she ages.[3]

Women who have positive serum screening for the prenatal detection of Down syndrome frequently have a difficult time discerning the significance of the test results. For the patient faced with having some quantified risk for Down syndrome, health care providers must provide a context in which to help the patient understand the degree of risk. The majority of those with positive serum screens for Down syndrome have perfectly normal fetuses that do not have Down syndrome. Much of our mandate for these patients is to educate them about what a positive serum screen means and to provide reasonable options for the patient and her partner according to their own concerns and values.

Second-Trimester Maternal Serum Screening Test

The maternal serum–α-fetoprotein test (MSAFP) was initially used as a screen for neural tube defects. Subsequently, a low MSAFP was shown to be associated with fetal Down syndrome, although the use of MSAFP and maternal age as a screening test for fetal Down syndrome was associated with a poor detection rate of ~20%.[4] Within a few years, an elevated maternal serum human chorionic gonadotropin (hCG) and a low maternal serum unconjugated estriol (uE3) were also found to be associated with Down syndrome. The use of maternal age and these three maternal serum analytes, MSAFP, hCG, and uE3, also known as the triple screen test, has been found to be effective as a screen for fetal Down syndrome. Sensitivities for the detection of fetal Down syndrome have been reported to be 50–90%, with false-positive rates of 3–6%.[4–6] Generally accepted as having a sensitivity of ~75% with a false-positive rate of 5%, the triple screen test has been commonly used as a screening tool for gravidas in the second trimester for over a decade.

Most recently, the inclusion of inhibin-A to the triple screen analytes has shown improved efficacy in screening for Down syndrome. The sensitivity for the detection of Down syndrome using MSAFP, hCG, uE3, and inhibin-A is ~80%, with a 5% false-positive rate and a positive predictive value of 1 in 51.[7] Given these encouraging results, the quadruple test has been increasingly used over the past few years as an initial screen for fetal Down syndrome in the second trimester.

Ultrasound Evaluation

As the serum screen was being developed into the currently used triple or quadruple serum analyte screens, great progress was made in the world of ultrasound with respect to the identification of factors associated with Down syndrome. Many structural defects have been shown to be associated with Down syndrome.[8] These include congenital heart defects, duodenal atresia

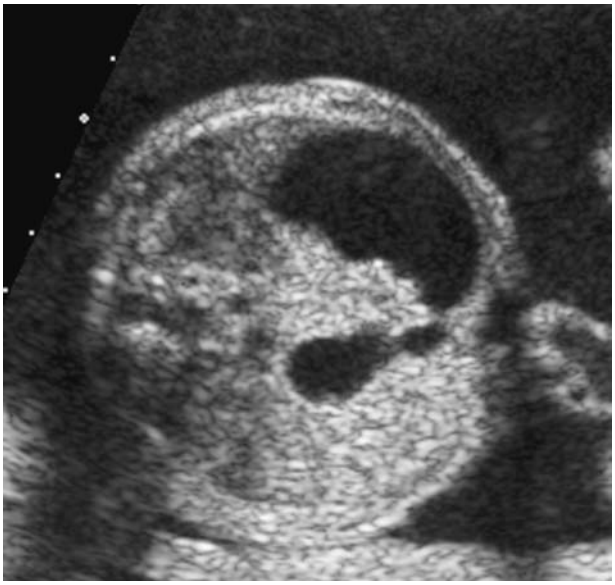

Figure 18–1 Transverse view of the fetal abdomen showing an enlarged, fluid-filled stomach and proximal duodenum secondary to duodenal atresia in a second-trimester fetus with Down syndrome.

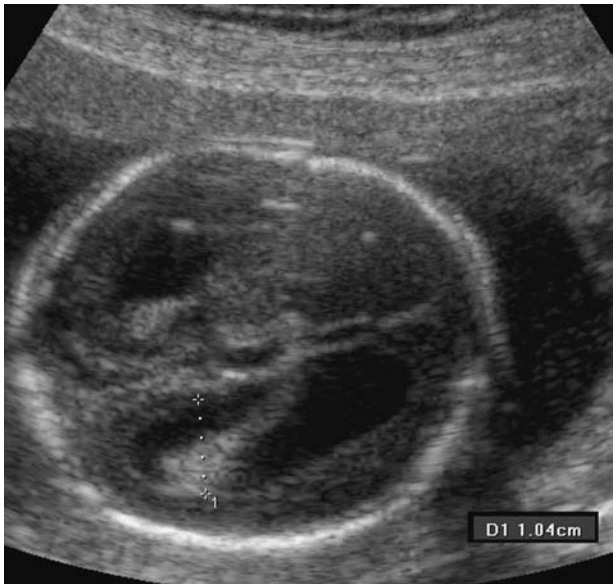

Figure 18–2 Transverse view of the fetal cranium of a second-trimester fetus with Down syndrome showing enlarged lateral ventricles consistent with ventriculomegaly.

(**Fig. 18–1**), cerebral ventriculomegaly (**Fig. 18–2**), and macroglossia (**Fig. 18–3**). The risk of Down syndrome is generally high enough for fetuses with congenital heart defects, such as tetralogy of Fallot and atrioventricular septal defects (**Fig. 18–4**), duodenal atresia, and cerebral ventriculomegaly, to warrant at least a consideration of karyotyping. Abnormal fluid collections in the fetus are similarly associated with Down syndrome. Fetuses in the second trimester with Down syndrome may show signs of generalized hydrops (**Fig. 18–5**), or even have more localized fluid collections, such as pleural effusions (**Fig. 18–6**) or small nuchal cystic hygromas (**Fig. 18–7**).

Benacerraf et al first reported the association of a thickened nuchal skin fold (**Fig. 18–8**) in the second trimester with Down syndrome in 1985.[9] Multiple authors have subsequently confirmed this association. Benacerraf et al were able to show that 40% of fetuses with Down syndrome had

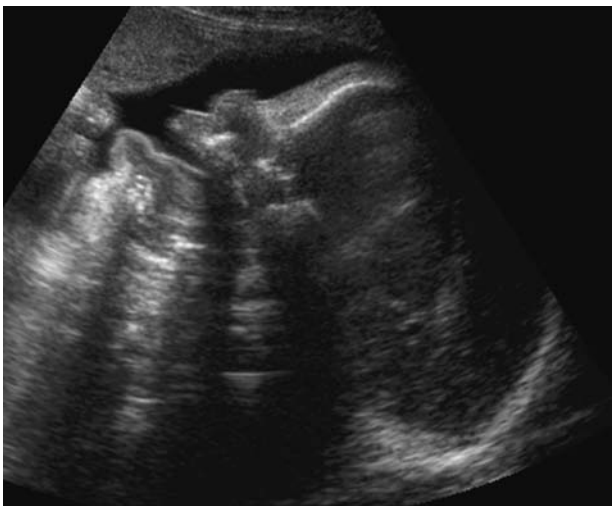

Figure 18–3 Midsagittal view of a third-trimester fetus with Down syndrome demonstrating macroglossia.

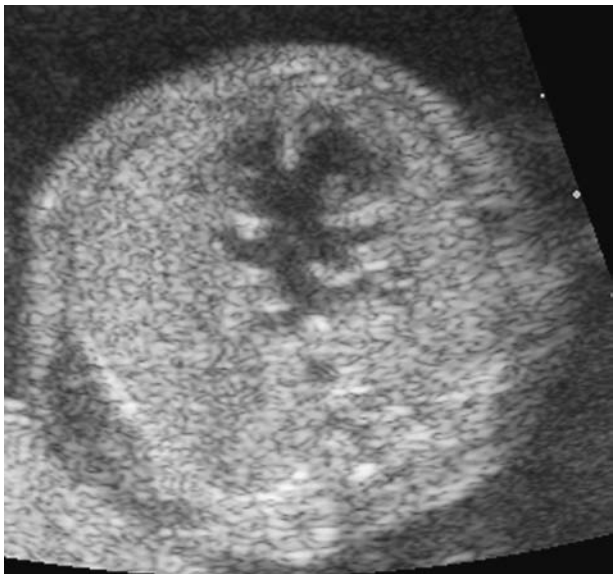

Figure 18–4 Transverse view of the fetal chest at the level of the four-chamber view. There are large ventricular and atrial septal defects in this second-trimester fetus with an atrioventricular septal defect and Down syndrome.

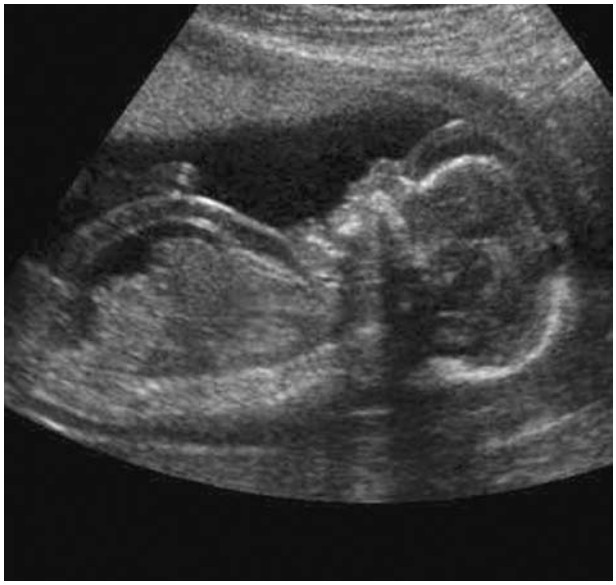

Figure 18–5 Midsagittal view of a second-trimester fetus with Down syndrome, demonstrating diffuse skin thickening and ascites consistent with hydrops fetalis.

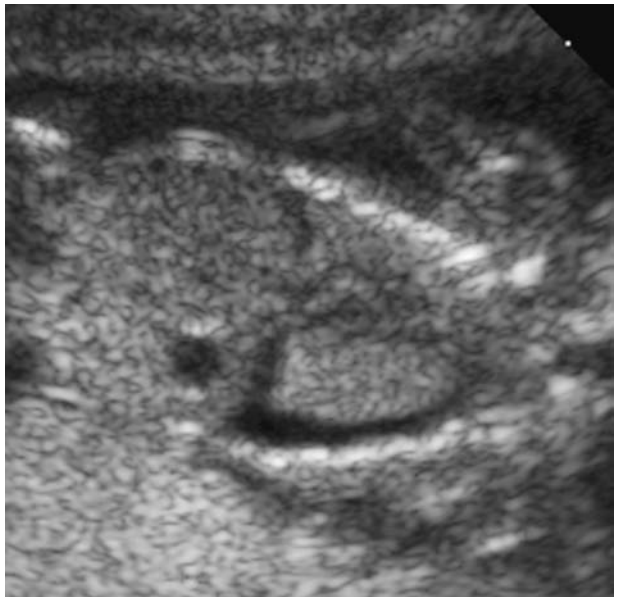

Figure 18–6 Coronal view of the second-trimester chest of a fetus with Down syndrome, demonstrating bilateral pleural effusions, left greater than right.

an abnormally thickened nuchal fold measurement of greater than 6 mm as did 0.1% of normal fetuses. There was a positive predictive value of 69% for those with a thickened nuchal skin fold in their high-risk population.[10] The thickened nuchal fold remains the most consistent sonographic sign associated with an increased risk for fetal Down syndrome.

Beyond structural defects and the thickened nuchal fold in the second-trimester fetus, many other sonographic

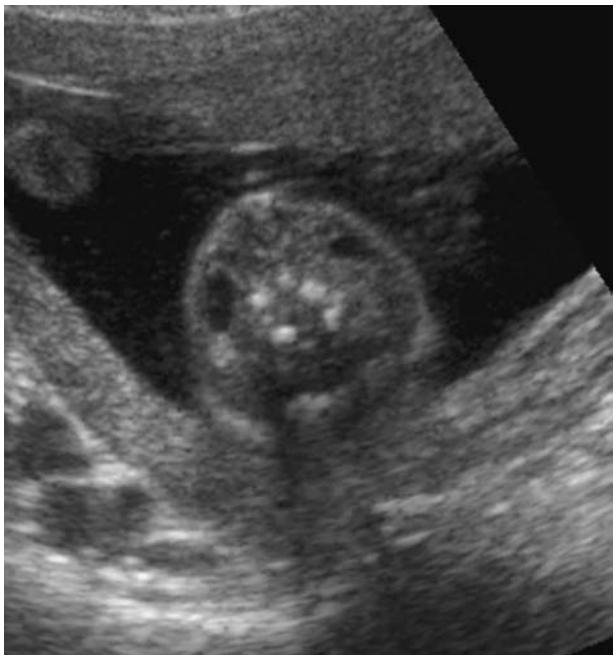

Figure 18–7 Transverse view of the fetal neck of a second-trimester fetus with Down syndrome, demonstrating small, bilateral cystic hygromas.

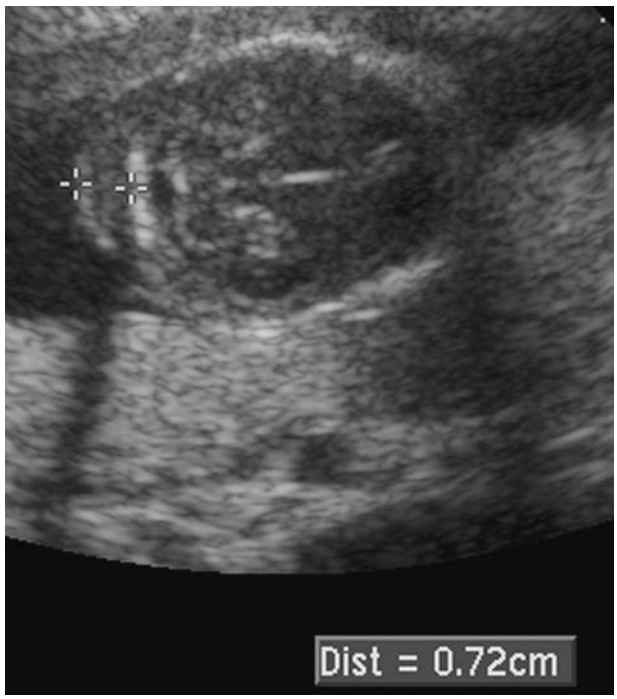

Figure 18–8 Transverse view of the fetal cranium, demonstrating a thickened nuchal fold in a second-trimester fetus with Down syndrome. The measurement is appropriately indicated by the calipers from the outer edge of the cranium to the outer edge of the skin fold.

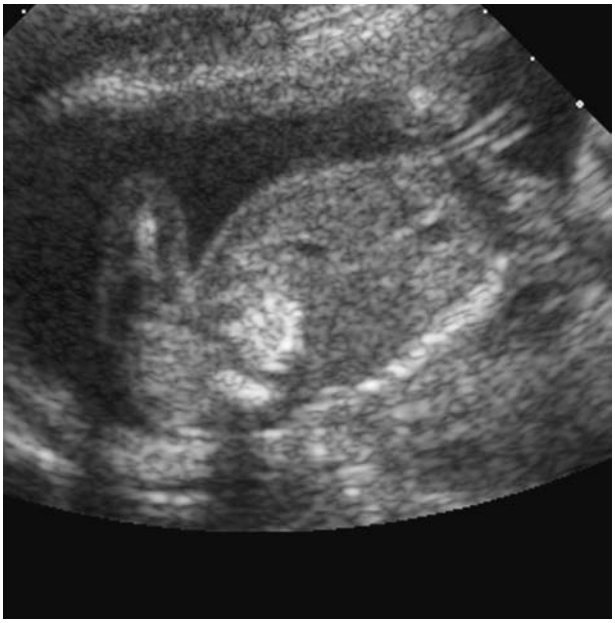

Figure 18–9 Oblique/sagittal view of the fetal abdomen demonstrating hyperechoic bowel in a second-trimester fetus with Down syndrome. The bowel is of similar echogenicity as that of surrounding bone.

signs have been reported that are associated with fetal Down syndrome.[11,12] Some of the most studied sonographic signs include hyperechoic bowel (**Fig. 18–9**), short femur, short humerus, renal pyelectasis (**Fig. 18–10**), echogenic intracardiac foci (**Fig. 18–11**), and choroid plexus cysts.[13] As

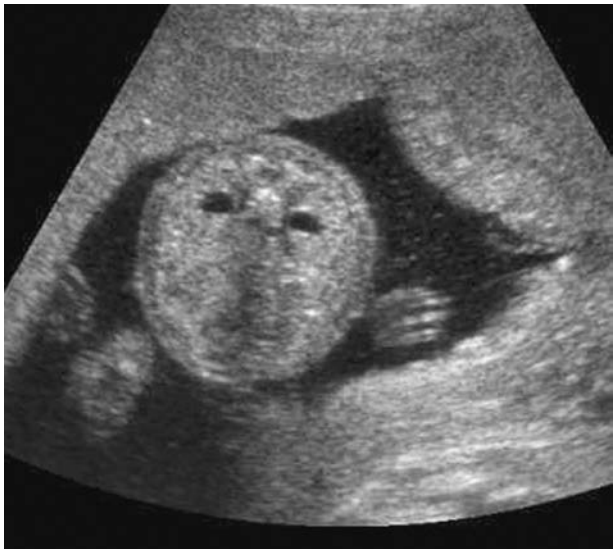

Figure 18–10 Transverse view of the fetal abdomen in a second-trimester fetus with Down syndrome, demonstrating bilateral renal pyelectasis.

isolated findings, a recent meta-analysis gave the following likelihood ratios (95% confidence intervals) for the above-noted sonographic signs for fetal Down syndrome in the second trimester: thickened nuchal fold—17 (8 to 38), hyperechoic bowel—6.1 (3.0 to 12.6), short femur—2.7 (1.2 to 6.0), short humerus—7.5 (4.7 to 12), renal pyelectasis—1.9 (0.7 to 5.1), echogenic intracardiac focus—2.8 (1.5 to 5.5), and choroid plexus cyst—1.0 (0.12 to 9.4).[13] This meta-analysis confirms many prior studies that have doc-

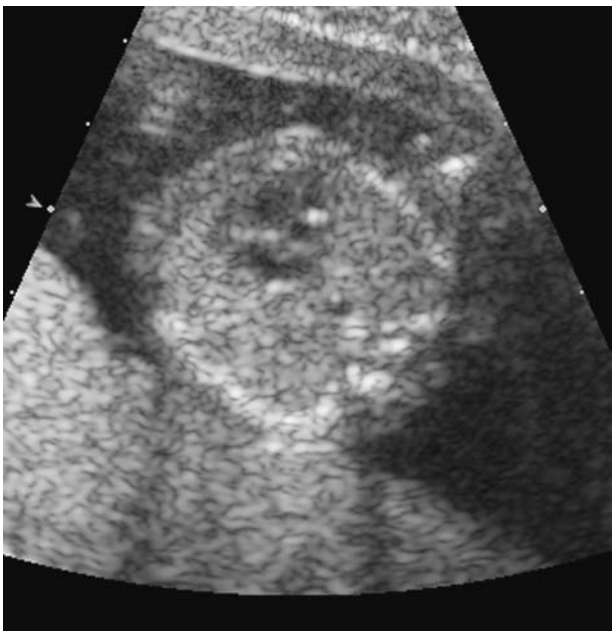

Figure 18–11 Transverse view of the fetal chest at the level of the four-chamber view in a second-trimester fetus with Down syndrome. An echogenic intracardiac focus is identified within the left ventricle, with a level of echogenicity similar to that of surrounding bone.

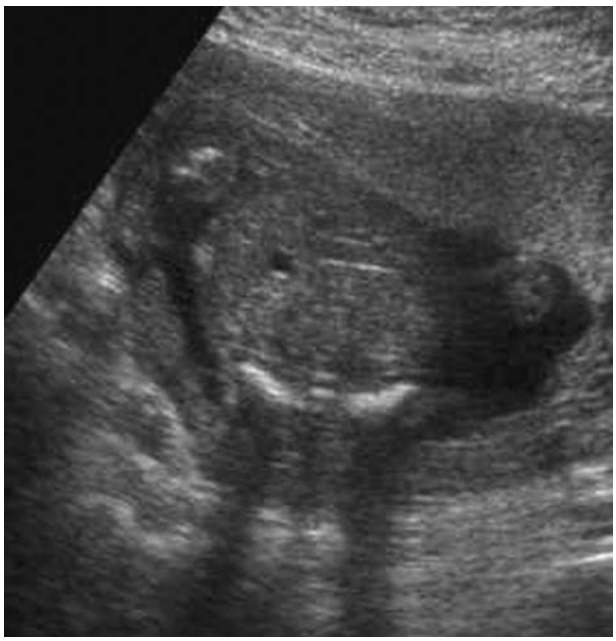

Figure 18–12 Transverse view of the lower fetal abdomen and upper pelvis in a second-trimester fetus with Down syndrome, demonstrating a wide iliac angle.

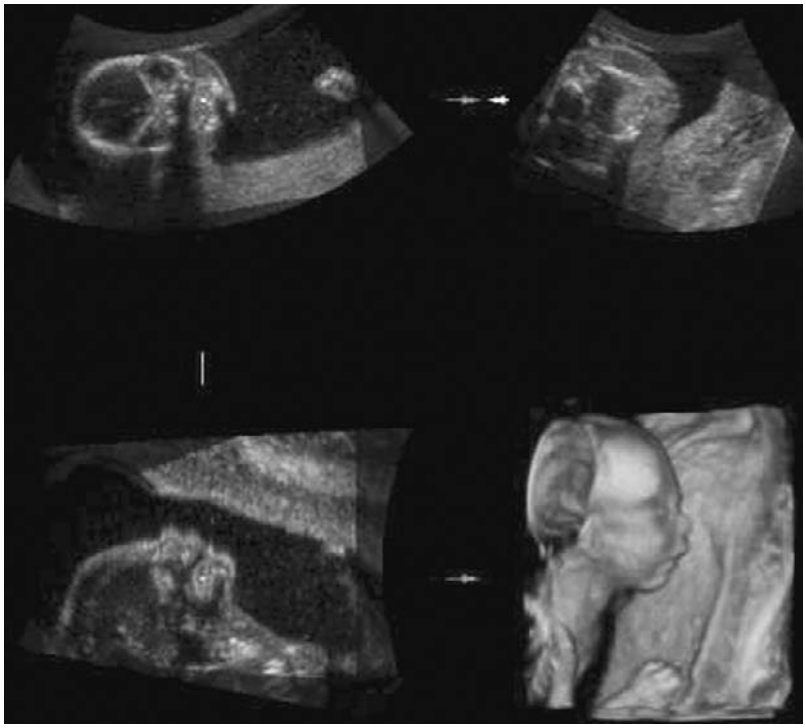

Figure 18–13 Three-dimensional reconstruction and rendering of a second-trimester fetus with Down syndrome. A small, thickened ear is shown on the rendered image.

umented an increased risk of Down syndrome among those fetuses with these isolated findings, except for choroid plexus cysts, which were not associated with Down syndrome. Further study is required to understand better how these sonographic signs should be used clinically. For example, fetal biometry, and even the prevalence of echogenic intracardiac foci, vary with maternal race.[12]

Many other sonographic signs have been associated with Down syndrome in the second trimester of pregnancy. Many, such as a wide iliac angle (**Fig. 18–12**), short ear lengths (**Fig. 18–13**), hypoplasia of the middle phalanx of the fifth digit (**Fig. 18–14**), clinodactyly, shortened frontal lobes, and a wide separation of the great toe (**Fig. 18–15**), have generally not proven useful as screening tools

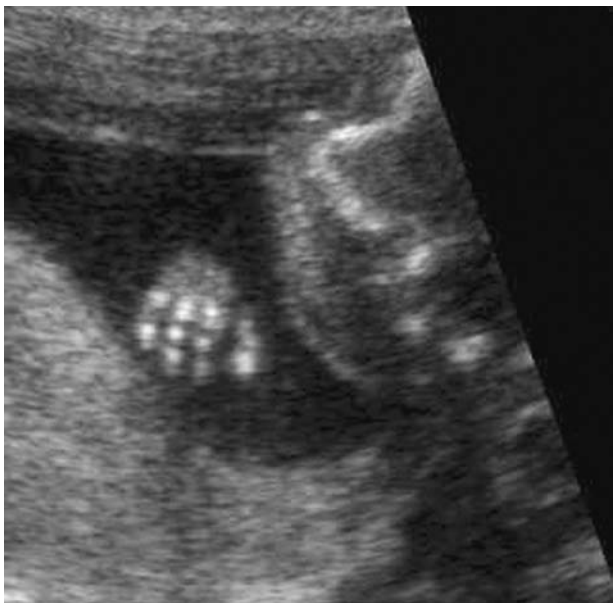

Figure 18–14 View of the fetal hand of a second-trimester fetus with Down syndrome demonstrating hypoplasia of the middle phalanx of the fifth digit.

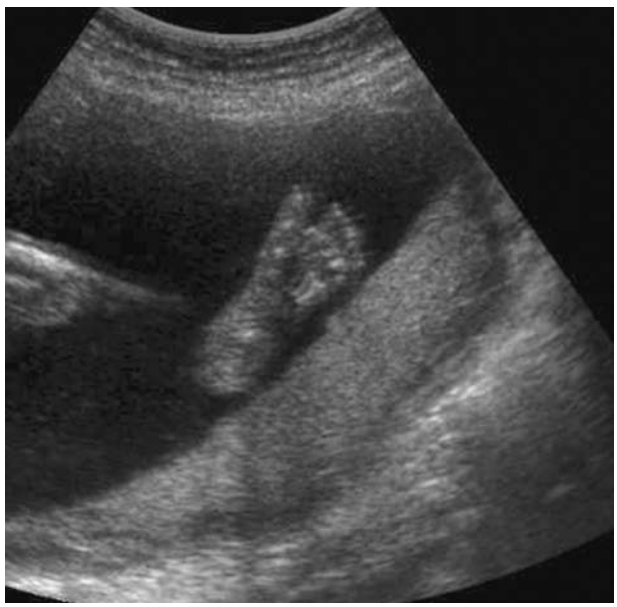

Figure 18–15 View of the base of the foot of a second-trimester fetus with Down syndrome demonstrating a wide separation between the first and second toes.

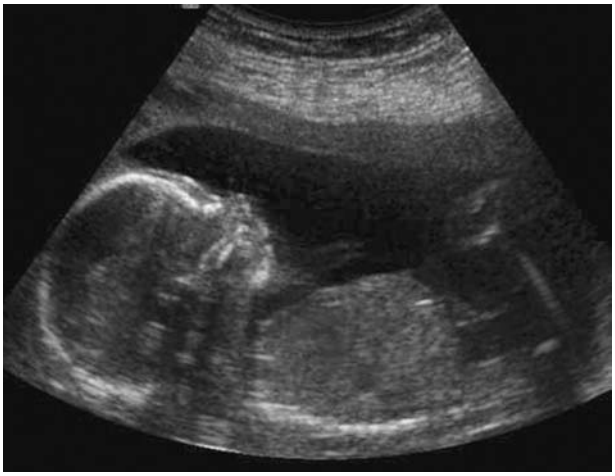

Figure 18–16 Midsagittal view of a fetus with normal chromosomes demonstrating a normal nasal bone.

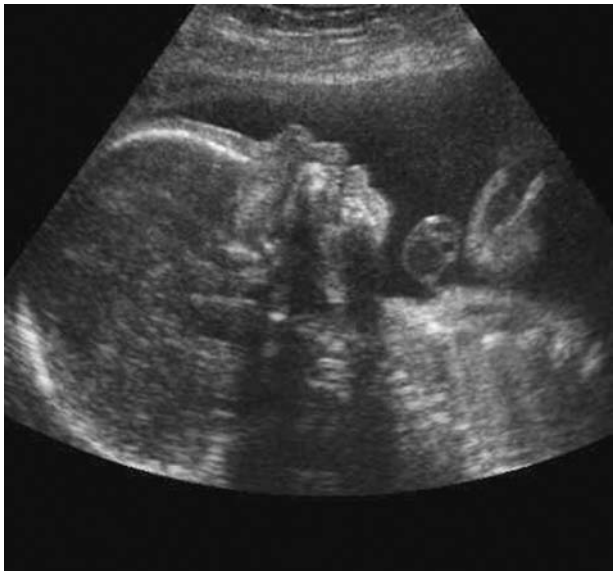

Figure 18–17 Midsagittal view of a fetus with Down syndrome demonstrating absence of the nasal bone.

due in great measure to their higher prevalence in fetuses with normal karyotypes.[12]

Other, more recent, sonographic signs may prove even more useful for screening for fetal Down syndrome. Hypoplasia of the nasal bone has been shown, in the second trimester, to be associated with an increased risk for Down syndrome.[14] Bromley et al reported an absent nasal bone (**Fig. 18–16** and **Fig. 18–17**) was found in 37% of fetuses with Down syndrome and 0.5% of control fetuses, yielding a likelihood ratio of 83.[14] How this sonographic sign will affect our current evaluation of the second-trimester fetus remains to be determined.

Genetic Sonogram

As already discussed, multiple authors from multiple ultrasound laboratories have shown that there are sonographic findings associated with fetal Down syndrome. Even though we have this information, many questions remain. How can we use this information to assist with our management of the gravida who undergoes second-trimester sonography? Can we use these sonographic signs to evaluate those at high risk for fetal Down syndrome? Can we use these sonographic signs to evaluate those at low risk for fetal Down syndrome? Can we modify the risk for fetal Down syndrome for those with abnormal maternal serum screens? These are the questions that we will endeavor to answer.

Initial work to evaluate the use of these sonographic markers among those undergoing second-trimester sonography was reported by Benacerraf et al in the early 1990s.[15,16] Their straightforward scoring index was described as follows: 2 points for a major congenital structural defect or a thickened nuchal fold; 1 point for short femur, short humerus, pyelectasis, hyperechoic bowel, or echogenic intracardiac focus. Amniocentesis was performed for those at low risk with a score of 2 or greater, and for those at high risk with a score of 1 or greater. The authors were able to show that 73% of fetuses with Down syndrome could be identified with a false-positive rate of ~4%. This uncomplicated method of screening for Down syndrome was better than screening using maternal age alone, and comparable to the use of the serum screen. Vintzileos et al subsequently coined the term *genetic sonogram* to denote the use of an ultrasound exam of the second-trimester fetus to modify the risk of Down syndrome.[17] Although various authors have included different sonographic markers, or soft signs, of Down syndrome in their models, the use of the genetic sonogram has changed the way in which sonologists practice sonography of the second-trimester fetus.

The simple scoring system proposed by Benacerraf et al was supplanted by a more mathematical approach for evaluating the risk of Down syndrome in the second-trimester fetus. Nyberg et al proposed an adjustment in the maternal age–based risk for Down syndrome by using the likelihood ratios of the second-trimester ultrasound-derived markers for Down syndrome.[18] Their so-called age-adjusted ultrasound risk assessment (AAURA) was used to evaluate the posttest risk for Down syndrome. This was calculated after second-trimester sonography was performed, and the findings modified the prior age-adjusted risk for Down syndrome. Using a threshold of 1:200, they were able to identify 61.5% of fetuses with Down syndrome among those less than 35 years of age, 67.2% of those with Down syndrome from women aged 35 to 39 years, and 100% of those fetuses with Down syndrome among women age 40 and older. The false-positive rates were 4% for those less than 35 years of age, 12.5% for those age 35 to 39 years, and 100% for those 40 years of age and older. A normal ultrasound exam with no markers identified was

assigned a likelihood ratio of 0.4. The likelihood ratios for those with isolated findings were as follows: structural defect—25, thickened nuchal fold—18.6, hyperechoic bowel—5.5, short humerus—2.5, short femur—2.2, echogenic intracardiac focus—2, pyelectasis—1.6. The calculated likelihood ratios from their population were as follows: structural defect—71, thickened nuchal fold—58, hyperechoic bowel—21.9, short humerus—15.8, short femur—4.6, echogenic intracardiac focus—5.1, pyelectasis—4.8.[18]

In our laboratory, we recently sought to determine the risk for Down syndrome in fetuses with sonographic markers using likelihood ratios.[19] In our population there were 164 fetuses with Down syndrome and 656 euploid fetuses. The likelihood ratios (95% confidence intervals) for the sonographic markers were as follows: anomaly—22 (10.6 to 45.8), thickened nuchal fold ≥ 6 mm—94.7 (30.2 to 296.7), thickened nuchal fold ≥ 5 mm—61.6 (25.3 to 149.7), hyperechoic bowel—14.4 (5.4 to 38.1), short humerus—23.5 (13.1 to 42.1), short femur—10.1 (7.1 to 14.3), echogenic intracardiac focus—8.0 (4.8 to 13.3), pyelectasis—8.8 (5.0 to 15.4), any marker—6.5 (5.3 to 8.1), no marker or anomaly identified—0.22 (0.16 to 0.30). When the markers were grouped as to present or absent, the presence of one of the markers was associated with a likelihood ratio of 1.9 (1.3 to 2.9), two markers had a likelihood ratio of 6.2 (3.1 to 12.1), and three markers had a likelihood ratio of 80 (19.5 to 327.6).

As more information becomes available with regard to the genetic sonogram and its use clinically, more detailed statistical information is necessary. If we are going to screen with sonographic markers, we must confirm that there are no significant correlations between the sonographic markers and biochemical markers and maternal age. Souter et al have critically evaluated the correlation of the sonographic markers with both maternal age and the biochemical markers. No correlation of the sonographic markers was identified with maternal age.[20] The authors were able to identify some weak correlations between a few of the markers. For example, there was a statistically significant correlation between both femur length and humerus length with human chorionic gonadotropin. Despite these few correlations, the authors concluded that the "sonographic and biochemical markers for trisomy 21 are largely independent in unaffected pregnancies."[21] Although more work must be done to determine the correlations in affected pregnancies, it appears that the sonographic markers can be used to modify the maternal age–specific risk for Down syndrome.

Genetic Sonogram for Those with Abnormal Second-Trimester Serum Screens

Literature is becoming increasingly available to guide us with respect to clinical management of those patients with abnormal serum screens indicating an increased risk for Down syndrome. Ten years ago, Nyberg et al evaluated 395 women with an abnormal triple marker screening test by prenatal sonography. The sonographic findings that were evaluated were structural defects, nuchal fold measurements, hyperechoic bowel, pyelectasis, and femur length measurements. Of this cohort, 18 (4.5%) had Down syndrome. At least one abnormal sonographic finding was found in 50% of those with Down syndrome. Having an abnormal sonographic exam increased the risk of Down syndrome 5.6-fold, or from 4.5 to 25%. A normal sonographic exam decreased the risk for Down syndrome by 45%, or from 4.5 to 2.5%. Although the authors identified an improvement in risk for Down syndrome with a normal ultrasound exam, they recommended amniocentesis for all patients in this cohort regardless of sonogram results.[22]

More recent data suggest that the risk for Down syndrome can be confidently modified using the genetic sonogram from the a priori risk estimate as determined from the serum screen. Bahado-Singh et al evaluated the risk of Down syndrome in pregnancies with abnormal serum screen results indicating an increased risk for Down syndrome. All patients received targeted sonograms searching for signs of Down syndrome. A normal ultrasound exam with no signs of Down syndrome reduced the risk of Down syndrome by a factor of 7.8. Overall, the risk for Down syndrome was 1.0%. If the sonographic findings were abnormal, the rate of Down syndrome was 8/127, or 6.3%. If there were no sonographic signs of Down syndrome identified on the sonographic exam, the risk of Down syndrome was 1/753, or 0.13%, yielding an odds ratio of 50.4 (95% confidence interval, 6.4 to 90.2) for those with sonographic findings suggestive of Down syndrome in a population of those with abnormal serum screen results.[23] Verdin and Economides reported on 463 fetuses with positive serum screens for Down syndrome. Eleven (2.4%) had Down syndrome. Nine of the 11 with Down syndrome (81.8%) had the presence of sonographic markers associated with Down syndrome. The presence of one or more sonographic markers was associated with a likelihood ratio of 8.4 (95% confidence interval 5.7 to 12.5) for Down syndrome, and the presence of two or more sonographic markers was associated with a likelihood ratio of 41 for Down syndrome. The absence of any markers was associated with a likelihood ratio of 0.2 for fetal Down syndrome. The authors concluded that the presence or absence of sonographic markers could modify the risk of Down syndrome among women at risk for Down syndrome based on an abnormal serum screen.[24]

As noted earlier, current data suggest that the genetic sonogram can modify the risk for Down syndrome from that obtained with the serum screen. It remains unclear which aspects of the genetic sonogram are most beneficial to this risk modification and how they should be incorporated into clinical use. Benn et al evaluated the use of second-trimester biochemical analysis, as well as the assessment of specific ultrasound marker, in determining the risk for Down syndrome, with the goal of developing

a model for obstetric practice.[25] They used the quadruple screen of MSAFP, hCG, uE3, and inhibin A, and the sonographic parameters of biparietal/femur length and biparietal/femur length ratios, as well as the nuchal fold measurement. Using the serum screen, the sensitivity for detection of Down syndrome was 81.5% with a false-positive rate of 6.9%, and positive predictive value of 1 in 42 for Down syndrome. From the ultrasound-derived factors, the sensitivity for the detection of Down syndrome was 79.7% with a false-positive rate of 6.7%, and, again, a positive predictive value of 1 in 42. Combining both tests led to a sensitivity of 90% with a false-positive rate of 3.1%, and a positive predictive value of 1 in 18. Combining the serum screen with the sonographically obtained data gives the best screening test for Down syndrome. Obviously, much more research is necessary to help us determine the best screening method or methods, giving us the highest sensitivity while keeping our false-positive rate to a minimum.

Diagnostic Evaluation for Those with Abnormal Second-Trimester Maternal Serum Screens

A patient with an abnormal serum screen result for Down syndrome is quite commonly surprised at this news. She has not had any antecedent abnormal signs or symptoms during the pregnancy to suggest that there could be a problem. Unfortunately, most women do not fully understand, at the time the test is taken, exactly what information this test provides. Because of this, those with an abnormal serum screen are faced with comprehending the intricacies of this screening test after the results have been given. It is the providers' obligation to explain precisely what information is given and to formulate a plan for the patient.

After the serum screen indicates an increased risk for Down syndrome, the patient is most commonly sent for an ultrasound exam. This exam fulfills two important goals. First, an assessment of gestational age is vital to interpret the results of the serum screen. This serum test is dependent upon gestational age. It is typically drawn from 15 to 22 weeks' gestation age based on last menses. If the patient is earlier in gestation than suspected, given her menstrual dates, the serum screen may not be accurate. Many laboratories will reassess the serum analytes when gestational age based on ultrasound differs from menstrual age by 10 days or more. If the ultrasound exam confirms the menstrual dates that were used for the calculation of the serum screen risk estimate, then the serum screen is considered accurate. The second role that ultrasound plays is in diligently searching for structural defects or sonographic signs suggestive of Down syndrome. If no signs of Down syndrome are identified by an experienced sonologist after an exhaustive sonographic search, the patient can be informed of an ~50% decrease in the risk for Down syndrome. As already discussed, much literature suggests that the modification of the serum screen–related risk may be as high as an 80% decrease in risk. Alternatively, the identification of any structural defects associated with Down syndrome would prompt a recommendation for karyotyping should the patient desire this information. Similarly, if any signs of Down syndrome were identified, the a priori serum screen–related risk could be modified and a posttest risk could be presented to the patient.

After the posttest risk is presented to the patient, it is important to acknowledge variability in decision making dependent on the patient's desires. The only way to determine that a fetus definitely has Down syndrome is via karyotype. Ultrasound does not diagnose nor exclude this diagnosis. The standard method for karyotype analysis in the second trimester is via amniocentesis. This typically simple, yet invasive procedure is generally well tolerated by the patient, but is associated with an excess risk of miscarriage of ~1/200 to 1/300 above the baseline risk. The karyotype generally requires approximately 2 weeks for final results. The patient must decide whether to have amniocentesis, a procedure with some inherent risk, for a definitive diagnosis of the fatal karyotype, or to forgo invasive testing. Given our current level of understanding, ultrasound plays an essential role in providing the patient with information she needs to help make this difficult decision.

Summary

There are many sonographic signs associated with Down syndrome. The use of a genetic sonogram is a way of modifying the risk for Down syndrome based on the presence or absence of sonographic signs of Down syndrome. The genetic sonogram can be used to as an aid to modify the risk for Down syndrome for those with abnormal second-trimester serum screens. Ultrasound is a vital procedure for those with abnormal second-trimester serum screens to assess gestational age and to search diligently for those structural defects and signs that can be seen in fetuses with Down syndrome.

References

1. Morris JK, Wald NJ, Mutton DE, et al. Comparison of models of maternal age-specific risk for Down syndrome live births. Prenat Diagn 2003;23:252–258
2. Biggio JR Jr, Morris TC, Owen J, et al. An outcome analysis of five prenatal screening strategies for trisomy 21 in women younger than 35 years. Am J Obstet Gynecol 2004;190:721–729
3. Mulvey S, Zachariah R, McIlwaine K, et al. Do women prefer to have screening tests for Down syndrome that have the lowest screen-positive rate or the highest detection rate? Prenat Diagn 2003; 23:828–832
4. Phillips OP, Elias S, Shulman LP, et al. Maternal serum screening for fetal Down syndrome in women less than 35 years of age using alpha-fetoprotein, hCG, and unconjugated estriol: a prospective 2-year study. Obstet Gynecol 1992;80:353–358

5. Burton BK, Prins GS, Verp MS. A prospective trial of prenatal screening for Down syndrome by means of maternal serum alpha-fetoprotein, human chorionic gonadotropin, and unconjugated estriol. Am J Obstet Gynecol 1993;169:526–530
6. Cheng EY, Luthy DA, Zebelman AM, et al. A prospective evaluation of a second-trimester screening test for fetal Down syndrome using maternal serum alpha-fetoprotein, hCG, and unconjugated estriol. Obstet Gynecol 1993;81:72–77
7. Benn PA, Fang M, Egan JFX, et al. Incorporation of inhibin-A in second-trimester screening for Down syndrome. Obstet Gynecol 2003;101:451–454
8. Nyberg DA, Resta RG, Luthy DA, et al. Prenatal sonographic findings of Down syndrome: review of 94 cases. Obstet Gynecol 1990; 76:370–377
9. Benacerraf BR, Barss VA, Laboda LA. A sonographic sign for the detection in the second trimester of the fetus with Down's syndrome. Am J Obstet Gynecol 1985;151:1078–1079
10. Benacerraf BR, Frigoletto FD Jr, Cramer DW. Down syndrome: sonographic sign for diagnosis in the second-trimester fetus. Radiology 1987;163:811–813
11. Nyberg DA, Souter VL, El-Bastawissi A, et al. Isolated sonographic markers for detection of fetal Down syndrome in the second trimester of pregnancy. J Ultrasound Med 2001;20: 1053–1063
12. Shipp TD, Benacerraf BR. Second trimester ultrasound screening for chromosomal abnormalities. Prenat Diagn 2002;22:296–307
13. Smith-Bindman R, Hosmer W, Feldstein VA, et al. Second-trimester ultrasound to detect fetuses with Down syndrome: a meta-analysis. JAMA 2001;285:1044–1055
14. Bromley B, Lieberman E, Shipp TD, et al. Fetal nose bone length: a marker for Down syndrome in the second trimester. J Ultrasound Med 2002;21:1387–1394
15. Benacerraf BR, Neuberg D, Bromley B, et al. Sonographic scoring index for prenatal detection of chromosomal abnormalities. J Ultrasound Med 1992;11:449–458
16. Benacerraf BR, Nadel A, Bromley B. Identification of second-trimester fetuses with autosomal trisomy by use of a sonographic scoring index. Radiology 1994;193:135–140
17. Vintzileos AM, Campbell WA, Rodis JF, et al. The use of second-trimester genetic sonogram in guiding clinical management of patients at increased risk for fetal trisomy 21. Obstet Gynecol 1996;87:948–952
18. Nyberg DA, Luthy DA, Resta RG, et al. Age-adjusted ultrasound risk assessment for fetal Down's syndrome during the second trimester: description of the method and analysis of 142 cases. Ultrasound Obstet Gynecol 1998;12:8–14
19. Bromley B, Lieberman E, Shipp TD, et al. The genetic sonogram: a method of risk assessment for Down syndrome in the second trimester. J Ultrasound Med 2002;21:1087–1096
20. Souter VL, Nyberg DA, El-Bastawissi A, et al. Correlation of ultrasound findings and biochemical markers in the second trimester of pregnancy in fetuses with trisomy 21. Prenat Diagn 2002;22: 175–182
21. Souter VL, Nyberg DA, Benn PA, et al. Correlation of second-trimester sonographic and biochemical markers. J Ultrasound Med 2004;23:505–511
22. Nyberg DA, Luthy DA, Cheng EY, et al. Role of prenatal ultrasonography in women with positive screen for Down syndrome on the basis of maternal serum markers. Am J Obstet Gynecol 1995; 173:1030–1035
23. Bahado-Singh RO, Tan A, Deren O, et al. Risk of Down syndrome and any clinically significant chromosome defect in pregnancies with abnormal triple-screen and normal targeted ultrasonographic results. Am J Obstet Gynecol 1996;175:824–829
24. Verdin SM, Economides DL. The role of ultrasonographic markers for trisomy 21 in women with positive serum biochemistry. Br J Obstet Gynaecol 1998;105:63–67
25. Benn PA, Kaminsky LM, Ying J, et al. Combined second-trimester biochemical and ultrasound screening for Down syndrome. Obstet Gynecol 2002;100:1168–1176

19 Diabetes Mellitus and Pregnancy

Peter W. Callen

It has been estimated that diabetes mellitus affects between 1 and 2 million women of childbearing age in the United States.[1] The management of this disease has evolved from an attempt to improve maternal survival in the 1900s and fetal survival in the middle part of the century to the prevention of fetal morbidity in the 1990s. The diagnosis and management of the maternal complications of diabetes mellitus are numerous and complex and will not be addressed in this discussion. Rather, the fetal complications, including fetal malformations; growth disturbances, including intrauterine growth restriction; macrosomia; and prematurity will be discussed.[2,3]

Pathophysiology and Classification

Pregnancy itself has often been referred to as diabetogenic. In fact, this is only partially true. In the first trimester, estrogen- and progesterone-induced pancreatic β-cell hyperplasia results in increased insulin production and a lowering of fasting blood sugar in both diabetic and nondiabetic pregnancies. In the second and third trimesters, the levels of human placental lactogen, a polypeptide hormone that is an insulin antagonist, rise. In addition, prolactin, cortisol, estrogen, and progesterone also exert a contrainsulin effect.

Diabetes mellitus occurring during pregnancy has been traditionally categorized according to the White classification. The basis of this system relied upon the fact that the severity of diabetes can be quantified and is directly related to both maternal and perinatal outcomes. The White classification grouped patients into classes A through F on the basis of the type of therapy administered, the duration of maternal diabetes before pregnancy, and the presence or absence of maternal vascular complications. Class A refers to those patients with gestational diabetes, whereas classes B, C, and D include patients with diabetes mellitus predating their pregnancies. Classes F, R, and H represent those diabetic women with evidence of vascular disease. Although the White classification has been useful for identifying women at risk for an adverse outcome, it has recently fallen into disuse. As our understanding of diabetes and pregnancy has improved it has become clear that most of the fetal risk is related to the time during pregnancy when diabetes is present, the degree of metabolic control achieved with therapy, the presence of maternal vascular complications, and the presence of medical complications, such as hypertension and urinary tract infections.

A more modern classification divides patients into two large groups: those whose diabetes antedated pregnancy (pregestational diabetes) and those whose diabetes was first diagnosed during gestation (gestational diabetes).[4] Fetal risks in the former group include those derived from maternal metabolic abnormalities during the first trimester (birth defects and spontaneous abortion), as well as during the second and third trimesters. (e.g., macrosomia, hyperinsulinemia, and stillbirth). Fetal risks in women with gestational diabetes are primarily derived from metabolic abnormalities in the second and third trimesters. In addition to the above classifications, diabetes mellitus may be characterized as type I, insulin-dependent diabetes mellitus (IDDM) and type II, noninsulin-dependent diabetes mellitus. Type I diabetes is the ketotic-prone form of the disorder, whereas type II is the so-called maturity-onset, nonketotic-prone form of the disease.

Ultrasound Evaluation

Through the use of fetal biometry, ultrasound is able to determine fetal age, weight, and growth. The accurate determination of fetal gestational age is important in the diabetic patient to aid in the timing and interpretation of maternal serum α-fetoprotein (AFP) levels, in the timing of third-trimester amniocentesis and delivery, and in the evaluation of fetal growth. In patients in whom the menstrual history is uncertain, first-trimester ultrasound may be necessary to establish the gestational age to aid in the timing of either maternal serum AFP testing or amniocentesis. Accuracy within 4 to 7 days may be achieved in most cases. As will be discussed later, although the accuracy for estimating gestational age is excellent, the ability to detect many significant fetal malformations is poor in the first trimester. A sonogram performed between 18 and 20 weeks of gestation will still have an accuracy of ± 1 week for defining gestational age, and greater than 90% likelihood of detecting serious fetal malformations.

Fetal Malformations

Perhaps the most significant fetal complication of pregnancy encountered by pregestational diabetic women is a significantly increased risk of fetal congenital malformations. An association between diabetes mellitus and congenital malformations was suspected as early as 1885, when it was reported that infants of diabetic mothers had an increased incidence of congenital malformations.[5–7] In a study done between 1926 and 1963, 6.4% of infants of diabetic mothers had major congenital malformations compared with 2.1% in the control group.[8] Virtually all other studies done subsequently have verified the increased incidence of congenital malformations in this population to be three to four times that of controls.[5,9,10] Congenital malformations account for 35 to 40% of all perinatal deaths and are the leading cause of death among infants of diabetic mothers. Despite routine widespread morphological ultrasound scans, the rates of perinatal death from congenital anomalies in diabetic pregnancies have not changed over the last decade.[11,12]

A study by Wong et al demonstrated that within the same institution the detection rate of congenital anomalies for diabetic women was significantly lower than that for the general population (30% vs 73%).[11] The authors postulated several reasons that might account for this difference. First, 30% of the major anomalies in the diabetic group were considered not detectable by current ultrasound technology at the gestational age when the scan was performed. This was higher than in the low-risk group. However, after excluding these anomalies, the detection rate was still lower than in the low-risk group (42% vs 86%). Second, the diabetic women were more obese, with an average body mass index (BMI) of 29 kg/m^2 versus 23 kg/m^2 in the nondiabetic group. It is well known that obesity is significantly associated with poor ultrasound imaging.[13] In one study, image quality was considered unsatisfactory in 37% of the diabetic women.

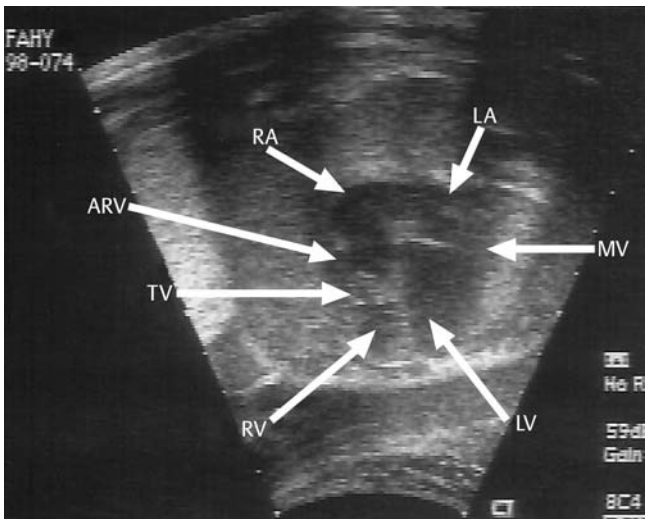

Figure 19–1 Four-chamber view from a fetal echocardiogram in a diabetic patient. Typical findings of inferior displacement of the tricuspid valve (TV) with an atrialized right ventricle (ARV) is seen. RA, right atrium; LA, left atrium; MV, mitral valve; RV, right ventricle; LV, left ventricle. (Case courtesy of Norman Silverman, M.D., Palo Alto, CA)

The detection rate of congenital anomalies may improve with technological advancements in ultrasound, such as harmonic imaging, which is available in most new ultrasound machines. Likewise, the use of transvaginal sonography at 14–16 weeks may overcome problems with excess subcutaneous tissue.[11]

The malformations most commonly observed in fetuses of diabetic mothers are cardiac defects, neural tube defects, caudal regression syndrome (sacral agenesis), and renal abnormalities (**Fig. 19–1, 19–2**). Although the focus of many clinical centers is on the detection of neural tube disease in pregestational diabetics, cardiac abnormalities are by far the most common abnormalities in these patients. The reported incidence of cardiac abnormalities is increased to between 2 and 4% in pregestational diabetics as compared with the incidence of 0.8% in the general nondiabetic population.[1,14] The abnormalities most commonly seen are conotruncal abnormalities, such as transposition of the great vessels (**Fig. 19–3**), truncus arteriosus (**Fig. 19–4**), tetralogy of Fallot (**Fig. 19–5**), and ventricular septal defects (**Fig. 19–6**). Many of the abnormalities will not be detected with just the standard four-chamber view of the heart. In a recent study by Smith et al,[15] the sensitivity of ultrasound for detecting an abnormal heart increased from 73% with the four-chamber view (**Fig. 19–7**) to 82% with the addition of the aortic outflow tract view (**Fig. 19–8**). There were two false-negative and no false-positive diagnoses. In their study, when the four-chamber view and outflow tracts appeared normal, additional views, such as the ductal and aortic arches, did not detect a cardiac defect. Additional cardiac abnormalities that may be seen in the diabetic patient include cardiomyopathy (**Fig. 19–9**) and aortic coarctation. Clearly, if a gravid diabetic patient is to have an ultrasound evaluation for the purpose of detecting morphological abnormalities, it should include an evaluation of the fetal heart by an experienced fetal and/or pediatric echocardiographer.

Neural tube defects are increased in the diabetic population. The incidence of neural tube defects is said to be 19.5 per thousand in diabetic mothers compared with one to two per thousand in the general population.[12] Anencephaly (**Fig. 19–10**) as well as myelomeningoceles (**Fig. 19–11**) may be seen in this population. Caudal regression syndrome (sacral agenesis) is wrongly often assumed to be an abnormality seen only in the diabetic population. Caudal regression, in which there is hypoplasia of the sacrum and lower extremities, was first described in 1964 as being more common in infants of diabetic mothers.[13] Associated

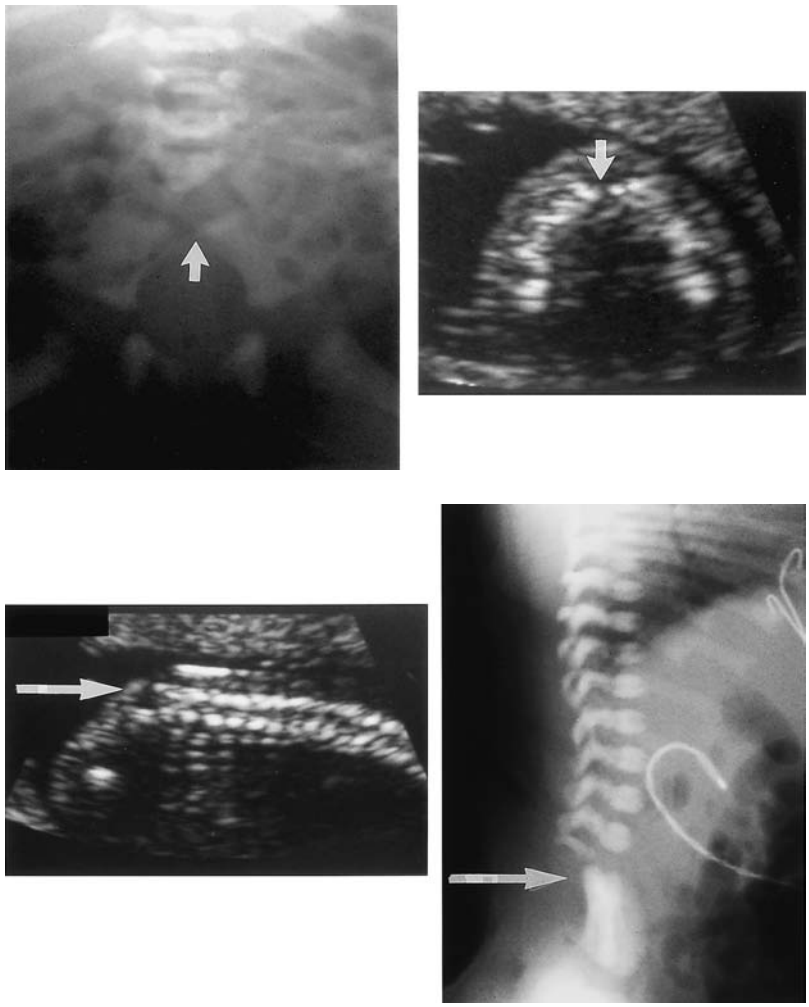

Figure 19–2 (A) Anteroposterior radiograph and sonographic transverse axial plane of section of a fetus with sacral agenesis and preconceptional diabetes at 26 weeks gestation. Medial aspects of the iliac wings are in close proximation to one another (arrow). **(B)** Sagittal plane of section sonogram and lateral radiograph from the same patient as in **(A).** Absence of the normal continuation of the spine into the sacrum is seen (arrow). (Courtesy of Nancy Budorick, M.D., New York, NY)

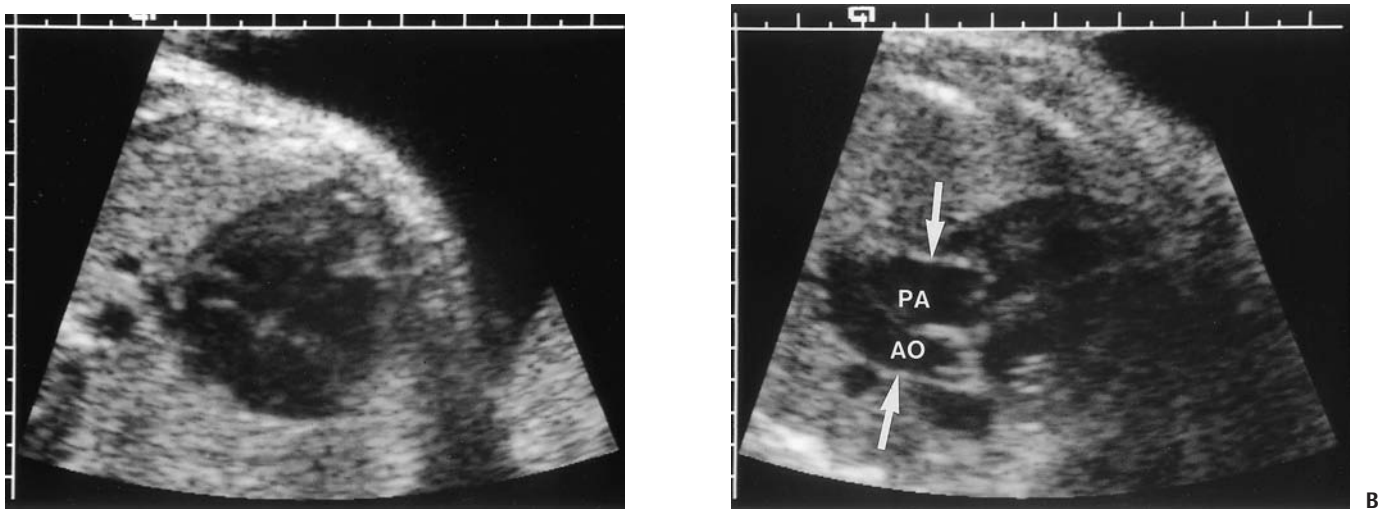

Figure 19–3 Transposition of the great vessels. **(A)** Normal four-chamber view of the fetal heart. **(B)** View of cardiac outflow tracts demonstrates the two great vessels arising from the heart in parallel to each other (arrows), with the aorta (AO) arising from the right ventricle and the pulmonary artery (PA) arising from the left ventricle. (Courtesy of Carol B. Benson, M.D., Boston, MA)

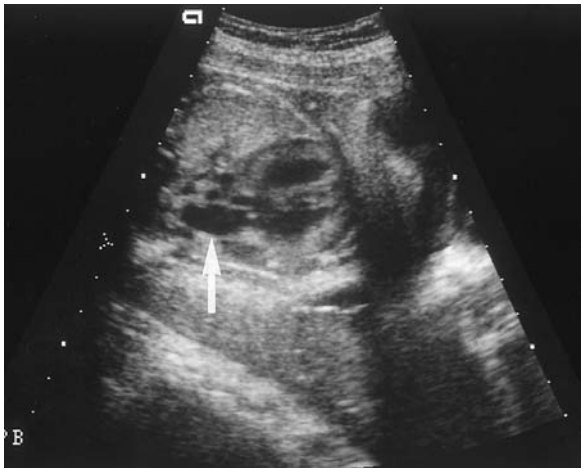

Figure 19–4 Truncus arteriosus. Long axis view of the fetal heart demonstrating a single large vessel (arrow) arising from both ventricles. (Courtesy of Carol B. Benson, M.D., Boston, MA)

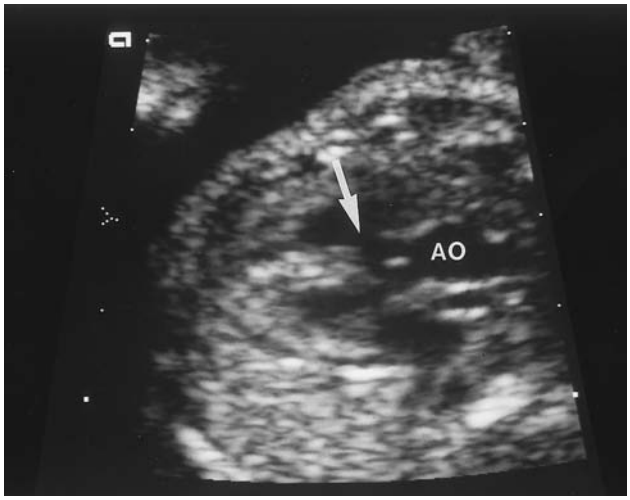

A

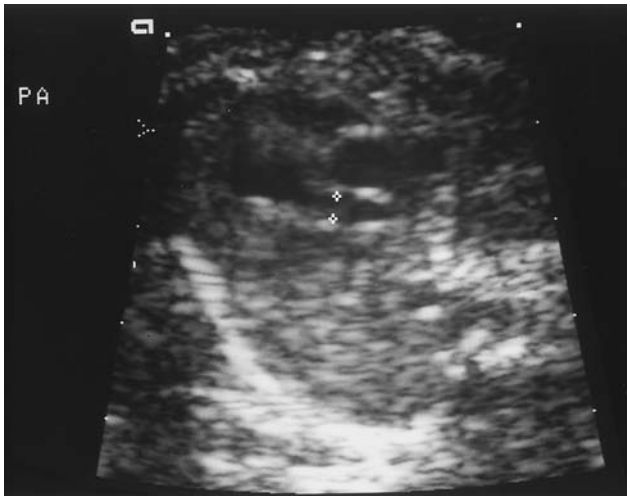

B

Figure 19–5 Tetralogy of Fallot **(A)** Long axis view of the fetal aortic outflow tract demonstrating overriding aorta (AO) and ventricular septal defect (arrow). **(B)** The pulmonary artery (calipers) was small. (Courtesy of Carol B. Benson, M.D., Boston, MA)

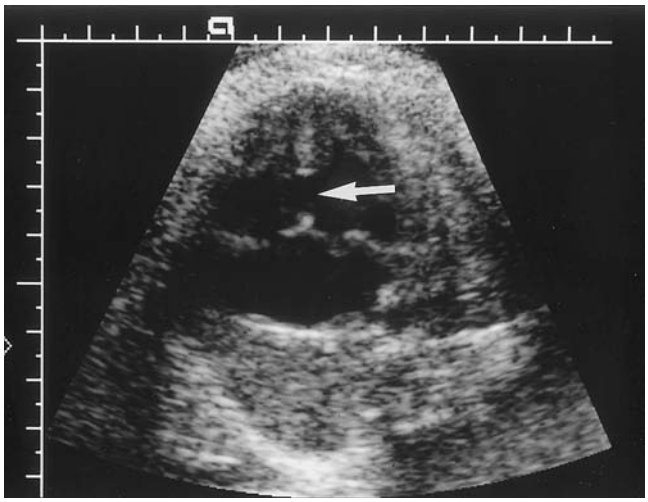

Figure 19–6 Ventricular septal defect. Four-chamber view of the fetal heart demonstrating a defect in the ventricular septum (arrow). (Courtesy of Carol B. Benson, M.D., Boston, MA)

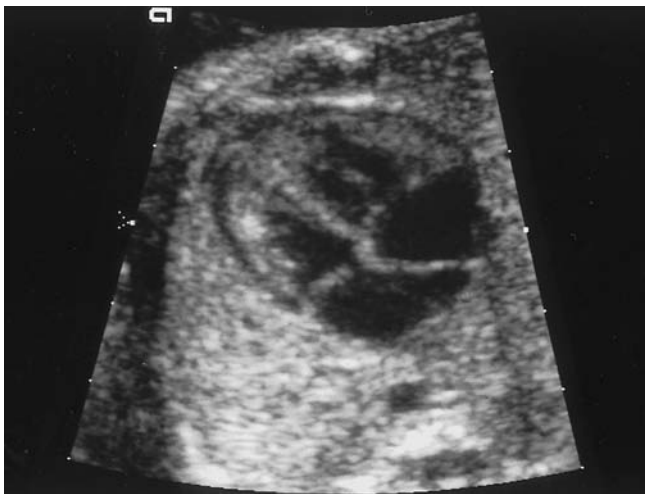

Figure 19–7 Normal four-chamber view of the fetal heart. (Courtesy of Carol B. Benson, M.D., Boston, MA)

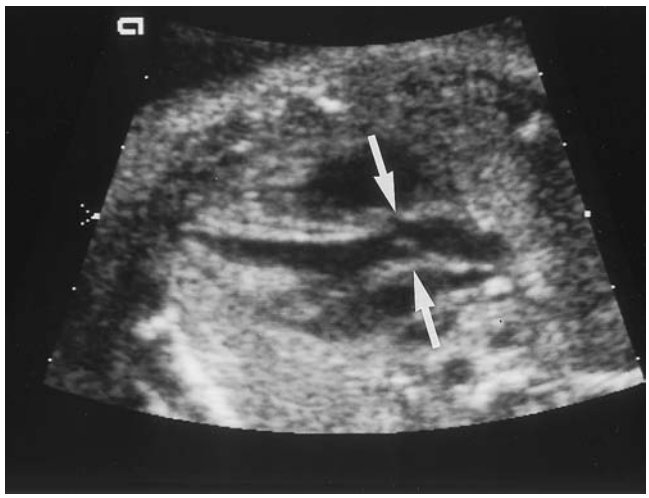

Figure 19–8 Normal aortic outflow tract (arrows) arising from the left ventricle. (Courtesy of Carol B. Benson, M.D., Boston, MA)

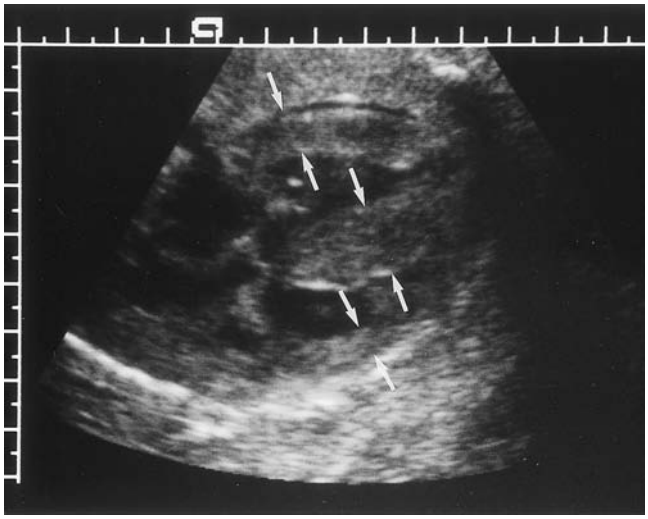

Figure 19–9 Cardiomyopathy. Four-chamber view of the fetal heart demonstrating thickening of the walls of both ventricles (arrows) and the septum. (Courtesy of Carol B. Benson, M.D., Boston, MA)

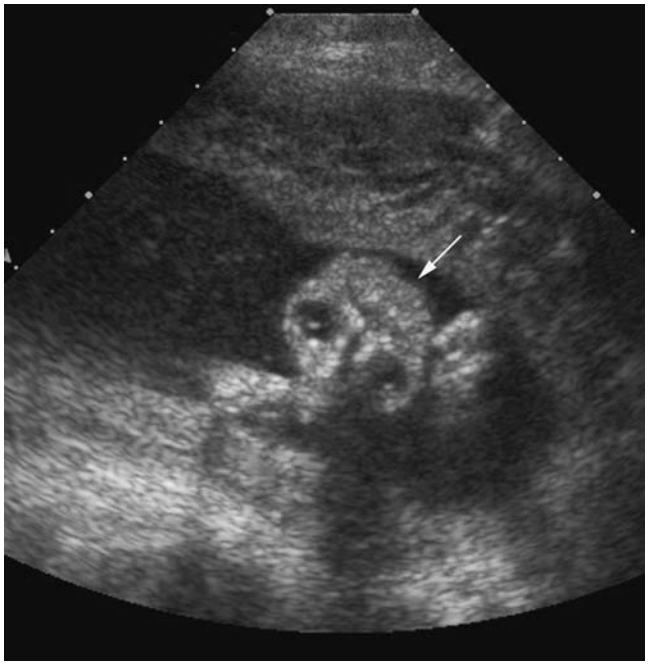

Figure 19–10 Anencephalic fetus. Sonogram demonstrates the fetal face with absence of the cranium. Abnormal brain (arrow) is seen above the orbits.

anomalies that may be seen at birth are fusion of the lower limbs (sirenomelia), absence of the bladder, imperforate anus, absence of external genitalia, renal agenesis (**Fig. 19–12**), hypospadias (**Fig. 19–13**), and single umbilical artery. As already stated, the abnormalities that form the basis of caudal regression syndrome may be seen in nondiabetics as well.

Several other abnormalities may also be seen in pregestational diabetics, including fetal hydronephrosis, skeletal abnormalities, and ocular and skin defects. A study by Petrikovsky et al evaluated a group of 12 patients with a hypoplastic umbilical artery (**Fig. 19–14**) (artery to artery difference of greater than 50%).[14] They found that one third of the patients was diabetic. Another study by Weissman et al found that the umbilical cord was significantly larger in fetuses of mothers with gestational diabetes than in the normal population.[16] The main increase in width was attributed to an increase in Wharton jelly content.

The exact mechanism leading to an increased incidence of congenital malformations is controversial. Insulin is unlikely to be the cause of malformations because it does not cross the placenta, and fetal insulin is not produced until

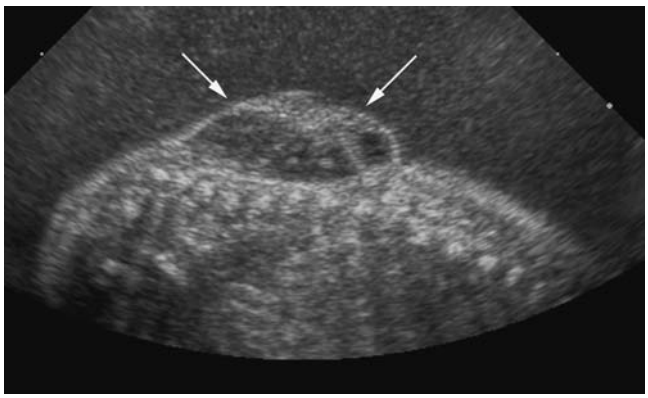

Figure 19–11 Myelomeningocele. Longitudinal view of the lower spine demonstrating disruption of the spine and posterior cystic mass (arrows).

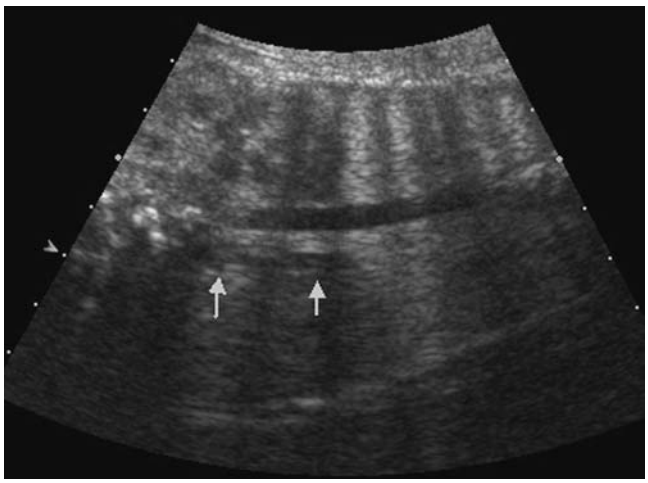

Figure 19–12 Renal agenesis. Coronal plane of section in a fetus with unilateral renal agenesis. No kidney is seen in the renal fossa and the adrenal gland has assumed an elongated shape (arrows) due to absence of the kidneys.

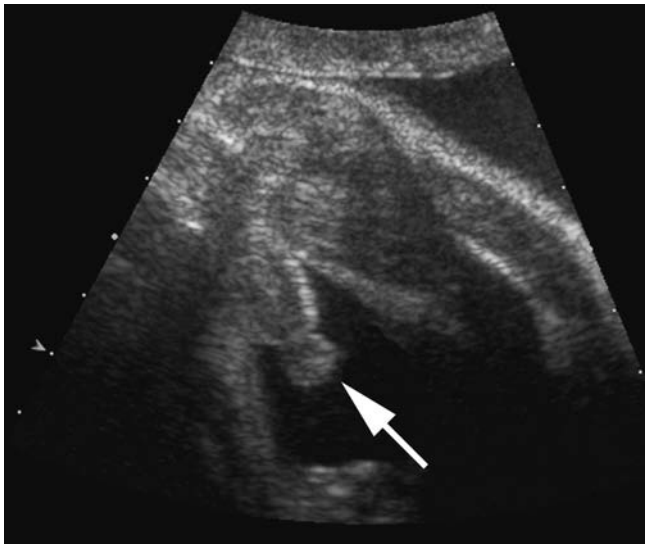

Figure 19–13 Hypospadias. Coronal plane of section in a male fetus. Abnormal blunt end of the penis (arrow) is identified.

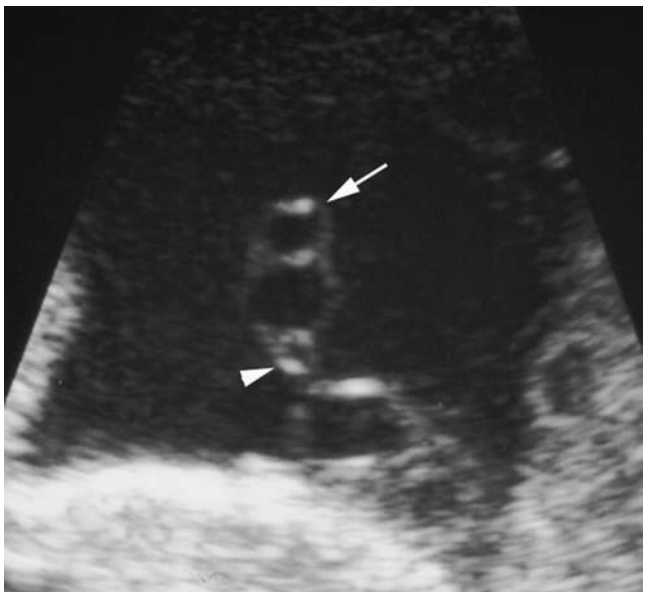

Figure 19–14 Hypoplastic umbilical artery. Transverse image of a three-vessel umbilical cord with one normal umbilical artery (arrow) and one hypoplastic (arrowhead). (Case courtesy of Carol B. Benson, M.D., Boston, MA)

after organogenesis. Hyperglycemia has been implicated as the main cause of malformations. Maternal glycosylated hemoglobin (Hb A1 c) is a reflection of average maternal glucose levels during the preceding 6 to 8 weeks. When these values are found to be elevated in the early second trimester, it raises the concern that the diabetes is poorly controlled and that hyperglycemia may have been present at the time of organogenesis. One study found a 22% incidence of congenital anomalies among infants of diabetic mothers if the Hb A1 c was greater than 8.5%, and a 3% incidence if the Hb A1 c was less than 8.5%.[16]

Although the foregoing risks and malformations apply to the pregestational insulin-dependent diabetic, they do not apply to the patient with gestational diabetes. Historically, the chance of fetal malformations in gestational diabetics has been reported as not being appreciably different from that of the general population. The Collaborative Perinatal Project, a prospective study of 48,437 subjects from 14 institutions, revealed that diabetic women with pregnancy-induced glucose intolerance were not at increased risk for producing infants with congenital malformations.[10] These facts strongly implicate a first-trimester metabolic teratogen contribution in the pregestational diabetic population and give further credence to the notion of attempting to achieve optimal preconceptional glucose control in an attempt to decrease the risk of fetal malformations. An interesting, study by Schaefer et al attempted to determine the risk of congenital malformations based upon the degree of hyperglycemia in women with gestational diabetes.[17] In their study, one or more major congenital anomalies were present in 2.9% of the newborns and an additional 2.4% had only minor abnormalities. In this study the highest fasting serum glucose level at diagnosis was the best predictor of the likelihood of congenital anomalies. When the authors stratified women into subgroups based upon the fasting serum glucose level at diagnosis, the incidence of major anomalies was as follows: 2.1% with a fasting serum glucose < 120 mg/dL, 5.2% with a fasting serum glucose level of 121 to 260 mg/dL, and 30.4% with a fasting serum glucose level > 260 mg/dL. Their conclusion was that a fasting glucose level below that of overt diabetes outside of pregnancy carries an important risk of major anomalies that should be considered in the counseling of gravid patients.

Growth Disturbances

Infants of diabetic mothers can be affected by major growth disturbances, most commonly macrosomia. The etiology of the macrosomia is thought to be due to excess levels of insulin resulting from maternal hyperglycemia. The accelerated fetal growth seen in macrosomia is likely due to the structural similarity of insulin to human growth hormone. It should be remembered that, although diabetic women have a higher incidence of macrosomia than nondiabetics, only ~2% of macrosomic fetuses will be born to mothers with diabetes mellitus.[18,19]

Macrosomia has been traditionally defined as a birth weight greater than the 90th percentile for gestational age or a birth weight greater than 4000 g. Ultrasound is capable of estimating fetal weight utilizing measurements of the fetus, of which the fetal abdomen is the most important. Although fetal weight estimates are fairly accurate

throughout pregnancy, they tend to be less so in the macrosomic fetus. One possible explanation is the greater amount of adipose tissue (not accounted for in most formulas for fetal weight estimation) in these fetuses.[18] A second problem is that because one of the definitions of macrosomia relates the weight to the menstrual age, when the menstrual age is not known this relationship is no longer meaningful. It is for this reason that menstrual age–independent indicators, such as the absolute measurement of the fetal abdomen or the relationship of the fetal abdomen to the fetal femur, have been used as methods of detecting these fetuses. These methods are far from perfect, however.

Because shoulder dystocia is a major problem in the macrosomic diabetic fetus, several investigators have recently evaluated the utility of ultrasound in predicting this condition. Studies have evaluated either fetal subcutaneous tissue around the extremities or abdomen or various combinations of relationships of the fetal abdomen to other fetal parts.[20–22] In several studies, humeral soft tissue thickness greater than 12 mm was predictive of macrosomia with sensitivities of 88 to 96%.[20,23] There are, however, several studies in which ultrasound is only marginally better than clinical evaluation for the prediction of macrosomia.[21]

Macrosomia is more common in women with gestational diabetes than in nondiabetic women.[22] Shoulder dystocia is more likely at a given birth weight in diabetic than nondiabetic pregnancies. As a result, some physicians recommend cesarean delivery without a trial of labor at a certain threshold of estimated fetal weight. However, the clinical utility of this has not been established. The American College of Obstetricians and Gynecologists has stated, "Although the diagnosis of fetal macrosomia is imprecise, prophylactic cesarean delivery may be considered for suspected fetal macrosomia with estimated fetal weights greater than 5000 grams in women without diabetes and greater than 4500 grams in women with diabetes."[24] In a 2001 issue of *Practice Bulletin*, the threshold estimated fetal weight for patients with gestational diabetes was lowered to 4000 g.[25]

A review of fetal weight estimation in diabetic pregnancies by Ben-Haroush et al resulted in the following conclusions. (1) Regardless of the formula used, the relative accuracy of the sonographic estimated fetal weight decreases with increasing birth weight. (2) The time elapsed between the fetal weight estimation and delivery may influence the accuracy and precision of the estimate. (3) The diagnosis of fetal macrosomia is imprecise. Some believe that for suspected fetal macrosomia, the estimated fetal weight using ultrasound biometry is no more accurate than the estimated fetal weight obtained by clinical palpation. (4) Ultrasound biometry, used to detect macrosomia, is characterized by low sensitivity, low positive predictive value, and high negative predictive value. Thus, the true value of the fetal weight estimate for fetal macrosomia may be its ability to rule out the diagnosis.[22]

Although macrosomia is the most common growth disturbance in diabetic pregnancies, intrauterine growth retardation can be seen in these patients as well. It is likely that the etiology in this population is decreased uteroplacental perfusion secondary to vascular compromise. The commonly used definition of fetuses below the 10% weight for gestational age is also used in this population.

Polyhydramnios

Virtually every discussion concerning polyhydramnios will list diabetes mellitus as a common etiology. Although it is true that polyhydramnios can be seen in patients with diabetes mellitus, it relates more to three factors than the actual disease itself: (1) patients with poor glycemic control are more likely to have polyhydramnios than those whose blood glucose is normal, (2) those patients with macrosomic fetuses (either diabetic or nondiabetic) are more likely to have polyhydramnios, and (3) fetuses with morphological abnormalities (which may be seen in the pregestational diabetic group) may have polyhydramnios.[26–28]

Prematurity

Diabetic patients tend to have an increased incidence of premature deliveries, two to three times that of the general population.[2,29] Many of these deliveries are due to maternal complications, including hypertension and preeclampsia. An additional problem is that insulin-dependent diabetic pregnancies have delayed lung maturation. A recent series demonstrated that ~23% of patients with insulin-dependent diabetes were negative for amniotic fluid phosphatidylglycerol as late as 39 weeks.[4] Because of the risk for prematurity and respiratory distress syndrome, it is important that gestational age be established as accurately as possible. In general, the earlier in pregnancy that fetal biometry is performed using ultrasound, the more accurate it is likely to be. Although early first-trimester ultrasound examinations are quite accurate for establishing gestational age, they do not allow accurate detection of fetal morphological abnormalities. A reasonable compromise is to obtain a sonogram at 18 to 20 weeks of gestation, when the sonographic accuracy is still within 1 week.

Summary

Knowledge that the gravid patient is diabetic will significantly alter the performance and interpretation of the sonogram. At the very least, the patient with post-conceptional diabetes will have frequent sonograms to monitor fetal weight and growth. The fetus of a mother with preconceptional diabetes will be carefully evaluated for fetal morphologic abnormalities. In both cases, the fetal weight and knowledge of the patient's diabetic status may alter the mode of delivery.

References

1. Reece EA. Diabetes-associated congenital anomalies: pathogenesis and prenatal diagnosis. In: Chervenak FC, Issacson GC, Campbell S, eds. Ultrasound in Obstetrics and Gynecology. Boston: Little, Brown; 1993:771–781
2. Macones G, Silverman N. Diabetes during pregnancy. In: Spitzer AR, ed. Intensive Care of the Fetus and Neonate. St. Louis: Mosby-Year Book; 1996
3. Costrini NV, Kalkhoff RK. Relative effects of pregnancy, estradiol, and progesterone on plasma insulin and pancreatic islet insulin secretion. J Clin Invest 1971;50:992–999
4. Buchanan TA, Coustan DR. Diabetes mellitus. In: Burrow GN, Ferris TF, eds. Medical Complications during Pregnancy. Philadelphia: WB Saunders; 1995
5. Shah DM. Sonography in diabetic pregnancies. In: Fleischer AC, et al, eds. Sonography in Obstetrics and Gynecology. 5th ed. Stamford: Appleton and Lange; 1996:531–546
6. Mills JL, Baker L, Goldman AS. Malformations in infants of diabetic mothers occur before the seventh gestational week: implications for treatment. Diabetes 1979;28:292–293
7. Mills JL. Malformations in infants of diabetic mothers. Teratology 1982;25:385–394
8. Pedersen LM, Tygstrup I, Pedersen J. Congenital malformations in newborn infants of diabetic women. Correlation with maternal diabetic vascular complications. Lancet 1964;13:1124–1126
9. Kucera J. Rate and type of congenital anomalies among offspring of diabetic women. J Reprod Med 1971;7:73–82
10. Chung CS, Myrianthopoulos NC. Factors affecting risks of congenital malformations, II: Effect of maternal diabetes on congenital malformations. Birth Defects Orig Artic Ser 1975;11: 23–38
11. Wong SF, Chan FY, Cincotta RB, et al. Routine ultrasound screening in diabetic pregnancies. Ultrasound Obstet Gynecol 2002;19: 171–176
12. Hawthorne G, Robson S, Ryall EA, et al. Prospective population based survey of outcome of pregnancy in diabetic women: results of the Northern Diabetic Pregnancy Audit, 1994. BMJ 1997;315: 279–281
13. DeVore GR, Medearis AL, Bear MB, et al. Fetal echocardiography: factors that influence imaging of the fetal heart during the second trimester of pregnancy. J Ultrasound Med 1993;12:659–663
14. Rowland TW, Hubbell JP Jr, Nadas AS. Congenital heart disease in infants of diabetic mothers. J Pediatr 1973;83:815–820
15. Smith RS, Comstock CH, Lorenz RP, et al. Maternal diabetes mellitus: which views are essential for fetal echocardiography? Obstet Gynecol 1997;90:575–579
16. Miller E, Hare JW, Cloherty JP, et al. Elevated maternal hemoglobin A1c in early pregnancy and major congenital anomalies in infants of diabetic mothers. N Engl J Med 1981;304:1331–1334
17. Schaefer UM, Songster G, Xiang A, et al. Congenital malformations in offspring of women with hyperglycemia first detected during pregnancy. Am J Obstet Gynecol 1997;177:1165–1171
18. Hadlock FP. Ultrasound evaluation of fetal growth. In: Callen PW, ed. Ultrasonography in Obstetrics and Gynecology. Philadelphia: W.B. Saunders; 1994:129–143
19. Boyd ME, Usher RH, McLean FH. Fetal macrosomia: prediction, risks, proposed management. Obstet Gynecol 1983;61:715–722
20. Mintz MC, Landon MB, Gabbe SG, et al. Shoulder soft tissue width as a predictor of macrosomia in diabetic pregnancies. Am J Perinatol 1989;6:240–243
21. Johnstone FD, Prescott RJ, Steel JM, et al. Clinical and ultrasound prediction of macrosomia in diabetic pregnancy. Br J Obstet Gynaecol 1996;103:747–754
22. Ben-Haroush A, Yogev Y, Hod M. Fetal weight estimation in diabetic pregnancies and suspected fetal macrosomia. J Perinat Med 2004;32:113–121
23. Sood AK, Yancey M, Richards D. Prediction of fetal macrosomia using humeral soft tissue thickness. Obstet Gynecol 1995;85:937–940
24. American College of Obstetricians and Gynecologists. Fetal Macrosomia. Practice Bulletin, No. 22. American College of Obstetricians and Gynecologists; 2000
25. American College of Obstetricians and Gynecologists. Gestational Diabetes. Practice Bulletin, No. 30. American College of Obstetricians and Gynecologists; 2001
26. Bar-Hava I, Scarpelli SA, Barnhard Y, et al. Amniotic fluid volume reflects recent glycemic status in gestational diabetes mellitus. Am J Obstet Gynecol 1994;171:952–955
27. Martinez-Frias ML, Bermejo E, Rodriguez-Pinilla E, et al. Maternal and fetal factors related to abnormal amniotic fluid. J Perinatol 1999;19:514–520
28. Varma TR, Bateman S, Patel RH, et al. The relationship of increased amniotic fluid volume to perinatal outcome. Int J Gynaecol Obstet 1988;27:327–333
29. Greene MF, Hare JW, Krache M, et al. Prematurity among insulin-requiring diabetic gravid women. Am J Obstet Gynecol 1989;161: 106–111

20 Teratogen Exposure

Mark A. Kliewer

The true risks of teratogen exposure are usually poorly understood by patients, and even by the physicians, nurses, and sonologists who attempt to provide counsel. Such misunderstandings can lead to both false assurances and false alarm, both unfounded dismissiveness and unwarranted anxiety.

Teratogenesis results from genetic and environmental factors that singly or in concert alter the normal development of the embryo. Those environmental agents that can cause developmental abnormalities include drugs, chemicals, infection, procedures, radiation, and hyperthermia. Genetic aberrations are determined before conception, or at least differentiation, and exert a preemptive governing effect on development. Considering that every neonate has at least a 5% risk of having a serious congenital abnormality, and that environmental teratogens account for ~10% of nongenetic human malformations, it is apparent that teratogenesis is a field of considerable importance for to those involved with prenatal diagnosis.[1,2]

Clinical Principles of Teratogenicity

There are four cardinal principles of teratogenicity.[3,4]

1. ***Teratogens exert their effects idiosyncratically across individuals of a population and between species.***

The expression of teratogenic effects is determined by a multitude of factors that interact in complex and unpredictable ways. The genetic constitutions of mother and fetus interact to create a unique background of resilience and vulnerability to a teratogen. Indeed, only a small minority of exposed fetuses will exhibit any adverse consequences, and the range of phenotypic expression is extremely broad.[3] Such variable susceptibility is not well understood. It is nonetheless incontrovertible that only small proportions of fetuses exposed to hydantoins or even thalidomide develop malformations. Some mothers can consume alcohol throughout pregnancy without apparent ill effect to the fetus, whereas others imbibe sparingly and their offspring suffer grievously.[3]

Teratogenic effects can be further modified by the size, metabolism, parity, age, social class, and nutritional state of the mother, as well as the ethnicity, race, and gender of the baby.[5] In addition, numerous environmental factors, such as season, temperature, and geography, have been shown to potentially influence the incidence of malformations.[4]

Interspecies differences are commonplace.[6] Though animal studies are invaluable for the investigation of mechanism and pathogenesis, the results of these studies are not always directly transposable to the human case. This was most tragically demonstrated in the case of thalidomide, where tests on rodents indicated the benignity of the drug prior to its release, with devastating consequences for thousands of human babies. Unfortunately, this event has prejudiced some against all animal studies, a position that is excessive, unreasoned, and ultimately dangerous.

2. ***Susceptibility of a developing fetus to a teratogenic agent depends on the developmental stage of the fetus at the time of exposure.***

The developmental effects of a teratogen exposure can include death, malformation, growth disturbance, and functional disorder. Three important stages are usually distinguished: predifferentiation, embryonic, and fetal (**Fig. 20–1**).

The first stage, encompassing the 2 weeks from fertilization to early implantation, is a period before cellular differentiation has occurred in the embryo and before the establishment of a placental connection to the blood supply of the mother. The embryo is relatively invulnerable to most teratogens during this period. Unless an agent can reach the embryo through the mucous blanket of the maternal genital tract or by other means independent of the maternal blood system, the embryo will not be affected. Those agents—such as radiation—that are not delivered by the maternal blood supply will result in embryonic death if significant cell loss or chromosomal defects are produced. Countervailing these effects is the plasticity of omnipotential embryonic cells, which can mount a potent reparative response. If affected at all, the embryo will tend to either recover or die. This binary response has been referred to as the "all or none" phenomenon. This is not to say that malformations cannot occur in this period, only that there is a propensity toward embryolethality rather than surviving malformed embryos.

The second stage of development extends from roughly the third to the eighth week. This is the embryonic period when organogenesis occurs. During this stage, cells take on specific roles, grouping together to form organs at prescribed critical periods of formation.[9] Each organ, then, has a window of particular vulnerability to teratogenic insult.

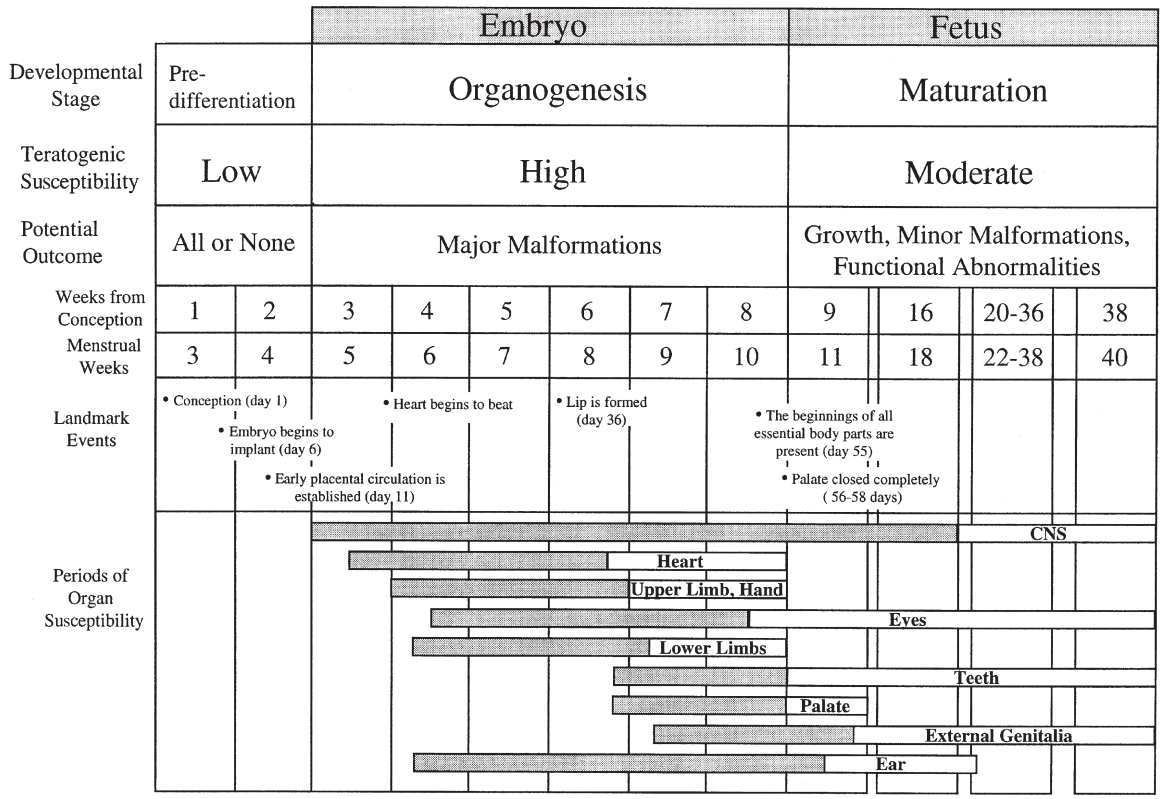

20–1 Human embryonic development. Periods of greatest sensitivity (shaded) and lesser sensitivity to malformation are shown for individual organs. (This chart is modified, from The causes of human congenital malformations. In: Moore KL, ed. The Developing Human: Clinically Oriented Embryology. 4th ed. Philadelphia: 1988:131–158; and Risks. In: Kelly-Buchanan C, ed. Peace of Mind during Pregnancy. Philadelphia: Dell; 1989:7–26)

Unfortunately, this period of greatest teratogenic susceptibility begins before most women know themselves to be pregnant, and sometimes even before the condition of pregnancy can be reliably ascertained.

The last stage of development, known as the fetal stage, begins after the ninth week of gestation. With the important exceptions of the genitourinary system, the palate, and the brain, most organs have formed and thereafter proceed to mature, function, and grow. Teratogenic insults during this period can lead to growth failure and eventual disturbances of behavior or fertility. Examples of behavioral teratogenicity include the hyperactivity, inattention, and tremulousness of children of narcotic-addicted mothers; the mental retardation of children of women exposed to anticonvulsants, alcohol, and lead; and the abnormal reflexes of children of mothers exposed to methyl mercury.[10]

3. *Teratogenic induction is a threshold phenomenon.*
A dosage threshold must be exceeded for irreparable damage to be done. This can occur either as a single large dose, or as repeated chronic exposure, and the interaction of two or more drugs or chemicals may be synergistic. Equally important, especially for the parents, is the inverse formulation of this principle: There is a level below which no embryopathic effects can be measured.[11] The concept of a placental barrier has been debunked as fallacious: Most drugs and chemicals readily reach the fetus in significant concentration soon after administration.[12]

4. *Typically, teratogens cause characteristic patterns of malformations rather than single defects.*
The final pattern of malformation represents not only the consequences of initial injury mediated through cell death and disruption of cell growth and metabolism, but also that of secondary reparative and regenerative processes. For example, the intraabdominal and intracranial calcifications characteristic of some viral infections represent a reparative response to initial injury.

Identifying Teratogens

Establishing the safety or risk of drugs is a daunting task fraught with many methodological problems. Even known teratogens do not affect the great majority of exposed fetuses because teratogenic effects are idiosyncratic and

mitigated by a wide range of genetic, environmental, developmental, and physiological factors.[13,14] Indeed, only a few of the most potent teratogens increase the background malformation rate by a factor of two or more.[13] To illustrate, if the background rate is 3%, then at least 220 exposed fetuses (and a similar number of nonexposed fetuses) would be needed to establish the risk of an agent that increases the malformation rate by a factor of 2.5, with a statistical power of 80%.[13] This is the level of teratogenicity seen only with the most severe and virulent agents, such as thalidomide and isotretinoin.

Teratogens are identified and characterized on the basis of case reports of individuals, epidemiological studies of populations, and controlled laboratory studies on animals. Clinical case reports serve to provide working hypotheses for the teratogenicity of an agent but cannot establish a quantitative index of risk. Case reports are rarely persuasive in themselves, except perhaps if the agent is a usually potent teratogen, few women have been exposed, and the consequent malformation is rare.[13] Such was the case with warfarin, diethylstilbestrol, and isotretinoin.[13] In most cases, however, the association of a congenital malformation and an environmental exposure is purely coincidental, especially if the exposure or the malformation is common. Such was the case with Bendectin and other drugs (**Table 20–1,** Exonerated drugs). An apparent association may result from the convergence of the baseline rate of malformations in the general population (estimated between 1 and 5%) and the widespread use of the agent.

Epidemiological studies are necessary to establish risk when the agent is widely used, the malformation is common, and the teratogenic potency of the drug is relatively weak. There are two types of epidemiological studies: case control and cohort. Case-control studies are retrospective: Investigators look backward into the histories of children with and without the malformation to determine if children with the malformation were more likely to have had an exposure. Cohort studies are prospective: Investigators look forward from records of exposure to rates of malformation. Retrospective studies can be skewed by recall or ascertainment biases. Prospective studies can be confounded by any number of incidental factors (such as the maternal illness that occasioned the exposure) if these factors are not distributed randomly between exposed and nonexposed groups.[15]

Though it is true that the results of animal studies cannot be extrapolated with certainty to humans, animal studies have proven invaluable in assessing developmental risks and preventing the catastrophic exposures in the human population.[13] Every true human teratogen has had parallel effects in animals, with two exceptions—thalidomide and misoprostol. In the case of isotretinoin, animal studies prevented a human disaster similar to that of thalidomide.[13] Indeed, controlled experimentation across a range of doses during the period of organogenesis can only be performed in animal models. Epidemiological studies alone are only conclusive once the agent has damaged many children. Still, caution is required in the interpretation of animal studies: dosages may be many times greater than those likely to occur in humans, and maternal toxicity may contribute to the observed effect. Further, teratogenic effects seen at high doses in animals may not be present at clinical dosage levels in humans (as is the case with benzodiazepines, salicylates, and glucocorticoids).

Meta-analyses combine similar studies to increase sample sizes. Such analyses, though, require that the combined studies be comparable in quality and methods, which may not always be the case. Further, there tend to be fewer studies in the literature that do not find an association because publication bias against negative studies leads to unbalanced reporting.

In the end, several conditions must be satisfied to establish the teratogenicity of an agent from available evidence. The evidence must be reproducible, consistent, and biologically plausible.[16] Epidemiological studies should be independent and demonstrate similar effects. Animal studies have greater credence if the exposure is

Table 20–1 Historical Recognition of Chemical Teratogenesis in Humans

Date Discovered	Drug	Approximate Number Cases Malformed
1903	Antithyroid compounds	140
1950	Aminoglycoside antibiotics	60
1952	Anticancer agents	50
1953	Androgenic hormones	250
1956	Tetracyclines	Thousands
1961	Thalidomide	7700
1963	Phenytoin	Hundreds
1965	Hypervitaminosis A	20
1966	Coumarin anticoagulants	55
1967	Alcohol	Thousands
1970	Methadione anticonvulsants	40
1970	Lithium	25
1970	Diethylstilbestrol	Hundreds
1971	Penicillamine	5
1976	Primidone	25
1982	Valproic acid	100
1983	Vitamin A analogues	115
1987	Cocaine	Hundreds
1988	Carbamazepine	70

Adapted from Turner GM, Twining P. The facial profile in the diagnosis of fetal abnormalities. Clin Radiol 1993;47:389–395 and from Schardein JL. Chemically Induced Birth Defects. 2nd ed. New York: Marcel Dekker; 1993:398641.

comparable in dose and route of exposure as in humans, and if the species is phylogenetically close to humans. And finally, the teratogenic effects must be biologically plausible: effects should be related to dose, timing during development, and presence at susceptible sites within the fetus.

Ultrasound Evaluation

The sonologist evaluating a patient with teratogen exposure will need to first assess the developmental risks of the exposure. This requires interviewing the patient to determine the agent, the dose, and the timing of the exposure. Specific agents tend to produce specific patterns of abnormality. Both the incidence and the severity of malformations tend to increase with the dose (**Table 20–1**). As stated earlier, timing is crucial. Teratogenic exposures in the first 2 weeks following conception are less likely to result in malformation in embryos that survive. Exposures occurring during the embryonic stage should be placed as precisely as possible in those critical 6 weeks so that the examination can be concentrated on those organs most susceptible to injury (**Fig. 20–1**).

Once risk is assessed, the sonologist will likely benefit from any of several information or consultative resources. Online databases provide perhaps the most current and readily accessible summaries of the medical literature and estimates of risk. Particularly valuable services are provided by the ReproTox system,[17] the Motherisk program (416–813–6780, www.motherisk, org), and the Organization of Teratogen Information Services (OTIS, 801–328–2229, http://orpheus.ucsd.edu/ctis). The OTIS Web site has very good fact sheets for many drugs that can be downloaded and printed in English, Spanish, and French, and which are written in accessible lay language.

Other useful electronic resources that can be accessed online are the Teratogen Information System (TERIS),[18] ReproRisk, and Shepards Catalog of Teratogenic Agents.[19] If an unusual abnormality or pattern of abnormalities is found in a fetus, possible etiologies can be found in such databases as POSSUM (Pictures of Standard Syndromes and Undiagnosed Malformations), Platypus, and the London Dysmorphology Database. Finally, there are several excellent books and review articles that list teratogens and their described effects, though these will be variably current.[20–25] Though dated, the book *Peace of Mind during Pregnancy* by Christine Kelley-Buchanan is particularly useful for counseling patients because it is written in direct and clear language that will be accessible to most patients.[26]

Ultimately, the sonographic study of a pregnancy with a known teratogenic exposure will need to be more comprehensive and meticulous than routine studies. In addition to the routine fetal survey, additional scrutiny will need to be directed to the face, calvarium, spine, heart, limbs, hands and feet, and genitalia, as well as to the measures of fetal growth, amniotic fluid volume, and placental function. Knowing the probable effects of a teratogen will help focus this rather formidable and extensive survey.

This said, one small study of 126 pregnancies studied by ultrasound for teratogen exposure found only one structural abnormality.[27] This study, however, made no accounting of the magnitude or the timing of the exposures and included a broad miscellany of agents, most of which contribute five or less episodes of exposure each. As discussed earlier, the likelihood that such a study would be able to identify the effects of even the most potent teratogen is extremely small. The value of this study is highly questionable, and its conclusions could be misleading.

Observed effects can be organized into four basic categories: malformation, growth retardation, death, and functional impairment.[4] Of these, growth disturbances are the most common and sensitive signs of exposure.[8]

Craniofacial anomalies can generally be depicted with routine imaging, though more subtle abnormalities may require morphometric analysis.[28] Standardized linear measurements have been proposed to describe the growth of normal craniofacial structures, including the mandible.[29–31] Even so, the morphometric approach has not been widely adopted in prenatal laboratories, partly due to the problem of obtaining reproducible planes of imaging and partly due to the inherent imprecision of the relatively small measurements. Nonetheless, these techniques have been well established in infants and children[32] and may yet prove to be transposable to the fetus.

Functional and neurobehavioral effects may be revealed in observations of fetal breathing, movement, behavior, and adaptability to stimulus. The agitated behavioral state of a cocaine-exposed fetus may be the only detectable abnormality. Choanal atresia in a coumarin-exposed fetus could theoretically be detected by an abnormal pattern of fetal breathing visible with color Doppler techniques. In cases of misoprostol exposure, Doppler techniques can demonstrate increased resistive indices in the uterine artery, an important indicator of compromise of the uteroplacental perfusion that is the presumed mechanism of fetopathy. Such observations test the limits of the capabilities, skills, and patience of the examiner. The success of the enterprise, however, will finally depend on the ability of the sonologist to make subtle and careful observations.

Classes of Teratogens

Pharmaceuticals

Despite the widespread recognition that drugs taken during pregnancy could affect the fetus, recent studies have shown that drug use during pregnancy is, in fact, increasing.[33] An average of 81% of pregnant women are exposed to

drugs sometime during their gestation, and the average number of drugs taken is approximately six.[34] Nonetheless, apart from exposures to established teratogens, the risk of a major fetal malformation following general maternal drug use is low: Case-control studies from large birth registries suggest an odds ratio of 1.2.[35]

The myth that the uterus is a privileged sanctuary for the fetus, largely impervious to the noxious agents of the maternal world, was shattered by the thalidomide catastrophe. To be sure, an association had already been reported between maternal rubella infection and severe fetal malformations as early as 1941, but the extreme vulnerability of the fetus to drugs and chemicals had not been widely suspected.[36–38] Indeed, essentially all drugs are transferred across the placenta to the fetus, with rare exception.[33] In subsequent years a broad spectrum of drugs have come under closer scrutiny. Even so, fewer than 30 drugs have been identified as human teratogens and many of these are no longer in clinical use (**Table 20–1**).[13] More recent entries to **Table 20–1** would include angiotensin-converting enzyme (ACE) inhibitors, angiotensin II receptor antagonists, fluconazole, systemic corticosteroids, misoprostol, and methimazole.[39]

It is equally important to recognize that several drugs had been initially identified as teratogens, but were subsequently shown not to be in larger and better-controlled studies.[13] These include diazepam (Valium) (reported to cause oral clefts); oral contraceptives (pseudohermaphroditism, various malformations in the VACTERL spectrum); spermicides (limb defects, tumors, hypospadius); salicylates (cleft palate, congenital heart disease); and Bendectin (cardiac and limb defects).[13]

Thalidomide

Once a popular tranquilizer outside the United States, thalidomide damaged an estimated 7700 children before its teratogenic effects were discovered.[40,41] Malformations occur in roughly 20% of exposed fetuses and include limb reduction defects, esophageal and duodenal atresia, tetralogy of Fallot, renal agenesis, facial hemangiomata, and anomalies of the external ear (**Fig. 20–2**). Following the catastrophe, the use of thalidomide as a sedative ended in the 1960s, but has been recently reinstituted in clinical practice for the treatment for leprosy and multiple myeloma. The drug is also being studied for use with several malignant diseases, such as myelofibrosis, renal cell cancer, prostate cancer, and Kaposi sarcoma.[42]

Angiotensin-Converting Enzyme Inhibitors and Angiotensin II Receptor Antagonists

Used for the treatment of hypertension, these drugs act on the renin-angiotensin system by different mechanisms to reduce angiotensin II production. Angiotensin II, though, is also a growth factor for the fetal kidney and is important for nephrogenesis.[15] These drugs do not appear to have teratogenic effects in the first trimester of pregnancy, but have been associated with renal dysgenesis, fetal oliguria (and oligohydramnios), skull defects, fetal growth restriction, and death when the fetus is exposed in the second and third trimesters[43,44] (**Fig. 20–3**). It has been suggested that hypotension is an important mechanism for the malformations.[45] Serial fetal sonograms for amniotic fluid volume and fetal growth are indicated for exposures later in pregnancy.

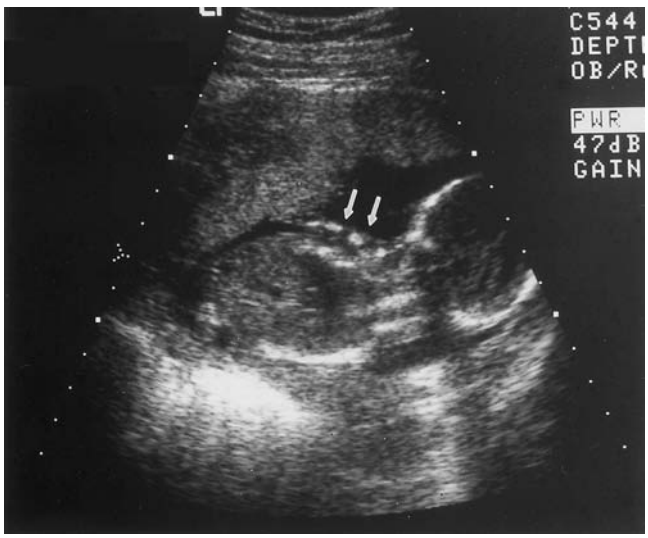

Figure 20–2 Phocomelia and micromelia. The upper limb of this fetus (arrows) is markedly short with complete or partial absence of individual bones. Such an abnormality was found in babies of mothers who had taken the sedative thalidomide. Though no longer used as a sedative, this drug is being reintroduced as a treatment for skin disease.

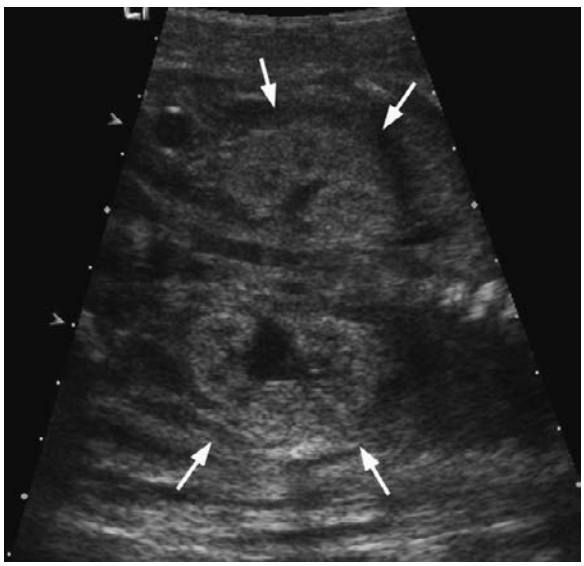

Figure 20–3 Renal dysgenesis. Echogenic and dysmorphic kidneys (arrows) are a feature of angiotensin-converting enzyme inhibitors and angiotensin II receptor antagonists, when exposure occurs in the second or third trimester.

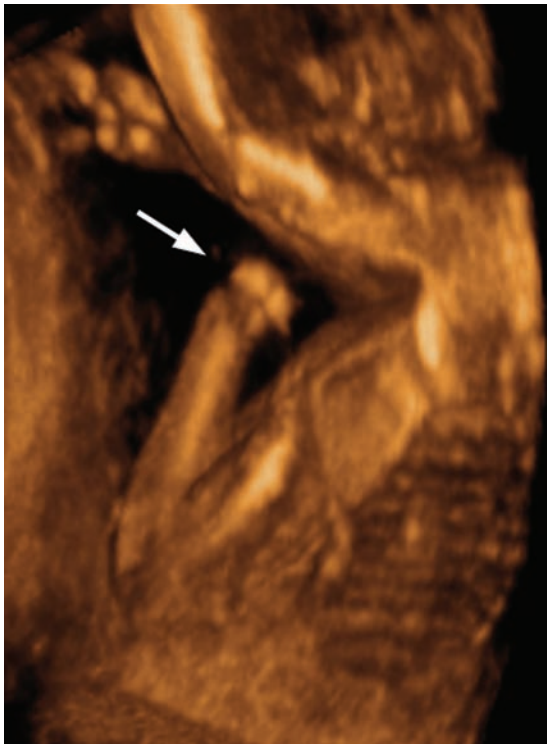

A

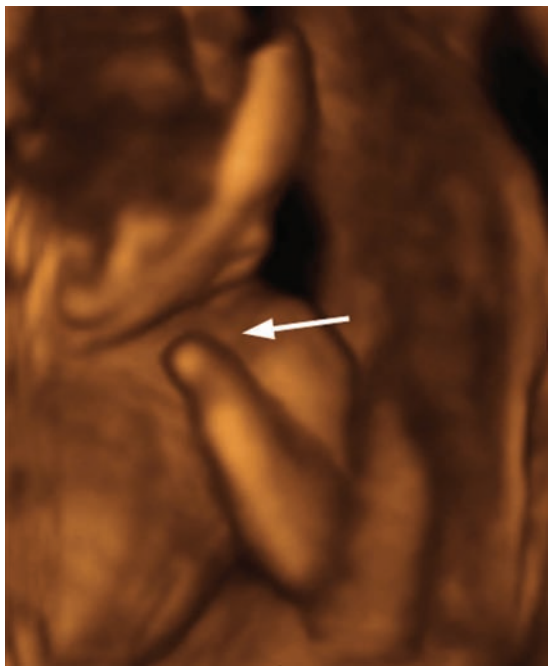

B

Figure 20–4 (A,B) Terminal transverse defect in the upper limb (arrow). Limb defects can be the result of dysmorphogenesis (thalidomide, warfarin, phenytoin), or vascular disruption of the limb that had formed normally (misoprostol, chorionic villus sampling). (Courtesy of Carol B. Benson, M.D., Boston, MA)

Misoprostol

When used in the treatment of peptic ulcer disease, misoprostol (a prostaglandin E1 analog) was found to also cause endometrial bleeding.[46] This led eventually to its use as an abortifacient in Brazil, where abortion is illegal and prescription drugs can be purchased over the counter. This confluence of factors led to the widespread popularity of the drug: fully 11% of women delivering in Rio de Janeiro in 1993 had used misoprostol in attempts to end their pregnancies.[46] Unfortunately, misoprostol alone will induce abortion in only 11 to 20% of cases, which resulted in a large number of exposed fetuses.[47] Though the frequency of malformation has not been established prospectively, one retrospective case-control study found an odds ratio of 29.7 (95% CI 11.6 to 76.0) comparing mothers who had used misoprostol in the first trimester to mothers who had given birth to infants with spina bifida.[48]

Misoprostol causes intense uterine contractions followed by bleeding.[49] This is postulated to lead to hypoperfusion of the fetus, and ischemia and infarction in tenuously perfused areas served by end arteries (limbs, brain stem, spinal cord, intestine, tongue). The resulting vascular disruption defects include cranial nerve hypoplasia and terminal transverse defects in the arms and legs (and other limb abnormalities) (**Fig. 20–4A,B).** This combination of abnormalities has been referred to as the Mobius sequence.[46,48]

Teratogen-induced limb defects, therefore, can be either the result of limb dysmorphogenesis (thalidomide, warfarin, phenytoin), or vascular disruption of a limb that had formed normally [misoprostol, chorionic villus sampling (CVS)].[46] The pathogenic hypothesis for misoprostol is supported by Doppler ultrasound studies showing an increase in the resistive indices of the uterine arteries in women taking misoprostol.[50]

Thyroid Agents

Antithyroid agents such as iodine-131 readily cross the placental membrane and are taken up by the fetal thyroid with an avidity that exceeds even that of the mother.[51] Methimazole, carbimazole, and propythiouracil (PTU) can cause fetal goiter and hypothyroidism if used after 10 weeks gestation when the fetal thyroid begins to concentrate iodide, though there is usually a return to the euthyroid state within days or weeks after birth.[52] The risk is probably minimal with methimazole and carbimazole and small with PTU. Prenatal ultrasound evaluation for fetal thyroid enlargement is indicated. Both methimazole and carcimazole have been associated with scalp defects (aplasia cutis), and therefore PTU is currently the drug of choice during pregnancy.[52]

Thyroid replacement agents, by distinction, are predominantly protein bound and, therefore, do not readily

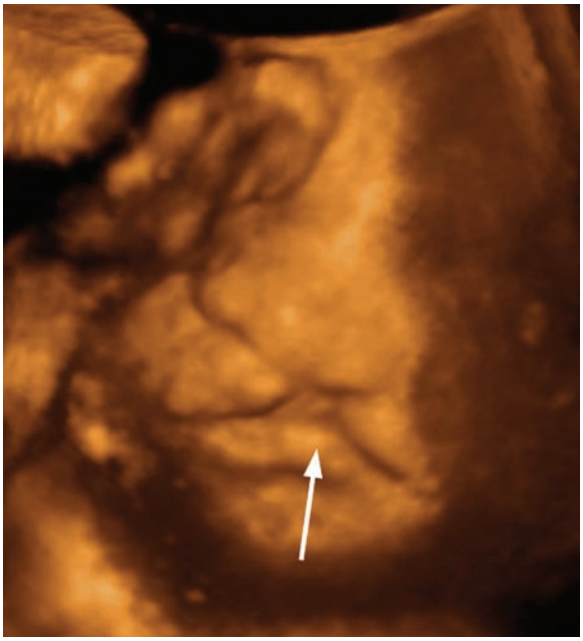

Figure 20–5 Cleft lip and palate. A complete unilateral defect (arrow) is seen in this modified coronal view. This finding can be found following exposure to hydantoins, valproic acid, trimethadione, retinoids, cyclophosphamide, ethanol, cocaine, glucocorticoids, and hyperthermia. (Courtesy of Carol B. Benson, M.D., Boston, MA)

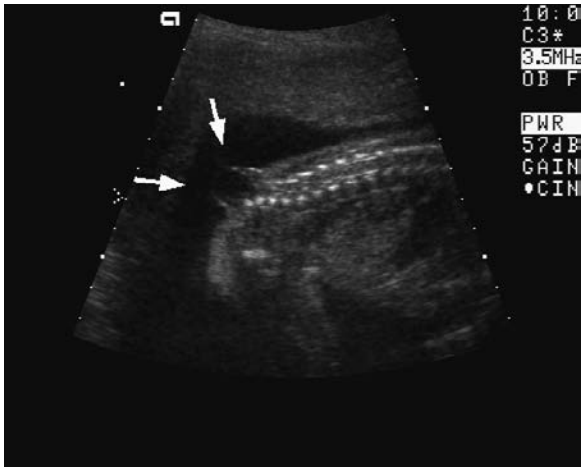

Figure 20–6 Neural tube defect. Spinal dysraphism and a meningomyelocele (arrows) is demonstrated in this fetus. This abnormality is a prominent feature of embryopathy resulting from valproic acid, carbamazepine, methotrexate, lithium, ethanol, and hyperthermia.

cross the placenta.[53] These agents are considered to have a low teratogenic potential.

Anticonvulsants

The rate of congenital malformation is increased 2 to 3 times for epileptics receiving anticonvulsant therapy over nonepileptics or epileptics who were not medicated.[54,55] Anticonvulsant therapy has been particularly implicated in the induction of cleft lip–cleft palate, and congenital heart disease (**Fig. 20–5**). More specific patterns of malformation have been attributed to five anticonvulsant drugs: phenytoin, trimethadione, valproic acid, primidone, and carbamazepine. The syndrome associated with hydantoins, such as Dilantin, is manifest by characteristic craniofacial features, which include hypertelorism and depressed nasal bridge, limb anomalies, such as digital and nail hypoplasia, and growth retardation. Many of these abnormalities are subtle, and at least one study indicated that sonograms at 18 to 20 weeks are unlikely to reveal the structural defects associated with this drug.[56]

Those abnormalities associated with valproic acid, however, have been described in the ultrasound literature. Specifically, these include lumbar meningomyelocele (1 to 2% incidence) and radial ray limb defects (**Fig. 20–6**).[57–59] Similar phenotypic changes are seen with primidone, phenobarbital, and carbamazepine (Tegretol). Some recent studies have suggested that valproic acid exposure in vitro is also associated with lower verbal IQ scores, though this is as yet unsubstantiated.[60] Trimethadione is the most potent teratogen of the anticonvulsant group. The trimethadione syndrome is manifested by intrauterine growth retardation, microcephaly, cardiac anomalies, renal malformations, and mental retardation.[61] The increased teratogenic risk estimates for anticonvulsants are 69 to 80% for trimethadione exposure, 6% for phenobarbital and hydantoin exposure, and ~1% for valproic acid.

Anticoagulants

Coumarin anticoagulants, such as warfarin, produce characteristic teratological abnormalities of the skeleton in ~10% of those fetuses exposed during the critical sixth to ninth weeks of gestation.[14] The most frequent abnormalities found in babies are stippled epiphyses, shortened fingers, and nasal hypoplasia (**Fig. 20–7A–C**). Stippled epiphyses are difficult to demonstrate prenatally by ultrasound, although one report does purport to depict this finding in a 22-week fetus with Conradi-Hünermann syndrome.[62] Brachydactyly with disordered chondrogenesis has been described in a case report of a 17-week abortus[63] and so may also be detectable with prenatal ultrasound. The nasal hypoplasia may be severe and associated with choanal atresia. Coumarin can cause intrauterine growth retardation and central nervous system (CNS) abnormalities such as microcephaly, Dandy-Walker malformation, eye defects, and agenesis of the corpus callosum.[64] Developmental retardation has been associated with second- and third-trimester exposure. In a small number of cases, congenital heart disease has been described.

Both the nasal hypoplasia and the stippled epiphyses likely result from disordered chondrogenesis rather than

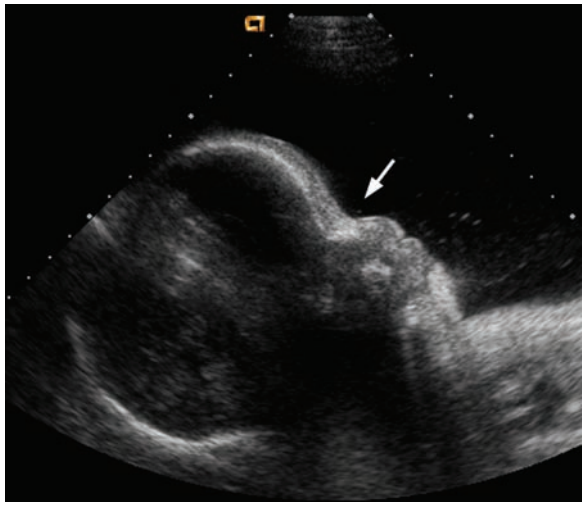

A

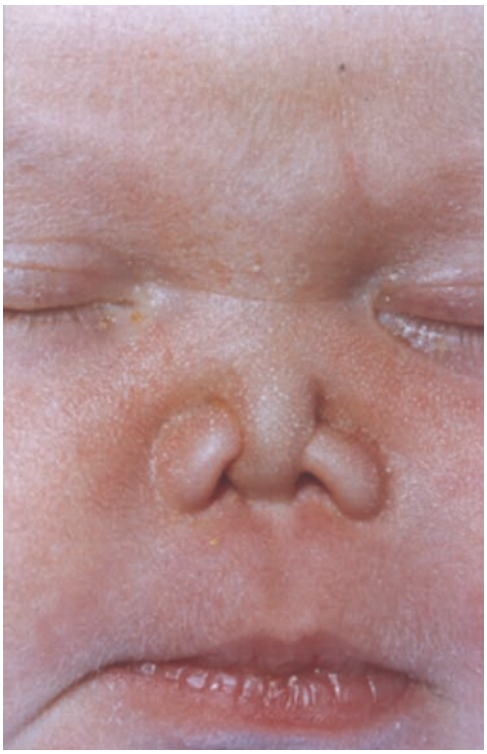

B

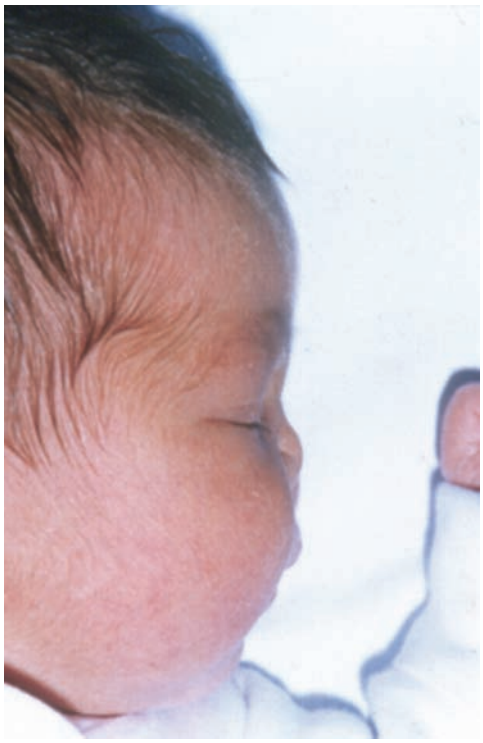

C

Figure 20–7 Midface hypoplasia in warfarin exposure. Nasal hypoplasia is a salient feature of exposure to coumarin anticoagulants in the first trimester. This malformation is thought to result from disordered chondrogenesis. **(A)** The depression of the midface (arrow) is seen in the prenatal sonogram at 32 weeks. **(B,C)** Postnatal images clearly demonstrate the dysmorphic features. (Courtesy of David Nyberg, M.D.)

hemorrha.[65,66] The CNS defects are probably caused by microhemorrhages in the developing tissues, although one case report does suggest a direct effect of warfarin on the developing CNS.[67] For the critical first-trimester period, many authorities recommend using heparin, which does not cross the placenta, as an alternative to warfarin.[68]

Vitamin A Congeners

Retinoids are among the most potent teratogens on the market. Used primarily in the treatment of severe acne and psoriasis, these vitamin A congeners carry an ~25% relative risk of malformation among fetuses that survive to 20 weeks of gestation following maternal exposure to therapeutic doses.[69] These malformations include craniofacial defects (small malformed ears, mandibular and midfacial underdevelopment, and wide palatal clefts), cardiovascular malformations (especially conotruncal defects, transposition of the great vessels, tetralogy of Fallot, ventricular septal defects (VSDs), and aortic arch abnormality), and central nervous defects (hydrocephalus and absence of the cerebellar vermis).

For some of the retinoids, it is unclear how long a couple should wait after termination of therapy to attempt pregnancy. One retinoid drug in particular, etretinate, is extremely lipophilic and can be stored in body fat and

produce measurable blood levels up to 1 year after cessation of treatment. Indeed, several cases of malformation have been reported in infants whose mothers discontinued etretinate treatment 7 to 12 months before their conceptions.[70] Other agents, such as isotretinoin, are effectively eliminated within a month.[71] Vitamin A itself has much less teratogenic potential, although hydronephrosis, hemifacial micromelia, microhydrocephaly, and partial sirenomelia have been described after massive doses.[72,73]

Anticancer Agents

Cyclophosphamide and other alkylating cancer therapeutic agents carry an estimated risk of malformation of one in every three exposures.[74] With first-trimester exposure, these malformations are typically skeletal and palate defects, as well as malformations of the limbs and eyes.[75] Exposure in the second and third trimesters is associated with a much smaller risk of malformation, though growth retardation and pancytopenia have been described.[76] Other alkylating agents, such as busulfan and chlorambucil, also produce malformations, but these more often cause abnormalities of the kidneys, ureters, and CNS closure.

Lithium

Lithium is the most controversial entry on the list of known teratogens. This drug has been associated with congenital heart disease, and in particular the rare Ebstein's anomaly (**Fig. 20–8**).[77–79] Although the true risk of congenital heart disease is unresolved, the repeated observation of heart defects appears to be more than coincidental. Although a 7 to 8% incidence has been cited, many believe a 1 to 5% range is more realistic.[17,80–82] More recent studies support a 1% or less risk estimate.[83] The issue is confounded by lack of a control population, the likely overreporting of abnormal cases, the prevalence of drug use and heavy smoking in this population, and a possible increased background risk of perinatal death and heart disease in the offspring of women with bipolar illness regardless of drug therapy. Second-trimester sonographic screening and fetal echocardiography have been recommended for any woman exposed to lithium in early pregnancy.[84,85] Exposures near term have been associated with neonatal cyanosis, hypotonia, cardiac dysrhythmia, diabetes insipidus, and hypothyroidism. The small reported risk of teratogenesis must be weighed against the potentially life-threatening consequences of recurrent material bipolar disease. This recurrence rate is ~50% following discontinuation of lithium therapy.[83]

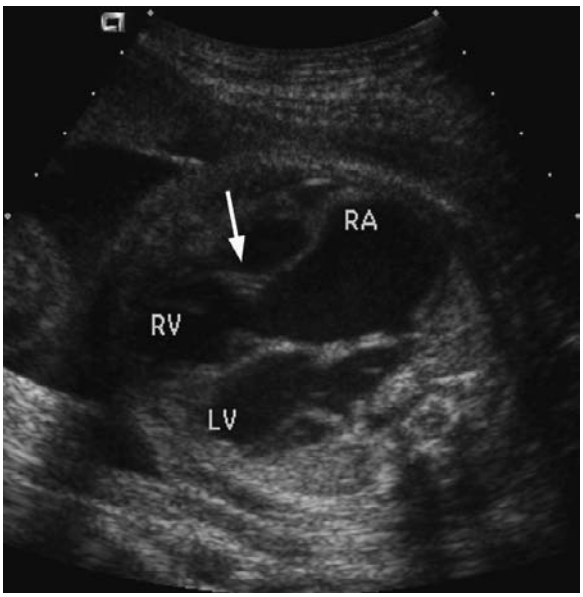

Figure 20–8 Ebstein's anomaly. This rare cardiovascular anomaly is characterized by displacement of the tricuspid valve into the right ventricle (arrow), creating a large right atrium (RA), a small right ventricle (RV), and right ventricular outflow obstruction. This anomaly has been reported in an unusually large number of lithium-exposed fetuses. LV, left ventricle. (Courtesy of Carol B. Benson, M.D., Boston, MA)

Tetracycline

Tetracycline has never been convincingly associated with major birth defects. Only minor defects have been described with consistency, the most common being discoloration of developing teeth. At high doses, there has been depression of skeletal bone growth, particularly the fibula, and hypoplasia of tooth enamel.[86] Case reports of limb reduction defects have not been supported by epidemiological or animal studies.

Hormones

Progestins and Estrogens

Exposure to progestins and estrogens usually results from the continued use of birth control pills following conception by women unaware that they are pregnant.[87] Alternatively, women are sometimes exposed to these hormones as treatment for threatened abortion in the first trimester. Early retrospective studies proposed an association between exposure to female sex hormones and abnormalities such as cardiovascular defects (particularly transposition of the great vessels), limb reduction defects, the VACTERL syndrome, and malformations of the external genitalia.[88] These studies were, however, limited retrospective studies with small sample sizes. In many reported cases, exposure occurred outside of the critical period of organ formation. Most authorities now believe that progesterones and progesterone–estrogen combinations represent an ~1% risk of clitoral hypertrophy in females, and that exposure during the 8th to 10th week of gestation is required for the effect.[89,90] There does not seem to be an increased incidence of hypospadias in male fetuses exposed to progestin, as once reported.[91] It is presumed that the

clitoromegaly results from the conversion of progestins to androgens in the mother and unborn baby.

Diethylstilbestrol

Diethylstilbestrol (DES) was widely prescribed before 1971 in the United States to prevent miscarriage, premature delivery, and other pregnancy complications. In utero exposure to DES has been associated with subsequent development of vaginal adenosis and carcinoma in young women of DES-exposed mothers. This association is an important example of the potential long-term and delayed effects of drugs given during pregnancy.[15] Further, these daughters have also been found to have increased incidence of premature deliveries associated with increased perinatal mortality.[89] Abnormal morphology of the uterus, the "T-shaped appearance," as well as other uterine lesions have been described in this population. Detection of abnormalities in utero, however, has not been described. At least 25% of women with first-trimester DES exposure develop genital tract anomalies, including vaginal adenosis, cervical malformations, vaginal septae, uterine cavity anomalies, and fallopian tube anomalies.[92] A parallel increase in male urogenital abnormalities has not been substantiated, though microphallus, cryptorchidism, and hypoplastic testes have been reported.[93] More recently, reports of potential transgenerational effects of DES have included an increased rate of hypospadius in sons of mothers who had had in utero exposure[94]; a third-generation case of vaginal adenocarcinoma[95]; and increased neurological injury to children of affected mothers.[96]

Glucocorticoids

Systemic corticosteroids (cortisone, prednosalone, prednisone) have been implicated in the causation of cleft lip or palate in animals and humans since the 1960s (**Fig. 20–5**). The increased risk in humans, however, seems to be so low that it has been difficult to substantiate above a background malformation rate of 3%.[83,97] Studies have produced widely disparate results. A recent meta-analysis has demonstrated a small, but statistically significant association with first-trimester exposures.[98] These authors estimate an increase of only one or two cases of oral clefts per 1000 treated women. Many authorities advise, therefore, that the benefits to the mother in certain circumstances far outweigh the risks.[83,99] This is undoubtedly true after 12 weeks gestation, the fetal age when the palate formation is complete. Screening ultrasound is often able to detect clefting prenatally and is indicated in mothers on systemic steroids. No effect has been attributed to topical or inhaled steroids, presumably because the systemic dose is so low.[97]

Alcohol and Recreational Drugs

Alcohol and recreational drugs are the most significant developmental toxicants of the modern day.

Alcohol

Alcohol consumption during pregnancy is the most frequent cause of mental retardation in the Western world.[100] Alcohol teratogenicity produces CNS dysfunction, prenatal and postnatal growth retardation, characteristic craniofacial abnormalities, and a variable number of major and minor malformations.[101–103] Described CNS abnormalities include microcephaly, hydrocephaly, neural tube defects, and holoprosencephaly (**Fig. 20–9A–D**). Facial features include midface hypoplasia, hypoplastic maxilla, micrognathia, cleft palate and lip, as well as short upturned nose, short palpebral fissures, thin upper lip, and flat philtrum. Other associated malformations include cardiac defects [VSD, atrial septal defect (ASD), great vessel anomalies, and tetralogy of Fallot], hydronephrosis, small kidneys, scoliosis, radial ulnar synostosis, polydactyly, hypoplastic external genitalia, and hernias of the diaphragm, umbilicus, or groin. Though the kidneys of ethanol-exposed infants are significantly smaller than normal controls, the prevalence of structural malformation may not be increased in the exposed group.[104]

Although only ~4% of women who drink will have a child that meets the criteria for fetal alcohol syndrome, it is clear that prenatal exposure to alcohol can produce severe brain damage and neurobehavioral dysfunction, even without facial dysmorphism.[105] Currently, the wider range of deleterious outcomes following alcohol exposure is called fetal alcohol spectrum disorder. Recent studies indicate that heavy maternal alcohol consumption is associated within 40% risk of fetal brain damage.[15] Binge drinking seems to be particularly dangerous for long-term behavioral and cognitive deficits.[83]

Prenatal detection of ethanol effects is often difficult, with subtle features appearing only late in pregnancy.[24] Quantitative characterization of the craniofacial dysmorphism has been reported in a nonblinded study of three fetuses at 16, 19, and 24 weeks of gestation.[106] These results have not been corroborated in all laboratories. Even so, there is no clear dosage threshold or period of susceptibility yet defined: The brain is both the first organ to begin development and the last organ to complete it, and it therefore remains vulnerable throughout gestation. With no safe dose threshold, most authorities now advocate total abstinence from ethanol during pregnancy.

Cocaine

Cocaine use during pregnancy is a serious public health problem: An estimated 10 to 15% of pregnant women in Western countries use cocaine. Although it is clear that cocaine is a significant developmental toxicant, the teratogenic potential of the drug is difficult to characterize. In part, it is because fetuses of cocaine-abusing mothers are also exposed to the potentially deleterious effects of malnutrition, polydrug abuse, and inadequate prenatal care.[107]

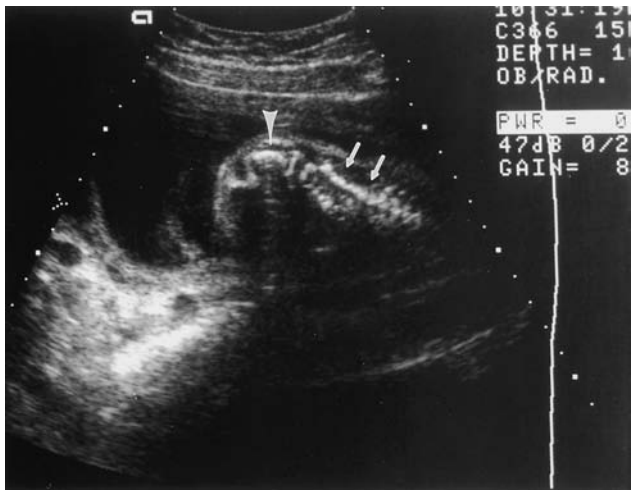

A

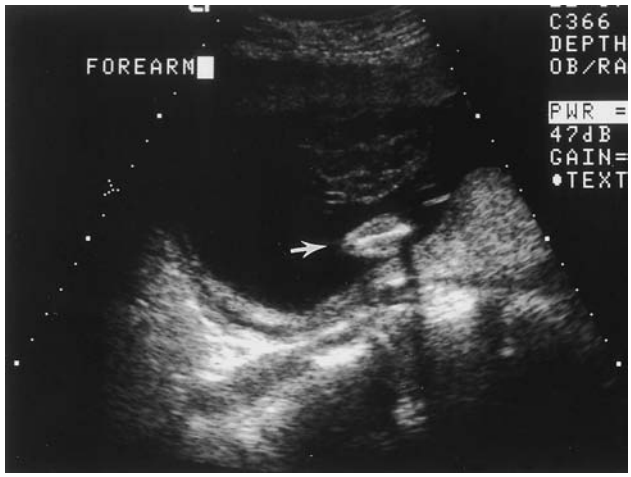

B

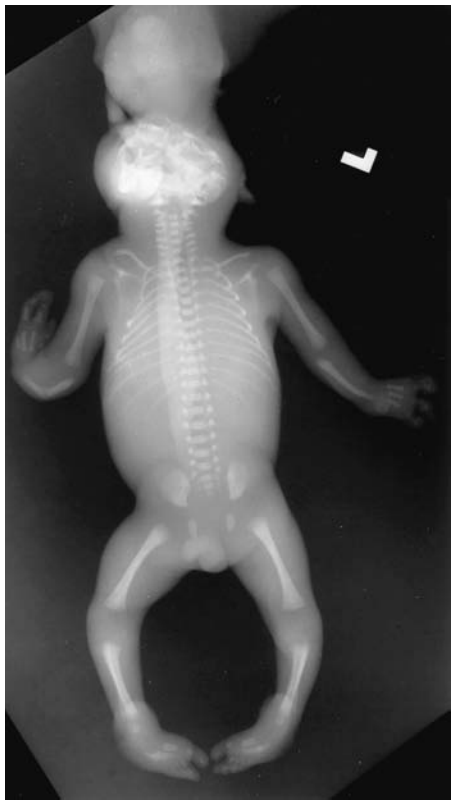

C

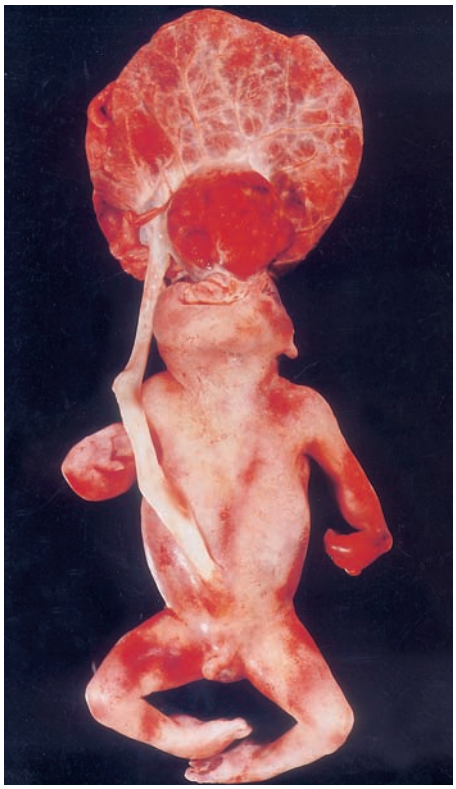

D

Figure 20–9 Ethanol exposure. The mother of this fetus was a chronic alcoholic who admitted to daily alcohol consumption. **(A)** Prenatal ultrasound demonstrated an intact cervical spine (arrows) and occiput (arrowhead), but absent anterior calvaria. Facial features could not be discerned. Disorganized neural tissue was seen arising above the expected level of the orbits. **(B)** Sonographic depictions of the forearms revealed only one bone (arrow) on each side. Abnormal hands and feet were seen on other views. **(C)** Postnatal radiography of the abortus demonstrates a large defect extending from the face to the cranium (faciocranioschisis), bilateral radial aplasia, ulnar bowing, bilateral ectrodactyly, and bilateral club feet. **(D)** Photograph of the abortus shows the extruded neural tissue from the head, which adheres to the placenta. (Courtesy of Martha Decker-Phillips, M.D.)

In addition, malformations resulting from cocaine abuse vary too widely between patients to constitute a recognized syndrome. Some studies have found a 15 to 20% incidence of congenital abnormalities in cocaine-abusing populations, and all such pregnancies are at increased risk of spontaneous abortion, stillbirth, premature rupture of membranes, placental abruption, premature labor and delivery, and intrauterine growth retardation.[108–110]

The teratogenic actions of cocaine likely stem from its physiological effects, specifically vasoconstriction, transient hypertension, and vascular disruption.[111] Cocaine use has been associated with reduction or disruption of blood

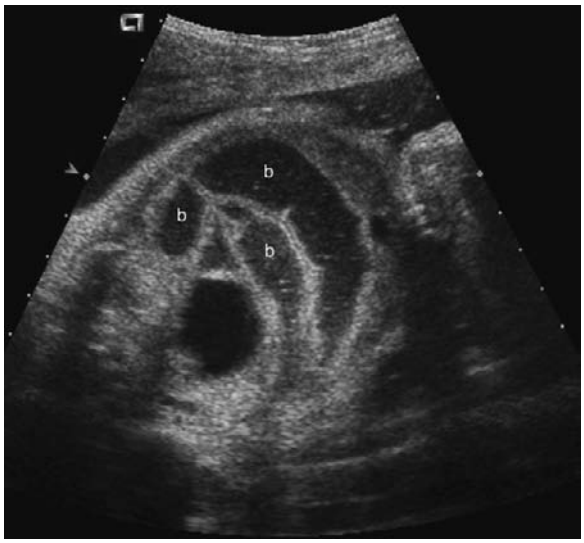

Figure 20–10 Dilated loops of bowel (b) in the fetal abdomen. Intestinal perforation, obstruction, and atresia are features found in the fetuses of cocaine-abusing mothers. Vascular disruption is presumed to cause ischemic and infarctive bowel injury in these fetuses.

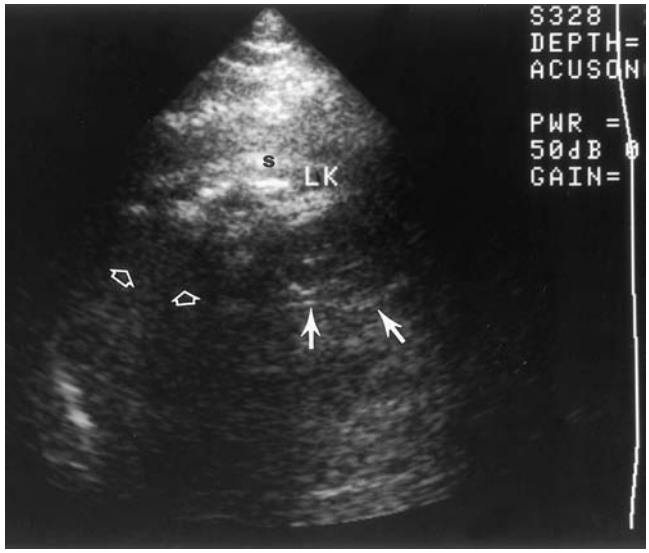

Figure 20–11 Renal agenesis. The left kidney is present (arrows), but the right is absent (open arrows) on this axial image with the spine (S) up. Malformations of the urinary tract, such as this, have been convincingly shown to have an increased incidence in fetuses exposed to cocaine. The urological abnormalities, however, are wide ranging and include malformation, infarction, and obstruction.

to the placenta, uterus, and fetus, making generalized intrauterine growth retardation a logical consequence. Specific malformations are multifarious and wide ranging, but can be broadly categorized as cranial defects (exencephaly, encephalocele, parietal bone defects); limb reduction defects; intestinal perforation, obstruction, or atresia; urogenital abnormalities; and cerebral infarction (**Fig. 20–10**, **Fig. 20–11**, **Fig. 20–12**).[17]

Neurosonographic studies on neonates have demonstrated subependymal germinal matrix cysts,[112,113] and prenatal studies have demonstrated choroid plexus cysts.[111] These cysts may represent focal ischemia or hemorrhage. The incidence of abnormality on postnatal neurosonographic studies varies between studies and may be quite low.[114] Heart abnormalities include transposition of the great vessels and hypoplastic right heart syndrome. The increased incidence of malformations of the urinary tract is perhaps the most convincingly demonstrated manifestation of exposure: The estimated risk is approximately four times that for the control.[115,116] Such urological abnormalities include hydronephrosis, renal infarction, crossed fused ectopic, prune belly syndrome, renal and ureteral agenesis, and hypospadius (**Fig. 20–10**). Cocaine also produces neurobehavioral disturbances, such as hypertomia

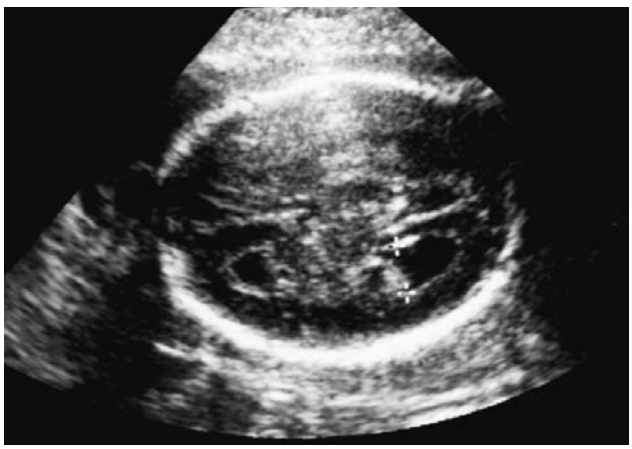

A

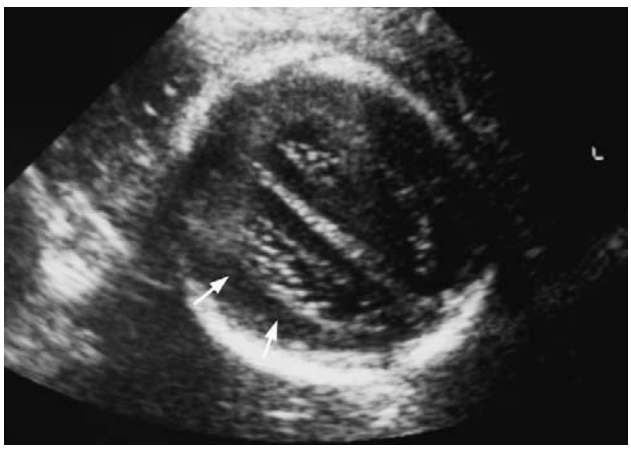

B

Figure 20–12 Cerebral infarction and periventricular leukomalacia in a cocaine-exposed fetus. Cocaine is believed to cause vascular disruption anomalies throughout the body. **(A)** In the brain, this can be manifest as ventriculomegaly and **(B)** abnormal increased echogenicity of the white matter tracks (arrows). (Courtesy of Carol B. Benson, M.D., Boston, MA)

and irritability, evidence for which has been seen even on prenatal ultrasound.[15,117]

Recreational Drugs

Toluene inhalation produces a pattern of congenital abnormality similar to fetal alcohol syndrome (microcephaly, CNS dysfunction, intrauterine growth restriction, craniofacial anomalies).[14] By distinction, teratogenicity has never been conclusively demonstrated for marijuana, heroin, opium, or lysergic acid diethylamide (LSD). To be sure, LSD use has been associated with limb defects, ocular defects, and CNS abnormalities. Heroin use has been associated with fetal growth retardation and neonatal withdrawal symptoms, but as yet no discernible pattern of defects has been identified.[118] Likewise, impaired fetal growth has been associated with marijuana, although this effect is difficult to substantiate when the confounding effects of social status and concurrent alcohol and drug use are considered. The growth impairment with marijuana use is comparable to that seen with cigarette smoking. Cigarette smoking itself is also associated with miscarriages, abnormal placentation, facial clefts, and clubfoot deformities.[83] The risks for oral clefts and foot abnormalities seem to be quite small, although recent studies have indicated that the incidence of these abnormalities is increased with particular genetic variants and familial susceptibilities.[83,119]

Obstetrical Intervention and Procedures

Methotrexate

Methotrexate is used to terminate ectopic pregnancies and induce abortions because of its toxicity to embryonic and trophoblastic tissues. If used inappropriately, an intrauterine embryo may be exposed during the critical period of 6 to 8 weeks after fertilization. If the embryo survives, a broad range of serious malformations can be found. These include malformations of the skull, such as sutural synostosis, defective ossification of the calvarium, micrognathia, brachycephaly, and a "clover leaf" configuration. Abnormalities of the CNS have included anencephaly, hydrocephaly, meningomyelocele, and cerebral hypoplasia. Ocular hypertelorism and a wide nasal bridge, and limb deformities such as syndactyly, talipes equinovarus, and mesomelic shortening of the forearms have been seen in several infants.[120,121] Growth retardation was also a feature of the few cases that have been reported to date. To be sure, several normal pregnancies have been reported after methotrexate and aminopterin exposure.

Much of what is known about the teratogenicity of methotrexate has been derived from case reports of mothers undergoing cancer treatment. A folic acid antagonist, methotrexate interferes with the replication of nucleic acid and consequently prevents the division and multiplication of cells. Aminopterin, a drug closely related to methotrexate, was at one time used in the first trimester for the purpose of inducing abortion. The anomalies identified in the abortuses and in the surviving babies represent one of the very few teratogenic experiments performed in humans.

Chorionic Villus Sampling and Amniocentesis

CVS, a technique of first-trimester genetic diagnosis, has been implicated in the production of limb defects. This association was suggested by population studies and CVS registries in which an unexpected number of mothers who had had a CVS gave birth to babies with transverse limb reduction defects and oromandibular–limb reduction hypogenesis syndrome, a syndrome characterized by limb deficiency, hypoglossia, and micrognathia.[122,123] Other studies have suggested an association with intestinal atresia, gastroschisis, and clubfoot.[124] This association is controversial and not corroborated by all studies.[125] Most investigators now believe that the risk, if real, is small (estimated at 1/1000 to 1/3000 births), and may be related to the technique and timing of the procedure. There is no convincing evidence for an increase in limb reduction defects following CVS when performed at 10 weeks of gestation or later, but there may be for procedures performed earlier than 10 weeks.[126,127] The proposed etiology of these malformations is vascular disruption and may be the result of embolization of trophoblastic tissue from the placenta to the fetus, resulting in ischemic or infarctive injury.[124] Other proposed mechanisms suggest that the function of the placenta is compromised, or that the release of vasoactive placental angiotensin initiates the fetal injury.

Amniocentesis performed before 13-weeks gestation has been associated with an increased risk of talipes equinovarus (club foot).[128,129] No added risk of fetal malformation has been shown when the procedure is performed at 15 weeks or later,[14] although there are case reports of limb malformation presumably due to direct injury by the amniocentesis needle itself.[46]

Radiation and Heat

Radiation

More than any single issue in teratology, misunderstanding of the risks of radiation exposure to the developing embryo and fetus has caused excessive and unnecessary anxiety.[26] A recent study demonstrated that family physicians and obstetricians tend to grossly overestimate the risks of diagnostic levels of radiation.[130] Radiation is certainly one of the best known and earliest recognized teratogens, but the effects of radiation have been documented in pregnant women who have received large amounts of ionizing radiation either as therapy for cervical cancer or as atomic bomb survivors. The principle effects include microcephaly, intrauterine growth retardation,

mental retardation, and eye malformations, but spina bifida cystica, cleft palate, and skeletal and visceral abnormalities have also been described. Studies indicate that microcephaly and mental retardation are associated with doses of 50 rad or greater, and no morphological abnormality has been substantiated in a fetus that has not exhibited growth retardation or a CNS abnormality. Radiation effects are clearly dose related: radiation risks to the embryo are negligible at doses of 5 rad or less, which is well within the range of typical exposures from diagnostic x-ray studies.[131] There is no proof that human congenital malformations have ever been caused by diagnostic levels of radiation.[132,133]

Hyperthermia

Hyperthermia was the first teratogen found to cause malformations in both animals and humans.[134] Defined as a core body temperature of at least 102°F (38.9°C), hyperthermia causes a range of effects from fetal loss to major malformation, but these effects are strongly dependent on the dose (≥ 38.9°C) and timing (first trimester). Although the brain is especially sensitive, epidemiological studies have also suggested an increase in abdominal wall defects, cardiovascular malformations (ASDs, hypoplastic left heart), and neural tube defects.[17] Exposures between 14 and 28 days after conception are thought to pose an increased risk for neural tube defects (spina bifida and anencephaly). From 4 to 14 weeks of pregnancy, there is an increased risk of mental retardation, hypotonia, and facial defects (cleft lip and palate, external ear abnormalities, and midface hypoplasia).[135] To be sure, considerable controversy exists surrounding the teratogenic affects of hyperthermia.[136] In most cases where birth defects have been reported, the mother had had a high fever that persisted for days. Potential confounding factors in this setting include the illness or infectious agent itself, poor maternal nutrition, and drugs and treatments the mother might use.[136]

Theoretical risks exist for heat exposures in hot tubs and saunas, although it has been suggested that a mother would find the hot tub or sauna intolerable before her temperature reached 102°F. Other studies have found the subjective assessment of overheating to be highly variable and cast doubt on whether all women feel uncomfortably hot at core temperatures exceeding 39°C.[134,137,138]

Infection

The collection of infectious agents into the TORCH acronym (toxoplasmosis–other–rubella–cytomegalovirus–herpes simplex virus) is convenient, but misleading. Certainly there is no recognizable TORCH syndrome per se, inasmuch as that implies a single entity, pattern of malformation, or clinical presentation. The types and frequencies of abnormalities vary from one agent to the next.[139]

Rubella

Rubella is a very efficient teratogen. The 1941 report that linked German measles to birth defects was the first to attribute congenital malformations in the human to an exogenous environmental agent.[36] Rubella infection causes detectable defects in 85% of fetuses for exposures in the first 8 weeks, 52% between 9 and 12 weeks, and 16% between 13 and 20 weeks. The consequences of infection tend to be severe: death, cardiac malformation (pulmonary artery stenosis, patent ductus arteriosus), deafness, eye defects (particularly cataracts), growth retardation, and mental retardation. Thankfully, with the advent of rubella vaccination, the incidence of infection has decreased by more than 99%, and the production of fetal malformations by the rubella virus has drastically decreased. Nonetheless, failure to be vaccinated has left 10 to 20% of the population susceptible to exposure, and this has not changed since the 1970s. The principle aim of the vaccination program is the prevention of congenital rubella.

Cytomegalovirus

The most common viral infection of the human fetus is cytomegalovirus (CMV) infection, occurring in some 1% of live births in the United States.[140] Infections in early pregnancy often result in embryonic death. Of those that survive, 90% of newborns are asymptomatic, although at least 10 to 15% of these will develop cognitive or sensorineural deficits later in life. Evidence of CMV infection by prenatal ultrasound includes intrauterine growth retardation, ascites, polyhydramnios or oligohydramnios, microcephaly, ventriculomegaly, calcifications in the fetal abdomen and brain, hepatosplenomegaly, hyperechoic bowel, cardiac dysrhythmia, hydronephrosis, and hydrops (**Fig. 20–13A–E**).[7,24,139] The findings of cerebral ventriculomegaly and decreased head circumference may be particularly ominous.[141] This said, many infected fetuses will appear normal until late in pregnancy.[140]

Toxoplasmosis

Toxoplasmosis, caused by a protozoan parasite, is a common infection, but a rare disease. Maternal infection is most often caused by eating poorly cooked meat, contact with infected cats, or contact with cat feces. Transmission of the infection from the mother to the fetus occurs only with primary infection during pregnancy, except when the mother has an immunosuppressive condition, such as acquired immunodeficiency syndrome (AIDS). With maternal infection, the rate of transmission to the fetus is ~17 to 25% in the first and second trimester and 65% in the third trimester. The majority of the fetuses, however, are asymptomatic, and the rate at which infection produces clinical illness is only 16% in the first and second trimesters and 5% in the third trimester. In the first trimester, the toxoplasma

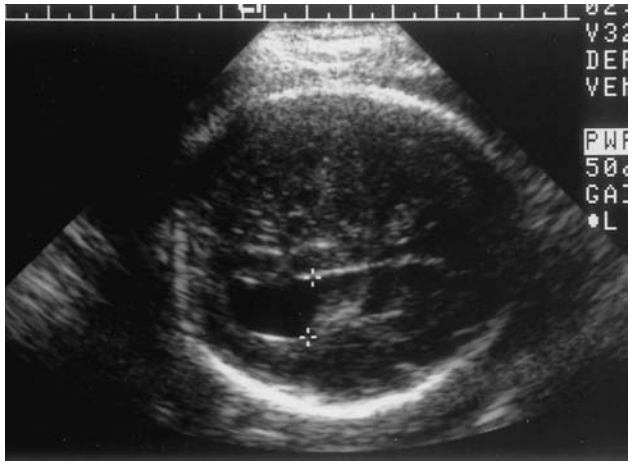

A

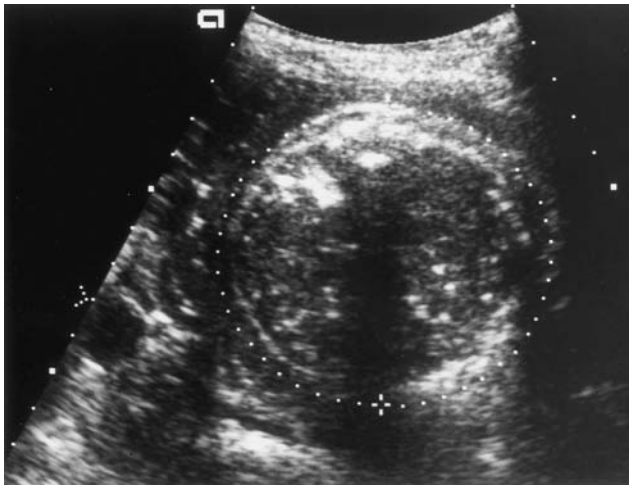

B

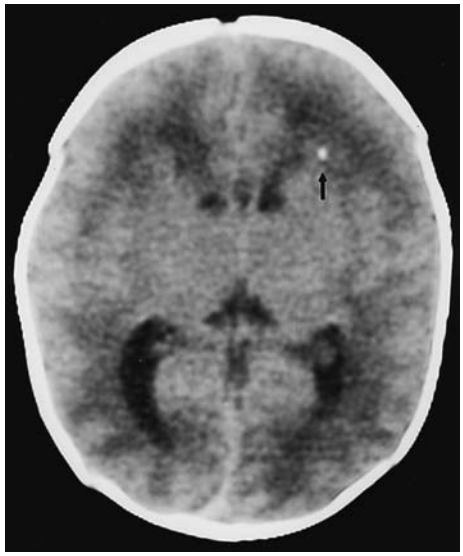

C

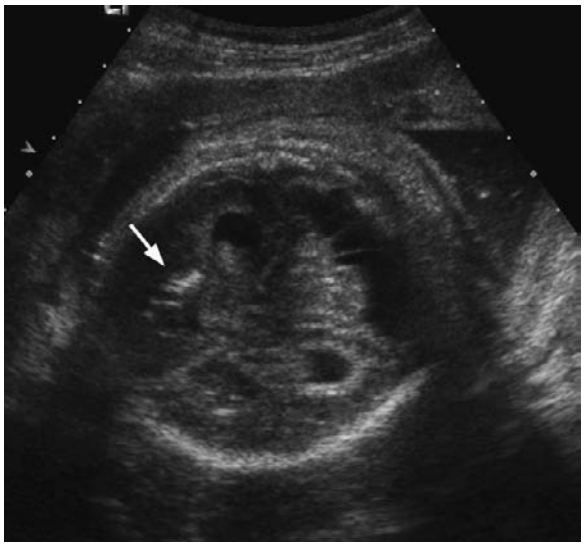

D

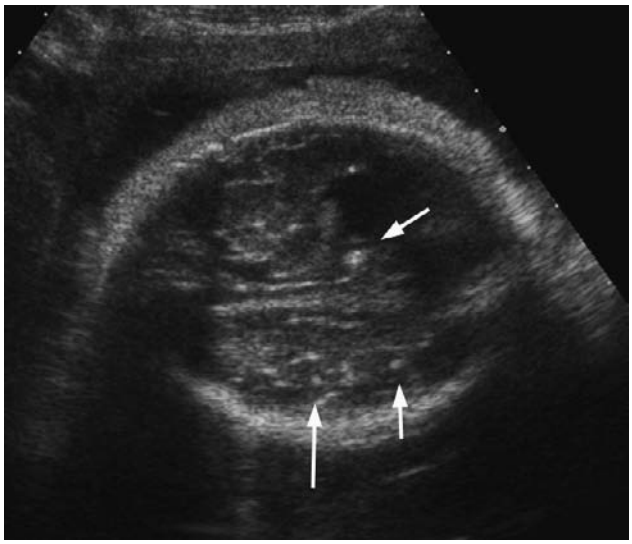

E

Figure 20–13 Fetal cytomegalovirus (CMV) infection. This is the most common viral infection of the human fetus. **(A)** In this case, the infection was evident by ventriculomegaly and **(B)** calcifications in the fetal abdomen. **(C)** Postnatal computed tomographic examination demonstrated periventricular cerebral calcification (arrow) as well. **(D)** A second case of CMV fetopathy demonstrates a hypoplastic posterior fossa and **(E)** multiple punctate echogenic foci throughout the brain (arrows), which indicate calcification.

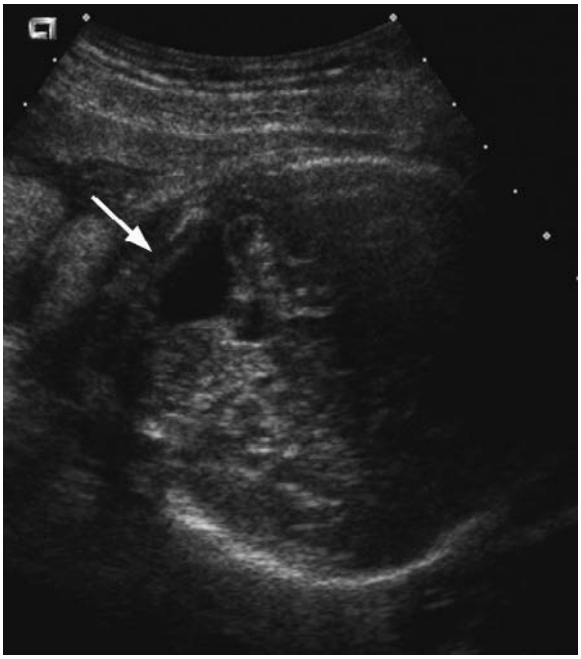

A

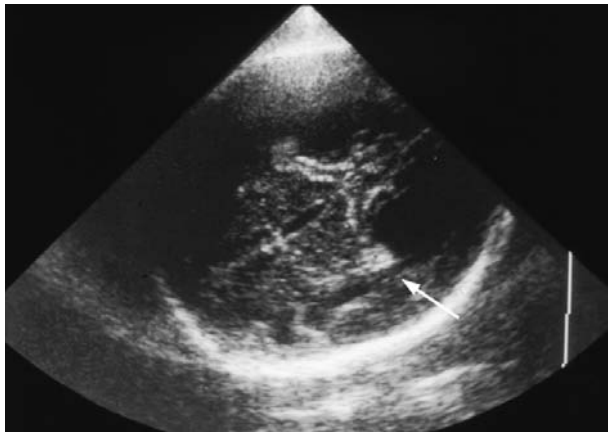

B

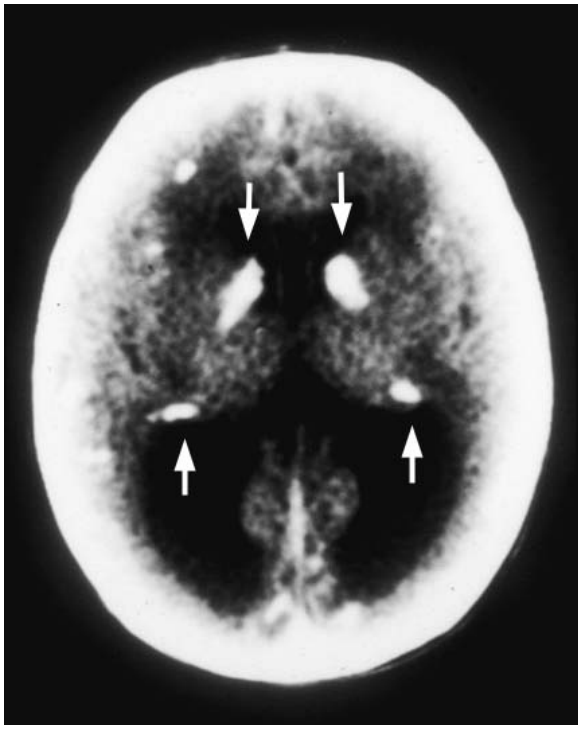

C

Figure 20–14 Toxoplasmosis infection. **(A)** The toxoplasma parasite can cause destructive changes of the brain, such as this area of focal tissue loss in the cerebellum (arrow). **(B)** Abnormal periventricular calcification and ventriculomegaly are demonstrated in a prenatal image (arrow) and **(C)** a postnatal computed tomographic scan (arrows). (Courtesy of Carol B. Benson, M.D., Boston, MA)

parasite can cause destructive changes of the brain and eyes, resulting in microcephaly, microphthalmia, and hydrocephalus[7] (**Fig. 20–14A–C**). Prematurity, growth retardation, cerebral calcification, hepatosplenomegaly, ascites, and pleural and pericardial fluid collection can also evolve.[24]

Varicella-Zoster

Varicella-zoster virus, which causes both chicken pox and shingles, is a neurotropic agent that causes abnormality when acquired by the fetus in the first trimester of pregnancy. The chance of abnormality is ~25% when infection occurs during this time, and these abnormalities include skin scarring, muscle atrophy, limb reduction defects, microcephaly, microphthalmia, ascites, liver calcifications, talipes equinovarus, hydrocephalus, and meningoceles.

Syphilis

The incidence of congenital syphilis has increased steadily from 1980. *Treponema pallidum* is an efficient teratogen, causing infection of nearly 100% of fetuses born to women

with untreated primary or secondary syphilis. Many pregnancies end in prenatal or perinatal fetal death, and the remainder demonstrate either congenital abnormality or later symptoms of infection. Manifestations of congenital syphilis seen with prenatal ultrasound include hepatosplenomegaly, hydrops, bowel obstruction, bone changes, and abnormally large placental size (**Fig. 20–15A–B**).[24,142,143] The bone changes are evident as surface irregularities and abnormal curvature and bowing in of the long bones of fetuses.[143] The classical stigmata of congenital syphilis infection, such as saddle nose, saber shin, and dental abnormalities, evolve from the destructive consequences of early childhood disease, and are seen only later in life.[17]

Herpes Simplex Virus

Infection of the fetus by herpes simplex virus usually occurs late in pregnancy. Described congenital abnormalities include microcephaly, microphthalmia, and mental retardation.

Parvovirus

Parvovirus is being increasingly recognized as the cause of previously unexplained nonimmune hydrops, spontaneous abortion, and stillbirth.[24] Infection typically results in spontaneous abortion in the first trimester, hydrops in the second trimester, and stillbirth in the third trimester. This said, one study has indicated that parvovirus is a relatively common cause of second-trimester fetal death, and most such cases do not demonstrate hydrops.[144] Parvovirus may also cause isolated pleural or pericardial effusion,[145] and possibly also structural malformations of the fetal brain and heart mediated by vasculitis.[146] Only 30 to 60% of adults are seropositive to the virus, leaving ~40 to 70% of the population susceptible to disease. Parvovirus appears to be, however, a relatively poor teratogen, causing congenital infection from an infected mother in only 10 to 20% of cases, and adverse outcome in only ~3% of pregnancies showing evidence of a recent maternal infection.[147]

Human Immunodeficiency Virus

The prenatal and perinatal transmission rate of the human immunodeficiency virus (HIV) is estimated to be at 40 to 50%. The effects of HIV infection on the outcome of pregnancy are controversial: some studies have noted premature rupture of membranes, premature birth, and growth retardation, but others find no such effects when the confounding factor of intravenous drug use is eliminated. Initial descriptions of an "AIDS embryopathy" have been disputed, and the diagnosis is now in disfavor. This syndrome was said to include growth failure, microcephaly, and a distinctive craniofacial dysmorphism (boxlike forehead, hypertelorism, flat nasal bridge, obliquity to the axis of the eyes).[148] Reports of such a craniofacial dysmorphism have been severely criticized for failing to control for ethnic variation, maternal substance abuse, and other potentially teratogenic agents.[149] At present there is no compelling evidence for an embryopathy that can be attributed to HIV alone.

Conclusion

Many embryos and fetuses exposed to teratogens will not have a demonstrable abnormality.[22] Even so, it is incumbent on the sonologist to be alert to potential teratogenic

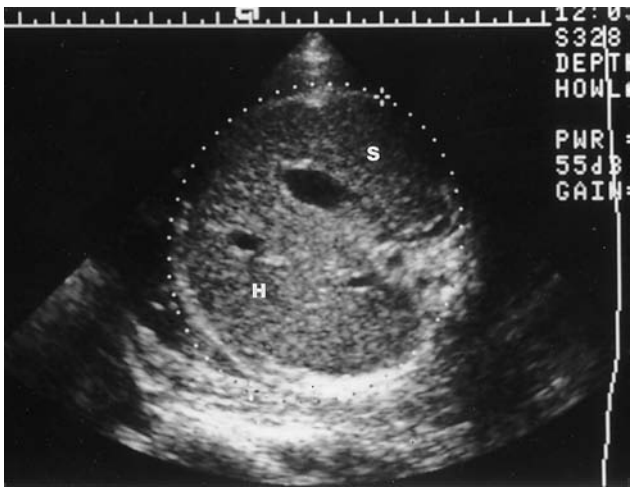

A

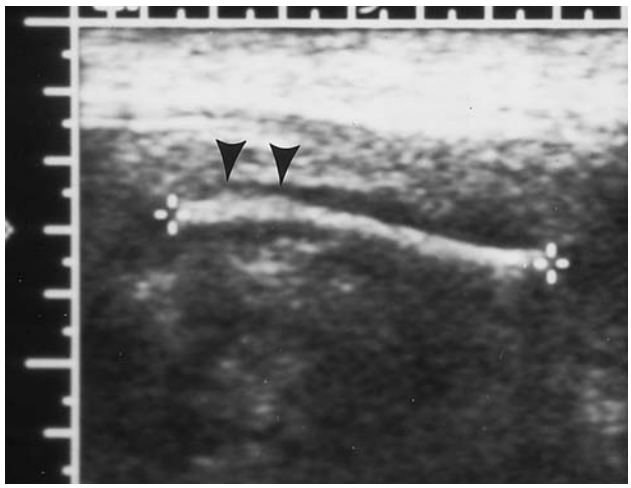

B

Figure 20–15 Congenital syphilis. **(A)** Hepatosplenomegaly is often the first, and sometimes the only, finding of infection (20). In this case, enlargement of the spleen causes displacement of the stomach (s) toward the midline. The liver (h) is also markedly enlarged. The measured abdominal circumference corresponds to ~35 menstrual weeks, although the fetus was only 22 weeks of age. **(B)** Views of the femurs showed surface irregularities of the bone (arrowheads) and abnormal bowing. These features have been described in a from 1982 case report.[84] (Courtesy of Sheryl Jordan, M.D.)

effects so that a purposeful and orderly survey of the fetus can be made for the often subtle signs, which may be the only indication of a teratogen. The use of ultrasound to establish the presence or absence of discernible abnormality may be the best—and only—reassurance available to parents tormented by the fear that they have brought harm to their unborn child through a potentially preventable exposure.

Acknowledgments

Thanks to Carol Benson, M.D. and David Nyberg, M.D. for case materials; Eileen P. Ahearn, M.D., Ph.D. for editing suggestions; and Carrie Poole for manuscript preparation.

References

1. Beckman DA, Brent RL. Mechanisms of teratogenesis. Annu Rev Pharmacol Toxicol 1984;24:483
2. Brent RL, Beckman DA. Environmental teratogens. Bull N Y Acad Med 1990;66:123–163
3. Finnell RH. Teratology: general considerations and principles. J Allergy Clin Immunol 1999;103:S337–S342
4. Principles of teratogenesis applicable to drug and chemical exposure. In: Schardein JL, ed. Chemically Induced Birth Defects. 2nd ed. New York: Marcel Dekker; 1993:1–62
5. Kalter H. Experimental investigation of teratogenic action. Ann N Y Acad Sci 1965;123:287–294
6. Kalter H. Teratology of the Central Nervous System. Chicago: University of Chicago Press; 1968
7. The causes of human congenital malformations. In: Moore KL, ed. The Developing Human: Clinically Oriented Embryology. 4th ed. Philadelphia: 1988:131–158
8. Risks. In: Kelly-Buchanan C, ed. Peace of Mind during Pregnancy. Philadelphia: Dell; 1989:7–26
9. Wilson JG. Experimental studies on congenital malformations. J Chronic Dis 1959;10:111–130
10. Tanimura T. Introductory remarks on behavioral teratology. Congenit Anom (Kyoto) 1980;20:301–318
11. Wilson JG. Mechanisms of abnormal development. In: Newburgh R, ed. Proceedings, Conference on Toxicology: Implications to Teratology. Washington, DC: NICHHD; 1971:81–114
12. Brent RL. Definition of a teratogen and the relationship of teratogenicity to carcinogenicity [editorial comment]. Teratology 1986a;34:359–360
13. Koren G, Pastuszak A, Ito S. Drugs in pregnancy. N Engl J Med; 338:1128–1137
14. Polifka JE, Friedman JM. Clinical teratology: identifying teratogenic risks in humans. Clin Genet 1999;56:409–420
15. Jacqz-Aigrain E, Koren G. Effects of drugs on the fetus. Semin Fetal Neonatal Med 2005;10:139–147
16. Brent RL. Evaluating the alleged teratogenicity of environmental agents. Clin Perinatol 1986;13:609
17. ReproTox (database). Columbia Women's Hospital, Washington, DC.
18. TERIS (database) Department of Pediatrics, University of Washington, Seattle.
19. Shepard TH, ed. Catalog of Teratogenic Agents. Baltimore: Johns Hopkins University Press; 1989
20. Schardein JL, ed. Chemically Induced Birth Defects. 2nd ed. New York: Marcel Dekker; 2000
21. Briggs GG, Freeman RK, Yaffe SJ, eds. Drugs in Pregnancy and Lactation. 5th ed. Baltimore: Williams & Wilkins; 2002
22. Gilstrap LC III, Little BB, eds. Drugs and Pregnancy. New York: Elsevier Science; 1998
23. Koren G, Edwards MB, Miskin M. Antenatal sonography of fetal malformations associated with drugs and chemicals: a guide. Am J Obstet Gynecol 1987;156:79–85
24. Sanders RC, ed. Structural Fetal Abnormalities: The Total Picture. St. Louis: Mosby-Year Book; 1996
25. Ultrasound of Fetal Syndromes (Benacerraf)
26. Kelly-Buchanan C, ed. Peace of Mind during Pregnancy. Philadelphia: Dell; 1989
27. Levine D, Filly RA, Goldberg JD. Teratogen exposure: lack of morphological abnormalities by detailed fetal sonography. Ultrasound Obstet Gynecol 1994;4:452–456
28. Turner GM, Twining P. The facial profile in the diagnosis of fetal abnormalities. Clin Radiol 1993;47:389–395
29. Escobar LF, Bixler D, Padilla LM, et al. Fetal craniofacial morphometrics: in utero evaluation at 16 weeks gestation. Obstet Gynecol 1988;72:674–679
30. Escobar LF, Bixler D, Padilla LM, et al. A morphometric analysis of the fetal craniofacies by ultrasound: fetal cephalometry. J Craniofac Genet Dev Biol 1990;10:19–27
31. Watson WJ, Katz VA. Sonographic measurement of the fetal mandible: standards for normal pregnancy. Am J Perinatol 1993; 10:226–228
32. Garn SM, Smith RH, La Velle M. Applications of pattern profile analysis to malformations of the head and face. Pediatr Radiol 1984;150:683–690
33. Yaffe SJ. Introduction
34. Drug use in pregnancy. In: Schardein JL, ed. Chemically Induced Birth Defects. 2nd ed. New York: Marcel Dekker; 1993:63–78
35. Queiber-Luft A, Eggers I, Stolz G, et al. Serial examination of 20,248 newborn fetuses and infants: correlations between drug exposure and major malformations. Am J Med Genet 1996;63: 268–276
36. Gregg NM. Congenital cataract following German measles in the mother. Trans Ophthalmol Soc Aust 1941;3:35–46
37. Lenz W. Kindichemissbildungen nach Medikamenteinnahme wahrend der Graviditat? Dtsch Med Wochenschr 1961;86: 2555–2556
38. McBride WG. Thalidomide and congenital abnormalities. Lancet 1961;2:1358
39. Briggs GG. Preface
40. Thalidomide symposium: Papers presented at the 26th meeting of the Teratology Society, July 6–10, 1986, Boston, MA. Teratology 1988;38:201–251
41. Gollop TR, Eigier A, Neto JG. Prenatal diagnosis of thalidomide syndrome. Prenat Diagn 1987;7:295–298
42. Dimopoulos MA, Eleutherakis-Papaiakovou V. Adverse effects of thalidomide administration in patients with neoplastic diseases. Am J Med 2004;117:508–515
43. Serreau R, Luton D, Macher MA, et al. Developmental toxicity of the angiotensin II type 1 receptor antagonists during human pregnancy: a report of 10 cases. Intl J Obstet Gyn 2005;112: 710–712
44. Ratnapalan S, Koren G. Taking ACE inhibitors during pregnancy: is it safe? Can Fam Physician 2002;48:1047–1049
45. Brent RL, Beckman DA. Angiotensin-converting enzyme inhibitors, an embryopathic class of drugs with unique properties: information for clinical teratology counselors. Teratology 1991; 43:543–546
46. Holmes LB. Teratogen-induced limb defects. Am J Med Genet 2002;112:297–303

47. Herting RI, Clay GA. Overview of misoprostol clinical experience. Dig Dis Sci 1986;31:47S–54S
48. Pastuszak AL, Schuler L, Speck-Martins C, et al. Use of misoprostol during pregnancy and Mobius' syndrome in infants. N Engl J Med 1998;338:1881–1885
49. Gonazlez CH, Marques-Dias MJ, et al. Congenital abnormalities in Brazilian children associated with misoprostol misuse in first trimester of pregnancy. Lancet 1998;351:1624–1627
50. Yip S-K, Tse AO-K, Haines CJ, et al. Misoprostol's effect on uterine arterial blood flow and fetal heart rate in early pregnancy. Obstet Gynecol 2000;95:232–235
51. Speert H, Quimby EH, Werner SC. Radioiodine update by the fetal mouse thyroid and resultant effects in later life. Surg Gynecol Obstet 1951;93:230
52. Diav-Citrin O, Ornoy A. Teratogen update: antithyroid drugs—methimazole, carbimazole, and propylthiouracil. Teratology 2002; 65:38–44
53. Fisher DA, Klein AH. Thyroid development and disorders of thyroid function in the newborn. N Engl J Med 1981;304: 702–712
54. Anticonvulsants. In: Schardein JL, ed. Chemically Induced Birth Defects. 2nd ed. New York: Marcel Dekker; 1993:157–207
55. Lindhout D, Omtzigt GC. Teratogenic effects of antiepileptic drugs: implications for the management of epilepsy in women of childbearing age. Epilepsia 1994;35(Suppl 4):S19–S28
56. Wladimiroff JW, Stewart PA, van Swaay RE, et al. The role of ultrasound in the early diagnosis of fetal structural defects following maternal anticonvulsant therapy. Ultrasound Med Biol 1988;14: 657–660
57. Sharony R, Garber A, Viskochil D, et al. Preaxial ray reduction defects as part of valproic acid embryofetopathy. Prenat Diagn 1993; 13:909–918
58. Langer B, Haddad J, Gasser B, Maubert M, Schlaeder G. Isolated fetal bilateral radial ray reduction associated with valproic acid usage. Fetal Diagn Ther 1994;9:155–158
59. Ylagan LR, Budorick NE. Radial ray aplasia in utero: a prenatal finding associated with valproic acid exposure. J Ultrasound Med 1994;13:408–411
60. Tomson T, Battino D. Teratogenicity of antiepileptic drugs: state of the art. Curr Opin Neurol 2005;18:135–140
61. Sharony R, Graham JM Jr. Identification of fetal problems associated with anticonvulsant usage and maternal epilepsy. Obstet Gynecol Clin North Am 1991;18:933–951
62. Avni EF, Rypens F, Zappa M, et al. Antenatal diagnosis of short-limb dwarfism: sonographic approach. Pediatr Radiol 1996;26: 171–178
63. Barr JM, Burdi AR. Warfarin-associated embryopathy in a 17-week old abortus. Teratology 1976;14:129–134
64. Harrod MJE, Sherrod PS. Warfarin embryopathy in siblings. Obstet Gynecol 1981;57:673–676
65. Howe AM, Webster WS. The warfarin embryopathy: a rat model showing maxillonasal hypoplasia and other skeletal disturbances. Teratology 1992;46:379–390
66. Van Driel D, Wesseling J, Sauer PJJ, et al. Teratogen update: fetal effects after in utero exposure to coumarins overview of cases, follow-up findings, and pathogenesis. Teratology 2002;66: 127–140
67. Kaplan LC. Congenital Dandy-Walker malformation associated with first trimester warfarin: a case report and literature review. Teratology 1985;32:333
68. Nageotte MP, et al. Anticoagulation in pregnancy. Am J Obstet Gynecol 1981;141:472
69. Sulik KK, Alles AJ. Teratogenicity of the retinoids. In: Saurat JH, ed. Retinoids: 10 Years On. Basel, Switzerland: S. Karger; 1991:282–295
70. Verloes A, Dodinval P, Koulischer L, et al. Etretinate embryotoxicity 7 months after discontinuation of treatment. Am J Med Genet 1990;37:437–438
71. Anonymous. Recommendations for isotretinoin use in women of childbearing potential. Teratology 1991;44:1–6
72. van Lennap E, et al. A case of partial sirenomelia and possible vitamin A teratogenesis. Prenat Diagn 1985;5:35–40
73. Rosa FW, et al. Teratogen update: vitamin A congeners. Teratology 1986;33:355–364
74. Schardein JL. Chemically Induced Birth Defects. 3rd ed. New York: Marcel Dekker; 2000:585
75. Greenberg LH, Tanaka KR. Congenital anomalies probably induced by cyclophosphamide. JAMA 1964;188:423–426
76. Nicholson HO. Cytotoxic drugs in pregnancy: review of reported cases. J Obstet Gynaecol Br Commonw 1968;75:307–312
77. Nora JJ, Nora AH, Toews WH. Lithium, Ebstein's anomaly and other congenital heart defects. Lancet 1974;??:594–595
78. Källén B, Tandberg A. Lithium and pregnancy: a cohort study on manic-depressive women. Acta Psychiatr Scand 1983;68:134–139
79. Källén B. Comments on teratogen update: lithium. Teratology 1988;38:597
80. Cohen LS, Friedman JM, Jefferson JW, et al. A reevaluation of risk of in utero exposure to lithium. JAMA 1994;271:146–150
81. Jacobson SJ, Jones K, Johnson K, et al. Prospective multicentre study of pregnancy outcome after lithium exposure during first trimester. Lancet 1992;339:530–533
82. Zalzstein E, Koren G, Einarson T, et al. A case-control study on the association between first trimester exposure to lithium and Ebstein's anomaly. Am J Cardiol 1990;65:817–818
83. Shepard TH, Brent RL, Friedman JM, et al. Update on new developments in the study of human teratogens. Teratology 2002;65: 153–161
84. Allan LD, et al. Prenatal echocardiographic screening for Ebstein's anomaly for mothers on lithium therapy. Lancet 1982;2:875–876
85. Loebstein R, Koren G. Pregnancy outcome and neurodevelopment of children exposed in utero to psychoactive drugs: the Motherisk experience. J Psychiatry Neurosci 1997;22:192–196
86. Rendle-Short TJ. Tetracycline in teeth and bone. Lancet 1962; 1:1188
87. Jones KL. Effects of therapeutic, diagnostic, and environmental agents. In: Creasy, Resnik, eds. Maternal–Fetal Medicine. 3rd edition. 1994
88. Katz Z, Lancet M, Skornik J, et al. Teratogenicity of progestogens given during the 1st trimester of pregnancy. Obstet Gynecol 1985;65:77–780
89. Hormones and hormonal antagonists. In: Schardein JL, ed. Chemically Induced Birth Defects. 2nd ed. New York: Marcel Dekker; 1993:271–339
90. Harlap S, Prywes R, Davies AM. Birth defects and oestrogens and progesterones in pregnancy. Lancet 1975;1:682–683
91. Harlap S, Shiono PH, Ramcharan S, et al. Chromosomal abnormalities in the Kaiser-Permanente birth defects study, with special reference to use around time of conception. Teratology 1985;31: 381–387
92. Senekjian EK, et al. Infertility among daughters either exposed or not exposed to diethylstilbestrol. Am J Obstet Gynecol 1988; 158:493–498
93. Stillman RJ. In utero exposure to diethylstilbestrol: adverse effects on the reproductive tract and reproductive performance in male and female offspring. Am J Obstet Gynecol 1982;142:905

94. Klip H, Werloop J, van Good JD, et al. Hypospadias in sons of women exposed to diethylstilbestrol in utero: a cohort study. Lancet 2002;359:1102–1107
95. Turusov VS, Trukhanova LS, Parfenov YuD, et al. Occurrence of tumours in the descendants of CBA male mice prenatally treated with diethylstilbestrol. Int J Cancer 1992;50:131–135
96. Brahams D. Diethylstilbestrol: third-generation injury claims. Lancet 1991;337:785
97. Oren D, Nulman I, Makhija M, et al. Using corticosteroids during pregnancy. Can Fam Physician 2004;150:1083–1085
98. Park-Wyllie L, Mazzotta P, Pastuszak A, et al. Birth defects after maternal exposure to corticosteroids: prospective cohort study and meta-analysis of epidemiologic studies. Teratology 2000;62: 385–392
99. Armenti VT, Mortiz MJ, Cardonick EH, et al. Immunosuppression in pregnancy: choices for infant and maternal health. Drugs 2002;62:2361–2375
100. Clarren SK, Smith DW. The fetal alcohol syndrome. N Engl J Med 1978;298:1063–1067
101. Clarren SK. Recognition of fetal alcohol syndrome. JAMA 1981;245:2436–2439
102. Day NL, et al. Prenatal exposure to alcohol: effect on infant growth and morphologic characteristics. Pediatr 1989;84: 536–541
103. Ernhart CB, et al. Alcohol teratogenicity in the human: a detailed assessment of specificity, critical period and threshold. Am J Obstet Gynecol 1987;156:33–39
104. Taylor CL, Jones KL, Jones MC, et al. Incidence of renal anomalies in children prenatally exposed to ethanol. Pediatr 1994;94: 209–212
105. Goodlett CR, Horn KH, Zhou FC. Alcohol teratogenesis: mechanisms of damage and strategies for intervention. Exp Biol Med 2005;230:394–406
106. Escobar LF, Bixler D, Padilla. Quantitation of craniofacial anomalies in utero: fetal alcohol and Crouzon syndromes and thanatophoric dysplasia. Am J Med Genet 1993;45:25–29
107. Chasnoff I, Burns W, Schnoll S, Burns K. Cocaine use in pregnancy. N Engl J Med 1985;313:666–669
108. MacGregor SN, Keith LG, Chasnoff IJ, et al. Cocaine use in pregnancy: adverse perinatal outcome. Am J Obstet Gynecol 1987; 157:686–690
109. Viscarello RR, Ferguson DD, Nores J, et al. Limb–body wall complex associated with cocaine abuse: further evidence of cocaine's teratogenicity. Obstet Gynecol 1992;80:523–526
110. Townsend RR, Laing FC, Jeffrey RB Jr. Placental abruption associated with cocaine abuse. AJR Am J Roentgenol 1988;150: 1339–1340
111. Hume RF Jr, Gingras JL, Martin LS, et al. Ultrasound diagnosis of fetal anomalies associated with in utero cocaine exposure: further support for cocaine-induced vascular disruption teratogenesis. Fetal Diagn Ther 1994;9:239–245
112. Cohen HL, Sloves JH, Laungani S, et al. Neurosonographic findings in full-term infants born to maternal cocaine abusers: visualization of subependymal and periventricular cysts. J Clin Ultrasound 1994;22:327–333
113. Dogra VS, Shyken JM, Menon PA, et al. Neurosonographic abnormalities associated with maternal history of cocaine use in neonates of appropriate size for their gestational age. AJNR Am J Neuroradiol 1994;15:697–702
114. Bebnke M, Eyler FD, Conlon M, et al. Incidence and description of structural brain abnormalities in newborns exposed to cocaine. J Pediatr 1998;132:291–294
115. Battin M, Albersheim S, Newman D. Congenital genitourinary tract abnormalities following cocaine exposure in utero. Am J Perinatol 1995;12:425–428
116. Chavez GF, et al. Maternal cocaine use during early pregnancy as a risk factor for congenital urogenital anomalies. JAMA 1989;262: 795–798
117. Hume RF Jr, O'Donnell KJ, Stanger CL, et al. In utero cocaine exposure: observations of fetal behavioral state may predict neonatal outcome. Am J Obstet Gynecol 1989;161:685–690
118. Personal and social drugs. In: Schardein JL, ed. Chemically Induced Birth Defects. 2nd ed. New York: Marcel Dekker; 1993: 398–641
119. Wyszynski DF, Beaty TH. Review of the role of potential teratogens in the origin of human nonsyndromic oral clefts. Teratology 1996;53:309
120. Milunsky A, et al. Methotrexate-induced congenital malformations with a review of the literature. J Pediatr 1968;72: 790–795
121. Goodman RM, Gorlin RJ, eds. The Malformed Infant and Child: An Illustrated Guide. New York: Oxford University Press; 1983
122. Firth HV, Chamberlain P, MacKenzie IZ, et al. Severe limb abnormalities after chorion villus sampling at 56–66 day's gestation. Lancet 1991;337:762–763
123. Burton BK, Schulz CJ, Burd LI. Limb anomalies associated with chorionic villus sampling. Obstet Gynecol 1992;79:726–730
124. Stoler JM, McGuirk CK, Lieberman E, et al. Malformations reported in chorionic villus sampling exposed children: a review and analytic synthesis of the literature. Genet Med 1999;1: 315–322
125. Olney RS, Khoury MJ, Alo CJ, et al. Increased risk for transverse digital deficiency after chorionic villus sampling: results of the United States multistate case-control study, 1988–1992. Teratology 1995;51:20–29
126. Rodeck CH. Fetal development after chorionic villus sampling. Lancet 1993;341:468–469
127. Firth H. Chorion villus sampling and limb deficiency: cause or coincidence? Prenat Diagn 1997;17:1313–1330
128. Canadian Early and Mid-Trimester Amniocentesis Trial (CEMAT) Group. Randomised trial to assess safety and fetal outcome of early and midtrimester amniocentesis. Lancet 1998;351: 242–247
129. Mennuti M. A 35-year-old pregnant woman considering maternal serum screening and amniocentesis. JAMA 1996;275: 1440–1446
130. Ratnapalan S, Bona N, Chandra K, et al. Physicians' perceptions of teratogenic risk associated with radiography and CT during early pregnancy. AJR Am J Roentgenol 2004;182:1107–1109
131. Brent RL. The effects of embryonic and fetal exposure to x-ray, microwaves, and ultrasound. Clin Obstet Gynecol 1983;26:484–510
132. Berlin L. Radiation exposure and the pregnant patient. AJR Am J Roentgenol 1996;167:1377–1379
133. Taylor L. Lauriston Taylor reviews radiation risks. J Nucl Med 1985;26:118–121
134. Graham JM Jr, Edwards MJ, Edwards MJ. Teratogen update: gestational effects of maternal hyperthermia due to febrile illnesses and resultant patterns of defects in humans. Teratology 1998;58: 209–221
135. Pleet H, Graham JM, Smith DW. Central nervous system and facial defects associated with maternal hyperthermia at 4 to 14 weeks gestation. Pediatr 1981;61:785–789
136. Moretti ME, Bar-Oz B, Fried S, et al. Maternal hyperthermia and the risk for neural tube defects in offspring: systematic review and meta-analysis. Epidemiology 2005;16:216–219

137. Milunsky A, Ulcickas M, Rothman KJ, et al. Maternal heat exposure and neural tube defects. JAMA 1992;268:882–885
138. Ridge BR, Budd GM. How long is too long in a spa pool? N Engl J Med 1990;323:835
139. Drose JA, Dennis MA, Thickman D. Infection in utero: US findings in 19 cases. Radiology 1991;178:369–374
140. Bar-Oz B, Berkovitch M, Ford-Jones L, et al. Congenital cytomegalovirus infection: is there a breakthrough? Can Fam Physician 2001;47:1179–1181
141. Twickler DM, Perlman J, Maberry MC. Congenital cytomegalovirus infection presenting as cerebral ventriculomegaly on antenatal sonography. Am J Perinatol 1993;10:404–406
142. Nathan L, Twickler DM, Peters MT, et al. Fetal syphilis: correlation of sonographic findings and rabbit infectivity testing of amniotic fluid. J Ultrasound Med 1993;2:97–101
143. Raafat NA, Birch AA, Altieri LA, et al. Sonographic osseous manifestations of fetal syphilis: a case report. J Ultrasound Med 1993;12:783–785
144. Wright C, Hinchliffe SA, Taylor C. Fetal pathology in intrauterine death due to parvovirus B19 infection. Br J Obstet Gynaecol 1996;103:133–136
145. Parilla BV, Tamura RK, Ginsberg NA. Association of parvovirus with isolated fetal effusions. Am J Perinatol 1997;14:357–358
146. Katz VL, McCoy C, Kuller JA, et al. An association between fetal parvovirus B19 infection and fetal anomalies: a report of two cases. Am J Perinatol 1996;13:43–45
147. Guidozzi F, Ballot D, Rothberg AD. Human B19 parvovirus infection in an obstetric population: a prospective study determining fetal outcome. J Reprod Med 1994;39:36–38
148. Marion RW, Wiznia AA, Hutcheon RG, et al. Fetal AIDS syndrome score: correlation between severity of dysmorphism and age at diagnosis of immunodeficiency. Am J Dis Child 1987;141: 429–431
149. Qazi QH, Sheikh TM, Fikrig S, et al. Lack of evidence for craniofacial dysmorphism in perinatal human immunodeficiency virus infection. J Pediatr 1988;112:7–11

21 Postpartum Complications

Donald N. Di Salvo

The sonographic diagnosis of maternal complications arising in the postpartum period, a time encompassing the puerperium and extending until roughly 6 to 8 weeks thereafter, is the focus of this chapter.

The postpartum period is a time of readjustment following the tremendous physiological upheaval of pregnancy.[1] Obstetrics Key organ systems (namely, genitourinary and circulatory) that have been affected by the hormonal and vascular changes which accompany pregnancy are all undergoing changes in size, function, and vascularity. Clinical problems that arise may be due to residua of pregnancy or a wholly unrelated, coincidental pathological process. Although radiological imaging can undoubtedly assist in uncovering the problem, it is important to be aware of the normal appearance of key organ systems to avoid misdiagnosis. This chapter focuses on the role of ultrasound in the diagnosis of postpartum clinical problems. Computed tomography (CT) and magnetic resonance imaging (MRI) are both useful complementary modalities, but their use should be reserved for specific problem solving (for instance, cases of suspected parametrial infection or postpartum ovarian vein thrombophlebitis) following initial investigation with ultrasound. Given that the average radiation dose to the ovaries is 2 to 3 rem with pelvic CT, MRI may be the preferred second-line imaging modality.[2] This chapter is organized into clinical symptoms and diagnoses, the normal appearance of the postpartum pelvis, and selected pathological diagnoses: retained products of conception (RPOC), postcesarean section (C-section) hematomas, postpartum ovarian vein thrombophlebitis (POVT), and endometritis.

Clinical Symptoms and Diagnostic Evaluation

Common yet nonspecific clinical symptoms and signs that may prompt an exam include blood loss (either occult or overt), pelvic pain, and fever, potential harbingers of the dreaded "lethal triad" of maternal peripartum morbidity: namely, obstetric hemorrhage, preeclampsia, and puerperal infection.3 Of these, hemorrhage is the most common problem, affecting 1 to 2% of all deliveries. It is usually divided into primary hemorrhage (beginning with the third stage of labor and extending to the first 24 hours) and secondary hemorrhage (beyond 24 hours and extending up to 6 weeks, with peak at between 5 and 15 days postpartum).4 Major diagnostic possibilities are shown in **Table 21–1.** Although overt blood loss is usually due to genital tract trauma (**Fig. 21–1**) and will generally prompt a quick investigation, occult bleeding may go unrecognized due to the 30 to 60% blood volume expansion during pregnancy, making hematocrit measurements less reliable in the estimation of blood loss.5 Occult blood loss, such as hemoperitoneum and periuterine and hepatic subcapsular

Table 21–1 Common Postpartum Clinical Signs and Diagnoses*

1 Postpartum Hemorrhage	2 Postpartum Hemorrhage	Fever	Pelvic Pain
Uterine atony	**RPOC**	Mastitis	**Uterine dehiscence**
Genital tract trauma	**Periuterine hematoma**	Pelvic infection	Pelvic infection
Episiotomy	Subfascial	**Metritis**	**Metritis**
Laceration	Bladder flap	Parametrial phlegmon	Parametrial phlegmon
Perineum, vagina, cervix	Broad ligament	Peritonitis	Peritonitis
Uterine rupture			
Clotting disorder	**Placental site subinvolution**	UTI/pyelonephritis	**Hematoma**
(**HELLP syndrome**)			
	Uterine dehiscence	**RPOC**	**RPOC**
		Thrombophlebitis (includes **POVT**)	**POVT**
		Hematoma	
		Pneumonia	

*Items in bold are illustrated. HELLP, hemolysis, elevated liver enzymes, and low platelets; POVT, postpartum ovarian vein thrombophlebitis; RPOC, retained products of conception; UTI, urinary tract infection.

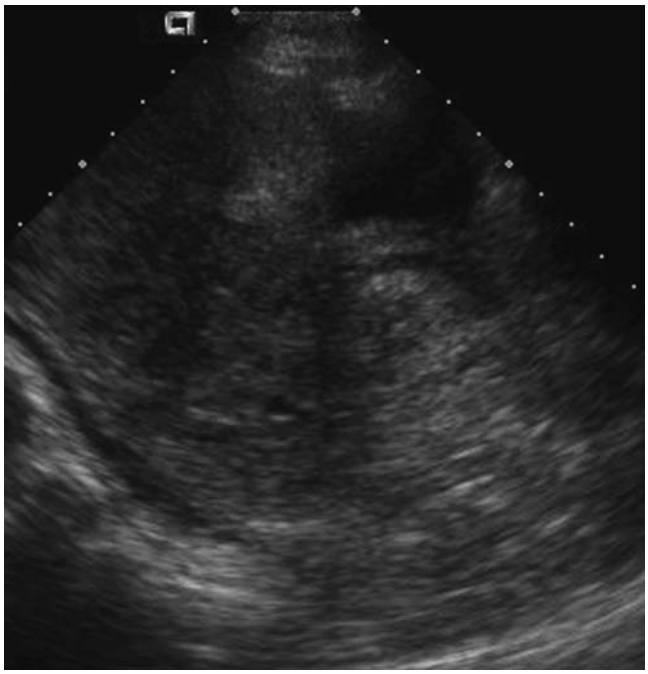

Figure 21–1 Cervical laceration. Forty-year-old woman with bleeding immediately following therapeutic abortion at 20 weeks. Sagittal transabdominal sonogram shows echogenic mass expanding the cervical area and extending into the vaginal fornices; the patient was treated with emergency uterine artery embolization.

hematoma (**Fig. 21–2**), is readily demonstrated with ultrasound and may indicate unrecognized hemolysis, elevated liver enzymes, and low platelets (HELLP syndrome). *Pelvic pain* or mass can be a manifestation of any of the hematomas listed above, as well as unrecognized uterine rupture, pelvic infection, or ovarian vein thrombophlebitis. *Postpartum fever* is generally defined as any temperature > 38°C (100.4°F) on any 2 days of the first 10 days after delivery, exclusive of the first day (due to the frequency of self-limiting mastitis in the first 24 hours).3 Clinical factors affecting the risk of postpartum infection include prolonged labor, preterm rupture of membranes, and C-section delivery. For example, postpartum endometritis has a 2 to 3% incidence following vaginal delivery, whereas the incidence following C-section is 6 to 10%; these incidences increase significantly in the face of preterm rupture of membranes or chorioamnionitis to 13% and 85% for vaginal delivery and C-section, respectively.4,6 As examination of **Table 21–1** shows, clinical manifestations in and of themselves are quite nonspecific and may have overlapping etiologies. Although a consideration of time of onset of symptoms can be helpful, pelvic ultrasound can often yield specific-enough findings to rule in or out many of these conditions.

Ultrasound and Imaging Technique

A brief review of sonographic technique follows. Even without a full bladder, transabdominal imaging gives the best overall view of the uterus and ovaries because the fundus is often beyond the reach of the transvaginal scan, especially in the first 4 weeks postpartum. Examination of the anterior wall C-section scar for subfascial collections can only be accomplished transabdominally (and may require higher frequency linear transducers for optimal visualization); frequently the lower uterine segment C-section site can be adequately seen as well. The transvagi-

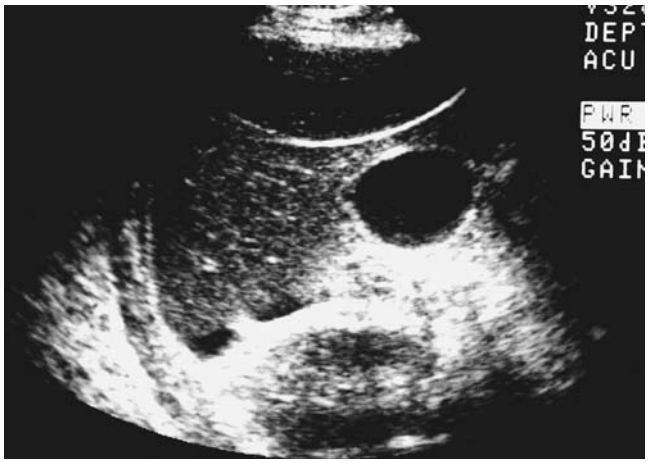

Figure 21–2 Postpartum hemolysis, elevated liver enzymes, and low platelets (HELLP syndrome) with hepatic subcapsular hematoma. Patient 8 days postpartum with fever, decreasing hematocrit level, and right upper quadrant pain. Transverse transabdominal sonogram shows complex subcapsular fluid collection, a small amount of ascites, and gallbladder sludge. (From Di Salvo DN. Sonographic imaging of maternal complications of pregnancy. J Ultrasound Med 2003;22:72. Reprinted by permission.)

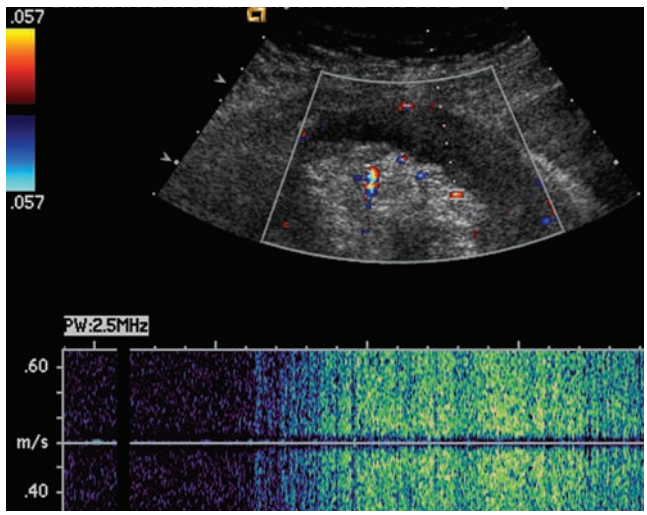

Figure 21–3 False-positive color Doppler signals in devitalized placenta accreta. Patient 3 weeks following bilateral uterine artery embolization, currently asymptomatic. Sagittal transabdominal ultrasound with color and pulsed Doppler shows spurious color flow signals and noise due to flash color artifacts.

nal approach is recommended in the latter half of the puerperium (weeks 4 to 8) for a detailed view of the endometrial cavity if retained products are suspected, especially to investigate blood flow. Transperineal imaging is an adequate alternative method to image the lower uterine segment/cervix and cul-de-sac in patients with an open wound in whom the transvaginal approach is not feasible. Proper Doppler technique to evaluate uterine blood flow includes attention to gain settings and interrogating frequency, as well as use of pulsed Doppler to elucidate the flow profiles of any color Doppler findings. Regarding the latter point, color "flash" artifacts should not be overinterpreted as evidence for true flow because hyperechoic foci due to air or calcifications, commonly seen in the postpartum uterus, can give rise to spurious color signals (**Fig. 21–3**).

Normal Postpartum Pelvis

The uterus does not return to its pregravid size and position until ~8 weeks after delivery, with the greatest decrease occurring during the first month.[7,8] The process of uterine involution involves both myometrial and endometrial changes. Hyalinization of pregnancy-hypertrophied myometrial vessels leads to ischemic atrophy of the fundus. The vascular basis for this process has been validated in Doppler studies of the uterine artery in the puerperium that show increase in resistive indices beginning by the second postpartum day and continuing for the next 6 weeks; these studies also suggest the vascular basis for subinvolution of the uterus in cases of secondary postpartum hemorrhage (see next section).[8–12] Concurrent with myometrial involution, sloughing of the decidua superficialis layer of the endometrium occurs, leading to vaginal discharge, termed *lochia rubra* in the first 3 to 4 days, changing to *lochia alba* thereafter. The regeneration of the endometrium from the remaining basalis layer is generally complete by the third week postpartum, except at the placental implantation site, which may take up to 8 weeks to fully heal. Histological studies have shown that inflammatory changes similar to those seen in endometritis are part of the normal reparative process.[1] One longitudinal sonographic study of the uterus in 42 women following uncomplicated vaginal delivery from day 1 to day 56 showed that the uterine fundus and corpus rotates 100 to 180 degrees relative to the lower uterine segment as follows: Beginning slightly retroverted on days 1 to 3, it becomes colinear on day 7, and finally slightly anteverted from week 2 on (**Fig. 21–4A,B**). The greatest size decrease, measured as maximal anteroposterior (AP) uterine thickness, occurred in the first 2 weeks, with a more gradual return to prepregnant dimensions between weeks 4 to 8. Findings in the endometrial cavity in this study were somewhat more complex: On day 1 the upper endometrial cavity was most often empty (93%), whereas debris and fluid were present in the cervical area in 79% (**Fig. 21–4C**). An increase in upper cavity size and contents was seen between days 7 and 14 in 90% of patients, likely reflecting necrotic deciduas superficialis, which was expelled by the time of follow-up at 4 weeks.[13] A later study included 40 postpartum women making an uncomplicated recovery following vaginal delivery, who were serially imaged at 1, 2, and 3 weeks. An echogenic intracavitary mass was seen in 51, 21, and 6% of women at the aforementioned times, but there was no correlation with amount or duration of bleeding[14] (**Fig. 21–4D**). CT and MRI studies have confirmed the frequent presence of fluid and blood in the postpartum uterus.[2,4,6] A small amount of air in the endometrial cavity, manifest as echogenic foci with ring-down artifacts, is not uncommon in the first several days after either vaginal delivery or C-section: it was present in 21% of healthy postpartum women and may persist for up to 3 weeks[4,15] (**Fig. 21–4E**).

Following a C-section, there are postsurgical changes in both the subfascial tissues as well as in the anterior lower uterine segment of the uterus. Subfascial and pelvic fluid collections at least 20 mL in volume were seen in 48% of 145 women following C-section: 58/145 in the abdominal wall and 11/145 in the deep pelvis.[16] Significantly, there was no correlation of febrile morbidity between women with or without these collections. The C-section site sonographically appears heterogeneous, with bright echogenic foci (sutures and/or air) intermixed with hypoechoic areas (blood) in the first several days[2,16,17] (**Fig. 21–5A,B**). Later, the site may be manifest as a thin discontinuity of the anterior lower uterine segment, best seen transvaginally when a tiny sliver of fluid may track within the myometrial defect (**Fig. 21–5C**). Postpartum physiological dilatation of the right ovarian vein may be observed by examining the region of the inferior vena cava (IVC) at the level of the renal hilus (**Fig. 21–5D,E**). Due to the expanded volume of blood that accompanies pregnancy, dilatation of ovarian veins without thrombosis may persist for several days following delivery, as MRI techniques have confirmed. Confirmation of patency can be made through use of Doppler techniques or time of flight MRI imaging.[17]

Retained Products of Conception

Retained products of conception represent a failure of the uterus to expel part or all of the placenta following delivery. Underlying predisposing factors include adhesions, succenturiate lobe, congenital uterine anomaly, uterine atony, and uterine scarring with placenta accreta. The clinical diagnosis of RPOC, based upon postpartum bleeding in the presence of fever, pain, and an open os, is unreliable; in one study, serology for elevated β HCG had low sensitivity for this diagnosis, being <30 mIU/ml in 43% of 26 patients with RPOC.[18] The diagnosis of RPOC and its distinction from intrauterine hematoma is not trivial because dilation and curettage (D&C) the standard treatment for RPOC, carries an overall complication rate of 7.3%, with such risks as cervical laceration, perforation, and synechiae.[19] Although

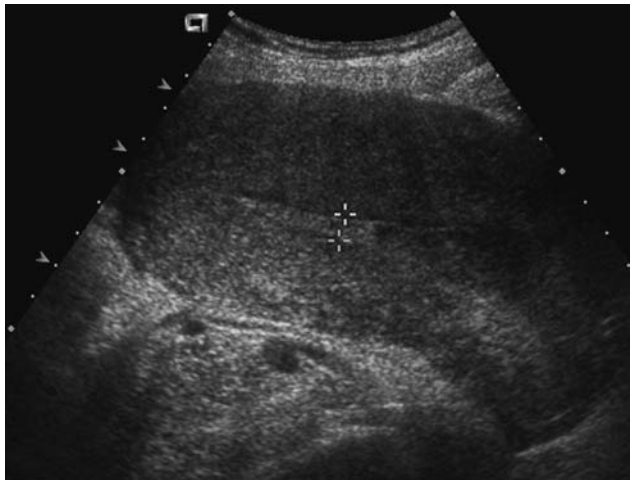

A

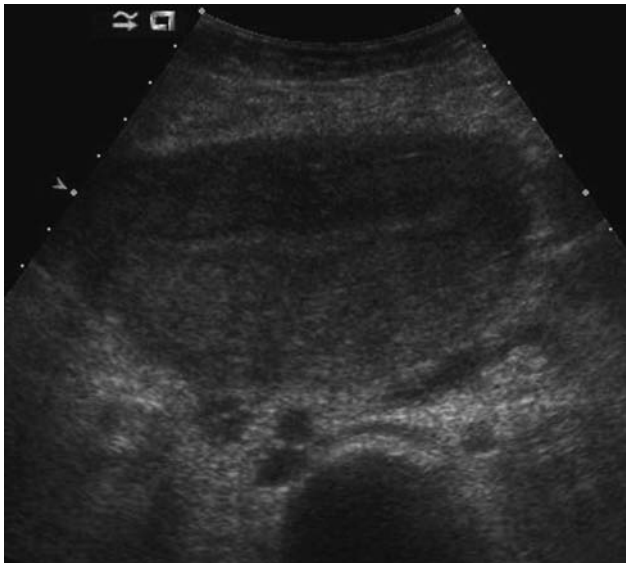

B

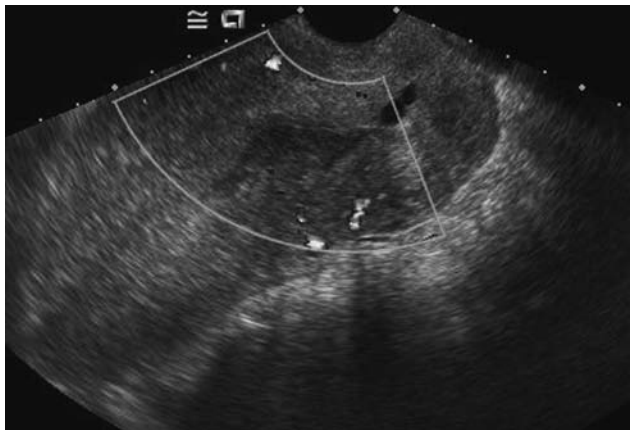

C

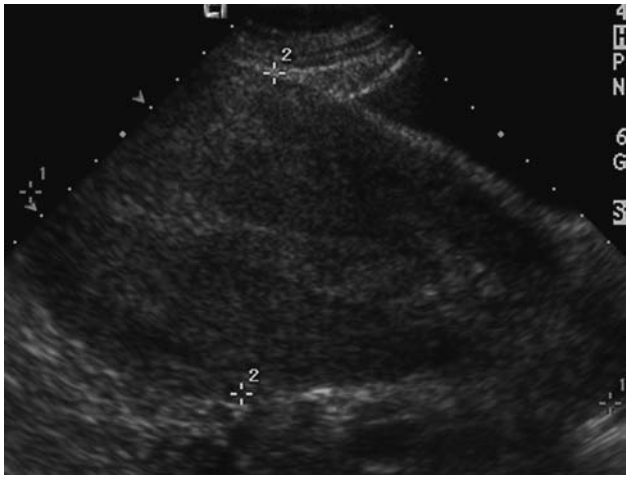

D

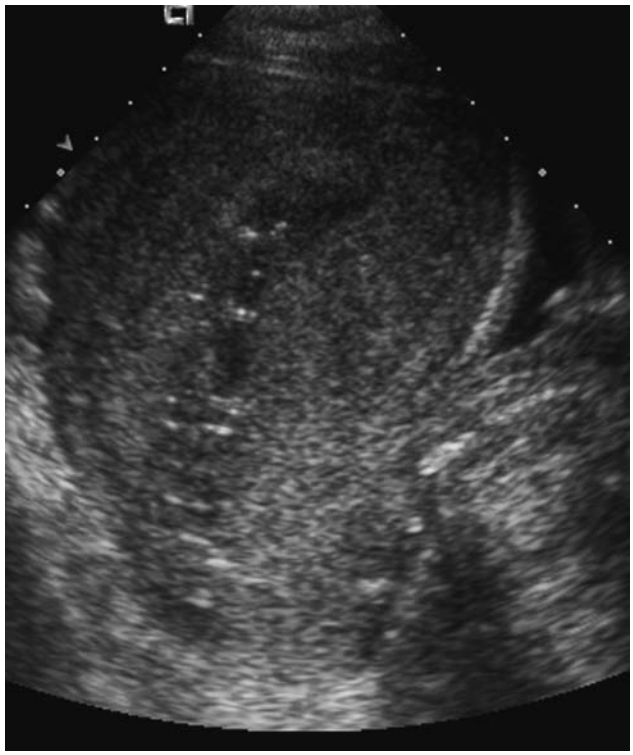

E

Figure 21–4 Range of normal findings postpartum from vaginal delivery. **(A,B)** Typical uterine enlargement in a patient presenting with bleeding on postpartum day 5, with the fundus retroflexed over the sacrum and extending above the level of the aortic bifurcation, as seen on the transverse image (between calipers, in **A**) **(B)**. Note the thin (6 mm) echogenic endometrial stripe in the corpus and hypoechoic material in lower uterine segment. **(C)** Transvaginal scan of the uterus [same patient as **(A)** and **(B)**] with color Doppler shows avascular material in the lower uterine segment consistent with clot and/or decidua. **(D)** Transabdominal sonogram (TAS) of the uterus in another patient postpartum day 4. Typical enlarged uterine dimensions outlined by calipers (sagittal = 16 cm, anteroposterior diameter = 8 cm), with diffusely thickened and echogenic endometrium (23 mm), avascular with Doppler (not shown). The patient spontaneously expelled solid material 2 days later, which was necrotic decidua at pathological examination. **(E)** TAS of the uterus in a different patient 1 day following delivery with manual extraction of the placenta performed. Small echogenic foci within the endometrial cavity are consistent with air.

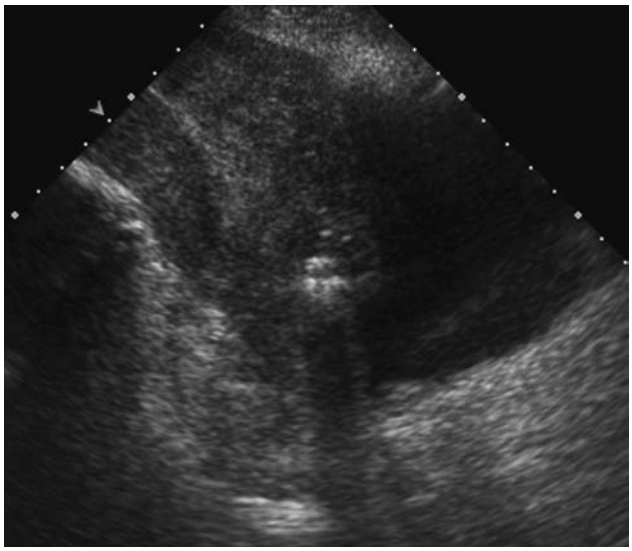

A

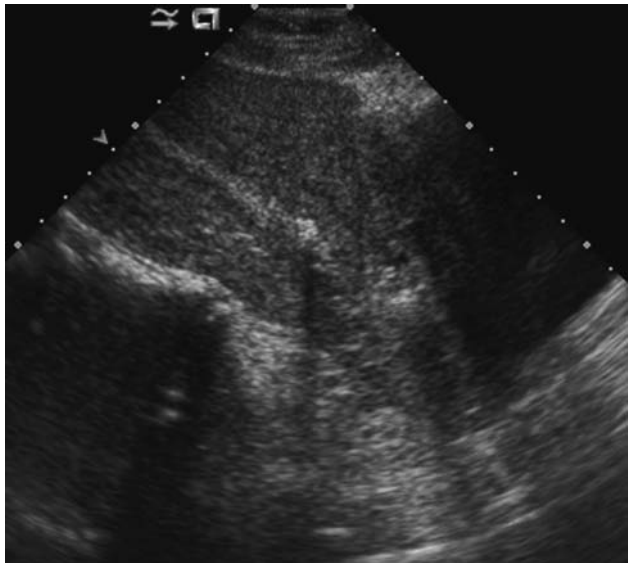

B

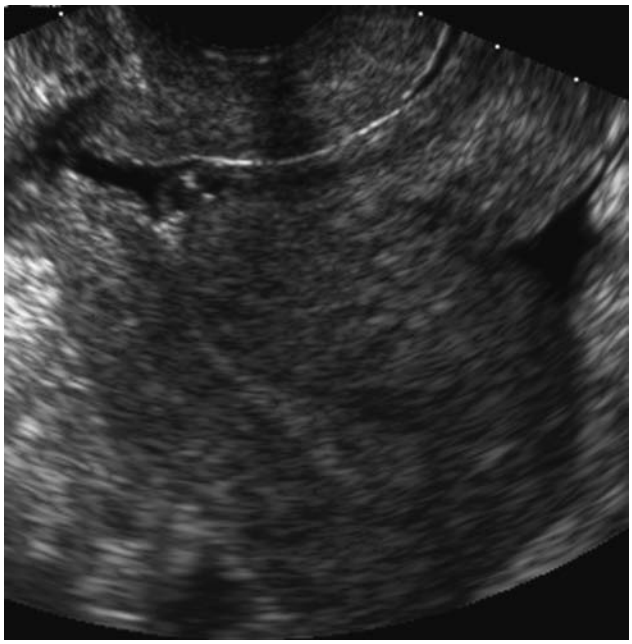

C

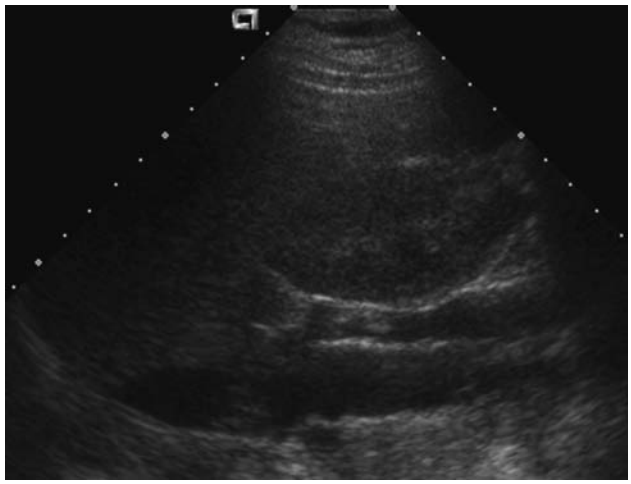

D

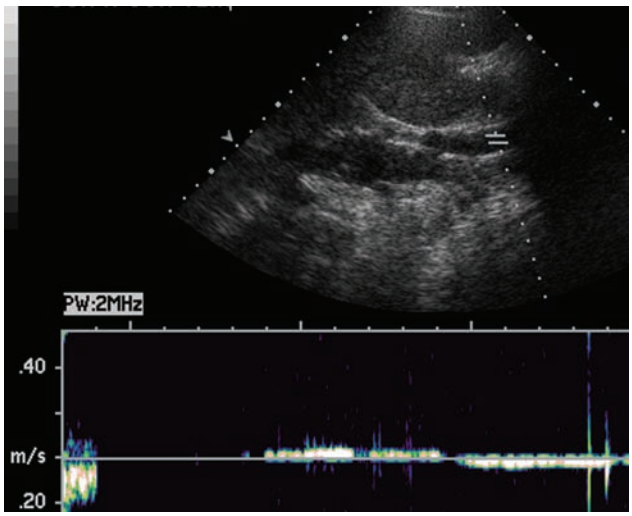

E

Figure 21–5 Range of normal findings post-cesarean section (C-section). **(A)** Transabdominal sonogram (TAS)- from a patient on day 4 with fevers shows echogenic foci in the lower uterine segment at the C-section site, consistent with air and/or suture material. **(B)** Echogenic foci in the endometrial cavity (in **B**) represent air bubbles from recent surgery. **(C)** Transvaginal scan of a retroflexed uterus from a different patient with a remote prior C-section shows fluid tracking into the surgical site. **(D)** TAS in a different patient presenting on day 3 with fever shows a dilated right ovarian vein anterior to the inferior vena cava. **(E)** Pulsed Doppler tracing with a sample gate in the ovarian vein shows normal venous flow, confirming patency. (This finding may also be seen following vaginal delivery.)

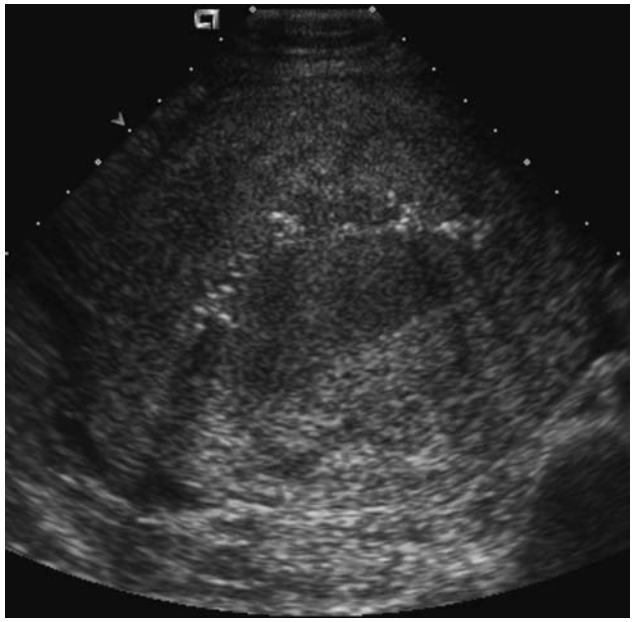

A

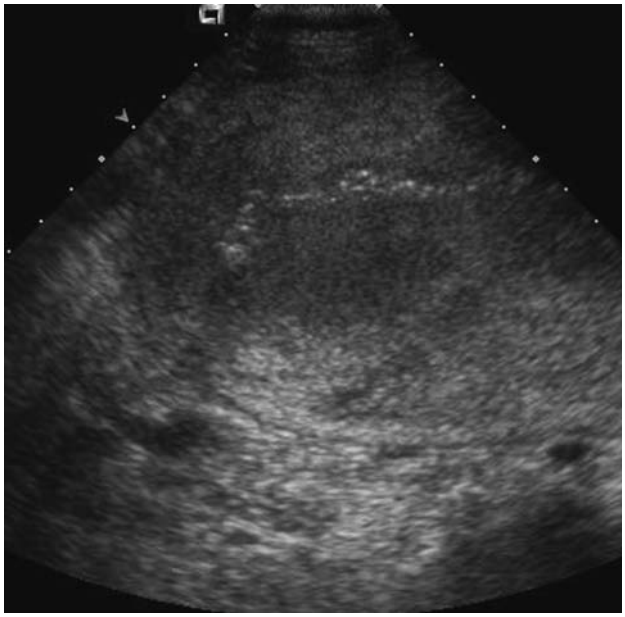

B

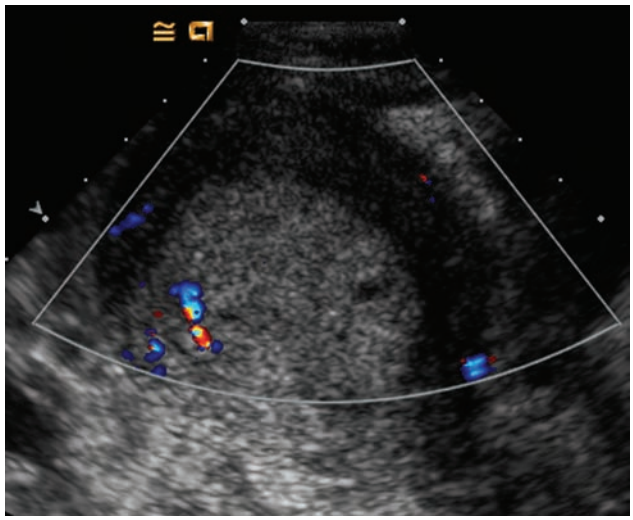

C

Figure 21–6 Retained placenta, missed diagnosis. **(A,B)** Transabdominal sonogram (TAS) in the delivery room immediately postpartum because the obstetrician suspected incomplete placental delivery. Cavity contents were incorrectly diagnosed as hematoma due to relative hypoechogenicity and absence of significant blood flow (not shown); also echogenic foci were all attributed to air rather than air and placental calcifications. **(C)** Follow-up TAS with color Doppler 6 weeks later for continued bleeding shows a hypovascular echogenic mass, which was removed with sonographic guidance; pathology showed necrotic placenta. This case illustrates some pitfalls with the diagnosis of retained products of conception.

placental tissue is readily recognizable with sonography during pregnancy, the appearance of residual placental tissue postpartum is complicated by the presence of coexisting blood products and necrotic decidua, which in themselves can range from echogenic to hypoechoic. Additionally, the endometrial cavity may be difficult to delineate due to the sloughing and regenerative process described earlier (see normal postpartum pelvis); on occasion, the inner myometrial layer itself may be hyperechoic, further obscuring the location of the endometrial stripe.[20] Ultrasound can readily exclude retained products when the endometrial cavity is thin (< 2 mm), or contains a small amount of fluid.[21] What constitutes an abnormal thickness is quite variable, with cutoff values ranging between 5 and 15 mm: Part of the confusion in the literature stems from variability of patient populations (postpartum vs postabortion) and the end points used (tissue sampling vs clinical outcome).[20] Although an echogenic intracavitary mass was present in 9/11 patients subsequently shown to have retained products, reliance on this feature alone resulted in a 34% false-positive rate in a later study because hematoma and necrotic decidua may also be echogenic.[22] The presence of calcifications within the intrauterine mass would favor retained products given that 50% of placentas have some sonographically visible calcifications after 33 weeks[23]; however, the sonographic distinction between small calcifications and foci of air can be difficult, especially if a D&C has been attempted prior to the ultrasound[21] (**Fig. 21–6**). Sonohysterography was helpful in two small series by demonstrating an attached endometrial mass in cases of RPOC in distinction to free-floating clot.[24,25]

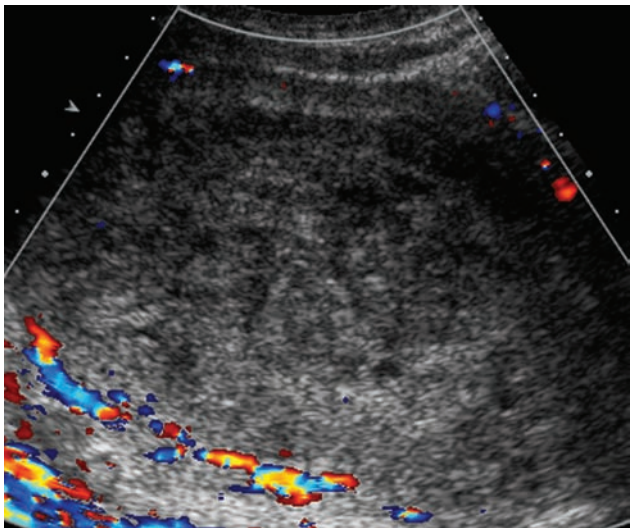

A

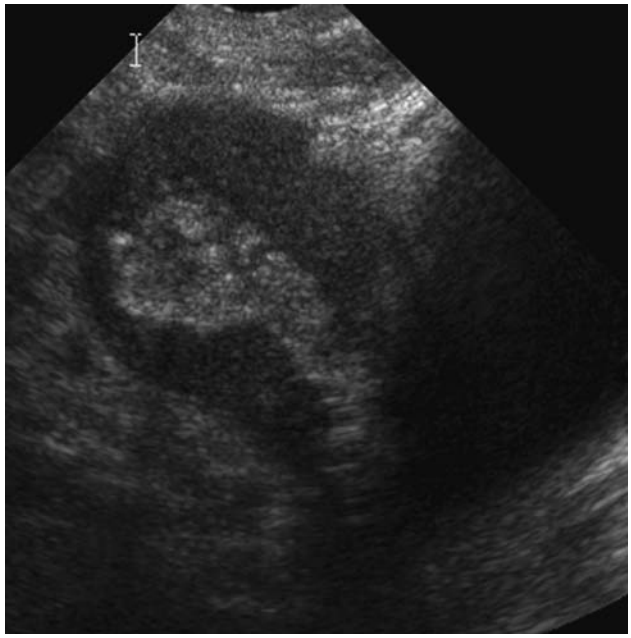

B

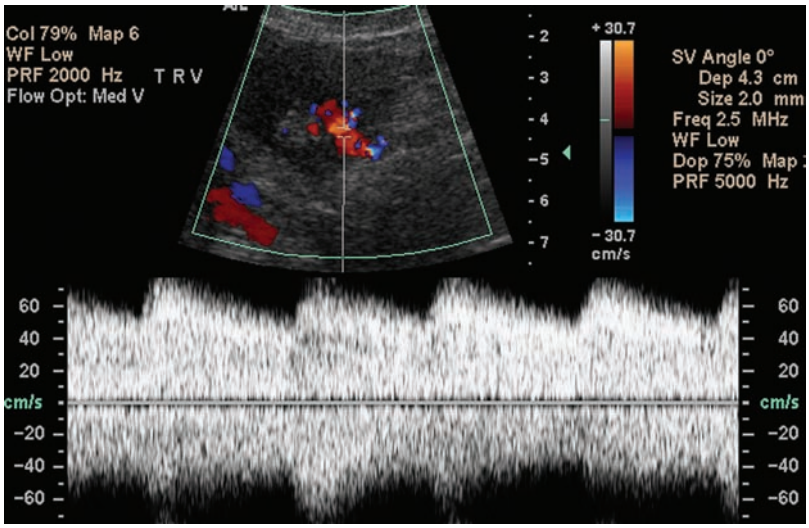

C

Figure 21–7 Avascular hematoma versus vascular retained products of conception. **(A)** Transabdominal sonogram (TAS) in a patient with heavy vaginal bleeding 1 day following therapeutic abortion shows a large (9 cm) avascular clot distending the uterine cavity, with normal flow signals in the posterior uterine wall at the former placental site. Bleeding resolved after methergin therapy. **(B,C)** TAS with color and pulsed Doppler in a different patient with bleeding 6 weeks postpartum shows an echogenic, partially calcified mass, (sagittal view, **A**) with abundant low-resistance flow (RI = .54) extending from the wall into the mass (transverse view, **B**). Retained products were confirmed pathologically.

The best discriminator between RPOC and hematoma should be Doppler techniques, with hematoma being avascular and retained products hypervascular (**Fig. 21–7**). Further, the vascularity associated with retained placental tissue displays typical low resistance flow seen in other situations involving vascularized trophoblast (e.g., early pregnancy and gestational trophoblastic disease).[26,27] In one study, a resistive index (RI) < 0.35 in myometrial arteries correctly identified all women with retained trophoblast in 28 women with postpartum or postabortion bleeding, whereas in a different study 14 of 15 patients with abundant myometrial color flow with RI < 0.45 had RPOC.[28,29] A later study of retained products showed color Doppler flow in 12 of 16 placental remnants presenting as an endometrial mass, but it was only present in 55% of the entire RPOC group. However, color flow interrogation was only performed in 17% of patients in that retrospective study.[30]

The concept of the placental implantation site involution, a process of sloughing of the infarcted superficial endometrial layers underlying the placenta, is well known to obstetricians.[1] The site begins as the size of the human palm at delivery and quickly shrinks to 3 to 4 cm by the end of the second week. Abnormal involution is a recognized cause of secondary postpartum hemorrhage, and it may be due to retained placenta or a primary process interfering with thrombosis of uteroplacental vessels themselves.[11,31] The normal gradual increase in uterine artery resistance that occurs in the puerperium may be delayed in cases of subinvolution.[9,10,12] Additional investigators of puerperial myometrial blood flow have shown an interest-

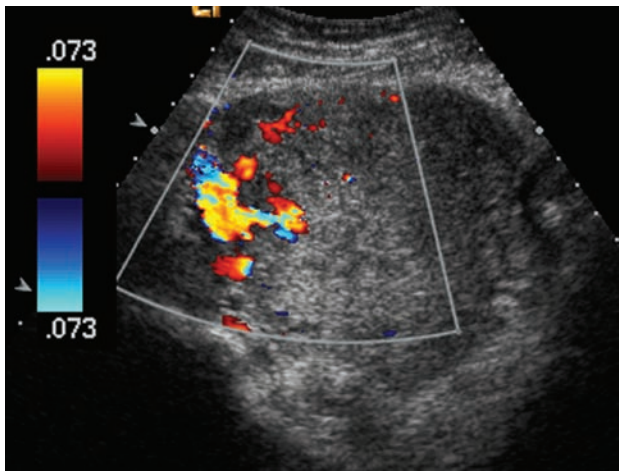

A

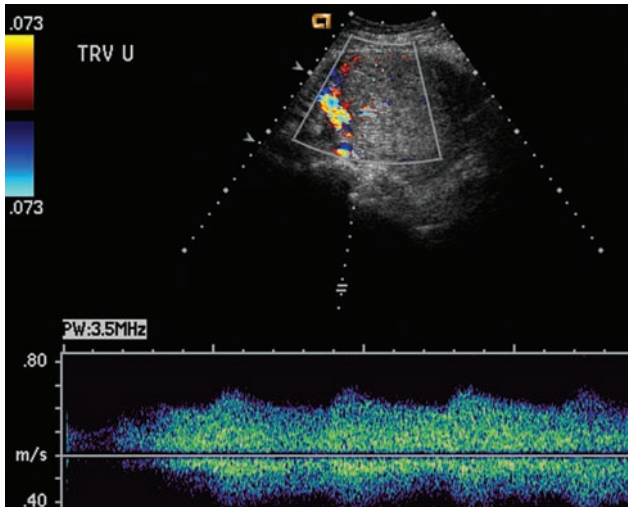

B

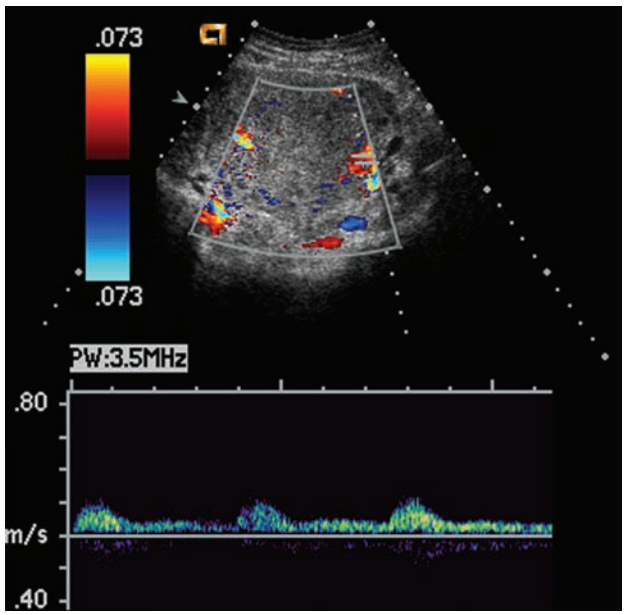

C

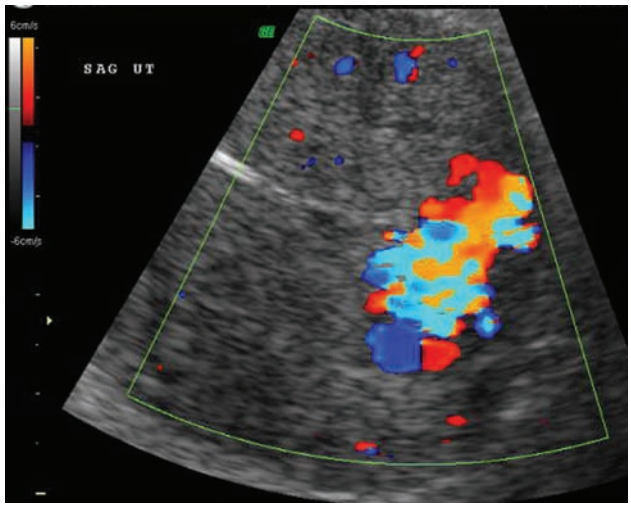

D

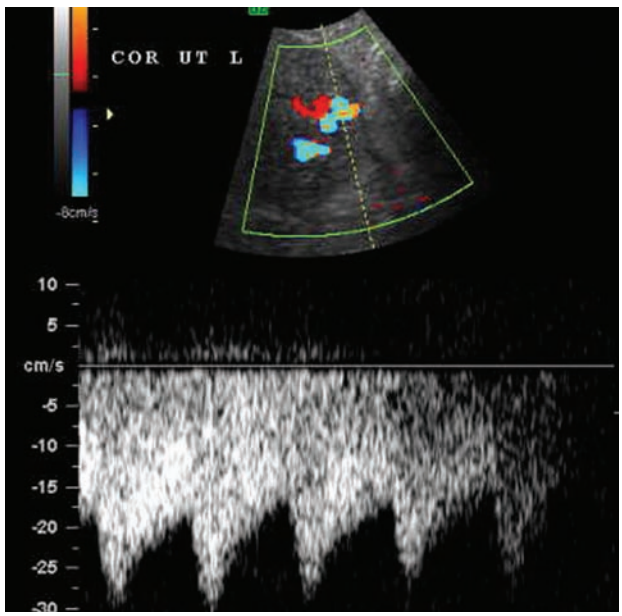

E

Figure 21–8 (A–C) Spectrum of focal versus **(D,E)** Diffuse appearance of enhanced myometrial vascularity (EMV) **(A)** Transabdominal sonogram (TAS) transverse color Doppler image in a patient with bleeding 5 days postvaginal delivery shows focal hypervascular focus in the right fundus. **(B)** Pulsed Doppler of the transmural vessel shows low resistance flow. **(C)** Comparison pulsed Doppler of the left fundal area shows a normal flow profile. Bleeding subsided spontaneously over the next few days without treatment. **(D)** Transvaginal scan in another patient 2 weeks post–therapeutic abortion with heavy vaginal bleeding shows a diffuse pattern of EMV in a retroverted fundus. **(E)** Pulsed Doppler shows high-velocity, low-resistance flow, suspicious for arteriovenous malformation. The patient was treated with methergin, and bleeding abated. Follow-up ultrasound 2 weeks later was normal.

ing phenomenon: the presence of focal zone(s) of high velocity, low-resistance flow in the myometrium strongly resembling an arteriovenous malformation (AVM). Although these foci of enhanced myometrial vascularity (EMV) have been seen in relation to RPOC, they may also be found in otherwise asymptomatic postpartum women as a transient phenomenon. One study found them in 32 out of 385 patients on an average of 5 weeks after delivery or spontaneous abortion (SAB) with an excellent correlation (90%) to former placental spontaneous abortion **(I)** position. The EMV was most commonly focal with a distinct vascular pedicle or less often a diffuse zone, extending from serosal to mucosal surface[18] (**Fig. 21–8**). Of 32 cases, 19 were associated with RPOC, whereas the remaining 13 were not; the foci resolved after removal of placental tissue in the first group and spontaneously in the second. A later study by the same investigators found EMVs in 46 of 93 women on day 3 after an uncomplicated vaginal delivery, decreasing to just three patients by 6 weeks. No abnormal bleeding or evidence for retained products was found.[32] It has been proposed that EMV represents delayed involution of the placental implantation site; although it may indicate the presence of RPOC, it is also a common transient finding following SAB or vaginal delivery and requires no specific therapy. Other investigators have noted seeming "AVMs" in connection with other pregnancy-related events; namely, following a spontaneous abortion, therapeutic abortion, recurrent gestational trophoblastic disease, or placental site trophoblastic tumor.[27,33–37]

These findings have led to a cautious redefinition of the diagnosis and therapy of uterine AVM, and by extension, retained products of conception: At present, no consistent Doppler criteria exist to separate true AVMs requiring embolization therapy from transient EMVs that may only require D&C or simple observation.[37,38] Careful consideration of both gray-scale and Doppler findings is needed; if low-resistance, high-flow signals are seen *both* in the myometrium and within an intracavitary mass in the setting of significant secondary postpartum hemorrhage, then D&C is suggested, with appropriate interventional backup available (in the unlikely event of a true AVM being uncovered). If the intracavitary mass is avascular and/or only myometrial hypervascularity is seen, then a trial of uterotonics (i.e., methylergonovine) may be more appropriate because many of these cases will resolve without intervention. It is still unclear the percentage of retained products that do not demonstrate blood flow, and further, if such cases require D&C (see **Fig. 21–6**).

Distinguishing retained placenta from placenta accreta or increta (i.e., placental tissue that has invaded the myometrium) is difficult. This rare condition (1/7000 pregnancies) may be suggested during pregnancy, when loss of the normally hypoechoic retroplacental clear space and prominent placental sinuses extending into the myometrium are seen, especially in the setting of placenta previa and prior C-section.[39] The postpartum diagnosis is suggested when residual placental tissue extends beyond the expected confines of the uterine cavity, although distinguishing myometrial invasion from simple myometrial thinning may be difficult (**Fig. 21–9**). Although MRI has been used to assist in this diagnosis, especially when the location of the abnormality is in the posterior fundus, the findings of myometrial thinning, loss of junctional zone,

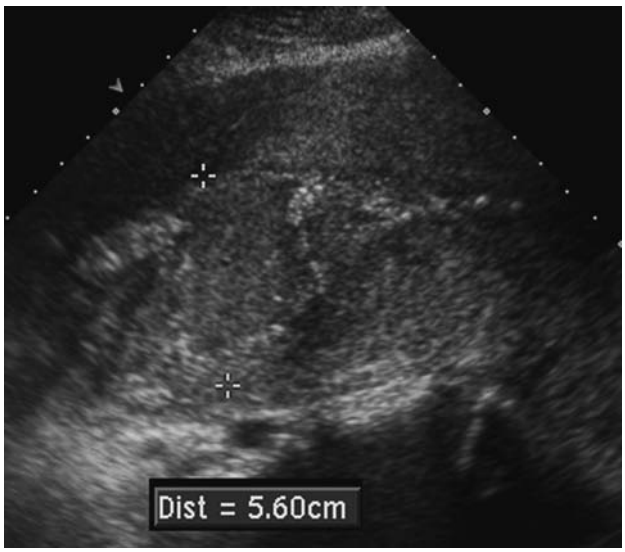

A

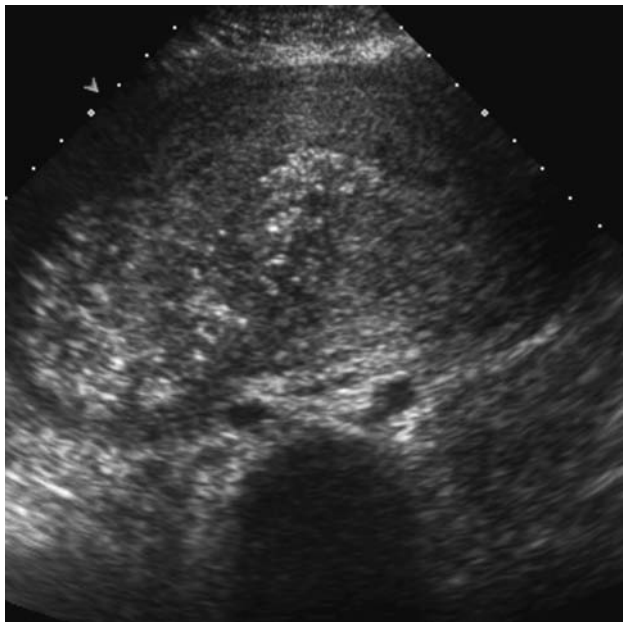

B

Figure 21–9 Placenta accreta. Transabdominal sonogram **(A)** sagittal and **(B)** transverse of the uterus in a patient who had retained placenta despite attempts at manual extraction 3 days previously. Calipers in the sagittal image measure a 5.6 cm thick placental remnant eccentrically placed in the right posterior fundus. Note the right posterior myometrial thinning in both images.

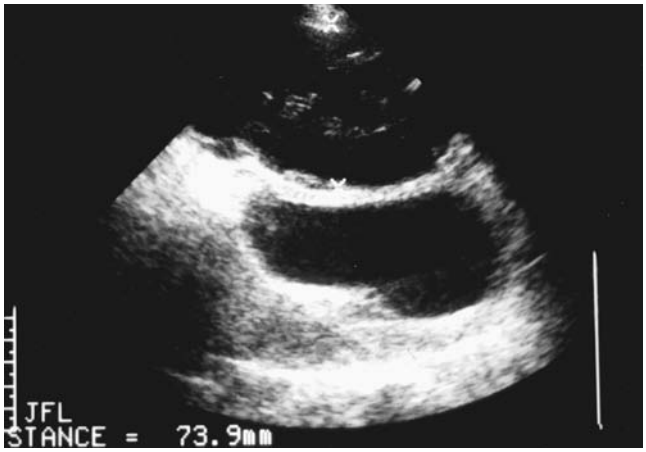

Figure 21–10 Subfascial hematoma following cesarean section. Transabdominal sonogram obtained in the sagittal midline plane in a patient with falling hematocrit shows a large, complex fluid collection (between calipers) beneath the anterior abdominal wall indenting the dome of the bladder. (Reprinted with permission from Di Salvo DN. Sonographic imaging of maternal complications of pregnancy. J Ultrasound Med 2003;22:84.)

and enhancement with gadolinium may all be seen with retained products of conception as well.[40,41]

Post–Cesarean Section Hematomas

Bladder flap, broad ligament, and subfascial hematomas are complications of C-sections; they are all also extraperitoneal fluid collections. The bladder flap is the potential space between the bladder and uterus created by the surgeon following the incision made into the parietal peritoneum that extends between these two organs, thus allowing access to the lower uterine segment; this vesicouterine peritoneal reflection is then resewn following closure of the uterine incision. Small collections of blood, likely due to incomplete hemostasis or periuterine vessels, are commonly seen here.[42] As they enlarge, these collections may readily extend over the uterine fundus, over the bladder dome, into the lateral pelvic peritoneal reflections (broad ligaments). The subfascial space is prevesical, posterior to the transversalis fascia, and anterior to the umbilicovesical fascia, it may extend inferiorly to the retropubic space of Retzius and can accommodate up to 2500 mL.[43] Because the rectus muscles and subjacent transversalis fascia have been surgically incised, the subfascial hematoma may dissect into the subcutaneous tissues behind the surgical wound; thus, a seeming superficial wound collection may in fact be the "tip of the iceberg," concealing a larger subfascial source (**Fig. 21–10**). The source for this collection is the inferior epigastric vessels. The bladder flap hematoma is thus retrovesical, whereas the subfascial is pre- or supravesical or both. Drainage of the former requires traversing the peritoneum, whereas the latter does not.

The frequency of these hematomas is variable depending on the study population, technique, and size criteria used. Fifty percent of patients in one study using transperineal ultrasound had a bladder flap hematoma.[44] The typical sonographic appearance is an echogenic mass in the vesicouterine space, centered on the lower uterine segment when small (< 3 cm) and extending cephalad over the fundus or bladder when large (**Fig. 21–11**). Subsequent series using MRI in postpartum patients have shown bladder flap hematomas in 13 of 14 asymptomatic women and 32 of 50 patients with suspected metritis; only two hematomas had a dimension greater than 5 cm.[2,17] Treat-

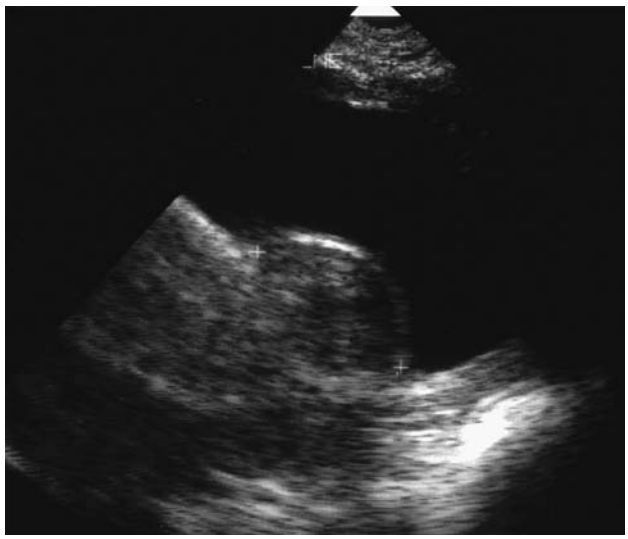

A

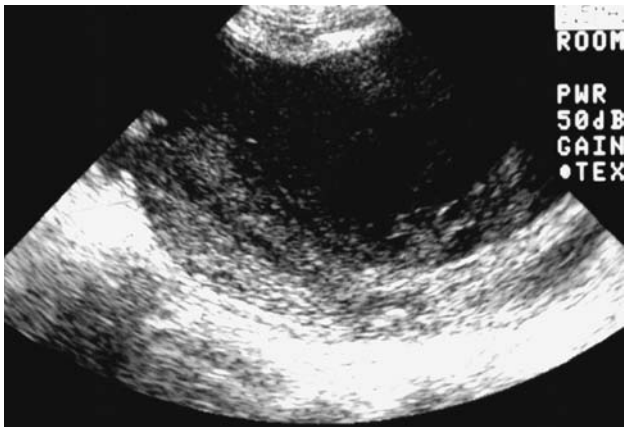

B

Figure 21–11 Bladder flap hematomas following cesarean section. **(A)** Sagittal midline sonogram shows a small isoechoic mass (between calipers) anterior to the lower midline segment and posterior to the bladder. (Reprinted with permission from Di Salvo DN. Sonographic imaging of maternal complications of pregnancy. J Ultrasound Med 2003;22:85.) **(B)** Sagittal midline sonogram shows a large, complex collection anterior to the uterus, extending over the fundus (bladder is displaced inferiorly and is not included on the image).

ment for extraperitoneal hematomas is expectant unless signs of infection are present; percutaneous sampling is required to determine if the hematoma is infected.

A persistent or enlarging bladder flap hematoma may rarely be a manifestation of postpartum uterine rupture or dehiscence.[45] Dehiscence is defined as a transmural myometrial defect covered by intact serosa, whereas rupture involves the serosal layer as well. Both processes most often affect a prior C-section, scar, which is vertically oriented in the uterine body in the now rarely performed classic C-section, and transversely oriented in the lower uterine segment in the more common transverse incision performed today. Although both are more likely to be intra- or prepartum events, patients may present in the immediate postpartum period with dropping hematocrit. Sonography may disclose a bladder flap hematoma with dehiscence only, or intraperitoneal/periuterine hematoma if complete rupture has occurred. It should be emphasized that both CT and MRI will readily disclose a myometrial defect as a normal postpartum finding post–C-section in the early puerperium (see earlier section titled, Normal Postpartum Pelvis). MRI provides more detail of serosal and endometrial contiguity and can show coaptation of the incision site, two features that argue against dehiscence.[6,17] Diagnosis of dehiscence in and of itself does not require surgical repair unless signs of concurrent infection are present (**Fig. 21–12**). However, knowledge of prior dehiscence does enter into counseling regarding future deliveries, especially given the widespread practice of encouraging vaginal birth after cesarean delivery.[46]

Postpartum Ovarian Vein Thrombophlebitis

Ovarian vein thrombophlebitis is an uncommon entity (estimated prevalence 1/600 deliveries), involving thrombosis of one or both ovarian veins, presumed due to retrograde extension of myometrial venous clot in the setting of placental or uterine infection. It is 10 times more common after C-section than after vaginal delivery. The right ovarian vein is three times more likely to be affected than the left, presumably due to uterine retroversion during pregnancy.[4] Clinical symptoms include fever, pelvic or flank pain, and pelvic mass. Treatment is generally directed to the predisposing pelvic infection, although anticoagulation is also indicated due to the risk of pulmonary embolism. Sonographic findings include ipsilateral ovarian enlargement with a dilated ovarian vein and absent flow signals; generally, only the proximal segment of the right ovarian vein is readily visible, near its junction with the IVC. Following the dilated vein to its junction with the IVC is important to avoid confusion with a dilated ureter (**Fig. 21–13**).[47] It is also important to check for flow because a dilated ovarian vein may be normally seen. In a study directly comparing ultrasound, MRI, and CT for the diagnosis of POVT in the clinical setting of puerperal fever refractory to antibiotics, sonography identified only six of 12 cases compared with the other modalities.[48] With currently available technology and pulse sequences, MR venography is the preferred modality when this diagnosis is considered to reduce unnecessary radiation exposure to the ovaries.

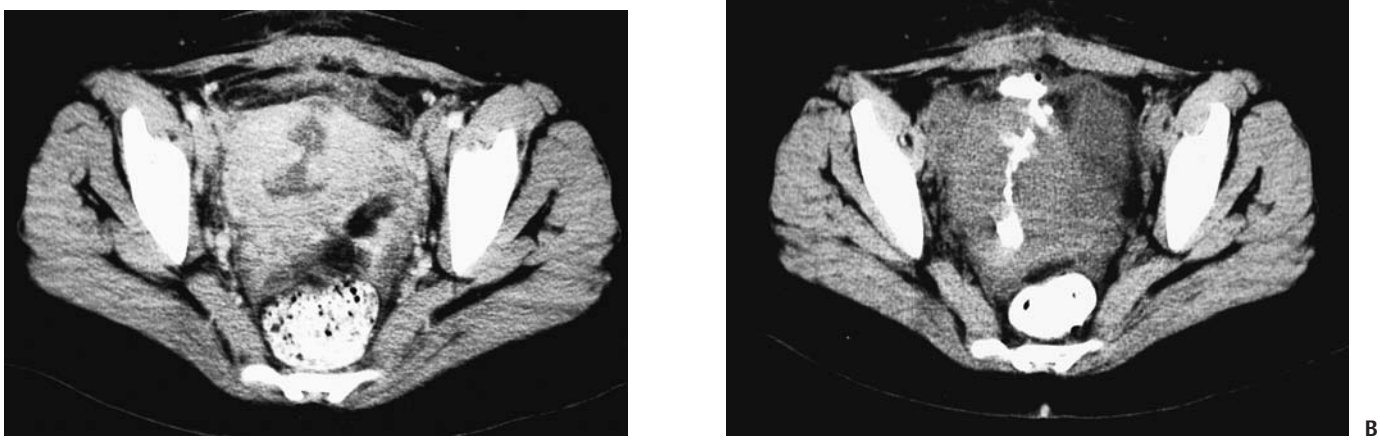

Figure 21–12 Infected bladder flap hematoma and uterine dehiscence following cesarean section. **(A)** Pelvic computed tomography post–contrast administration in a patient with fever shows a stellate, nonenhancing area in the anterior uterus, extending from the uterine cavity into the small bladder flap hematoma. **(B)** Fistulogram obtained after percutaneous drainage of the infected hematoma shows injected contrast outlining the area of dehiscence. The patient was treated with antibiotics; the follow-up sonogram was normal. (Reprinted with permission from Di Salvo DN. Sonographic imaging of maternal complications of pregnancy. J Ultrasound Med 2003;22:85.)

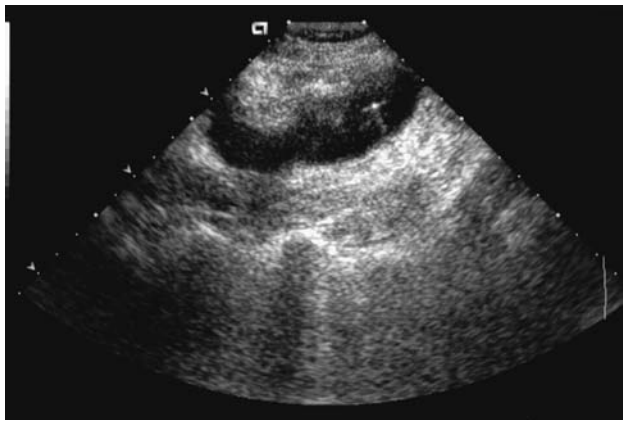

A

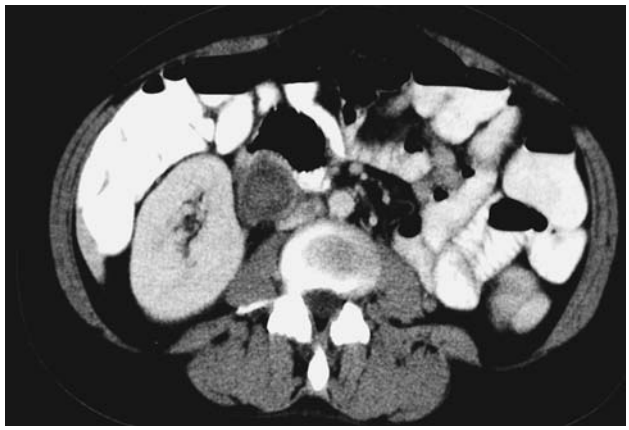

B

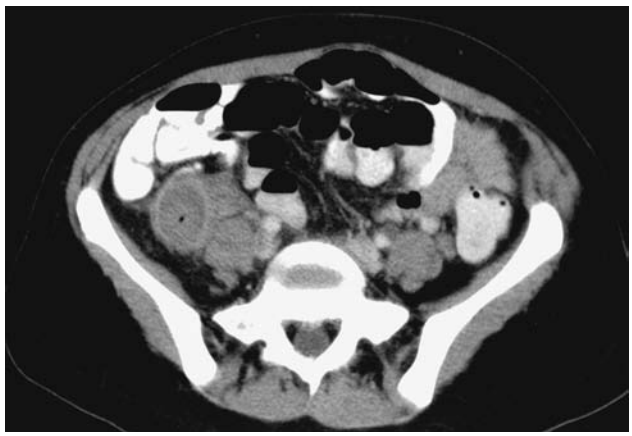

C

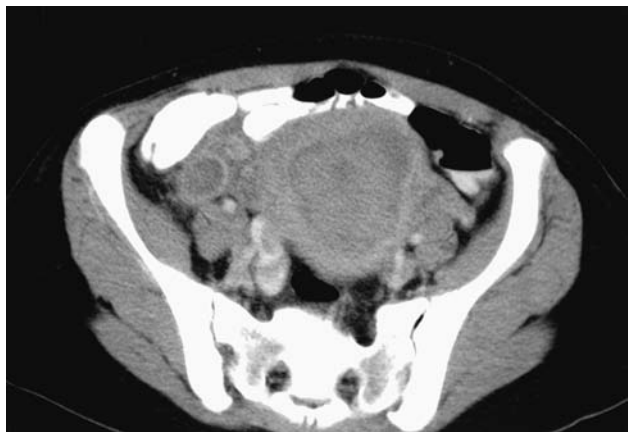

D

Figure 21–13 Postpartum ovarian vein thrombophlebitis and retained products in a patient with postpartum fever and vaginal discharge. **(A)** Coronal sonogram of the right flank shows a tubular structure without flow containing a hyperechoic focus with ringdown artifact consistent with air. **(B–D)** Sequence of postcontrast computed tomographic images shows a dilated, clot-filled right ovarian vein extending from the renal hilus into the pelvis. **(B)** The occluded vein compresses the inferior vena cava. **(C)** A focus of air in the vein is shown. **(D)** The uterus distended with retained products. (Reprinted with permission from Di Salvo DN. Sonographic imaging of maternal complications of pregnancy. J Ultrasound Med 2003;22:87.)

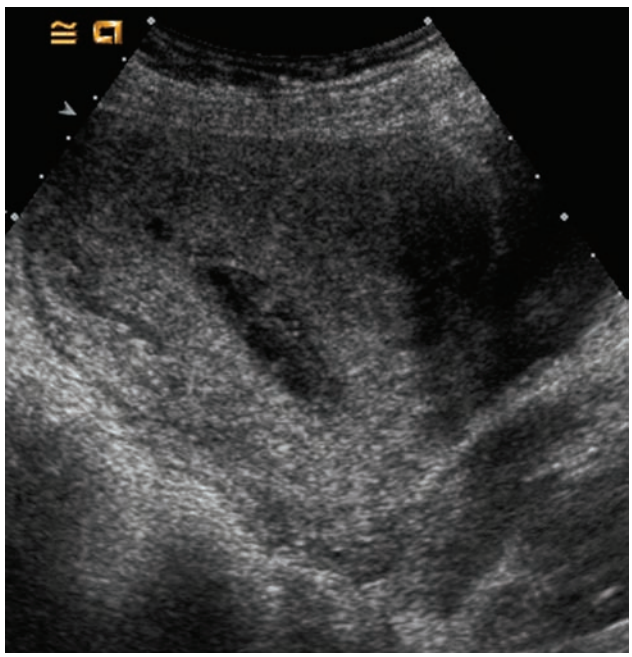

A

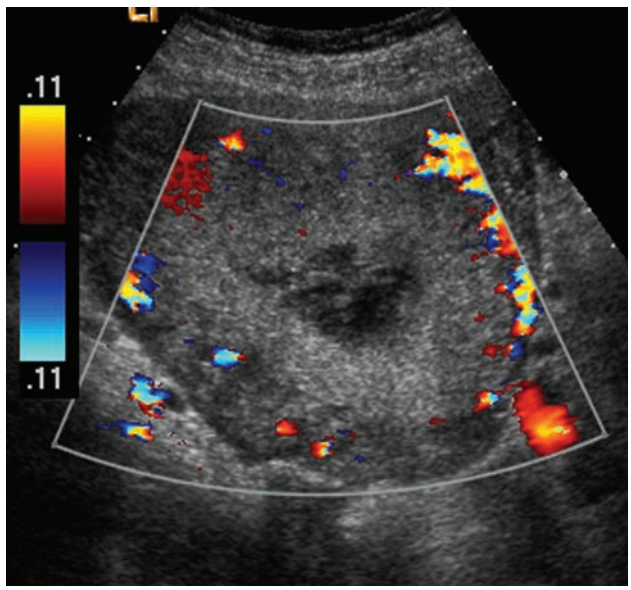

B

Figure 21–14 Postpartum endometritis. Patient presenting with fever and discharge 2 weeks after vaginal delivery. **(A)** Sagittal and **(B)** transverse sonograms show complex fluid and stranding within the uterine cavity and generalized myometrial hyperemia. Patient defervesced following treatment with broad spectrum antibiotics.

Postpartum Pelvic Infection

Postpartum metritis complicates 1 to 6% of all deliveries and is more common after C-section than vaginal delivery, despite the use of prophylactic perioperative antibiotics. As noted in the earlier "clinical" section, fever in the first postoperative day is generally not due to pelvic infection: Only 20% of such patients ultimately prove to have pelvic infection, whereas 70% of patients with fever after the second postoperative day do.[3] Roughly 10% of these patients are at risk for the more serious complications of parametrial phlegmon/abscess, dehiscence, peritonitis, and POVT. Infection usually spreads laterally to the pelvic sidewalls (similar to the spread of bladder flap hematoma), along the broad ligaments, or posteriorly to the rectovaginal septum. Sonographic findings are nonspecific because pelvic fluid collections, central cavity debris, clot, and air are all common findings postpartum (**Fig. 21–14**) (see Normal Postpartum Pelvis section). More specific findings include adnexal involvement such as pyosalpinx or tubo-ovarian abscess, whereas CT and MRI excel at demonstrating parametrial extension. Due to the nonspecificity of imaging findings, empirical antibiotic treatment may need to be started on clinical grounds alone, with imaging reserved for failure of response to therapy.

Summary

Clinical signs and symptoms in postpartum patients, typically bleeding, pain, and fever, are common and nonspecific. In most cases they likely reflect physiological response to the recent vaginal delivery or C-section. Although pelvic ultrasound is the best initial imaging modality for detecting many postpartum complications, it is important to be aware of the broad spectrum of normal findings in these patients to avoid misdiagnosis. This is especially true given current obstetric practice in the United States, where the C-section rate has reached 29%.[49] For practitioners, often the greatest utility of pelvic sonography may be the ability to exclude significant abnormalities related to the uterus and surrounding pelvic compartments. Careful analysis of both gray-scale and color Doppler findings is needed to maximize detection of retained placenta; cognizance of subinvolution of the placental site should prompt avoidance of unnecessary instrumentation and institution of appropriate medical treatment. Extra- and intrauterine hematomas have characteristic locations and sonographic appearances. Pelvic parametrial infection and POVT are uncommon but potentially significant complications; whereas sonography may be able to make these diagnoses, MRI and CT have greater diagnostic accuracy and may be preferable as the initial imaging study, or for follow-up if the pelvic ultrasound appears normal.

References

1. The puerperium. In: Cunningham FG, Leveno KJ, Bloom SL, Hanth JC, Gilstap L, Wenstrom K, eds. Williams Obstetrics. 22nd ed. New York: McGraw-Hill; 2005:695–710
2. Woo GM, Twickler DM, Stettler RW, et al. The pelvis after cesarean section and vaginal delivery: normal MR findings. AJR Am J Roentgenol 1993;161:1249–1252
3. Puerperal infection. In: Cunningham FG, Leveno KJ, Bloom SL, Hanth JC, Gilstap L, Wenstrom K, eds. Williams Obstetrics. 22nd ed. New York: McGraw-Hill; 2005:711–724
4. Zuckerman J, Levine D, McNicholas MM, et al. Imaging of pelvic postpartum complications. AJR Am J Roentgenol 1997;168: 663–668
5. Obstetric hemorrhage. In: Cunningham FG, Leveno KJ, Bloom SL, Hanth JC, Gilstap L, Wenstrom K, eds. Williams Obstetrics. 22nd ed. New York: McGraw-Hill; 2005:809–854
6. Twickler DM, Setiawan AT, Harrell RS, et al. CT appearance of the pelvis after Cesarean section. AJR Am J Roentgenol 1991;156: 523–526
7. Wachsberg RH, Kurtz AB, Levine CD, et al. Real-time ultrasonographic analysis of the normal postpartum uterus: technique, variability, and measurements. J Ultrasound Med 1994;13:215–221
8. Reles A, Ertan AK, Kainer F, et al. Doppler ultrasound images of the uterine artery and uterine involution in normal puerperium. Gynakol Geburtshilfliche Rundsch 1992;32:66–72
9. Sohn C, Fendel H, Kesternich P. Involution-induced changes in arterial uterine blood flow. Z Geburtshilfe Perinatol 1988;192: 203–209
10. Kirkinen P, Dudenhausen J, Baumann H, et al. Postpartum blood flow velocity waveforms of the uterine arteries. J Reprod Med 1988;33:745–748
11. Khong TY, Khong TK. Delayed postpartum hemorrhage: a morphologic study of causes and their relation to other pregnancy disorders. Obstet Gynecol 1993;82:17–22
12. Tekay A, Jouppila P. A longitudinal Doppler ultrasonographic assessment of the alterations in peripheral vascular resistance of uterine arteries and ultrasonographic findings of the involuting uterus during the puerperium. Am J Obstet Gynecol 1993;168: 190–198
13. Mulic-Luvica A, Bekuretsion M, Bakos O, et al. Ultrasonic evaluation of the uterus and uterine cavity after normal, vaginal delivery. Ultrasound Obstet Gynecol 2001;18:491–496
14. Edwards A, Ellwod DA. Ultrasonographic evaluation of the postpartum uterus. Ultrasound Obstet Gynecol 2000;16:640–643
15. Wachsberg RH, Kurtz AB. Gas within the endometrial cavity at postpartum US: a normal finding after spontaneous vaginal delivery. Radiology 1992;183:431–433
16. Antonelli E, Morales MA, Dumps P, et al. Sonographic detection of fluid collections and postoperative morbidity following Cesarean section and hysterectomy. Ultrasound Obstet Gynecol 2004;23: 388–392
17. Maldjian C, Adam R, Maldjian J, et al. MRI appearance of the pelvis in the post–Cesarean-section patient. Magn Reson Imaging 1999;172:223–227
18. Van den Bosch T, Van Schoubroeck D, Lu C, et al. Color Doppler and gray-scale ultrasound evaluation of the postpartum uterus. Ultrasound Obstet Gynecol 2002;20:586–591
19. Kurtz AB, Shlansky-Goldberg RD, Choi HY, et al. Detection of retained products of conception following spontaneous abortion in the first trimester. J Ultrasound Med 1991;10:387–395
20. Brown D. Pelvic ultrasound in the postabortion and postpartum patient. Ultrasound Q 2005;21:27–37

21. Hertzberg BS, Bowie JD. Ultrasound of the postpartum uterus: prediction of retained placental tissue. J Ultrasound Med 1991;109: 451–456
22. Sadan O, Golan A, Girtler O, et al. Role of sonography in the diagnosis of retained products of conception. J Ultrasound Med 2004; 23:371–374
23. Spirt BA, Cohen WN, Weinstein HM. The incidence of placental calcification in normal pregnancies. Radiology 1982;142:707–711
24. Wolman I, Jaffa AJ, Pauzner D, et al. Transvaginal sonography: a new aid in the diagnosis of residual trophoblastic tissue. J Clin Ultrasound 1996;24:257–261
25. Wolman I, Hartoov J, Pauzner D, et al. Transvaginal sonohysterography for the early diagnosis of residual trophoblastic tissue. J Ultrasound Med 1997;16:257–261
26. Laing FC, Frates MC. Ultrasound evaluation during the first trimester of pregnancy. In: Callen PW, ed. Ultrasonography in Obstetrics and Gynecology. Philadelphia: Saunders; 2000:127–128
27. Keogan MT, Hertzberg BS, Kliewer MA. Low resistance Doppler waveforms with retained products of conception: potential for diagnostic confusion with gestational trophoblastic disease. Eur J Radiol 1995;21:109–111
28. Achiron R, Goldenburg M, Lipitz S, et al. Transvaginal duplex Doppler ultrasonography in bleeding patients suspected of having residual trophoblastic tissue. Obstet Gynecol 1993;81:507–511
29. Alcazar JL. Transvaginal ultrasonography combined with color velocity imaging and pulsed Doppler to detect residual trophoblastic tissue. Ultrasound Obstet Gynecol 1998;11:54–58
30. Durfee SA, Frates MC, Luong A, et al. Sonographic and Color Doppler features of retained products of conception. J Ultrasound Med 2005;24:1181–1186
31. Andrew AC, Bulmer JN, Wells M, et al. Subinvolution of the uteroplacental arteries in the human placental bed. Histopathology 1989;15:395–405
32. Van Schoubroeck D, Van den Bosch T, Scharpe K, et al. Prospective evaluation of blood flow in the myometrium and uterine arteries in the puerperium. Ultrasound Obstet Gynecol 2004;23:378–381
33. Kelly SM, Belli AM, Campbell S. Arteriovenous malformation of the uterus associated with secondary postpartum hemorrhage. Ultrasound Obstet Gynecol 2003;21:602–605
34. Ichikawa Y, Nakauchi T, Sato T, et al. Ultrasound diagnosis of uterine arteriovenous fistula associated with placental site trophoblastic tumor. Ultrasound Obstet Gynecol 2003;21:606–608
35. Mungen E, Yergok YZ, Ertekin AA, et al. Color Doppler sonographic features of uterine arteriovenous malformations: report of two cases. Ultrasound Obstet Gynecol 1997;10:215–221
36. Timmerman D, Van den Bosch T, Peeraer K, et al. Vascular malformations in the uterus: ultrasonographic diagnosis and conservative management. Eur J Obstet Gynecol Reprod Biol 2000;92: 171–178
37. Mungen E. Vascular abnormalities of the uterus: have we recently over-diagnosed them? Ultrasound Obstet Gynecol 2003;21: 529–531
38. Timmerman D, Wauters J, Van Calenbergh S, et al. Color Doppler imaging is a valuable tool for the diagnosis and management of uterine vascular malformations. Ultrasound Obstet Gynecol 2003;21:570–577
39. Avva R, Shah HR, Angtuaco TL. US case of the day. Radiographics 1999;19:1089–1092
40. Noonan JB, Coakley FV, Qayyum A, et al. MR imaging of retained products of conception. AJR Am J Roentgenol 2003;181:435–439
41. Levine D, Hulka CA, Ludmir J, et al. Placenta accreta: evaluation with color Doppler US, power Doppler US, and MR imaging. Radiology 1997;205:773–776
42. Winsett MZ, Fagan CJ, Bedi DG. Sonographic demonstration of bladder-flap hematoma. J Ultrasound Med 1986;5:483–487
43. Weiner DM, Bowie JD, Baker ME, et al. Sonography of subfascial hematoma after cesarean delivery. AJR Am J Roentgenol 1987;148: 907–910
44. Hertzberg BS, Bowie JD, Kliewer MA. Complications of cesearean delivery: role of transperineal US. Radiology 1993;188:533–536
45. Maldjian C, Milestone B, Schnall M, et al. MR appearance of uterine dehiscence in the post-cesarean section patient. JCAT YEAR;22: 738–741
46. Kieser K, Baskett TF. A 10-year population-based study of uterine rupture. Obstet Gynecol 2002;100:749–753
47. Kaakaji Y, Nghiem HV, Nodell C, et al. Sonography of obstetric and gynecologic emergencies, I: Obstetric emergencies. AJR Am J Roentgenol 2000;174:641–649
48. Twickler DM, Setiawan AT, Evans RS, et al. Imaging of puerperal septic thrombophlebitis: prospective comparison of MR imaging, CT, and sonography. AJR Am J Roentgenol 1997;169:1039–1043
49. Goldberg C. NIH rethinks elective caeserean births. Boston Globe 2006;269:A2

Index

Note: Page numbers followed by *f* and *t* represent figures and tables respectively.

A
Abdomen
  ectopic pregnancy in, 107
  fetal, ultrasound assessment of, 168–172, 168*f*–171*f*
  right lower quadrant pain, appendicitis and, 18, 18*f*
Abdominal circumference, in fetal gestational age estimation, 138–139
Abdominal wall, fetal
  defects in
    elevated MS-AFP and, 189*t*, 193–194, 193*f*–194*f*
    gastroschisis. *See* Gastroschisis
    omphaloceles. *See* Omphaloceles
    polyhydramnios and, 145*f*, 146
  with normal umbilical cord insertion, 171, 171*f*
Abortion
  clinical classification of, 35
  outcome studies of, 35–36, 35*t*, 36*t*
  probability predictions, 35
  teratogenic drugs inducing, 228
Abscess, tubo-ovarian, 11, 16–17, 16*f*
Acardiac twin, 145
  nonimmune hydrops and, 148
ACE (angiotensin-converting enzyme) inhibitors, teratogenic effects of, 220, 220*f*
Acute pelvic pain
  appendicitis and, 18, 18*f*
  diagnostic evaluation in
    nonimaging tests, 11
    sonographic, 11–19, 12*f*–19*f*
  differential diagnosis of, 11
  ectopic pregnancy and, 13–14, 13*f*–14*f*
  endometrioma and, 17, 17*f*
  endometriosis and, 17, 17*f*
  inflammatory disease and, 16–17, 16*f*
  ovarian cysts and, 11–13, 12*f*–13*f*
  ovarian torsion and, 11, 14–15, 16*f*
  in postpartum patient, 238
  ureteral calculus and, 18–19, 19*f*
Adenocarcinoma, endometrial, tamoxifen therapy and, 91
Adenoma, pituitary, amenorrhea and, 58, 58*f*
Adenomyosis
  cause of, 26
  common complaints in, 26–27
  pathology of, 26, 27*f*
  sonographic diagnosis of, criteria for, 28–29, 29*t*
  sonographic features of, 27–28, 28*f*
  fibroids *vs.*, 29*t*
  treatment of, 29
Adnexa, TVS evaluation in ectopic pregnancy, 47, 47*f*
Adnexal masses
  asymptomatic palpable. *See* Palpable adnexal masses, asymptomatic
  in ectopic pregnancy evaluation, 105–106, 105*f*–107*f*
Adnexal torsion, first-trimester, 109, 109*f*
Adnexal tumors, 17–18
Adolescents
  amenorrhea in, 50–53. *See also* Amenorrhea
  virilization in, 60
Adrenal tumors, 17–18
  testosterone-producing, 60
AF-AFP. *See* Amniotic fluid-alpha-fetoprotein
AFP (alpha-fetoprotein)
  fetal gestational age and, 208
  maternal serum. *See* Maternal serum-alpha-fetoprotein
Alcohol, teratogenic effects on fetus, 225, 226*f*
Alpha-fetoprotein
  fetal gestational age and, 208
  maternal serum. *See* Maternal serum-alpha-fetoprotein
Amenorrhea
  definitions of, 50
  with delayed sexual development, 57–59, 57*f*–59*f*
  diagnostic evaluation in, 56–57, 56*t*
  eugonadism estrogenization and, 61–62, 61*f*–62*f*
  female adolescence with virilization and, 60
  in polycystic ovarian syndrome, 60–61, 60*f*
  primary, etiologies for, 56*t*
  pseudohermaphroditism and, 59–60, 59*f*
  secondary, 50
    causes of, 62–63, 62*f*
  vaginal obstruction and, 61–62, 61*f*–62*f*
Aminopterin, teratogenic effects of, 228
Amniocentesis
  amniotic fluid-AFP and, 188
  circumventing, cautions against, 188–189
  clubfoot risk and, 228
  in Down syndrome screening, 204
  fetal gestational age and, 208
  fetal loss rates following, 188
  following elevated MS-AFP, 188, 189
  indications for, 189
  in twin pregnancy, 144
Amniotic band syndrome, elevated MS-AFP and, 191, 191*f*
Amniotic fluid
  testing of. *See* Amniocentesis
  volume estimation, 145. *See also* Polyhydramnios
Amniotic fluid-alpha-fetoprotein
  elevated, follow-up sonography and, 188, 189
  testing for. *See* Amniocentesis
Amniotic Fluid Index, 145
Anembryonic pregnancy, outcome studies, 35–36, 35*t*
Anencephaly
  in diabetic pregnancy, 209, 212*f*
  elevated MS-AFP and, 190, 190*f*
Angiotensin-converting enzyme inhibitors, teratogenic effects of, 220, 220*f*
Angiotensin II receptor antagonists, teratogenic effects of, 220, 220*f*
Annular pancreas, fetal, polyhydramnios and, 169
Anomalous pulmonary venous return, in fetal heart examination, 176, 181
Anorexia nervosa, amenorrhea and, 57–58
Anticancer agents, teratogenic effects of, 224
Anticardiolipin antibodies, early pregnancy loss and, 34
Anticoagulants, teratogenic effects of, 222–223, 223*f*
Anticonvulsants, teratogenic effects of, 222, 222*f*
Antiphospholipid antibodies, early pregnancy loss and, 34
Antithyroid agents, teratogenic effects of, 221
Aorta, fetal heart
  coarctation of the. *See* Coarctation of the aorta
  normal, 209, 211*f*
  overriding, 183–184, 183*f*
  parallel pulmonary artery and, 184, 184*f*
Aortic arch abnormality
  teratogen-induced, 223
  type B interrupted, chromosome deletions and, 175
Aortic valve stenosis
  in congenital heart disease, 174–175
  in fetal heart examination, 176
    critical form, 182, 182*f*
APAs (antiphospholipid antibodies), early pregnancy loss and, 34
Appendicitis, acute pelvic pain and, 18, 18*f*
Arnold-Chiari malformation. *See* Chiari II malformation
ARPD. *See* Autosomal recessive polycystic disease
Arteriovenous malformations, myometrial, in postpartum patient, 244*f*, 245
ASD (atrial septal defect), in fetal heart examination, 176
Atrial septal defect, in fetal heart examination, 176
Atrioventricular canal defect, fetal
  in Down syndrome, 200, 200*f*
  in heart assessment, 180, 180*f*
Atrophy, endometrial, in postmenopausal women, 94
Autosomal recessive polycystic disease, fetal, 170, 170*f*
AVCD. *See* Atrioventricular canal defect
AVMs (arteriovenous malformations), myometrial, in postpartum patient, 244*f*

B
Ballooning membranes, in evaluation of cervix, 123, 123*f*
"Banana" sign, fetal head, 165, 165*f*
  elevated MS-AFP and, 191, 191*f*, 192
Bed rest, for incompetent cervix, 127
Benign ovarian tumors, ultrasound evaluation of, 6–7, 6*f*–7*f*
Bicornuate uterus, 52–53, 53*f*

Binocular distance, in fetal gestational age estimation, 140, 140*f*
Biopsy, endometrial. *See* Endometrial biopsy
Biparietal diameter
in fetal gestational age estimation, 135*t*, 136, 136*f*
difficulties measuring perimeter, 136–137
in fetal head assessment, 161–162, 162*f*
in spina bifida, 192
Biparietal perimeter, difficulties measuring, 136–137
Bladder. *See* Urinary bladder
Bladder flap hematomas, post-Cesarean section, 246–247, 246*f*–247*f*
Bleeding
menstrual. *See* Menstrual bleeding
in obstetric patient
causes of, 32
and early pregnancy failure. *See* Early pregnancy failure
extrauterine gestation and, 37, 37*t*
in first trimester. *See* First-trimester bleeding
in heterotopic pregnancy, 37
intrauterine gestation and, 32–37, 32*f*, 33*f*
in second and third trimesters. *See* Second/third trimester bleeding
postmenopausal. *See* Postmenopausal vaginal bleeding
in postpartum patient, 237–238, 238*f*
Blighted ovum. *See* Early pregnancy failure
Bowel
hyperechoic, in fetal Down syndrome, 202, 202*f*
obstructed, in cocaine-exposed fetus, 227, 227*f*
Brain, fetal, circle of Willis and, 157
Brain-sparing reflex, fetal growth restriction and, 158
BRCA 1 and BRCA 2 genes, and increased ovarian cancer risk, 76
Breast cancer
morbidity and mortality in, 90
tamoxifen therapy for, 90
and endometrial cancer risk, 91–92

C

Calcifications
adenomyosis and, 28
uterine fibroids, 26
Calculus disease, ureteral, 18–19, 18*f*
Cancer antigen 125
adnexal lesions and, 1
ovarian cancer and, 77
Carcinoma
breast. *See* Breast cancer
endometrial. *See* Endometrial cancer
ovarian. *See* Ovarian carcinoma
Cardiac abnormalities, fetal
chromosome deletions and, 175
in diabetic mother, 209, 209*f*
polyhydramnios and, 150, 152*f*
Cardiac outflow tracts, fetal, 167–168, 168*f*
abnormalities in, 183–184, 183*f*–184*f*
considerations, 178*t*
left ventricular, 177, 177*f*
normal aortic, 209, 211*f*
right ventricular, 177, 178*f*
Cardiac tumors, in fetal heart examination, 182–183, 183*f*
Cardiac ventricles, fetal, hypoplastic, 167, 167*f*
Cardiomyopathy, fetal, in diabetic pregnancy, 209, 212*f*
Cardiovascular malformations, teratogen-induced, 223–224
Caudal regression syndrome, in fetus of diabetic mother, 209, 210*f*
CDS. *See* Color Doppler sonography
Central nervous system abnormalities, fetal
polyhydramnios and, 148, 149*f*
teratogen-induced, 223
Central vascularity, in adenomyosis, 28
Cephalocele, elevated MS-AFP and, 192–193
occipital, 193, 193*f*
prognosis for, 193
Cerclage placement, for incompetent cervix, 127, 127*f*
Cerebellar diameter, transverse, in fetal gestational age estimation, 139, 140*f*
Cerebral infarction, in cocaine-exposed fetus, 227, 227*f*
Cerebral ventricles, in fetal head assessment, 161, 163–164, 163*f*–164*f*
Cerebral ventriculomegaly, fetal
in fetal Down syndrome, 200, 200*f*
posterior fossa deformity and, 192
Cervical length, measurement of, 124, 124*f*
with cervical sonography, 125
in normal pregnancy, 124–125
pitfalls in, 123, 123*f*
Cervical sonography
cervical length measurements with, 125
fetal fibronectin test with, 125
in incompetent cervix, 125–128, 126*f*–128*f*
in premature labor, 121, 121*f*–122*f*
cervical length, 124, 124*f*
technical aspects, 122*f*–124*f*, 123–124
in premature rupture of fetal membranes, 128–129
preterm delivery prediction by, 125
Cervix
imaging criteria, 124
incompetent, 125–128, 126*f*–128*f*
lacerated, in postpartum patient, 237, 238*f*
in normal pregnancy, 124–125
in premature labor, sonographic evaluation of, 121, 121*f*–122*f*
cervical length, 124, 124*f*
technical aspects, 122*f*–124*f*, 123–124
role in pregnancy, 121
Cesarean section
hematomas after, 246–247, 246*f*–247*f*
normal postsurgical pelvic changes, 239, 241*f*
prior, placenta accreta association with, 116
CHD. *See* Congenital heart disease
Chiari II malformation, fetal, 165, 165*f*, 192
Chlamydia trachomatis, pelvic inflammatory disease and, 16
Chorioangioma, 150, 152, 153*f*
Chorionic villus sampling, 228
Choroid plexus, in fetal head assessment, 163, 163*f*, 164–165, 164*f*
Choroid plexus cysts
in fetal Down syndrome, 202
in fetal head assessment, 164–165, 164*f*
Chromosomal abnormalities, fetal
cardiac anomalies and, 175
polyhydramnios and, 148, 150, 151*f*–152*f*
Cigarette smoking, teratogenic effects on fetus, 228
Circle of Willis, fetal brain and, 157
Circumvallate placenta, 116–117, 117*f*
Clavicular length, in fetal gestational age estimation, 139
Cleft lip and palate
in fetal head assessment, 165
polyhydramnios and, 151*f*
Clubfoot
amniocentesis and, 228
in fetal extremity assessment, 172, 172*f*
polyhydramnios and, 152*f*
CMV (cytomegalovirus), teratogenic effects of, 229, 230*f*
Coarctation of the aorta, in fetal heart examination, 176
false-positive diagnosis, 180–181
four-chamber view, 180–181, 180*f*–181*f*
Cocaine, teratogenic effects of, 225–228, 227*f*
Cog wheel appearance, hydrosalpinx and, 4
Color Doppler sonography
in ectopic pregnancy evaluation, 103, 104*f*–107*f*, 105–106
following methotrexate treatment, 106
of female reproductive organs, 56
of fetal heart, 177
in gestational trophoblastic disease, 108, 108*f*
in ovarian cancer screening, 85–87, 86*f*
in postpartum patient, 238–239, 238*f*
of uterine arteries, 95
Complete abortion
defined, 35
incomplete abortion *vs.,* 107*f*, 108
outcome studies of, 35–36, 35*t*
Complete central placenta previa, 114, 114*f*
Complete heart block, fetal, 152*f*
Computed tomography, pelvic, in uterine dehiscence, 247, 247*f*
Congenital anomalies
in diabetic pregnancy, 209, 210*f*–213*f*, 212–213
detection rate, 209
mechanisms, 212–213
risk estimates, 209
gynecologic, 52
renal agenesis associated with, 52, 52*f*
Congenital (Finnish) nephrosis, elevated MS-AFP and, 195
Congenital heart disease
aortic valvular stenosis and, 174–175
family history of, 174–184
hereditary issues for, 174–175
prenatal ultrasound examination for. *See* Fetal heart
prevalence of, 174
risks factors for, 174–175
Congenital syphilis, 231–232, 232*f*
Conjoined twins, 143, 144*f*
Contact bleeding, 32
Contractions
low uterine, simulating placenta previa, 114*f*, 115
myometrial retroplacental, hematoma and, 111
Controlled ovarian stimulation, ultrasound monitoring and, 44, 44*f*

Corpus luteal cysts, 2, 12–13, 12*f*
hemorrhagic, 13, 13*f*
Corpus luteum
in ectopic pregnancy evaluation, 105–106, 105*f*
in normal menstrual cycle, 50–51, 51*f*
Corrected transposition, fetal heart, 184
Corticosteroids, systemic, teratogenic effects of, 225
Craniofacial defects, teratogen-induced, 223–224
Crown-rump length, in fetal gestational age estimation, 134*f*, 134*t*.320, 136
CT (computed tomography), pelvic, in uterine dehiscence, 247, 247*f*
CVS (chorionic villus sampling), 228
Cyclophosphamide, teratogenic effects of, 224
Cystic hygroma. *See* Hydroma, cystic fetal
Cyst(s)
choroid plexus. *See* Choroid plexus cysts
corpus luteum. *See* Corpus luteal cysts
myometrial, in adenomyosis, 27–28
Nabothian, 128, 128*f*
ovarian. *See* Ovarian cysts
as palpable adnexal masses
dermoid, 5–6, 5*f*–6*f*, 7
hemorrhagic, 2–3, 2*f*
paraovarian and paratubal, 3–4, 3*f*
peritoneal inclusion cysts, 4, 4*f*
physiological, 1–2, 3*f*–4*f*
in premenarchal ovaries, 55, 55*f*
Cytologic examination, in abnormal uterine bleeding evaluation, 21
Cytomegalovirus, teratogenic effects of, 229, 230*f*

D

Dandy-Walker malformation, in fetal head assessment, 164*f*, 165
Dating, of pregnancy. *See* Pregnancy dating
Dermoid cysts, as palpable adnexal masses, 5–6, 5*f*–6*f*, 7
Dermoid plug, 5
ovarian teratomas and, 82–83, 84*f*
DES (diethylstilbestrol), teratogenic effects of, 225
Diabetes
gestational. *See* Gestational diabetes
pregestational. *See* Diabetic pregnancy
Diabetic pregnancy
classification of, 208
fetal biometry evaluation in, 208
fetal congenital malformations in, 209, 210*f*–213*f*, 212–213
detection rate, 209
mechanisms, 212–213
risk estimates, 209
fetal growth disturbances in, 213–214
fetal risks and, 208
fetal weight estimation and, 213, 214
pathophysiology, 208
polyhydramnios and, 146
Diaphragmatic hernia, fetal heart displacement by, 167, 167*f*
Diethylstilbestrol, teratogenic effects of, 225
DiGeorge syndrome, chromosome deletions and, 175
Dilatation and curettage
in abnormal uterine bleeding evaluation, 22
retained placenta and, 242, 242*f*, 245
"Discriminatory zone," in ectopic pregnancy evaluation, 103
Doppler flow imaging
in infertility evaluation, 41
in postpartum uterine evaluation
hematoma, 243, 243*f*
retained placenta, 242*f*
in pregnancy dating, 156
fetal growth restriction and. *See* Intrauterine growth restriction
middle cerebral circulation and, 157–158, 157*f*
umbilical arterial circulation and, 156–157, 157*f*
DORV (double-outlet right ventricle), in fetal heart examination, 184
"Double bubble" sign, elevated MS-AFP and, 195, 195*f*
Double-outlet right ventricle, in fetal heart examination, 184
Down syndrome, fetal
diagnostic evaluation in, 206
genetic sonogram and. *See* Genetic sonogram, of second-trimester fetus
maternal age and, 199
risk estimate for, 199
serum screens for, 199
abnormal, 205–206
and sonographic signs in second-trimester fetus, 201–204, 202*f*–204*f*
structural defects, 199–201, 200*f*–201*f*
Duodenal atresia, fetal
elevated MS-AFP and, 195, 195*f*
in fetal Down syndrome, 199, 200*f*
polyhydramnios and, 146–147, 146*f*, 168*f*, 169
Dysfunctional uterine bleeding, 29
Dysmenorrhea, in adenomyosis, 26
Dyspareunia, in adenomyosis, 26–27
Dysplastic kidney, fetal, 170, 170*f*
multicystic, 170, 170*f*

E

Ear length, in fetal Down syndrome, 203, 203*f*
Early pregnancy, diagnosis of, 46
Early pregnancy failure
assessment of, 46
with bleeding, 35
classification, 35
clinical outcome studies, 35–36, 35*t*, 36*t*
sonographic findings, 36–37, 37*f*
causes of, 34
without bleeding, 34, 34*t*
Ebstein's anomaly
in fetal heart assessment, 167
four-chamber view, 182, 182*f*
teratogen-induced, 224, 224*f*
Echocardiography, M-Mode, in fetus, 152*f*
Echogenicity
in adenomyosis, 27, 27*f*–28*f*
of endometrial polyps, 29–31, 30*f*–31*f*
of fetal heart tumors, 183
of intracardiac foci, in fetal Down syndrome, 202, 202*f*
of premenarchal ovaries, 55, 55*f*
of uterine fibroids, 22, 23*f*–25*f*
Echotexture
endometrial, 96, 97*f*
of ovarian mass, 82–84, 82*f*–84*f*
Ectopic kidney, fetal, 169, 169*f*
Ectopic pregnancy, 13–14, 13*f*–15*f*, 37
abdominal, 107
assessment of, 46–47, 47*f*
clinical findings for, 103
interstitial, 106
secondary amenorrhea and, 62–63, 62*f*
sonographic criteria for, 37*t*
termination of, methotrexate for, 228
"bizarre" response to, 106
ultrasound evaluation of, 103–107, 104*f*–107*f*
uncommon types of, 106–107
Effusions, pleural, in fetal Down syndrome, 200, 201*f*
Embryology, genital, 52–53, 52*f*–53*f*
Embryonic demise, in threatened abortion, 108, 108*f*
EMV (enhanced myometrial vascularity), 245
Encephalocele, 162, 162*f*
Endocervical canal, normal changes *vs.* polyps within, 30, 30*f*
Endometrial biopsy
in abnormal uterine bleeding evaluation
postmenopausal, 71
premenopausal, 21
in diagnostic workup algorithm, 71, 73*f*
tamoxifen therapy and, 101
Endometrial cancer
tamoxifen therapy and, 91–92
transvaginal sonography evaluation of, 95–96, 96*f*–97*f*
benefits, 96, 97*f*–98*f*
Endometrial fluid, in postmenopausal patients, 95
Endometrial polyps, 29–31, 30*f*–31*f*, 95, 95*f*–96*f*
with complex hyperplasia, 98*f*
with cystic change, 97, 99, 99*f*–100*f*
histology of, 29–30
sonographic diagnosis of
criteria for, 30–32, 30*f*–31*f*
hysteroscopy in, 30–31
hysterosonography technique in, 30–31
3-D sonography and, 70, 70*f*
treatment of, 31
Endometrial thickness, postmenopausal
carcinoma and, 94–95
hormone replacement therapy and, 67–68, 93, 94
outcome studies of, 66–67, 67*f*, 67*t*
sonographic evaluation of
benefits, 71
diagnostic workup algorithm for, 71, 72*f*
diffuse thickening and, 69–70, 69*f*
in endometrial hyperplasia, 68, 68*f*
in malignancy, 68, 68*f*
Endometriomas
acute pelvic pain and, 17, 17*f*
appearance of, 43, 43*f*
as palpable adnexal masses, 5, 5*f*
Endometriosis, 17, 17*f*
Endometriosis interna. *See* Adenomyosis
Endometritis, in postpartum patient, 248*f*, 249
Endometrium
in postmenopausal women, sonographic evaluation of
transabdominal, 92, 92*f*
transvaginal, 92–93, 93*f*
response to tamoxifen. *See* Tamoxifen, endometrial responses to

Endovaginal sonography, 11, 19, 19*f*
in abnormal uterine bleeding evaluation, 22
adenomyosis diagnosis with, criteria for, 28–29
in endometrial polyp diagnosis, 28–29
in placenta previa, 115–116, 116*f*
Enhanced myometrial vascularity, 245
Epiphyses, stippled, teratogen-induced, 222–223, 223*f*
Esophageal atresia, fetal
elevated MS-AFP and, 195, 195*f*
polyhydramnios and, 146–147, 146*f*, 147*f*
Estrogenization, eugonadism, amenorrhea and, 61–62, 61*f*–62*f*
Estrogens, teratogenic effects of, 224–225
Ethanol exposure, teratogenic effects on fetus, 225, 226*f*
Eugonadism estrogenization, amenorrhea and, 61–62, 61*f*–62*f*
EVS. *See* Endovaginal sonography
Exophytic myoma, ovarian, 7–8
Extrauterine pregnancy. *See* Ectopic pregnancy
Extremities, fetal
lower
clubfoot and. *See* Clubfoot
normal, 172, 172*f*
ultrasound assessment of, 172, 172*f*
upper, defects of. *See* Upper limb defects

F

Fallopian tube(s)
dilated, as palpable adnexal mass, 4–5, 4*f*
evaluation in infertility, 41–42, 41*f*
False-positives
in coarctation of the aorta, 180–181
in devitalized placenta accreta, 238*f*, 239
in endometrial malignancy, 95
in fetal Down syndrome, 199
in incompetent cervix, 122*f*, 128, 128*f*
and maternal serum-AFP, 188
in placenta previa, 115
in retained products of conception, 242, 242*f*
Feet. *See* Clubfoot
Female pseudohermaphroditism (intersex), 59
Femur length
in fetal gestational age estimation, 137–138, 138*t*, 139*f*
short, in fetal Down syndrome, 202
Fetal alcohol syndrome, 225, 226*f*
Fetal anomalies
anatomical structures to be assessed for, 161, 161*t*
etiology of, 161
incidence of, 161
Fetal biometry, 133
abdominal circumference in, 138–139
best parameters to use, 141
binocular distance in, 140, 140*f*
biparietal diameter in, 135*t*, 136, 136*f*
difficulties measuring perimeter, 136–137
cerebellar diameter in, transverse, 139, 140*f*
clavicular length in, 139
crown-rump length in, 134*f*, 134*t*.320, 136
femur in, 137–138, 138*t*.325*f*
head circumference in, 136*f*, 137, 137*f*
humerus length in, 138, 138*t*, 139*f*
long bones in, 137–138, 138*t*.325*f*
mean gestational sac diameter in, 133–134, 133*t*
measurement errors in, 141
nuchal translucency in, 139–140, 140*f*
other measures in, 140
placental thickness in, 140
problems raised in, 141
renal length in, 140
Fetal brain, circle of Willis and, 157
Fetal fibronectin test, with cervical sonography, 125
Fetal gestational age, estimating, methods for, 133. *See also* Fetal biometry
best parameters to use, 141
in diabetic mother, 208
where parameters suggest different age, 141
Fetal heart, ultrasound evaluation of, 167–168, 167*f*–168*f*
for congenital heart disease
four-chamber view, abnormalities found on, 178*t*, 179–183, 179*f*–183*f*. *See also* Four-chamber view
general aspects of, 176–179, 176*f*–178*f*, 178*t*
identification sensitivity, 175–176
timing of, 175
Fetal spine
dysraphism of
detection of, 190–192, 191*f*
teratogen-induced, 222, 222*f*
ultrasound assessment of, 166–167, 166*f*–167*f*
elevated MS-AFP and, 190–192, 191*f*
Fetus. *See also* Fetal *entries*
demise of, 36
early pregnancy loss and, 34
genital embryology in, 52–53, 52*f*–53*f*
growth restriction in. *See* Intrauterine growth restriction
teratogen exposure and
alcohol and recreational drugs, 225–228
hormones, 224–225
identifying, 217–219, 218*t*
infectious agents, 229–232
in obstetrical intervention and procedures, 228
pharmaceuticals, 219–224
principles, 216–217, 217*f*
radiation and heat, 228–229
ultrasound evaluation in, 219
tumors in, polyhydramnios and, 150, 152, 153*f*
ultrasound assessment of
abdomen, 168–172, 168*f*–171*f*
for Down syndrome. *See* Down syndrome, fetal
extremities, 172, 172*f*
face, views for examining, 165–166, 165*f*–166*f*
genetic sonogram. *See* Genetic sonogram
head, 161–166, 161*f*–166*f*
heart. *See* Fetal heart
recommended anatomical structures in, 161, 161*t*
spine. *See* Fetal spine
weight estimation, 213–214
Fever, in postpartum patient, 238
Fibroid tumors, uterine, 152, 153*f*, 154
Fibroids, uterine, 40, 40*f*
diagnosis of, 26
IVF and pregnancy success rates with, 40
pathology of, 22, 23*f*
sonographic findings in, 22, 23*f*–25*f*, 25–26, 29*t*
adenomyosis *vs.*, 29*t*
treatment of, 26
Fibroma, benign ovarian, 7, 7*f*
Finger, fifth digit phalanx, in fetal Down syndrome, 203, 203*f*
Finnish nephrosis, elevated MS-AFP and, 195
First-trimester bleeding
adnexal torsion and, 109, 109*f*
ectopic pregnancy and, 103–107, 104*f*–107*f*
in gestational trophoblastic disease, 108, 108*f*
threatened abortion and, 107–108, 107*f*–108*f*
ultrasound evaluation modalities used in, 103
First-trimester pregnancy loss. *See* Early pregnancy failure
Fluid collections, abnormal, in fetal Down syndrome, 200–201, 201*f*
Follicle stimulating hormone, 50
Follicular cysts, ovarian, 12–13, 12*f*
Follicular phase, in normal menstrual cycle, 50, 51*f*
Foot. *See* Clubfoot
Four-chamber view, fetal heart, 167, 176, 176*f*, 177, 177*f*
abnormalities to be considered in, 178, 178*t*
cardiomyopathy in, 209, 212*f*
in diabetic mother, 209*f*
enlarged right atrium in, 182, 182*f*
key features of, 177–178
left ventricle smaller than right ventricle in, 180–181, 180*f*–181*f*
masses within cardiac chambers in, 182–183, 183*f*
normal, 209, 211*f*
right vertical smaller than left ventricle in, 181–182, 181*f*–182*f*
septal defects in, 179–180, 179*f*–180*f*
Frontal bones, flattened, of fetal head, 162, 163*f*
FSH (follicle stimulating hormone), 50

G

Gastrointestinal obstruction, fetal, polyhydramnios and, 145*f*–147*f*, 146–147
Gastroschisis, in fetal abdominal wall, 171–172, 171*f*
elevated MS-AFP and, 189*t*, 193–194, 194*f*
Genetic sonogram, of second-trimester fetus, 204–205
following abnormal serum screens, 205–206
Germ cell tumors, ovarian, 7–8, 7*f*
Gestational age, fetal. *See* Fetal gestational age
Gestational diabetes
fetal congenital malformations in, 213
fetal macrosomia associated with, 214
fetal risks and, 208
Gestational sac, intrauterine, in pregnancy diagnosis, 46
Gestational trophoblastic disease, 108, 108*f*

Glucocorticoids, teratogenic effects of, 225
Gonadotropin releasing hormone, 50, 52
Graafian follicle, 50, 51*f*
Gray-scale morphology, in ovarian cancer screening, 78–84, 78*f*
  ovarian mass and
    echotexture, 82–84, 82*f*–84*f*
    septa within, 78, 81*f*–82*f*
    wall features, 78, 80*f*
  ovary size and, 78
Great vessels, fetal heart, 167–168, 168*f*
  transposition of, 184, 184*f*
"Ground-glass" appearance, of endometrioma, 5, 5*f*, 43, 43*f*

H
hCG. *See* Human chorionic gonadotropin
Head circumference, in fetal gestational age estimation, 136*f*, 137, 137*f*
Heart, fetal. *See* Fetal heart, ultrasound evaluation of
Heat exposure, fetal, 229
  teratogenic effects of, 228–229
HELLP syndrome, in postpartum patient, 238, 238*f*
Hematoma
  avascular, *vs.* vascular retained products of conception, 243, 243*f*
  post-Cesarean section, 246–247, 246*f*–247*f*
  retroplacental, 111–112, 111*f*–112*f*, 113
Hematometrocolpos, amenorrhea and, 61–62, 61*f*–62*f*
Hemorrhage, subchorionic, normal intrauterine gestation with, 33, 33*f*
Hemorrhagic cysts, as palpable adnexal masses, 2–3, 2*f*
Hereditary nonpolyposis colorectal cancer syndrome, and increased ovarian cancer risk, 76
Hernia, diaphragmatic, fetal heart displacement by, 167, 167*f*
Heroin, teratogenic effects of, 228
Herpes simplex virus, teratogenicity of, 232
Heterotopic pregnancy, 37
High-intensity focused ultrasound, for fibroid ablation, 26
High-risk patients, ovarian carcinoma screening in, 77
  history and physical examination, 77
  serum CA 125 levels, 77
  sonographic, 77–87, 78*f*–86*f*
HIV (human immunodeficiency virus), teratogenic effects of, 232
HLHS (hypoplastic left heart syndrome), in fetal heart examination, 180, 180*f*
Holoprosencephaly, 163–164, 164*f*
Hormone exposure, teratogenic effects of, 224–225
Hormone replacement therapy, postmenopausal
  bleeding and, 93–94
  endometrial thickness and, 67–68
Human chorionic gonadotropin, 103
  in gestational trophoblastic disease, 108, 108*f*
  maternal serum, fetal Down syndrome and, 199
Human immunodeficiency virus, teratogenic effects of, 232
Humerus length
  in fetal gestational age estimation, 138, 138*t*, 139*f*
  short, in fetal Down syndrome, 202
Hydrocephalus, 163, 163*f*
  teratogen-induced, 223
Hydroma, cystic fetal, elevated MS-AFP and, 194, 194*f*
Hydronephrosis, fetal, diagnostic criteria for, 169–170, 169*f*
Hydrops
  nonimmune, 147–148, 147*f*–148*f*
  polyhydramnios and, 148
Hydrops fetalis, in fetal Down syndrome, 200, 201*f*
Hydrosalpinx, 41–42, 41*f*
  as palpable adnexal mass, 4–5, 4*f*
Hygroma, cystic fetal, 153*f*
  nuchal, in Down syndrome, 200, 201*f*
Hyperglycemia, fetal congenital malformations and, 213
Hypermenorrhea, 22–29, 23*f*–25*f*, 27*f*–28*f*, 29*t*
Hyperplasia, endometrial, 67, 68, 68*f*
Hyperthermia, effect on fetus, 229
Hypervascularity, endometrial, 95–96, 95*f*–97*f*
Hypogonadism
  hypergonadotropic, 58–59, 59*f*
  hypogonadotropic, 57–58, 58*f*
Hypomenorrhea, 29
Hypoplastic left heart syndrome, in fetal heart examination, 180, 180*f*
Hypoplastic mandible, in fetal head assessment, 165, 166
Hypospadias, in diabetic pregnancy, 212, 213*f*
Hypothalamic dysfunction, amenorrhea and, 57
Hysterosalpingography
  in abnormal uterine bleeding evaluation, 21
  in postmenopausal vaginal bleeding evaluation, 66
Hysteroscopy
  in endometrial evaluation, 99–100
  in endometrial polyp diagnosis, 30–31
  in postmenopausal vaginal bleeding evaluation, 71
Hysterosonography. *See* Sonohysterography

I
Iliac angle, in fetal Down syndrome, 202*f*, 203
Immunologic disorders, early pregnancy loss and, 34
In vitro fertilization
  pregnancy dating and, 46
  pregnancy success rates and, 40
  transvaginal sonography role in, 45, 45*f*
Incompetent cervix, 125–128, 126*f*–128*f*
Incomplete abortion
  defined, 35
  outcome studies of, 35–36, 35*t*
  vs. complete abortion, 107*f*, 108
Inevitable abortion
  defined, 35
  outcome studies of, 35–36
Infants, preterm. *See* Premature infants
Infected abortion
  defined, 35
  outcome studies of, 35–36
Infection
  pelvic inflammatory disease and, 16
  postpartum pelvic, 248*f*, 249
Infectious agents, teratogenic effects of, 229–232
  parasitic, 229, 231*f*
  viral. *See* Viral infections, fetal exposure to
Infertility
  age and, 39
  defined, 39
  diagnosis of, 39
  and early pregnancy diagnosis, 46
  treatments for, monitoring, 43
    ovarian response, 44–45, 44*f*–46*f*
    uterine response, 43–44
  ultrasound evaluation in
    fallopian tubes, 41–42, 41*f*
    ovaries, 42–43, 42*f*–43*f*
    transvaginal sonography, 39
    uterus, 39–41, 39*f*–41*f*
Inflammatory bowel disease, amenorrhea in, 57, 58*f*
Inhibin-A, fetal Down syndrome screening and, 199
Intermenstrual bleeding, 29–31, 30*f*–31*f*
Interocular distance, in fetal gestational age estimation, 140, 140*f*
Interstitial ectopic pregnancy, 106
Intestinal obstruction, in cocaine-exposed fetus, 227, 227*f*
Intrauterine gestation, bleeding and, 32–37
  early pregnancy failure, 34. *See also* Early pregnancy failure
  normal, 32, 32*f*
    with subchorionic hemorrhage, 33, 33*f*
Intrauterine growth restriction
  cardiac anomalies in, 181
  defined, 156
  in diabetes pregnancy, 214
  Doppler flow imaging in
    arterial, 158
    findings, 158–159
    venous, 158, 158*f*
  pathophysiology of, 159
Intrauterine mass, subchorionic hematoma mimicking, 112–113, 112*f*–113*f*
Intrauterine membranes, subchorionic hematoma and, 112, 112*f*
Involution, placental implantation site, 243–244
Iodine-131, teratogenic effects of, 221
Ischemia, uterine fibroid sensitivity to, 26
IUGR. *See* Intrauterine growth restriction
IVF. *See* In vitro fertilization

K
Kidneys. *See also* Renal *entries*
  fetal, ultrasound assessment of, 169, 169*f*
    autosomal recessive polycystic, 170, 170*f*
    dysplastic, 170, 170*f*
    multicystic dysplastic, 170, 170*f*

L
Laparoscopic surgery
  for asymptomatic palpable adnexal masses, 1, 8–9
  for ectopic pregnancy, 14
Lateral ventricles, in fetal head assessment, 163, 163*f*
Left ventricle, fetal heart
  right ventricle smaller than, 181–182, 181*f*–182*f*
  smaller than right ventricle, 180–181, 180*f*–181*f*

Legs. *See* Lower extremities
Leiomyoma(s). *See also* Fibroids, uterine
  retroplacental, 111, 112*f*
  uterine, 95–96, 96*f*
"Lemon" sign, fetal head, 162, 163*f*
  elevated MS-AFP and, 191–192, 191*f*
LH (luteinizing hormone), 50
Limb defects
  chorionic villus sampling implicated in, 228
  upper. *See* Upper limb defects
Limb–body wall complex, elevated MS-AFP and, 191, 191*f*
Lithium, teratogenic effects of, 224, 224*f*
LMP (low malignant potential lesions), ovarian, 6
Long bone length, in fetal gestational age estimation, 137–138, 138*t*, 139*f*
Low birth-weight infants. *See* Premature infants
Low uterine contractions, simulating placenta previa, 114*f*, 115
Lower extremities, fetal
  clubfoot and. *See* Clubfoot
  normal, 172, 172*f*
LSD (lysergic acid diethylamide), teratogenic effects of, 228
Luteal phase, in normal menstrual cycle, 50–51, 51*f*
Luteinizing hormone, 50
Lymphoma, ovarian mass and, 84, 84*f*
Lynch II syndrome, and increased ovarian cancer risk, 76
Lysergic acid diethylamide, teratogenic effects of, 228

M
Macroglossia, in fetal Down syndrome, 200, 200*f*
Macrosomia, fetal, in diabetic pregnancy, 213–214
Magnetic resonance imaging
  of adnexal lesions, 1
  in congenital uterine anomalies, 54, 55*f*
  of pituitary adenoma, 58, 58*f*
  in postmenopausal vaginal bleeding evaluation, 66
Magnetic resonance venography, in postpartum ovarian vein thrombophlebitis, 247, 248*f*
Male pseudohermaphroditism (intersex), 59–60
Mandible, hypoplastic, in fetal head assessment, 165, 166
Marginal placenta previa, 115–116, 115*f*
Marijuana, teratogenic effects of, 228
Maternal age, early pregnancy loss and, 34
Maternal serum-alpha-fetoprotein
  decreased, Down syndrome and, 199. *See also* Down syndrome, fetal
  elevated
    amniocentesis following, 188, 189
    fetal defects observed with, 189–196, 189*t*, 190*f*–195*f*
    targeted sonography following, 188, 189
  screening programs with, 187
    patient triage in, 188–189
  sources of, 187–188
Maternal serum radioassay, 103
Mayer–Rokitansky-Küster-Hauser syndrome, 52, 62
MDS. *See* Mullerian duct system
Mean gestational sac diameter, in fetal gestational age estimation, 133–134, 133*t*
Meckel's syndrome, occipital cephalocele and, 193
Membranes
  fetal, premature rupture of, 128–129
  intrauterine, subchorionic hematoma and, 112, 112*f*
Menarche, 52
Meningomyelocele. *See* Myelomeningocele
Menometrorrhagia, 32
Menorrhagia
  in adenomyosis, 26
  uterine fibroids and. *See* Fibroids, uterine
Menses. *See* Menstrual bleeding
Menstrual bleeding
  abnormal flow in, 22. *See also* Nonpregnant patient, bleeding in
  absence of
    in adolescent or young adult. *See* Amenorrhea
    at menopause. *See* Postmenopausal women
    defined, 50
    in menstrual cycle, 50–51, 51*f*
    physiology of, 51–52
Menstrual cycle, 50–51, 51*f*
  folliculogenesis in, 42, 42*f*
  in infertility evaluation, 40*f*, 41
Methotrexate
  for ectopic pregnancy termination, 228
    "bizarre" response to, 106
  teratogenic effects of, 228
Metrorrhagia, 29–31, 30*f*–31*f*
Microcysts, in premenarchal ovaries, 55, 55*f*
Micromelia, thalidomide exposure and, 220, 220*f*
Middle cerebral circulation, Doppler flow imaging of, 157–158, 157*f*
Miscarriage rates, 35
Misoprostol, teratogenic effects of, 221, 221*f*
Missed abortion. *See also* Early pregnancy failure
  defined, 35
  outcome studies of, 35–36, 35*t*
Mittelschmerz, 11–12
Mobius sequence, misoprostol exposure and, 221, 221*f*
Molar pregnancy, 35*t*, 152, 153*f*
Monochorionic-diamniotic twin pregnancy, 143–145, 144*f*
Monochorionic twinning process
  complications of, 143–145, 144*f*
  determining, 143, 144*f*
MORE (Multiple Outcomes of Raloxifene evaluation) trial, 90
MRI. *See* Magnetic resonance imaging
MS-AFP. *See* Maternal serum-alpha-fetoprotein
Mucinous tumors, ovarian, 6–7
  echotexture of, 82, 83*f*
Mullerian duct system
  anomaly, vaginal obstruction in, 54, 55*f*
  development of, 52–53
Multicystic dysplastic kidney, fetal, 170, 170*f*
Multicystic ovaries, premenarchal, 55–56
Multiple Outcomes of Raloxifene evaluation trial, 90
Multiple pregnancy, 143–145, 144*f*
  maternal serum-AFP detecting, 189*t*
Myelomeningocele
  Chiari II malformations and, 165
  deformities associated with, elevated MS-AFP and, 190–192, 191*f*
  in diabetic pregnancy, 209, 212*f*
  fetal spine, 166*f*, 167, 190–192, 191*f*
  "lemon" sign and. *See* "Lemon" sign, fetal head
  teratogen-induced, 222, 222*f*
Myoma(s)
  exophytic ovarian, 7–8
  in infertility evaluation, 40, 41, 41*f*
Myometrial cysts, in adenomyosis, 27
Myometrial thickening, in adenomyosis, 27
Myometrial vascularity, in postpartum patient
enhanced, 245
  focal *vs.* diffuse, 244*f*, 245
Myometrium
  focal *vs.* diffuse vascularity, in postpartum patient, 244*f*, 245
  in infertility evaluation, 40, 40*f*

N
Nabothian cysts, 128, 128*f*
Nasal bone, evaluation in fetal Down syndrome, 204, 204*f*
National Institute of Child Health and Human Development Network, cervical length study, 124–125
Neisseria gonorrhoeae, pelvic inflammatory disease and, 16
Neoangiogenesis, in endometrial cavity, 95
Neonates, preterm. *See* Premature infants
Neovascularity, in malignant ovarian lesions, Doppler imaging of
  color, 85–87, 86*f*
  spectral, 84–85, 85*f*
Neural tube defects, in fetus. *See also specific defects*
  amniotic fluid-AFP detecting, 188
  in diabetic pregnancy, 209, 209*f*–210*f*, 212*f*
  involving head, 161–162, 162*f*
  involving spine, 166–167, 166*f*
  maternal serum-AFP detecting, 187, 189–193, 189t, 190*f*–193*f*
  polyhydramnios and, 148, 149*f*
  teratogen-induced, 222, 222*f*
  trisomy 9 and 13 and, 148, 150, 151*f*–152*f*
NICHD (National Institute of Child Health and Human Development Network), cervical length study, 124–125
Nonimmune hydrops
  polyhydramnios and, 147–148, 147*f*–148*f*
  uterine masses and, 152
Nonmenstrual bleeding, causes of, 32
Nonpregnant patient, bleeding in
  abnormal menstrual flow, causes of, 22–32, 23*f*–31*f*, 29*t*
  contact bleeding, 32
  nonmenstrual, causes of, 32
Nuchal cystic hygromas, in fetal Down syndrome, 200, 201*f*
Nuchal skin fold, thickened, in fetal Down syndrome, 200–201, 201*f*
Nuchal translucency, in fetal gestational age estimation, 139–140, 140*f*

O
Obstruction, fetal duodenal. *See* Duodenal atresia, fetal
Office hysteroscopy, in abnormal uterine bleeding evaluation, 21–22
OHSS (ovarian hyperstimulation syndrome), 44*f*, 45
Oligomenorrhea, 32
Omphaloceles, in fetal abdominal wall, 171, 171*f*
  elevated MS-AFP and, 189*t*, 193, 193*f*
Oocyte retrieval, TVS role in, 45, 45*f*–46*f*
Ossification centers, fetal spine, 166, 166*f*
Outflow tracts, fetal cardiac. *See* Cardiac outflow tracts, fetal
Ovarian carcinoma, 76
  family history and, 76
  heritable syndromes correlated with, 76
  prevalence of, 76
  risk factors for, 76
  screening in high-risk women, 77
    history and physical examination, 77
    serum CA 125 levels, 77
    sonographic, 77–87, 78*f*–86*f*
  stage at detection, 76
Ovarian cysts, 11–13, 12*f*–13*f*, 80*f*
  echotexture of, 82, 82*f*
Ovarian folliculogenesis, 52
Ovarian hyperstimulation syndrome, 44*f*, 45
Ovarian lesions
  neoplastic, 6–8, 6*f*–8*f*
  sonographic evaluation of, 8
Ovarian masses, gray-scale morphology and echotexture, 82–84, 82*f*–84*f*
  septa within, 78, 81*f*–82*f*
  wall features, 78, 80*f*
Ovarian torsion, 11, 14–15, 16*f*
Ovarian tumors
  benign, ultrasound evaluation of, 6–7, 6*f*–7*f*
  classification, 6
  germ cell, 7–8, 7*f*
  mucinous, 6–7, 82, 83*f*
Ovarian vein thrombophlebitis, in postpartum patient, 247, 248*f*
Ovary(ies). *See also* Ovarian *entries*
  in infertility, ultrasound evaluation in, 42–43, 42*f*–43*f*
  in infertility treatment
    controlled stimulation, 44, 44*f*
    monitoring, 44–45, 44*f*–46*f*
  masses associated with. *See* Ovarian masses, gray-scale morphology and
  mobility of, 43
  postmenarchal, cyclical changes in, 50–51, 51*f*
  premenarchal, 54–56, 55*f*
  size estimation of, 78, 79*f*
  tumors of. *See* Ovarian tumors
Overriding aorta, in fetal heart examination, 183–184, 183*f*
Ovulation
  in normal menstrual cycle, 42, 50–51, 51*f*
  transvaginal sonography following, 42, 42*f*
Ovulatory cycle, 52

P
PA. *See* Pulmonary artery
PACs, fetal biometry and, 141
Pain
  in obstetric patient. *See* First-trimester bleeding; Second/third trimester bleeding
  pelvic
    acute. *See* Acute pelvic pain in postpartum patient, 238
  right lower quadrant, appendicitis and, 18, 18*f*
Palpable adnexal masses, asymptomatic
  differential diagnosis of, 1
  imaging of, 1
  laparoscopic surgery for, 1, 8–9
  management guidelines for, 8–9
  ultrasound diagnostic evaluation of, 1–6, 1*f*–6*f*
Pancreas, fetal annular, polyhydramnios and, 169
Paraovarian cysts, as palpable adnexal masses, 3–4, 3*f*
Parasitic infections, fetal exposure to, 229, 231*f*
Paratubal cysts, as palpable adnexal masses, 3–4, 3*f*
Parvovirus, teratogenicity of, 232
Patency, of fallopian tube, 42
Patent ductus arteriosus, in fetal heart examination, 176
Patient history
  in abnormal uterine bleeding evaluation, 21
  ovarian cancer and, 77
PCOS. *See* Polycystic ovarian syndrome
PDA (patent ductus arteriosus), in fetal heart examination, 176
Pediatric patients
  adolescent. *See* Adolescents
  prematurity and. *See* Premature infants
Pelvic inflammatory disease, 16–17, 16*f*
  transvaginal ultrasound in, 56
Pelvic kidney, fetal, 169, 169*f*
Pelvic pain
  acute, 11–19. *See also* Acute pelvic pain in postpartum patient, 238
Pelvic tenderness, in adenomyosis, 26–27
Pelvis. *See also* Pelvic *entries*
  adnexal masses in, asymptomatic palpable, 1–9
  ovarian carcinoma in, 76–87
  pain in. *See* Pelvic pain
  tamoxifen therapy and. *See* Tamoxifen
  ultrasound evaluation of
    approaches to, 92–96, 92*f*–96*f*
    in infertility. *See* Infertility
  vaginal bleeding and
    abnormal premenopausal, 21–37
    postmenopausal, 65–73
Peritoneal inclusion cysts, as palpable adnexal masses, 4, 4*f*
Periventricular leukomalacia, in cocaine-exposed fetus, 227, 227*f*
Phacomelia, thalidomide exposure and, 220, 220*f*
Phalanx, fifth digit, in fetal Down syndrome, 203, 203*f*
Pharmaceuticals, teratogenic effects of, 219–224
Physical examination
  in abnormal uterine bleeding evaluation, 21
  in ovarian cancer, 77
Physiological cysts, as palpable adnexal masses, 1–2, 3*f*–4*f*
PI (pulsatility index), in ovarian mass vascularity evaluation, 84–85, 85*f*
Pituitary adenoma, amenorrhea and, 58, 58*f*
Pituitary dysfunction, amenorrhea and, 57, 58, 58*f*
Placenta
  abnormalities of, elevated MS-AFP and, 195–196
  implantation site involution, 243–244
  retained. *See* Retained placenta
  thickness of, in fetal gestational age estimation, 140
Placenta abruption, sonographic findings in, 111–113, 111*f*–113*f*
Placenta accreta
  devitalized, false-positive Doppler signals in, 238*f*, 239
  placenta previa with, 116, 116*f*
  and prior C-section association, 116
  retained placenta *vs.*, 245–246, 245*f*
Placenta increta, retained placenta *vs.*, 245–246
Placenta previa
  complete central, 114, 114*f*
  marginal, 115–116, 115*f*
  with placenta accreta, 116, 116*f*
  "pseudo," 107
  sonographic findings in, 113–116, 114*f*–116*f*
Pleural effusions, in fetal Down syndrome, 200, 201*f*
Polycystic ovarian syndrome
  amenorrhea in, 60–61, 60*f*
  in infertility evaluation, 43, 43*f*
  palpable adnexal masses in, 3, 3*f*
Polyhydramnios, 145
  in diabetes pregnancy, 214
  malformations associated with, 145*f*–147*f*, 146–147
  mild, 146
Polymenorrhea, 31
Polyps, endometrial. *See* Endometrial polyps
Posterior fossa, in fetal head, 161, 164*f*, 165, 165*f*
  ventriculomegaly and, 192
Postmenopausal vaginal bleeding, 65
  endometrial pathology and. *See* Endometrial thickness, postmenopausal
  hysterosalpingography in, 66
  MRI in, 66
  nonimaging test in, 65–66
  sonographic evaluation in, 66–70, 66*f*–70*f*. *See also* Sonohysterography
    benefits of, 71
    diagnostic workup algorithm, 71, 72*f*
  transvaginal sonographic evaluation of, 93
Postmenopausal women
  breast cancer in, tamoxifen therapy for, 90–91. *See also* Tamoxifen
  normal uterus in, 92, 92*f*
  osteoporosis in, raloxifene for, 90
  palpable adnexal masses in, 2
    management guidelines, 9
  vaginal bleeding in. *See* Postmenopausal vaginal bleeding
Postpartum fever, 238
Postpartum ovarian vein thrombophlebitis, 247, 248*f*
Postpartum patient
  complications in

Postpartum patient (*continued*)
clinical signs and diagnoses, 237–238, 237*t*, 238*f*
endometritis, 248*f*, 249
hematomas, post-Cesarean section, 246–247, 246*f*–247*f*
imaging modalities used, 237
imaging modalities used, ultrasound technique, 238–239, 238*f*
ovarian vein thrombophlebitis, 247, 248*f*
retained products of conception, 239, 242–246, 242*f*–245*f*
normal pelvic changes in
after C-section, 239, 241*f*
after vaginal delivery, 239, 240*f*
POVT (postpartum ovarian vein thrombophlebitis), 247, 248*f*
Pregnancy
adverse outcomes in, MS-AFP and, 187
bleeding in
causes of, 32
and early pregnancy failure. *See* Early pregnancy failure
extrauterine gestation and, 37, 37*t*
in first trimester. *See* First-trimester bleeding
in heterotopic pregnancy, 37
intrauterine gestation and, 32–37, 32*f*, 33*f*
in second and third trimesters. *See* Second/third trimester bleeding
cervical role in, 121
dating of. *See* Pregnancy dating
diabetes mellitus in. *See* Diabetic pregnancy
diabetogenic nature of, 208
early. *See* Early pregnancy; Early pregnancy failure
extrauterine. *See* Ectopic pregnancy
Pregnancy dating
AFP testing for, 208
amniocentesis and, 208
fetal biometry for. *See* Fetal biometry
in vitro fertilization and, 46
large uterine size in
incorrect dates and, 143
large uterine masses and, 152, 153*f*, 154
multiple pregnancy and, 143–145, 144*f*
polyhydramnios and, 145–152, 145*f*–153*f*
small uterine size in
cerebral circulation and, 157–158, 157*f*
fetal growth restriction, 158–159, 158*f*
umbilical circulation and, 156–157, 157*f*
Pregnancy test(s), 103
in abnormal uterine bleeding assessment, 21
Premature delivery
cervical sonography predicting, 125
defined, 121
in diabetes pregnancy, 214
Premature infants
cost of care for, 121
morbidity and mortality trends for, 121
Premature labor
evaluation of cervix in, 121, 122*f*
technical aspects, 122*f*–124*f*, 123–124
role of cervical sonography in, 125
findings, 125–129, 126*f*–128*f*
Premature rupture of fetal membranes, 128–129
Premenopausal women
abnormal vaginal bleeding in. *See* Nonpregnant patient, bleeding in; Pregnancy, bleeding in
palpable adnexal masses in, 1*f*, 2, 2*f*
management guidelines, 8
Presacral tumors. *See* Sacrococcygeal teratoma
Preterm infants. *See* Premature infants
Primary amenorrhea
defined, 50
etiology of, 56*t*
Progestins, teratogenic effects of, 224–225
"Pseudo placenta previa," 107
Pseudohermaphroditism, amenorrhea and, 59–60, 59*f*
Pseudoventricular septal defect, in fetal heart assessment, 179, 179*f*
Pubarche, 52
Pulmonary artery, fetal heart, 177, 178*f*
overriding aorta and, 184
parallel aorta and, 184, 184*f*
Pulmonary atresia
chromosome deletions and, 175
in fetal heart examination
with intact ventricular septum, 181, 181*f*
with ventricular septal defect, 181–182
Pulmonary valve stenosis, in fetal heart examination, 176
Pulsatility index, in ovarian mass vascularity evaluation, 84–85, 85*f*
PVL (periventricular leukomalacia), in cocaine-exposed fetus, 227, 227*f*

R

Radiation exposure, teratogenic effects on fetus, 228–229
Raloxifene, for postmenopausal osteoporosis, 90
Recreational drugs, teratogenic effects of, 225–228
Renal abnormalities
chromosome deletions and, 175
elevated MS-AFP and, 195
Renal agenesis
congenital gynecologic anomaly and, 52, 52*f*
in diabetic pregnancy, 212, 212*f*
Renal collecting system, in fetal abdomen assessment, 169–170, 169*f*
Renal dysgenesis, teratogen-induced
ACE inhibitors and angiotensin II receptor antagonists, 220, 220*f*
cocaine, 227, 227*f*
Renal length, in fetal gestational age estimation, 140
Renal pyelectasis, in fetal Down syndrome, 202, 202*f*
Reproductive organs
genital embryology and, 52–53
maturation of, 52
ultrasound imaging techniques, 56
Resistive index
in ovarian mass vascularity evaluation, 84–85, 85*f*
vascularized trophoblast and, 243
Retained placenta
dilatation and curettage and, 242, 242*f*, 245
in postpartum patient, 242, 242*f*
vs. placenta accreta or increta, 245–246, 245*f*
Retained products of conception, 239, 242–246, 242*f*–245*f*
Retinoids, teratogenic effects of, 223–224
Retroplacental hematoma, 111–112, 111*f*–112*f*
Retroplacental leiomyoma, 111, 112*f*
Retzius, space of, post-Cesarean section hematomas and, 246, 246*f*
Reversed diastolic flow, in umbilical arterial circulation evaluation, 157, 157*f*
Rhabdomyomas, in fetal heart examination, 183, 183*f*
RI. *See* Resistive index
Right atrium, fetal heart, 182, 182*f*
Right lower quadrant pain, appendicitis and, 18, 18*f*
Right ventricle, fetal heart
double-outlet, 184
left ventricle smaller than, 180–181, 180*f*–181*f*
overriding aorta and, 184
smaller than left ventricle, 181–182, 181*f*–182*f*
"Ring of fire" appearance
in ectopic pregnancy evaluation, 103
ovarian follicular cyst and, 12–13, 12*f*
RLQ (right lower quadrant) pain, appendicitis and, 18, 18*f*
Rokitansky nodule, 5
ovarian teratomas and, 82–83, 84*f*
RPOC (retained products of conception), 239, 242–246, 242*f*–245*f*
Rubella, teratogenic effects of, 229
Rupture
premature, of fetal membranes, 128–129
uterine. *See* Uterine rupture
RV. *See* Right ventricle

S

Sacral agenesis, in fetus of diabetic mother, 209, 210*f*
Sacrococcygeal teratoma, fetal, 152, 153*f*, 172, 172*f*
elevated MS-AFP and, 194–195–380*f*
Saline infusion sonohysterography-transvaginal sonography. *See also* Sonohysterography
of endometrium, 94*f*, 95, 97
Salpingectomy/Salpingostomy, 14
Screening
for fetal Down syndrome, in second trimester. *See* Second-trimester screening, for fetal Down syndrome
maternal serum-alpha-fetoprotein, 187
patient triage in, 188–189
for ovarian carcinoma, 77
history and physical examination, 77
serum CA 125 levels, 77
sonographic, 77–87, 78*f*–86*f*
Second/third trimester bleeding
circumvallate placenta and, 116–117, 117*f*
diagnostic considerations in, 110
nonimaging evaluation of, 110
placenta abruption and, 111–113, 111*f*–113*f*
placenta previa and, 113–116, 114*f*–116*f*

uterine rupture and uterine dehiscence and, 117–118
vasa previa and, 117, 117*f*
Second-trimester screening, for fetal Down syndrome, 199
genetic sonogram in, 204–205
following abnormal serum screens, 205–206
sonographic findings, 201–204, 202*f*–204*f*
structural defects, 199–201, 200*f*–201*f*
Secondary amenorrhea, 62–63, 62*f*
defined, 50
Secundum atrial septal defect, in fetal heart examination, 176
Selective estrogen receptor modulators, 90. *See also* Tamoxifen
Septa, within ovarian mass, 78, 81*f*–82*f*
Septic abortion
defined, 35
outcome studies of, 35–36
SERMS (selective estrogen receptor modulators), 90. *See also* Tamoxifen
Serous cystadenocarcinoma, ovarian, 6–7, 7*f*
Serous cystadenoma, benign ovarian, 6, 6*f*
septa within, 78, 81*f*
Serum screens, in fetal Down syndrome testing, 199
abnormal, 199
diagnostic evaluation, 206
genetic sonogram following, 205–206
sonographic findings following, 199–204, 200*f*–204*f*
Sex cord tumors, ovarian, 7
Sexual development, delayed
amenorrhea and, 57, 57*f*
hypergonadotropic hypogonadism and, 58–59, 59*f*
hypogonadotropic hypogonadism and, 57–58, 58*f*
Shoulder dystocia, in macrosomic diabetic fetus, 214
Shpintzen's syndrome, chromosome deletions and, 175
SIS (saline infusion sonohysterography)-transvaginal sonography. *See also* Sonohysterography
of endometrium, 94*f*, 95
Skeletal dysplasias, fetal, polyhydramnios and, 148, 151*f*
Small bowel obstruction, fetal, polyhydramnios and, 146–147, 146*f*
Society of Radiologists in Ultrasound, on transvaginal sonography role in postmenopausal bleeding, 93
Sonohysterography
in endometrial polyp diagnosis, 30–31
in infertility evaluation, 41, 41*f*
in postmenopausal vaginal bleeding evaluation, 68–70, 69*f*–70*f*
benefits, 71
diagnostic workup algorithm, 71, 72*f*
3-D, 70, 70*f*
in postpartum uterine evaluation, 242–243
Space of Retzius, post-Cesarean section hematomas and, 246, 246*f*
Spectral Doppler imaging, in ovarian cancer screening, 84–85, 85*f*
Spina bifida
elevated MS-AFP and, 191
open, cranial findings in, 191–192, 191*f*
Spinal dysraphism, fetal
detection of, 190–192, 191*f*
teratogen-induced, 222, 222*f*
Spine, fetal. *See* Fetal spine
Spontaneous abortion, 35
outcome studies of, 35–36, 35*t*
rates of, 36*t*
subclinical, 35
SRU (Society of Radiologists in Ultrasound), on transvaginal sonography role in postmenopausal bleeding, 93
Stenosis, aortic valve. *See* Aortic valve stenosis
Stippled epiphyses, teratogen-induced, 222–223, 223*f*
Stomach bubble, absence in fetus, polyhydramnios and, 147, 147*f*
Streaky shadowing, in adenomyosis, 28
Stromal tumors, ovarian, 7
Subchorionic hematoma
intrauterine membrane and, 112, 112*f*
mimicking intrauterine mass, 112–113, 112*f*–113*f*
Subchorionic hemorrhage
normal intrauterine gestation with, 33, 33*f*
in threatened abortion, 107–108, 107*f*
Subfascial hematoma, post-Cesarean section, 246, 246*f*
Submucous uterine fibroids
sonographic findings in, 22, 24*f*–25*f*
treatment of, 26
Syphilis, fetal exposure to, 231–232, 232*f*
Systemic corticosteroids, teratogenic effects of, 225
Systemic diseases, amenorrhea and, 57, 58*f*

T

Tachycardia, fetal, 152*f*
TAH-BSO (total abdominal hysterectomy-bilateral salpingo-oophorectomy), 17
Tamoxifen
endometrial responses to, 91–92
with long-term use, 101
ultrasound evaluation of, 92–96, 92*f*–96*f*
estrogenic effects of, 90–91
mechanism of action of, 90–91
prophylactic use of, 92
TAPVR (total anomalous pulmonary venous return), in fetal heart examination, 181
TAS. *See* Transabdominal sonography
Teratogen exposure, fetal, 219
Teratogenesis, factors associated with, 216
Teratogenicity
of alcohol and recreational drugs, 225–228
of hormones, 224–225
of infections agents, 229–232
of interventional measures, 228
nature of, 218–219
of pharmaceuticals, 219–224
principles of, 216–217, 217*f*
of radiation and heat exposure, 228–229
Teratogens
fetal exposure to, assessment of, 219
identification of, 218, 218*t*
idiosyncratic effects of, 217–218
potency and risk of, 218
Teratoma
mature cystic, as palpable adnexal mass, 5–6, 5*f*–6*f*, 7
sacrococcygeal. *See* Sacrococcygeal teratoma
Testicular feminization syndrome, 60, 60*f*
Tetracycline, teratogenic effects of, 224
Tetralogy of Fallot, fetal
chromosome deletions and, 175
in diabetic pregnancy, 209, 211*f*
in Down syndrome, 200
overriding aorta and, 183–184, 183*f*
severe form of, 181–182
teratogen-induced, 223
Thalidomide, teratogenic effects of, 220, 220*f*
Thanatophoric dysplasia, fetal, polyhydramnios and, 148, 151*f*
Thelarche, 52
Therapeutic abortion, outcome studies of, 35*t*
Thorax
fetal abnormalities of, polyhydramnios and, 148, 150*f*
normal fetal heart in, 167, 167*f*, 176–177
Threatened abortion
defined, 35
outcome studies of, 35–36, 35*t*
transvaginal sonography in, 107–108, 107*f*
Thrombophlebitis, ovarian vein, in postpartum patient, 247, 248*f*
Thyroid agents, teratogenic effects of, 221–222
Thyroid replacement agents, teratogenic effects of, 221–222
TOA (tubo-ovarian abscess), 11, 16–17, 16*f*
Toes, gap between, in fetal Down syndrome, 203, 203*f*
TOF. *See* Tetralogy of Fallot, fetal
Toluene inhalation, teratogenic effects of, 228
Torsion
adnexal. *See* Adnexal torsion
ovarian, 11, 14–15, 16*f*
Total abdominal hysterectomy-bilateral salpingo-oophorectomy, 17
Total anomalous pulmonary venous return, in fetal heart examination, 181
Toxoplasmosis, teratogenic effects of, 231, 231*f*
Transabdominal sonography
in cervix evaluation, 122*f*, 123
of female pelvis, 92, 92*f*
of female reproductive organs, 56
in incompetent cervix, 126*f*, 127
in placenta previa, 115
in vasa previa, 117, 117*f*
Translabial sonography, female reproductive organs, 56
Transperineal sonography
in cervix evaluation, 121, 122*f*, 123
of female reproductive organs, 56
in placenta previa, 115–116, 116*f*
Transposition of the great arteries, fetal heart, 184, 184*f*
corrected transposition and, 184
in diabetic pregnancy, 209, 210*f*
teratogen-induced, 223
Transvaginal sonography
of adnexal lesions, 1
in anencephaly, 149*f*
in cervix evaluation, 121, 121*f*, 123, 123*f*

Transvaginal sonography (*continued*)
in ectopic pregnancy evaluation, 103, 104*f*
of female pelvis, 92–96, 92*f*–96*f*
benefits, 92–96–269, 97*f*–100*f*, 99, 101
tamoxifen therapy and, 101
of female reproductive organs, 56
in fetal heart evaluation, 175
in incompetent cervix, 122*f*, 126*f*, 127
in infertility evaluation, 39
endometrium, 40–41, 40*f*–41*f*
fallopian tubes, 41–42, 41*f*
ovaries, 42–43, 42*f*–43*f*
uterine anomalies, 40–41, 40*f*–41*f*
in lumbosacral neural tube defect, 149*f*
in postmenopausal bleeding, 93
role in infertility treatment monitoring
ovaries, 44–45, 44*f*–46*f*
uterus, 43–44
with saline infusion sonohysterography. *See* Saline infusion sonohysterography-transvaginal sonography
in threatened abortion, 107–108, 107*f*–108*f*
Treponema pallidum, fetal exposure to, 231–232, 232*f*
Tricuspid valve
atresia of, 182
congenital absence of leaflets in, 182
Triplet pregnancy, 143, 144*f*
Trisomy 9, polyhydramnios and, 150, 151*f*–152*f*
Trisomy 13, polyhydramnios and, 148, 150, 151*f*–152*f*
Trisomy 18, polyhydramnios and, 148
Trisomy 21, polyhydramnios and, 148
Trophoblast, vascularized, 243
Truncus arteriosus, fetal
chromosome deletions and, 175
in diabetic pregnancy, 209, 211*f*
overriding aorta and, 184
Tubo-ovarian abscess, 11, 16–17, 16*f*
Tumors. *See also individually named tumors*
adrenal, 17–18, 60
cardiac, in fetal heart examination, 182–183, 183*f*
fetal, polyhydramnios and, 150, 152, 153*f*
ovarian. *See* Ovarian tumors
presacral. *See* Sacrococcygeal teratoma
uterine fibroid, 152, 153*f*, 154
Turner's syndrome, amenorrhea in, 58–59, 59*f*
TVS. *See* Transvaginal sonography
TVUS (transvaginal ultrasound). *See* Transvaginal sonography
Twin pregnancy, 143, 144*f*
acardiac twin, 145
complications associated with, 143–145, 144*f*
conjoined twins, 143, 144*f*
Twin-to-twin transfusion syndrome, 143–145, 144*f*
nonimmune hydrops and, 148

U

uE3 (unconjugated estriol), maternal serum, fetal Down syndrome and, 199
Uhl's anomaly, 182, 182*f*
Umbilical artery(ies)
Doppler flow imaging of, 156–157, 157*f*
hypoplastic, in diabetic pregnancy, 212, 213*f*
and umbilical cord, normal insertion of, 171, 171*f*
Umbilical cord, normal insertion, 171, 171*f*
Umbilicus, abdominal wall defects at, 171, 171*f*
Unconjugated estriol, maternal serum, fetal Down syndrome and, 199
Upper limb defects, fetal
misoprostol exposure and, 221, 221*f*
thalidomide exposure and, 220, 220*f*
Ureteral calculus, acute pelvic pain and, 18–19, 19*f*
Ureteropelvic junction obstruction, in fetal renal collecting system, 169
Urethral valves, fetal, 171, 171*f*
Urinary bladder, fetal, 170–171, 170*f*
Urinary enzyme-linked immunosorbent assay, 103
Uterine aplasia, amenorrhea due to, 62
Uterine artery flow, color Doppler TVS assessing, 95
Uterine bleeding, abnormal
diagnostic evaluation of, 21–22
initial assessment of, 21
sonographic, 22
dysfunctional, 29
menstrual flow and, 22–32. *See also specific conditions*
in pregnant patient, 32–37. *See also* Early pregnancy failure; Pregnancy, bleeding in
Uterine dehiscence
defined, 118, 247
diagnosis of, 247
post-Cesarean section, 247, 247*f*
second/third-trimester bleeding and, 117–118
sonographic diagnosis of, 118
Uterine fibroids, 152, 153*f*, 154
Uterine hypoplasia, amenorrhea due to, 62
Uterine leiomyomata. *See* Fibroids, uterine
Uterine mass, pregnancy dating and, 152, 153*f*, 154
Uterine rupture
defined, 118
second/third-trimester bleeding and, 117–118
sonographic diagnosis of, 118
Uterine size
after puberty, 54
in obstetric patient
greater than dates, 143–154
less than dates, 156–159
Uterine tenderness, on palpation, in adenomyosis, 28
Uterus. *See also* Uterine *entries*
in amenorrhea patients, ultrasound evaluation of, 53–54, 54*f*
bicornuate, 52–53, 53*f*
congenital anomalies of, imaging evaluation of, 54, 55*f*
infantile, 57, 57*f*
in Turner's syndrome, 59, 59*f*
in infertility evaluation, 39–41, 39*f*–41*f*
monitoring of, in infertility treatment, 43–44
neonatal, 53, 53*f*
postmenarchal, 53, 54*f*
premenarchal, 53–54, 54*f*
size of. *See* Uterine size

V

Vaginal bleeding
in menstrual cycle. *See* Menstrual bleeding
placenta previa severity and, 114
postmenopausal. *See* Postmenopausal vaginal bleeding
premenopausal, abnormal, evaluation of, 21–22. *See also* First-trimester bleeding; Nonpregnant patient, bleeding in; Pregnancy, bleeding in; Second/third trimester bleeding
Vaginal delivery, normal pelvic findings after, 239, 240*f*
Vaginal obstruction, amenorrhea and, 61–62, 61*f*–62*f*
Mullerian duct anomaly and, 54, 55*f*
Varicella-zoster virus, teratogenic effects of, 231
Vasa previa, 117, 117*f*
Velocardiofacial syndrome, chromosome deletions and, 175
Ventricles, fetal heart. *See* Left ventricle, fetal heart; Right ventricle, fetal heart
Ventricular septal defect, fetal heart, 167
for congenital heart disease, 176, 179–180, 179*f*–180*f*
in diabetic pregnancy, 209, 211*f*
pulmonary atresia with, 181–182
teratogen-induced, 223
Vesicoureteral reflux, in fetal renal collecting system, 169
Viral infections, fetal exposure to
cytomegalovirus, 229, 230*f*
herpes simplex, 232
HIV, 232
parvovirus, 232
rubella, 229
varicella-zoster, 231
Virilization, in female adolescence, 60
Vitamin A congeners, teratogenic effects of, 223–224
VSD. *See* Ventricular septal defect, fetal heart
VUR (vesicoureteral reflux), in fetal renal collecting system, 169

W

White classification, of diabetes mellitus in pregnancy, 208
White matter damage. *See* Periventricular leukomalacia

Y

Young adults, amenorrhea in, 50–63. *See also* Amenorrhea